Solid-state properties of pharmaceuticals

Marius Brits
B.Pharm., M.Sc. (Pharmaceutics)

Thesis submitted in the Department of Pharmaceutics in the School of Pharmacy at the North-West University, Potchefstroom Campus for the degree **Doctor Philosophiae** in Pharmaceutics.

Supervisor: **Prof. W. Liebenberg**
Co-Supervisor: **Prof. M.M. de Villiers**

POTCHEFSTROOM

2008

Table of contents

TABLE OF CONTENTS I

ABSTRACT XI

UITTREKSEL XIII

Aims and objectives XV

CHAPTER 1: IMPORTANCE OF POLYMORPHISM AND PSEUDOPOLYMORPHISM TO PRODUCT DEVELOPMENT AND LIFE CYCLE MANAGEMENT 1

Introduction 1

1.1 Polymorphism, psuedopolymorphism, amorphism and pharmaceutical co-crystals: the art of crystal engineering and the importance thereof 2

1.1.1 Importance of polymorphism and pseudopolymorphism to drug development 6

1.1.2 Importance of polymorphism and pseudopolymorphism to product Life Cycle Management (LCM) 7

1.2 Stability and thermodynamic relationship between polymorphs 10

1.3 Factors that may influence the thermodynamic stability of crystal forms 17

1.3.1 Manufacturing activity induced polymorphic transitions 19

1.3.2 Effect of granulation on stability of polymorphic forms 20

1.3.3 Effect of drying on stability of polymorphic forms 24

1.3.4 Effect of excipients on stability of polymorphic forms 26
1.3.5 Effect of grinding and compression on stability of polymorphic forms 28
1.3.6 Role of moisture in polymorphic stability (moisture induced polymorphic transitions. 31

1.3.6.1 Water-solid interactions 31
1.3.6.2 Water-solid interactions for freely water soluble API's 36
1.3.6.3.Water-solid interactions for slightly soluble to very slightly water soluble API's 40
1.3.6.4 Water-solid interactions for API's that are practically insoluble in water 41

Conclusion 44

CHAPTER 2: GENERAL METHODS UTILISED DURING STUDIES FOR CHARACTERISATION AND ANALYTICAL PURPOSES 45

Introduction 45

2.1 Identification and characterisation methods used in this study 45

2.1.1 Crystallographic methods 47

2.1.1.1 X-ray powder diffraction (XRPD) 47
2.1.1.2 Variable temperature X-ray powder diffraction (VT-XRPD) 48

2.1.2 Thermal methods 49

2.1.2.1 Differential scanning calorimetry (DSC) 49
2.1.2.2 Thermogravimetric analysis (TGA) 49

2.1.3 Infrared spectroscopy (DRIFT-IR) 50

2.1.4 Microscopy 51

2.1.4.1 Thermal microscopy (TM) 51
2.1.4.2 Scanning electron microscopy (SEM) 51

2.1.5 Particle size analysis 51

2.1.6 Specific surface area analysis 52

2.1.7 Moisture sorption analysis 54

2.1.8 Karl Fischer analysis 56

2.1.9 Heat of solution studies 56

Conclusion 57

CHAPTER 3: THERMODYNAMIC STABILITY OF MEBENDAZOLE POLYMORPHIC FORMS IN TABLETS UNDER HIGH HUMIDITY CONDITIONS 59

Introduction 59

3.1 Materials and methods 60

3.1.1 Products 60
3.1.2 Stability testing 66
3.1.3 High pressure liquid chromatography analysis (HPLC) 66
3.1.4 Infrared spectroscopy (DRIFT-IR) 67

3.1.5 X-ray powder diffraction (XRPD) 69
3.1.6 Dissolution testing 73
3.1.7 Calculations 74

3.2 Results 76

3.2.1 Polymorphic stability of mebendazole in Product 1 80
3.2.1.1 Summary of polymorphic stability in Product 1 87
3.2.2 Polymorphic stability of mebendazole in Product 2 88
3.2.2.1 Summary of polymorphic stability in Product 2 95
3.2.3 Polymorphic stability of mebendazole in Product 3 95
3.2.3.1 Summary of the polymorphic stability in Product 3 103
3.2.4 Polymorphic stability of mebendazole in Product 4 103
3.2.4.1 Summary of the polymorphic stability in Product 4 109
3.2.5 Polymorphic stability of mebendazole in Product 5 110
3.2.5.1 Summary of the polymorphic stability in Product 5 117
3.2.6 Polymorphic stability of mebendazole in Product 6 119
3.2.6.1 Summary of the polymorphic stability in Product 6 125
3.2.7 Polymorphic stability of mebendazole in Product 7 125
3.2.7.1 Summary of the polymorphic stability in Product 7 131
3.2.8 Summary of results obtained: Products 1 - 7 131
3.2.9 Polymorphic stability of mebendazole in Product 2A 132
3.2.9.1 Summary of the polymorphic stability in Product 2A 141

3.3 Discussion of the polymorphic transitions observed in the various commercially available products 142

3.3.1 Quantitative investigation of the conversion of mebendazole polymorph C → polymorph A in commercially available tablets 142
3.3.1.1 Calculating the ratio of polymorph A and C content relative to the total polymorph content in the tablet from XRPD data 142

3.3.1.2 Calculating the ratio of polymorph A and C content relative to the total polymorph content in the tablet from DRIFT-IR data 144

3.3.2 Kinetics of mebendazole polymorph C → polymorph A in commercially available tablets 151

3.3.2.1 Models for polymorphic conversion 152

3.3.2.1.1 Prout-Tompkins model 153

3.3.2.1.2 Johnson-Mehl-Avrami-Erofeev-Kolmogorov (JMAEK) model 154

Discussion and Conclusion 162

CHAPTER 4: THE INFLUENCE OF MOISTURE AND INCREASED TEMPERATURE ON MEBENDAZOLE POLYMORPHS 165

Introduction 165

4.1 The influence of moisture and heat on the stability of mebendazole polymorph B and polymorph C raw materials 166

4.1.1 Materials and methods 166

4.1.2 The influence of moisture and heat on the stability of mebendazole polymorph C 169

4.1.3 The influence of moisture and heat on the stability of mebendazole polymorph B 184

4.1.4 The effect of moisture on the stability of mebendazole polymorphs 201

4.1.5 Theory of the aqueos mediated phase transformation of mebendazole polymorphic forms 207

Conclusion 212

CHAPTER 5: VENLAFAXINE HYDROCHLORIDE **215**

Introduction 215

5.1 Intellectual property: Venlafaxine HCl polymorphic and pseudopolymorphic forms 215

5.2 Introduction to venlafaxine hydrochloride Form 1 and Form 5 225

5.2.1 Preparation of venlafaxine hydrochloride Form 1 and Form 5 225
5.2.2 Solid state properties of venlafaxine hydrochloride Form 1 and Form 5 226
5.2.2.1 X-ray powder diffractometry (XRPD) 226
5.2.2.2 Diffuse reflectance infrared Fourier transform spectroscopy (DRIFT-IR) 233
5.2.2.3 Thermal analysis 235
5.2.2.4 Heat of solution of venlafaxine HCl polymorphs – Form 1 and Form 5 241
5.2.2.5 Thermodynamic stability of venlafaxine HCl polymorphs – Form 1 and Form 5 246
5.2.2.5.1 Thermodynamic stability of venlafaxine HCl Form 1 247
5.2.2.5.2 Thermodynamic stability of venlafaxine HCl Form 5 250

Conclusion 262

CHAPTER 6: MOISTURE SORPTION PROPERTIES OF VENLAFAXINE HYDROCHLORIDE CRYSTAL FORMS **265**

Introduction 265

6.1 Method and materials for the moisture uptake measurement of the venlafaxine hydrochloride polymorphic forms 265

6.2 Moisture uptake measurements of venlafaxine hydrochloride polymorphic forms 267

6.2.1 Particle size and specific surface area analysis results 267
6.2.2 Moisture sorption analysis results 268
6.2.3 Total moisture content – Karl Fischer (KF) results 270
6.2.4 Polymorphic stability of venlafaxine hydrochloride Form 1 273
6.2.5 Polymorphic stability of venlafaxine hydrochloride Form 5 278
6.2.5.1 Venlafaxine hydrochloride Form 5 - 30°C & 0% RH 278
6.2.5.2 Venlafaxine hydrochloride Form 5 - 30°C & 65% RH 285
6.2.5.3 Venlafaxine hydrochloride Form 5 - 30°C & 75% RH 294
6.2.5.4 Venlafaxine hydrochloride Form 5 - 30°C & 85% RH 300
6.2.5.5 Morphological behaviour of the venlafaxine hydrochloride polymorphs when exposed to increased relative humidities 315
6.2.5.6 Dehydration of the hydrated venlafaxine hydrochloride Form 5 318

6.3 Hydration kinetics of Form 5 319

6.4 Summary of results 325

Conclusion 328

CHAPTER 7: FLUCONAZOLE 329

Introduction 329

7.1 Literature overview of fluconazole 330

7.2 Introduction to fluconazole crystal forms investigated in this study: Form I, and monohydrate (FormMH) 341

7.2.1 Preparation of fluconazole Form I and the monohydrate (Form MH) 341
7.2.2 Solid state properties of fluconazole Form I and monohydrate (Form MH) 342
7.2.2.1 X-ray powder diffractometry (XRPD) 342
7.2.2.2 Diffuse reflectance infrared Fourier transform spectroscopy (DRIFT-IR) 347
7.2.2.3 Thermal analysis 349
7.2.2.4 Thermodynamic stability of fluconazole crystal modifications – Form I and Form MH 354
7.2.2.4.1 Thermodynamic stability of fluconazole Form I 355
7.2.2.4.2 Thermodynamic stability of fluconazole Form MH 358

Conclusion 362

CHAPTER 8: MOISTURE SORPTION PROPERTIES OF FLUCONAZOLE CRYSTAL FORMS 363

Introduction 363

8.1 Moisture uptake measurement of the fluconazole anhydrous Form I and monohydrate Form MH 363

8.2 Moisture uptake measurement of the fluconazole polymorphic forms 364

8.2.1 Moisture sorption analysis results 367
8.2.2 Total moisture content – Karl Fischer results 369
8.2.3 Polymorphic stability of fluconazole Form I 371

8.2.4 Polymorphic stability of fluconazole Form MH 381
8.2.5 Comparison of fluconazole Form MH and the hydrated Form I 385

8.3 Summary of results 398

Conclusion 401

CHAPTER 9: SUMMARY AND CONCLUSION **403**

Part I – Mebendazole 404

Part II – Venlafaxine HCl 407

Part III – Fluconazole 411

BIBLIOGRAPHY **415**

ACKNOWLEDGEMENTS **437**

ANNEXURES **439**

Annexure 1: Article in the process of submission: *Thermodynamic stability of mebendazole polymorph C in solid dosage forms* 441

Annexure 2: Article in the process of submission: *Aqueous mediated phase transformation of mebendazole polymorphic form* 473

Annexure 3: Article in the process of submission: *Thermodynamic stability of two venlafaxine HCl polymorphic forms* 497

Annexure 4: Article in the process of submission: *Effect of moisture sorption on the stability of fluconazole crystal forms* 517

ABSTRACT

Solid-state properties of pharmaceuticals

The complexity of polymorphic interconversions emphasized the need for a well defined study to investigate the solid-state properties of selected pharmaceutical solids, the thermodynamic stability of various polymorphic forms and to explore the effect of heat and moisture on the stability of these polymorphic forms. It was decided to embark on such studies focusing on the following active pharmaceutical ingredients: venlafaxine HCl (freely water soluble), fluconazole (slightly water soluble) and mebendazole (practically insoluble in water).

Three of the seven commercially available mebendazole products (tablets) contained polymorph C and traces of polymorph A, the other four products contained mebendazole polymorph C. Moisture, increased temperatures and the presence of polymorph A traces in products played an integral role in the thermodynamic stability of mebendazole polymorph C fraction in the tablets. The three mentioned factors influenced the dissolution behaviour negatively. The rate of the polymorph C → polymorph A conversion was investigated and found to be higher for tablets stored at 40°C & 75% RH, compared to those stored at 30°C & 65% RH.

Products which contained traces of polymorph A revealed a higher rate of polymorph transformation (polymorph C → polymorph A) compared to those who initially contained only polymorph C.

Kinetic analysis of the transformations abided JMAEK fits for the isothermal conversion of mebendazole polymorph C → A in the tablets. From the Avrami exponent (n) it could be suggested that the rate-limiting step for the formation of polymorph A in these products was diffusion. The importance of these transformations were illustrated by the changes in the half-life ($t_{1/2} = 0.693/k$) and shelf-life ($t_{90} = 0.105/k$) of the polymorph C fractions in the products.

It was also observed that the metastable polymorphic forms of mebendazole (i.e. polymorphs B & C) undergo an aqueous mediated phase transition (at increased temperatures) to convert to the thermodynamic stable, polymorph A.

A new crystal form of venlafaxine HCl (Form 5) was successfully prepared and characterised. Form 5 was classified as a metastable polymorph of venlafaxine HCl which is enantiotropically related to Form 1, and converts to Form 1 when heated at 150°C or converts to Form 2 when heated at 175°C for two hours.

Solution microcalorimetry revealed that the dissolution of Form 1 and Form 5 in water was an exothermic reaction and that an increase in temperature inhibits the dissolution reaction of the mentioned crystal forms, decreasing the solubility thereof.

Exposure of venlafaxine HCl Form 1 to moisture did not induce any polymorphic transition. However, the metastable form, Form 5 absorbed moisture and transformed into a monohydrate when exposed to 85% RH at 30°C. The hydration of Form 5 when exposed to 85% RH & 30°C (anhydrous form → monohydrated form) was accompanied by a morphological change to accommodate the absorbed water molecules in the hydrated Form 5. Form 5 did not undergo any polymorphic transition when exposed to 65 & 75% RH at 30°C but revealed unpredictable thermal behaviour. VT-XRPD studies revealed that when the hydrated Form 5 was dehydrated it converted to the anhydrous Form γ.

The monohydrated crystal from (Form MH) and the anhydrous form (Form I) of fluconazole were successfully prepared and VT-XRPD studies confirmed that dehydration of Form MH resulted in the formation of the thermodynamic stable Form I.

Form MH and Form I remained stable when exposed to 0-85% RH & 30°C and 0-75% RH & 30°C respectively. Upon exposure to 85% RH & 30°C for 7 days, Form I incorporated water molecules into the crystal lattice and transformed into a hydrated Form I.

The dehydration mechanism and kinetic parameters for the hydrated Form I and Form MH were compared. It was revealed that the activation energy for dehydration of the hydrated Form I was slightly higher compared to that for Form MH due to the fact that dehydration and an endothermic rearrangement occurred simultaneously, contributing to the slightly higher dehydration activation energy observed for the hydrated Form I, also explaining the absence of the rearrangement endotherm in the DSC thermogram of the hydrated Form I at 101°C. The DSC thermogram for the dehydration of Form MH revealed two separate endothermic events (a dehydration and a rearrangement endotherm) showing that dehydration of Form MH occurred in two steps and dehydration of the hydrated Form I in one step. A monohydrated crystal structure proves to be the highest and most stable hydration level for fluconazole.

UITTREKSEL

Vaste toestand eienskappe van farmaseutiese middels

Die kompleksiteit van polimorf omskakelings het hierdie studie genoodsaak om die vaste toestand eienskappe en termodinamiese stabiliteit van 'n groep geneesmiddels te ondersoek, asook om die invloed van verhoogde temperature en vog op die stabiliteit van die polimorfiese vorme te ondersoek. Vir die studie was die volgende geneesmiddels gekies: venlafaksien HCl (hoogs wateroplosbaar), flukonasool (geredelik wateroplosbaar) en mebendasool (prakties onoplosbaar in water).

Drie van die sewe kommersieël beskikbare mebendasool produkte (tablette) het mengsels van polimorf C en polimorf A bevat, terwyl die ander vier produkte slegs polimorf C bevat het. Die teenwoordigheid van vog, verhoogde temperature en spore van polimorf A, het 'n belangrike rol gespeel in die termodinamiese stabiliteit van die polimorf C fraksie teenwoordig in die tablette. Die drie genoemde faktore het die dissolusie profiel negatief beïnvloed.

Die tempo van die polimorf C → polimorf A omskakeling was ondersoek en daar is gevind dat die tempo van omskakeling hoër was vir die produkte wat gestoor was by 40°C & 75% RH in vergelyking met die produkte wat by 30°C & 65% RH gestoor was.

Die tempo van die polimorf omskakeling (polimorf C → polimorf A) was ook hoër in die produkte wat polimorf A spore bevat het, in vergelyking met die produkte wat slegs polimorf C bevat het.

Die kinetika van die isotermiese polimorf omskakeling in die tablette het voldoen aan die JMAEK-model en die Avrami eksponent (n) het aangedui dat die tempo-bepalende stap vir die vorming van polimorf A in die produkte - diffusie was. Die belangrikheid van die polimorfiese omskakeling was geïllustreer deur die invloed wat dit op die half-leeftyd ($t_{1/2} = 0.693/k$) en rakleeftyd ($t_{90} = 0.105/k$) van die polimorf C fraksie gehad het.

Die studie het ook aangedui dat die meta-stabiele vorme van mebendasool (polimorf B en polimorf C) 'n water-bemiddelde omskakeling ondergaan het (by verhoogde temperature) en polimorf A (termodinamiese stabiele vorm) gevorm het as produk.

'n Nuwe metastabiele polimorf van venlafaksien HCl (Vorm 5) was berei en gekarakteriseer. Vorm 5 is enantiotropies verwant aan Vorm 1. Vorm 5 skakel om na Vorm 1 indien dit verhit word by 150°C of skakel om na Vorm 2 indien dit verhit word by 175°C vir twee ure.

Vloeistof mikro-kalorimetriese analises het aangetoon dat die oplos proses van Vorm 1 en Vorm 5 in water eksotermies van aard is, en dat 'n verhoging in die temperatuur van die oplosmiddel, die oplosbaarheid van die genoemde vorme verlaag.

Vorm 1 het geen polimorfiese omskakeling ondergaan nadat dit blootgestel was aan vog nie. Die metastabiele Vorm 5 het egter vog geabsorbeer (by 85% RH by 30°C) en het 'n polimorfiese omskakeling ondergaan en 'n monohidraat as produk opgelewer. Tydens die hidrerings-proses het Vorm 5 morfologiese veranderinge ondergaan om die geabsorbeerde water molekules te kan huisves in die kristal-latwerk. Die bewaring van Vorm 5 by 65 & 75% RH & 30°C het geen polimorfiese omskakeling tot gevolg gehad nie, maar het daartoe gelei dat verskeie monsters (van Vorm 5) onvoorspelbare termiese gedrag geopenbaar het.

Variërende temperatuur x-straal poeier diffraktometriese studies (VT-XRPD) het aangetoon dat die dehidrering van die gehidreerde Vorm 5, Vorm γ opgelewer het as produk.

Flukonasool monohidraat (Vorm MH) en die anhidraat (Vorm I) was suksesvol berei. VT-XRPD studies het bevestig dat die Vorm I die produk is van die dehidrering van Vorm MH.

Vorm MH en Vorm I het geen polimorf-omskakeling getoon nadat hulle onderskeidelik blootgestel is aan die volgende kondisies nie: 0-85% RH & 30°C en 0-75% RH & 30°C. Blootstelling van Vorm I aan 85% RH & 30°C het daartoe gelei dat Vorm I na 7 dae omgeskakel het na 'n monohidraat.

Die meganisme en kinetika van dehidrasie vir Vorm MH en die gehidreerde Vorm I was ondersoek. Daar is gevind dat die aktiverings energie benodig vir die dehidrering van die gehidreerde Vorm I hoër was i.v.m. die energie benodig vir die dehidrering van Vorm MH. Die rede vir die verskil in die dehidrasie aktiverings energieë is omdat die dehidrering- en herrangskikking-prosesse gelyktydig plaasgevind het tydens dehidrering van die gehidreerde Vorm I.

Differensiële skanderingskalorimetriese (DSC) termogramme van Vorm MH het twee aparte termiese aktiwiteite aangetoon ('n dehiderings endoterm en herrangskikkings endoterm by 101°C). Dit verklaar dus dat die dehidrering van Vorm MH in twee onderskeidende stappe plaasvind en die dehidrering van die gehidreerde Vorm I in een stap plaasvind. Die studie dui ook aan dat die hoogste vlak van hidrasie vir flukonasool 'n monohidraat is.

AIMS AND OBJECTIVES

Solid-state properties of active pharmaceutical ingredients with varying degree of water solubility

Formulation design relies heavily on the basic solid-state properties of polymorphic forms due to the fact that these properties may differ significantly (Grant, 1999:7). Regulatory bodies require that the crystalline form used during the development should be well cross-examined to ensure the safety and efficacy of the active pharmaceutical ingredient (API) in the final product. Polymorphic transformations of API's may occur not only during the manufacturing process of the product, but also post-production. Unexpected polymorphic transformations may have severe practical (i.e. manufacturing) and economic implications for the pharmaceutical manufacturer.

The solid-state properties of three API's with varying degree of water solubility were investigated and the susceptibility of these polymorphic forms to moisture and heat induced phase transitions. The British Pharmacopoeia (BP) classification for water solubility (BP 2007) was used to identify the three prototype API-groups: (1) practically insoluble in water (mebendazole), (2) slightly water soluble to very slightly water soluble (fluconazole) and (3) freely water soluble (venlafaxine HCl).

This study consisted of three parts: **Part I:** Mebendazole, **Part II:** Venlafaxine HCl and **Part III:** Fluconazole. Due to the fact that the physico-chemical properties of the three API's differ significantly and that the outcomes of the moisture stability testing might differ, a unique set of analytical techniques and methodologies were selected for each API, to ensure that a lucid understanding regarding the solid-state properties of the different polymorphic forms of each API can be obtained.

To achieve this, the following study objectives were set and pursued:

Part: I

(1) Determine the mebendazole polymorphic forms present in mebendazole generic products (tablets) available in South Africa, and determine the thermodynamic stability of the polymorph C present in the tablets when stored at 30°C & 65% RH and 40°C & 75% RH respectively for a period of 6 months.

(2) Investigate the influence of polymorphic conversions (polymorph C→ polymorph A) on the dissolution profiles of mebendazole tablets.

(3) Quantify the degree of polymorphic conversion observed in the mebendazole tablets and determine a kinetic model to characterise the phase transformation(s) observed.

(4) Determine the influence of moisture exposure on the rate of the polymorphic conversion in the tablets when exposed directly to 30°C & 65% RH and 40°C & 75% RH respectively.

(5) Investigate the influence of heat and moisture on the stability of the metastable mebendazole polymorphs i.e. polymorphs B and C.

Part: II

(1) Prepare, identify and characterise a novel crystal form of venlafaxine HCl (Form 5). Investigate the solid-state properties and thermodynamic stability of this new form.

(2) Determine the influence of increased temperatures on the solubility of Form 5 and Form 1 using isothermal high sensitivity microcalorimetry at 20, 30 and 40°C.

(3) Determine the thermodynamic relationship between Form 5 and Form 1, and investigate the influence of increased temperatures on the stability of Form 5.

(4) Generally, for polymorphic forms of the same API the unit cell volume differ, that may induce differences in the surface areas of the crystals. Exposure of the two venlafaxine hydrochloride polymorphic forms (i.e. Form 1 and Form 5), with similar particle sizes to similarly relative humidity conditions would provide an insight to the sorption- and phase-stability of these crystal forms. Thus, investigate moisture sorption (ab-/adsorption) of venlafaxine HCl Form 1 and Form 5, and investigate the influence of moisture sorption on the physico-chemical properties and the morphological properties of the crystal forms.

(5) Investigate the thermal stability of the hydrated Form 5.

Part: III

(1) Prepare and identify fluconazole crystal Form I (anhydrous form) and Form MH (monohydrate), investigate the solid-state properties and thermodynamic stability of these two forms.

(2) Investigate moisture sorption (ab-/adsorption) of fluconazole Form I and the Form MH respectively, and investigate the influence thereof on the physico-chemical properties and the morphological properties of the mentioned crystal forms.

(3) Compare the stability of the hydrated Form I and Form MH.

(4) Investigate the kinetic parameters for the dehydration of fluconazole Form MH and the hydrated Form I utilising the Ozawa method (Ozawa, 1965:1881) to determine the dehydration activation energy (E_A) for the mentioned hydrates.

Figure 1 provides a schematic overview of this study.

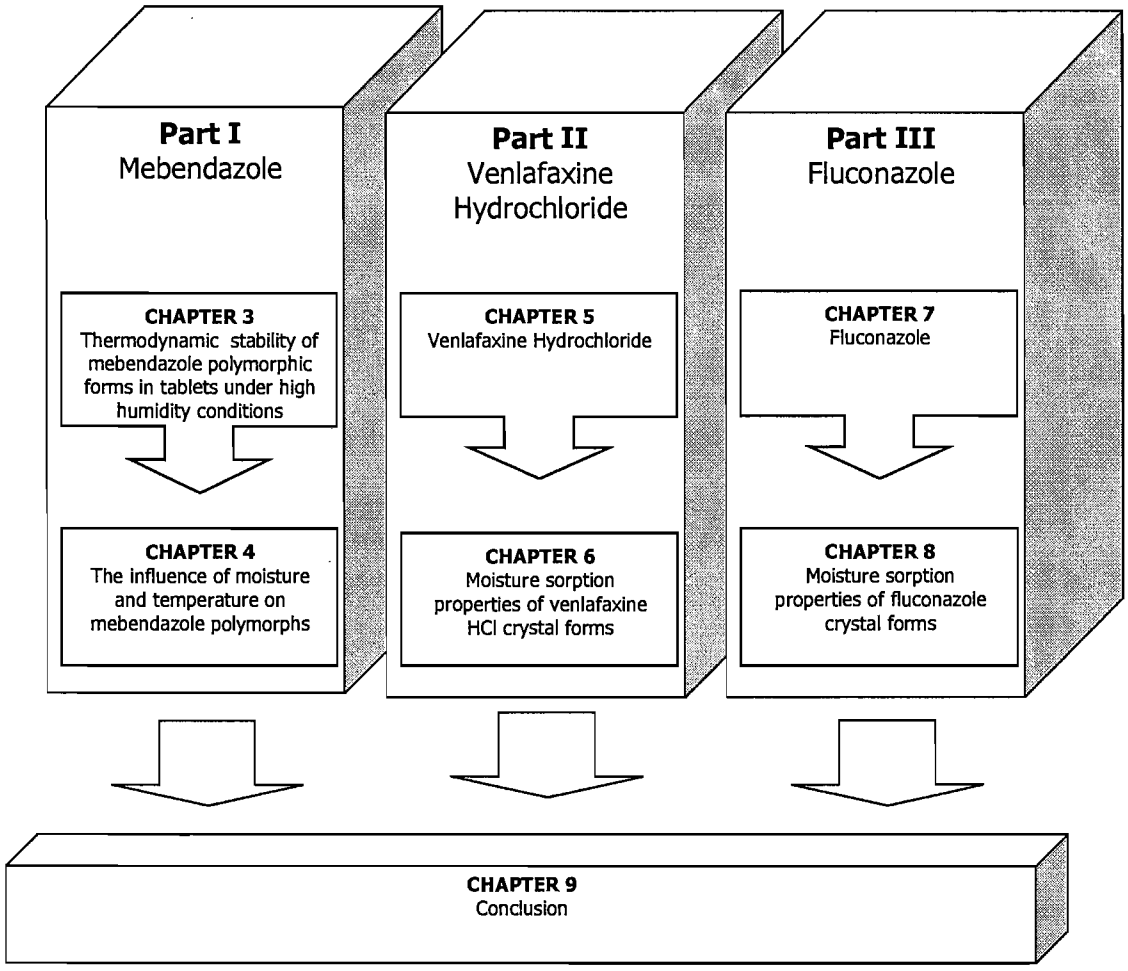


Figure 1 Overview of this study.

This study was conducted to further the knowledge and understanding of the solid-state properties of the three active pharmaceutical ingredients with varying degree of water solubility, and to identify new potential research opportunities.

CHAPTER 1

Importance of polymorphism and pseudopolymorphism to product development and life cycle management

Introduction

Polymorphism and pseudopolymorphism of active pharmaceutical ingredients [API's] and drug excipients are of considerable interest, as they can affect the production of dosage forms, the biological behaviour of the final form in which the drug substance is presented, and plays an imperative role in the life cycle management (LCM) of innovator products.

The early and comprehensive exploration of possible crystalline forms is advised to ensure that the best (most stable crystal modification, with most favoured biopharmaceutical and manufacturing properties) crystal form is selected for the manufacturing process, to enable a proactive and value-maximizing approach to product life cycle management and to secure appropriate and timely intellectual property protection (Requadt, 2004:2).

For the approval of a new drug substance, the drug substance guideline of the United States Food and Drug Administration (FDA) states that "appropriate" analytical procedures need to be used to detect polymorphs, pseudopolymorphs and amorphous forms of the API. The FDA also stresses the importance of controlling the crystal form of the API during the various stages of product development (Byrn *et al.*, 1995:945-954). It is therefore important to identify and control the crystal form of the API during the various stages of product development and storage.

Phase transitions may alter the physico-chemical properties of the API that may have severe cost implications for the pharmaceutical manufacturer.

1.1 Polymorphism, pseudopolymorphism, amorphism and pharmaceutical co-crystals: the art of crystal engineering and the importance thereof

API's and excipients (in the solid phase) can be classified as either crystalline or amorphous solids. Crystalline implies an ideal crystal in which the structural units, named unit cells, are repeated regularly and indefinitely, and three-dimensionally in space. Each crystal can be classified as a member of one of seven possible crystal systems or crystal classes, that are defined by the relationships between the individual dimensions, *a, b* and *c*, of the unit cell, and between the individual angles, α, β and γ, of the unit cell (Byrn *et al.*, 1999:48).

Some API's and excipients may, however, not be arranged in one of the seven fundamental crystalline forms, but may recrystallise into a non-ordered, random system, related to the liquid state. These API's and excipients are then classified as *amorphous* solids. According to Giron (1995:2), the term *"amorphate"* is used to describe these drug substances.

Polymorphism is the phenomenon where polymorphs are different crystalline forms of the same chemical entity, in which the atoms or molecules of this entity has different arrangements (Grant, 1999:2). The difference in internal crystal structure in polymorphs arises when the drug substance crystallises in different crystal packing arrangements and / or different conformations.

Configurational polymorphism has been defined as "a type of polymorphism in which one labile isomer of a compound (eg. a keto form) is present in one polymorph and another labile isomer (eg. an enol form) is present as another form" (Byrn *et al.*, 1999:506). Byrn *et al.* (1999:506) also defined *conformational polymorphism* as: "a type of polymorphism in which the conformation of the independent molecule in each polymorph is different."

Other variations in the crystal structures of the same chemical entity are encountered where the entity is defined by other unit cells, but these unit cells

differ in elemental composition through the inclusion of one or more solvent molecules. Solvent inclusion can be in stoichiometric or non-stoichiometric order. In the past, solvent inclusion has been considered to be a mechanism of polymorphism (due to changes / differences in the unit cell of a solid) but was dubbed *pseudopolymorphism*, due to the fact that the composition of the pseudopolymorph differs chemically (due to the presence of solvent molecules) from the unsolvated form. Brittain (2007:705) suggested that the terms *solvatomorphs* and *solvatomorphism* should be used to avoid issues associated with inconsistent nomenclature.

When water is incorporated in stoichiometric proportions into the crystal lattice of the compound, the molecular adduct(s) formed is referred to as *hydrate* (Grant *et al.*, 1999:61). Although most hydrates exhibit a whole number ratio stoichiometry, an unusual case is the metastable hydrate of caffeine, which contains only 0.8 moles of water per mole of caffeine. Only in a saturated water vapour atmosphere will additional amounts of water be adsorbed at the surface of the 4 or 5-hydrate to yield a 5 or 6-hydrate (Pirttimaki & Laine, 1994:203).

Sometimes a compound of a given hydration state may crystallise into more than one crystalline form, thus producing hydrates that exhibit polymorphism themselves, which is known as *polymorphic pseudopolymorphs*. An example of this phenomenon is nitrofurantoin (Pienaar, 1994:50). Nitrofurantoin can be crystallised as two monohydrous forms (polymorphs I and II), and two anhydrous species (designated polymorphs α and β). Solvated forms (from different solvents) that do not exhibit significant differences in XRPD patterns and crystal packing (i.e. hydrate and isopropanolate of hexakis(2,3,6-tri-O-acetyl)-α-cyclodextrin (Beettinetti *et al.*, 2006:1209) are called *isostructural pseudopolymorphs*.

The term *desolvated solvates* has been used to classify a compound that was originally crystallised as a solvate but when the incorporated solvent is removed, the crystal lattice of the solvated and desolvated crystal lattices do not show any

or relatively small differences for example: desolvated monohydrate of terazosin HCl (Bauer *et al.*, 2006:923).

Amorphous forms of API's and excipients are of substantial interest because they are usually more soluble than their crystalline counterparts, but are considered to be thermodynamically less stable (Byrn *et al.*, 1995:952). Solid state properties of amorphous forms of the same chemical entity (melting behaviour, solubility profile, etc.) may differ; this phenomenon is referred to as *poly-amorphism* (Byrn *et al.*, 1995:952).

Another interesting phenomenon of crystal engineering is that of *pharmaceutical co-crystals*. *Pharmaceutical co-crystals* can be defined as crystalline materials comprised of an API and one or more unique co-crystal formers, which are solids at room temperature (Peterson *et al.*, 2006:320), thus it is suggested that co-crystal formation could be considered a sub-division of pseudopolymorphism.

Figure 1.1 provides a summary of the groups wherein solids can be classified.

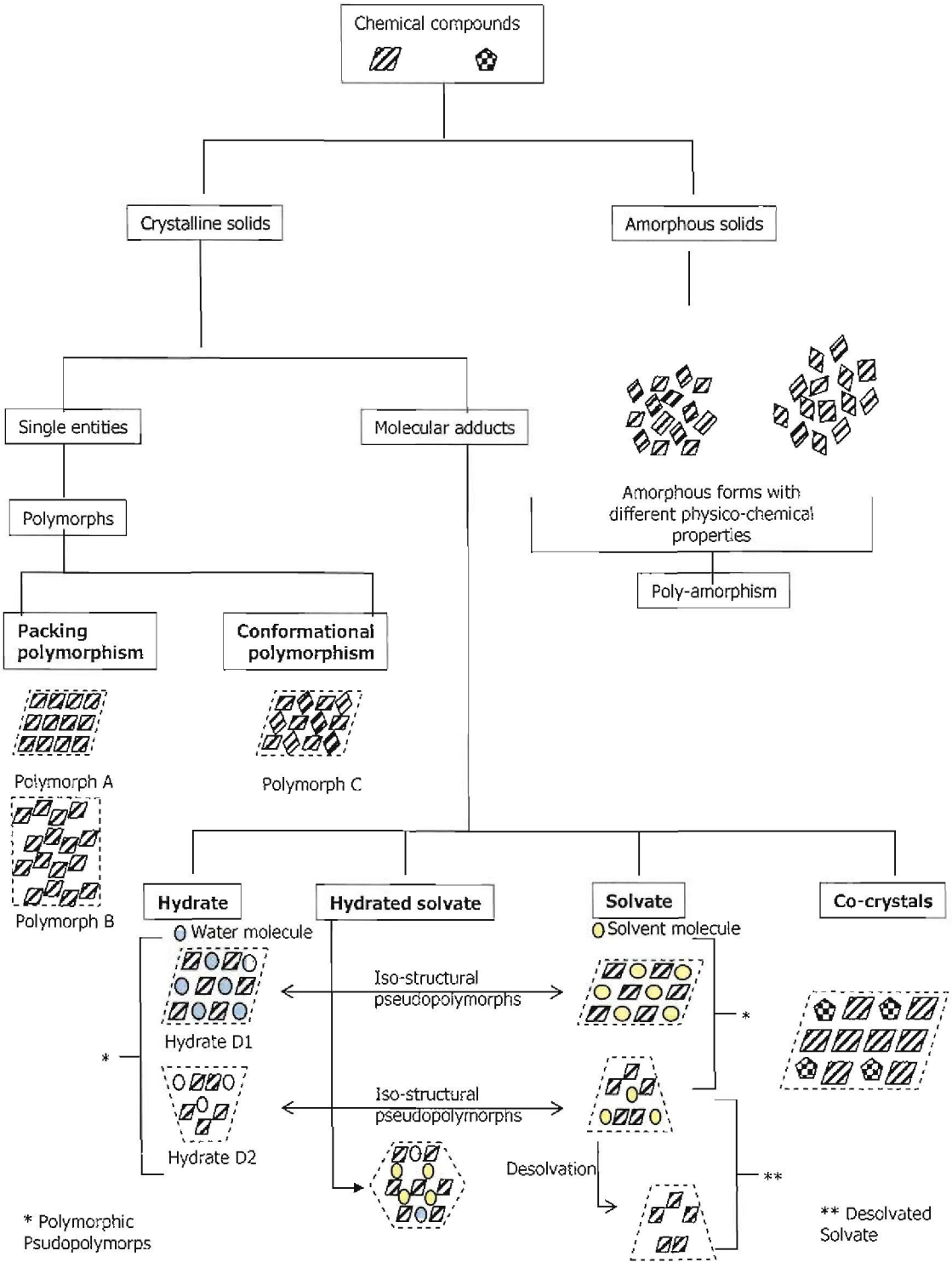


Figure 1.1 Summary of the groups wherein solids can be classified.

1.1.1 Importance of polymorphism and pseudopolymorphism to product development

Crystalline forms are characterised based on the differences of their physical properties. Table 1.1 lists some of the properties that may differ among different polymorphs (Grant, 1999:7).

Table 1.1 List of physical properties that may differ among various polymorphs (Grant, 1999:7)

1. **Packing properties**
   a. Molar volume and density;
   b. Refractive index;
   c. Conductivity (electrical and thermal);
   d. Hygroscopicity.

2. **Thermodynamic properties**
   a. Melting and sublimation temperatures;
   b. Internal energy (i.e. structural energy);
   c. Enthalpy (i.e. heat content);
   d. Heat capacity;
   e. Entropy;
   f. Free energy and chemical potential;
   g. Thermodynamic activity;
   h. Vapour pressure;
   i. Solubility.

3. **Spectroscopic properties**
   a. Vibrational transitions (i.e. infrared absorption spectra and raman spectra);
   b. Rotational transitions (i.e. far infrared or microwave absorption spectra);
   c. Nuclear spin transitions (i.e. solid state nuclear magnetic resonance spectra).

4. **Kinetic properties**
   a. Dissolution rate;
   b. Rates of solid state reactions;
   c. Stability.

5. **Surface properties**
   a. Surface-free energy;
   b. Interfacial tensions;
   c. Habit (i.e. shape).

6. **Mechanical properties**
   a. Hardness;
   b. Tensile strength;
   c. Compactibility, tabletting;
   d. Handling, flow, and blending.

The selection of the most favourable crystal form (i.e. thermodynamically most stable form with optimal dissolution properties) for manufacturing is important, to ensure the efficacy of the final product. Failure to identify the most favourable crystal form during production caused market shortages and financial repercussions for pharmaceutical companies. An example of this is the Norvir® brand of ritonavir. The commercial start-up of the mentioned product was initiated in 1996, and during 1998 ritonavir began to precipitate in the capsules. The precipitation lead to dissolution failures for the capsules and product recalls. Investigation revealed that the Form I polymorph (initially used in the manufacturing process) transformed into the less soluble Form II (Snider *et al.*, 2004:392 & Bauer *et al.*, 2001:861-862).

Zhang *et al.* (2004:386) revealed that various crystalline forms of API's can differ in their tabletting properties such as: brittleness, deformation and compressibility. A good example to illustrate the importance of polymorphism and pseudopolymorphism to product development is paracetamol. Paracetamol exhibits poor flow and compression properties, thus forcing manufacturers to make use of wet-granulation to produce a solid dosage form. However, the sintered-like crystals produced when the dioxane hemisolvate is desolvated, reveal a rounded shape with good flow and compressibility (*Fachaux et al.*, 1995:129-132).

It remains an important aspect of the preformulation studies to select the most favoured crystal form for manufacturing and also to ensure that the selected crystal form remains stable during and after manufacturing.

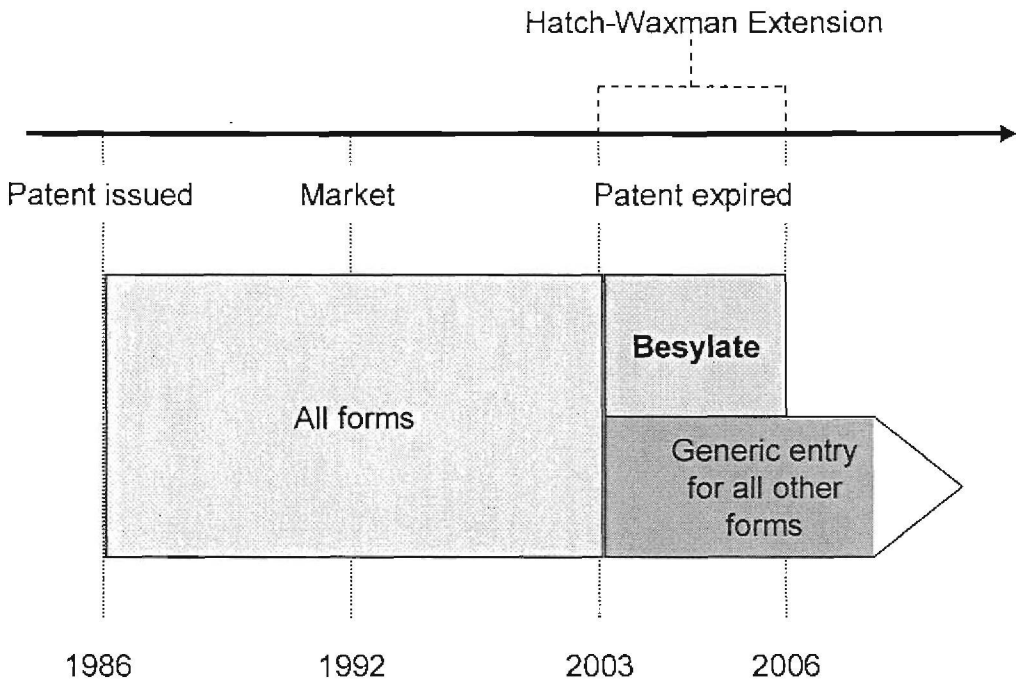
1.1.2 Importance of polymorphism and pseudopolymorphism to product Life Cycle Management (LCM)

Patent law often treats different crystal forms of API's as being potentially distinct entities (Requadt, 2004:3), thus in order to remain competitive in the pharmaceutical industry, innovator companies need to explore the true potential

of existing molecules to counter the competition from generic companies. The quest to stretch the life cycle of API's starts around clinical phase II and sometimes even as early as the pre-clinical stage (Blomsma, 2006:32).

Generic companies are increasingly making use of opportunities offered by polymorphic forms of API's to circumvent patents in order to bring products to the market earlier.

It is important to file an application on a polymorphic form in good time. An example of where the marketed form was filed too early is that of Norvasc® (amlodipine) by Pfizer (figure 1.2) (Lucas & Burgess, 2004:56-57).



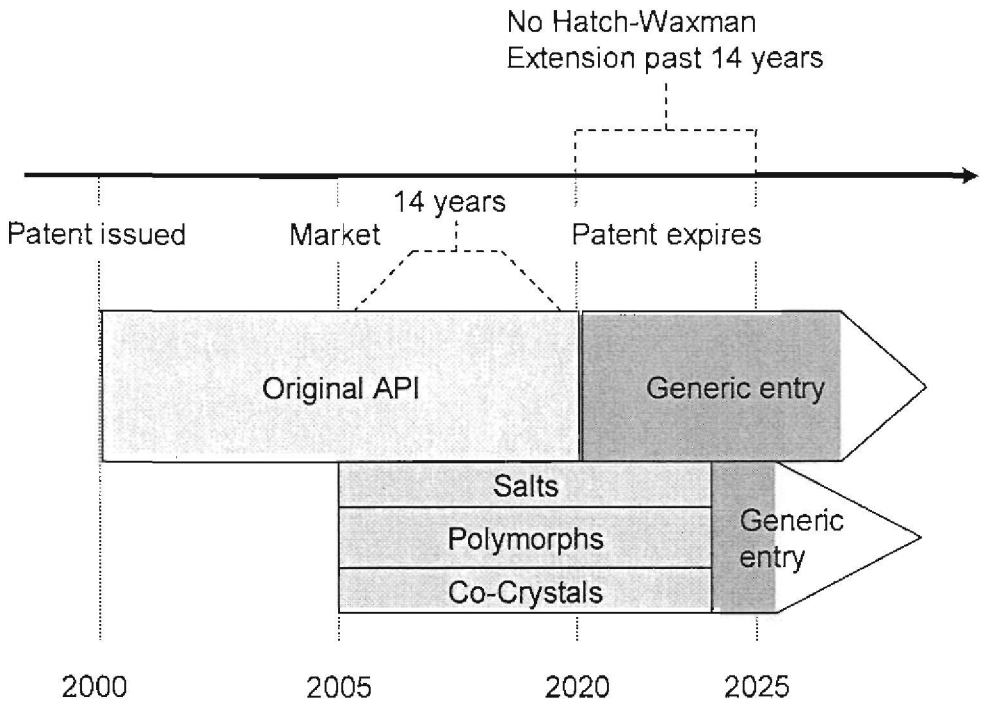
Pfizer's original API patent was issued in 1986 and expired in 2003. Norvasc was approved by the FDA in 1992. Pfizer had 11 years of patent protected market product sales. The court extended Pfizer's patent only for the besylate salt until 2006. Thus all other salts were available for generic drug entry beginning 2003.

Figure 1.2 Schematic presentation of LCM of Norvasc® of Pfizer [reproduced from Lucas & Burgess (2004:56-57)].

The amlodipine maleate salt was disclosed in the core new chemical entity (NCE) patent. This premature disclosure resulted in protection for the maleate salt ending at the same time as the NCE, thus the innovator (Pfizer) could not protect the salt (amlodipine maleate) for a period of time equal to its protection of the amlodipine besylate salt (Lucas & Burgees, 2004:56-57).

The Hatch-Waxman extension selection will determine the timely filing of the polymorph. If the polymorph patent is extended by the Hatch-Waxman extension the additional polymorph(s) patent(s) must be filed after the marketed polymorph patent to ensure that the patents will run concurrently during at least part of the extension (figure 1.2) (Lucas & Burgess, 2004:56-57).

If the polymorph patent is not selected for the extension (figure 1.3), the additional polymorphs can be filed at the same time or later than the marketed API polymorph patent.



In this example, the drug product had market sales of a patent-protected product for more than 14 years. Thus, this drug was not eligible for a patent extension. A form screen covering all salts, polymorphs, and co-crystals would function Similar to the original API patent and provide patent coverage until 2025.

Figure 1.3 Schematic presentation of an API without the Hatch-Waxman extension [reproduced from Lucas & Burgess (2004:56-57)].

1.2 Stability and thermodynamic relationship between polymorphs

An energy-temperature diagram of a crystalline solid under constant pressure is illustrated in figure 1.4.

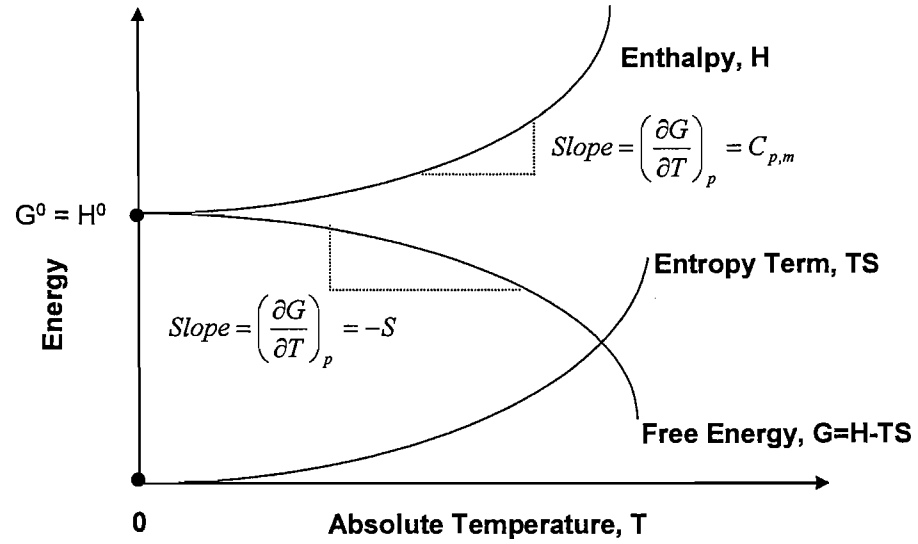


Figure 1.4 Energy-temperature diagram of a crystalline solid under constant pressure (Adapted from Lohani & Grant, 2006:25).

From figure 1.4 it is clear that the entropy term (TS) increases with increasing temperature, and that the free energy (G) decreases with increasing temperature, because the slope of the free energy curve is equal to the negative value of the entropy (Lohani & Grant, 2006:25).

The thermodynamic relationship between polymorphs (A and B) of the same chemical entity can be classified as *enantiotropic* or *monotropic.*

A pair of polymorphs is said to be *enantiotropically* related if there exists a transition point at which the two polymorphs can undergo reversible solid-solid transformation at a transition point (T_t) that is below the melting point of both polymorphs (A and B) (Lohani & Grant, 2006:25).

Figures 1.5 and 1.6 resemble energy-temperature plots for enantiotropic (figure 1.5) and monotropic (figure 1.6) systems.

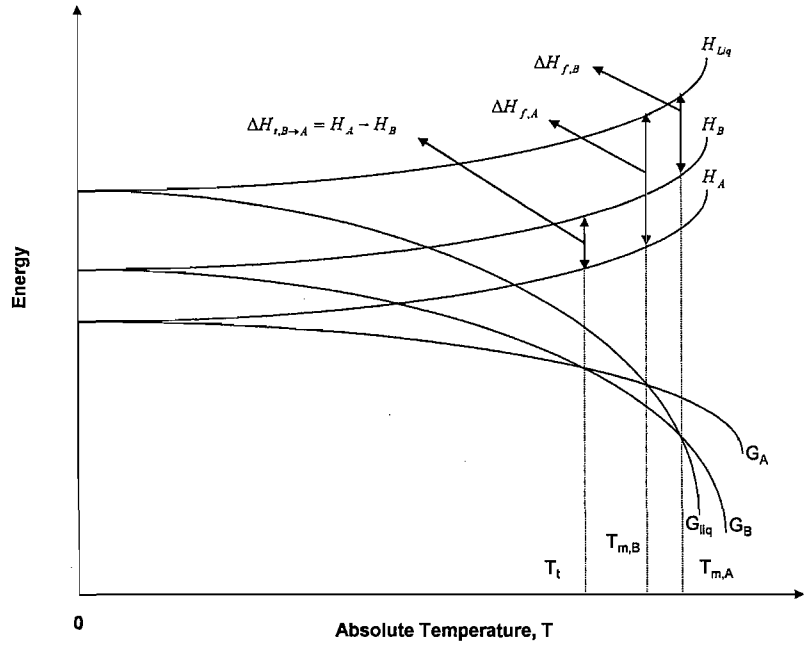


Figure 1.5 Energy-temperature plots for an enantiotropic system. G is the free energy, H is the enthalpy, T is the temperature, sub-scripts A and B and Liq refer to the polymorph A, polymorph B and liquid phase respectively, while scripts f, t and m refer to fusion, transition point, and melting point, respectively (adapted from Lohani & Grant, 2006:26).

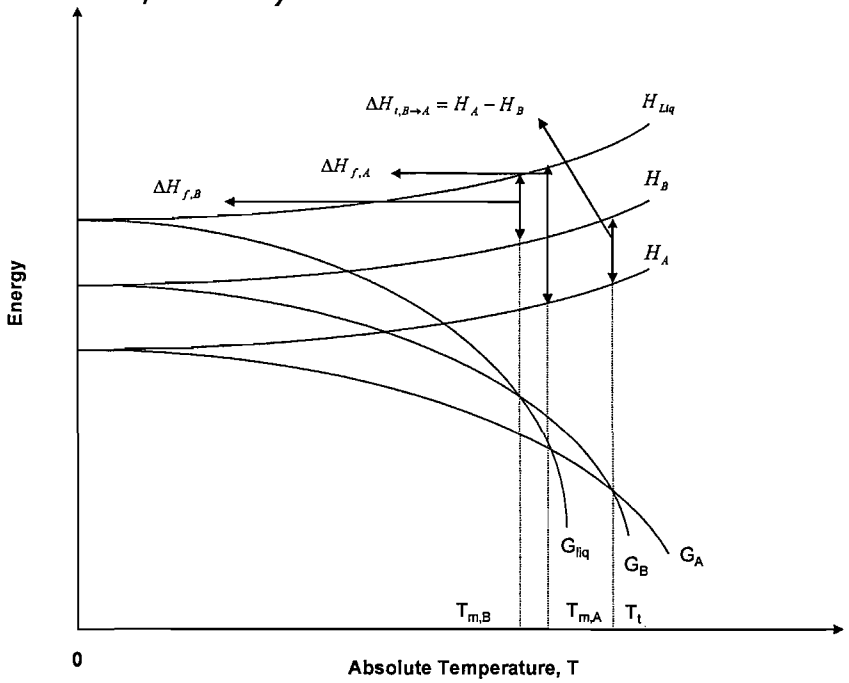


Figure 1.6 Energy-temperature plots for a monotropic system. G is the free energy, H is the enthalpy, T is the temperature, sub-scripts A and B and Liq refer to the polymorph A, polymorph B and liquid phase respectively, while scripts f, t

and m refer to fusion, transition point, and melting point, respectively (adapted from Lohani & Grant, 2006:26).

In figures 1.5 and 1.6 the melting point of the polymorphs (A and B) can be regarded as the temperature at which the free energy isobar of the polymorph intersects with the free energy isobar of the liquid, and the transition temperature (T_t) can be defined as the temperature at which the free energy isobar of polymorph A intersects the free energy isobar of polymorph B (Lohani & Grant, 2006:25).

From the energy-temperature plots for enantiotropic related polymorphs, A and B, in figure 1.5 it is clear that the free energy of A is lower than that of B ($G_A < G_B$), thus polymorph A will be the thermodynamic stable form at temperatures below T_t. Polymorph B can thus undergo a spontaneous exothermic transformation into polymorph A bellow T_t, and above T_t, polymorph B can be considered the thermodynamic stable form due to the fact that its free energy is lower than that of polymorph A (i.e. $G_B < G_A$). Above T_t polymorph A can undergo spontaneous endothermic transformation into polymorph B (Lohani & Grant, 2006:27).

For polymorphs that are monotropically related, one polymorph is always stable below the melting point of both polymorphs (figure 1.6). At temperatures below $T_{m,A}$, the free energy of polymorph A is always less than that of polymorph B ($G_A < G_B$), thus making it possible for polymorph B to undergo spontaneous exothermic transformation into polymorph A (Lohani & Grant, 2006:27).

The solid-solid transformations are kinetically hindered in monotropic systems due to the fact that the activation energy needed for the transition (i.e. the temperature at which sufficient thermal energy can cross the activation energy barrier) exceeds the melting points of both polymorphs. Thus the transition point (T_t) in a monotropic system is considered to be a virtual point (Lohani & Grant, 2006:27).

The polymorph with the highest free energy (i.e. metastable polymorph) will have a higher fugacity, vapour pressure, thermodynamic activity, solubility rate per unit surface area, and rate of reaction. The mentioned statement has been summarised by Lohani & Grant (2006:27-28) using equations 1-4 as follows:

The ratio of the fugacities (escaping tendency) (*f*) of polymorphs are reflected by the Gibbs free energy difference between two polymorphs. The fugacity (*f*) can be approximated from the vapour pressure (*p*), thus:

$$\Delta G_{B\to A} = RT \ln\left(\frac{f_A}{f_B}\right) \approx RT \ln\left(\frac{p_A}{p_B}\right) \qquad (1)$$

The fugacity is proportional to the thermodynamic activity (*a*) where the constant of proportionality depends on the choice of standard state. The thermodynamic activity can be approximated from the solubility (*s*), thus:

$$\Delta G_{B\to A} = RT \ln\left(\frac{a_A}{a_B}\right) \approx RT \ln\left(\frac{s_A}{s_B}\right) \qquad (2)$$

According to the Noyes-Whitney equation the dissolution rate per unit area (*J*) is proportional to the solubility under sink conditions and constant hydrodynamic flow, thus:

$$\Delta G_{B\to A} = RT \ln\left(\frac{J_A}{J_B}\right) \qquad (3)$$

According to the law of mass action the rate of a chemical reaction (r) is proportional to the thermodynamic activity of the reacting polymorph, thus:

$$\Delta G_{B\to A} = RT \ln\left(\frac{r_A}{r_B}\right) \qquad (4)$$

Six rules are defined to assist in the characterisation and prediction of the stability of polymorphs, which include the following: heat-of-transition rule, heat of fusion rule, entropy-of-fusion rule, heat-capacity rule, density rule and infrared rule. Table 1.2 summarises the basics of the mentioned rules.

Table 1.2 Six rules for the characterisation of polymorphic forms

Rule	Principal of the rule
Heat-of-transition	If an *endothermic* phase transition is observed at a certain temperature, the point of transition lies below that temperature, and these two polymorphs can be considered being enantiotropically related. If an *exothermic* transition is observed, there is no transition point below the transition temperature, thus these forms could be considered being monotropically related or enantiotropically related forms where the point of transition is higher than the measured transition temperature (Burger & Ramberger 1979a:259-272, 1979b:273-316).
Heat-of-fusion	In an enantiotropic system the higher-melting polymorph will have the lower heat of fusion. In a monotropic system the higher-melting polymorph will have the higher heat of fusion (Burger & Ramberger, 1979b:273-316).
Entropy-of-fusion	Two modifications are enantiotropically related if the higher-melting polymorph has the lower entropy of fusion. If the lower melting form has the lower entropy of fusion, these two forms are monotropically related (Burger & Ramberger 1979a:259-272, 1979b:273-316).
Heat-capacity	For an enantiotropic system the higher-melting polymorph has a higher heat capacity at a given temperature than the lower-melting polymorph and vice versa (Burger 1982a:158-163, 1982b:1-20).
Density	Kitaigorodskii (1961) announced that the mutual '*orientation of molecules in a crystal is conditioned by the shortest distance between atoms of adjacent molecules*' and due to the fact that periphery molecules is often dominated by hydrogen atoms that these distances will '*be determined by the interactions between hydrogen atoms or the interaction of hydrogen atoms with other atoms of other elements*'.
Infrared	The hydrogen-bonded polymorphic structure with the higher frequency in the bond stretching modes may be assumed to have the higher entropy (Burger & Ramberger, 1979a:259-272).

Gu & Grant (2001:1277-1287) described how the heat of solution and the solubility of polymorphs may be utilised to estimate the relative stability of polymorphic forms. Polymorphic transition temperatures and the thermodynamic stability relationship between polymorphs can be estimated from their melting data using the following equation derived by Yu (1995:966-974):

$$T_t = \frac{\Delta H_{A-B}}{\Delta S_{A-B}}$$

$$= \frac{\Delta H_{mA} - \Delta H_{mB} + 0.003 \cdot \Delta H_{mA} \cdot (T_{mB} - T_{mA})}{\frac{\Delta H_{mA}}{T_{mA}} - \frac{\Delta H_{mB}}{T_{mB}} + 0.003 \cdot \Delta H_{mA} \cdot \ln\left(\frac{T_{mB}}{T_{mA}}\right)} \qquad (5)$$

Where ΔH_{mA} and ΔH_{mB} are the enthalpies of fusion of polymorphs A and B respectively, and T_{mA} and T_{mB} are the absolute melting temperatures of polymorphs A and B respectively.

1.3 Factors that may influence the thermodynamic stability of crystal forms

Formulation design relies heavily on the basic physico-chemical properties of the polymorphic forms due to the fact that the properties of the polymorphic forms may differ significantly (Grant, 1999:7). Regulatory bodies require that the crystalline form used during the development should be well interrogated to ensure the safety and efficacy of the API in the final product. The requirements set by the International Conference on Harmonisation for the polymorphic form (that is undissolved or in the solid state in the final product) to be used in the design of a formulation are summarised in the Q6A specifications (ICH, 1999:27).

Figure 1.7 provides an indication when acceptance criteria should be set for the control of the polymorph content in solid dosage forms or liquids containing undissolved API's.

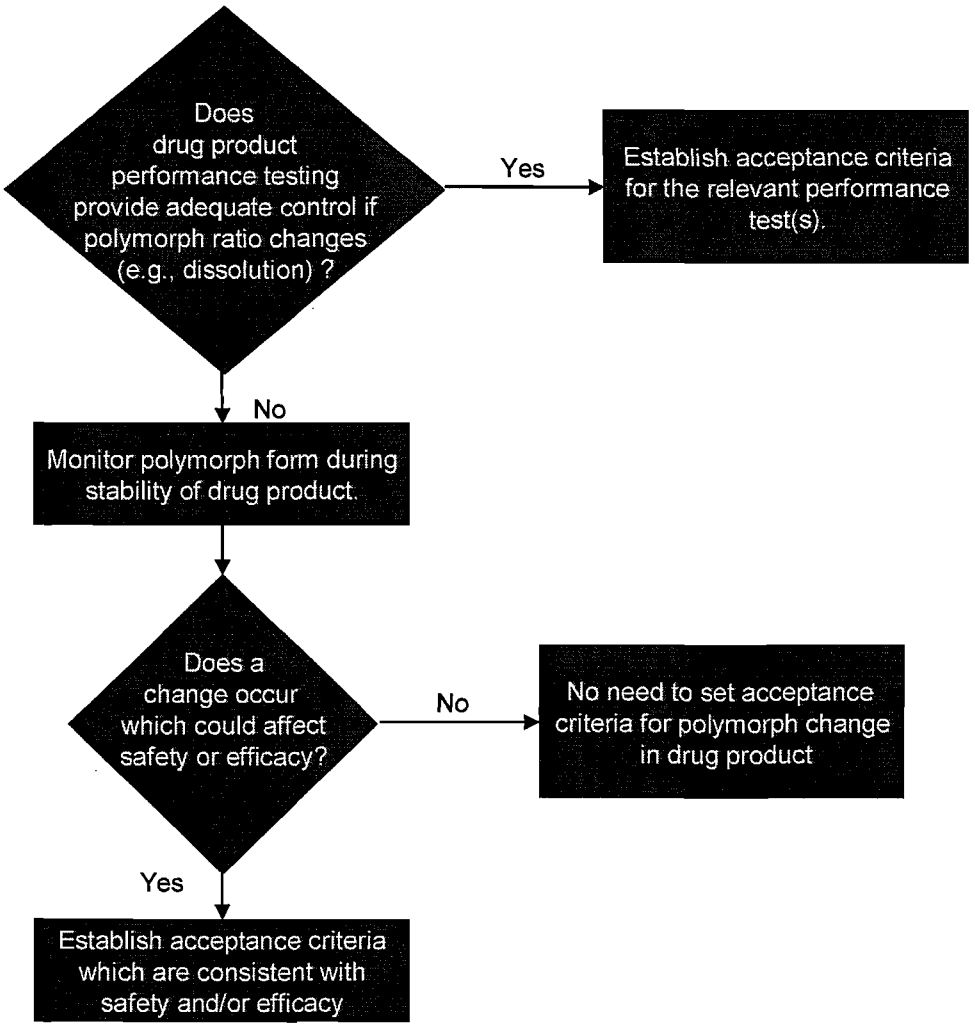


Figure 1.7 Regulatory decision tree for solid dosage forms or liquids containing undissolved API's (adapted from ICH, 1999:27).

If the performance and safety of the product can be affected by the polymorphic form present in the dosage form (i.e. the polymorphic forms reveal significant differences in physical and chemical properties), acceptance criteria should be set to determine the extent of allowed polymorphic transformation which may occur in the product, that will not influence the efficacy or safety of the product.

It is important to remember that polymorphic transformations may occur not only during the manufacturing process of the product, but also during post-production. During the manufacturing process the stability of the polymorphic

forms can be manipulated to ensure stability, by controlling exposure to: heat, moisture, granulation solvent, compression-pressure etc. Two vital components of the current Good Manufacturing Procedures (cGMP) of the manufacturer include: (1) the testing and conformity of all in-coming batches of raw material to appropriate written specifications, including any specification for polymorphic form (if applicable), prior to release thereof for production; and (2) demonstration that the manufacturing process is reproducible and if critical factors or variables are present, that they are well-understood and controlled to ensure the stability of the polymorphic forms present in the final product (Raw *et al.*, 2003:402).

During the post-production period, the efficacy of the packaging material and environmental conditions (i.e. temperature and relative humidity where the product is stored) will play an integral role in the stability of the polymorph.

Several articles have been published describing factors that influence the stability of API-polymorphic forms. Some of these factors include granulation, drying of solids / granules (exposure to increased temperatures), excipients that influence the stability of polymorphic forms, compression, exposure to moisture etc.

1.3.1 Manufacturing activity induced polymorphic transitions

Various manufacturing activities (figure 1.8) such as granulation, drying of solids / granules (exposure to increased temperatures), addition of excipients to API's and grinding and compression may influence the thermodynamic stability of polymorphs (Yu *et al.*, 1998:119).

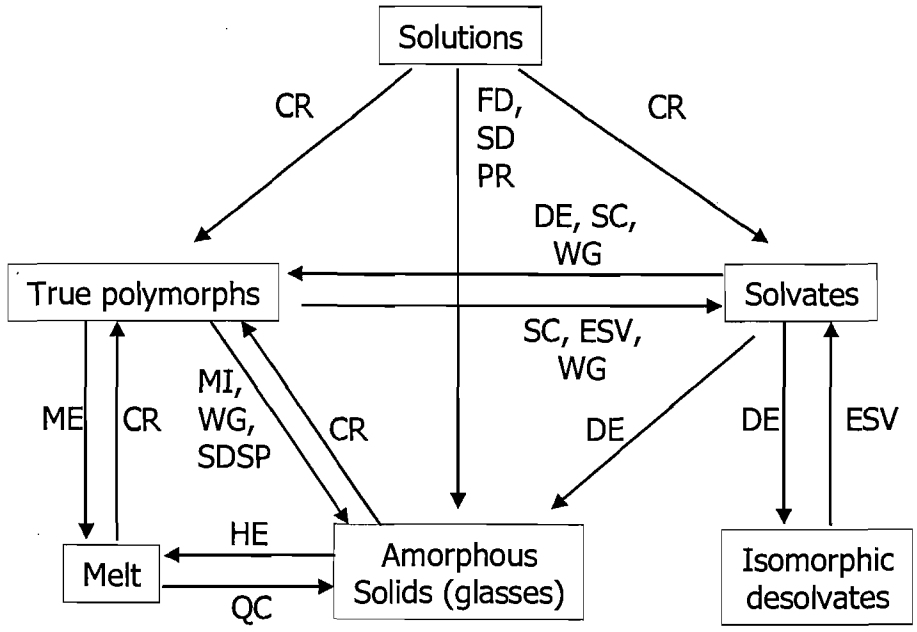


Figure 1.8 Types of polymorphs that can be produced by standard pharmaceutical processes. Crystallisation (CR); desolvation (DE), exposure to solvent vapour (ESV); freeze drying (FD); heating (HE); melting (ME); milling (MI); precipitation (PR); quench cooling (QC); slurry conversion (SC); spray drying (SD); solid dispersion (SDSP); wet granulation (WG) (reproduced from Yu *et al.*, 1998:119).

In the sections to follow the influence of the mentioned activities will be discussed.

1.3.2 Effect of granulation on stability of polymorphic forms

Figure 1.9 summarises the potential effects that granulation may have on a solid API.

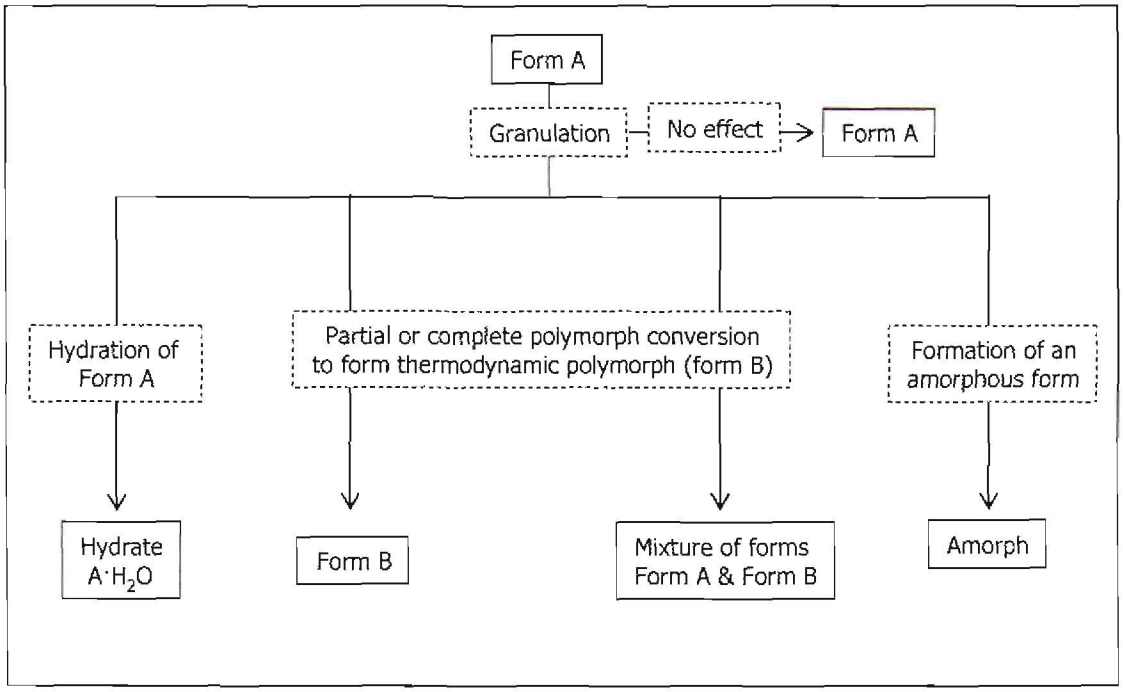


Figure 1.9 Potential effects of granulation on the stability of polymorphic forms.

Initial pre-formulation studies of Abbott-232 (a chemically stable, highly water soluble, non-hygroscopic compound) with various excipients indicated that no incompatibilities existed, and the company proceeded with the granulation and tabletting process. However, the prototype IR tablets designed for the clinical trials were found to be chemically unstable. Investigation using various analytical techniques indicated that the degradation was due to a solution-mediated phase transformation from the anhydrate to amorphous Abbott-232 during the wet granulation process (figure 1.10). A new direct compression formulation was created, and the observed chemical instability was solved (Wardrop *et al.*, 2006:2389).

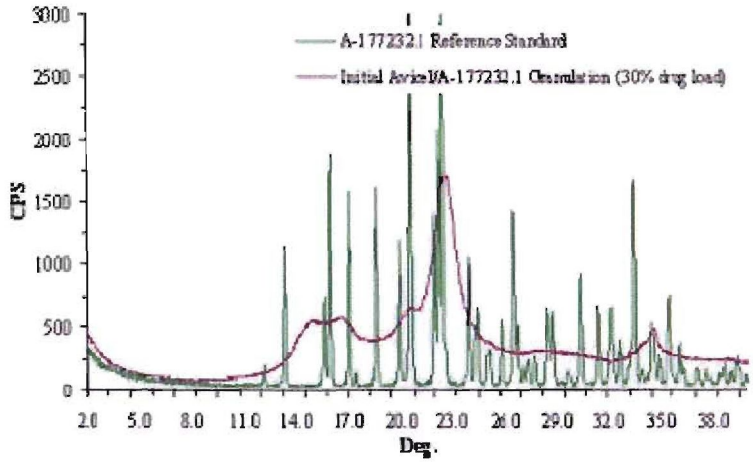
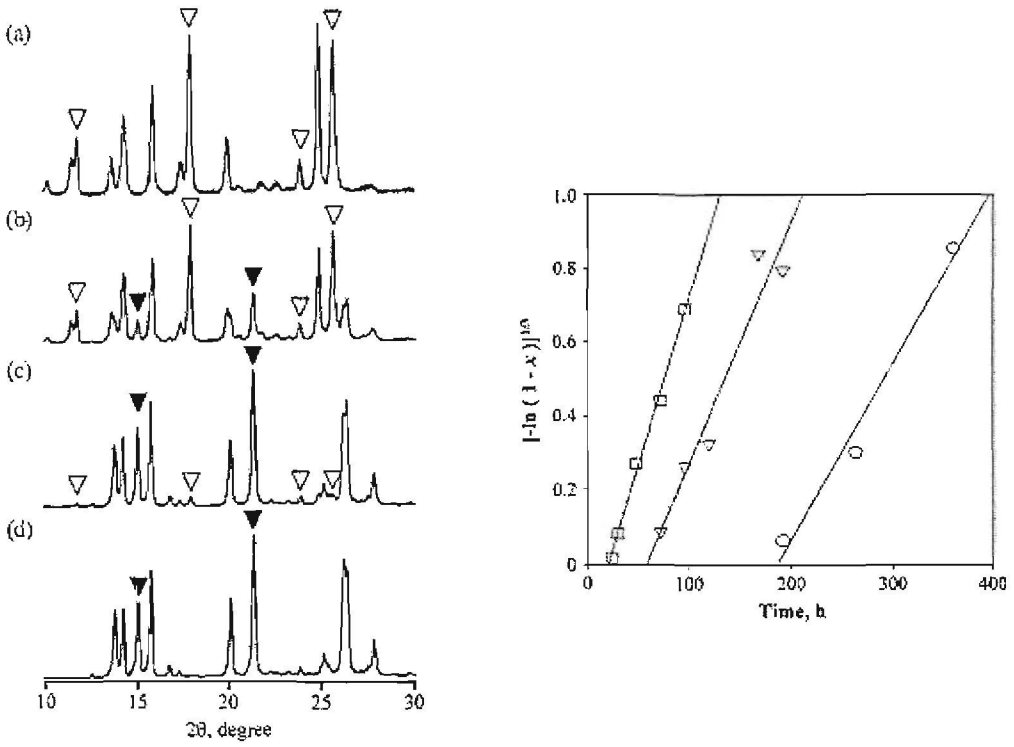


Figure 1.10 XRPD of the crystalline Abbott-232 raw material (green) and the Abbott-232 wet granulated amorphous sample (purple) (Wardrop *et al.*, 2006:2389).

An in-line monitoring of the hydrate formation of anhydrous theophylline indicated that the midpoint of conversion occurred 3 minutes after the binder solution was added to the anhydrous theophylline (Wikström *et al.*, 2005:209). The mentioned authors also indicated that an increase in the mixing speed shortened the onset time and increased the hydration process of the theophylline. The influence of processing-induced phase transformations (hydration) on the dissolution of theophylline tablets (lowered dissolution of theophylline) was also investigated by Debnath and Suryanarayanan (2004:1-11).



(i) (ii)

Figure 1.11 (i) XRPD patterns of mefenamic acid Form II after suspended in water at 28°C (a) 0 hours; (b) 192 hours; (c) 312 hours; (d) 456 hours. Open and closed triangles represent the characteristic peaks of Form I and Form II, respectively. (ii) Dependence of the function g(x) on time for the content of form II suspended in water. The o, Δ and □ represent temperatures: 28, 33 and 37°C respectively. $A3=[-\ln(1-x)]^{1/3}$ (Otsuka *et al.*, 2004:452).

Mefenamic acid, form II transformed into Form I when kneaded in water at 25, 35 and 37°C as illustrated in figure 1.11 (Otsuka *et al.*, 2004:452). The transformation followed the three-dimensional growth of nuclei equation. It was found that the transformation rate of Form II in ethanol was the fastest and that in distilled water the slowest (Otsuka *et al.*, 2004:452).

Some polymorphic forms remain unaffected by the granulation process as was observed for erythromycin A dihydrate. Römer *et al.* (2007:249) indicated that

erythromycin A dihydrate did not undergo any phase transition during the blending, wetting, extrusion or spheronisation processes.

1.3.3 Effect of drying on stability of polymorphic forms

The drying process of granules is usually associated with an increase in the temperature of the granules and or lowered relative humidity, which might thus cause a thermal phase transition (i.e. meta-stable polymorph converts to stable polymorph), desolvation of solvated crystal structures or dehydration of hydrated crystal structures (Römer *et al.*, 2007:250).

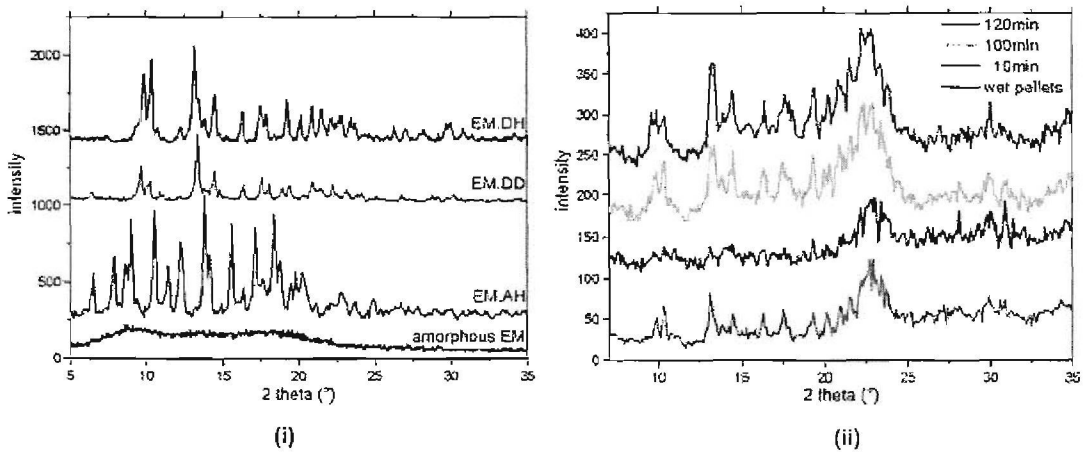


Figure 1.12 (i) XRPD patterns of amorphous erythromycin (amorphous EM), erythromycin anhydrate (EM.AH), erythromycin dehydrate (EM.DD) and erythromycin dihydrate (EM.DH) (Römer *et al.*, 2007:248). (ii) XRPD patterns for the erythromycin & micro crystalline cellulose pellets obtained at different intervals during drying in an oven at 60°C (Römer *et al.*, 2007:250).

Partial transformation of erythromycin E dihydrate to erythromycin dehydrate was observed when the granules containing erythromycin dihydrate was dried at 60°C. Near infrared and XRPD (figure 1.12) confirmed this dehydration observed.

Upon heating of polymorph III of cyclopentazide for 10 minutes at 180°C, a transition of Form III took place into polymorphic Form I (Gerber, 1989:48).

An increase in temperature can lead to the desolvation of drug pseudopolymorphs, or the modification of drug polymorphic forms. Terblanche (2001:110-139) illustrated that zopiclone crystal Forms B, C, D and E had undergone two distinctive crystal / phase changes with an increase in temperature. The first phase change resulted in the formation of crystal Form F at 70-90°C.

Figure 1.14 (i) illustrates the first phase change (Form B ⇒ Form F), using variable temperature XRPD (VT-XRPD) patterns.

The second crystal change occurred at 135-145°C, where Form F was transformed into Form A. Figure 1.14 (ii) illustrates the second phase change (Form F ⇒ Form A), using VT-XRPD patterns.

De Villiers *et al.* (1991:1295) investigated the interconversions of chloramphenicol palmitate as a function of environmental temperature. From the mentioned study it became clear that when the most soluble polymorph, Form C, was exposed to 75°C it converted to the less soluble polymorph, Form A, via the intermediate polymorph, Form B, as illustrated in figure 1.13.

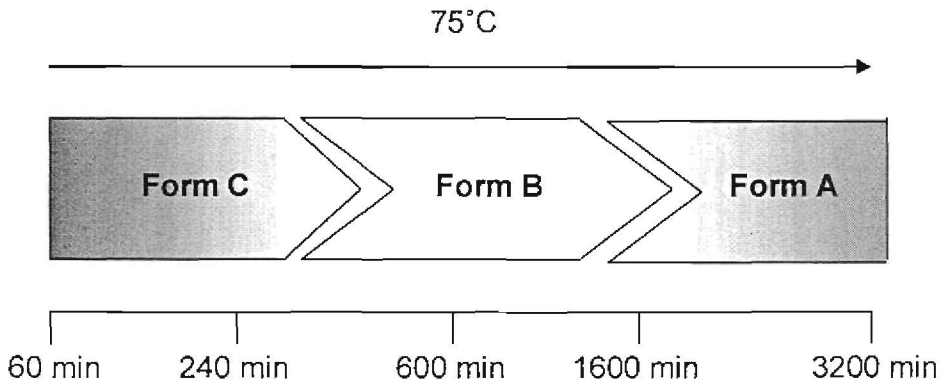
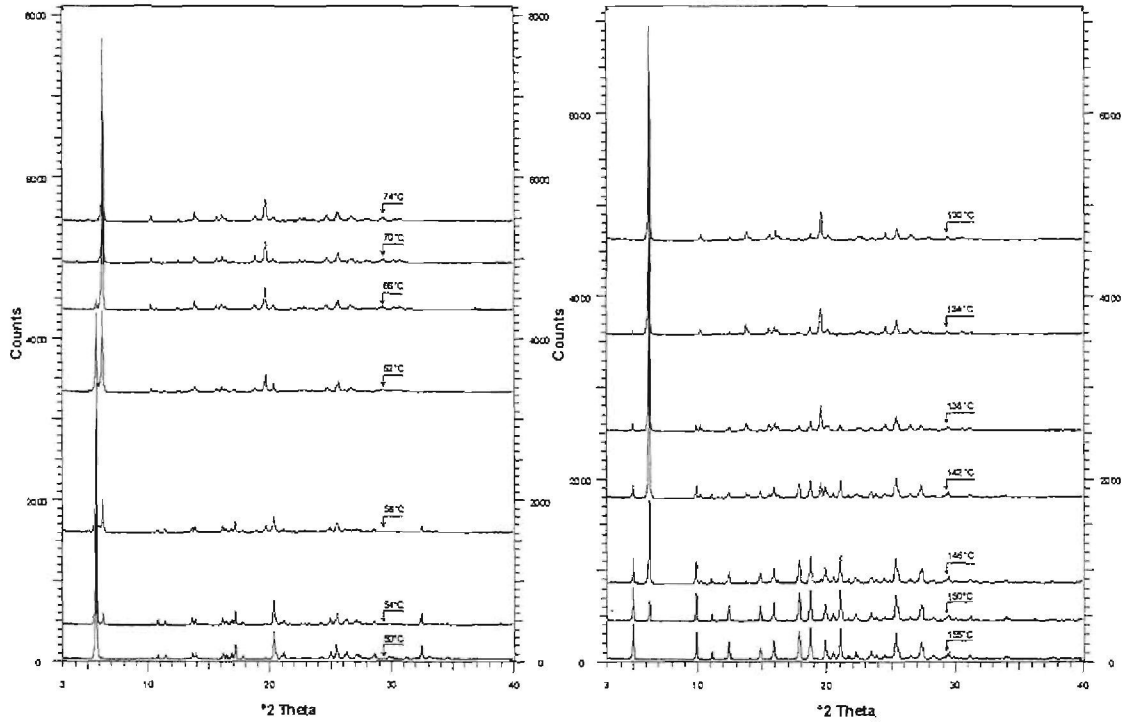


Figure 1.13 Schematic presentation of chloramphenicol palmitate polymorphic conversion when Form C is exposed to 75°C (constructed using information from De Villiers *et al.*, 1991:1301).



(i) (ii)

Figure 1.14 (i)The first phase change of zopiclone (Form B ⇒ Form F), using VT-XRPD patterns (Terblanche, 2001:116). (ii) The second phase change of zopiclone (Form F ⇒ Form A), using VT-XRPD patterns (Terblanche, 2001:117).

1.3.4 Effect of excipients on stability of polymorphic forms

Pienaar *et al.* (1993:739 & 1993:785) and Caira *et al.* (1996:241) studied and characterised the polymorphic and pseudopolymorphic behaviour of nitrofurantoin. Four new crystal forms were described: Two monohydrated forms (i.e. Form I and Form II) and two anhydrous forms (Form **α** and Form β). Otsuka and Matsuda (1994:158) revealed that the anhydrous forms of nitrofurantoin converted to the monohydrated crystal form when exposed to increased humidity.

In 2005 Airaksinen *et al.* (2005:E311-E322) investigated the influence of crystalline and amorphous excipients on the hydrate formation of nitrofurantoin

in wet masses. Airaksinen *et al.* (2005:E311-E322) used four excipients with varying crystallinity, i.e. amorphous-, less crystalline-, hygroscopic partially crystalline- and crystalline- excipients. From this study it became clear that the less crystalline excipient used in the formulation the more water is absorbed into the excipient crystal structure. The amorphous excipient used during the wet granulation retarded the hydration of the anhydrous nitrofurantoin. The use of a hygroscopic partially crystalline excipient hindered the hydrate formation of nitrofurantoin at low water contents. The crystalline excipient used was unable to retard the hydration process (Airaksinen *et al.*, 2005:E311-E322).

Airaksinen *et al.* (2003:516) investigated the ability of **α**-lactose monohydrate and silicified microcrystalline cellulose to retard the hydration of anhydrous theophylline. The **α**-lactose monohydrate (with a minimal absorbing potential) was not able to prevent but enhanced the hydration of anhydrous theophylline. Silicified microcrystalline cellulose (which is able to incorporate a large amount of water into its internal structure) was able to inhibit the formation of theophylline monohydrate at low moisture contents. XRPD analysis (figure 1.15) revealed that theophylline anhydrate converted to theophylline monohydrate with the first (0.03 g/g) addition of water (A1).

The XRPD-patterns of the theophylline-lactose monohydrate granules revealed that theophylline anhydrate also converted to theophylline monohydrate with the first (0.03 g/g) addition of water (E1), however the first trace of the monohydrate conversion in the theophylline-silicified microcrystalline cellulose granules was only observed after the addition of 0.07 g/g water (E2) (Airaksinen *et al.*, 2003:521-522).

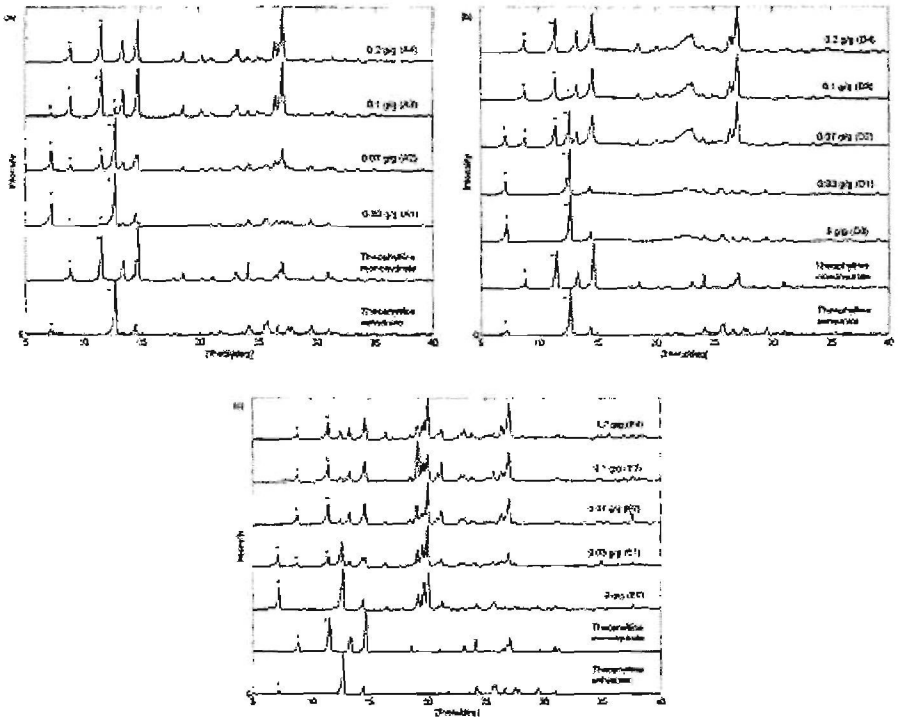


Figure 1.15 XRPD patterns of formulations after addition of different amounts of water: (a) theophylline (masses A1-A4), (b) theophylline-silicified microcrystalline cellulose (1:1) (masses D0-D4), and (c) theophylline-lactose monohydrate (1:1) (masses E0-E4). The characteristic peaks of theophylline anhydrate (7.1°2θ and 12.6°2θ) (+) and theophylline monohydrate (8.8°2θ and 11.4°2θ) (*) (Airaksinen *et al.*, 2003:522).

1.3.5 Effect of grinding and compression on stability of polymorphic forms

Chan & Doelker (1985:315) performed an extensive study on the effect of compression and grinding on stability of polymorphic forms. Table 1.3 provides an extraction of some of the observations made by the mentioned authors.

Table 1.3 API's tested for polymorphic transformations during grinding (reproduced from Chan & Doelker 1985:316)

API	Polymorphic transformation[a]	Number[b] before grinding	Number[b] after grinding
Acetohexamide	-		
Azaperone	-		
Barbitone	+	2	1
Caffeine	+	2	1
Diazepam	-		
Dipyridamole	+	2	3
Flunanisone	-		
Maproteline HCl	+	3	1
Nafoxidine HCl	+	4	3
Trimethoprim	-		

a (+) undergoes a polymorphic transformation upon grinding; (-) does not undergo a polymorphic transformation upon grinding. *b* Number of polymorphs.

Chan & Doelker (1985:316) illustrated that maproteline HCl form III converted to form II when exposed to increased pressures during tablet compression. Boldyreva *et al.* (2006:51) investigated the polymorph A → polymorph C conversion of chlorpropamide upon tabletting, and illustrated that this conversion might be attributed to local heating effects.

A study on the transformation of pharmaceuticals upon milling and co-milling (Descamps *et al.*, 2007:1405-1406) revealed that:

(i) Milling of crystalline compounds below the glass transition temperature of the corresponding liquid induces a direct solid state vitrification of lactose, trehalose and budesonide.

(ii) Milling of crystalline compounds above the glass transition temperature induces polymorphic transformations which generally place the system in a metastable state.

The milling of crystalline D-sorbitol (Form Γ) for 10 hours at room temperature (above Tg (Tg=0°C)) promoted the progressive conversion to the metastable crystalline Form A (figure 1.16).

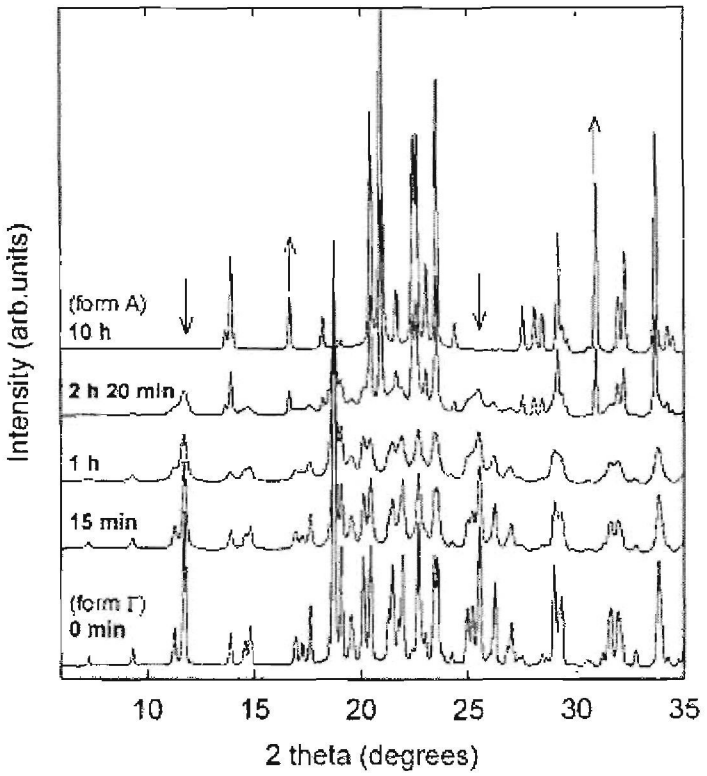


Figure 1.16 XRPD patterns of D-Sorbitol (Form Γ) in the course of a 10 hour milling process (Descamps *et al.*, 2007:1401).

In the first stage of the milling of D-sorbitol (Form Γ) (t < 1 hour) the crystallites revealed a state of nanostructuration. This nanostructuration was illustrated by the broadening of the diffraction peaks and was confirmed by the decrease of the melting temperature of D-sorbitol (Form Γ) (figure 1.16) - (Descamps *et al.*, 2007:1401).

1.3.6 Role of moisture in polymorphic stability (moisture induced polymorphic transitions)

1.3.6.1 Water-solid interactions

Water molecules consist of two hydrogen atoms which are covalently bound to a central oxygen atom (figure 1.17). Due to the electron-density distribution in the water molecule, water molecules attract each other through a dipole-dipole interaction (δ^- - δ^+) which is also known as a hydrogen bond.

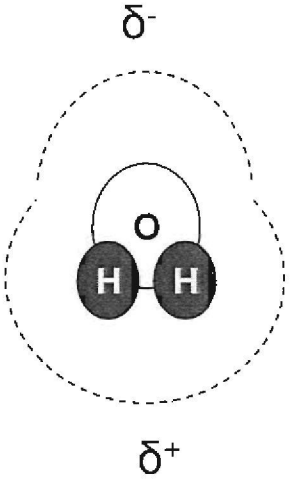


Figure 1.17 Schematic presentation of water molecule, illustrating the dipole moments present in the molecule (reproduced from Pidwirny, 2007).

The prolonged exposure of pharmaceutical solids to a water-vapour containing atmosphere might lead to moisture *sorption* by the solids. The USP (2007) describes the interaction of water with solids as: (i) water can interact at the surface of solids (known as *adsorption*) and (ii) water can penetrate the bulk solid structure (known as *absorption*). *The* general model for the interaction of water with water-soluble solids (Zografi *et al.*, 1991:1459) can be summarised as illustrated in figure 1.18:

(i) *Adsorption of water onto the surface of a crystalline solid* can take place at a relative humidity (RH_i) that is lower than that of the critical relative humidity of the solid (RH_0) (thus: $RH_i < RH_0$). Moisture

adsorption may lead to the formation of a mono-layer of water molecules on the surface of the solid. With an increase of the relative humidity there may be a tendency for multi-layer sorption of water due to the dipole-dipole moments present in the water molecules (figure 1.17), leading to the formation of a liquid film on the surface of the solid.

(ii) The vapour pressure over the sorbed film of water will be depressed relative to that of pure water due to the saturated solution of solute that will most likely exist in the film of water. This vapour pressure may be expressed as the critical relative humidity (RH_0). *Deliquescence* of solids may occur due to the continuous uptake of water at the critical relative humidity (RH_0) of the solid, which leads to the dissolution of the solid within the adsorbed moisture (Zografi *et al.*, 1991:1459).

Kontny & Zografi (1995:401-405) revealed that water sorption below RH_0 can be divided into two groups: (1) water sorption onto non-hydrates and (2) water sorption onto hydrates.

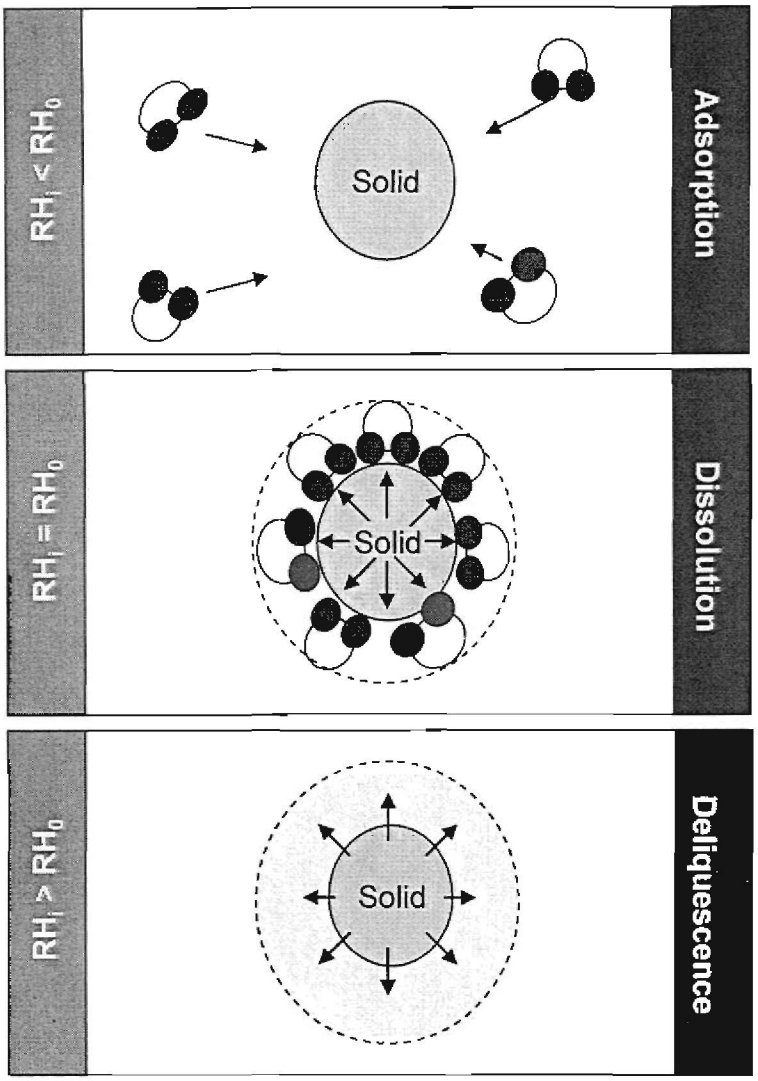


Figure 1.18 General model for the interaction of water with water-soluble solids (reproduced from Kontny & Zografi, 1995:399).

Water sorption onto non-hydrates below RH_0:

Due to the polar and dipole-dipole behaviour of water molecules (figure 1.17) the sorption of water vapour onto non-hydrating crystalline solids (i.e. adsorption) will depend on the polarity of the surfaces of the solid (Kontny & Zografi, 1995:399). For example water exhibits a greater tendency to sorb to polar and organic salts, and little tendency to sorb to non-polar surfaces.

Water sorption onto hydrates below RH_0:

When a hydrated solid is dried to it's anhydrous state and exposed to water vapour, the anhydrous specie shows a similar water sorption behaviour as non-hydrates (i.e. sorb very little water on the surface of the solid). When exposed to increasing relative humidities the surface of the solid will discontinue the adsorption of water molecules on the surface of the solid, and will incorporate the water vapour molecules into the crystal lattice (i.e. absorption). The strength of the water-solid interaction will depend on the level of the potential hydrogen bonding (Kontny & Zografi, 1995:401).

The moisture sorption will provoke the hydration of the anhydrous lattice and result in a hydrated crystal lattice. Depending on the properties of the crystal lattice, the moisture absorption process may continue and increase the stoichiometric / non-stoichiometric hydration status of the hydrated-solid, for example a monohydrated crystal lattice may be converted to a di-hydrated crystal lattice. An example of this is lactitol monohydrate which converts to lactitol dihydrate when stored at 95% RH (Halttunen *et al.*, 2005:285).

Thus, it can be concluded that water sorption on solid-surfaces can occur via three models: (1) monomolecular adsorption on the surface of the solid, (2) multi-molecular adsorption (or condensation) on the surface of the solid and (3) incorporation of water molecules into (i.e. absorption) the crystal lattice (figure 1.19).

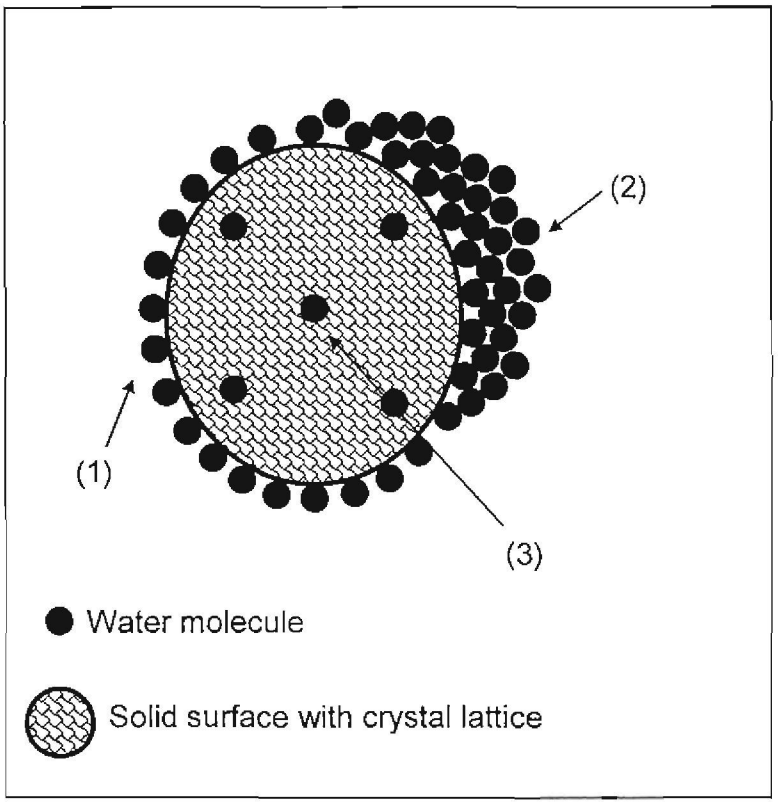


Figure 1.19 Schematic presentation of potential water-solid interactions: (1) monomolecular adsorption on the surface of the solid, (2) multi-molecular adsorption (or condensation) on the surface of the solid and (3) incorporation (absorption) of water molecules into the crystal lattice.

The BP classification for water solubility (BP, 2007) was used to investigate the effect and/or mechanism of moisture induced polymorphic transformation for three groups of solids, with different water solubilities. Table 1.4 summarises the three classes and model API's investigated.

Table 1.4 Polymorphic conversions observed in three classes

Class	Water solubility	Model API's
I	Freely soluble	• Anhydrous Lactose
		• Mannitol
		• Venlafaxine HCl
II	Slightly soluble to very slightly soluble	• Ampicillin
		• Theophylline
		• Fluconazole
III	Practically insoluble	• Phenylbutazone
		• Niclosamide
		• Mebendazole

One of the aims of this study was to investigate the thermodynamic stability of venlafaxine HCl, fluconazole and mebendazole when exposed to increased relative humidities. The results obtained will be discussed in the chapters to follow. A literature overview of the other API's tabulated in table 1.4 will now be briefly discussed.

1.3.6.2 Water-solid interactions for freely water soluble API's

Price & Young (2004:155-164) investigated the morphology and crystalline state of amorphous lactose as a function of relative humidity. The mentioned authors indicated that only a fraction of the amorphous lactose sample underwent recrystallisation transformation (i.e. nucleation and growth) during moisture uptake at 58 and 75% RH. The irregular surface morphology of the recrystallised particles (figure 1.20) suggested a secondary nucleation and growth process. The vapour sorption profile of the amorphous lactose (figure 1.21) revealed a rapid increase in moisture uptake over the range of 0-50% RH (~ 11% w/w at 50% RH), and at a partial water vapour pressure exceeding 50% RH led to a dramatic weight loss, which was attributed to the expulsion of water during the recrystallisation process. Subsequent increments above 60% RH resulted in

equilibrium adsorption of water uptake, indicative of a crystalline material (figure 1.21).

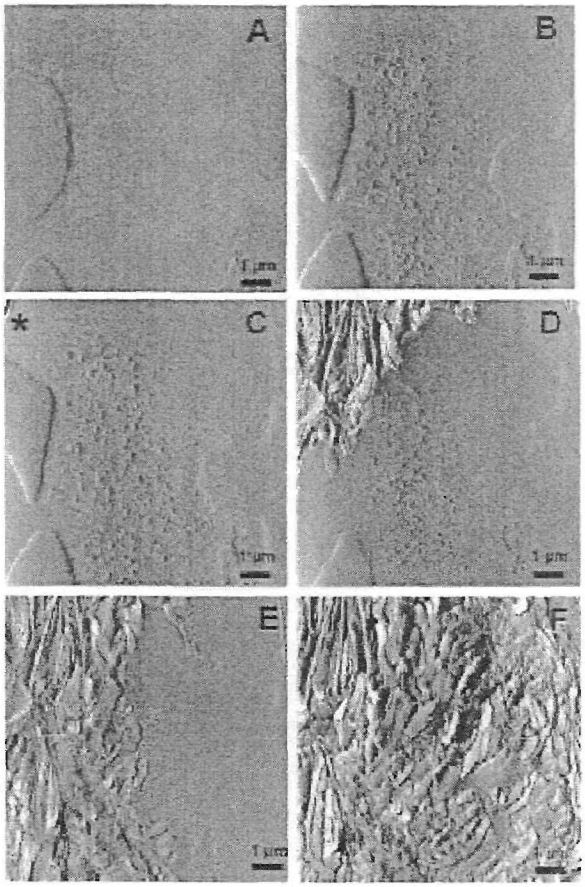


Figure 1.20 Topographical AFM amplitude images of the surface reconstruction of amorphous lactose during exposure to 58% RH: (A) 60 min; (B) 120 min; (C) 128.5 min; and (D-F) sequential downscan images (Price & Young, 2004:160).

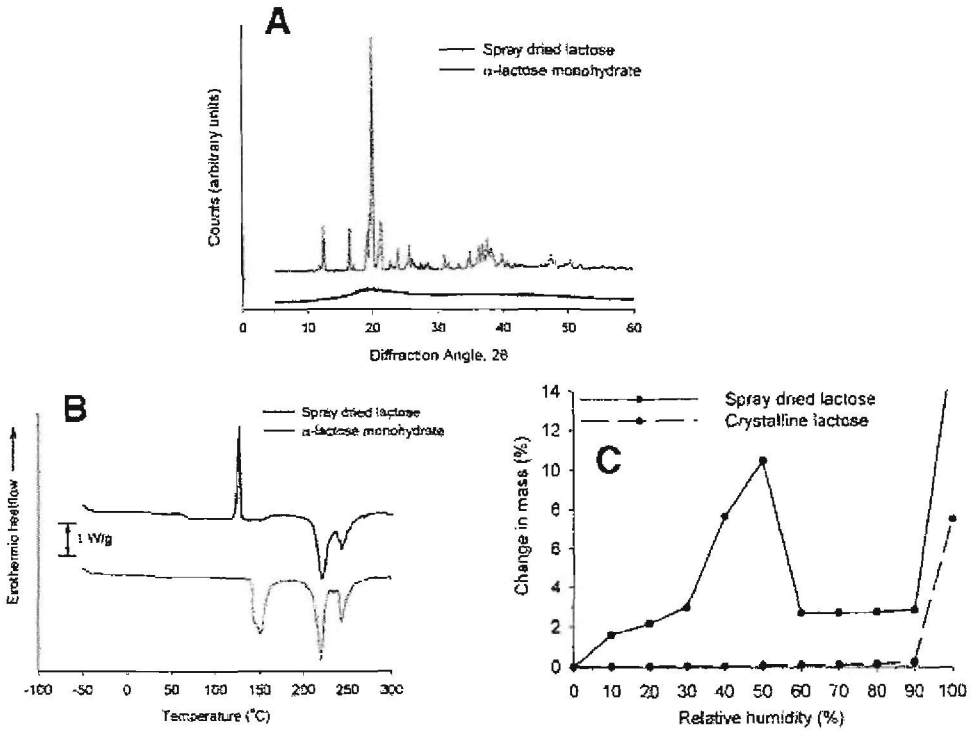


Figure 1.21 (A) XRP diffractograms of spray dried lactose (bottom) and α-lactose monohydrate (top). (B) DSC thermograms of spray dried lactose (top) and α-lactose monohydrate (bottom) at 10°C/min heating rate. (C) Water vapour sorption profile of spray dried lactose (bottom) and α-lactose monohydrate (top) (Price & Young, 2004:155).

Price & Young (2004:155) indicated that the primary nucleation of α-lactose monohydrate occurred in the non-crystallised particles at 94% RH.

Yoshinari *et al.* (2002:69-77; 2003:121-131) revealed that mannitol Form δ converted to Form β when stored at 97% RH at 25°C. It was indicated that upon exposure to the mentioned conditions, both samples started to adsorb moisture after a lag time of about 30 minutes (figure 1.22), and that the rate and extend of moisture sorption of Form δ was greater compared to that of Form β. The mentioned authors indicated that the moisture induced polymorphic conversion caused a morphological change bringing about an almost 6-fold increase in the

surface area of the newly formed Form β. The morphological change (figure 1.23) was considered to be brought about by the water molecules acting to disrupt the hydrogen bonds of the mannitol at multiple sites, which induced the immediate reconstruction of a hydrogen network to form the Form β lattice. Yoshinari *et al.* (2003:121) indicated that the moisture induced polymorphic conversion improved the compaction properties of the mannitol.

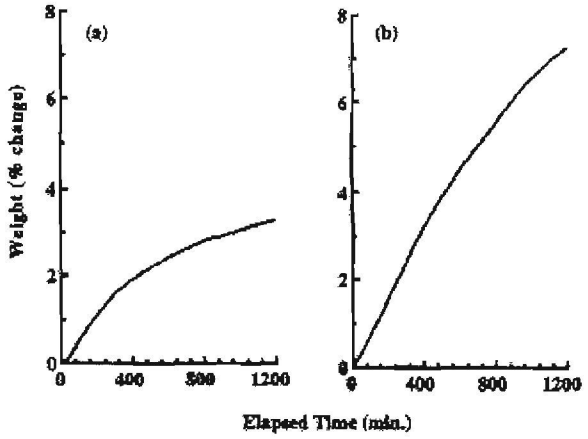


Figure 1.22 Moisture sorption profiles of mannitol (a) Form β and (b) Form δ when exposed to 97% RH & 25°C (Yoshinari *et al.*, 2002:73).

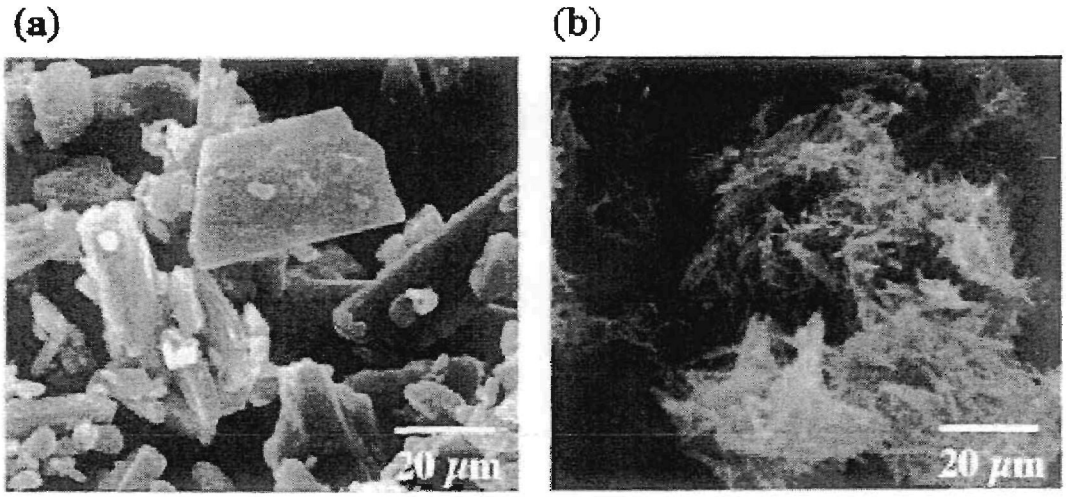


Figure 1.23 Scanning electron-micrographs of δ-crystal; (a) before and (b) after exposure to 97% RH for 20 hours (Yoshinari *et al.*, 2002:76).

1.3.6.3 Water-solid interactions for slightly soluble to very slightly water soluble API's

Examples of slightly soluble to very slightly water soluble API's are: ampicillin and theophylline. The anhydrous crystal forms of both these active pharmaceutical ingredients converted to hydrated species upon exposure to increased relative humidities.

Anhydrous theophylline converted to the monohydrate form when exposed to > 80% relative humidity (Fokkens & Blaey, 1984:127-138; Rodrigues-Hernando *et al.*, 1992:149-162; Lehto and Laine, 2000:701-706; Zhu *et al.*, 1996:151-160).

The anhydrous forms of ampicillin prepared at various dehydration temperatures showed that the anhydrous form prepared at 100°C had a higher hydration (anhydrous → trihydrate) rate compared to the anhydrous form prepared at 160°C (figure 1.24) – Moribe *et al.*, 2005:248. Atomic force microscopy (AMF) showed that the surface of the anhydrous form prepared at 100°C was coarse and rough [figure 1.25 (A) & (B)] and that the surface of the anhydrous form prepared at 160°C was rather smooth [figure 1.25 (C) & (D)].

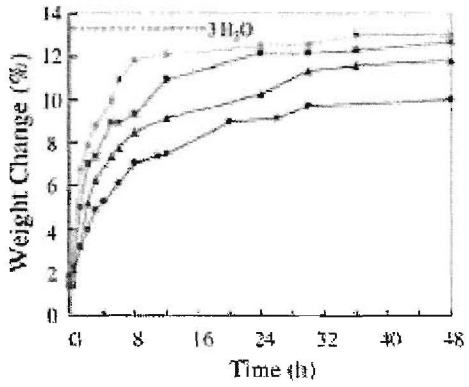


Figure 1.24 Isothermal hydration profiles (at 89% RH at 40°C) of ampicillin anhydrous forms prepared at various temperatures: (◇) 100°C, (▪) 120°C, (Δ) 140°C and (●) 160°C (Moribe *et al.*, 2005:248). The broken line in the figure shows the calculated water content for the trihydrate (13.4%).

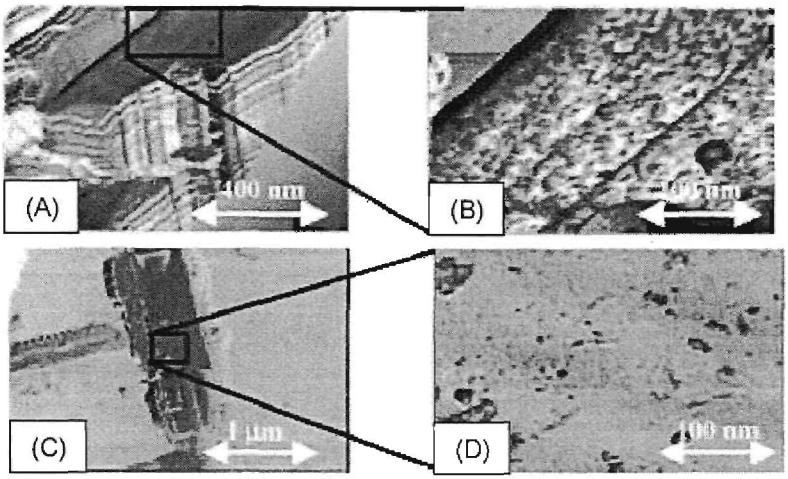


Figure 1.25 AMF topography images of the ampicillin anhydrous forms prepared at 100°C (A & B) and 160°C (C & D) respectively (Adapted from Moribe *et al.*, 2005:249 – 250).

Matsuo & Matsuoka (2007:413) indicated that during the hydration of theophylline anhydrous Form III (upon exposure to increased relative humidities) water facilitated the molecular loosening in the crystal, causing the crystal surface to change from a relatively smooth surface to an assembly of small platelike flakes piling on each other.

1.3.6.4 Water-solid interactions for API's that are practically insoluble in water

According to Matsuda *et al.* (1984:1453-1460), the exposure of phenylbutazone polymorphs to water vapour caused polymorphic conversions: Form β→ Form δ and Form α → Form δ (figure 1.26).

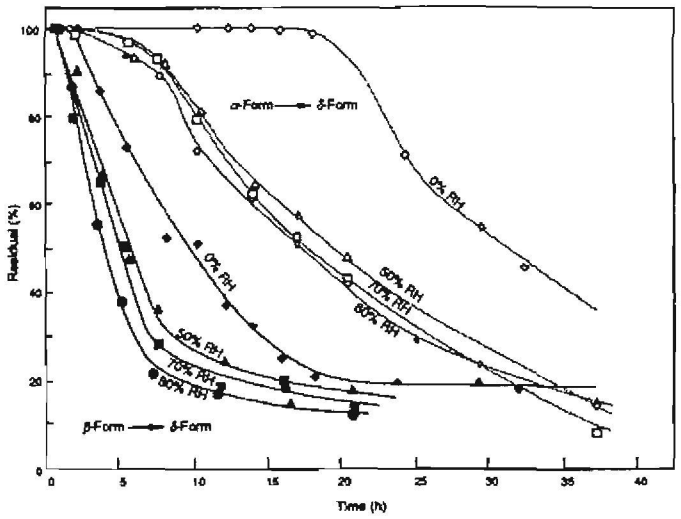


Figure 1.26 Time course for phenylbutazone Form β→ Form δ and Form α → Form δ transformations at 60°C and various relative humidities (Adapted from Byrn *et al.*, 1999:267).

Another example of a moisture induced polymorphic transition of a practically water insoluble API, is that of the anthelmintic, niclosamide (5-chloro-N-(2-chloro-4-nitrophenyl)-2-hydroxy-benzamide) – Manek & Kolling (2004:1-8). Figure 1.27 provides a summary of the moisture stability study performed by Manek & Kolling (2004:1-8).

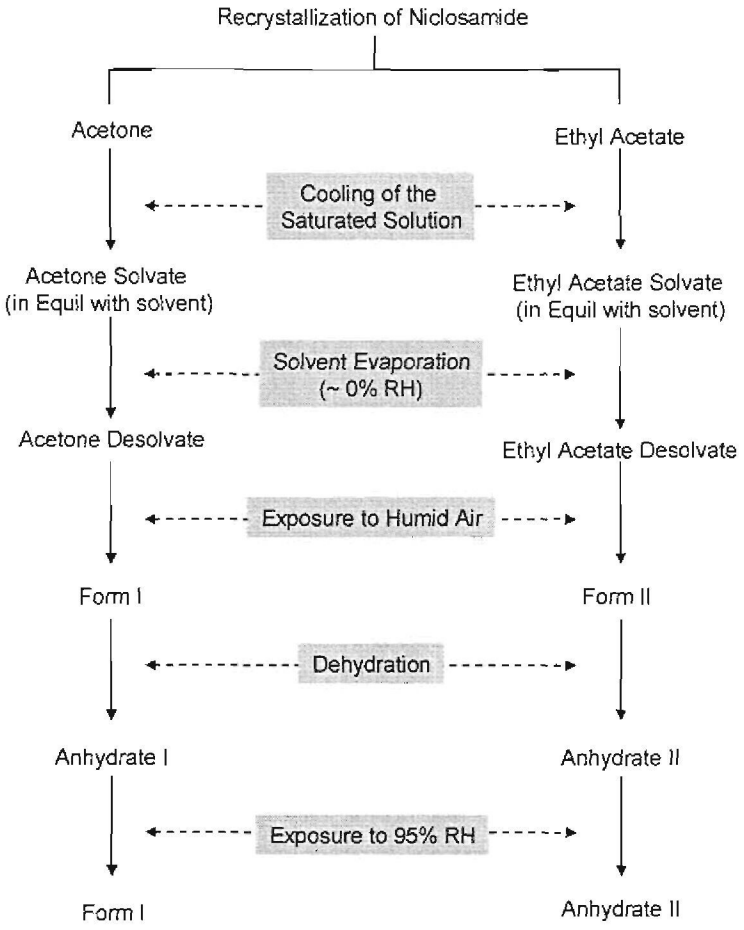


Figure 1.27 Schematic representation of the formation of pseudopolymorphs of niclosamide (reproduced from Manek & Kolling, 2004:1-8).

Desolvation of the acetone and ethyl acetate solvates produced two desolvated-solvate crystal forms. These two forms seemed to maintain the structure of the parent solvate, yet no longer possess the solvent of crystallisation (i.e. acetone and ethyl acetate) - Manek & Kolling (2004:1-8).

Upon exposure to humid air, the desolvated solvates (i.e. acetone and ethyl acetate desolvates) converted to monohydrate Form I and Form II respectively, in order to stabilise the high-energy desolvated crystal lattices. Exposure of Form I and Form II to increased temperatures caused dehydration of the mentioned crystal forms, and form anhydrate I and anhydrate II respectively (Manek &

Kolling, 2004:1-8). Anhydrate I converted to monohydrate Form I when exposed to 95% RH, however anhydrate II remained unaffected.

Manek & Kolling (2004:1-8) attributed the difference in the moisture sorption profiles of the 2 anhydrates to the differences in the ease of molecular diffusion through the crystal lattice. Dehydration of Form I occurs at low temperatures and the unit cell probably does not attain maximum packing density, as illustrated by the rehydration of anhydrate I at 95% RH. Dehydration of Form II occurs at elevated temperatures with structural rearrangement to maximize the packing efficiency, thus leading to a comparatively stable anhydrate (anhydrate II) which does not interact with moisture at 95% RH.

Conclusion

This chapter highlighted the importance of the early and comprehensive exploration of possible polymorphism and/or pseudopolymorphism to ensure that the best (most stable crystal modification, with most favoured biopharmaceutical and manufacturing properties) crystal form is selected for the manufacturing process, to enable a proactive and value-maximizing approach to product life cycle management and to secure appropriate and timely intellectual property protection.

Many factors may influence the thermodynamic stability of API's, for example moisture. It was decided to investigate the effect of moisture on the following polymorphic API's with different water solubilities: venlafaxine HCl (freely water soluble), fluconazole (slightly water soluble) and mebendazole (practically insoluble in water).

CHAPTER 2

General methods utilised during studies for characterisation and analytical purposes

Introduction

Polymorphic forms of API's can display a wide and largely unpredictable variety of solid state and chemical properties (Byrn *et al.*, 1999:4). Application of basic physico-chemical principles, combined with appropriate analytical methodologies, can provide a powerful tool to investigate the solid state properties of solid drug substances and assist in the prediction of the stability of various crystalline phases.

This chapter will describe the methods used for the characterisation and identification of the polymorphic forms of mebendazole, venlafaxine HCl and fluconazole.

2.1 Identification and characterisation methods used in this study

The methods and techniques used for the characterisation of the different crystal forms are shown in table 2.1.

Table 2.1 Methods used for the characterisation of the various crystal forms (adapted from Yu *et al.*, 1998:124 – unless otherwise indicated).

Type of crystal modification	XRPD	Thermal methods	DRIFT-IR	Microscopy	Particle size analysis	Specific surface analysis	Moisture sorption analysis	KF	Heat of solution studies
True polymorphs	Unique diffraction peaks. Useful for determination of phase purity and % crystallinity.	Unique mp, heat capacity, heats of fusion / transition, solubility. Useful for determining relative stability of forms.	Characteristic spectra. Sensitive to H bonding.	Characteristic indices of refraction, birefringence, dispersion, colour, crystal habit.	Different polymorphs may exhibit morphological differences, which may cause differences in particle sizes (Newman & Brittian, 1995:151).	Differences in crystal packing lead to differences in void spaces and surface differences that may influence the dissolution rate, crushing strength and powder density (Brittain, 1995:18-20).	The sorption and desorption moisture transformation has been used to evaluate the thermodynamically favoured state that will result after the equilibrium process is finalised (Brittain, 1995:29).	NA	Each crystal phase is characterized by a well-defined heat of solution as it dissolves in a given solvent, the difference between the heats of solution of each phase equals the heat of transition between them at the temperature of measurement (Grant & Brittain, 1995:368-369).
Solvates	Same as true polymorphs.	Low temperature transitions due to desolvation (TGA loss)	Unique solvent bands. Shifted molecular bands. Sensitive to H bonding.	Same as true polymorphs. Desolvation observable by hot stage microscopy.	Same as true polymorphs.	Same as true polymorphs.	Same as true polymorphs.	Moisture content of hydrated crystal forms can be determined.	Same as true polymorphs.
Isomorphic desolvates	NA	Low temperature desolvation absent. Events due to crystalisation or lattice relaxation.	Solvent bands disappear. Molecular bands shifted.	Birefrigent microcrystalline domain, with cracks and fissures.	Same as true polymorphs.	Same as true polymorphs.	Same as true polymorphs.	NA	Same as true polymorphs.
Amorphous solids	NA	Glass transition seen. Often followed by crystallization and melting. 'Fragility' related to with of Tg.	Broadened spectra.	No birefringence, irregular particle shape.	Same as true polymorphs.	Same as true polymorphs.	Amorphous solids are considered more susceptible to moisture sorption (Brittain, 1995:29).	NA	Same as true polymorphs.
Polymorphic mixtures	NA	Thermal behaviour indicative of phase diagram (e.g. *mp*-depression, eutectic melting, dissolution).	Composite spectrum of all components.	Composites of distinct crystalline and amorphous particles.	Particle size distribution may consist of composite sizes of all components (Newman & Brittian, 1995:151).		Composites moisture sorption behaviour of all components.	Moisture / water content can be determined.	Same as true polymorphs.

2.1.1 Crystallographic methods

X-ray powder diffraction (XRPD) and variable temperature X-ray powder diffraction (VT-XRPD) were used in this study to investigate crystallographic properties of the pharmaceutical solids.

2.1.1.1 X-ray powder diffraction (XRPD)

XRPD was used due to its efficacy to distinguish between different solid phases in different or the same powdered samples. The advantage of using X-ray powder diffraction is that this method does not require large single crystals, but instead can be readily applied to any powdered sample (Byrn *et al.*, 1999:52-55).

The X-ray powder diffractogram yields information about the diffraction characteristics of the sample. These diffraction characteristics include the intensities of the maxima diffraction peaks and the angles at which they occur. The values of the *d* spacings reflect the dimensions of the unit cell, while the intensities are due to the contents of the unit cell and the manner in which the different atoms and molecules are arranged in the unit cell. X-ray powder diffraction can be used for qualitative and quantitative analysis of polymorphs or mixtures of polymorphic forms (Bernstein, 2002:112-122).

X-ray powder diffraction patterns in this study were obtained at room temperature using a Bruker D8 Advance diffractometer (Bruker, Germany). Approximately 200 mg samples were weighed into aluminium sample holders, taking care not to induce a preferential orientation of crystals. The measurement conditions were: target, Cu; voltage, 40 kV; current, 30 mA; divergence slit, 2 mm; antiscatter slit, 0.6 mm; detector slit, 0.2 mm; monochromator; scanning speed, 2°/min (step size, 0.025°; step time, 1.0 sec.).

Samples were lightly ground in an agate mortar and pestle to reduce the particle size to prevent or reduce the effect of preferred orientation.

The XRPD traces of the powders and crystals were compared with regard to peak position and relative intensity, peak shifting and the presence or lack of peaks in certain regions of °2θ values. This was achieved by the preparation of overlays of the various XRPD patterns of the various crystal forms, or the simulation of Guinier films using EVA® and Powder3D 1.1® software.

2.1.1.2 Variable temperature X-ray powder diffraction (VTXRPD)

Diffractometers can be fitted with environmental chambers to control the temperature of the sample being analysed, that may be used to investigate the interconversions of crystal forms or the desolvation of solvated phases under different conditions. VTXRPD is useful in conjunction with differential scanning calorimetry to elucidate thermal events (such as desolvation endotherms, recrystallisation exotherms etc.) observed in thermograms.

Variable temperature X-ray powder diffraction (VT-XRPD) patterns were recorded with an Anton Paar TTK 450 low-temperature camera (Anton Paar, Austria) attached to a Bruker D8 Advance diffractometer (Bruker, Germany). The specific temperatures used during the studies will be specified in the relevant sections. A heating rate of 10°C/min was used during all of these determinations.

The isothermal measurement conditions were: target, Cu; voltage, 40 kV; current, 30 mA; divergence slit, 2 mm; antiscatter slit, 0.6 mm; detector slit, 0.2 mm; monochromator; scanning speed, 2°/min (step size, 0.025°; step time, 1.0 sec.). Approximately 200 mg samples were weighed into aluminium sample holders, taking care not to induce a preferential orientation of crystals.

2.1.2 Thermal methods

DSC and TGA analyses are commonly used for purity and solvent determinations, polymorphism studies, polymorphic-transition studies and quantitative analysis (Giron-Forest *et al.*, 1989:1421-1433).

2.1.2.1 Differential scanning calorimetry (DSC)

Differential scanning calorimetry is used to investigate the changes in the energy flow in samples when exposed to increased temperatures.

DSC thermograms of the venlafaxine hydrochloride samples were recorded with a Shimadzu DSC-50 instrument (Shimadzu, Kyoto, Japan). Samples weighing 3-5 mg were heated in closed aluminium crimp cells at a rate of 10°C/min under a nitrogen purge of 35 ml/min.

DSC studies on the fluconazole crystal forms were recorded with a Mettler-Toledo DSC 822e/700 (Microsep, Switserland). Samples weighing 3-5 mg were heated in closed aluminium crimp cells with pierced lids at a rate of 1°C/min under a nitrogen purge of 50 ml/min.

DSC results were used to identify possible polymorphs and pseudo polymorphs (hydrates or solvates), to characterise the different forms in view of their melting points and to investigate the relationship between polymorphs.

2.1.2.2 Thermogravimetric analysis (TGA)

Thermogravimetric analysis is used to investigate the change in mass with an increase in the temperature and is usually used to study the desolvation process in solvated crystal forms.

The TGA thermograms of the venlafaxine hydrochloride samples were recorded with a Shimadzu TGA-50 instrument (Shimadzu, Kyoto, Japan). Approximately 5-8 mg samples were weighed and heated in an open platinum cell, at a heating rate of 10°C/min under a nitrogen purge of 35 ml/min.

The TGA thermograms of the fluconazole samples were recorded with a Mettler-Toledo TGA/SDTA 851e/LF/1100 instrument (Microsep, Switzerland). Approximately 5-8 mg samples were weighed and heated in an open platinum cell, at a heating rate of 10°C/min under a nitrogen purge of 50 ml/min.

Thermogravimetric analysis was performed on all samples which indicated a possible pseudopolymorphic behaviour. These samples were heated to 160°C.

The theoretical weight loss for solvated samples were calculated, using the following equation:

$$\%\ Weight\ loss = \frac{Molecular\ weight(solvent)}{Molecular\ weight(solvent) + Molecular\ weight(API)}\ x\ 100\%$$

The experimental weight loss (in percentage) recorded by the instruments, was compared with the theoretical weight loss (in percentage), calculated for a solvate or hydrate using the above equation.

2.1.3 Infrared spectroscopy (DRIFT-IR)

The infrared spectrum of an organic compound is extremely sensitive to structure and confirmation thereof and thus is a powerful method for the characterisation and identification of different crystal phases (Byrn *et al.*, 1999: 111).

IR-spectra were recorded on a Nicolet Nexus 470-FT-IR spectrometer (Nicolet intrument corporation, Maddison, USA) over a range of 400 – 4000 cm^{-1}. The diffuse reflectance method was used. KBr was used as background material. The main absorptions in the IR-spectral results of all the samples were compared to determine possible significant differences with regard to polymorphic form or polymorphic modifications.

2.1.4 Microscopy

Microscopic methods are used to explain some of the thermal events detected by the DSC and TGA thermograms, such as desolvation, melting and recrystallisation events. It also provides information on the morphology of crystals.

2.1.4.1 Thermal microscopy (TM)

TM analysis was performed on small amounts of sample with a Nikon Eclipse E400 microscope (Nikon, Japan), equipped with a Metratherm 1200d heating stage and a Nikon Coolpix 5400 digital camera (Nikon, Japan). The effects of an increase in temperature on the crystal behaviour of the samples were studied by gradually increasing the temperature.

Observations that can be made from TM include the following: sublimation, desolvation of solvated crystal forms, melting, decomposition, formation of intergrowth crystals and polymorph-polymorph interconversions (Brandstätter, 1971:14-19).

2.1.4.2 Scanning electron microscopy (SEM)

The information obtained from SEM is visual and descriptive of nature. The particle morphology of the pharmaceutical solids was investigated using SEM. A FEI Quanta 200 ESEM & Oxford INCA 400 EDS system (FEI, USA) was used to obtain photomicrographs of the various crystal forms studied. The samples were adhered to a small piece of carbon tape, mounted onto a metal stub and coated with a gold-palladium film (Eiko Engineering ion Coater IB-2, USA).

2.1.5 Particle size analysis

Particle size plays an important role in the dissolution and moisture sorption properties of solids. Particle size distributions in suspension were measured with a Galai-Cis-1 (Galai-Cis-1, Israel) particle size analyser. This analyser uses dual discipline analysis, integrating laser diffraction and image analysis for particle

sizing. Samples of powder suspended in a dispersing solution were each placed in a small cuvette and fitted into the analyser.

A small magnetic stirrer was placed inside the cuvette to prevent sedimentation of the particles during the measurement. The acquired data was used to compute means, medians and standard deviations, based on the total particle population.

2.1.6 Specific surface area analysis

The specific surface area of powders can be determined by the adsorption of a gas on the surface of the solid and by calculating the amount of adsorbate gas corresponding to a monomolecular layer on the surface using the BET (Branauer, Emmet and Teller) theory. The data obtained are treated according to the BET adsorption isotherm equation:

$$\frac{1}{\left[V_a\left(\frac{P_0}{P}-1\right)\right]} = \frac{C-1}{V_m C} x \frac{P}{P_0} + \frac{1}{V_m C}$$

Where:

P = Partial vapour pressure of adsorbate in equilibrium with the surface at 77.4 K (boiling point of liquid nitrogen), in Pa,

$\mathbf{P_0}$ = Saturated pressure of adsorbate gas, in Pa,

$\mathbf{V_a}$ = Volume of gas adsorbed at standard temperature and pressure (STP), which is 273.15 K and atmospheric pressure (1.013×10^5 Pa), in ml,

$\mathbf{V_m}$ = volume of gas adsorbed at STP to produce an apparent monolayer on the sample surface, in ml,

C = dimensionless constant that is related to the enthalpy of adsorption of the adsorbate gas on the powder sample (USP, 2006).

The value of V_a is measured at each of not less than three values of P/P_0. Then the BET value ($\frac{1}{\left[V_a\left(\frac{P_0}{P}-1\right)\right]}$) is plotted against P/P_0.

This plot usually yields a straight line in the approximate relative pressure range 0.05 to 0.3. Data considered acceptable produces a linear coefficient (r^2) of not less than 0.9975. From the linear plot the slope (m) and intercept (y) is calculated by linear regression analysis, where:

$$m = \frac{(C-1)}{V_m C} \quad \text{and;} \quad y = \frac{1}{V_m C}$$

From these values, C, V_m and the specific surface are (S, in m^2/g) is calculated using the following equations:

$$C = \left(\frac{m}{y}\right) + 1$$

$$V_m = \frac{1}{m+y}$$

$$S = \frac{V_m N a}{m \; x \; 22400}$$

Where:

N = Avogadro constant (6.023×10^{23} mol^{-1}),

a = effective cross-sectional area of one adsorbate molecule, in square meters ($a_{Nitrogen}$=0.162 nm^2),

m = mass of test sample, in g,

22 400 = volume, in ml, occupied by one mole of the adsorbate gas at STP allowing for minor departures from the ideal (USP, 2006).

The specific surface area of the powdered samples was determined using a Micrometrics Flowsorb II2300 surface analyser (Norcross, GA, USA). Nitrogen was used as adsorbate. All pre-adsorbed gases and vapours were removed from the surface of the samples by means of out-gassing at 40°C, for 180 minutes. Samples weighing 200-900 mg were used for specific surface area analysis.

2.1.7 Moisture sorption analysis

Byrn *et al.* (1999:24) stated that the plot of vapour pressure versus relative humidity is an excellent way to determine the nature of a solid with respect to water sorption (figure 2.1).

The basic behaviour of moisture sorption depicted in figure 2.1 include the following:

(1) Virtually no water uptake;
(2) Gradual water uptake, characteristic of amorphous material or a non-stoichiometric hydrate;
(3) "Stair-step" – water uptake, characteristic of stoichiometric hydrates.

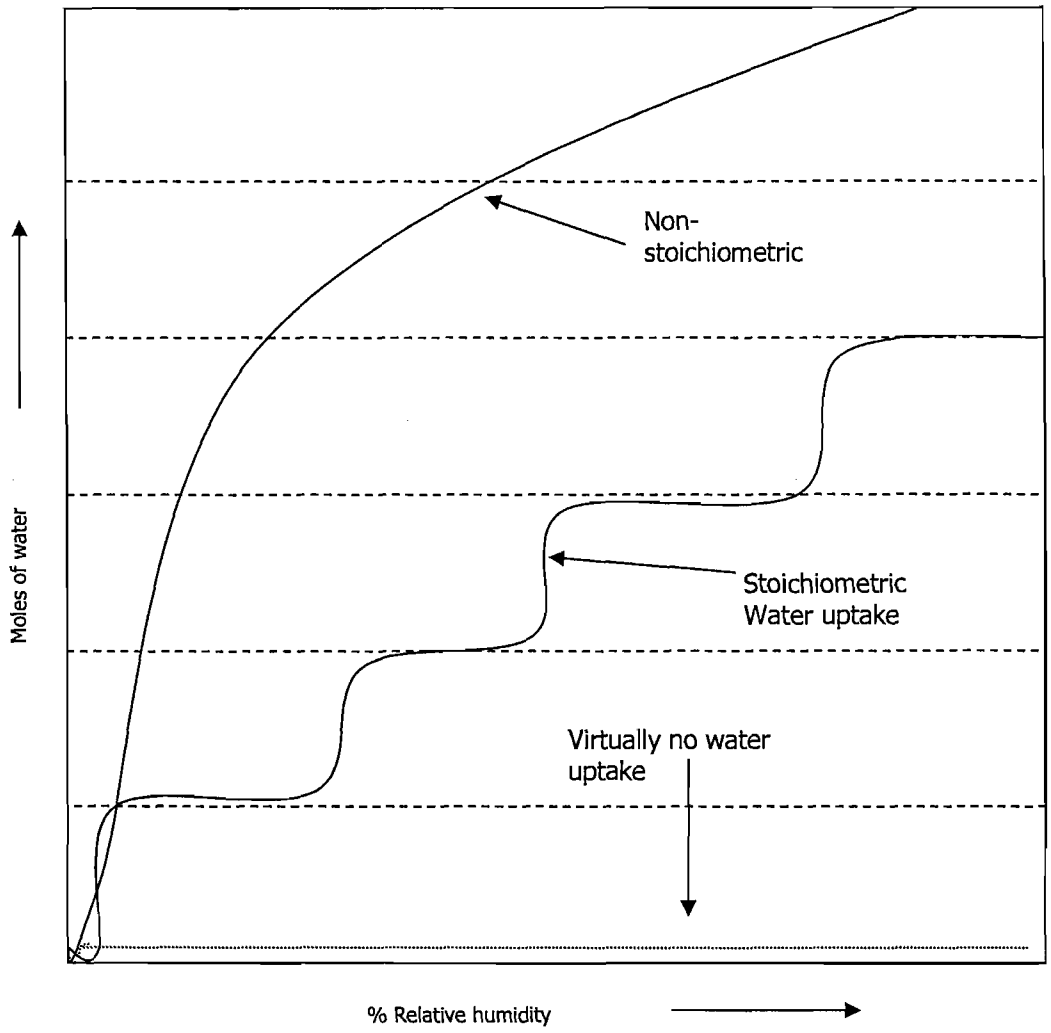


Figure 2.1 Idealised vapour pressure versus relative humidity plot (reproduced from Byrn *et al.,* 1999:24).

Anhydrous samples were vacuum dried at 50°C for three days prior to inducing the sample in the sorption analyser. Moisture sorption isotherms were generated at 25°C using a Symmetric Vapour Sorption Analyser (model SGA-100, VTI, Hialeah, FL). The SGA-100 is equipped with an electronic microbalance (CI Electronics, Wiltshire, UK) and dew point analyser (Edgetech, Milford, MA) for the accurate measurement of weight and relative humidity (RH), respectively. The instrument was calibrated using sodium chloride and polyvinylpyrrolidone (PVP) K30. The procedure involved drying the samples in the VTI instrument at 60°C and ~ 0 % RH until the instrument recorded a weight loss of less than 1 µg over

a period of 5 minutes. This was followed by exposing the samples to 10 % steps in RH from 0 to 95 % RH. Equilibrium was assumed when there was no weight change of more than 1 µg over a period of 5 minutes.

2.1.8 Karl Fischer analysis

Karl Fischer titrations were performed on samples to determine the total moisture content of the samples. The total moisture content of the samples was determined with a Metrohm 701 KF Titrino autotitrator (Metrohm, Switzerland). The instrument was calibrated using a predetermined mass of water and sodium tartrate dihydrate dibasic reference standard. Approximately 50 mg of each sample was used for the moisture determination. The titration experiment was performed in at-least duplicate for each analysis, and the total moisture content (% - m/m) was calculated from the results obtained.

2.1.9 Heat of solution studies

Each distinct crystal phase can be characterised by a heat of solution as it is dissolved into a given solvent system. Solution calorimetry studies can be used to describe the relationship between a given set of polymorphs (i.e. monotropic or enantiotropic), and to deduce the heat of transitions between the various forms (Grant & Brittain, 1995:369). The heats of solution of the various crystal forms were determined by isothermal high sensitivity microcalorimetry (MicroDSC III, Setaram, France) at 20, 30 or 40°C. Samples weighing approximately 2 mg were analysed in a mixing "batch" vessel under nitrogen purging with about 0.15 g deionised water used as the solvent (Nanopure, Barnstead International, Dubuque, Iowa). The vessel is composed of a cylinder and a set of parts mounted on a rod provided for dividing the experimental volume into two distinct chambers with a volume of 0.2 cm^3 for the upper chamber and 0.55 cm^3 for the lower chamber. The powder was placed in the bottom of the mixing vessel while the solvent was added to the top reservoir. Once the instrument was equilibrated at 20, 30 or 40°C, the rod was pushed down allowing the solvent to come in

contact with the sample powder. The heat measured, once corrected for the heat involved in stirring; represent the heat involved in the dissolution of the powders in water. All measurements were repeated 6 times.

The heat of solution, ΔH, is calculated using the following equation:

$$\Delta H = \frac{q}{mol}$$

Since the heat (q) comes from the chemical reaction of the solute, ΔH is per moles solute, not per mol solution.

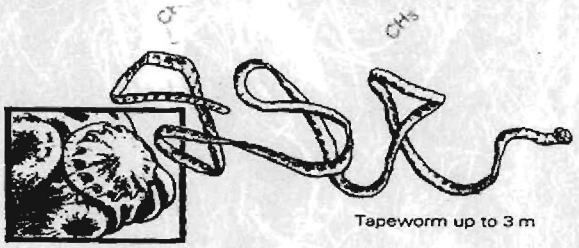
Applications of the results obtained will be discussed in the chapters to follow.

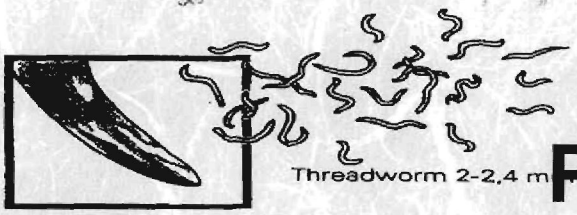
Conclusion

The methods and techniques of characterisation and analysis described in this chapter (as summarised in section 2.1) will be utilised to investigate and elucidate the observations made during this study.

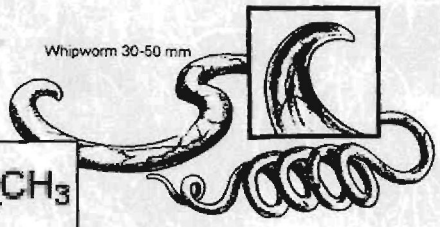
From a manufacturing point of view it is important to be fully acquainted with the solid-state properties and thermodynamic behaviour of the API to be used during the manufacturing process. Phase transitions such as the formation of hydrates may occur during various pharmaceutical processes (i.e. manufacturing, packaging and storage of the final product), which may alter tabletting properties, dissolution rates and stability of the drug substance remarkably.

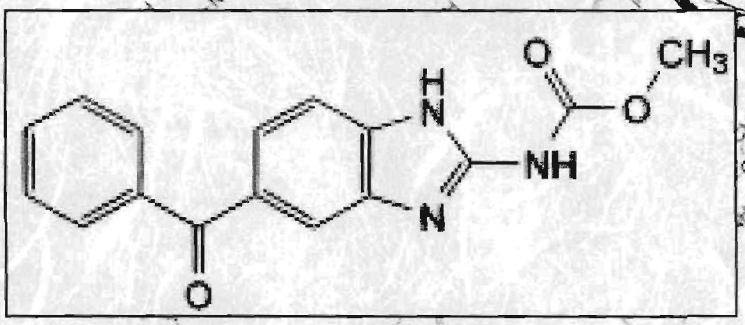
Potential phase transitions, factors inducing these transitions and the effect thereof on molecular level will be discussed in the chapters to follow.

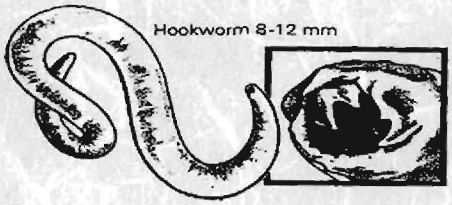


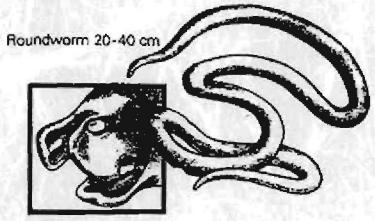


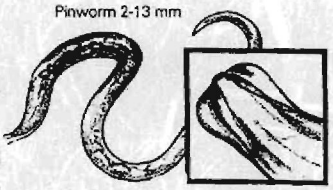
PART 1
Mebendazole











CHAPTER 3

Thermodynamic stability of mebendazole polymorphic forms in tablets under high humidity conditions

"Most people believe that if something costs more it has to be better quality. In the case of generic drugs, this is not true."

Gary Buchler, Director of FDA's Office of Generic Drugs

Introduction

The three polymorphic forms of mebendazole (i.e. A, B and C) display significant differences in solubility and therapeutic efficacy. The solubility of the three mebendazole polymorphs in physiological media has been reported as: Form B > Form C > Form A (Costa *et al.*, 1991:415). Polymorph C is the preferred form to be used clinically due to its optimal bioavailability and reduced toxicity compared to the more soluble Form B (Charoenlarp *et al.*, 1993:712).

The order of the mebendazole polymorph stability has been described as: polymorph A > polymorph C > polymorph B (Himmelreich *et al.*, 1977:123). Terblanche (2001:139-147) showed that polymorph C transformed into the thermodynamically more stable polymorph A at temperatures exceeding 175°C. This transformation was a first-order process with activation energy of 238±16 kJ/mole.

It has been documented that polymorph A had no anthelmintic activity when administered alone or when present above 30% in polymorphic mixtures (Ren *et al.*, 1987:356). It is thus important to ensure the stability of polymorph C in the final product to prevent the transformation of polymorph C into polymorph A that might result into a product with little or no clinical efficacy.

Therefore, it was imperative to initiate a study to determine the mebendazole polymorphic forms present in the mebendazole generic products available in

South Africa, and to determine the thermodynamic stability of these forms in the commercially available tablets.

3.1 Materials and methods

The following materials and methods were used in the study of the polymorphic stability of mebendazole in commercially available tablets in South Africa.

3.1.1 Products

Commercially available mebendazole tablets were obtained from local pharmacies (Table 3.1).

Table 3.1 Commercially available mebendazole tablets

Product	Manufacturing company
Rolab-Anthex 100 mg tablets	Rolab
D-Worm 100 mg tablets	Triomed
Adco-Wormex 100 mg tablets	Adcock Ingram
Worm Stop 100 mg tablets	Be-Tabs
Worm-Go 100 mg tablets	Aspen Pharmacare
Cipex 100 mg tablets	Cipla Medpro (Pty) Ltd.
Vermox 100 mg tablets	Janssen-Cilag

The products were randomly numbered: Product 1 – Product 7, to conceal the product identity. Table 3.2 provides a basic summary of the composition of the various tablets.

A battery of analytical tests was performed on the procured tablets to identify the mebendazole polymorph present in the tablets (XRPD and DRIFT-IR). The methods used to determine the polymorphic content of the various products will be discussed in sections 3.1.4 - 3.1.6.

Table 3.2 Content of the various mebendazole containing tablets

Product	Mebendazole content (mg/tab)	Polymorph	Moisture content (% m/m)	Average tablet weight (mg)	Excipient weight (mg)	Filler
1	105.48 mg/tab	C	4.37	288.72	183.24	Microcrystalline cellulose
2	103.49 mg/tab	C	3.89	298.02	194.53	Microcrystalline cellulose
3	99.93 mg/tab	C with traces of A	2.50	302.26	202.33	α-Monohydrate –lactose
4	101.52 mg/tab	C	4.19	317.00	215.48	α-Monohydrate –lactose
5	100.44 mg/tab	C with traces of A	1.82	301.65	201.21	Other
6	100.96 mg/tab	C with traces of A	2.66	313.41	212.45	Microcrystalline cellulose
7	101.93 mg/tab	C	3.93	350.62	248.69	α-Monohydrate –lactose

As discussed in Chapter 1, moisture may induce polymorphic transitions, thus the moisture content of the tablets were determined using Karl Fischer (KF) titrations, to investigate the potential influence of the manufacturing process on the moisture content of the tablet and the potential impact thereof on the stability of the polymorph C in the tablets.

The moisture content of the tablets as determined by KF was in the following order: Product 1 > Product 4 > Product 7 > Product 2 > Product 6 > Product 3 > Product 5.

The amount of water associated with solids at a specific relative humidity and temperature depends on the chemical affinity of the solids present in the tablets, the nature of the solids (amorphous vs. crystalline) and the number of sites available for the moisture sorption (Dawoodbhai and Rhodes, 1989:1577-1600). Dawoodbhai and Rhodes (1989:1590) revealed that water soluble excipients (e.g. lactose or mannitol) showed crystal growth when exposed to increased

relative humidities and might thus influence the properties of other crystal entities present in a tablet containing the water soluble excipients. The total % water-soluble excipients (% m/m) in each product were determined. The initial mass of a tablet was determined (m_0). The tablet was then transferred into a glass beaker containing 100 ml distilled water and sonicated for 10 minutes to allow the water-soluble excipients to dissolve in the water. The solution was thereafter filtered and the dried mass of the water-insoluble matter (m_i) was determined. The total % water-soluble excipient (% WSE) in each product was calculated using the following equation:

$$\%\text{WSE} = \frac{m_0 - m_i}{m_0} x\,100$$

The % WSE, % mebendazole and % water insoluble excipients (% WISE) for the products are tabulated in table 3.3.

Table 3.3 % WSE, % mebendazole and % WISE per tablet for each product

Product	% WSE (% m/m)	% Mebendazole (% m/m)	% WISE (% m/m)
1	3.62	36.53	59.85
2	1.34	34.73	63.93
3	12.15	33.06	54.79
4	2.02	32.03	65.95
5	13.29	33.30	53.41
6	0.52	32.21	67.27
7	16.01	29.07	54.92

Product 7 contained the highest percentage water soluble excipients (16.01 % m/m) and Product 6 the lowest percentage (0.52% m/m). The potential effect of the % WSE will be discussed in the conclusion of this chapter.

The XRPD patterns of the products were investigated and it was found that Products 3, 4 and 7 had diffraction peaks communal to α-lactose monohydrate (figure 3.1). Lactose is usually used for direct compression or in the wet-granulation process during tablet manufacturing.

The XRPD patterns of Products 1, 2 and 6 revealed broad halo-shaped peaks between 13-18°2θ and 18-25°2θ characteristic to microcrystalline-cellulose (figure 3.2). Microcrystalline-cellulose is used in both wet-granulation and direct-compression processes. Due to confidentiality reasons the manufacturers were not able to provide information regarding procedures followed during manufacturing; whether wet-granulation or direct-compression was followed.

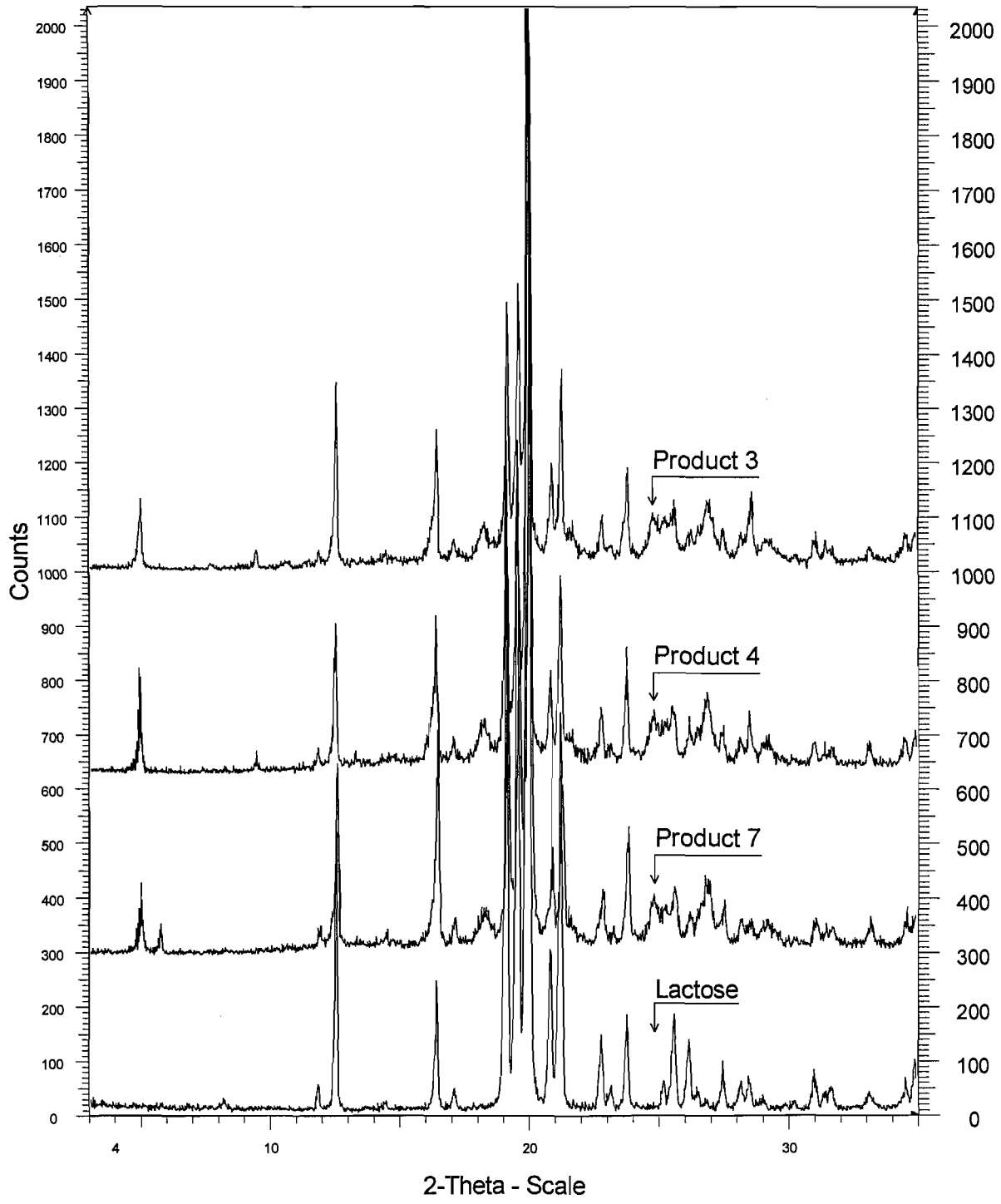


Figure 3.1 XRPD patterns of Product 3, Product 4, Product 7 and α-lactose monohydrate.

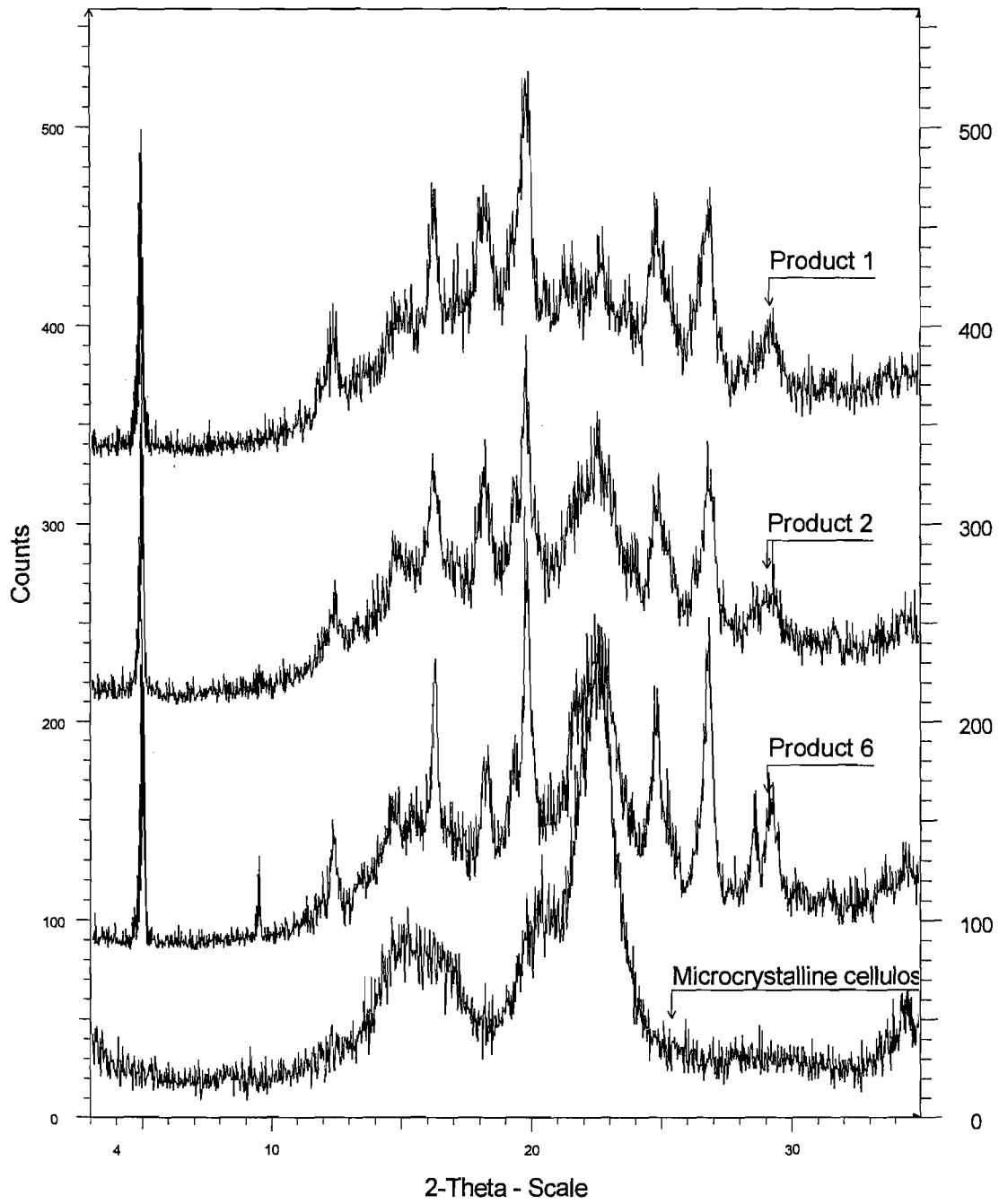


Figure 3.2 XRPD patterns of Product 1, Product 2, Product 6 and microcrystalline-cellulose.

3.1.2 Stability testing

The products were stored in controlled climate rooms at conditions in accordance to ICH stability guidelines (ICH, 2003) for intermediate and accelerated stability testing as indicated in table 3.4.

Table 3.4 Storage conditions of the mebendazole products

Climate-rooms	Temperature	Relative humidity (RH)
1	30°C	65%
2	40°C	75%

Tablets in the original commercial packaging of the mentioned products (table 3.1) were exposed to the conditions as mentioned in table 3.4 and the stability of the mebendazole polymorphs in the tablets was investigated at the following predetermined intervals: 0 months (initial), 1 month, 2 months, 3 months, 4 months, 5 months and 6 months. Product 2 was selected to be tested in duplicate, where the one set of the tablets was exposed to the mentioned conditions in the original packaging (will be referred to as Product 2), and the other set of tablets were removed from the original packaging and stored at the same conditions (will be referred to as Product 2A). See section 3.2.9 for more information.

XRPD and DRIFT-IR spectroscopy were used to evaluate the polymorphic composition of the mebendazole in the tablets. The dissolution profiles of the tablets were also evaluated at the mentioned intervals to determine the influence of polymorphic transitions on the dissolution behaviour of the tablets.

3.1.3 High pressure liquid chromatographic analysis (HPLC)

The mebendazole content of each product was determined using HPLC analysis. The mebendazole assays were performed according to the method described in USP 26 (2006), "Mebendazole Tablet" monograph under the following conditions:

Mobile phase: A mixture of methanol and 0.05 M mono-basic potassium phosphate (60:40), adjusted with 0.1 M phosphoric acid or 0.1 N sodium hydroxide to a final pH of 5.5.

Chromatographic system: A liquid chromatograph equipped with a 247 nm detector, a pre-column that contained packing L1, and a 3.9 mm x 30 cm analytical column that contained packing L1 and was maintained at about 30°C. Flow rate: 1.5 ml per minute. Injection volumes: 15 µl.

The amount of mebendazole (in mg) present in the tablets was calculated using the following formula:

$$mg/tablet = \frac{Au\ x\ mgStd\ x\ C\ x\ 1000\ x\ mgAtm}{As\ x\ 500\ x\ 100\ x\ mgSa}$$

Where:

Au	=	Area of sample solution peak
mgStd	=	Mass (mg) mebendazole reference standard used
C	=	Potency of mebendazole (%) reference standard
mgAtm	=	Average mass (mg) of tablets
As	=	Area of standard solution peak
mgSa	=	Mass (mg) of powdered tablets used

3.1.4 Infrared spectroscopy (DRIFT-IR)

The IR-spectra of the products were recorded on a Nicolet Nexus 470-FT-IR spectrometer as described in Chapter 2. Infrared spectroscopy has emerged as the preferred method to identify the mebendazole polymorphic forms (Liebenberg *et al.*, 1998:487 and Bunaciu *et al.*, 2002:647). Table 3.5 lists the characteristic frequencies (cm^{-1}) used to identify the mebendazole polymorphic forms in raw materials and tablets. The DRIFT-IR spectra of the three mebendazole polymorphs are depicted in figure 3.3.

Table 3.5 Characteristic IR frequencies (cm^{-1}) of C=O and N-H stretching used to identify the mebendazole polymorphs (Himmelreich *et al.*, 1977:123)

Polymorph	-NH	>C=O
A	3370 cm^{-1}	1730 cm^{-1}
B	3340 cm^{-1}	1700 cm^{-1}
C	3410 cm^{-1}	1720 cm^{-1}

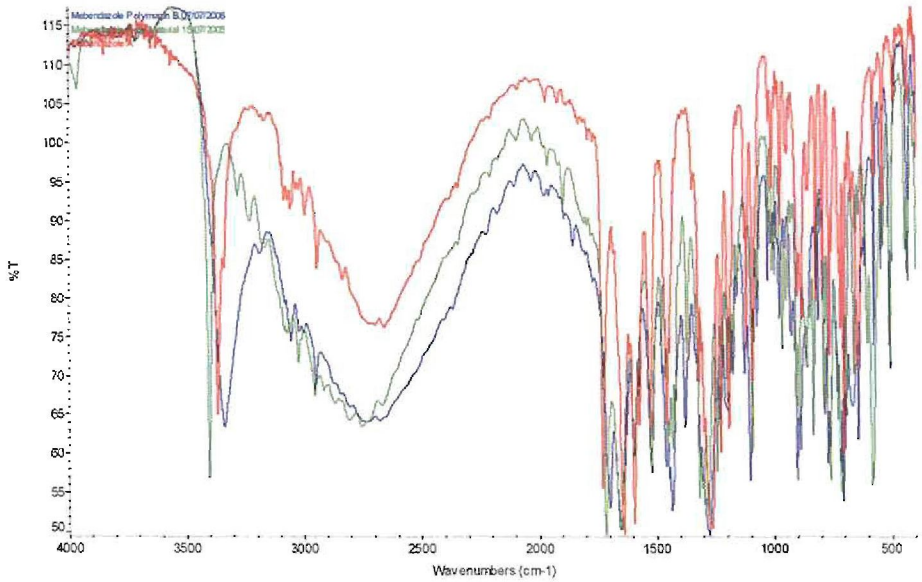


Figure 3.3 Overlay of the DRIFT-IR spectra of mebendazole polymorphs: A, B & C.

The areas of the characteristic absorption bands of the different polymorphs (table 3.5) in the DRIFT-IR spectra of the products were determined and used to calculate the relative polymorph A and polymorph C ratios present in the tablets at the various intervals (see section 3.3.1.2) and to investigate the rate of the polymorphic transition.

For example: Figure 3.4 illustrates an overlay with the DRIFT-IR spectra of Product 3 at months 0, 3 and 6. The polymorphic transition (polymorph C → polymorph A) observed in Product 3 (figure 3.4) revealed that the polymorph C

content decreased and the polymorph A content of the product increased during the 6 months when stored at 40°C & 75% RH.

The DRIFT-IR spectra of the products will be displayed and discussed in the results section.

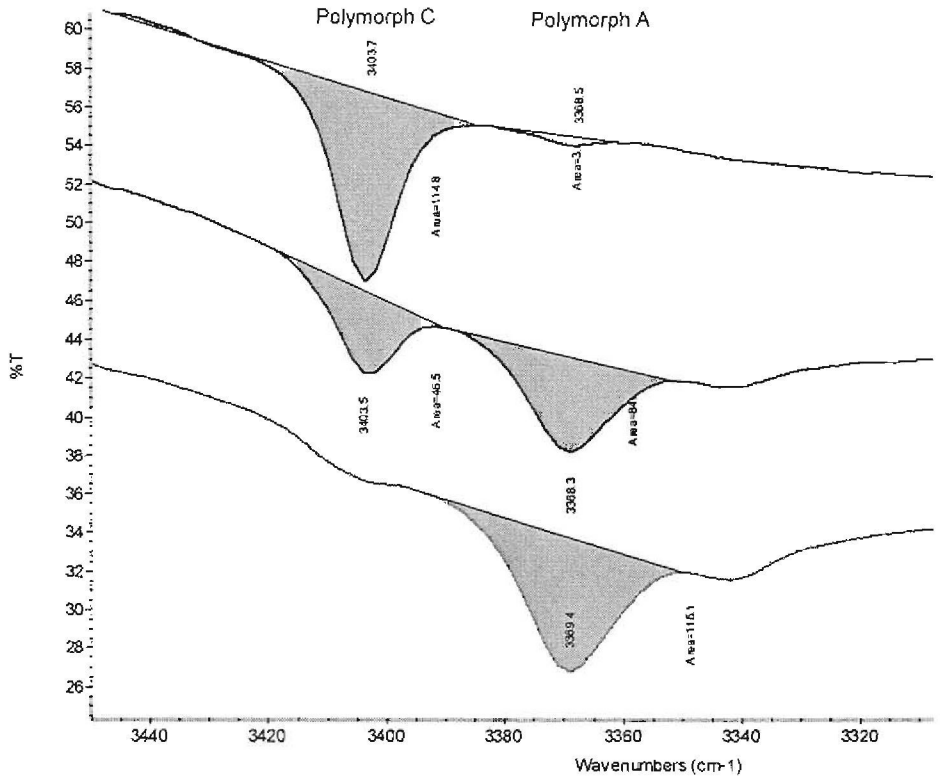


Figure 3.4 Characteristic stretching frequencies / bandwidths (cm^{-1}) and the areas thereof in the DRIFT-IR spectra of Product 3 at 0 (top), 3 (middle) and 6 (bottom) months stored at 40°C & 75% RH.

3.1.5 X-ray powder diffraction (XRPD)

From the XRPD results published by De Villiers *et al.* (2005:433) it was observed that the main XRPD peaks present for the mebendazole polymorph A, B and C were at the following positions: 7.67, 19.07 and 19.80 °2θ respectively. Closer inspection of the XRPD patterns of the mebendazole polymorphs (figure 3.5) indicated that the peaks in the 3–10 °2θ region, may also be regarded as

characteristic peak positions for polymorph B and C: 5.84 and 4.93 °2θ respectively (table 3.6).

Table 3.6 Characteristic peak positions in XRPD patterns of mebendazole polymorphs

Polymorph A		**Polymorph B**		**Polymorph C**	
7.67	7.67 *	5.84	19.07 *	4.93	19.80*

(* = 100% I/Io Peak according to De Villiers *et al.*, 2005:433)

The X-ray powder diffraction patterns of the products were recorded at room temperature using a Bruker D8 Advance diffractometer (Bruker, Germany) as described in Chapter 2. The XRPD patterns of the products were compared to the peak position and relative intensities of the characteristic peaks in the XRPD patterns of the mebendazole polymorphs (figure 3.5 and table 3.6). The intensities of the characteristic peaks (figure 3.6) were used to calculate the relative polymorph A and polymorph C ratios present in the tablets during the various intervals (see section 3.3.1.1) of the stability testing. The XRPD observations for each product will be discussed in the sections to follow.

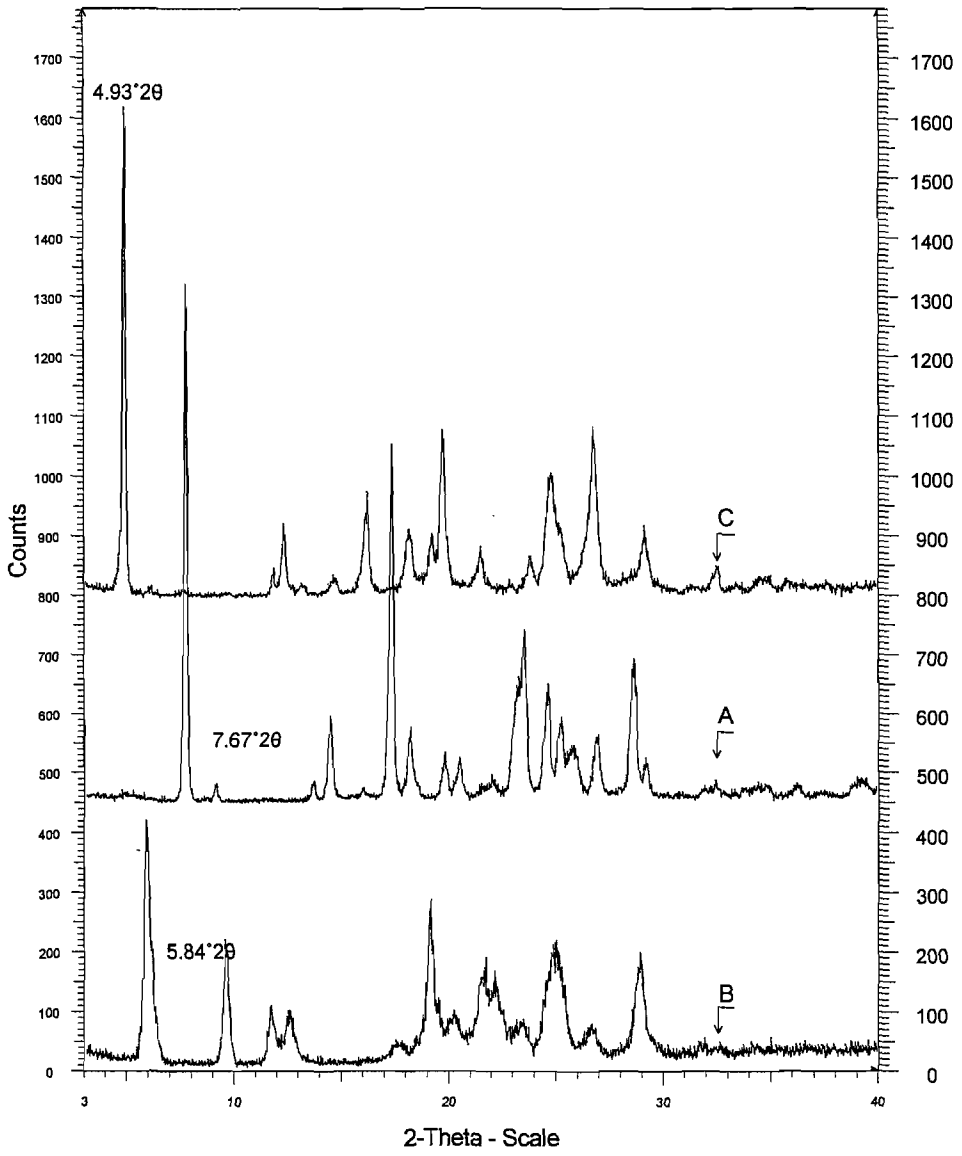


Figure 3.5 Overlay of the XRPD patterns of mebendazole polymorphs: A, B & C with the characteristic peak positions indicated.

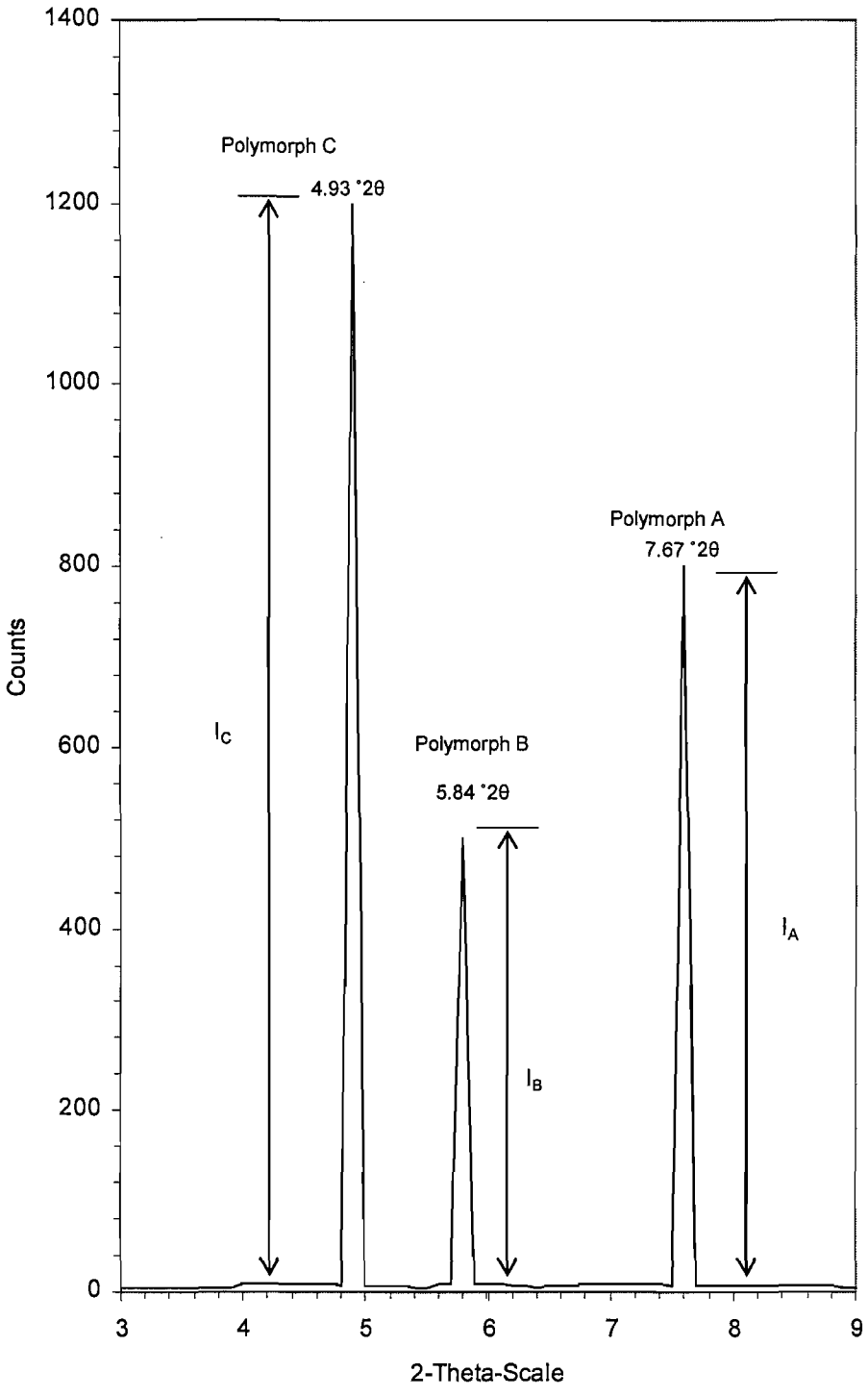


Figure 3.6 Theoretical XRPD pattern of a mixture of mebendazole polymorphs: A, B & C and the intensities of the characteristic peaks (I_A, I_B and I_C) indicated.

3.1.6 Dissolution testing

Swanepoel *et al.* (2003:345) suggested changes to be made to the USP dissolution medium to be able to distinguish between the active and favoured (polymorph C) and non-favoured and inactive mebendazole polymorphs (polymorphs B and A). It was suggested that SLS be excluded from the USP dissolution medium (0.1 N HCl & 1% SLS). When SLS was removed from the dissolution medium, the percentage dissolved versus time profiles changed and indicated that the dissolution rate to be: C > B > A (figure 3.7). Dissolution studies were therefore conducted on the tablets according to the USP 26 (2006) specifications for mebendazole tablets, without adding SLS to the dissolution medium.

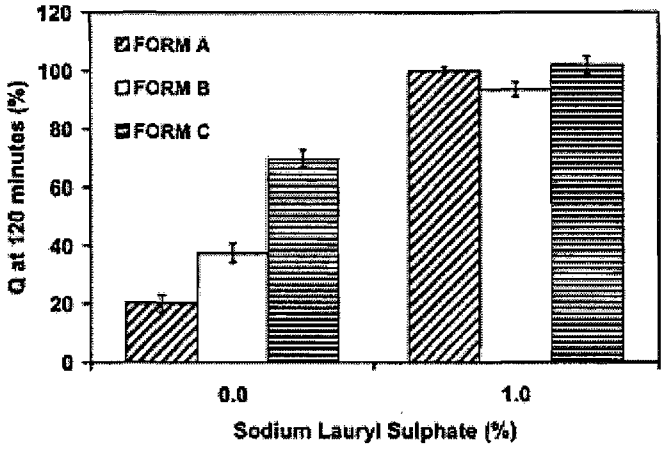


Figure 3.7 Effect of 1 % SLS in the dissolution medium on Q at 120 min for mebendazole polymorphs (Swanepoel *et al.*, 2003:348).

The dissolution conditions were as follows:

Apparatus : USP paddle assembly (Apparatus 2)
Medium : 900 ml 0.1 N HCl preheated and maintained at 37°C
Paddle speed : 75 rpm
Time : 120 minutes
Filters : 0.45 micron filters

The amount of mebendazole dissoluted at the various intervals (i.e.: 7.5, 15, 30, 60, 90 and 120 minutes) was calculated from the uv-absorbance of the suitably diluted samples at 254 nm.

3.1.7 Calculations

Dissolution profiles of the percentage mebendazole dissolved *versus* time were plotted and compared. The similarities between the dissolution profiles at the various intervals of a product relative to that of the same product at 0 months were calculated, using the equation described by Moore *et al.* (1996:64-67):

$$f2 = 50 \bullet \log\left(\left[1+\left(\frac{1}{n}\right)\sum_{t=1}^{n} wt(Rt-Tt)^2\right]^{-0.5} \bullet 100\right)$$

Where:

n	=	Number of dissolution time points.
Rt	=	Reference dissolution value, at time t.
Tt	=	Test dissolution value, at time t.
wt	=	Optional weighing factor.

The value of f2 is 100 when the test and reference mean profiles are identical. Values of f2 between 50 and 100 indicate similarity of the two dissolution profiles. Microsoft® Office Excel 2003 software was used for all calculations and graphs plotted.

Several models have been developed to account for the polymorphic transitions observed in solid-state studies. All of these methods assume a certain geometry and rely on some consistency of the system as the process proceeds. The kinetics of the polymorphic transition (polymorph C → polymorph A) observed in the tablets was investigated using the kinetic models summarised in table 3.7.

Table 3.7 Equations used during a kinetic study (Agbada *et al.*, 1994:33-40)

Rate controlling process and equation describing the process	
1. Prout Tompkins equation $\ln\left(\frac{x}{1-x}\right) = kt + c$	7. Two-dimensional diffusion equation $(1-x)\bullet\ln(1-x)+x = kt$
2. Avrami Efofe'ev equations $[-\ln(1-x)]^n = kt$ n = ¼ n = 1/3 n = 1/2 n = 2/3 n = 1	8. Three-dimensional diffusion equation $1-\frac{2}{3}x-(1-x)^{\frac{2}{3}} = kt$
3. One-dimensional advancement of a phase boundary equation $1-x = kt$	9. Power law equation $x^n = kt$ n = ¼ n = 1/3 n = ½ n = 1
4. Two-dimensional advancement of a phase boundary equation $1-(1-x)^{1/2} = kt$	10. Equations based on the concept of the order of the reaction (a) Zero order reaction $1-x = kt$
5. Three-dimensional advancement of a phase boundary equation $1-(1-x)^{1/3} = kt$	(b) First order reaction $\ln(x) = kt$
6. One-dimensional diffusion equation $x^2 = kt$	(c) Second order reaction $\frac{1}{(1-x)} = kt$

3.2 Results

From the results summarised in table 3.2 it can be concluded that only four of the seven commercially available mebendazole products contained primarily mebendazole polymorph C; three polymorph C with traces of polymorph A.

Due to a limited number of available tablets (same batch from the same supplier) the polymorphic stability of Product 4 was only evaluated over a period of 5 months.

The stability of the products at accelerated stability testing conditions (30°C & 65% RH and 40°C & 75% RH respectively) was investigated and will be discussed in the sections to follow. Tables 3.8 and 3.9 summarises the polymorphic content present in the products at the various intervals derived from the DRIFT-IR and XRPD results obtained.

Table 3.8 Mebendazole polymorphic forms present in commercially available products during the 6 month stability study derived from DRIFT-IR data

Product	Time (months)	30°C & 65% RH			40°C & 75% RH		
		-NH	>C=O	Polymorph Content	-NH	>C=O	Polymorph Content
1	0	3403	1717	C	3403	1717	C
	1	3403	1716	C	3403	1716	C
	2	3403	1716	C	3403 3368	1716 1732	C with traces of A
	3	3403	1716	C	3403 3368	1717 1732	C with traces of A
	4	3403	1716	C	3403 3368	1717 1732	Mixture of C & A
	5	3403	1717	C	3403 3368	1717 1732	Mixture of C & A
	6	3403 3369*	1716 1733*	C with traces of A	3403 3368 3342*	1717 1732 1701*	Mixture of C & A with traces of B

Table 3.8 continued...

Product	Time (months)	30°C & 65% RH			40°C & 75% RH		
		-NH	>C=O	Polymorph Content	-NH	>C=O	Polymorph Content
2	0	3403	1716	C	3403	1716	C
	1	3403	1717	C	3403	1716	C
	2	3403	1716	C	3403	1716	C
	3	3403	1716	C	3403	1716	C with traces of A
	4	3403	1716	C	3403 3369*	1716 1731*	Mixture of C & A
	5	3403	1716	C	3403 3369	1717 1731*	Mixture of C & A
	6	3403	1716	C	3403 3369	1717 1731	Mixture of C & A
3	0	3403 3369*	1716	C with traces of A	3403 3369*	1716	C with traces of A
	1	3403 3369*	1716	C with traces of A	3403 3369	1716	C with traces of A
	2	3403 3369*	1716	C with traces of A	3403 3369	1717 1731	Mixture of C & A
	3	3403 3369	1716	Mixture of C & A	3403 3369	1717 1732	Mixture of C & A
	4	3403 3369	1716	Mixture of C & A	- 3369	- 1732	Mixture of C & A
	5	3403 3369	1716	Mixture of C & A	- 3368	- 1732	Mixture of C & A
	6	3403 3369	1716	Mixture of C & A	- 3369	- 1731	A
4	0	3403	1716	C	3403	1716	C
	1	3403	1716	C	3403	1716	C
	2	3403	1716	C	3403	1716	C
	3	3403	1716	C	3403 3369*	1716 -	C with traces of A
	4	3403	1716	C	3403 3369	1716 1731	Mixture of C & A
	5	3403	1716	C	3403 3368	1716 1731	Mixture of C & A
5	0	3403 3367*	1716	C with traces of A	3404 3366*	1717 -	C with traces of A
	1	3403 3367*	1716	C with traces of A	3404 3366*	1716 1732*	C with traces of A
	2	3403 3367*	1716	C with traces of A	3404 3366*	1717 1732*	C with traces of A
	3	3403 3367*	1716	C with traces of A	3404 3366*	1716 17328	C with traces of A
	4	3403 3367*	1716	C with traces of A	3404 3366*	1716 1732*	C with traces of A
	5	3403 3367*	1716	C with traces of A	3404 3366*	1716 1732*	C with traces of A
	6	3403 3367*	1716	C with traces of A	3404 3366*	1716 1732*	C with traces of A

Table 3.8 continued...

Product	Time (months)	30°C & 65% RH			40°C & 75% RH		
		-NH	>C=O	Polymorph Content	-NH	>C=O	Polymorph Content
6	0	3404 3367*	1717 -	C with traces of A	3404 3368*	1717 -	C with traces of A
	1	3404 3367*	1716 -	C with traces of A	3404 3368*	1716 -	C with traces of A
	2	3404 3367*	1717 -	C with traces of A	3404 3368*	1716 -	C with traces of A
	3	3404 3367*	1716 -	C with traces of A	3404 3368*	1716 -	C with traces of A
	4	3404 3367	1716 -	C with traces of A	3404 3368	1716 1732*	C with traces of A
	5	3404 3367	1716 -	C with traces of A	3404 3368	1716 1732*	C with traces of A
	6	3404 3367	1716 -	C with traces of A	3404 3368	1716 1732*	C with traces of A
7	0	3403	1717	C	3403	1717	C
	1	3403	1717	C	3403	1717	C
	2	3403	1717	C	3403	1717	C
	3	3403	1717	C	3403	1717	C
	4	3403	1717	C	3403	1717	C
	5	3403	1717	C	3403	1717	C
	6	3403	1717	C	3403	1717	C

* Small traces detected = peak shoulder appeared

Table 3.9 Mebendazole polymorphic forms present in commercially available products during the 6 month stability study derived from XRPD data

Product	Time (months)	30°C & 65% RH			40°C & 75% RH		
		A (°2θ)	C (°2θ)	Polymorph Content	A (°2θ)	C (°2θ)	Polymorph Content
1	0	-	4.89	C	-	4.89	C
	1	-	4.88	C	-	4.87	C
	2	-	4.95	C	-	5.03	C with traces of A
	3	-	4.94	C	-	4.95	C with traces of A
	4	-	4.94	C	7.71	4.93	Mixture of C & A
	5	-	4.90	C	7.66	4.91	Mixture of C & A
	6	7.68	4.81	C with traces of A	7.69	4.89	Mixture of C & A

Table 3.9 continued...

Product	Time (months)	30°C & 65% RH			40°C & 75% RH		
		A (°2θ)	C (°2θ)	Polymorph Content	A (°2θ)	C (°2θ)	Polymorph Content
2	0	-	4.92	C	-	4.92	C
	1	-	4.93	C	-	4.90	C
	2	-	4.94	C	-	4.96	C
	3	-	4.89	C	7.66*	4.87	C with traces of A
	4	-	4.86	C	7.62	4.90	Mixture of C & A
	5	-	4.84	C	7.63	4.90	Mixture of C & A
	6	-	4.83	C	7.64	4.88	Mixture of C & A
3	0	7.69	4.95	C with traces of A	7.69	4.95	C with traces of A
	1	7.70	4.93	C with traces of A	7.70	4.93	C with traces of A
	2	7.70	4.94	C with traces of A	7.72	4.95	Mixture of C & A
	3	7.68	4.93	Mixture of C & A	7.68	4.92	Mixture of C & A
	4	7.65	4.87	Mixture of C & A	7.70	4.94	Mixture of C & A
	5	7.68	4.90	Mixture of C & A	7.64	4.86	Mixture of C & A
	6	7.67	4.89	Mixture of C & A	7.64	4.86	A
4	0	-	4.89	C	-	4.89	C
	1	-	4.94	C	-	4.83	C
	2	-	4.93	C	-	4.97	C
	3	-	4.91	C	7.63*	5.02	C with traces of A
	4	-	4.92	C	7.63	4.88	Mixture of C & A
	5	-	4.87	C	7.69	4.94	Mixture of C & A
5	0	-	4.91	C	-	4.91	C
	1	-	4.96	C	-	4.90	C
	2	-	4.94	C	-	49.2	C
	3	-	4.95	C	-	4.93	C
	4	7.58	4.90	C with traces of A	-	4.92	C
	5	-	4.88	C	-	4.89	C
	6	-	4.88	C	-	4.90	C

Table 3.9 continued...

Product	Time (months)	30°C & 65% RH			40°C & 75% RH		
		A (°2θ)	C (°2θ)	Polymorph Content	A (°2θ)	C (°2θ)	Polymorph Content
6	0	-	4.94	C	-	4.94	C
	1	-	4.89	C	-	4.91	C
	2	-	5.03	C	-	4.91	C
	3	-	4.95	C	7.68	4.92	C with traces of A
	4	-	4.92	C	-	4.92	C
	5	7.67*	4.89	C with traces of A	7.60	4.91	C with traces of A
	6	7.62*	4.89	C with traces of A	7.59	4.85	C with traces of A
7	0	-	4.94	C	-	4.94	C
	1	-	4.90	C	-	4.88	C
	2	-	4.94	C	-	4.89	C
	3	-	4.92	C	-	4.91	C
	4	-	4.90	C	-	4.91	C
	5	-	4.92	C	-	4.88	C
	6	-	4.83	C	-	4.88	C

* Small traces detected = peak shoulder appeared

3.2.1 Polymorphic stability of mebendazole in Product 1

The IR-spectrum of Product 1 is shown in figure 3.8. The IR-spectrum showed strong peaks at 3403 and 1717 cm^{-1}, which are distinctive infrared absorption peaks of mebendazole polymorph C.

The DRIFT-IR spectra of the tablets remained relatively unchanged for the period of the stability evaluation i.e. no significant peak appearances or disappearances were observed in the –NH stretch or the >C=O band region. The mebendazole crystal modification (i.e. polymorph C) remained unaffected during the first 4 months of the study when exposed to 30°C & 65% RH (figure 3.8). The appearance of a shoulder-peak at 1733 cm^{-1} and the (insignificantly) small peak at 3369 cm^{-1} after six months suggested that a very small fraction of the

polymorph C underwent a polymorphic transition producing traces of polymorph A in the tablets (polymorph C >>>> polymorph A).

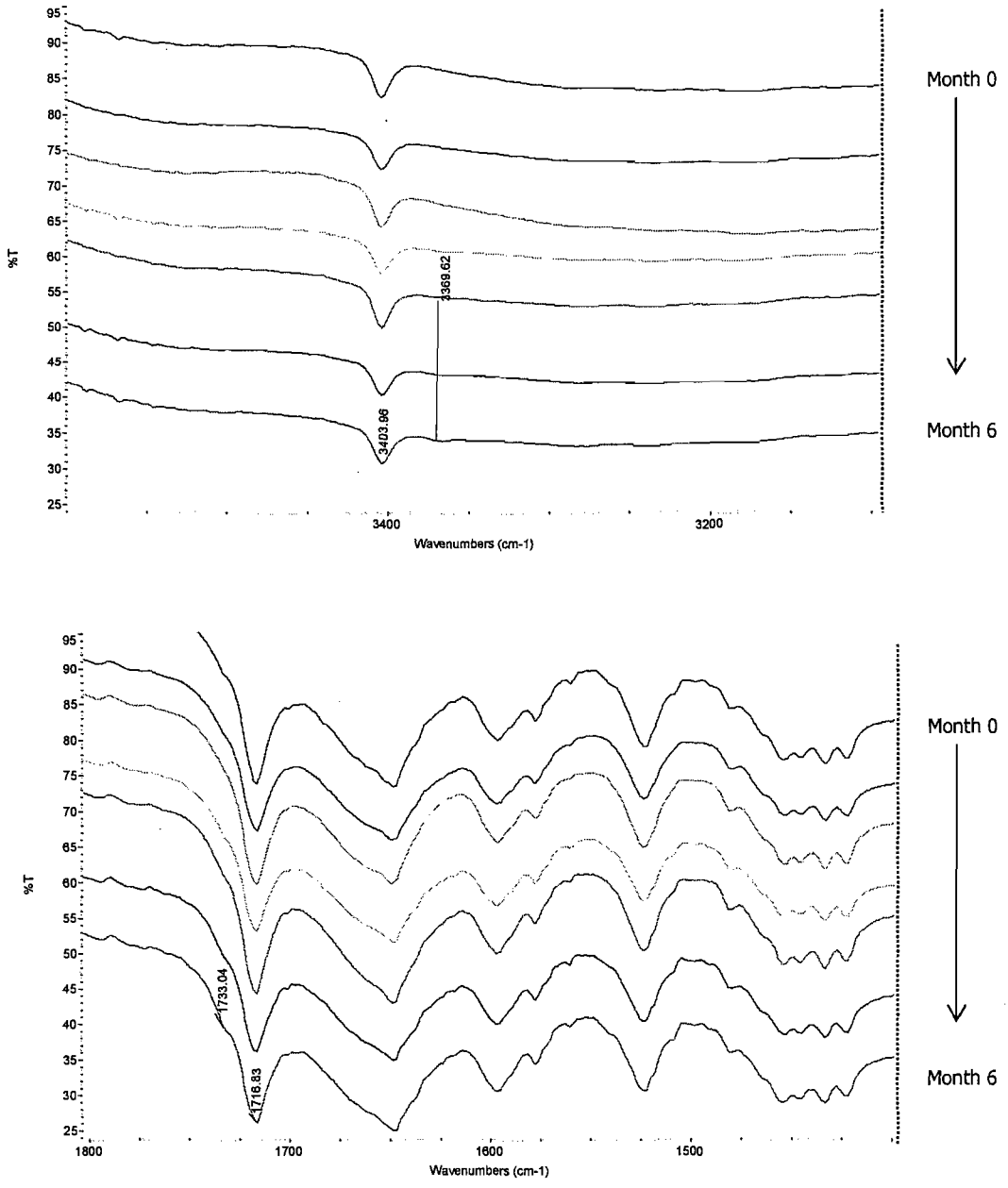


Figure 3.8 IR spectra (superimposed) of the powdered tablets of Product 1 over a period of six months – stored at 30°C & 65% RH, indicating small differences in the main absorptions at the –NH stretch and the >C=O band, after 6 months only.

The superimposed DRIFT-IR spectra of Product 1, stored at 40°C & 75% RH are displayed in figure 3.9. The appearance of absorption peaks at 3368 cm^{-1} at months 2–6, suggested that a polymorphic transition had occurred, and that the samples contained mebendazole polymorph C with small traces of polymorph A. The intensity of the mentioned peak increased with time, which indicated that the fraction of mebendazole polymorph A increased.

In the DRIFT-IR spectrum of the sample during month 6, very small peaks were detected at 3341 cm^{-1} and 1700 cm^{-1}, which are characteristic peaks of polymorph B. Thus it seemed as if the sample (at 6 months) contained primarily polymorph C and polymorph A and possible traces of polymorph B (polymorph C >>>> polymorph A >> polymorph B). The appearance of the mebendazole polymorph B traces will be discussed in Chapter 4.

The XRPD patterns of Product 1 samples at the various intervals are shown in figure 3.10. The characteristic peak angles (°2θ) presented in table 3.9 confirmed that the initial tablets contained mebendazole polymorphic form C, due to the presence of the strong peak at 4.93±0.1°2θ.

The absence of peaks at 7.67±0.1°2θ in the x-ray powder diffraction patterns (figure 3.10) during the first 5 months indicated that no significant polymorphic transformation occurred. A peak with a very weak intensity ($I/I_0 < 10$) at 7.68 °2θ indicated that a mixture of polymorphs (polymorph C >>>> polymorph A) was present in the samples stored at 30°C & 65% RH after 6 months.

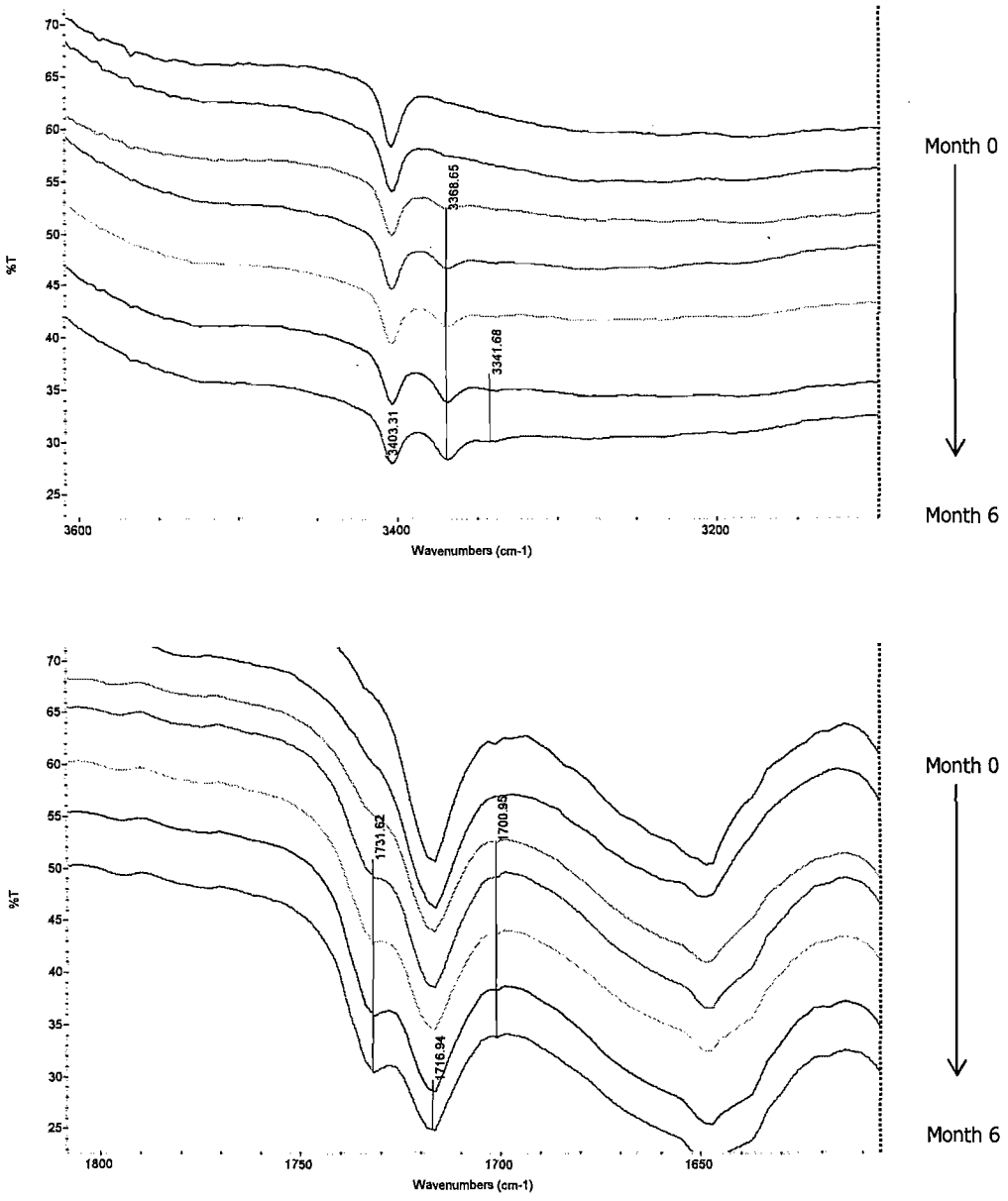


Figure 3.9 IR spectra (superimposed) of the powdered tablets of Product 1 over a period of six months – stored at 40°C & 75% RH, indicating differences in the main absorptions at the –NH stretch and the >C=O band.

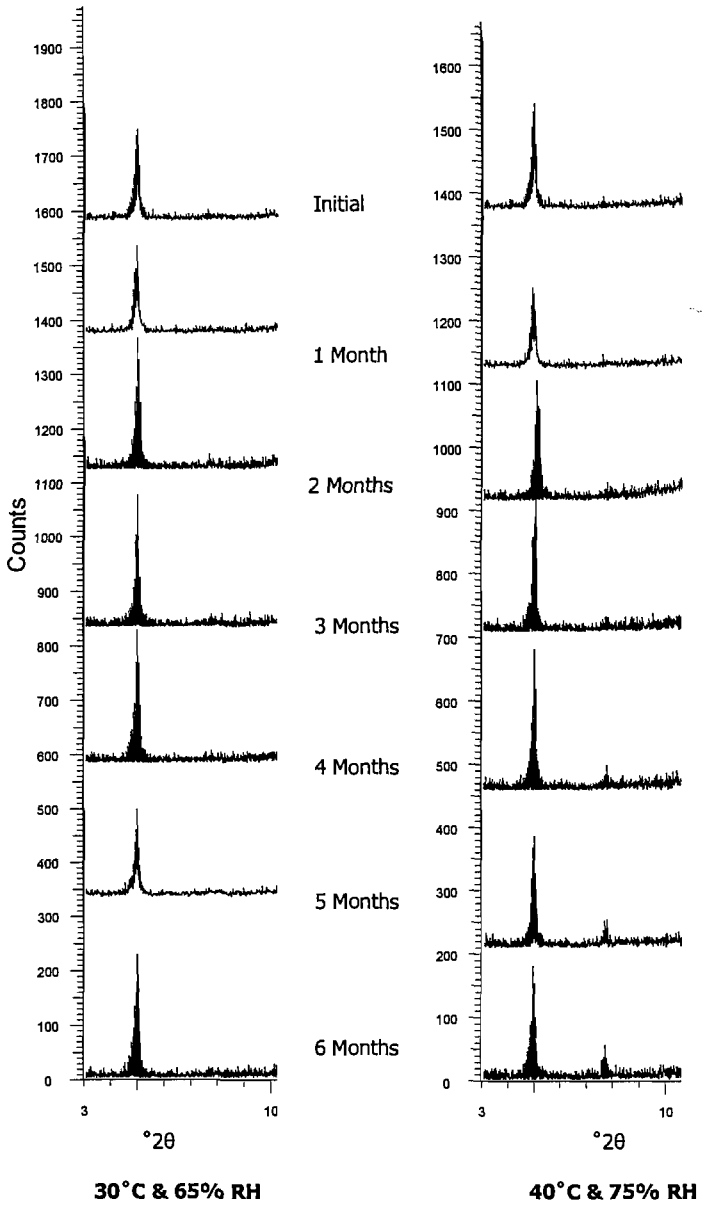


Figure 3.10 XRPD patterns of Product 1 over a period of six months – stored at 30°C & 65% RH and 40°C & 75% RH.

The XRPD patterns of Product 1 exposed to 40°C & 75% RH (figure 3.10) remained relatively unchanged during the first 3 months of the study. The diffraction peak at 19.80±0.1°2θ was not clearly detectable during month 2 and month 6 due to the amorphous character of the tablet contents (tablet excipients). Thus it should be emphasized that the detection of mebendazole

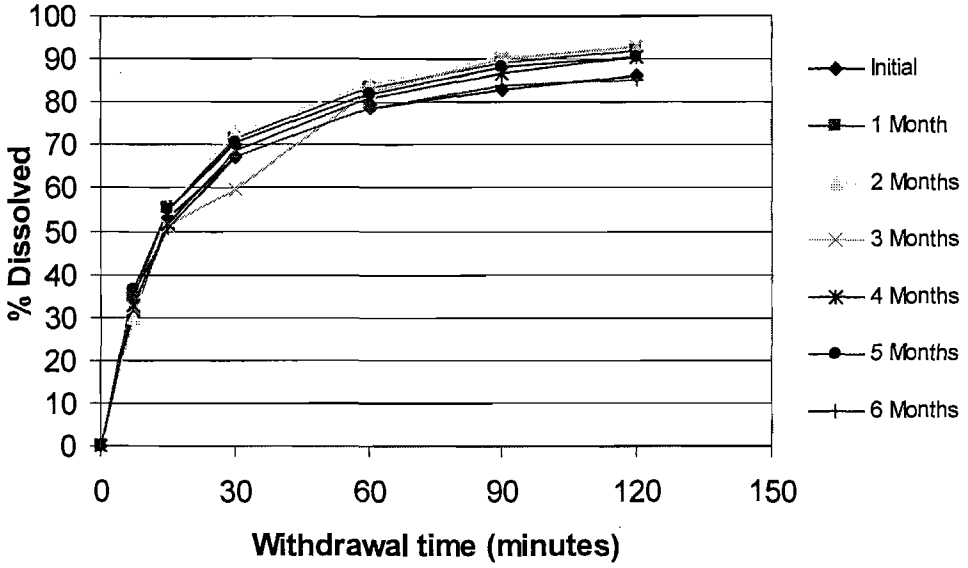
polymorphs using XRPD data in tablets might not be as sensitive compared to DRIFT-IR due to the interference of tablet excipients.

The appearance of the peak at 7.67±0.1°2θ during the 4-6 months period, confirmed the presence of mebendazole polymorph A in the tablets as observed in the DRIFT-IR spectra. No significant traces of mebendazole polymorph B were detected in the XRPD pattern due to the small traces thereof and the poor crystalline properties of polymorph B (Chapter 4 – section 4.1.2).

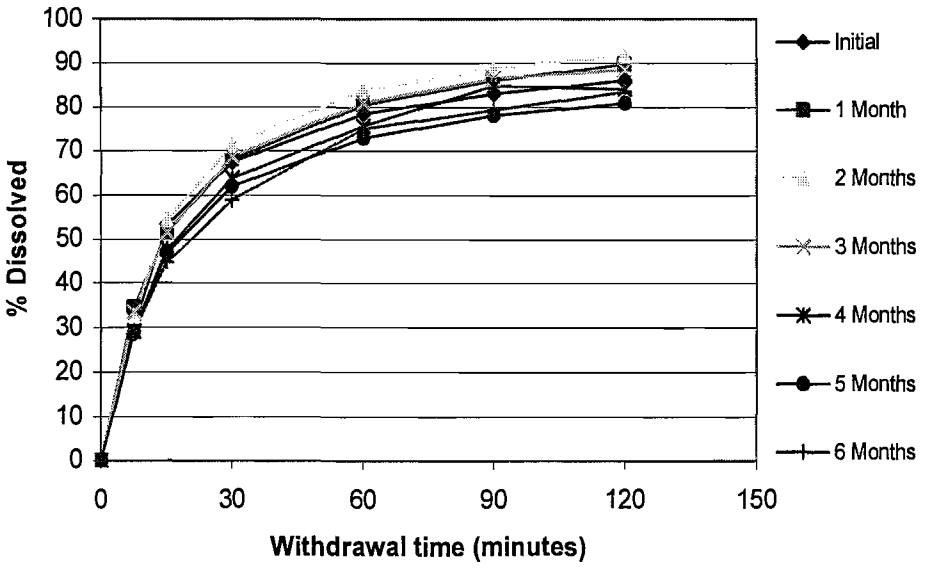
The influence of the mebendazole polymorphic transitions on the dissolution behaviour of the tablets was investigated (figure 3.11).

Similarities between the various dissolution curves (at time=t) and that of the initially procured product (at time = 0) were calculated using the equation described by Moore *et al.* (1996:64-67). Table 3.10 indicates the f_2-values calculated.

The dissolution profiles of the tablets stored over the 6 months period at 30°C & 65% RH were comparable ($100 > f_2$ values > 50) to the dissolution profile of the initially procured tablets (age = 0 months). The traces of polymorph A detected in the tablets stored at 30°C & 65% RH (after 6 months) did not have a profound influence on the dissolution behaviour of the product.



(A)



(B)

Figure 3.11 Dissolution profiles (in 0.1 M HCl) of Product 1 when stored at (a) 30°C & 65% RH and (b) 40°C & 75% RH for a period of six months.

Table 3.10 Similarity factors (f_2-values) of dissolution profiles of Product 1 when stored at 30°C & 65% RH and 40°C & 75% RH for a period of six months (in 0.1 M HCl)

Time	30°C & 65% RH	40°C & 75% RH
1 Month	66.25	75.89
2 Months	62.97	67.23
3 Months	62.96	77.93
4 Months	75.36	74.07
5 Months	67.82	64.62
6 Months	79.65	62.93

The dissolution profiles of the tablets stored for the duration of the study (6 months) at 40°C & 75% RH were comparable (100 > f_2 values > 50) to the dissolution profile of the initially procured tablets (age = 0 months). The solubility of mebendazole polymorphs in 0.1 N HCl has been reported to be in the order: B > C > A (Swanepoel *et al.,* 2003:347). The presence of mebendazole polymorph B traces, and its relatively high solubility in 0.1 M HCl, could thus have compensated for the traces of poorly soluble polymorph A in the tablets, thus explaining why no significant differences were observed in the dissolution profiles of Product 1 during the 6 month stability study testing despite the polymorphic transitions that occurred.

3.2.1.1 Summary of the polymorphic stability of Product 1

The XRPD and DRIFT-IR studies performed on the tablets revealed that the tablets initially procured, contained polymorph C. This study indicated that Product 1 revealed polymorphic transitions when exposed to increased temperatures and relative humidities. The rate and extend to which the transitions occurred seemed to be higher at 40°C & 75% RH. The effectiveness of DRIFT-IR spectroscopy in the detection of mebendazole polymorphs in tablets was once again highlighted.

3.2.2 Polymorphic stability of mebendazole in Product 2

The main IR absorption peaks and their corresponding wavenumbers (cm^{-1}) of Product 2 are listed in table 3.8. From table 3.8 it can be concluded that the initial product contained mebendazole polymorph C. The IR spectrum of the tablets stored at 30°C & 65% RH remained unchanged during the 6 months of stability evaluation (see figure 3.12), which indicated no polymorphic changes.

The main DRIFT-IR absorption peaks of mebendazole and their corresponding wavenumbers (cm^{-1}) present in Product 2 when stored at 40°C & 75% RH are listed in table 3.8. An overlay of the DRIFT-IR spectra indicating the –NH and >C=O stretch regions is depicted in figure 3.13. The intensity of the shoulders present at 3368 and 1731 cm^{-1} (distinctive to polymorph A) increased significantly and the absorption peaks at 3403 and 1716 cm^{-1} (distinctive of polymorph C) decreased slightly as a function of time, which indicated that a polymorph transition occurred (figure 3.13).

The appearance and progressive increasing of the intensity of the characteristic absorption bands of mebendazole polymorph A at 3369 cm^{-1} and 1716 cm^{-1} suggested that the samples contained polymorph C and traces of polymorph A after 3 months. A mixture of polymorph A and C was detected in the tablets after five months of storage at 40°C & 75% RH.

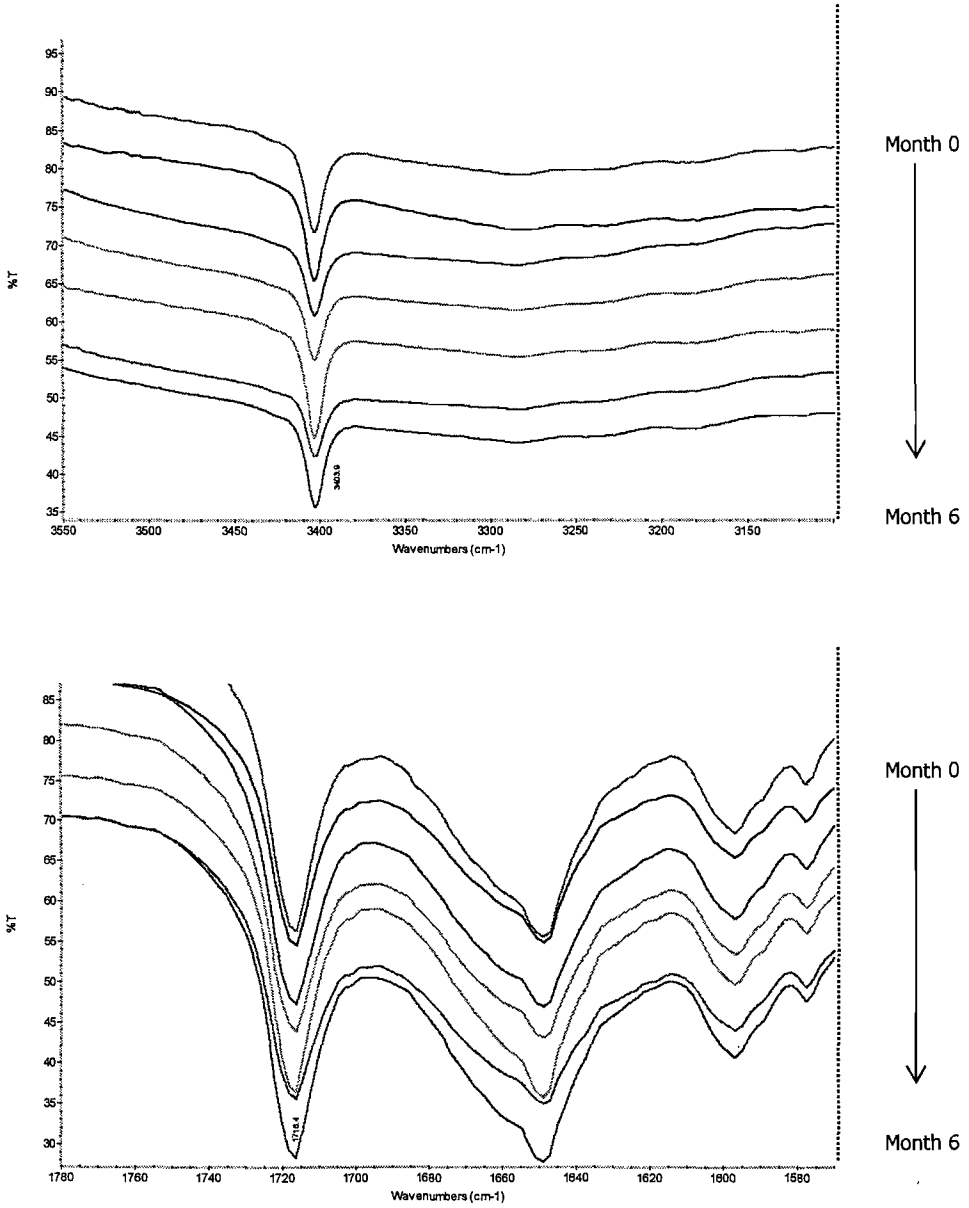


Figure 3.12 IR spectra (superimposed) of the powdered tablets of Product 2 over a period of six months – stored at 30°C & 65% RH, indicating no changes in the main absorptions at the –NH stretch and the >C=O band.

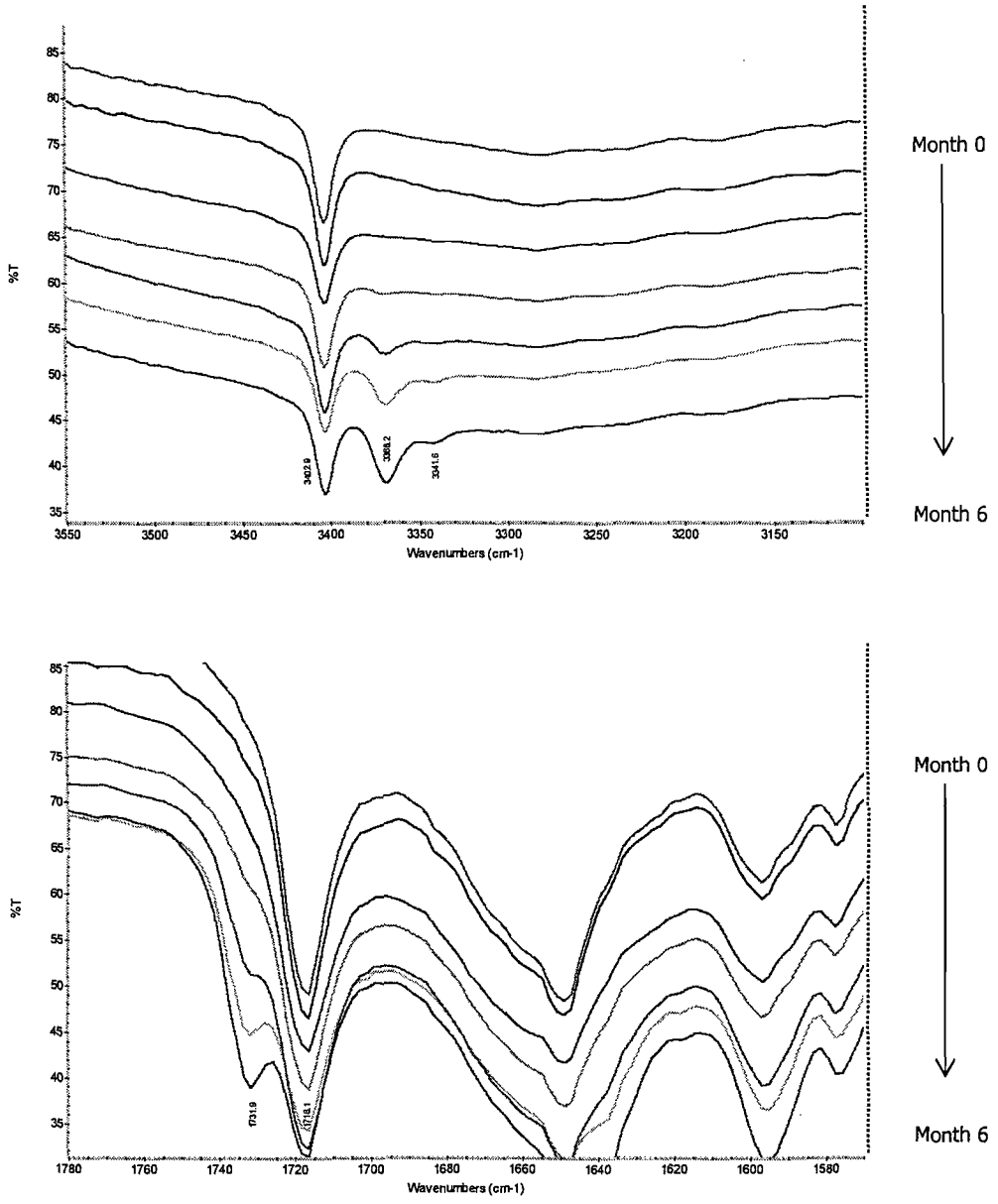


Figure 3.13 IR spectra (superimposed) of the powdered tablets of Product 2 over a period of six months – stored at 40°C & 75% RH, indicating changes in the main absorptions at the –NH stretch and the >C=O band.

The XRPD diffractograms of Product 2 when exposed to 30°C & 65% RH and 40°C & 75% RH for a period of 6 months are illustrated in figure 3.14.

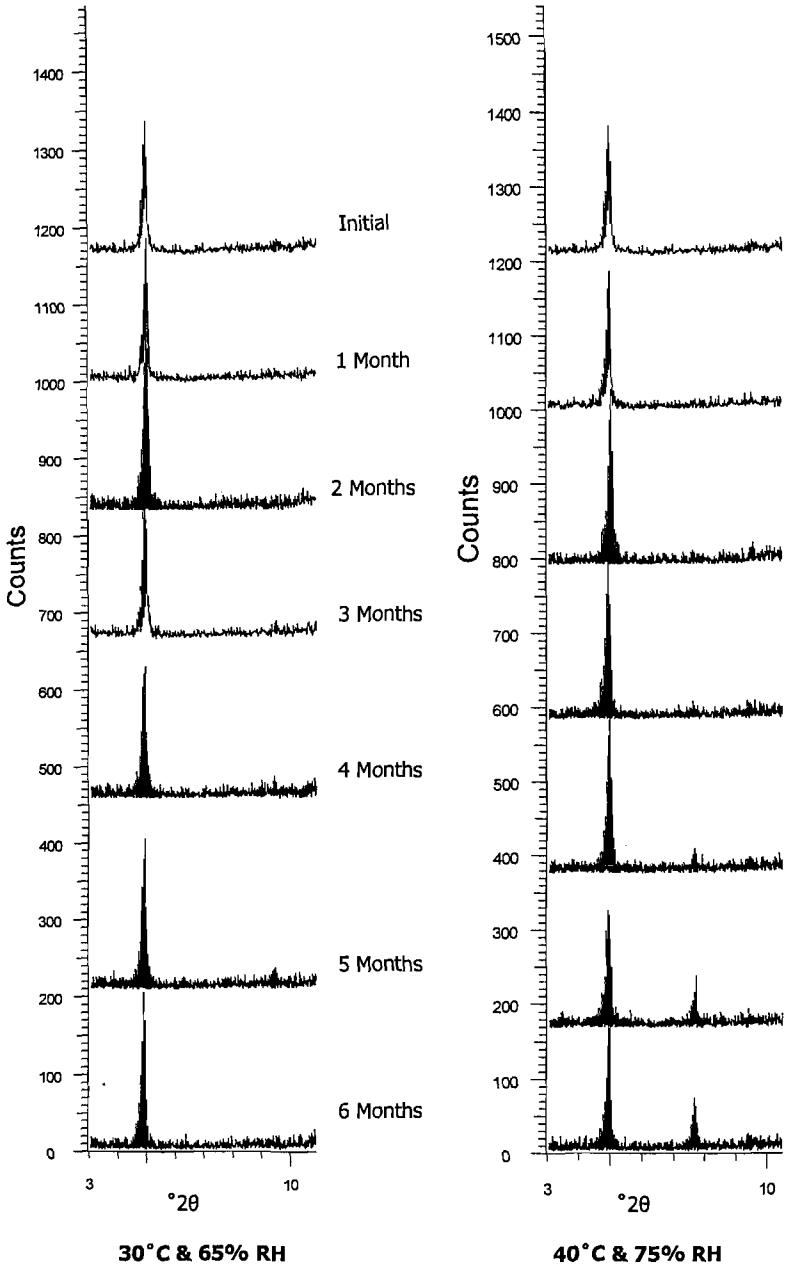
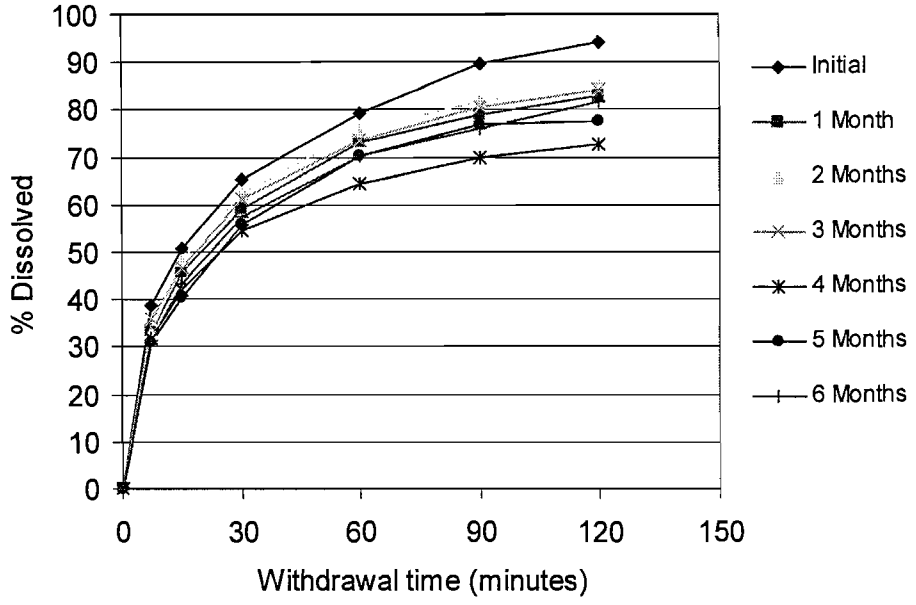


Figure 3.14 XRPD patterns of Product 2 over a period of six months – stored at 30°C & 65% RH and 40°C & 75% RH.

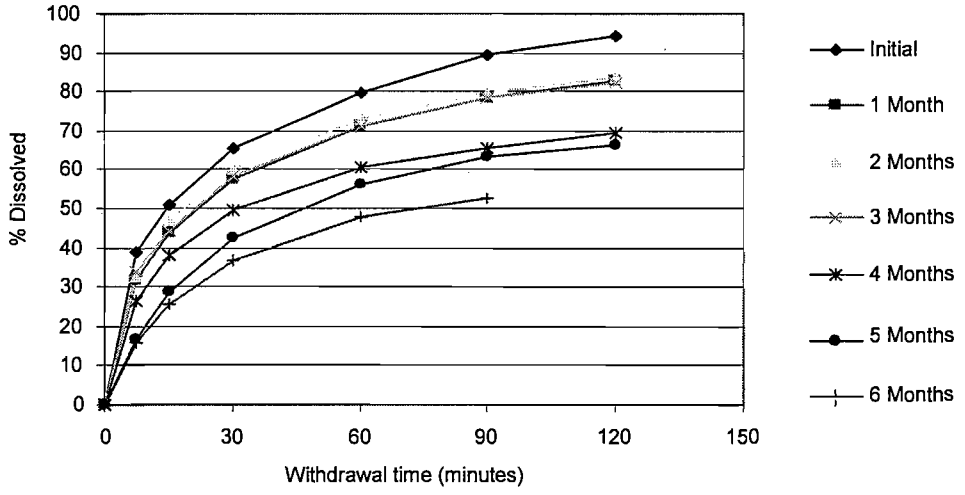
The characteristic polymorph C peak at 4.83°2θ was detected during the six months for Product 2 exposed to 30°C & 65% RH (figure 3.14). The absence of any other peaks in the 3-10°2θ region supported the DRIFT-IR observations that

polymorph C present in the tablets did not undergo polymorphic transitions. However, the XRPD patterns of the samples stored at 40°C & 75% RH showed weak diffraction peaks present at 7.67±0.1°2θ after 3 months (table 3.9), which confirmed that small traces of mebendazole polymorph A were present in the tablets. The intensities of the mentioned Bragg peaks notably increased as a function of time (figure 3.14) which confirmed the polymorphic transformation as observed using DRIFT-IR spectroscopy. An evident decrease in the intensity of the diffraction peaks at 4.93°2θ were visible from months 4 – 6, which indicated that the mebendazole polymorph C fraction had transformed into mebendazole polymorph A.

Similarities between the various dissolution curves (at time = t) and that of the initially procured product (at time = 0) were calculated using the equation described by Moore *et al.* (1996:64-67). In table 3.11 the calculated f_2-values of Product 2 are shown.



(A)



(B)

Figure 3.15 Dissolution profiles (in 0.1 M HCl) of Product 2 when stored at (a) 30°C & 65% RH and (b) 40°C & 75% RH for a period of six months.

Table 3.11 Similarity factors (f_2-values) of dissolution profiles of Product 2 tablets when stored at 30°C & 65% RH and 40°C & 75% RH for a period of six months (in 0.1 M HCl)

Time	30°C & 65% RH	40°C & 75% RH
1 Month	54.85	52.02
2 Months	62.08	56.09
3 Months	58.84	52.98
4 Months	41.44	36.26
5 Months	47.03	30.77
6 Months	50.12	28.05

The dissolution profiles of the tablets stored during the first 3 months at 30°C & 65% RH were comparable ($100 > f_2$ values > 50) to the dissolution profile of the initially procured tablets (age = 0 months).

The tablets stored at 30°C & 65% RH for 4-6 months revealed significant differences in their dissolution profiles ($0 < f_2$ values < 50) when compared to that of the initially procured tablets (age = 0 months). The variance (%CV) between the dissolution values for the respective dissolution vessels of Product 2 at 30°C & 65% RH after 4-6 months were small. The DRIFT-IR and XRPD results showed no significant transformation of polymorph C into polymorph A, thus the changes in the dissolution profiles could be either experimental error or be attributed to potential changes in the physical properties of the tablets. The general trend is a decrease in the dissolution values. Future studies should focus on the influence of the tablet excipients and physical properties such as hardness and disintegration that might have influenced the dissolution behaviour.

The dissolution profiles of the tablets stored at 40°C & 75% RH at the various time intervals confirmed the XRPD and IR results that polymorphic

transformations had occurred that influenced the dissolution behaviour of the tablets. The dissolution data for the tablets after 6 months at 120 minutes is not available due to an experimental error. The dissolution profiles of the tablets stored at 40°C & 75% RH during the first three months were comparable (100 > f_2 values > 50) to the dissolution profile of the initially procured tablets (age = 0 months).

The tablets stored for 4-6 months revealed significant differences in their dissolution profiles (0 < f_2 values < 50) when compared to that of the initially procured tablets (age = 0 months). The significant changes in the dissolution profiles thus supported the polymorphic transition (Polymorph C transformed into Polymorph A) observed using DRIFT-IR and XRPD.

3.2.2.1 Summary of the polymorphic stability of Product 2

From the results obtained it was evident that this product did not show a polymorphic instability when stored at 30°C & 65% RH, however the tablets stored at 40°C & 75% RH showed a polymorph C → polymorph A transition. The tablets stored at 30°C & 65% RH after 4 months revealed significant differences in their dissolution profiles (0 < f_2 values < 50) when compared to that of the initially procured tablets (age = 0 months). The DRIFT-IR and XRPD results showed no significant transformation of polymorph C into polymorph A, thus the changes in the dissolution profiles could be either experimental error or be attributed to potential changes in the physical properties of the tablets. The general trend is a decrease in the dissolution values. The tablets stored at 40°C & 75% RH showed a polymorph C → polymorph A transition which altered the dissolution profile of this product significantly.

3.2.3 Polymorphic stability of mebendazole in Product 3

The characteristic IR absorption peaks of the mebendazole polymorph present in Product 3 are listed in table 3.8. From this table it can be concluded that the initial product contained mebendazole polymorph C and traces of polymorph A.

When Product 3 was exposed to 30°C & 65 % RH and 40°C & 75% RH the intensity of the shoulders present at 3369 and 1732 cm^{-1} (distinctive to polymorph A) increased as a function of time, which indicated that a mebendazole polymorph transition occurred in the tablets, and that the tablets consisted of a mixture of polymorph C and A (figure 3.16).

The DRIFT-IR spectra of Product 3 exposed to 40°C & 75% RH (figure 3.17) suggested that the rate at which the fraction of polymorph C transformed to polymorph A was higher than that observed when Product 3 was exposed to 30°C & 65% RH. The rate of this transformation will be discussed in section 3.3.2.

The XRPD diffractograms of Product 3 when exposed to 30°C & 65% RH and 40°C & 75% RH for a period of 6 months are illustrated in figure 3.18. The x-ray powder diffraction analysis revealed weak diffraction peaks present at 7.67±0.1°2θ indicative of polymorph A. The intensities of the mentioned peaks increased as a function of time (figure 3.18) which confirmed the polymorphic transformation that occurred as observed using the DRIFT-IR spectroscopy.

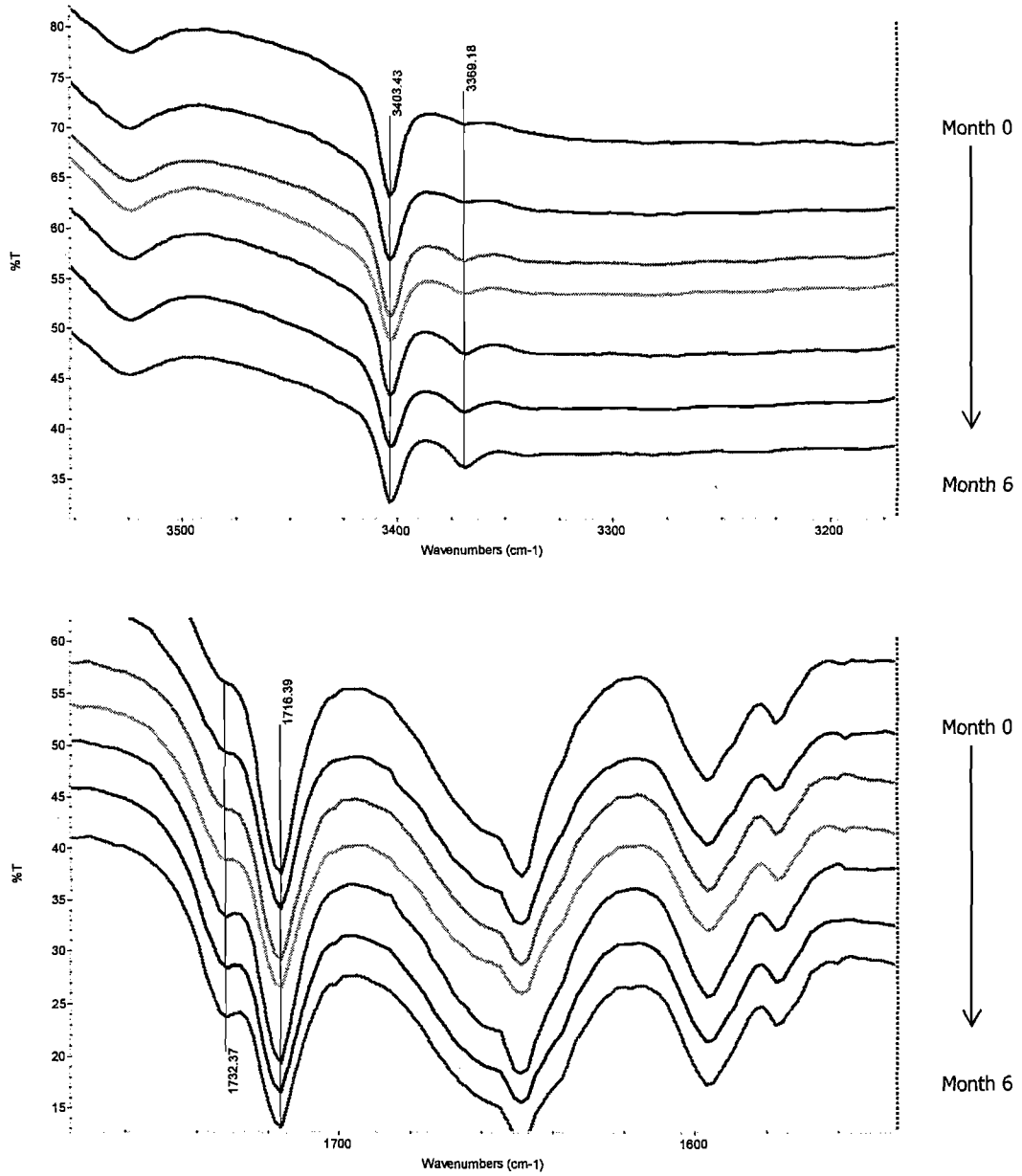


Figure 3.16 IR spectra (superimposed) of the powdered tablets of Product 3 over a period of six months – stored at 30°C & 65% RH, indicating differences in the main absorptions at the –NH stretch and the >C=O band.

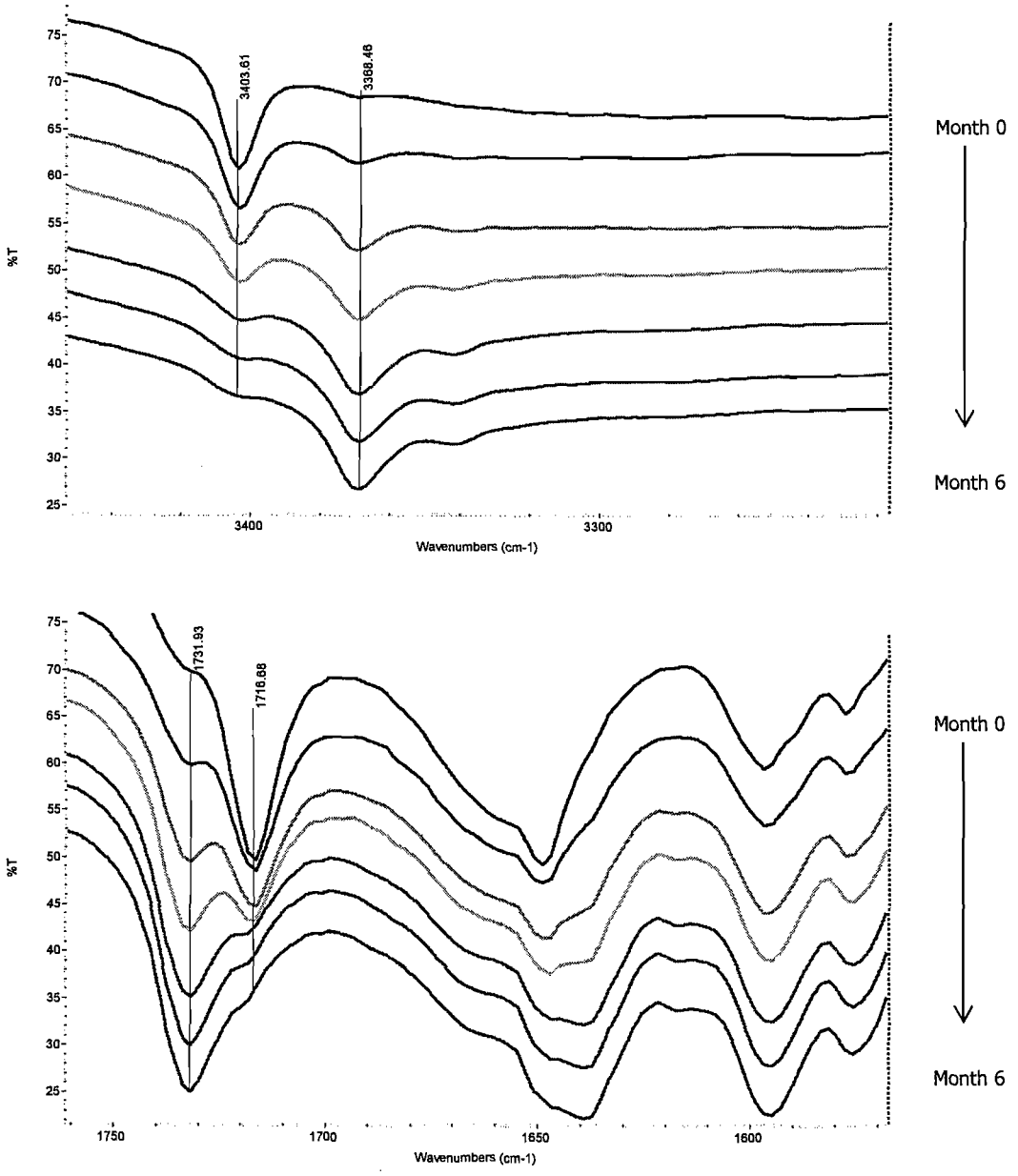


Figure 3.17 IR spectra (superimposed) of the powdered tablets of Product 3 over a period of six months – stored at 40°C & 75% RH, indicating differences in the main absorptions at the –NH stretch and the >C=O band.

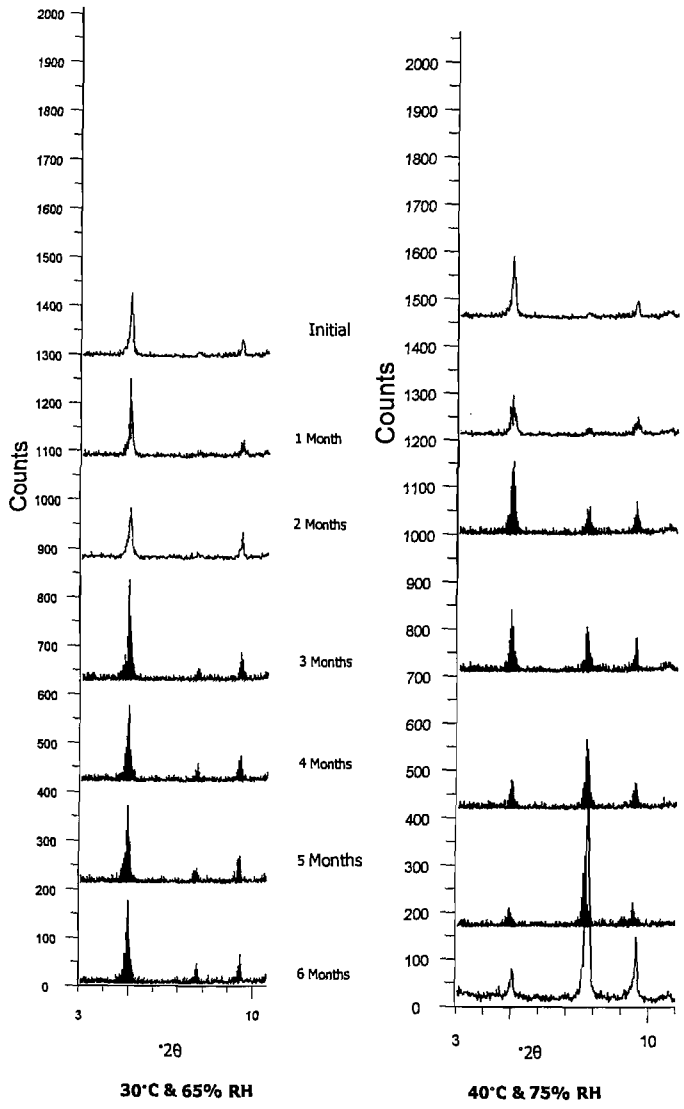


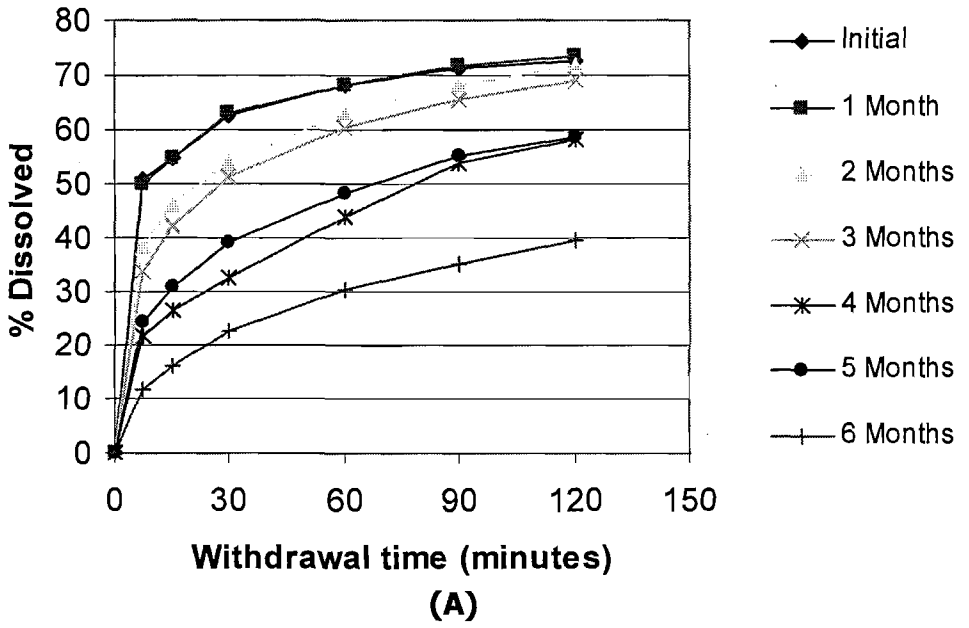
Figure 3.18 XRPD patterns of Product 3 over a period of six months – stored at 30°C & 65% RH and 40°C & 75% RH.

The polymorphic transitions influenced the dissolution behaviour of the tablets significantly i.e. the dissolution rate and extend of dissolution were significantly reduced (figure 3.19). Table 3.12 indicates the f_2-values calculated when the dissolution profiles of the products at the various intervals were compared to the dissolution profile of the initially procured Product 3.

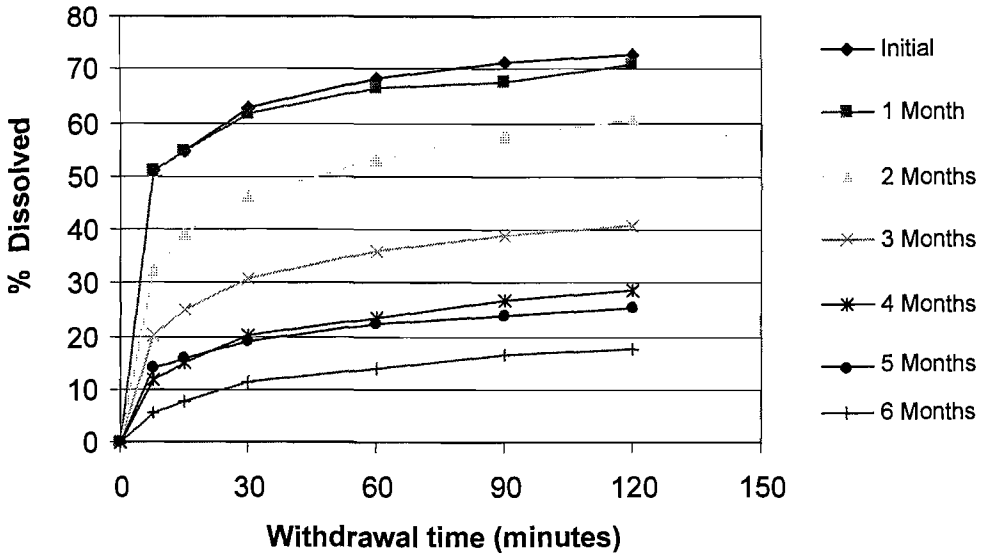
Table 3.12 Similarity factors (f_2-values) of dissolution profiles (in 0.1 M HCl) of Product 3 when stored at 30°C & 65% RH and 40°C & 75% RH for a period of six months

Time	30°C & 65% RH	40°C & 75% RH
1 Month	96.56	82.95
2 Months	55.61	40.59
3 Months	48.33	25.01
4 Months	30.28	18.56
5 Months	33.65	18.04
6 Months	21.19	14.40

The dissolution profiles of the tablets stored for 1 and 2 months at 30°C & 65% RH and that of the tablets stored at 40°C & 75% RH for 1 month were comparable (100 > f_2 values > 50) to the dissolution profile of the initially procured tablets (age = 0 months).



(A)



(B)

Figure 3.19 Dissolution profiles (in 0.1 M HCl) of Product 3 when stored at (a) 30°C & 65% RH and (b) 40°C & 75% RH for a period of six months.

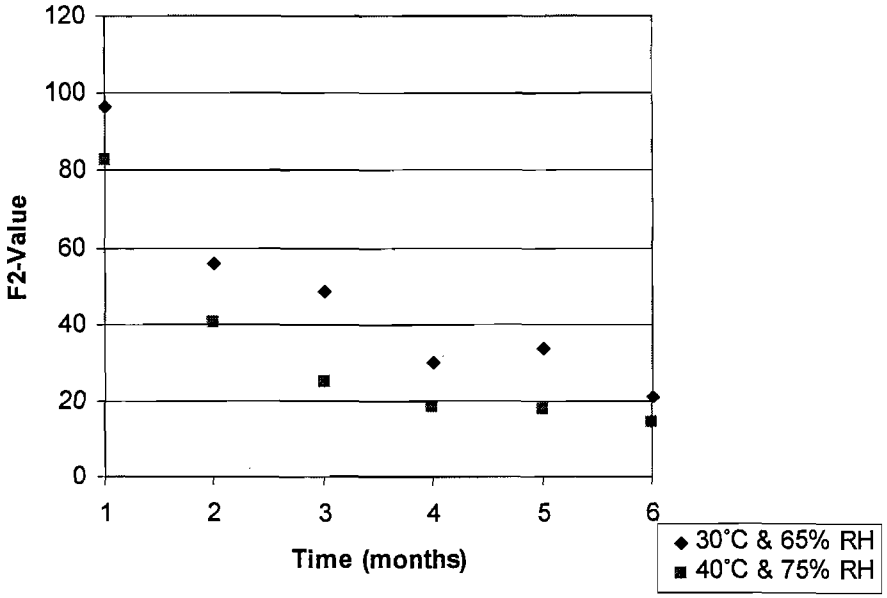


Figure 3.20 Calculated F2-values for Product 3 stored at (a) 30°C & 65% RH and 40°C & 75% RH versus the period of exposure.

The tablets stored for 3-6 months at 30°C & 65% RH and 2-6 months at 40°C & 75% RH revealed a significant decrease in the % mebendazole dissoluted (Q) after 120 minutes. The decrease in Q at 120 minutes could be attributed to the formation of mebendazole polymorph A in the tablet matrix and thus supported the DRIFT-IR and XRPD observations that polymorphic transitions (polymorph C transformed into polymorph A) occurred.

The *dissimilarity* between the dissolution profiles of Product 3 exposed to 40°C & 75% RH and that of the initial Product 3 was greater at the various intervals compared to that observed for Product 3 stored at 30°C & 65% RH (figure 3.20). Supporting the hypothesis that the rate and extend of the polymorphic conversion observed in Product 3 (polymorph C → polymorph A) was higher at 40°C & 75% RH compared to that at 30°C & 65% RH.

3.2.3.1 Summary of the polymorphic stability of Product 3

The analysis on the initial tablets showed that it contained mostly polymorph C and a small fraction of polymorphic form A.

The polymorphic transformation had a significant influence on the dissolution properties (dissolution rate and dissolution extend) of the tablets when stored at 30°C & 65% RH and 40°C & 75% RH.

The polymorphic transformation rate and extend of transformation at 40°C & 75% RH seemed to be higher compared to that observed at 30°C & 65% RH.

3.2.4 Polymorphic stability of mebendazole in Product 4

Due to a limited number of available tablets (same batch from the same supplier) the polymorphic stability of Product 4 was only evaluated over a period of 5 months.

The presence of the absorbance peaks at 3403 and 1716 cm^{-1} in the DRIFT-IR results signified that the initial product contained mebendazole polymorph C (table 3.8).

The IR spectrum of the tablets exposed to 30°C & 65% RH remained relatively unchanged during the 5 months of the stability evaluation (figure 3.21), which suggested mebendazole polymorph stability.

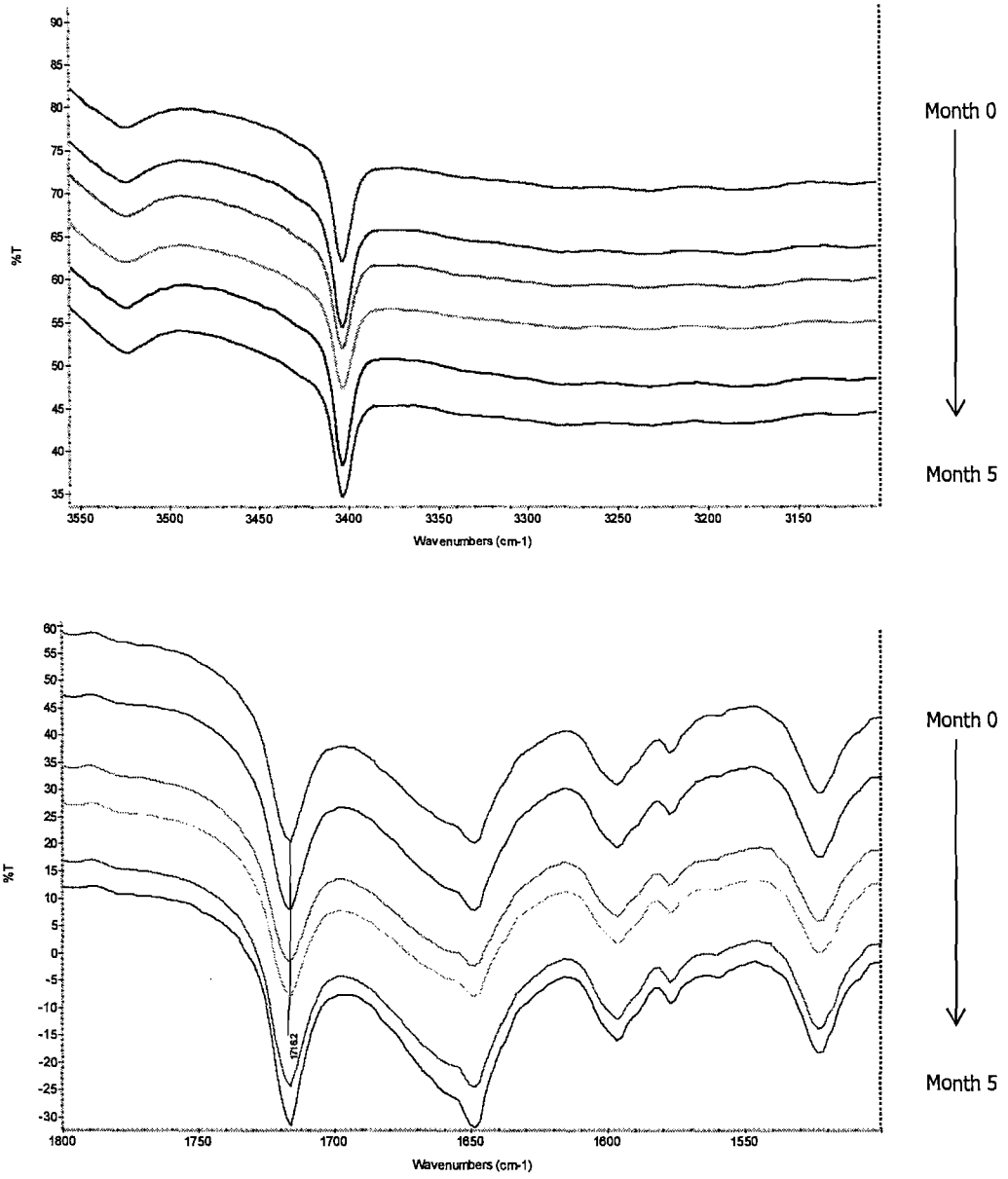


Figure 3.21 IR spectra (superimposed) of the powdered tablets of Product 4 over a period of five months – stored at 30°C & 65% RH, indicating the main absorptions at the –NH stretch and the >C=O band.

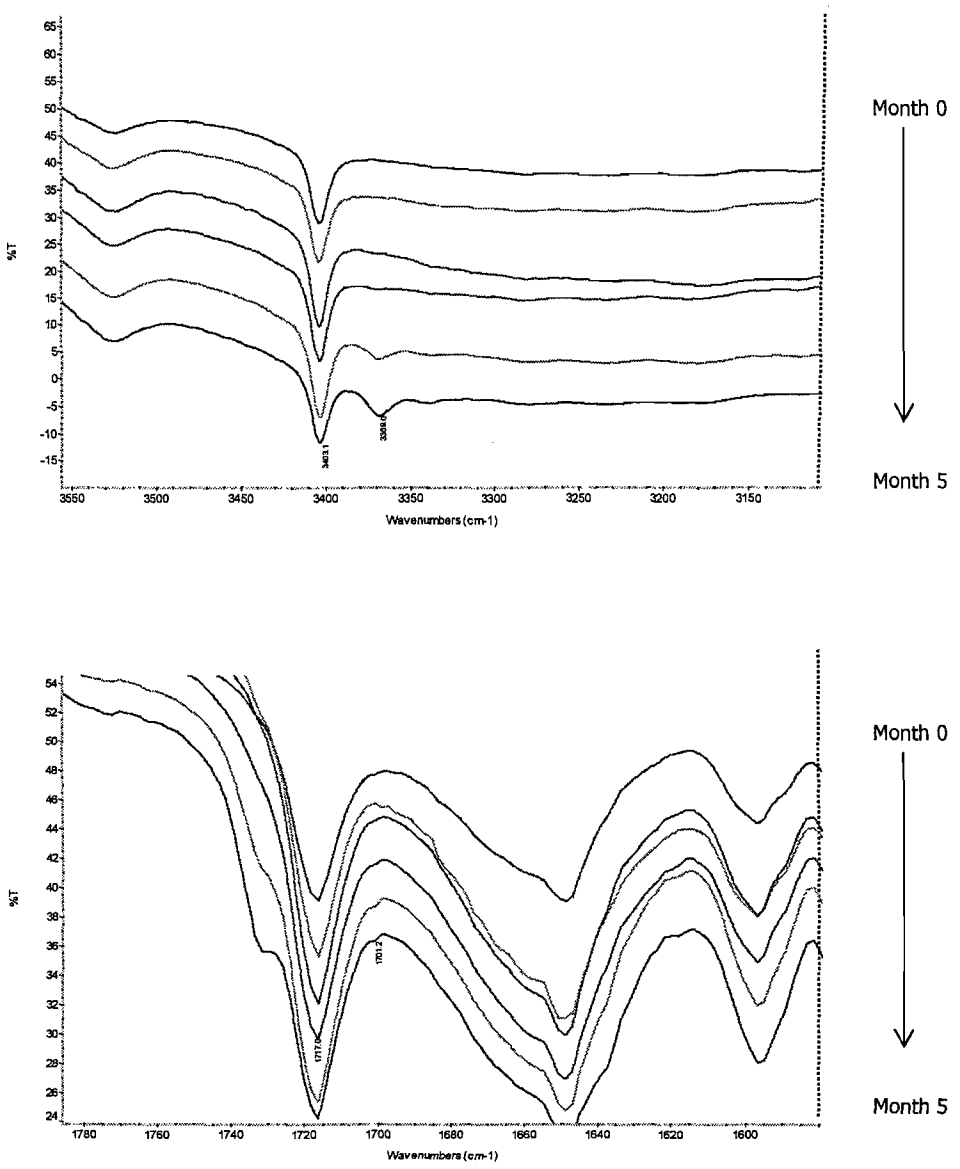


Figure 3.22 IR spectra (superimposed) of the powdered tablets of Product 4 over a period of five months – stored at 40°C & 75% RH, indicating differences in the main absorptions at the –NH stretch and the >C=O band.

The IR-spectra of the Product 4 samples exposed to 40°C & 75% RH remained relatively unchanged during the first 0 – 3 months. The appearance of the peak at 3368 cm^{-1} (at month 4) signified the commencement of the polymorphic transformation (i.e. polymorph C → polymorph A). The presence of the peaks at

3368, 3403 and 1716 cm^{-1} indicated that a mixture of mebendazole polymorphs (polymorph A <<< polymorph C) existed in the tablets after 5 months (figure 3.22).

The XRPD patterns of Product 4 stored at 30°C & 65% RH and 40°C & 75% RH at the various intervals are shown in figure 3.23. The characteristic XRPD peaks in table 3.9 confirmed that the initially procured tablets contained mebendazole polymorphic form C, due to the presence of the peak at 4.93±0.1°2θ.

The absence of peaks at 7.67±0.1°2θ in the x-ray powder diffraction patterns (figure 3.23) confirmed the DRIFT-IR observations that no mebendazole polymorph transformation occurred in the tablets when they were exposed to 30°C & 65% RH.

The XRPD diffractograms of Product 4 when exposed to 40°C & 75% RH for a period of 5 months are illustrated in figure 3.23.

The intensity of the 4.93±0.1°2θ Bragg peak (characteristic to polymorph C) did not reveal any significant changes in intensity which indicated that the tablets exposed to 40°C & 75% RH contained mebendazole polymorph C. The appearance of a very weak diffraction peak at 7.67±0.1°2θ during month 4, and the progressive increase in the intensity of the mentioned peak indicated the appearance and growth of mebendazole polymorph A phase, thus the tablets contained a mixture of mebendazole polymorphs A & C (polymorph C >>>> polymorph A).

The overall XRPD pattern displayed several well-defined peaks, with relatively high counts (counts ≥ 1200 cps) which suggested that the tablets contained crystalline excipients.

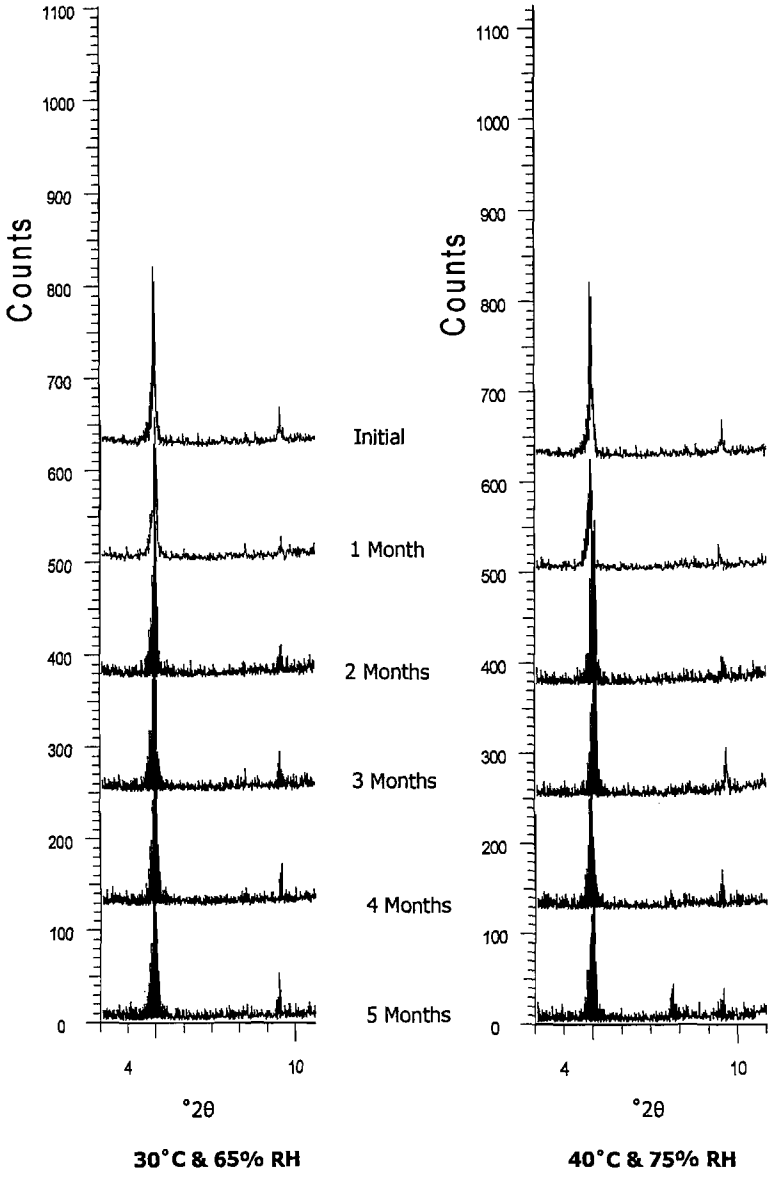
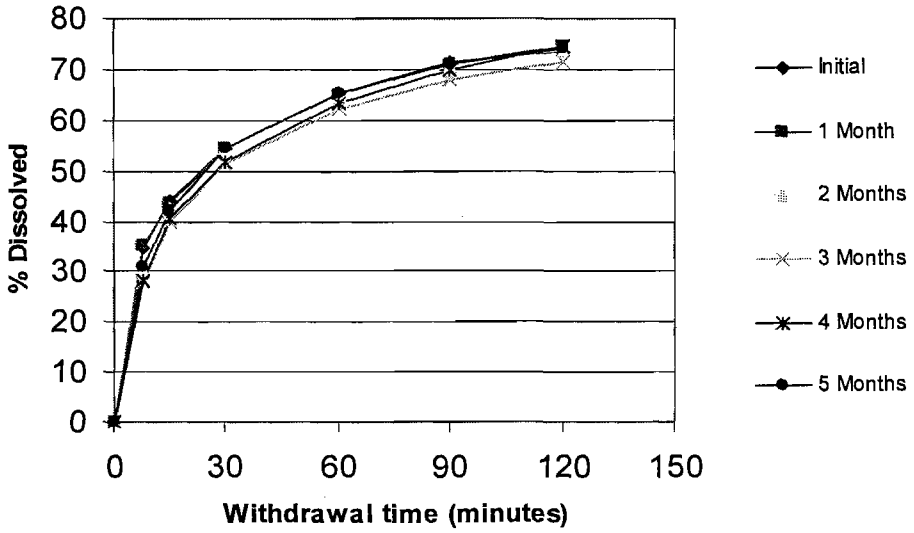
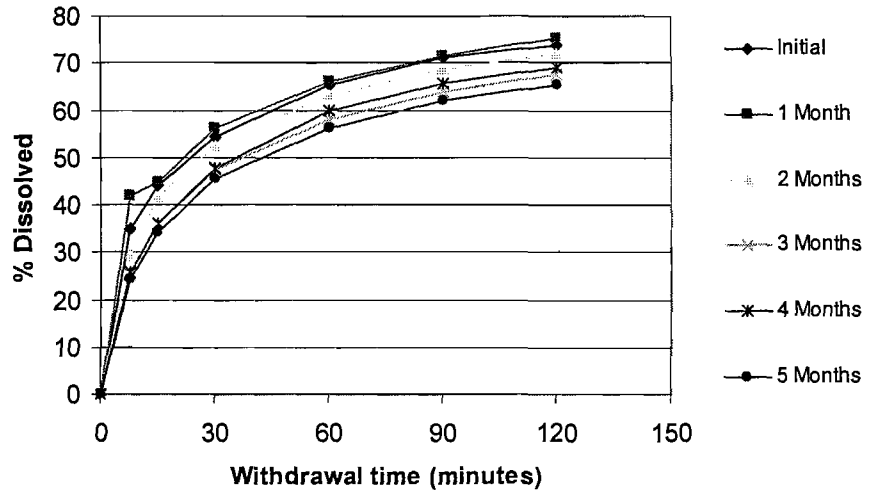


Figure 3.23 XRPD patterns of Product 4 over a period of five months – stored at 30°C & 65% RH and 40°C & 75% RH.

Based on the XRPD and DRIFT-IR observations it could be assumed that the dissolution profiles of the tablets exposed to 30°C & 65% RH should remain unchanged. The dissolution profiles (figure 3.24) of the tablets (kept at 30°C & 65% RH) confirm that no polymorphic transformation occurred. The dissolution profiles of the tablets at the various intervals may be considered to be identical.



(A)



(B)

Figure 3.24 Dissolution profiles (in 0.1 M HCl) of Product 4 when stored at (a) 30°C & 65% RH and (b) 40°C & 75% RH for a period of 5 months.

Table 3.13 Similarity factors (f_2-values) of dissolution profiles of Product 4 tablets when stored at 30°C & 65% RH and 40°C & 75% RH for a period of five months.)

Time	30°C & 65% RH	40°C & 75% RH
1 Month	97.07	75.08
2 Months	82.19	75.57
3 Months	68.86	55.73
4 Months	72.59	58.34
5 Months	84.38	51.30

The dissolution profiles of the tablets stored over the period of 5 months at 30°C & 65% RH were comparable (100 > f_2 values > 50) to the dissolution profile of the initially procured tablets (age = 0 months) as illustrated by the calculated f2-values in table 3.13.

The dissolution profiles of the tablets exposed to 40°C & 75% RH (figure 3.24 – b) confirmed that polymorphic transformations had occurred which influenced the dissolution behaviour of the tablets. Both the dissolution rate and extend of dissolution were lowered by the polymorphic transformation, due to the presence of the poorly-soluble mebendazole polymorph A in the tablet matrix.

The dissolution profile of the tablets stored at 40°C & 75% RH for the 5 months were comparable (100 > f_2 values > 50) to the dissolution profile of the initially procured tablets (age = 0 months), but the decrease in the calculated f_2 values of the tablets at 3 months and older, indicated that the tablets contained a mixture of polymorph C and polymorph A, and thus supported the DRIFT-IR and XRPD observations.

3.2.4.1 Summary of the polymorphic stability of Product 4

The initial analysis performed on the tablets revealed that the tablets contained mebendazole polymorph C. Product 4 showed a polymorphic instability at 40°C & 75% RH. A mixture of polymorph A and C were detected in the tablets after 3

months. No significant polymorphic transformations were observed for the tablets stored at 30°C & 65% RH after 5 months.

3.2.5 Polymorphic stability of mebendazole in Product 5

From table 3.8 it can be concluded that Product 5 contained mainly polymorph C with traces of polymorph A. Traces of polymorph A were detected in the DRIFT-IR spectra of the samples stored at 30°C & 65% RH during months 1-6 (figure 3.25).

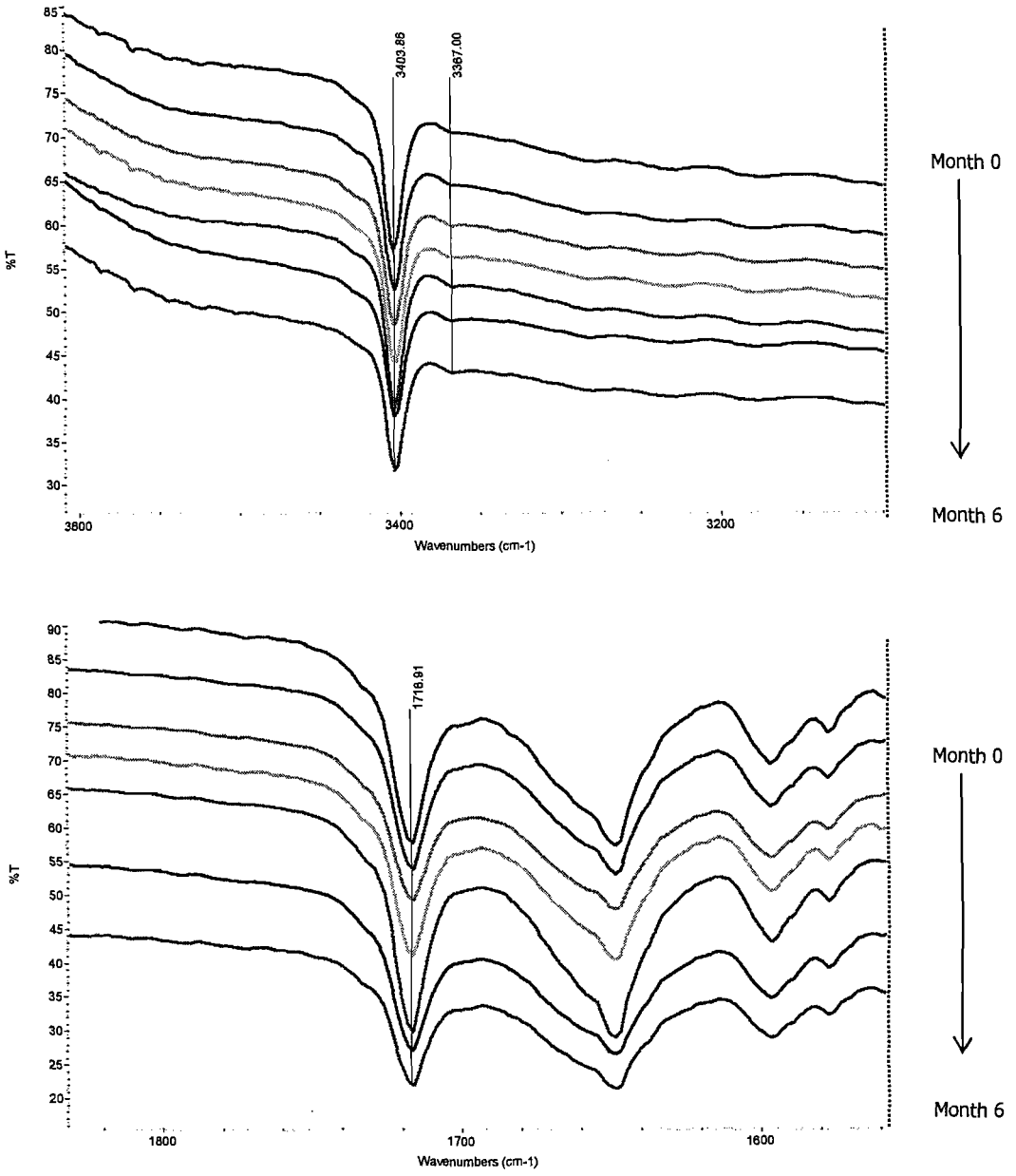


Figure 3.25 IR spectra (superimposed) of the powdered tablets of Product 5 over a period of six months – stored at 30°C & 65% RH, indicating polymorph C and traces of polymorph A in the main absorptions at the –NH stretch and the >C=O band.

The IR spectra of the product at 40°C & 75% RH (figure 3.26) indicated that the tablets contained mainly mebendazole polymorph C. Small shoulder peaks were observed in the 3367 cm^{-1} region (distinctive to polymorph A) during the stability

testing and the intensity thereof increased fairly during months 5 and 6. It was also observed that the peak appearance in the 1731 cm^{-1} region (distinctive to polymorph A) supported the polymorphic transition observed in the 3368 cm^{-1} region.

Thus, the product initially obtained contained polymorph C with traces of polymorph A, and the product revealed a partial polymorphic transformation during months 5 and 6, which lead to the formation of a mixture of mebendazole polymorphs in the product (polymorph C >>> polymorph A).

The XRPD diffractograms of Product 5 when exposed to 30°C & 65% RH and 40°C & 75% RH for a period of 6 months are illustrated in figure 3.27.

The samples of Product 5 revealed amorphous-like XRPD patterns with counts not exceeding 180 cps, which suggested that the tablet excipients showed a more amorphous character compared to the excipients used in Products 1-4. The traces of polymorph A in the initially procured tablets were not clearly detected in the XRPD patterns of Product 5. The detection of small traces of mebendazole polymorph A was complicated due to the presence of the amorphous tablet excipients.

After 4 months at 30°C & 65% RH the XRPD showed a weak diffraction peak (I/I_0 = 0.24%) at 7.58°2θ which indicate that small traces of mebendazole polymorph A were present in the tablets.

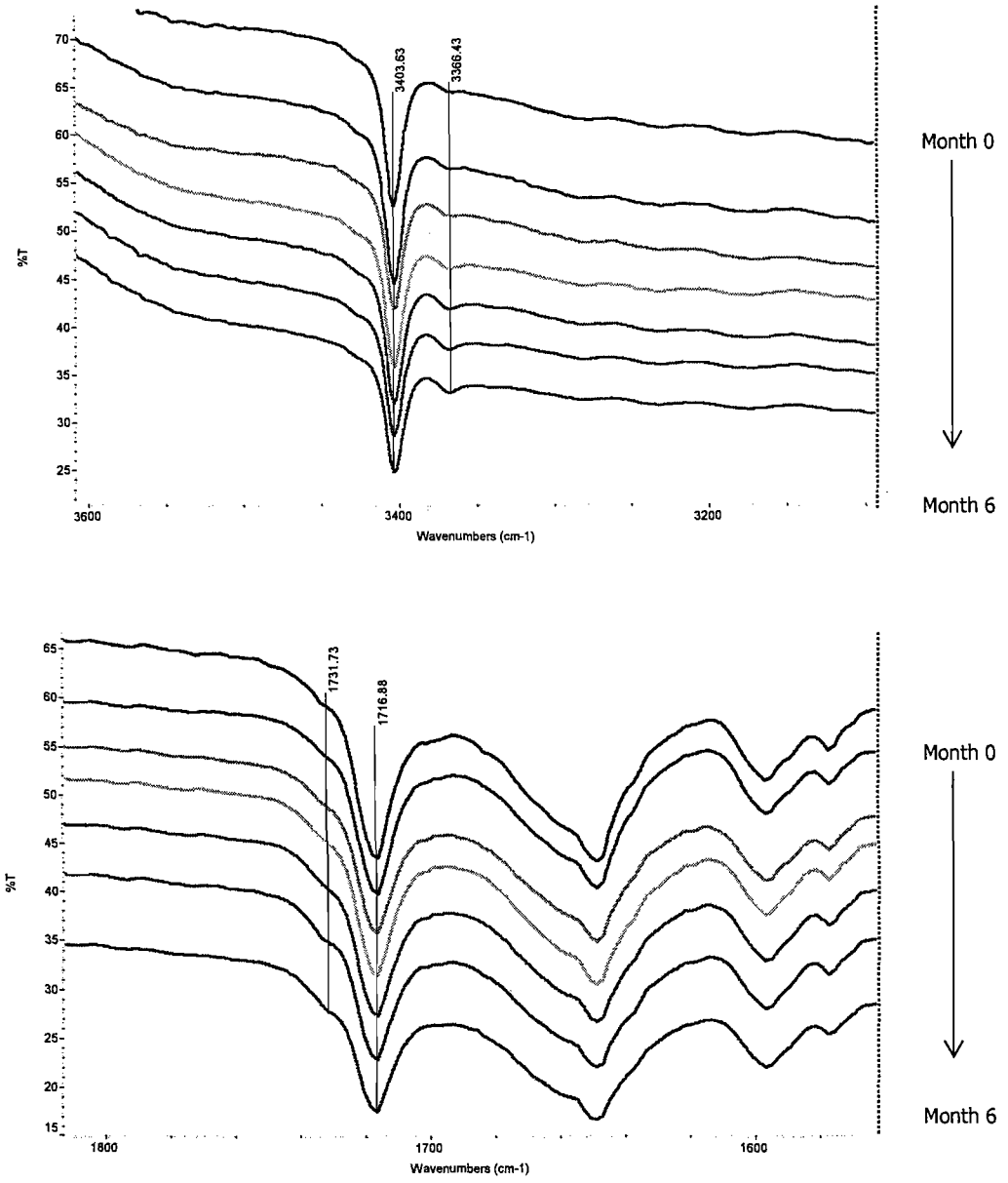


Figure 3.26 IR spectra (superimposed) of the powdered tablets of Product 5 over a period of six months – stored at 40°C & 75% RH, indicating differences in the main absorptions at the –NH stretch and the >C=O band.

The XRPD pattern of Product 5 stored at 40°C & 75% RH (figure 3.27) remained relatively unchanged, which suggested that no significant mebendazole polymorphic transformation occurred during the stability testing. Once a background subtraction and $K\alpha_2$-strip was performed on the XRPD patterns of

the samples for quantitative analysis, small diffraction peaks were observed at 7.70°2θ and 7.66°2θ with weak intensities during month 4 and month 6 respectively, indicating the presence of mebendazole polymorph A in the tablet matrixes.

The presence of the amorphous-like tablet excipients suppressed the detection of the characteristic diffraction peak of polymorph A at 6.67±0.1°2θ. Infrared spectroscopy has emerged as the preferred method to identify the mebendazole polymorphic forms (Liebenberg *et al.*, 1998:487 and Bunaciu *et al.*, 2002:647), and this study supports the authors' observations.

The dissolution profiles of Product 5 kept at 30°C & 65% RH at the various time intervals are illustrated in figure 3.28. The dissolution profiles revealed a slight decrease in the amount of mebendazole dissolved after 120 minutes as a function of time. The traces of mebendazole polymorph A detected using DRIFT-IR (figure 3.25) might thus have induced the changes observed in the dissolution behaviour of the product. Table 3.14 indicates the f_2-values calculated when the dissolution profiles of the samples at the various intervals were compared to the dissolution profile of the initially procured tablets of Product 5.

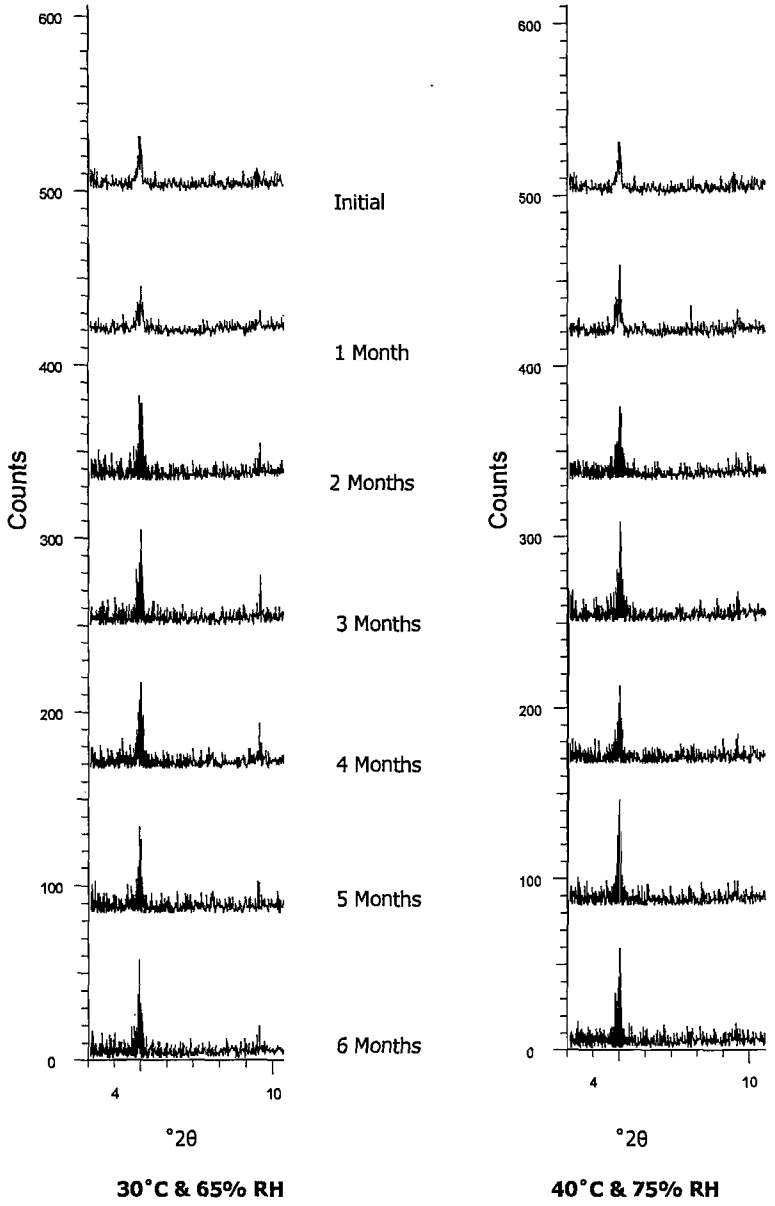
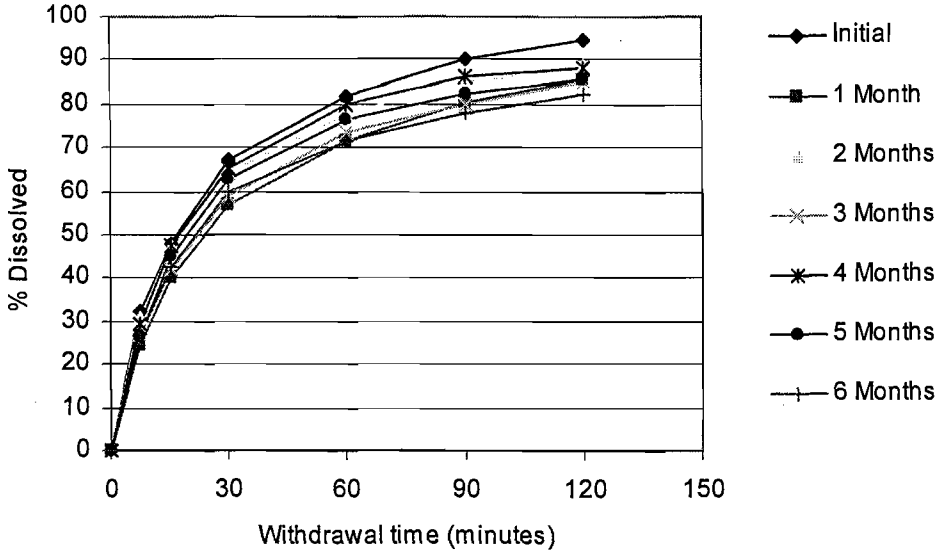
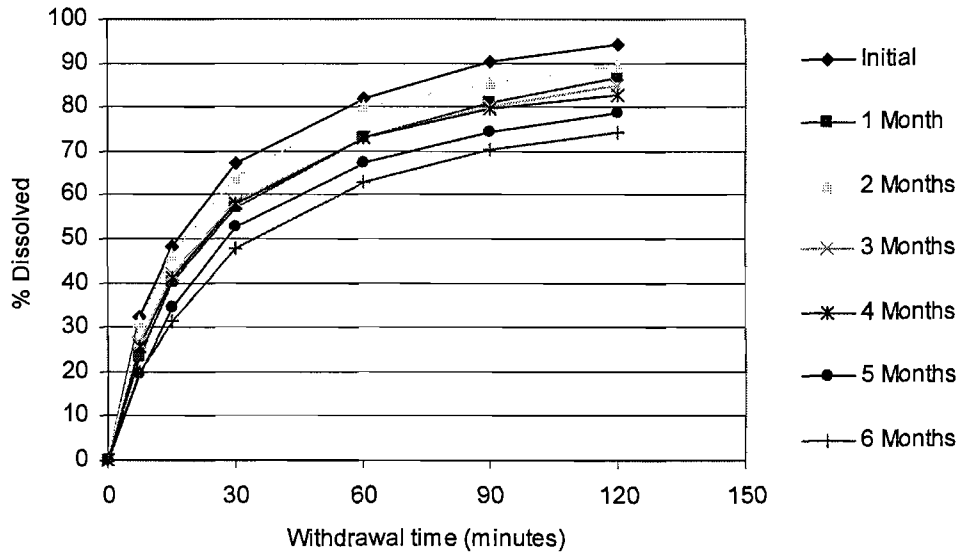


Figure 3.27 XRPD patterns of Product 5 over a period of six months – stored at 30°C & 65% RH and 40°C & 75% RH.



(A)



(B)

Figure 3.28 Dissolution profiles (in 0.1 M HCl) of Product 5 when stored at (a) 30°C & 65% RH and (b) 40°C & 75% RH for a period of 6 months.

Table 3.14 Similarity factors (f_2-values) of dissolution profiles of Product 5 when stored at 30°C & 65% RH and 40°C & 75% RH for a period of six months (in 0.1 M HCl)

Time	30°C & 65% RH	40°C & 75% RH
1 Month	51.57	52.63
2 Months	69.59	73.06
3 Months	54.65	53.56
4 Months	72.47	51.72
5 Months	59.98	41.76
6 Months	51.51	37.00

The dissolution profiles of the tablets stored at 30°C & 65% RH for the 6 months remained comparable ($100 > f_2$ values > 50) to the dissolution profile of the initially procured tablets (age = 0 months).

The similarity factors calculated for Product 5 during the first four months ($100 > f_2 > 50$) when stored at 40°C & 75% RH revealed that the dissolution profiles may be considered to be equivalent to that of the initially procured tablets.

The similarity factors calculated for Product 5 during the months 5 and 6 ($50 > f_2 > 0$) indicated that the dissolution profiles differed significantly when compared to that of the initially procured tablets, which correlated with the DRIFT-IR findings, that a polymorphic transformation did occur that lead to the formation of the less soluble polymorph A.

3.2.5.1 Summary of the polymorphic stability of Product 5

The polymorphic screening performed with DRIFT-IR spectroscopy on the tablets revealed that the tablets contained mainly mebendazole polymorphic Form C with traces of polymorph A.

No significant increases of the polymorph A fractions were observed when Product 5 was stored at 30°C & 65% RH for a period of 6 months.

Investigation of the XRPD patterns of Product 5 stored at 40°C & 75% RH revealed that the traces of polymorph A could not be detected except at months 4 and 6 after a background subtraction and $K\alpha_2$-stripping of the XRPD patterns has been performed. The detection of small fractions of mebendazole polymorph A in XRPD patterns was complicated due to the presence of amorphous tablet excipients. Quantitative XRPD techniques rarely detect traces of crystalline phases bellow 10% in a matrix (USP, 2006), thus DRIFT-IR spectroscopy is the preferred method of detection of mebendazole polymorphs in tablet matrixes, due to the fact that mebendazole reveals poor crystalline properties (this will be discussed in chapter 4).

From the results obtained it was evident that this product showed a polymorphic instability at 40°C & 75% RH which had a significant influence on the dissolution properties (dissolution rate and dissolution extend), due to the progressive increase of mebendazole polymorph A fraction in the tablet matrix.

3.2.6 Polymorphic stability of mebendazole in Product 6

The characteristic IR absorbance peaks and their corresponding wavenumbers (cm^{-1}) of the mebendazole polymorphs present in Product 6 when exposed to 30°C & 65% RH and 40°C & 75% RH are listed in table 3.8.

Investigation of the DRIFT-IR spectrum of Product 6 at an increased sensitivity (figure 3.29) revealed that traces of polymorph A (small peak at 3367 cm^{-1}) might have been present in the product initially procured.

The intensity of the shoulders present at 3367 cm^{-1} (distinctive to polymorph A) increased with time when exposed to 30°C & 65% RH, which indicated that a polymorphic transition occurred (figure 3.29). No absorbance bands were however detected in the >C=O band (1730 cm^{-1}) region which is characteristic to polymorph A.

The IR-spectra of samples exposed to 40°C & 75% RH (figure 3.30) remained relatively unchanged during the period 0-4 months, which clearly indicated that no or very little polymorphic transformation had occurred during this period. The presence of the peaks at 3368, 3404, 1732 and 1716 cm^{-1} indicated that a mixture of mebendazole polymorphs (polymorph A <<< polymorph C) existed in the tablets after 4 months.

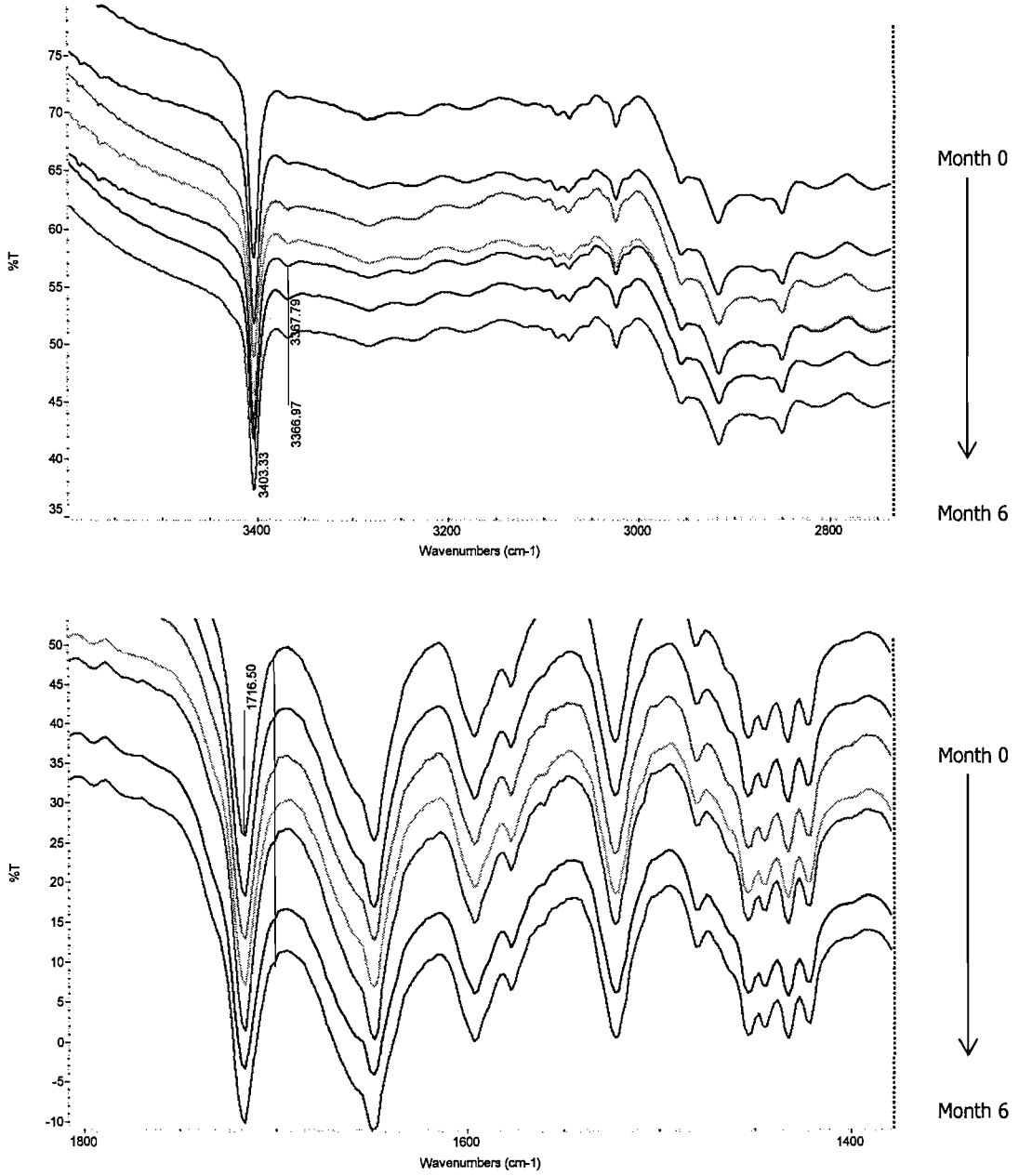


Figure 3.29 IR spectra (superimposed) of the powdered tablets of Product 6 over a period of six months – stored at 30°C & 65% RH, indicating differences in the main absorptions at the –NH stretch and the >C=O band.

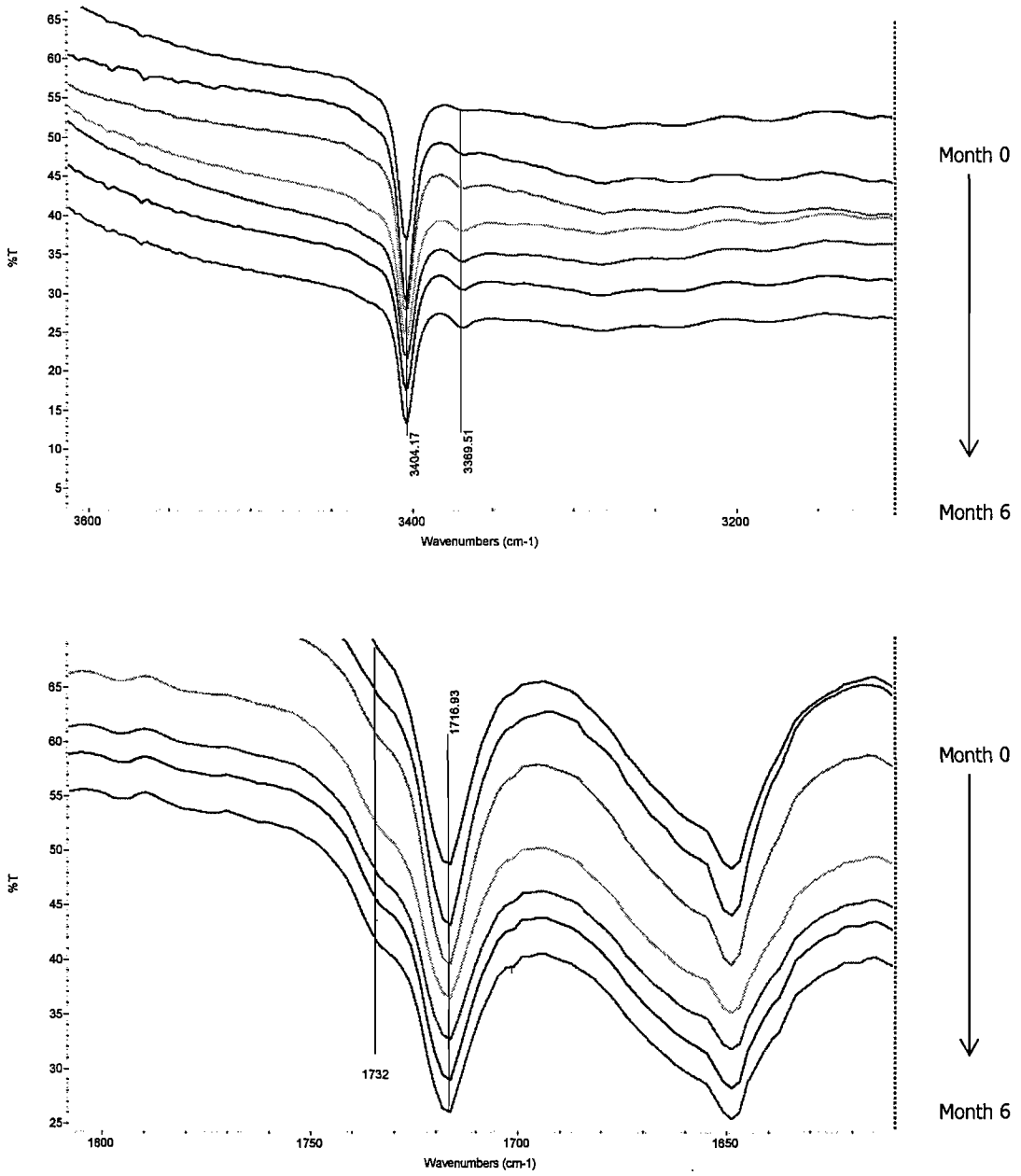


Figure 3.30 IR spectra (superimposed) of the powdered tablets of Product 6 over a period of six months – stored at 40°C & 75% RH, indicating differences in the main absorptions at the –NH stretch and the >C=O band.

The XRPD patterns of Product 6 samples exposed to 30°C & 65% RH and 40°C & 75% RH at the various intervals are depicted in figure 3.31. The characteristic peaks presented in table 3.9 confirmed the presence of mebendazole polymorphic form C in the initial tablets obtained, due to the presence of the peak at 4.93±0.1°2θ, no peak was detected at 7.67±0.1°2θ

to indicate the traces of polymorph A in the initial product due to the presence of the small, undetectable traces of polymorph A. The XRPD pattern of the sample at 30°C & 65% RH - month 2 revealed a slight shift of all peaks to the right (towards 35°2θ), this might have been due to a difference in the height of the powder bed in the sample holder. This peak shift was clearly indicated by the peak positions at: 9.54°2θ and 5.03°2θ.

The pulverised tablets of Product 6 had amorphous-like XRPD patterns with counts not exceeding 340 cps, which suggested that the tablet contained amorphous excipients.

After a background subtraction and $K\alpha_2$-strip have been performed on the XRPD patterns of Product 6 exposed to 30°C & 65% RH and 40°C & 75% RH after 5 months and 3 months, respectively; weak peaks at 7.67±0.1°2θ were detected. The appearance of these peaks supported the DRIFT-IR finding that the polymorphic transition occurred in the tablets.

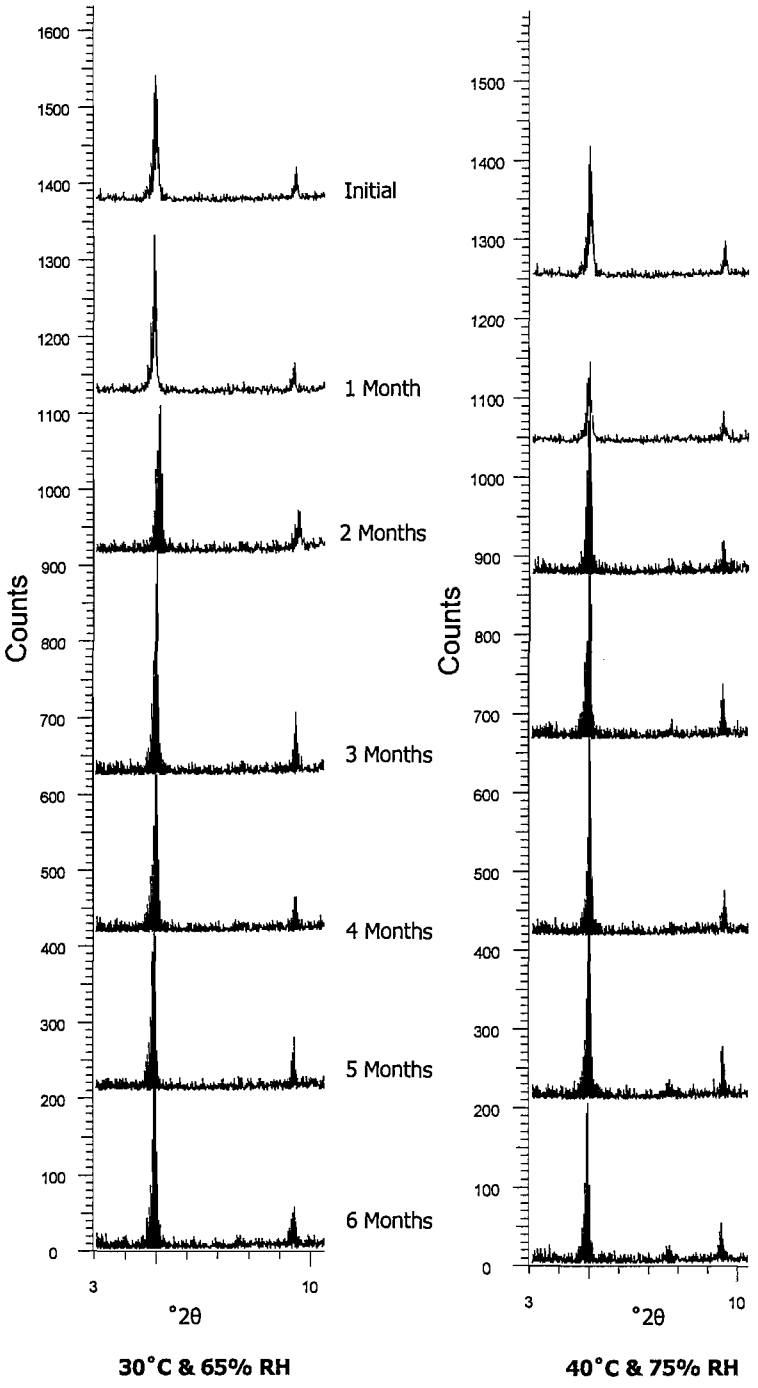


Figure 3.31 XRPD patterns of Product 6 over a period of six months – stored at 30°C & 65% RH and 40°C & 75% RH.

The dissolution profiles of Product 6 stored at 30°C & 65% RH and 40°C & 75% RH are illustrated in figure 3.32. The dissolution profiles of the tablets (stored at 30°C & 65% RH) at the various intervals may be considered to be similar ($100 > f_2 > 50$) compared to the dissolution profile of the initially procured tablets. The partial polymorphic transition that occurred during the

study did not have a profound influence on the dissolution behaviour of the tablets.

Similarities between the dissolution curves were calculated using the equation described by Moore *et al.* (1996:64-67). Table 3.15 indicates the f_2-values calculated.

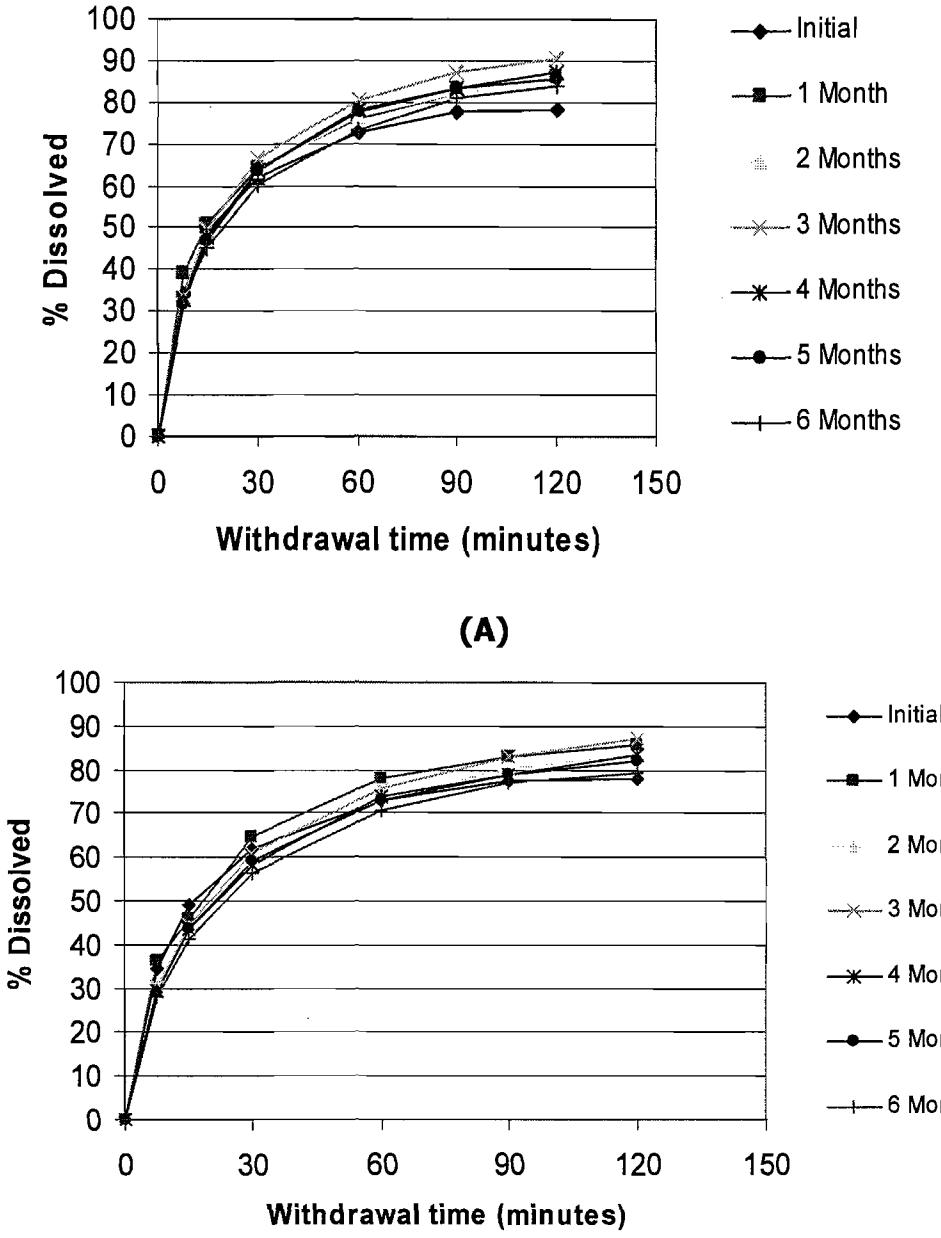


Figure 3.32 Dissolution profiles (in 0.1 M HCl) of Product 6 tablets when stored at (a) 30°C & 65% RH and (b) 40°C & 75% RH for a period of six months.

Table 3.15 Similarity factors (f_2-values) of dissolution profiles of Product 6 tablets when stored at 30°C & 65% RH and 40°C & 75% RH for a period of six months

Time	30°C & 65% RH	40°C & 75% RH
1 Month	66.16	65.74
2 Months	68.63	65.74
3 Months	55.95	63.88
4 Months	64.93	68.75
5 Months	66.83	69.74
6 Months	73.21	65.41

The dissolution profiles of the tablets stored at 40°C & 75% RH over the period of 6 months were comparable (100 > f_2 values > 50) to the dissolution profile of the initially procured tablets (age = 0 months).

3.2.6.1 Summary of the polymorphic stability of Product 6

The initial analysis performed on the tablets revealed that the tablets primarily contained mebendazole polymorphic form C and small traces of polymorph A.

A small increase in polymorph A content was detected in the tablets after 4 months, especially when kept at 40°C & 75% RH.

The dissolution behaviour of Product 6 was not significantly influenced by the small increase in polymorph A content.

3.2.7 Polymorphic stability of mebendazole in Product 7

The presence of the absorbance peaks at 3403 and 1717 cm^{-1} respectively in the DRIFT-IR spectra of Product 7 (figure 3.33) indicated that the product initially obtained, contained mebendazole polymorph C.

The IR spectra and the XRPD patterns of the tablets remained unchanged for the period of the stability evaluation (figures 3.33 to 3.35). The XRPD diffraction peak observed at 5.8°2θ could be attributed to a tablet excipient used in the formulation, due to the fact that DRIFT-IR analysis did not detect any traces of polymorph A and B in the product.

The XRPD patterns displayed several well-defined peaks, with relatively high intensities (counts ≥ 1200 cps) that suggested that the tablets contained more crystalline excipients.

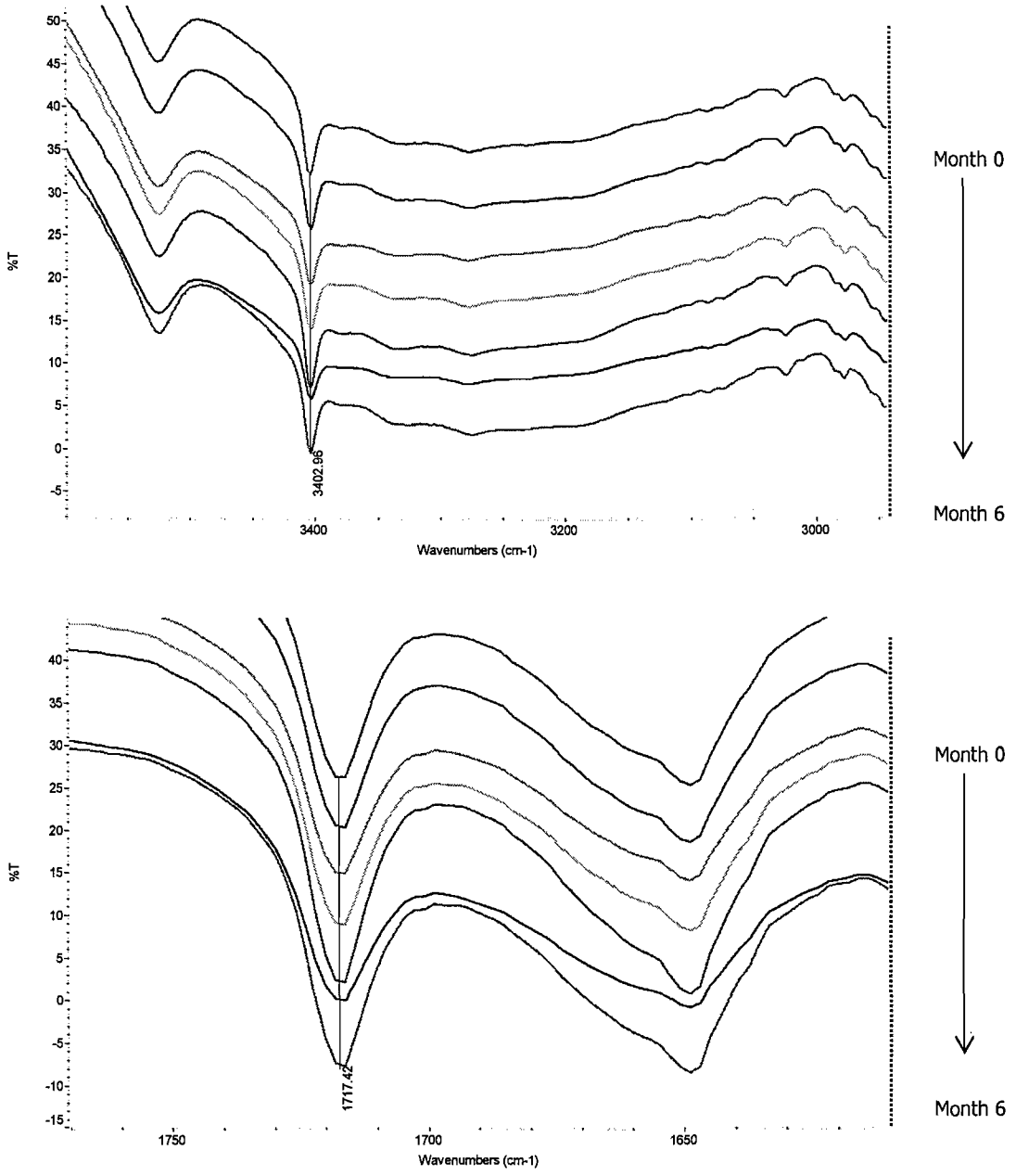


Figure 3.33 IR spectra (superimposed) of the powdered tablets of Product 7 over a period of six months – stored at 30°C & 65% RH, indicating no changes in the main absorptions at the –NH stretch and the >C=O band.

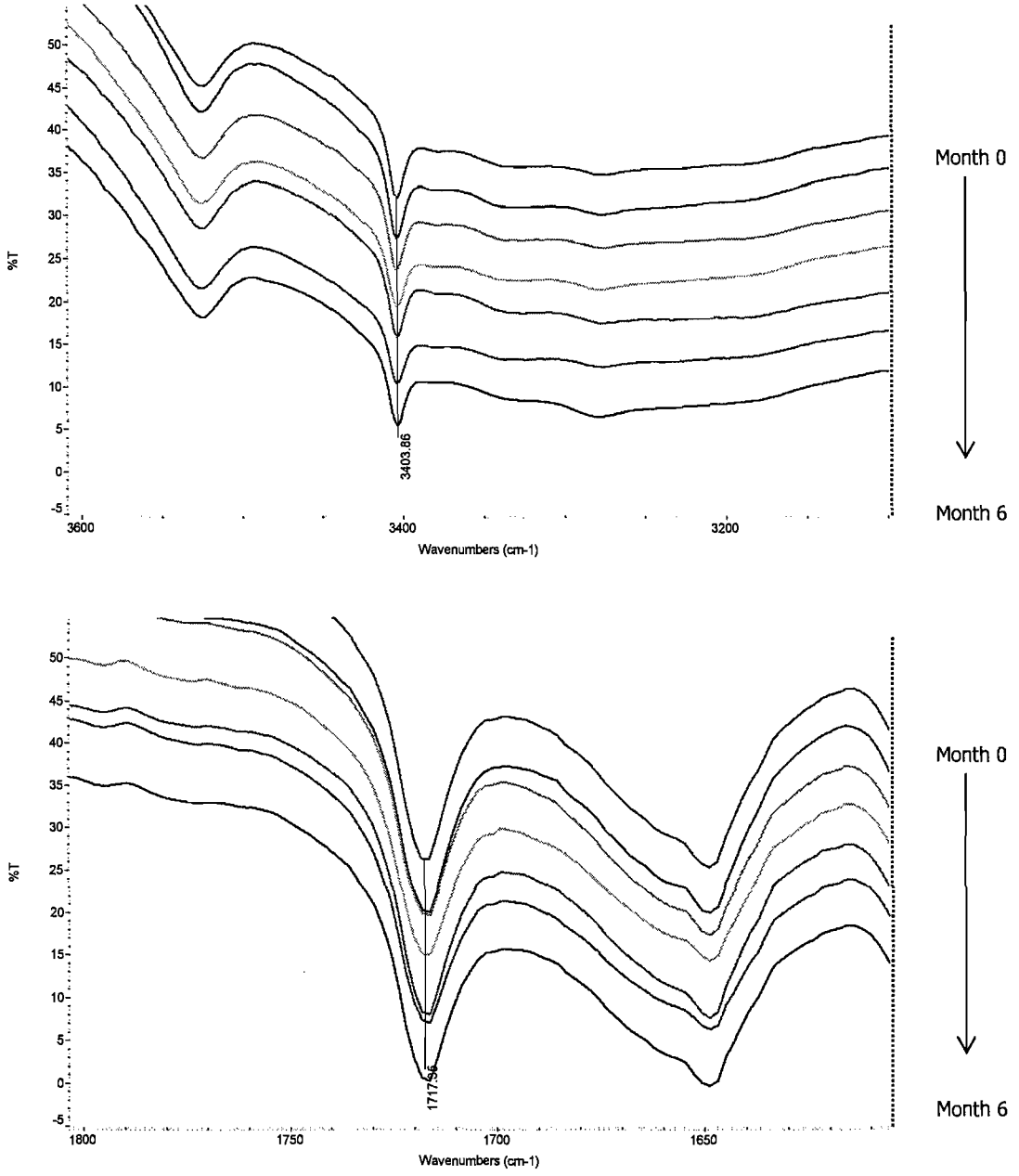


Figure 3.34 IR spectra (superimposed) of the powdered tablets of Product 7 over a period of six months – stored at 40°C & 75% RH, indicating no changes in the main absorptions at the –NH stretch and the >C=O band.

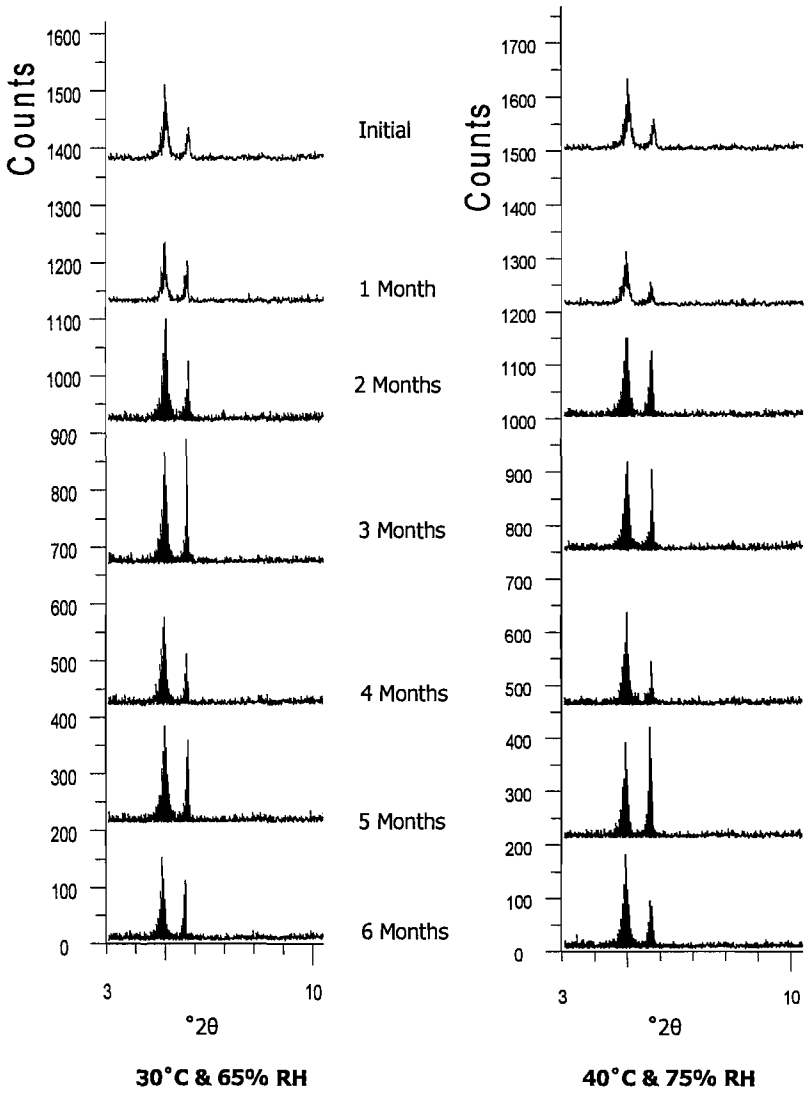
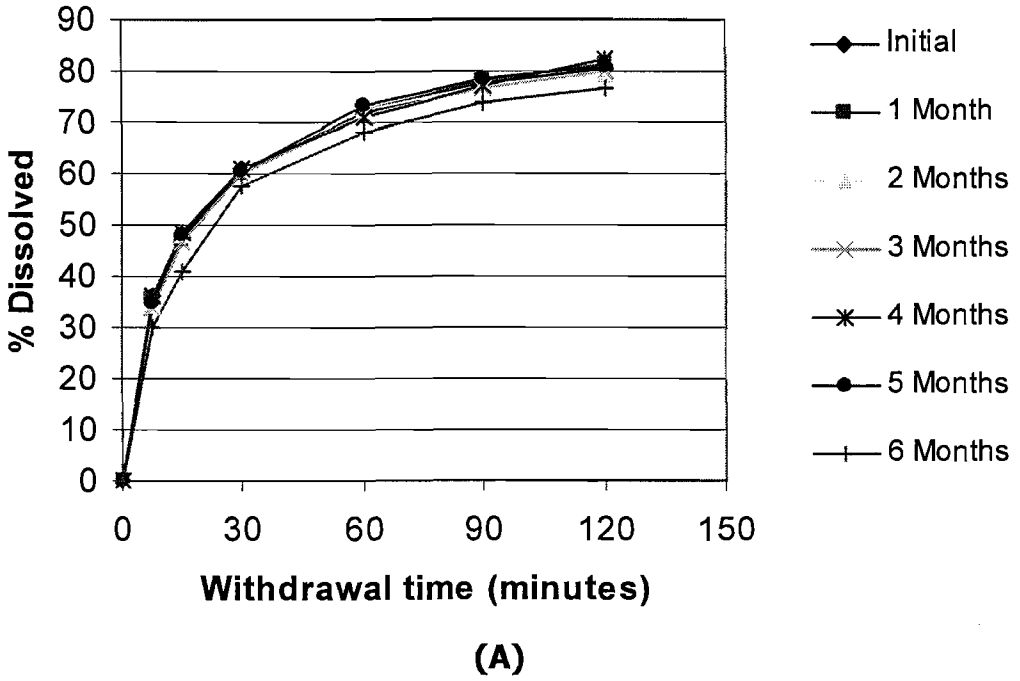
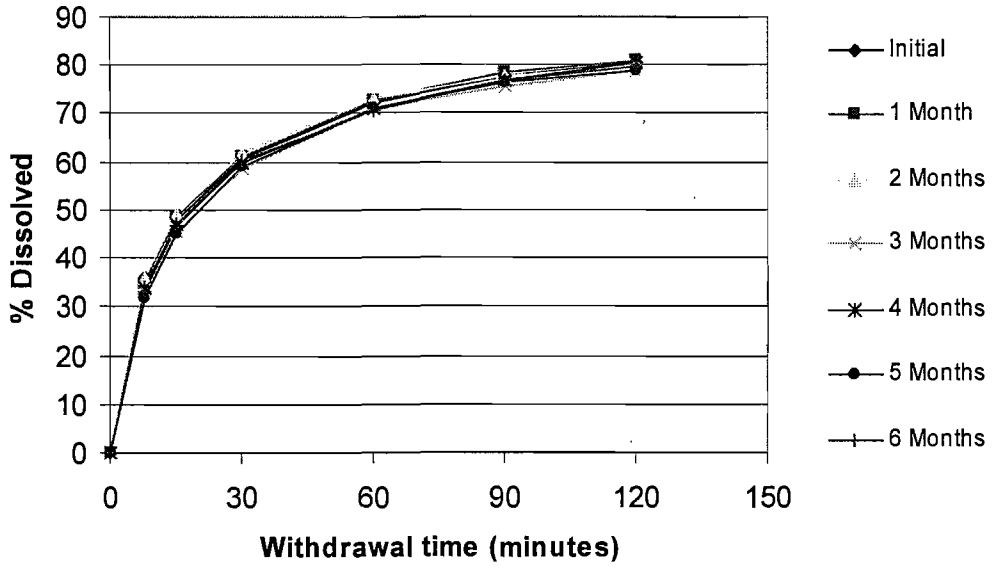


Figure 3.35 XRPD patterns of Product 7 over a period of six months – stored at 30°C & 65% RH and 40°C & 75% RH.

The dissolution profiles (figure 3.36) of the tablets confirmed that no mebendazole polymorphic transformation occurred. The dissolution profiles of the tablets at the various intervals could be considered to be similar. Similarities between the dissolution curves were calculated using the equation described by Moore *et al.* (1996:64-67). Table 3.16 indicates the f_2-values calculated.



(A)



(B)

Figure 3.36 Dissolution profiles (in 0.1 M HCl) of Product 7 when stored at (a) 30°C & 65% RH and (b) 40°C & 75% RH for a period of six months.

Table 3.16 Similarity factors (f_2-values) of dissolution profiles of Product 7 tablets when stored at 30°C & 65% RH and 40°C & 75% RH for a period of six months

Time	30°C & 65% RH	40°C & 75% RH
1 Month	96.94	94.42
2 Months	94.40	94.31
3 Months	90.27	83.34
4 Months	93.52	91.07
5 Months	94.18	79.12
6 Months	65.53	86.75

The dissolution profiles of the tablets stored at 30°C & 65% RH and 40°C & 75% RH over the period of 6 months were comparable ($100 > f_2$ values > 50) to the dissolution profile of the initially procured tablets (age = 0 months).

3.2.7.1 Summary of the polymorphic stability of Product 7

The XRPD and DRIFT-IR studies performed on the tablets revealed that the tablets primarily contained polymorph C.

This study indicated that the mebendazole present in Product 7 did not undergo any polymorphic transformations. The dissolution profiles of the tablets remained unchanged.

3.2.8 Summary of results obtained: Products 1 - 7

From the observations made during the stability studies of Products 1 - 7 it became evident that the rate and extend of the polymorphic transitions (polymorph C → polymorph A) seemed to be higher at 40°C & 75% RH compared to that observed at 30°C & 65% RH.

All products were stored in the original (intact) packaging. Products 1-6 were presented in clear blisters with foil seals, Product 7 however was presented in a HDPE securitainer. HDPE containers are renowned for their ability to protect their contents from moisture sorption due to their low moisture permeability (USP, 2006). Polyvinyl chloride (PVC) is the most commonly used blister material, which provides a nominal or zero barrier to moisture (USP, 2006). It

is interesting to note that at certain conditions Products 1-6 revealed polymorphic transition, but Product 7 remained stable, suggesting that moisture and traces of polymorph A might be catalysts for the polymorph conversions observed.

The effect of the elevated humidity on the polymorphic transition was also investigated.

3.2.9 Polymorphic stability of mebendazole in Product 2A

Product 2 was removed from its original packaging and subjected to the stability conditions (30°C & 65% RH and 40°C & 75% RH), this product will be referred to as Product 2A. The reason for the selection of Product 2, is because it did not contain any traces of polymorph A which might act as catalyst for the polymorph C → polymorph A transition. Comparison of the polymorphic transition kinetics in this product (Product 2A) to that of the product in its original packing (Product 2) will provide an insight to the effect of moisture on the stability of mebendazole polymorph C in the tablets.

The results obtained for the exposed Product 2, will now be discussed. A comparison of the polymorphic transition kinetics for the exposed (Product 2A) and unexposed (closed) Product 2, will be presented in section 3.3.

The mebendazole polymorphs present in Products 2 and 2A during the stability testing were analysed using DRIFT-IR data and are summarised in table 3.17.

As mentioned in section 3.2.2, Product 2 did not reveal any remarkable polymorph transition when exposed to 30°C & 65% RH for 6 months. Traces of mebendazole polymorph A were detected in Product 2A after 5 months as indicated by the presence of weak absorption bands at 3369 and 1731 cm^{-1} respectively (figure 3.37). Thus it seemed as if moisture played a catalytic role in the transformation of mebendazole polymorph C → polymorph A in the tablets.

The samples of Product 2 revealed traces of mebendazole polymorph A after 3 months when exposed to 40°C & 75% RH, whilst the samples of Product 2A

revealed traces of polymorph A after only one month at the same conditions. The appearance of the peaks at 3369 and 1731 cm^{-1} signified the presence of polymorph A in the tablets. The intensity of the peaks at 3369 and 1731 cm^{-1} increased significantly over the 6 month stability period. The appearance of the small peaks at 3340 and 1700 cm^{-1} after 4 months (in the exposed samples) signified that small traces of polymorph B might have been present in the tablets.

Table 3.17 Mebendazole polymorphic forms present in Product 2 and Product 2A during the 6 month stability study derived from DRIFT-IR data

Condition	Time (months)	Product 2			Product 2A		
		-NH	>C=O	Polymorph Content	-NH	>C=O	Polymorph Content
30°C & 65% RH	0	3403	1716	C	3403	1716	C
	1	3403	1717	C	3403	1716	C
	2	3403	1716	C	3403	1716	C
	3	3403	1716	C	3403	1716	C
	4	3403	1716	C	3403	1716	C
	5	3403	1716	C	3403 3369*	1716 1731*	C with traces of A
	6	3403	1716	C	3403 3369*	1716 1731*	C with traces of A
40°C & 75% RH	0	3403	1716	C	3403	1716	C
	1	3403	1716	C	3403 3369*	1716 1731*	C with traces of A
	2	3403	1716	C	3403 3369*	1716 1731*	C with traces of A
	3	3403	1716	C with traces of A	3403 3369	1717 1731	Mixture of C & A
	4	3403 3369*	1716 1731*	Mixture of C & A	3403 3369	1717 1731	Mixture of C & A
	5	3403 3369	1717 1731*	Mixture of C & A	3403 3369	1717 1731	C with traces of A
	6	3403 3369	1717 1731	Mixture of C & A	3403 3369	1717 1731	C with traces A

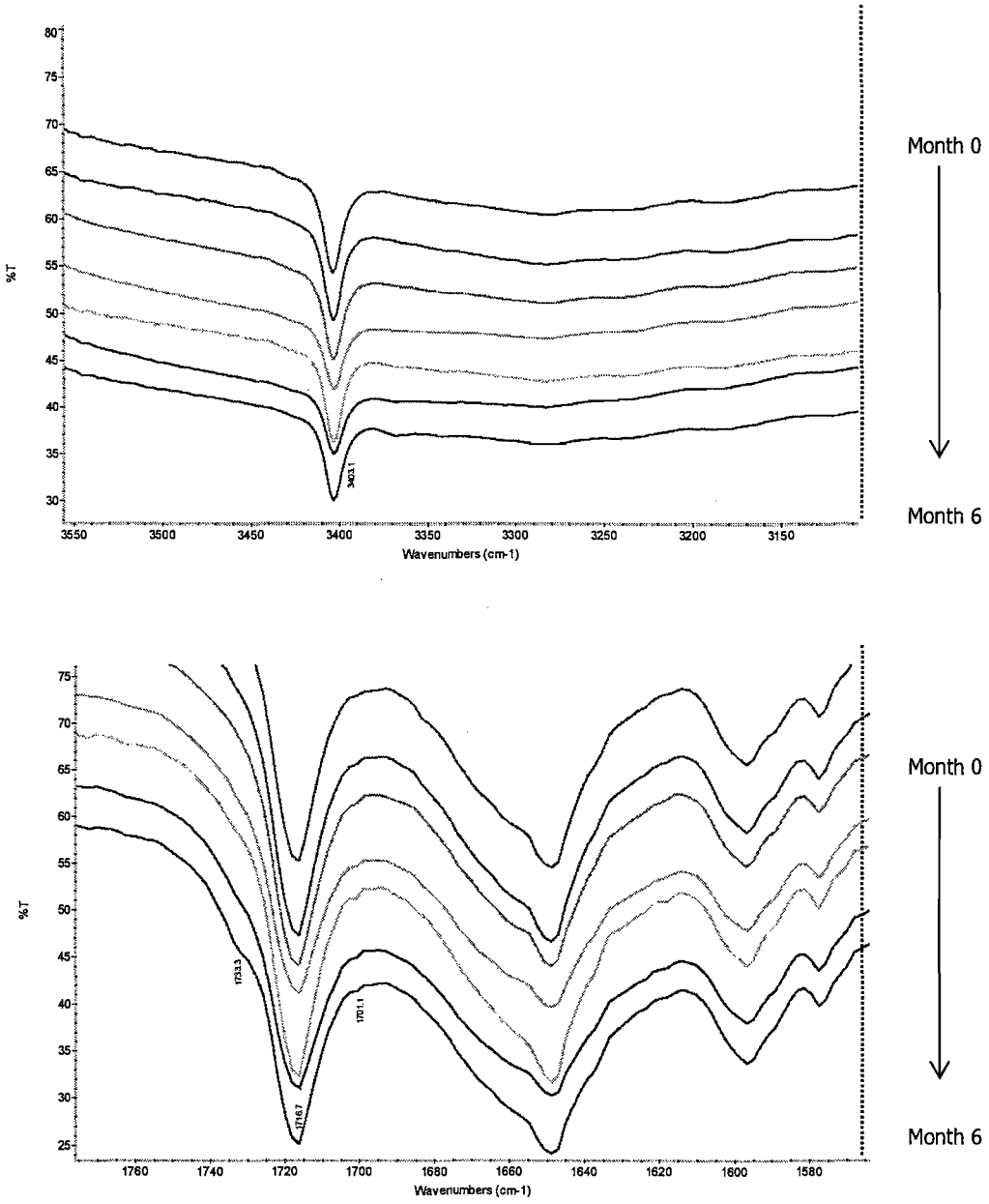


Figure 3.37 IR spectra (superimposed) of the powdered tablets of Product 2A over a period of six months – stored at 30°C & 65% RH, indicating differences in the main absorptions at the –NH stretch and the >C=O band.

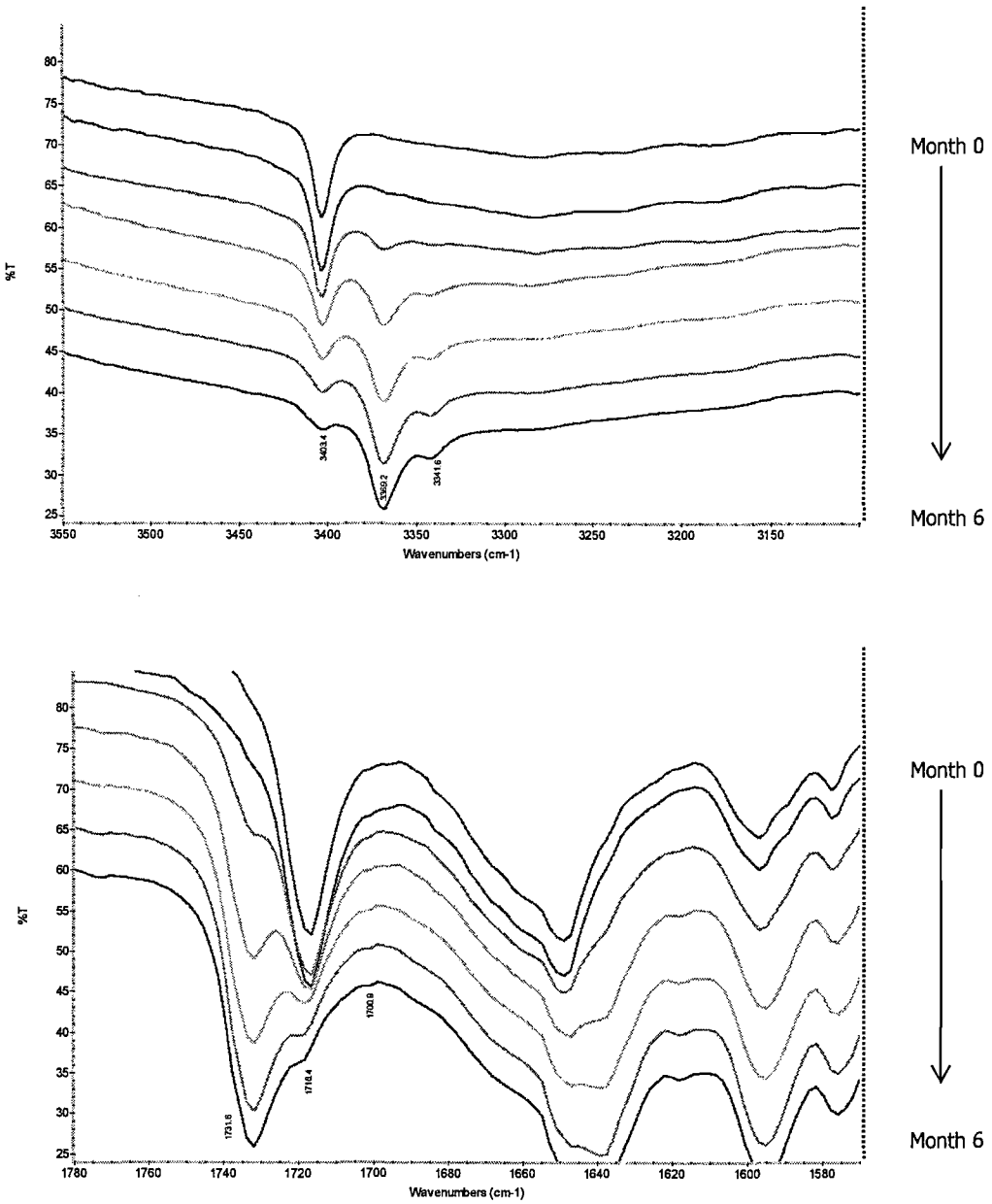


Figure 3.38 IR spectra (superimposed) of the powdered tablets of Product 2A over a period of six months – stored at 40°C & 75% RH, indicating differences in the main absorptions at the –NH stretch and the >C=O band.

The XRPD patterns of Product 2A at 30°C & 65% RH and 40°C & 75% RH during the various intervals are depicted in figure 3.39. Peak angles (°2θ) of the characteristic peaks of the mebendazole polymorphs present in the tablets are summarised in table 3.18. The characteristic peaks presented in table 3.18 confirmed that the initially procured tablets contained mebendazole polymorphic form C, due to the presence of the peak at 4.93±0.1°2θ.

Table 3.18 Mebendazole polymorphic forms present in Product 2 and Product 2A samples during the 6 month stability study derived from XRPD data

Condition	Time (months)	Product 2			Product 2A		
		A (°2θ)	C (°2θ)	Polymorph Content	A (°2θ)	C (°2θ)	Polymorph Content
30°C & 65% RH	0	-	4.92	C	-	4.92	C
	1	-	4.93	C	-	4.92	C
	2	-	4.94	C	-	4.96	C
	3	-	4.89	C	-	4.89	C
	4	-	4.86	C	7.62*	4.90	C with traces of A
	5	-	4.84	C	7.74*	4.89	C with traces of A
	6	-	4.83	C	7.63*	4.87	C with traces of A
40°C & 75% RH	0	-	4.92	C	-	4.92	C
	1	-	4.90	C	-	4.92	C
	2	-	4.96	C	7.69	4.94	C with traces of A
	3	7.66*	4.87	C with traces of A	7.68	4.93	Mixture of C and A
	4	7.62	4.90	Mixture of C & A	7.64	4.87	Mixture of C and A
	5	7.63	4.90	Mixture of C & A	7.63	4.87	Mixture of C and A
	6	7.64	4.88	Mixture of C & A	7.64	4.89	Mixture of C and A

The appearance of the very weak peaks at 7.67±0°2θ (only detectable once a $K\alpha_2$-strip and background subtraction performed on raw data) in the XRPD patterns of the exposed sample stored at 30°C & 65% RH revealed the presence of mebendazole polymorph A traces in the tablets after 4 months, confirming the DRIFT-IR observations. No significant traces of mebendazole polymorph A were detected in the XRPD patterns of Product 2 when stored at 30°C & 65% RH.

Traces of mebendazole polymorph B were detected in the DRIFT-IR spectra of the tablets of Product 2A stored at 40°C & 75% RH (figure 3.38), however due to the poor crystalline properties of mebendazole polymorph B, these traces were not easily detected by XRPD analysis. The poor crystalline properties of polymorph B will be discussed in section Chapter 4.

It can thus be concluded that the tablets subjected to 40°C & 75% RH for the first month contained mebendazole polymorph C. After 1 month the tablets consisted mainly of polymorph C, traces of polymorph A and small traces of polymorph B (Polymorph C >>>> Polymorph A >> Polymorph B). The intensity of the 4.93±0.1°2θ peak decreased and that of the 7.67±0.1°2θ peak increased as a function of time, indicating that the fraction of mebendazole polymorph C in the tablet was transformed into polymorph A. The formation of the polymorph B fractions will be investigated and discussed in chapter 4.

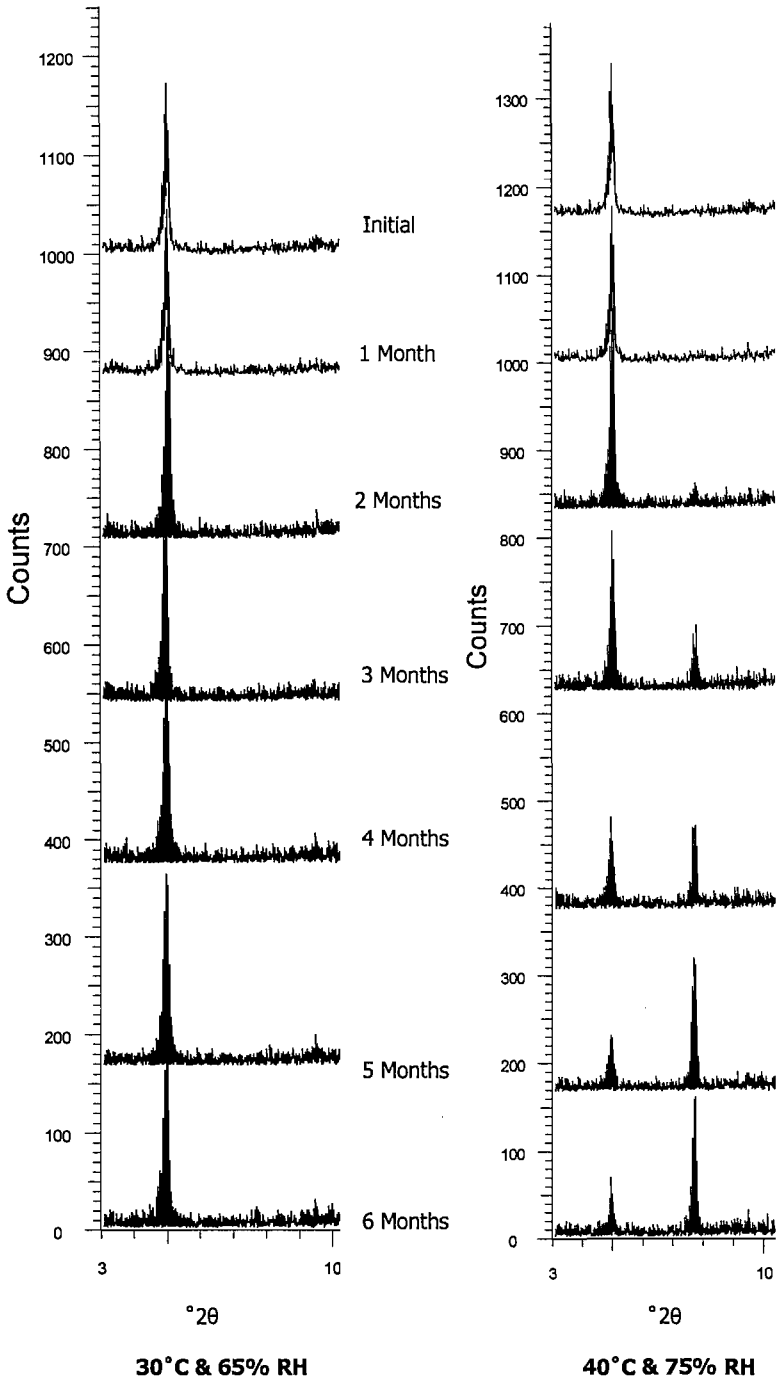


Figure 3.39 XRPD patterns of Product 2A over a period of six months – stored at 30°C & 65% RH and 40°C & 75% RH.

The dissolution profiles of Product 2A kept at 30°C & 65% RH and 40°C & 75% RH at the various time intervals are illustrated in figure 3.40. A slight decrease in the % mebendazole dissolved (Q) after 120 minutes was observed for the exposed tablets stored at 30°C & 65% RH compared to Q at

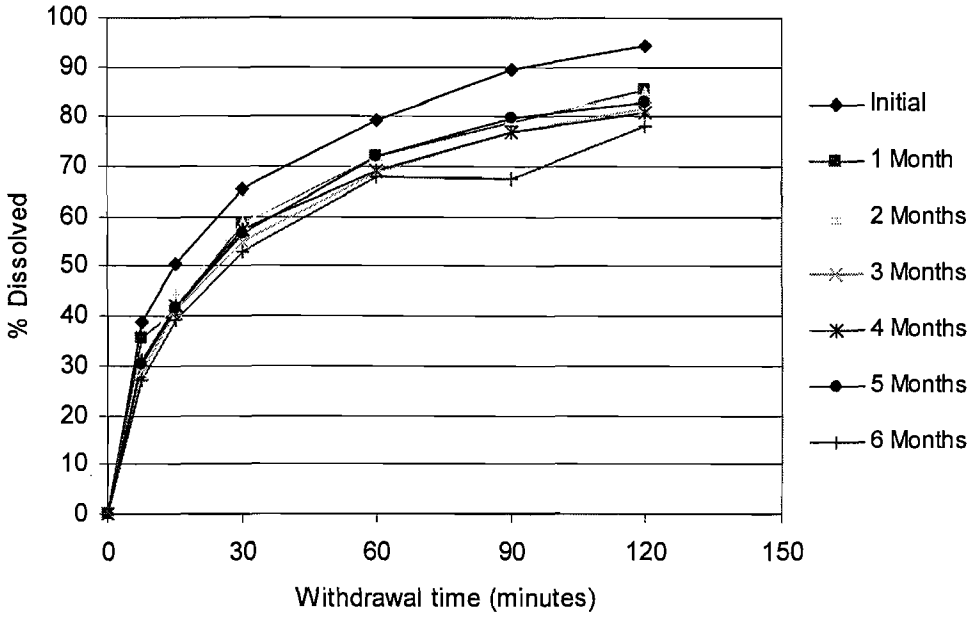
120 minutes for the initially procured tablets (age = 0 months), confirming the polymorph transition observed. Table 3.19 indicates the f_2-values calculated.

Table 3.19 Similarity factors (f_2-values) of dissolution profiles (in 0.1 M HCl) of Product 2A when stored at 30°C & 65% RH and 40°C & 75% RH for a period of six months

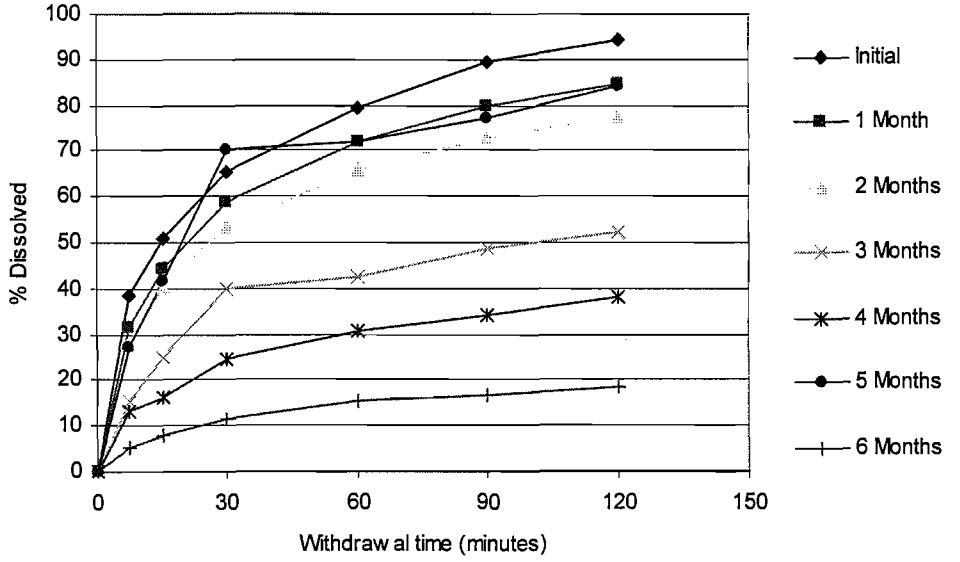
Time	30°C & 65% RH	40°C & 75% RH
1 Month	54.44	54.71
2 Months	54.61	43.12
3 Months	47.96	23.84
4 Months	49.00	17.35
5 Months	51.52	50.85
6 Months	41.64	11.34

The similarity between the dissolution profiles of the test samples at the various intervals and that of the initial dissolution profile decreased due to the appearance of the mebendazole polymorph A in the tablets stored at 30°C & 65% RH.

The dissolution profiles of the tablets stored at 40°C & 75% RH (figure 3.40 - b) were significantly reduced due to the polymorphic transformation (polymorph C → polymorph A).



(A)



(B)

Figure 3.40 Dissolution profiles (in 0.1 M HCl) of Product 2A tablets when stored at (a) 30°C & 65% RH and (b) 40°C & 75% RH for a period of six months.

The dissolution profile of the tablets stored at 40°C & 75% RH for the first month was comparable (100 > f_2 values > 50) to the dissolution profile of the initially procured tablets (age = 0 months). The dissolution profile of the samples after two months (2-4 months) revealed a lower Q at 120 minutes due to the presence of the less soluble polymorph A. The increase in f_2 values observed for the sample at 5 months (stored at 40°C & 75% RH) could be attributed to the presence of the more soluble polymorph B (Himmelreich *et al.*, 1977:123) in the tablets or a potential experimental error.

After six months the intensity of the 7.67±0.1°2θ peak (characteristic of polymorph A) in the XRPD pattern (figure 3.39) was significantly higher compared to that of the 4.93±0.1°2θ peak (characteristic of polymorph C), suggesting that the tablet contained polymorph A >>> polymorph C > polymorph B, thus explaining the decrease in the Q at 120 minutes after 6 months.

3.2.9.1 Summary of the polymorphic stability of Product 2A

The initial analysis performed on the tablets revealed that the tablets contained mebendazole polymorph C.

The tablets of Product 2A showed polymorphic instability, especially when stored at 40°C & 75% RH, where traces of polymorph A were detected in the tablets after 1 month, and possible traces of polymorph B after 5 months, as indicated by DRIFT-IR data.

Traces of polymorph A were detected in the exposed tablets stored at 30°C & 65% RH after 4 months.

From the results obtained in this section it can be concluded that the storage of mebendazole tablets at elevated temperatures and relative humidities induced polymorphic transitions which influenced the dissolution behaviour significantly. It was also clear that the packaging of Product 2 provided some protection against the polymorph transformation (polymorph C→ polymorph A), when compared to the increased rate and extend of polymorph transformation observed in Product 2A. Moisture seemed to be a catalyst for

this polymorphic transformation process, however no reference could be found in the literature available at the time of this study to substantiate the hypothesis. This hypothesis will be investigated in Chapter 4.

3.3 Discussion of the polymorphic transitions observed in the products

From the results discussed in section 3.2 it became clear that mebendazole polymorph C present in some of the commercially available products underwent polymorphic transition that lead to the formation of mebendazole polymorph A or mixtures polymorph A, B and C in the products.

In this section the kinetics of the polymorph transition (polymorph C → polymorph A) that occurred in some of the products will be investigated and discussed.

3.3.1 Quantitative investigation of the conversion of mebendazole polymorph C → polymorph A in commercially available tablets

The relative ratios of mebendazole polymorph A and C present in the tablets were calculated from the XRPD and DRIFT-IR data.

3.3.1.1 Calculating the ratio of polymorph A and C content relative to the total polymorph content in the tablet from XRPD data

The ratios of polymorph A and C content relative to the total polymorph content in a product were calculated from the XRPD data using the following equations:

$$Polymorph\ A/(A+C) = \frac{I_A}{I_A + I_C}$$

$$Polymorph\ C/(A+C) = \frac{I_C}{I_A + I_C}$$

Where:

Polymorph A/(A+C) : ratio of polymorph A content relative to the total mebendazole polymorph content in the product

Polymorph C/(A+C) : ratio of polymorph C content relative to the total mebendazole polymorph content in the product

I_A : Intensity of the 7.67±0.1°2θ diffraction peak, characteristic of polymorph A

I_C : Intensity of the 4.93±0.1°2θ diffraction peak, characteristic of polymorph C

For example: Figure 3.41 illustrates the characteristic diffraction peaks of polymorph C and A (at 4.93±0.1°2θ and 7.67±0.1°2θ respectively) and their intensities for mebendazole polymorph A and C in Product 3 at month: 0, 3 and 6 at 40°C & 75% RH. The decrease in the polymorph C content is not clearly visible in figure 3.41, due to differences in the crystallinity of the samples at the various intervals. The *fractions of the polymorphic forms relative to the total content* was used for quantification, which clearly indicated the decrease.

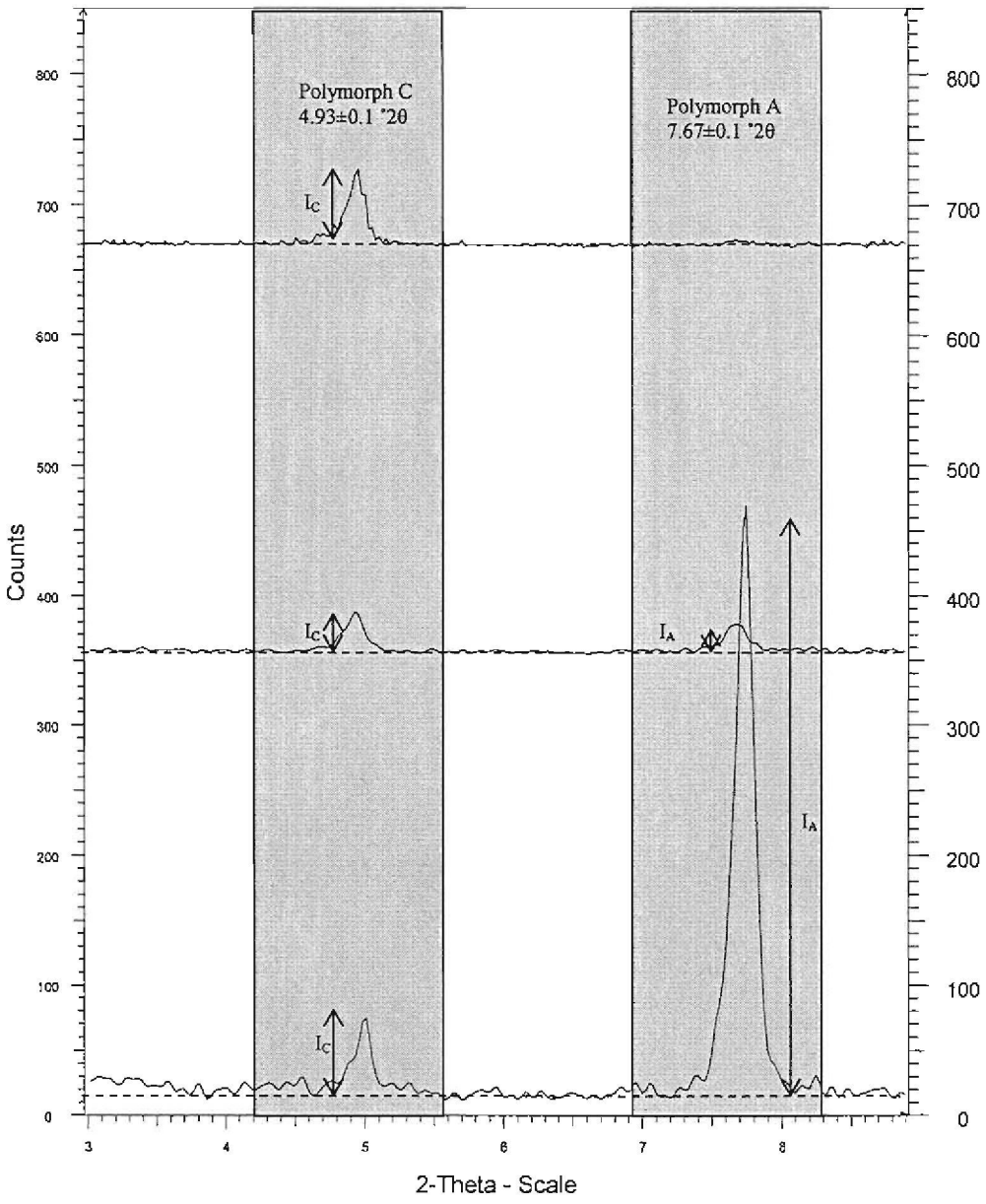


Figure 3.41 Characteristic diffraction peaks and their intensities for mebendazole polymorphs A and C present in Product 3 at 0 (top), 3 (middle) and 6 (bottom) months when stored at 40°C & 75% RH.

3.3.1.2 Calculating the ratio of polymorph A and C content relative to the total polymorph content in the tablet from DRIFT-IR data

The ratios of polymorph A and C content relative to the total polymorph content in the product were calculated from the DRIFT-IR data using the following equations:

$$Polymorph\ A/(A+C) = \frac{AUC_A}{AUC_A + AUC_C}$$

$$Polymorph\ C/(A+C) = \frac{AUC_C}{AUC_A + AUC_C}$$

Where:

Polymorph A/(A+C) : ratio of polymorph A content relative to the total mebendazole polymorph content in the product

Polymorph C/(A+C) : ratio of polymorph C content relative to the total mebendazole polymorph content in the product

AUC_A : Area of the absorption peak present at 3370 cm^{-1}, characteristic of polymorph A

AUC_C : Area of the absorption peak present at 3410 cm^{-1}, characteristic of polymorph C

For example: figure 3.42 illustrates the characteristic frequencies at 3370 cm^{-1} and 3410 cm^{-1} of polymorph A and polymorph C respectively and the areas thereof observed in the DRIFT-IR spectra of Product 3 at 0, 3 and 6 months, when stored at 40°C & 75% RH.

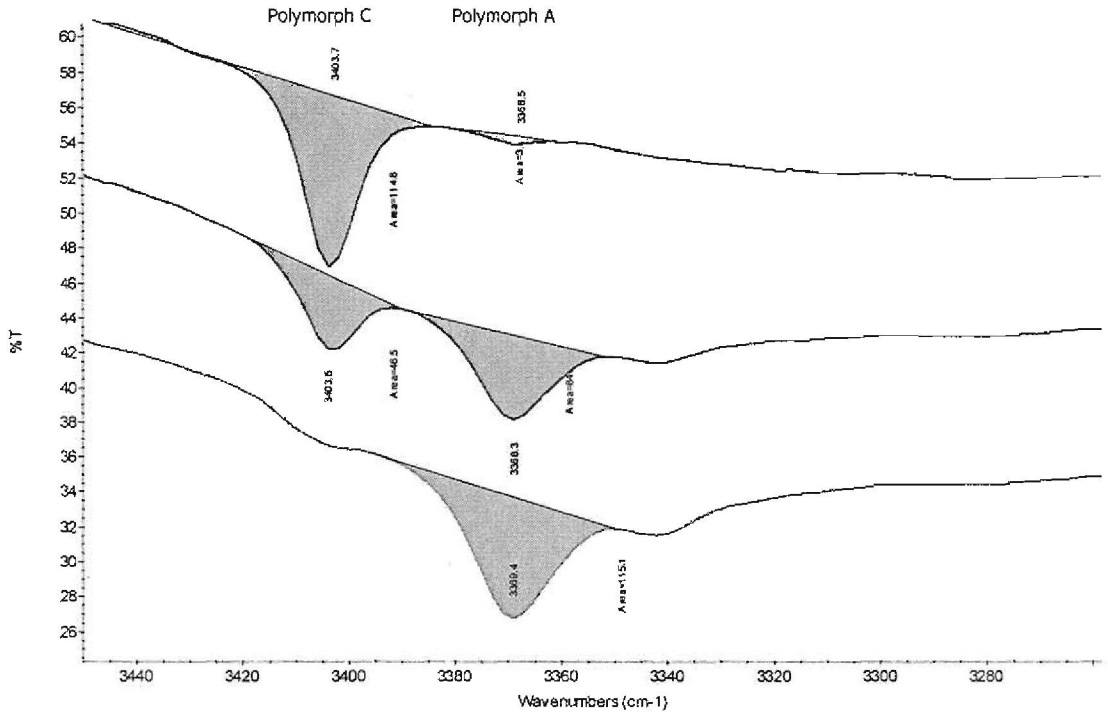


Figure 3.42 Characteristic stretching frequencies (cm^{-1}) and the areas thereof in the DRIFT-IR spectra Product 3 at 0 (top), 3 (middle) and 6 (bottom) months indicating the decreasing polymorph C and increasing polymorph A content (stored at 40°C & 75% RH).

The polymorph A/(A+C) and polymorph C/(C+A) were calculated for all the products and plotted against time (0-6 months). This provided an indication of the relative mebendazole polymorph content in a product at a given time. Figure 3.43 illustrates the ratio of polymorph A and C content relative to the total mebendazole polymorph content in Product 7 (at 30°C & 65% RH) and Product 3 (at 40°C & 75% RH) calculated from the DRIFT-IR and XRPD data respectively.

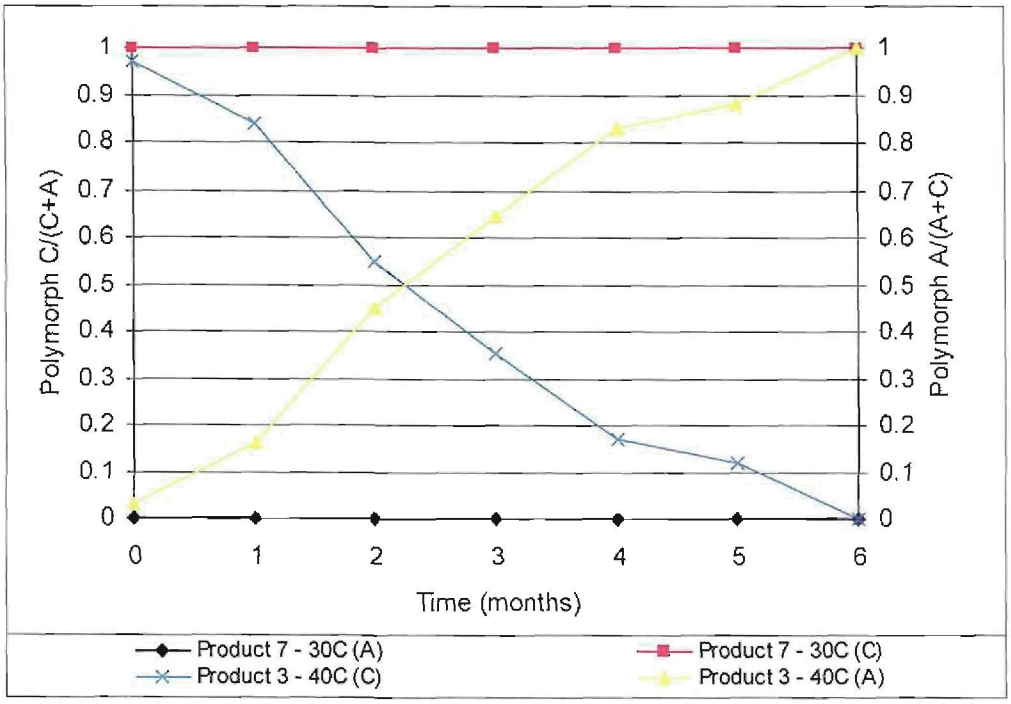
The polymorph A/(A+C) values of Product 7 (calculated from the DRIFT-IR data) remained 0.00, and that of polymorph C/(A+C) = 1.00 during the six months, which indicated that no polymorphic transition occurred when Product 7 was stored at 30°C & 65% RH. The transformation of the mebendazole polymorph C fraction into polymorph A in Product 3 (stored at 40°C & 75% RH) during the six months is illustrated in figure 3.43 (b). The decrease in the polymorph C content (polymorph C/(A+C) from 0.97 to 0.00

and simultaneous increase in polymorph A content (polymorph A/(A+C) from 0.03 to 1.00) is illustrated.

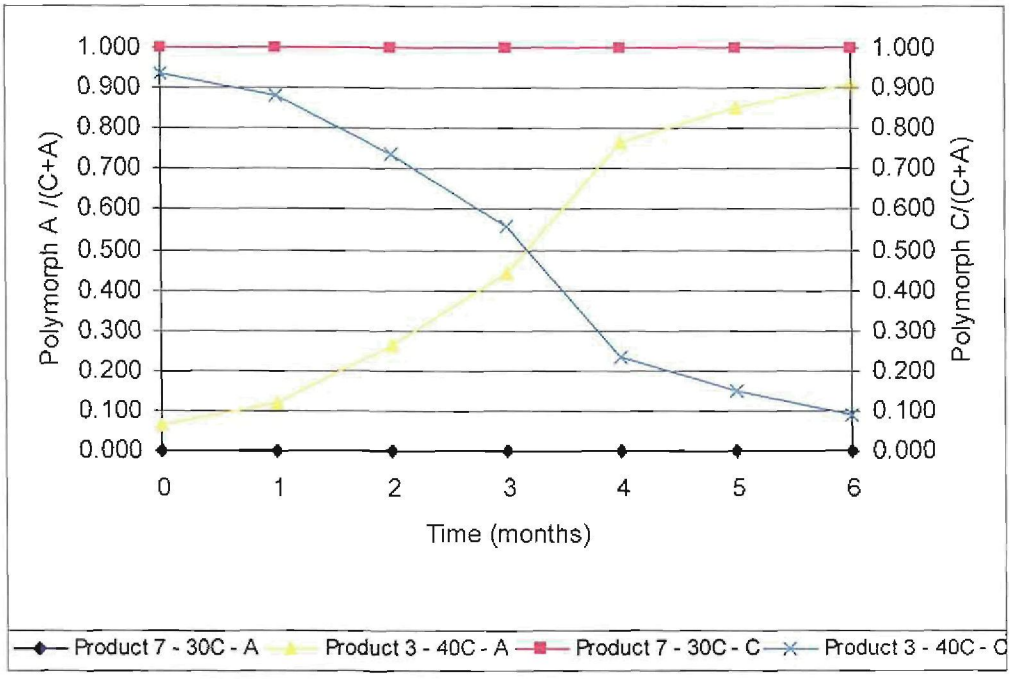
The overall-shape and distribution of polymorph A/(A+C) and polymorph C/(A+C) vs. time graphs for Product 7 and Product 3 calculated from the DRIFT-IR and that XRPD data were comparable.

The polymorph ratio (calculated from DRIFT-IR and XRPD data for polymorph A & C) at the various intervals differed slightly. Quantitative analysis of the mebendazole phases present in solids using XRPD techniques may be complicated due to the absorption effect which is normally different for phases with different chemical composition and gravimetric density (Pecharsky and Zavalij, 2005:385). The presence of the various unknown tablet excipients may therefore interfere with the detection of the mebendazole crystal phases that can introduce detection errors.

However, due to the features of the infrared spectra of the mebendazole polymorphs it has emerged as the preferred method to identify mebendazole polymorphic forms (Liebenberg *et al.*, 1998:487 and Bunaciu *et al.*, 2002:647). These studies have also shown that DRIFT-IR data for the polymorphs are not influenced by commercially used pharmaceutical excipients.



(a)



(b)

Figure 3.43 Ratio of the polymorph A and polymorph C content relative to the total mebendazole polymorph content in Product 7 (30°C & 65% RH) and Product 3 (40°C & 65% RH) calculated from (a) DRIFT-IR and (b) XRPD data.

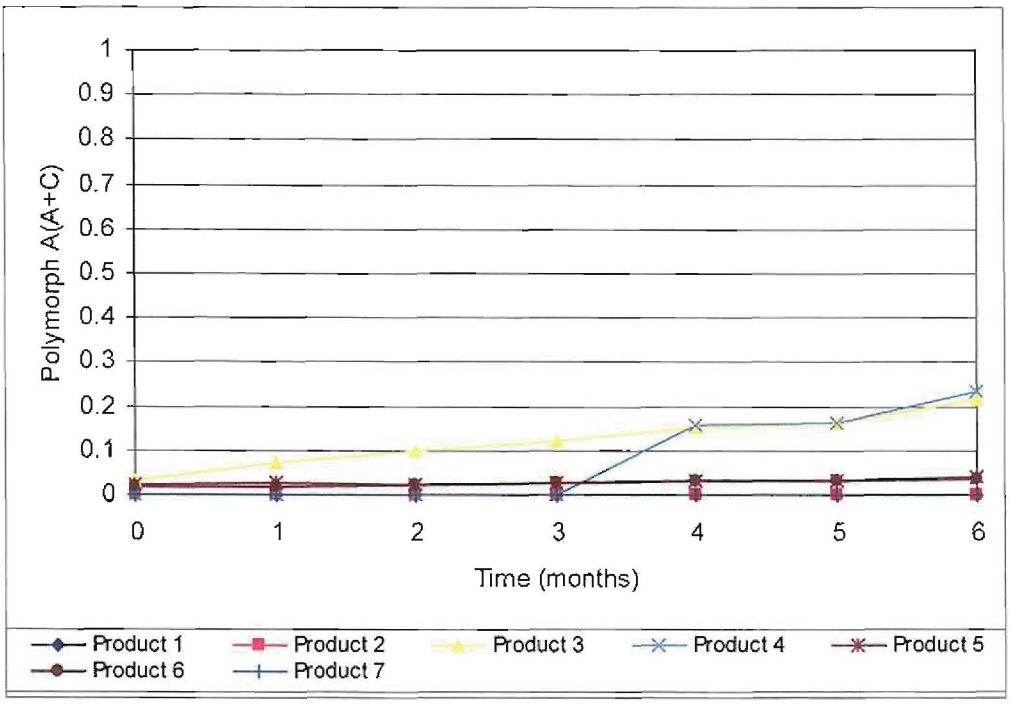
Based on these initial observations it was decided to use polymorph A/(A+C) ratios (calculated from the DRIFT-IR data) vs. time as a way to compare the transformation of polymorph C to polymorph A in the various products. The polymorph A/(C+A) vs. time plots (figure 3.44) indicates the progressive increase of the mebendazole polymorph A content in the products due to the polymorph transition (polymorph C → polymorph A). Overall the transformation of polymorph C to A was more pronounced in the products stored at 40°C & 75% RH compared to those stored at 30°C & 65% RH.

From a closer inspection of the graphs the following observations were made from the polymorph stability testing of the various products at 30°C & 65% RH and 40°C & 75% RH (figure 3.44):

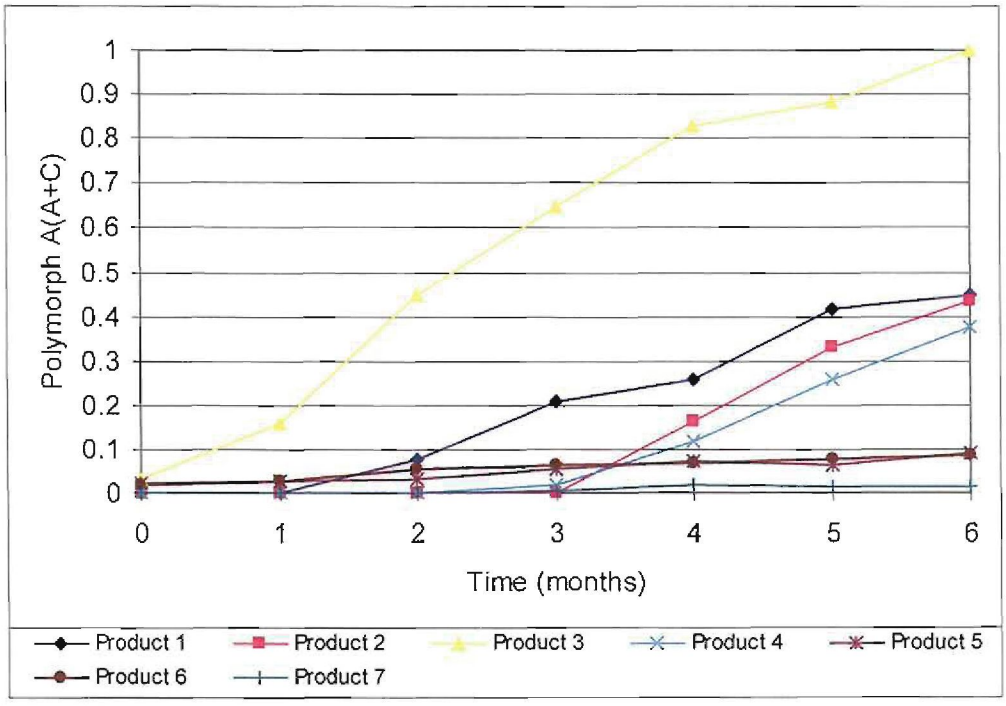
- Products 1,2,4,5 and 7 did not reveal significant polymorphic transition during the 6 months when stored at 30°C & 65%RH.

  The polymorphic transition in Product 3 and Product 4 at 30°C & 65% RH was only detected after 1 month for Product 3 and after 3 months for Product 4. All the products, except Product 7 revealed polymorphic transitions when exposed to 40°C & 75% RH for 6 months.

- The rate and extend of the polymorphic transitions of polymorph C to polymorph A at 40°C & 75% RH was faster and more pronounced compared to the transitions observed at 30°C & 65% RH, for example the ratio of polymorph A relative to the total polymorph content (i.e. A/(A+C)) for Product 3 was found to be approximately five times higher (1.00) at 40°C & 75% RH compared to the ratio (0.21) at 30°C & 65% RH.



(A)

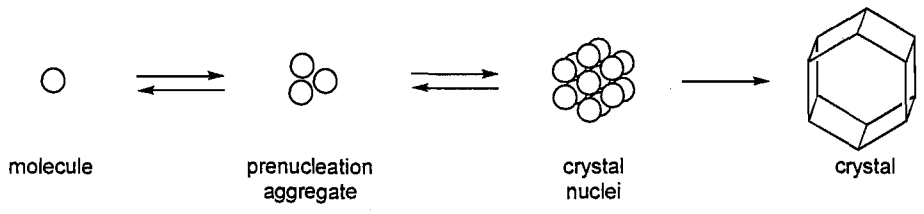


(B)

Figure 3.44 Ratio of polymorph A relative to the total polymorph content for Products 1-7 using DRIFT-IR data at : (a) 30°C & 65% RH and (b) 40°C & 75% RH.

3.3.2 Kinetics of mebendazole polymorph C → polymorph A conversion in commercially available tablets

Recrystallisation occurs through nucleation as illustrated in figure 3.45 which shows that overall crystallisation, r_C, depends on nucleation and occurs at a temperature intermediate between the preferred temperatures for nucleation and growth (Johnson & Mehl, 1939:416-446). Within this model, three types of recrystallisation can be distinguished: static recrystallisation, metadynamic recrystallisation and dynamic recrystallisation. A minimum strain (deformation) is needed to initiate *static recrystallisation*. This deformation must be sufficient to create the recrystallising nuclei and to sustain their growth. Increasing the deformation reduces the incubation period and increases the rate of recrystallisation. Eventually a critical strain is reached above which recrystallisation starts before the end of deformation. *Metadynamic recrystallisation* refers to the case in which, the nuclei are formed during deformation and consequently no incubation period is observed. In the case of *dynamic recrystallisation*, repeated nucleation and growth occur during deformation.(Hancock & Zografi, 1997:9)



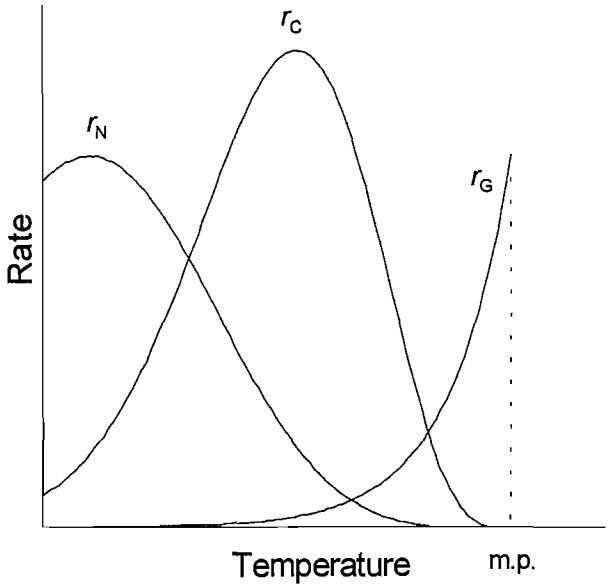


Figure 3.45 Theoretical representation showing that recrystallisation occurs through nucleation (applicable to the Prout-Tompkins and JMAEK kinetic models). When the rate of crystallisation is plotted as a function of temperature then the plot r_G represents the crystal growth rate, r_N the crystal nucleation rate, and r_C the overall crystallisation rate (adapted and reproduced from Hancock & Zografi, 1997:9).

3.3.2.1 Models for Polymorphic Conversion

When we look at the transformation of mebendazole polymorph C it can be considered that the growth stage of the parent phase (polymorph C) will undergo a complete transformation to a new equilibrium phase (polymorph A). The amount of new equilibrium phase will depend on time, growth rate and the number of nuclei. Most often the equations used to describe the kinetics of transformation are grouped according to the shape of the isothermal extent of transformation (fraction, α) versus time curves as acceleratory, sigmoid or deceleratory. In the case of the transformation of mebendazole polymorph C to polymorph A in the tablets (figure 3.43 and figure 3.44) the shape of the curves approximates that of sigmoidal curves.

Two equations for the kinetics of reactions involving nucleation according to sigmoidal α-time curves have been derived and are commonly used to describe the kinetics of polymorphic transformations (Byrn *et al.*, 1999:444).

3.3.2.1.1 Prout-Tompkins model

If the rate of the polymorphic transformation is assumed to be controlled by linearly growing nuclei that branch into chains and are terminated more rapidly as the number of nuclei increase, then the kinetics of transformation can be described by the Prout-Tompkins equation (Prout and Tompkins, 1944:488-498; Brown and Glass, 1999:129-137).

$$\frac{d\alpha}{dt} = k\alpha(1-\alpha) \qquad (1)$$

This equation upon integration gives

$$\ln\left[\frac{\alpha}{1-\alpha}\right] = kt + c \qquad (2)$$

where *c* is a constant. This derivative form shows clearly the dependence of the rate on both the amount of original crystal form left and the amount of the new crystal form produced. The transformation is therefore an autocatalytic process. Sometimes the kinetics of certain transformations are better described by a *modified* Prout-Tompkins equation

$$\ln\left[\frac{\alpha}{1-\alpha}\right] = k\ln(t) + c \qquad (3)$$

Where sigmoid α-time curves have been obtained there has been a surprising lack of examination of alternative kinetic expressions, with the Prout-Tompkins equation being accepted as an empirical method of comparing this type of transformations (Brown and Glass, 1999:130). However, the equation is not particularly convenient for application in kinetic analysis because of its indeterminate nature at small and large extremes of the extent of transformation, α. This is important for comparing the mebendazole

polymorph C → A conversion in the tablets since this conversion was limited in some products, $\alpha_{max} \approx 10$ %.

3.3.2.1.2 *Johnson-Mehl-Avrami-Erofeev-Kolmogorov* (JMAEK) model

Another very popular kinetic model applied to solid state transformations has been the Avrami model, developed independently by several workers and thus referred to as the Johnson-Mehl-Avrami-Erofeyev-Kolmogorov (JMAEK) model (Avrami, 1939:1103-1112, Avrami, 1940:212-224, Avrami, 1941:177-184, Johnson & Mehl, 1939:416, Erofeev, 1946:513, Kolmogorov, 1937:355-359). First, for simplicity, suppose that all the nuclei grow as spheres with constant velocity, *v*, and are nucleated at some different time *T*. The nucleus which nucleated at some time *T* will have a volume at time, *t*:

$$V(t,T) = \frac{4\pi}{3} R^3 = \frac{4\pi}{3} v^3 (t-T)^3 \tag{4}$$

If the nuclei do not interfere (collide during growth), then the total volume of transformed material is the sum of all the nuclei (N) which have created at times T

$$V_{total}(t) = \int_0^t \frac{4\pi}{3} v^3 (V_{total} N)(t-T)^3 \, dt \tag{5}$$

The volume fraction, α, of transformed material is:

$$\alpha = \frac{\pi}{3} N v^3 t^4 \tag{6}$$

If the nuclei do interfere with each other, a condition which would apply at either high density of nucleation sites or long times, i.e. during stability testing, then the above equation must be modified to account for volumes of particles which are changing. If the particles are nucleated independently, then the volume fraction is given by the *Avrami* equation:

$$\alpha = 1 - \exp(-\frac{\pi}{3} N v^3 t^4) \quad (7)$$

This equation represent site saturated 3D growth. However, depending on whether all the nuclei appear at one time, or growths dimensionally, the general equation for volume transformed transformation looks like:

$$\alpha = 1 - \exp(-kt^n) \quad (8)$$

Upon integration

$$[\ln(1-\alpha)]^n = kt \quad (9)$$

This equation summarizes transformation kinetics for any case where $\alpha \rightarrow 1$ as $t \rightarrow \infty$. The characteristics of the kinetics is that of a "S-curve", i.e. slow at first, then accelerating, then decelerating. Values of *k* and *n* are diagnostic of the crystallisation mechanism. The equation has been derived for spheres, discs and line segments, representing three-, two- and one-dimensional form of isotropic constant rate growth. In the case of two dimensional (planar) growth *n = 3* for sporadic nucleation and *n = 2* for predetermined nucleation. A very useful way to analyze the kinetics of transformation is to plot the quantity $-\ln(1-\infty)$ versus time on a double logarithmic plot. The slope of the line is then the exponent *n*. To do this the Avrami equation can be linearized to:

$$\ln\left(\ln\frac{1}{1-\alpha}\right) = \ln k + n \ln t \quad (10)$$

In figures 3.46 and 3.47 the Prout-Tompkins and JMAEK fits for the isothermal conversion of mebendazole polymorph C → A in the tablets are shown for those products where at least 5 % transformation was observed within 3 months. In table 3.20 the fit parameters for the two models are compared.

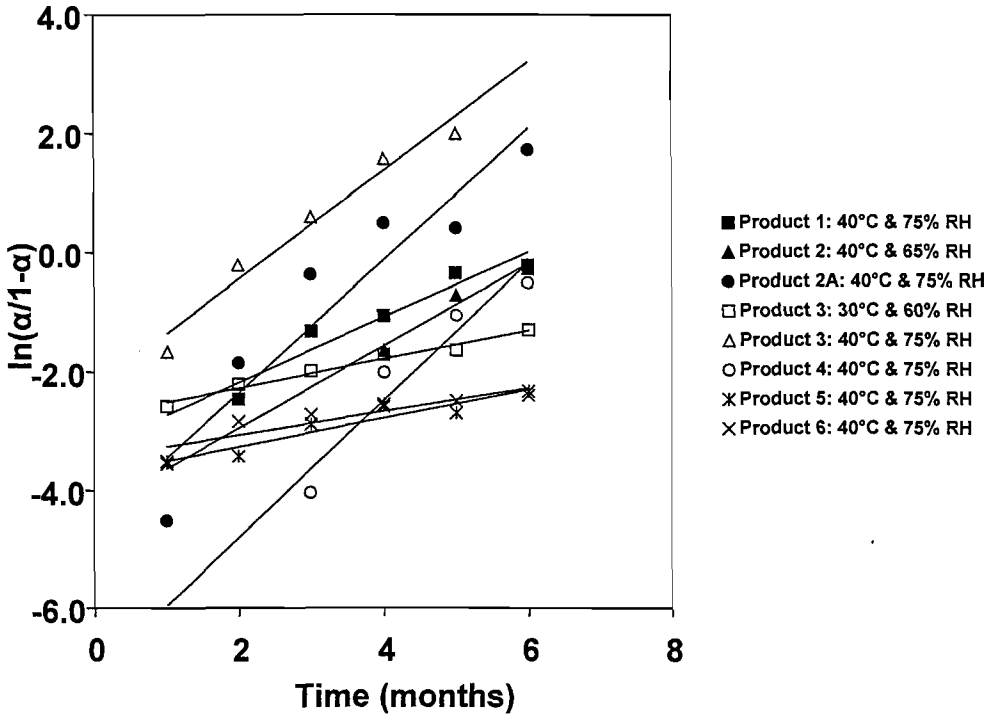


Figure 3.46 Prout-Tompkins plots for mebendazole products. The slopes of the fitted lines represent the rate constant for polymorph C → A conversion.

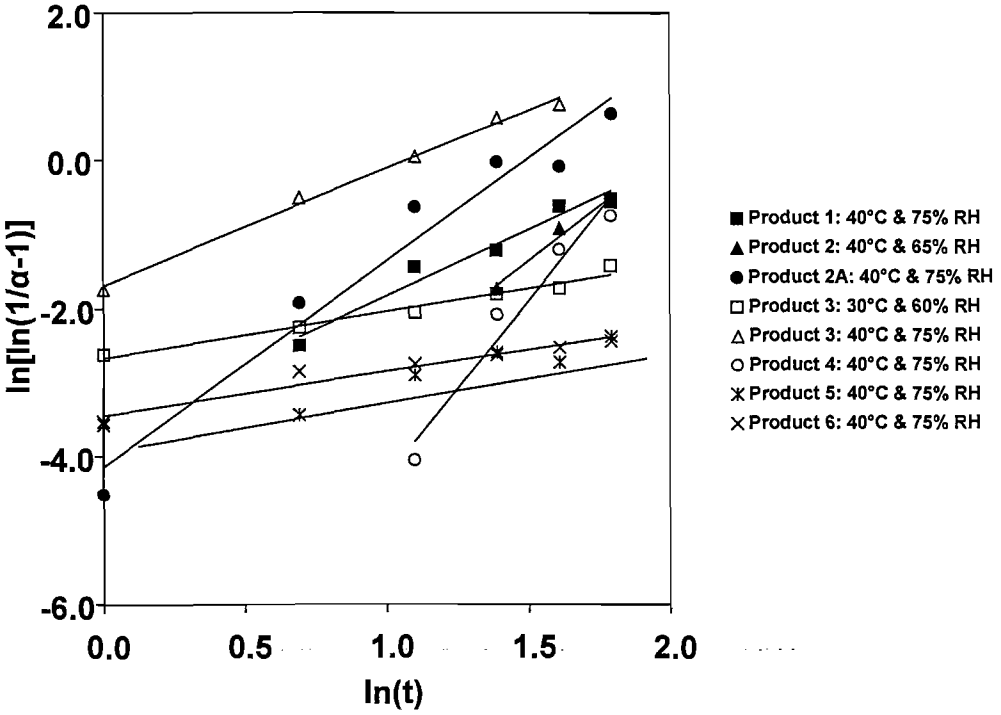


Figure 3.47 Avrami plots for the mebendazole products. Data shown correspond to the transformed A-volume fraction between 3% and 90 %. The slopes of the lines represent the Avrami exponents, n, and the y-intercept the natural logarithm of the rate constant.

Table 3.20 Comparison of the fit parameters for mebendazole polymorph C → polymorph A conversion in commercial products according to the Prout-Tompkins and JMAEK models of solid-state transformation

Product	Storage Conditions	Prout-Tompkins		JMAEK		
		k	r^2	ln*k*	*n*	r^2
1	40°C & 75% RH	0.547	0.9204	-3.623	1.8	0.9645
2	40°C & 75% RH	0.692	0.9625	-5.735	2.9	0.9746
2A	40°C & 75% RH	1.108	0.8788	-4.147	2.8	0.9603
3	30°C & 65% RH	0.318	0.9049	-2.675	0.6	0.9694
3	40°C & 75% RH	1.576	0.9943	-1.689	1.6	0.9943
4	40°C & 75% RH	1.158	0.9222	-6.871	1.1	0.9069
5	40°C & 75% RH	0.243	0.8955	-3.660	0.7	0.9420
6	40°C & 75% RH	0.600	0.9375	-3.728	0.3	0.9177

For several products at 30°C & 65% RH and some at 40°C & 75% RH no crystal transformation was observed. In addition for all the products that showed polymorph C → A conversion the start of the crystallisation process was found to be preceded by a temperature-dependent *incubation time*, this leads to the sigmoidal curves shown in figure 3.43 and figure 3.44. The *incubation time*, by definition, is the time that passes before the first nuclei of the new phase are formed. In table 3.20 the model fit results for those products showing significant transformation within 6 months, are listed. The data in table 3.20 show that for the transformation of mebendazole polymorph C to polymorph A in tablets the JMAEK model gives better and less variable correlation constants (0.954±0.030) compared to the Prout-Tompkins model (0.927±0.037). For this reason the results obtained from the JMAEK model was used to calculate stability constants (table 3.21) and to determine

difference in the rate of polymorph C → A conversion in the seven products stored at 30°C & 65 % RH and 40°C & 75 % RH. In table 3.20 for the JMAEK equation fit the isothermal parameters, *k* is known as the Avrami coefficient (also the rate constant) and n as the Avrami exponent.

Table 3.21 Stability parameters calculated using the JMAEK model for the mebendazole polymorph C → A conversion in the tablets

Product	Storage Conditions	JMAEK Stability Parameters		
		k **($month^{-1}$)**	**$t_{1/2}$ (months)**	**t_{90} (months)**
1	40°C & 75% RH	0.0267	26.0	3.9
2	40°C & 75% RH	0.0032	216.6	32.8
2A	40°C & 75% RH	0.0158	43.9	6.6
3	30°C & 65% RH	0.0689	10.1	1.5
3	40°C & 75% RH	0.1848	3.8	0.6
4	40°C & 75% RH	0.0011	630.0	95.5
5	40°C & 75% RH	0.0258	26.9	4.1
6	40°C & 75% RH	0.0240	28.9	4.4

When the rate constants, *k*, calculated using JMAEK kinetics (table 3.21) are compared it is clear that the rate of polymorph C → A conversion was faster at 40°C & 75% RH than at 30°C & 65% RH and that Product 3 was the least stable. Even at 30°C the rate constant for polymorph transformation in Product 3 was 2.5 times faster than for the next fastest transformation Product 1 at 40°C & 75% RH. The fastest conversation was observed for Product 3 at 40°C & 75% RH. The rate of conversion when the tablets were stored under these conditions was 2.7 times faster than at 30°C & 65 % RH.

Overall Product 7 was the most stable with no mebendazole polymorph A detected at both storage temperatures within the 6 months of testing. Product 4 was the second most stable with no polymorph C → A conversion at 30°C & 65% RH and the slowest measured conversion rate, 0.0011 month^{-1}, at 40°C & 75% RH. The third most stable product was Product 2 (stored as sealed samples). However, at 40°C & 75% RH the polymorph C → A conversion in this product was almost 3 times faster than for Product 4. For product 2A, protecting it by storing it in a sealed container at 40°C & 75% RH slowed down the polymorph C → A conversion by a factor of 5.

In practical terms the importance of these results are shown by changes in the half-life ($t_{1/2}$ = 0.693/k) and shelf-life (t_{90} = 0.105/k) listed in table 3.21. These values show that, except for Products 4 and 7 that showed little or no polymorph conversion, when stored at high temperature and high humidity conditions mebendazole polymorph C → A conversion is fast when the products are not completely sealed from the environment that most have shelf-lives of less than 7 months. This means that after these products enter the supply chain the possibility is great that patients will receive therapeutically ineffective tablets. This could explain the high variability in the success rate of treatment with mebendazole products (Fincham *et al.*, 2005: 13) in third world countries where environmental control of storage conditions in the supply chain is not always adequate.

The classic JMAEK model describes the kinetics of isothermal transformation from a parent phase to an equilibrium phase, by nucleation (the process by which the formation of a new phase begins), growth, and impingement (the restriction of transformed region growth by other transformed regions). This model decouples the kinetics of nucleation and growth from the geometric constraints of impingement, greatly simplifying analysis of the problem (Christian, 1975 & Stumpter, 2004:13). The theory is based on three main assumptions: an infinite volume available for transformation, random nucleation, and growth of transformed regions without preference of direction (see figure 3.48). Specific simplifying assumptions have also been made

about geometry and kinetics of nucleation and growth, in order to derive analytical solutions for special cases, such as zero-nucleation rate (pre-existing nuclei), constant nucleation rate, linear growth velocity, diffusion-limited growth, and growth of crystals in needle- or plate-like configurations (Christian, 1975 & Stumpter, 2004:13).

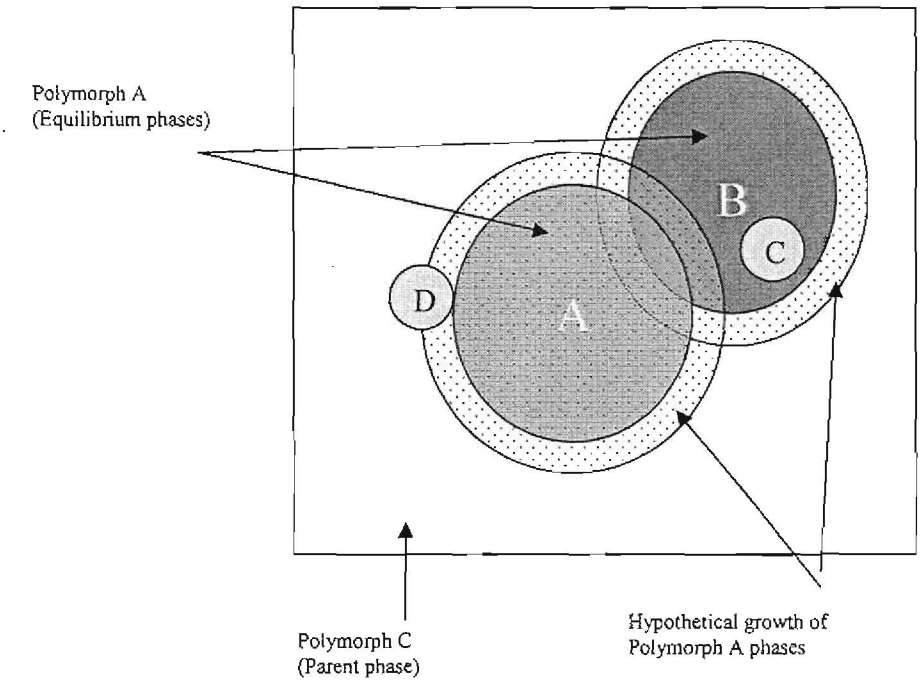


Figure 3.48 Schematic presentation of a two-dimensional phase transformation according to JMAEK theory. The spheres A and B represent regions of the transformed phase (polymorph A), growing from the parent phase (polymorph C). The shells represent the hypothetical growth of A and B during an infinitesimal time interval, ignoring impingement. The spheres C and D represent nascent nuclei appearing during this time interval, neglecting impingement (adapted and reproduced for mebendazole, using a schematic presentation by Sumpter, 2004:13).

Therefore, to get a better understanding of the actual process involved in mebendazole polymorph C → polymorph A conversion the results obtained from the JMAEK model should be studied closer, especially the importance of

the Avrami exponent, *n*. According to the original theory this exponent, listed in table 3.20, should be an integer from 0.5 to 4 (Avrami, 1939:1103-1112, Avrami, 1940:212-224, Avrami, 1941:177-184, Johnson *et al.*, 1939:416, Erofeev & Compt, 1946:513, Kolmogorov, 1937:355-359). Values of $n \approx 0.5$ to 1 (Product 3 at 30°C & 65% RH and Products 4, 5 and 6 at 40°C & 75% RH) would be characteristic of linear (rodlike) crystal growth and a thermal (spontaneous) nucleation rate-limited by diffusion (Smith *et al.*, 2005:3037). Values of $n \approx 2$ (Products 1 and 3 at 40°C & 75% RH) could indicate either sporadic nucleation and linear growth with the rate limited by diffusion or spontaneous nucleation and spherical growth with the rate limited by diffusion. Both cases would suggest two-dimensional diffusion and a constant or decelerating nucleation rate. This means that the rate-limiting step for the formation of polymorph A in these products was diffusion. Product 2 and Product 2A at 40°C & 75% RH (closed and exposed to the atmosphere) represents an example of a case in which the (local) nucleation rate is a decreasing function of time ($n \approx 3$). In the limiting case of site-saturation the nucleation rate decreases very rapidly. As a result, one may assume that all of the nuclei were formed at the start of recrystallisation. The JMAEK exponent would lie between 3 and 4 if the decrease in the nucleation rate was finite.

In this study the observed values of n were not exact numbers. However, many authors have suggested possible causes for the observed discrepancies between the JMAEK model and experimental data, including non-linear growth of crystals (Van Siclen, 1996:11845-11848), non-random nucleation (Clemente and Saleh, 2002:132102), and effect of finite sample size (Weinberg and Kapral, 1989:7146-7152). However, recently Cahn (1999:3-14) demonstrated that the JMAEK approach is accurate provided that the nuclei are randomly distributed. The requirement of a random distribution of nuclei is, therefore, the most serious limitation of the JMAK approach. Since the mebendazole in the products are randomly distributed throughout the tablet matrixes we assume that this requirement was met and therefore the JMAEK model is applicable to estimate the rate and type of polymorphic transformation observed for mebendazole because the basic assumptions of

the model were met. These results showed the Avrami exponent, n, ranged from ~ 1 to 3 for mebendazole polymorph C in tablets with different compositions. Within the JMAEK approach differences in the calculated *n*-values for the polymorph C→ polymorph A conversion in the products could be explained by a difference in the number of nucleation sites, differences in nucleation rate compared to growth velocity, and the presence of an incubation time before the beginning of nucleation.

Discussion and Conclusion

The aim of this chapter was to investigate the influence of moisture and heat on the stability of mebendazole polymorph C in randomly selected commercially available tablets in South Africa. From the results obtained it became clear that moisture and the presence of polymorph A traces in the product played an integral role in the thermodynamic stability of mebendazole polymorph C. Products which contained traces of polymorph A revealed a higher rate of polymorph transformation (polymorph C → polymorph A). All the products packed in blisters revealed polymorphic transformation when stored at 40°C & 75% RH for 6 months. Product 7, which was packed in a HDPE securitainer, did not reveal any polymorph transformation when stored at 30°C & 65% RH nor at 40°C & 75% RH for 6 months.

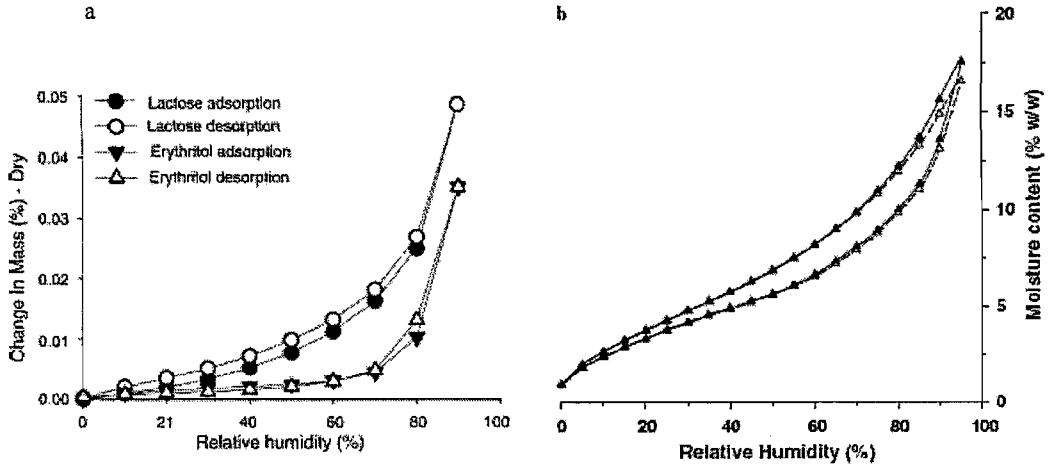


Figure 3.49 Dynamic vapour sorption profiles of (a) lactose monohydrate (Traini *et al.*, 2006:247) and (b) microcrystalline cellulose (dotted line) (Kachrimanis *et al.*, 2006:311).

From figure 3.49 it is clear that lactose monohydrate is less hygroscopic compared to microcrystalline cellulose. It is also clear that the vapour sorption profile of microcrystalline cellulose reveals a grater hysterisis (which may originate from the water liquefaction due to capillary condensation into pores) compared to lactose monohydrate (Kachrimanis *et al.*, 2006:311). The liquefied water present in these pores is thus freely available in the tablet matrix and may act as a catalyst for moisture-induced polymorph transitions. Thus it can be assumed that the polymorph C fraction in Product 7 was protected from moisture-induced polymorph transition by a dual mechanism: the formulation contained the less hygroscopic monohydrate lactose and was stored in a container with low water vapour permeation (i.e. HDPE securitainer).

The accelerated stability testing of Product 2 samples in their blisters at 30°C & 65% RH did not reveal any polymorphic transitions but the significant changes in the dissolution profiles suggested that changes in the physical properties occurred. The Product 2 samples which were removed from their blisters revealed that a polymorphic transition occurred after 6 months, when traces of mebendazole polymorph A were detected in the tablets, and lower dissolution properties observed.

The accelerated stability testing of the exposed samples of Product 2 at 40°C & 75% RH revealed a remarkable polymorphic instability. After 4 months polymorphic transitions caused significant changes in the dissolution profiles of the samples. The exposed sample of Product 2 revealed that a polymorphic transition occurred after 3 months when traces of polymorph A were detected and possible traces of polymorph B after 5 months.

Kinetic analysis of the transformations abided JMAEK fits for the isothermal conversion of mebendazole polymorph C → A in the tablets. The conversion profiles of the products showed that the start of the crystallisation process was preceded by a temperature-dependent *incubation time*, which lead to the formation of the sigmoidal curves.

From the results obtained in this chapter it can be concluded that the storage of mebendazole tablets at elevated temperatures and relative humidities induced polymorphic transitions which influenced the dissolution behaviour significantly.

CHAPTER 4

The influence of moisture and increased temperature on mebendazole polymorphs

Introduction

The effect of moisture on the solid-state properties of some active pharmaceutical ingredients and tablet excipients has been described in chapter 1. Moisture induced transformations could include: hydrate formation, desolvation and hydration of an anhydrous form, polymorphic transformation, crystallisation of amorphous phases etc.

Al-Badr & Tariq (1987:294) described mebendazole as an off-white to slightly yellow amorphous powder and not unpleasant to taste, which is almost *insoluble in water, not hygroscopic* and is stable in air. Terblanche (2001:139-147) indicated that mebendazole polymorph C remained stable between room temperature and ± 179 °C, and revealed that no crystal transformation had occurred between the mentioned temperatures.

The results obtained in chapter 3 showed that the stability of mebendazole polymorph C in some products showed instability at 30°C & 65% RH and 40°C & 75% RH, which had a significant influence on the dissolution behaviour of the tablets. From the results obtained it seemed as if some products were more susceptible to the polymorphic transformation at 40°C & 75% RH than at 30°C & 65% RH.

The aim of this chapter was to investigate the influence of heat and moisture on the stability of mebendazole polymorphs B and C.

The polymorphic stability testing in chapter 3 revealed that Product 2 (without original packaging, i.e. Product 2A) showed polymorphic instability. The instability was mainly exhibited when the tablets were stored at 40°C & 75% RH,

where a mixture of polymorph A and C were detected in the tablets after 1 month, and possible traces of polymorph B after 4 months.

Polymorphic transformations were observed for the tablets (Product 2A) stored at 30°C & 65% RH only after 5 months.

From the results obtained in chapter 3 it can be suggested that the storage of mebendazole tablets at elevated temperatures and relative humidities induced polymorphic transitions which influenced the dissolution behaviour significantly. Moisture seemed to be a catalyst for this polymorphic transformation process, however no reference could be found in the literature available at the time of this study to substantiate the hypothesis. This hypothesis will be investigated in the following sections.

4.1 The influence of moisture and heat on the stability of mebendazole polymorph B and polymorph C

The thermodynamic stability of mebendazole polymorph C has been described by Terblanche (2001:139-147). It has been indicated that mebendazole polymorph C remained stable between room temperature and ± 179°C. It was also shown that polymorph C transformed into the thermodynamically more stable polymorph A at higher temperatures. This transformation is a first-order process with activation energy of 238±16 kJ/mole (Terblanche, 2001:139-147).

4.1.1 Materials and methods

Mebendazole polymorph C (batch number: F10958, expiry date: 30/09/2006) and polymorph B (batch number: MWB/M-007/2006, expiry date: 30/04/2011) were obtained from Rolab, South-Africa and Exim-Pharm International, Mumbai, India respectively.

Approximately 500 mg mebendazole of each polymorph was transferred into amber 30 glass bottles with tight fitting caps. Water was added to 15 of these bottles (will be referred to as *suspended samples*), the other 15 bottles (will be referred to as *dry samples*) were tightly sealed. The samples were then divided

into 3 temperature groups: 5±3°C, 50±3°C and 100±2°C. Five suspended samples and five dry samples were stored at the mentioned temperatures in incubators for 75 hours. Two bottles (one dry sample and one suspended sample) were removed from each incubator at the following intervals: 1 hour, 6 hours, 25 hours, 50 hours and 75 hours (figure 4.1). The suspended samples were filtered and the mebendazole residues were allowed to dry at ambient conditions for 12 hours. XRPD and DRIFT-IR analysis were performed on all samples to investigate the stability of mebendazole polymorphs B and C.

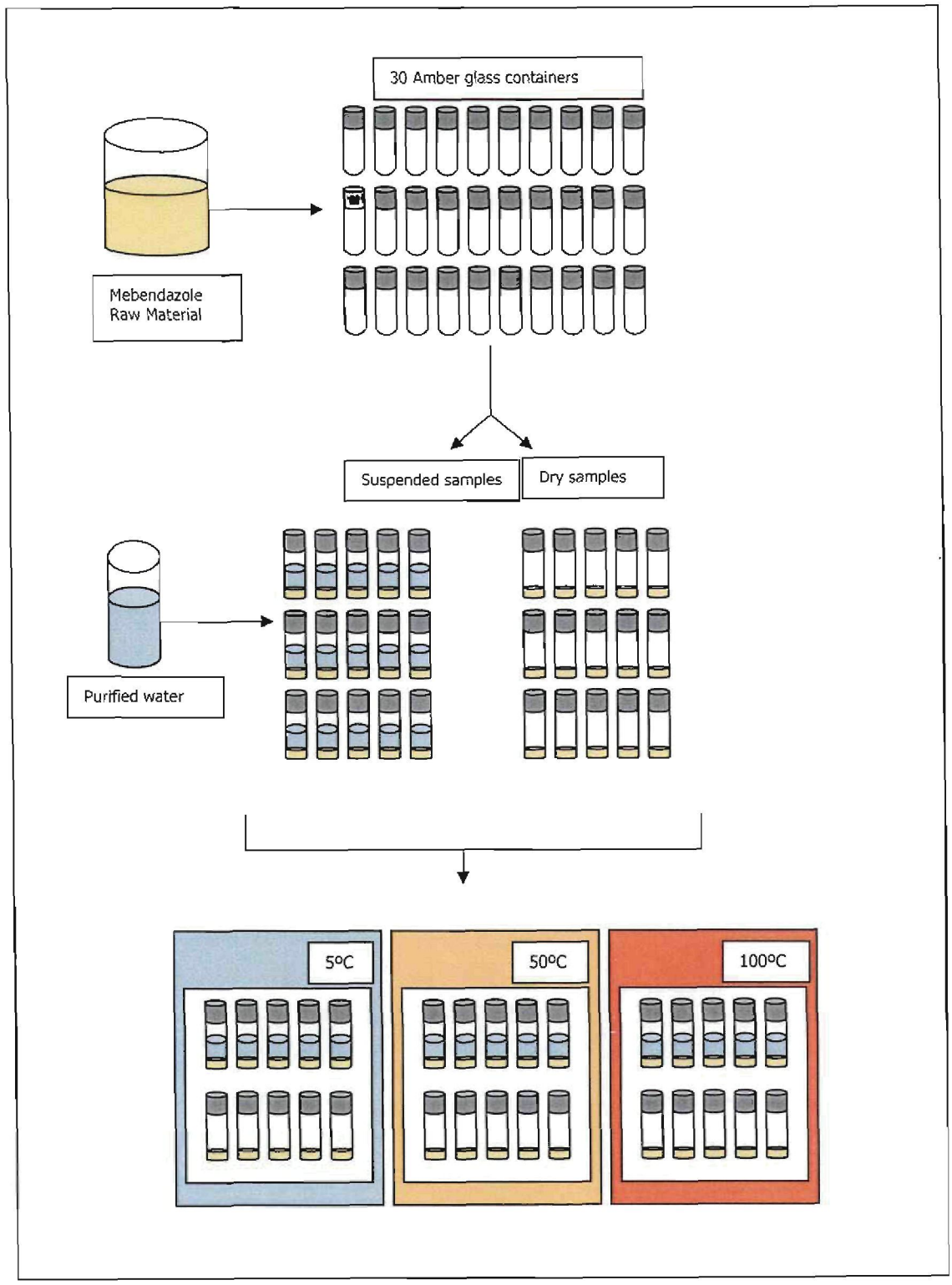


Figure 4.1 Investigating the influence of moisture and increased temperature on the stability of mebendazole polymorphs B & C.

4.1.2 The influence of moisture and heat on the stability of mebendazole polymorph C

The XRPD of the raw material obtained is illustrated in figure 4.2. The main peak positions (°2θ) and the relative intensities (I/I_0) thereof are tabulated in table 4.1.

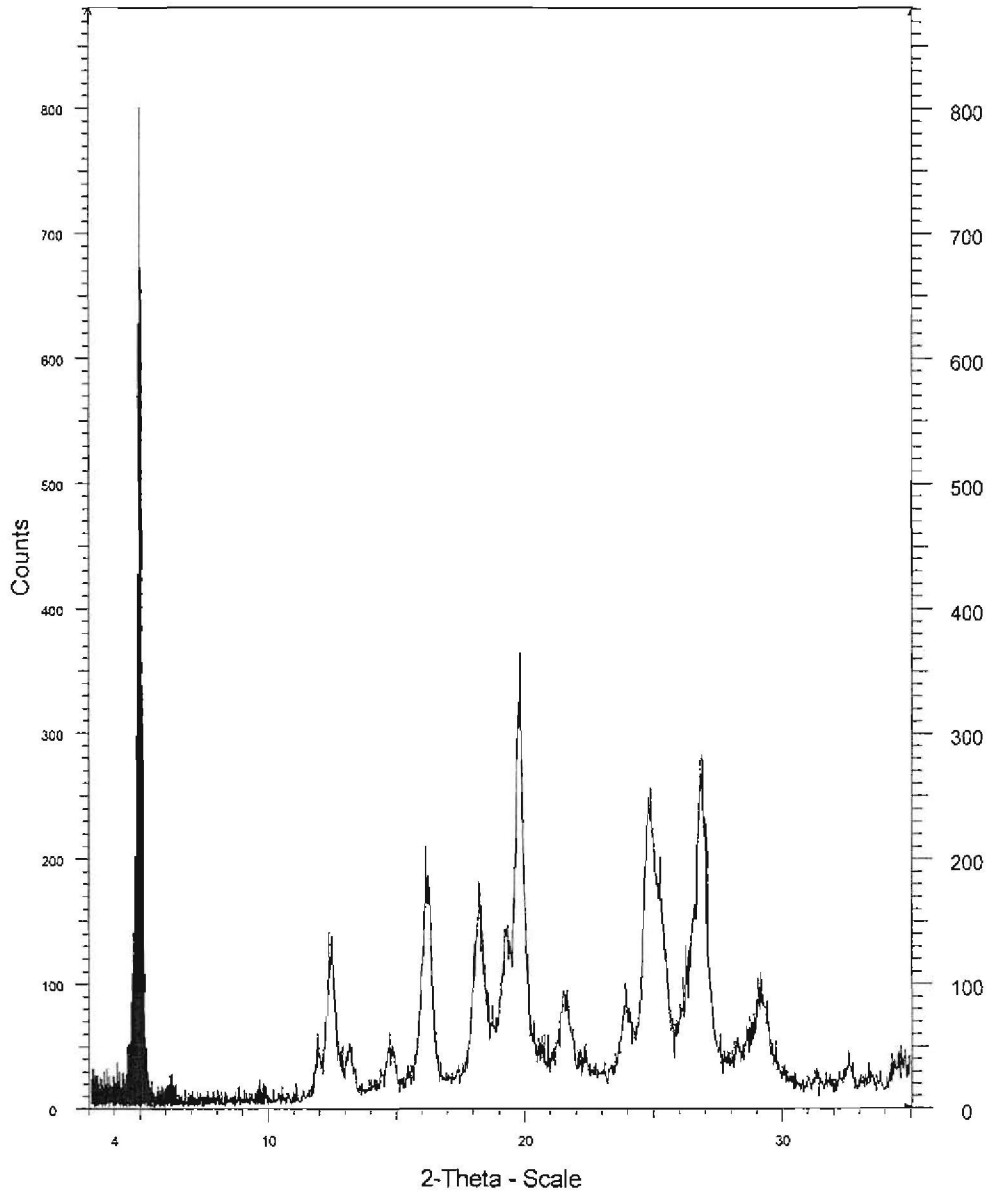


Figure 4.2 XRPD pattern of mebendazole polymorph C.

Table 4.1 Main peak positions (°2θ) and the relative intensities (I/I_0) of polymorph C.

Peak position (°2θ)	Intensity (I/I_0)
4.93	100.0
6.10	3.1
8.80	2.0
9.83	2.0
11.04	2.4
11.88	7.2
12.42	17.1
13.12	6.4
14.83	6.1
16.18	22.8
18.00	16.2
18.22	22.5
19.28	18.2
19.78	45.4
21.49	11.6
23.92	12.4
24.85	29.8
25.23	22.3
26.85	33.8
28.25	6.9
29.15	13.2
29.43	10.6
32.60	5.6

The DRIFT-IR spectrum of the mebendazole polymorph C (figure 4.3) was found to be concurrent to that of the spectrum described in the literature (Himmelreich *et al.*, 1977:123). The –NH and >C=O – stretching was observed at 3403 cm^{-1} and 1717 cm^{-1} respectively, no traces of polymorph A or B were detected.

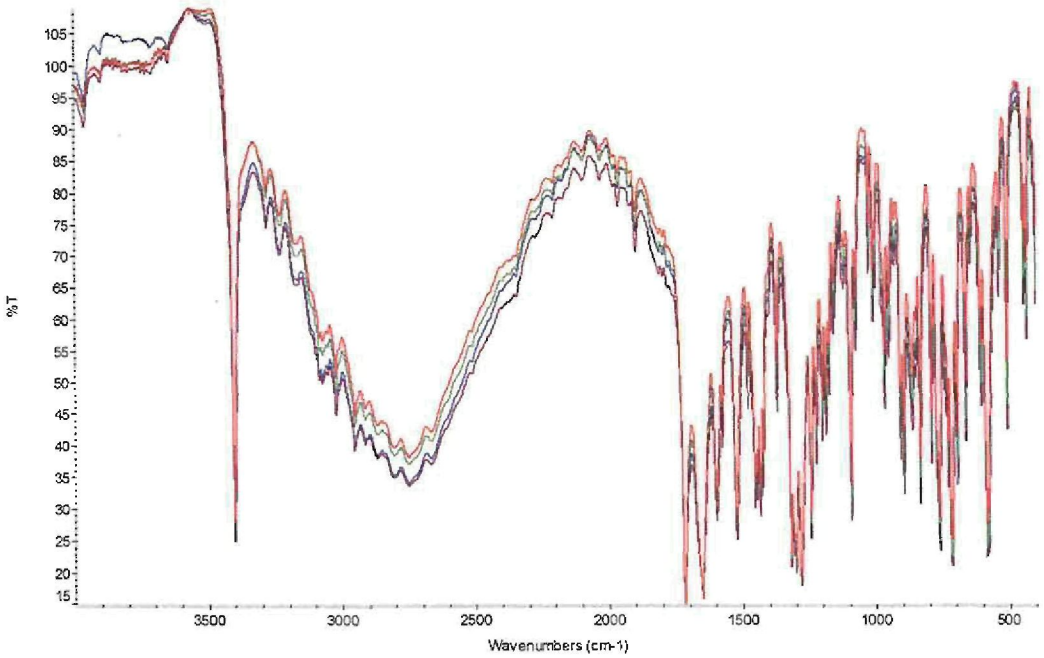


Figure 4.3 DRIFT-IR spectra of the dry mebendazole polymorph C samples stored at: 5, 50 and 100°C after 75 hours.

The effect of heat on the polymorph will be discussed first. The DRIFT-IR and XRPD results indicated that the exposure of mebendazole polymorph C to 5°C, 50°C and 100°C in the absence of water for 75 hours did not induce a polymorphic transition (figures 4.3 and 4.4).

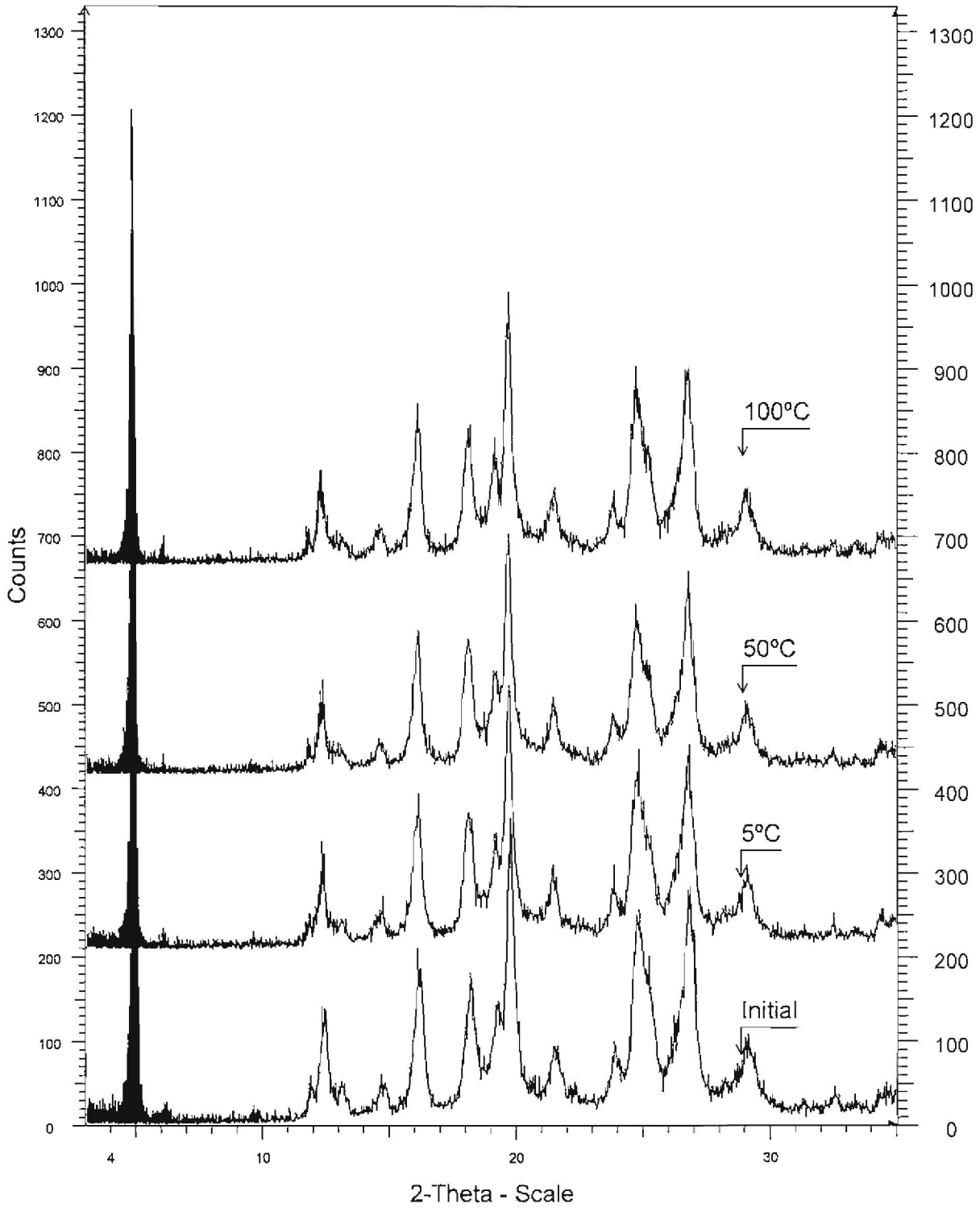


Figure 4.4 Overlay of the XRPD patterns of dry mebendazole polymorph C samples exposed to 5, 50 and 100°C for 75 hours.

This correlated with the results obtained by Terblanche (2001:139-147) who stated that mebendazole polymorph C remained stable between room temperature and ± 179°C.

The results obtained when the mebendazole polymorph C samples were suspended in water and exposed to 5, 50 and 100°C respectively will now be discussed.

No significant changes in the DRIFT-IR spectra (figure 4.5) and XRPD patterns were observed when the suspended mebendazole polymorph C samples were exposed to 5°C and 50°C over for a period of 75 hours. No traces of mebendazole polymorph A or B were detected in the samples. Slight differences in the peak positions of the peaks in the 4.93±0.1°2θ and 19.80±0.1°2θ regions might be attributed to small differences in the powder-bed height.

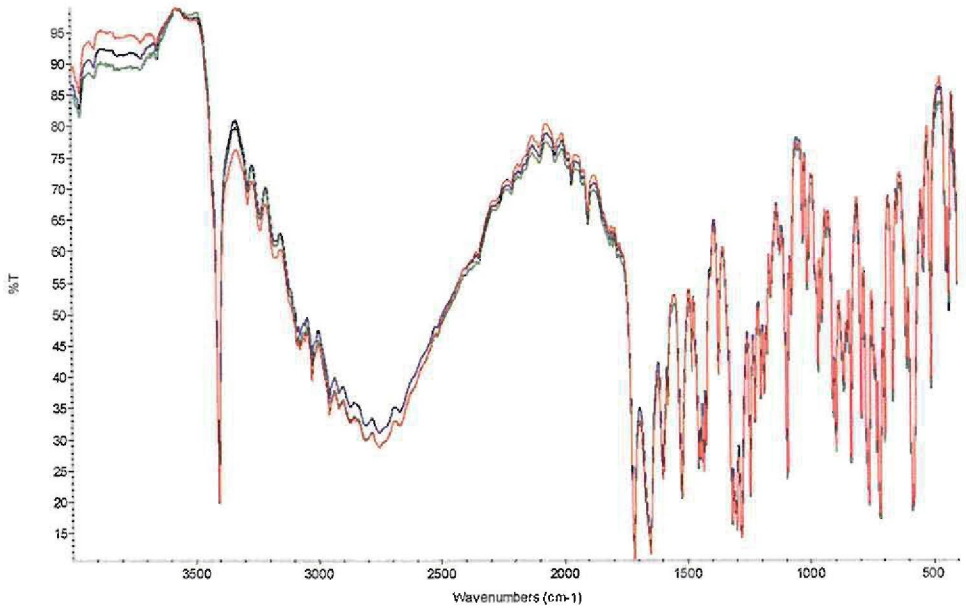


Figure 4.5 DRIFT-IR spectra of the suspended mebendazole polymorph C samples stored at: 5 and 50°C after 75 hours.

Polymorphic transitions occurred when the suspended mebendazole polymorph C samples were exposed to 100°C for 75 hours. The DRIFT-IR spectra of the samples revealed significant changes during the 75 hours in the 3550-3150 cm^{-1} (-HN stretch) region (figure 4.6). Initially, a sharp absorption peak, characteristic of polymorph C, was detected at 3403 cm^{-1}.

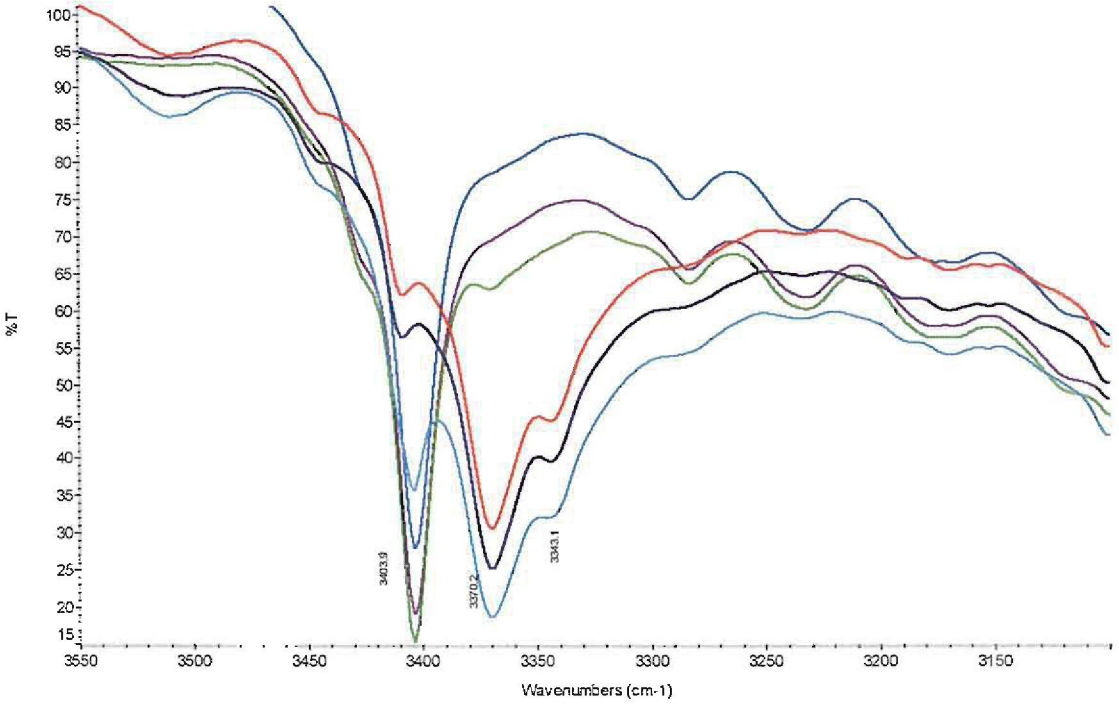


Figure 4.6 Overlay of DRIFT-IR spectra of the suspended mebendazole polymorph C sample – stored at 100°C over a period of 75 hours (initial, 1 hour, 6 hours, 25 hours, 50 hours, 75 hours) indicating differences in the main absorptions at the –NH stretch.

The commencement of the polymorphic transformation was observed after six hours, with the appearance of a shoulder peak at 3370 cm^{-1} indicative of polymorph A traces. After 25 hours the intensity of the 3403 cm^{-1} peak decreased significantly and the intensity of the 3370 cm^{-1} peak increased. The appearance of a shoulder peak at 3343 cm^{-1} was also observed after 25 hours, which suggested that the sample might have contained polymorph A and traces of polymorphs C and B (polymorph A >>> polymorph C >>> polymorph B).

The spectra of the samples after 50 and 75 hours were comparable in the 3550-3150 cm^{-1} region which indicated that the fraction of polymorph C in the sample has decreased significantly and mainly consisted of polymorph A and possible small traces of polymorph B. The following observations were made in the >C=O band (1780-1700 cm^{-1}) region (figure 4.7): The band present at 1717 cm^{-1} in the initial sample indicated that the sample consisted of polymorph C. After 6 hours at 100°C no changes were observed in the mentioned region. After 25 hours the intensity of the 1717 cm^{-1} band was significantly reduced and the absorption band at 1731 cm^{-1} appeared which confirmed the polymorphic transition observed in the –NH stretch region. The band at 1717 cm^{-1} disappeared after 50 hours which indicated that the sample primarily contained polymorph A. After 75 hours no absorption peak was detected at 1717 cm^{-1}. The >C=O absorption band of polymorph B (1700 cm^{-1}) was not clearly detected during the 75 hours. A summary of the DRIFT-IR observations is tabulated in table 4.2.

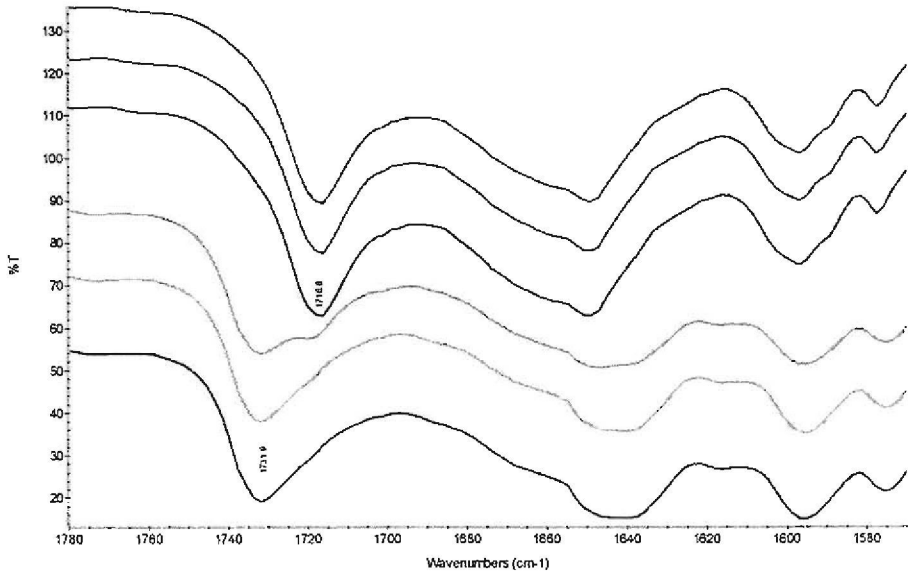


Figure 4.7 Overlay of DRIFT-IR spectra of the suspended mebendazole polymorph C sample – stored at 100°C over a period of 75 hours (initial, 1 hour, 6 hours, 25 hours, 50 hours, 75 hours) indicating differences in the main absorptions at the >C=O band.

The XRPD patterns of the suspended mebendazole polymorph C samples exposed to 5, 50 and 100°C for 75 hours are depicted in figure 4.8. The samples stored at 5 and 50°C did not reveal any polymorph transition during the 75 hours.

The characteristic Bragg peaks of mebendazole polymorphs A, B and C in the 3.1-9.8 °2θ region are indicated in figure 4.9. The intensities of these three peaks are in the order: A > C > B. The following observations were made:

(i) The detection of mebendazole polymorph B in the presence of amorphous solids or in the presence of highly crystalline solids (such as tablet excipients) will be complicated due to the fact that polymorph B reveals an XRPD pattern with weak intensities – as seen in chapter 3.

(ii) Weak intensities usually signify the absence of numerous crystal faces, for example: a sample with an XRPD pattern with low peak intensities (counts) could be considered to be less crystalline compared to a sample with an XRPD pattern with well-defined, intensified Bragg peaks. From figure 4.9 it can thus be proposed that the order of crystalinity (and therefore stability) for the three polymorphs is: A > C > B. Himmelreich *et al.* (1977:123) also stated that the order of thermal stability of the polymorphic forms is: A > C > B.

Table 4.2 Position of the –NH and >C=O stretch observed in the DRIFT-IR spectra of the suspended mebendazole polymorph C samples exposed to 100°C at various time intervals (⊙ indicates the presence of traces of the specific polymorph)

	-NH			>C=O		
	C	A	B	A	C	B
	3410 cm^{-1}	3370 cm^{-1}	3340 cm^{-1}	1730 cm^{-1}	1720 cm^{-1}	1700 cm^{-1}
Initial	3403 ●				1717 ●	
1 Hour	3403 ●				1717 ●	
6 Hours	3403 ●	3370 ⊙			1717 ●	
25 Hours	404 ●	3370 ●	3343 ⊙	1731 ●	1717 ●	
50 Hours	3404 ⊙	3370 ●	3341 ⊙	1731 ●		
75 Hours	3404 ⊙	3370 ●	3341 ⊙	1731 ●		

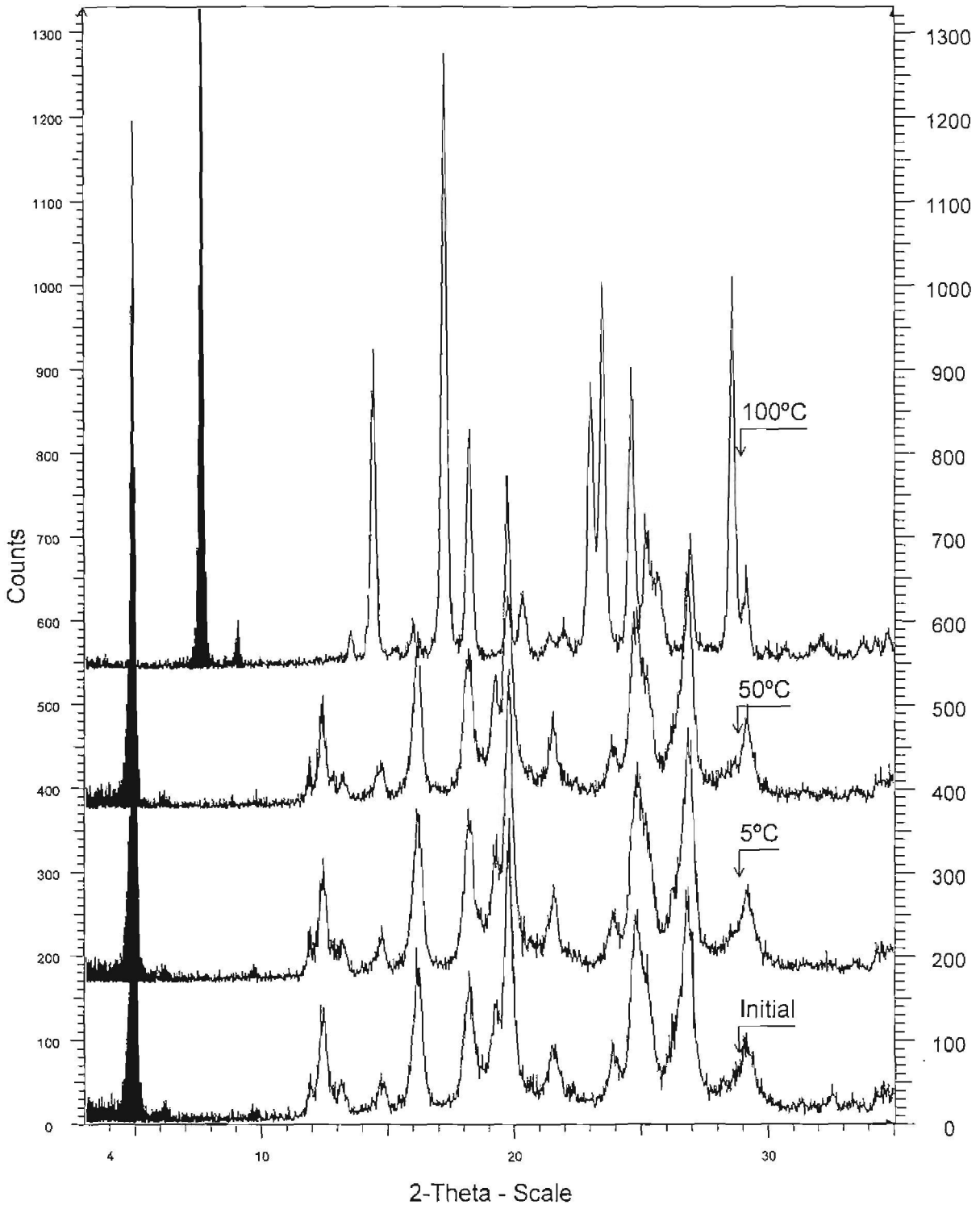


Figure 4.8 Overlay of the XRPD patterns of the suspended mebendazole polymorph C samples exposed to 5, 50 and 100°C for 75 hours.

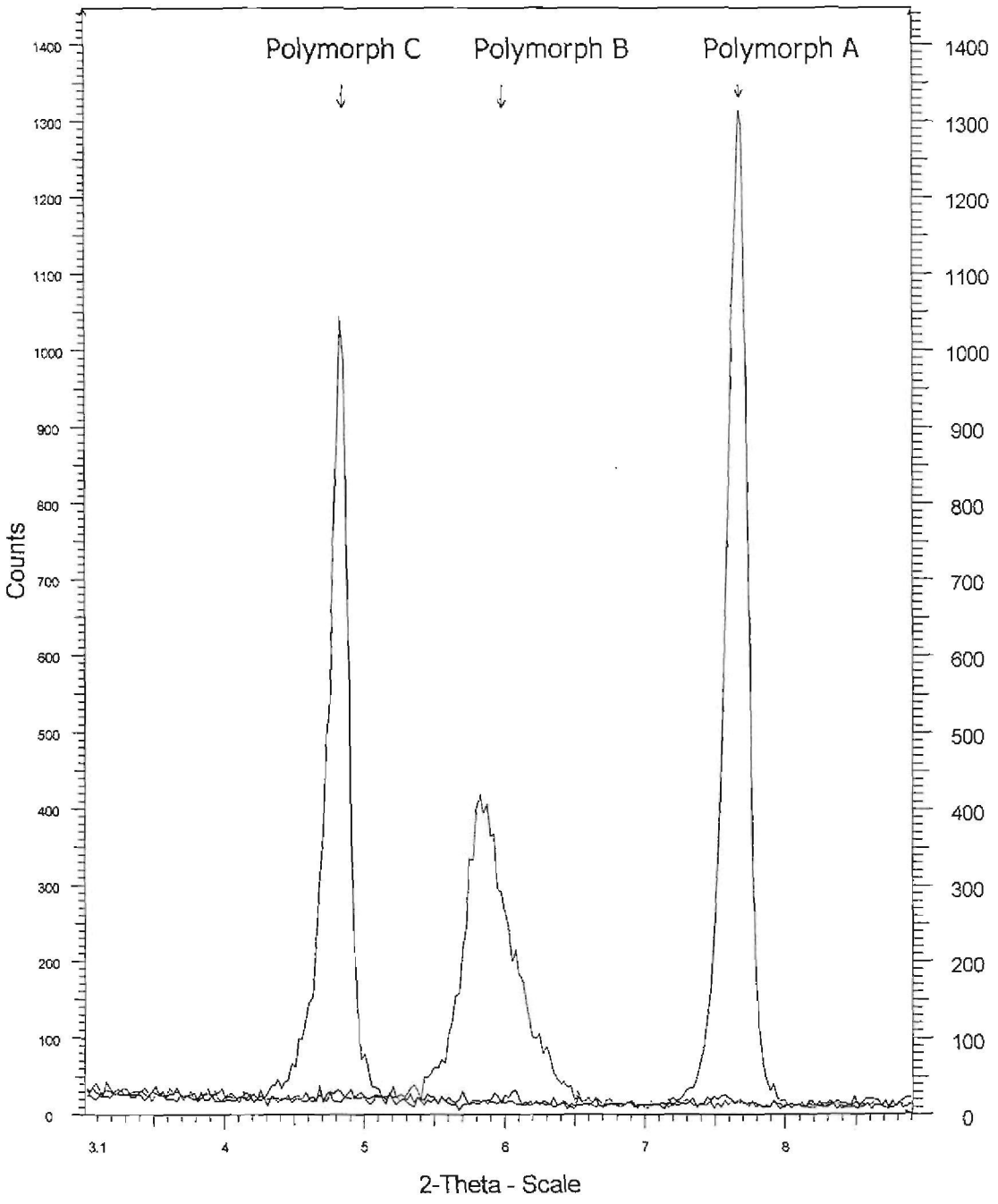


Figure 4.9 XRPD overlay of the characteristic XRPD peaks of mebendazole polymorphic forms A, B & C in the 3.1 – 8.9 °2θ region.

The XRPD pattern of the suspended sample exposed to 100°C for 1 hour (figure 4.10) was comparable to the XRPD pattern of the initial sample with the exception that the 1 hour sample revealed a peak shift of all the peaks towards 35°2θ. As mentioned the DRIFT-IR spectra of the 1 hour and initial sample were comparable.

A general decrease in the intensities of the peaks in the region of 15-30 °2θ was observed after 6 hours, which indicated that changes were occurring in the crystal lattice due to the polymorphic transition. The effect of the polymorphic transition was clearly visible after 25 hours. Figure 4.11 indicates that the XRPD pattern of the sample had peaks characteristic to both polymorph A and C, supporting the DRIFT-IR observations.

The XRPD patterns of the 50 & 75 hours samples were comparable and resembled that of polymorph A (figure 4.12). The small traces of polymorph C, and possible traces of polymorph B were not detected in the diffractograms.

The fact that DRIFT-IR only detected the –NH stretch absorption peaks, and that neither the >C=O band nor clearly detectable crystallographic (XRPD) traces of polymorph B were detected could indicate that the presence of polymorph B could be considered trivial.

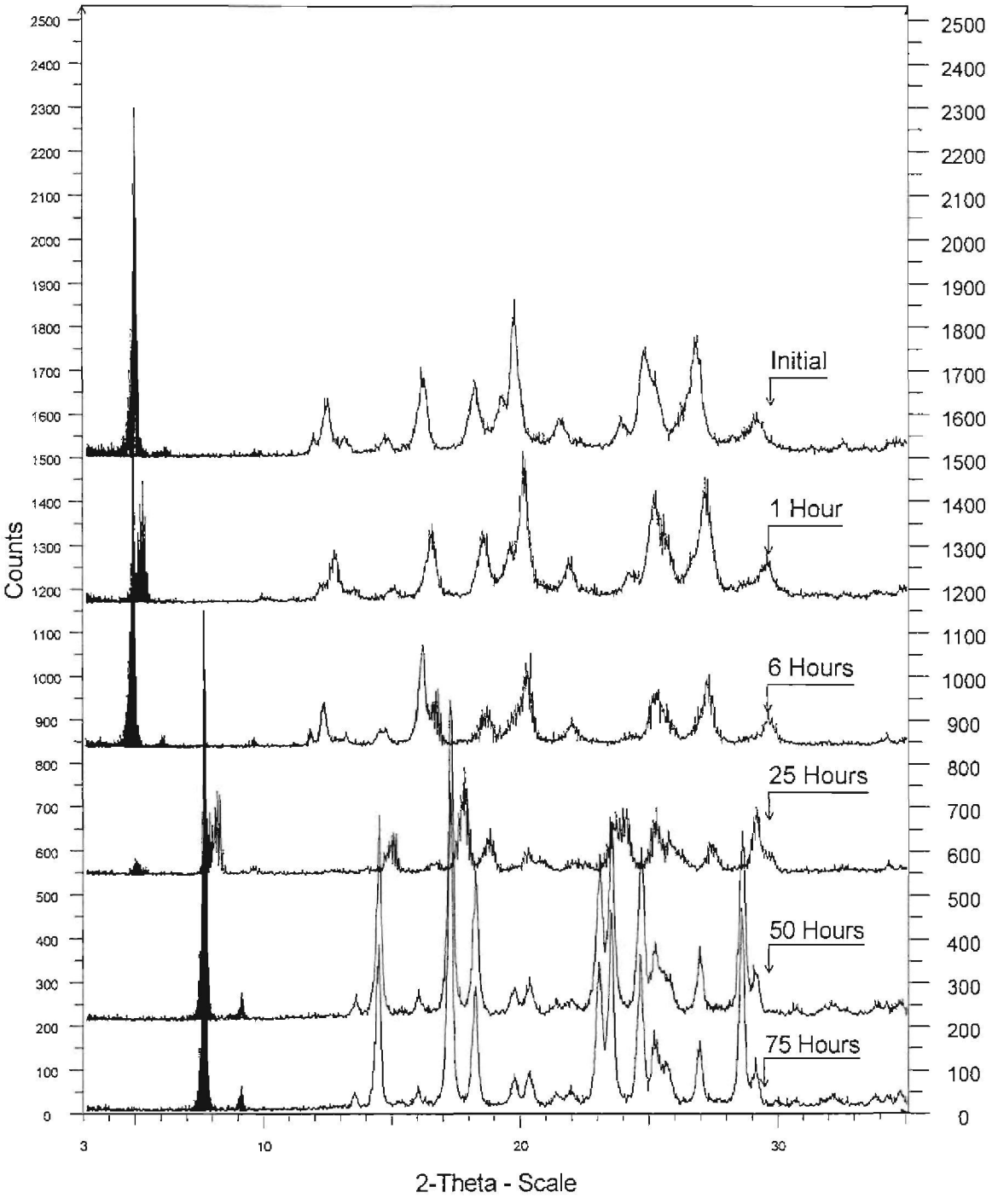


Figure 4.10 Overlay of the suspended mebendazole polymorph C samples exposed to 100°C at various time intervals.

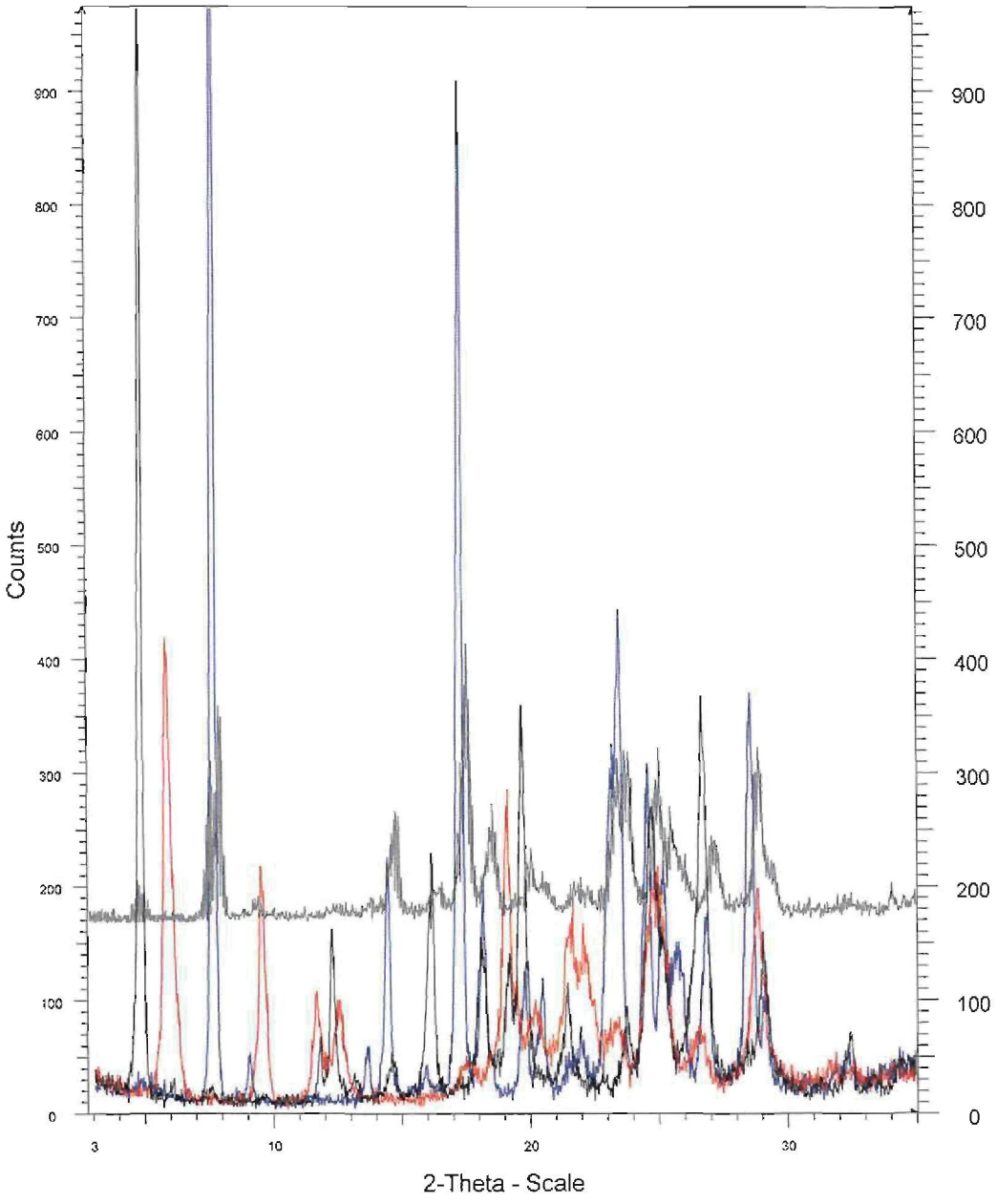


Figure 4.11 Overlay of XRPD patterns of: suspended mebendazole sample stored at 100°C (25 hours) – polymorph C, polymorph B and polymorph A.

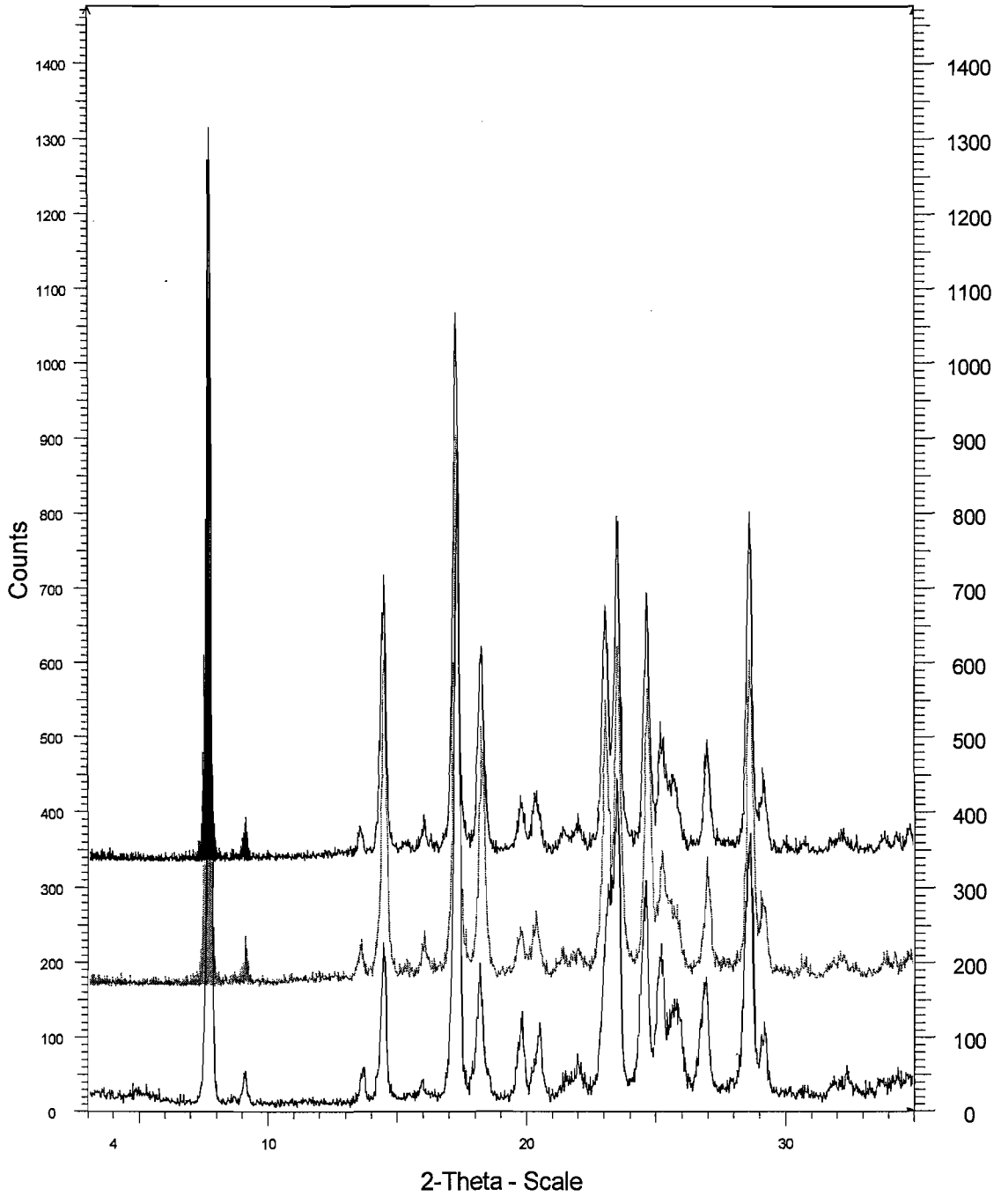


Figure 4.12 Overlay of XRPD patterns of suspended sample at 100°C after 75 hours (top), 50 hours (middle) and mebendazole polymorph A (bottom).

It can thus be concluded that the exposure of mebendazole polymorph C to increased temperatures (up to 100°C) for a period of 75 hours did not induce polymorphic transition and correlated well with the observations made by Terblanche (2001:139-147). However, in the presence of moisture (water) polymorphic transformations were observed at 100°C after only 6 hours, which produced polymorph A as final product after 50 hours.

4.1.3 The influence of moisture and heat on the stability of mebendazole polymorph B

The XRPD of the raw material obtained is illustrated in figure 4.13. The main peak positions (°2θ) and the relative intensities (I/I_0) thereof are tabulated in table 4.3.

Table 4.3 Main peak positions (°2θ) and the relative intensities (I/I_0) of mebendazole raw material : polymorph B.

Peak position (°2θ)	Intensity (I/I_0)
5.84	100.0
9.55	51.2
11.66	25.4
112.55	23.4
19.11	64.1
20.20	23.4
21.50	36.8
21.63	40.7
22.13	39.5
23.37	19.1
24.58	38.0
24.81	46.4
25.03	51.7
26.75	16.0
28.90	47.1
31.68	11.0

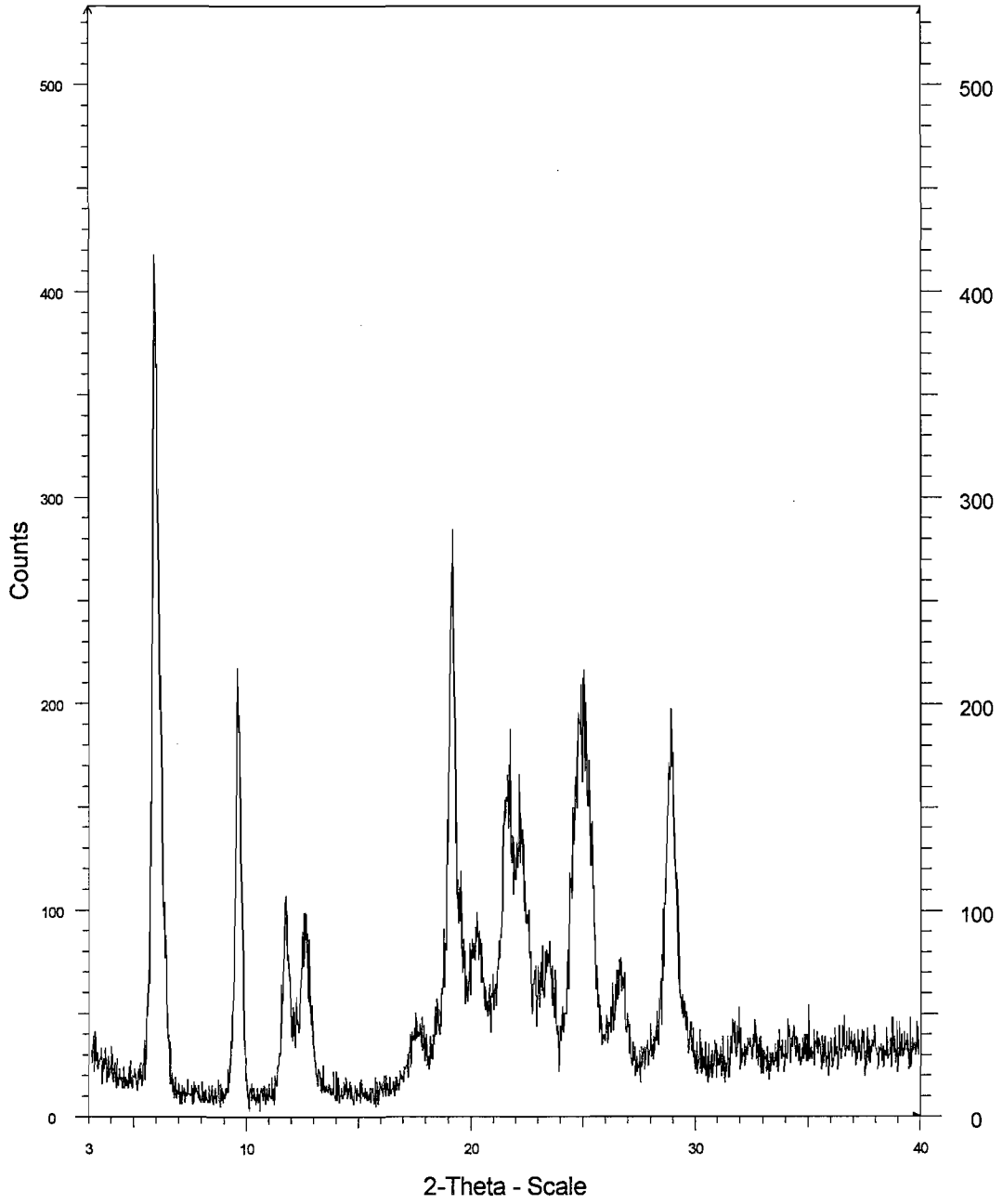


Figure 4.13 XRPD pattern of mebendazole polymorph B.

The DRIFT-IR spectrum of mebendazole polymorph B (figure 4.14) was found to be concurrent to that of the spectrum described in the literature (Himmelreich *et*

al., 1977:123). The –NH and >C=O – stretching was observed at 3339 cm^{-1} and 1700 cm^{-1} respectively, no traces of polymorph A or C were detected.

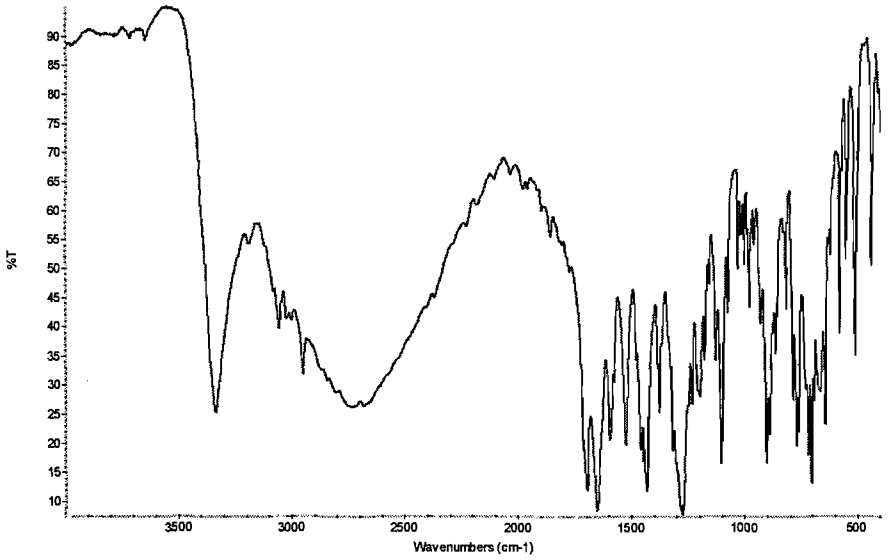


Figure 4.14 DRIFT-IR spectrum of mebendazole polymorph B.

The effect of heat on the polymorph will be discussed first. Mebendazole polymorph B was exposed to increased temperatures and the stability of the crystal form was investigated by means of VT-XRPD. An investigation into the behaviour of solid drugs at elevated environmental temperatures is important in ensuring the stability, efficacy and safety of the drug (Byrn *et al.*, 1999:443).
An overlay of the XRPD patterns obtained during the VT-XRPD study is depicted in figure 4.15.

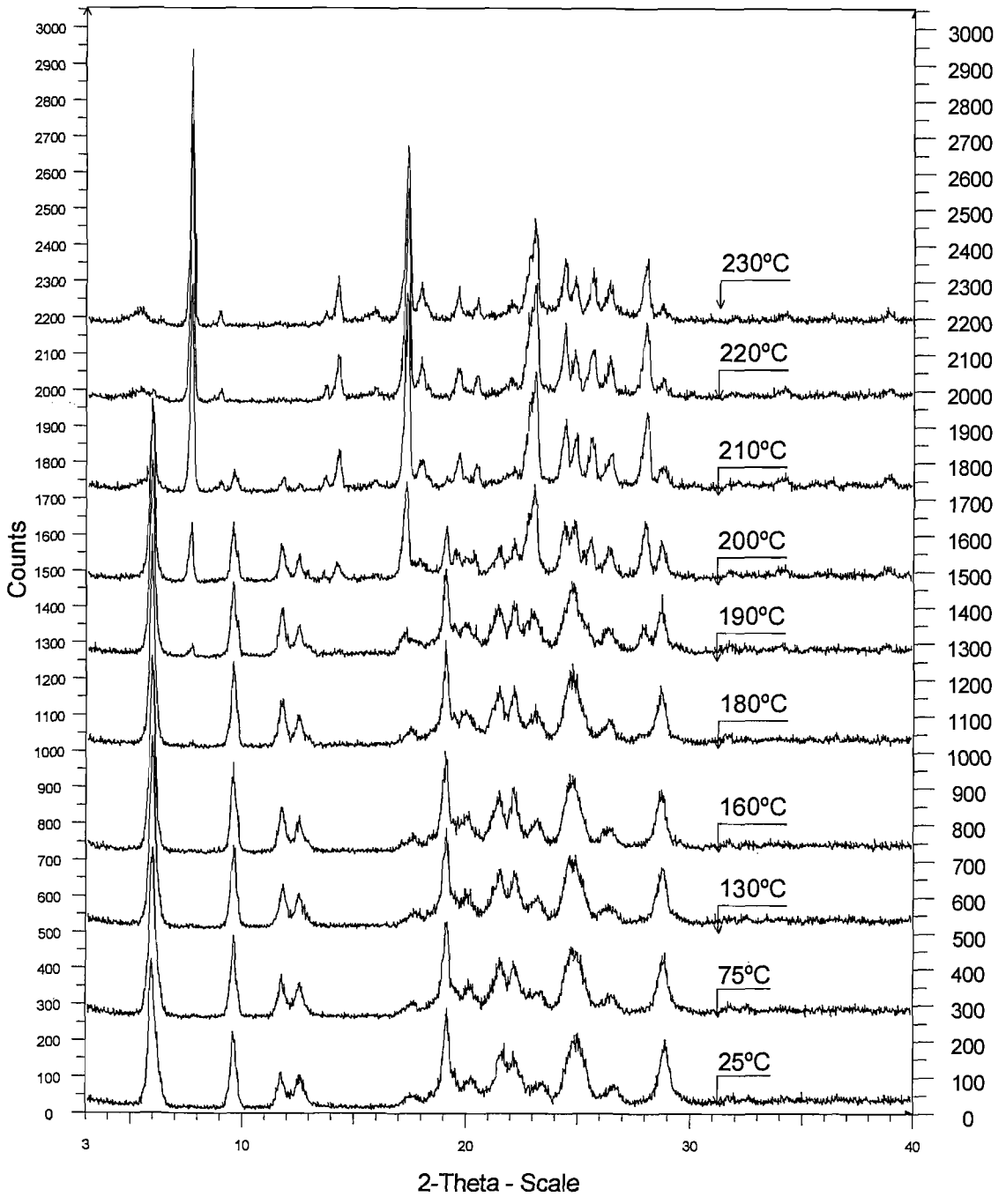


Figure 4.15 VT-XRPD patterns of mebendazole polymorph B at 25-230°C.

Himmelreich *et al.* (1977:124) stated that the heating of polymorph B below 235°C caused the transformation to polymorph A; however no VT-XRPD data was available to illustrate this transformation process.

The XRPD pattern of polymorph B remained relatively unchanged when exposed to 25-180°C. After 190°C the following events occurred which illustrated the transformation of polymorph B to form the more stable polymorph A:

- The 5.84°2θ peak of polymorph B revealed a decrease in intensity during the temperature range: 190-210°C and eventually disappeared at 220°C.
- The peak at 7.67°2θ which is characteristic to form A, emerged at 190°C and revealed an increase in intensity when exposed to elevated temperatures.
- The intensity of the 9.55°2θ peak decreased significantly when heated from 200-210°C and vanished at 220°C. The small peak at 8.94°2θ of mebendazole polymorph A appeared at 210°C.
- The peak at 14.18°2θ appeared.
- The intensities of the two overlapping Bragg peaks at 21.63 and 22.13 °2θ (characteristic to form B) decreased when the sample was exposed to temperatures exceeding 190°C, and disappeared at 210°C.

The XRPD patterns of the sample at 220°C and 230°C were found to be comparable to that of mebendazole polymorph A (figure 4.16). The VT-XRPD thus indicated that mebendazole polymorph B converted to the thermodynamically more stable polymorph A when exposed to 220°C.

The influence of moisture and heat on the stability of mebendazole polymorph B was also investigated using the method described in section 4.1.1.

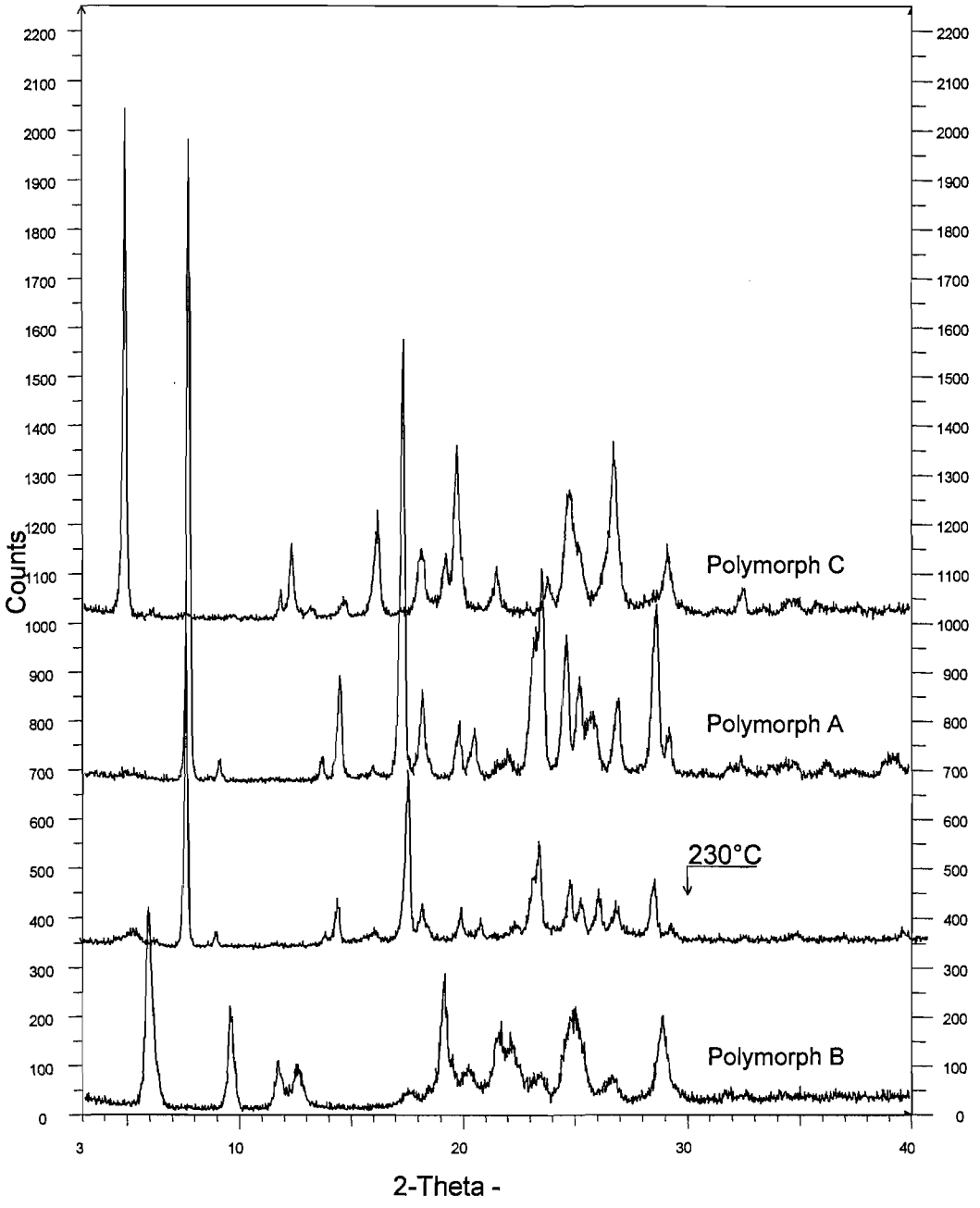


Figure 4.16 Overlay XRPD patterns of mebendazole polymorphs A, B and C and polymorph B at 230°C.

The DRIFT-IR results (figure 4.17) indicated that the exposure of mebendazole polymorph B to 5°C, 50°C and 100°C for 75 hours did not induce any significant polymorphic transition. The position of the –NH stretch and >C=O band was detected at 3340 cm^{-1} and 1700 cm^{-1} respectively, which is characteristic of mebendazole polymorph B throughout the study. No traces of polymorphs A or C were detected in any of the samples.

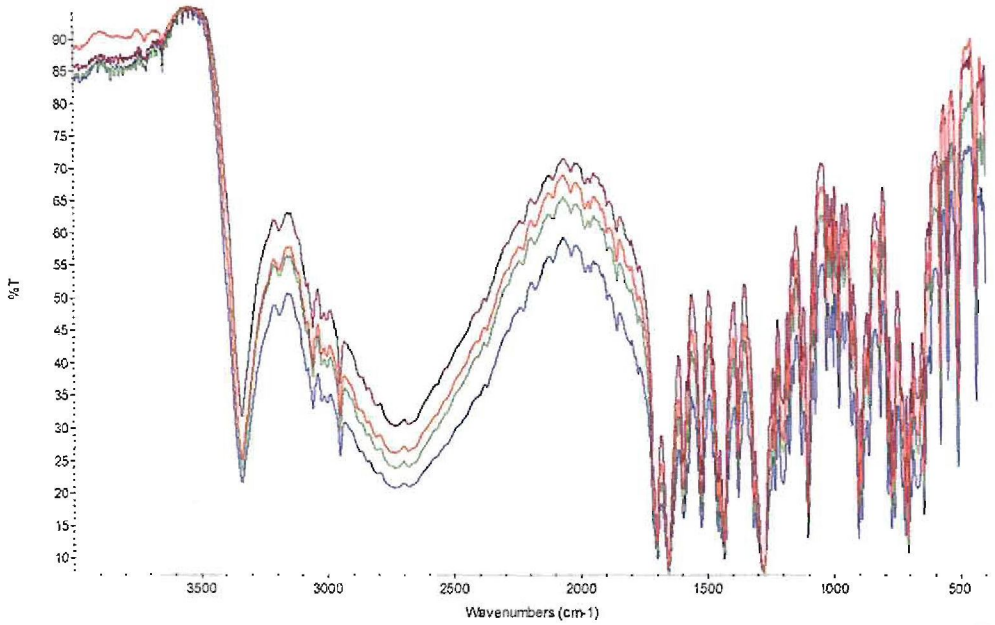


Figure 4.17 Overlay of DRIFT-IR spectra of dry mebendazole samples (Initial polymorph B) stored at 5, 50 and 100°C for 75 hours.

The XRPD patterns of the samples (figure 4.18) supported the DRIFT-IR observations that no polymorphic transformation has occurred during the stability testing. Slight differences in the peak positions of the peaks in the 5.84±0.1°2θ and 19.07±0.1°2θ regions might be attributed to small differences in the powder-bed height. This correlated with the results observed in the VT-XRPD study (figure 4.15) which indicated that mebendazole polymorph B remained stable between room temperature and ± 180°C.

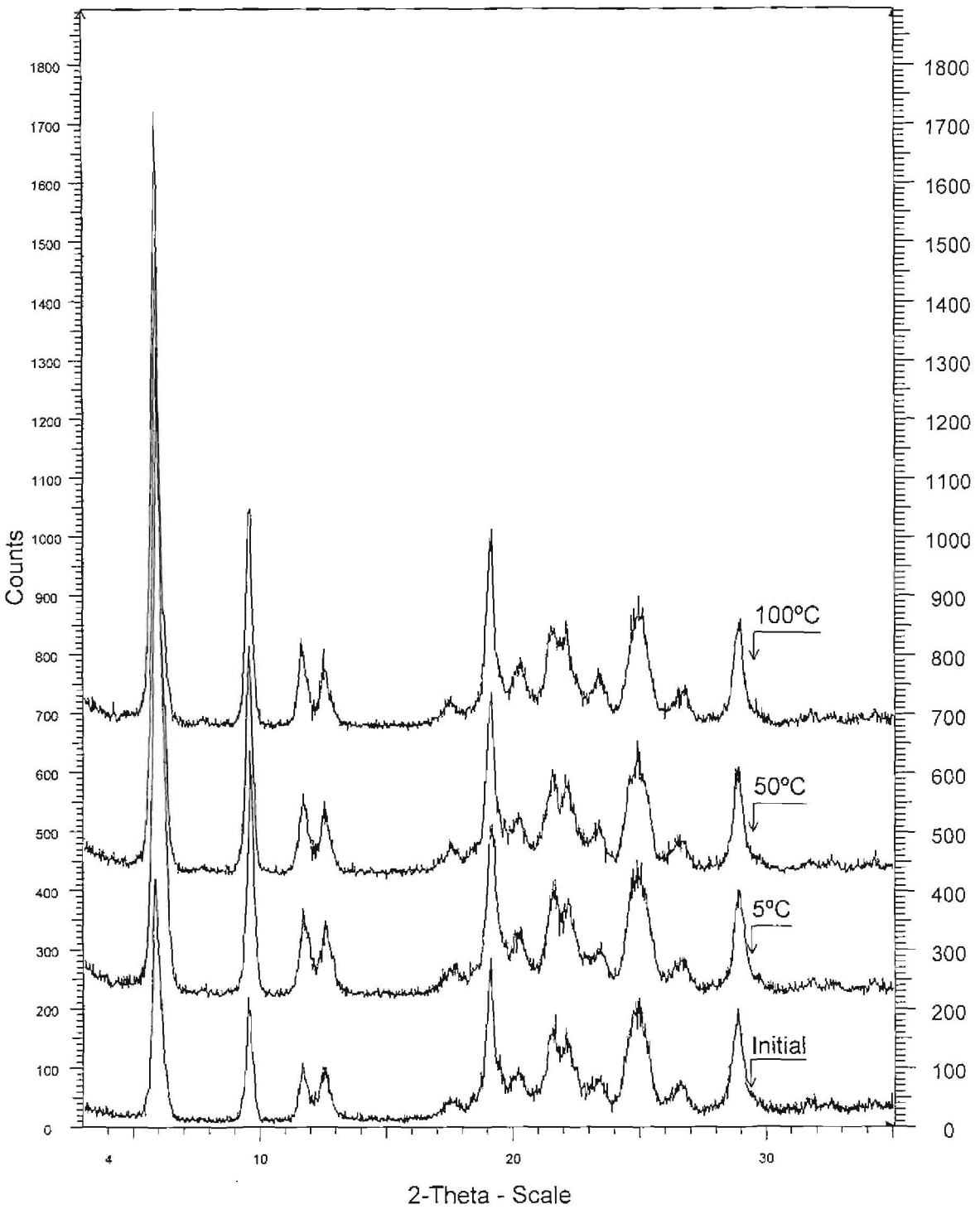


Figure 4.18 Overlay of the XRPD patterns of dry mebendazole polymorph B samples exposed to 5, 50 and 100°C for 75 hours.

The stability of mebendazole polymorph B suspended in water and stored at elevated temperatures was investigated.

From figure 4.19 it became clear that the storage of the suspended mebendazole polymorph B samples at 5°C did not induce any polymorphic transition. No changes (peak appearances or disappearances) were observed in the XRPD patterns (figure 4.20) of the suspended mebendazole polymorph B sample at 5°C, thus confirming the DRIFT-IR observations.

The DRIFT-IR spectra of the suspended mebendazole polymorph B exposed to 50°C revealed that the crystal form remained relatively unchanged during the first six hours of the study, and minor shoulder peaks appeared after 25 hours at 3401 and 1716 cm^{-1} which suggested that a fraction of polymorph B transformed into polymorph C (figure 4.21 and figure 4.22).

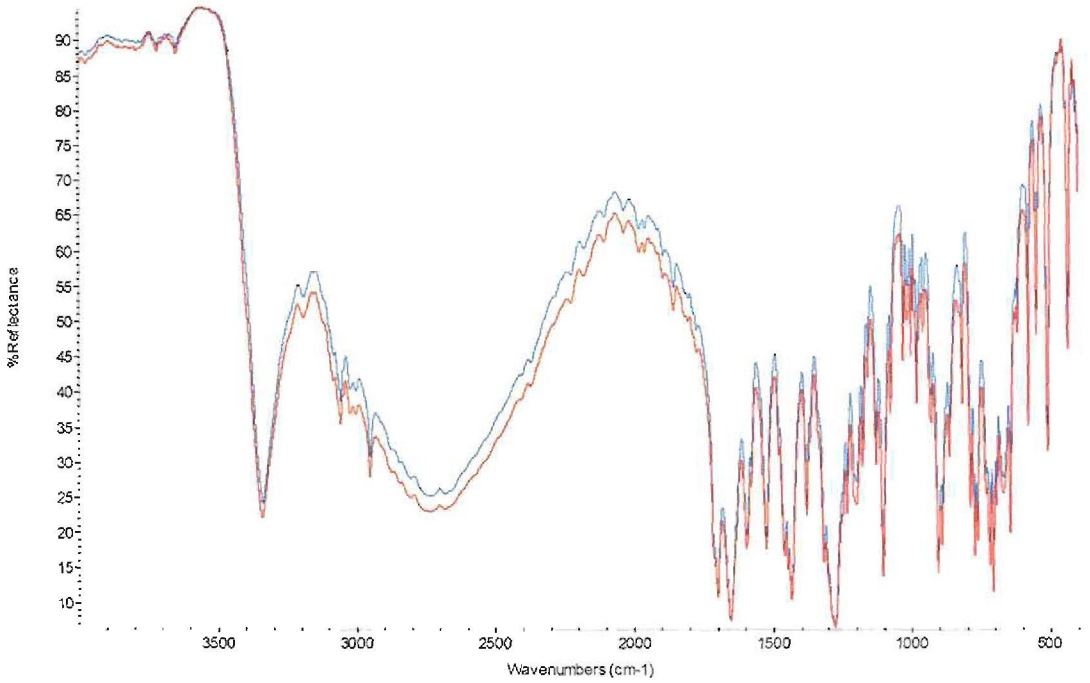


Figure 4.19 Overlay of DRIFT-IR spectra of the suspended mebendazole samples (Initial polymorph B) stored at 5°C for 75 hours.

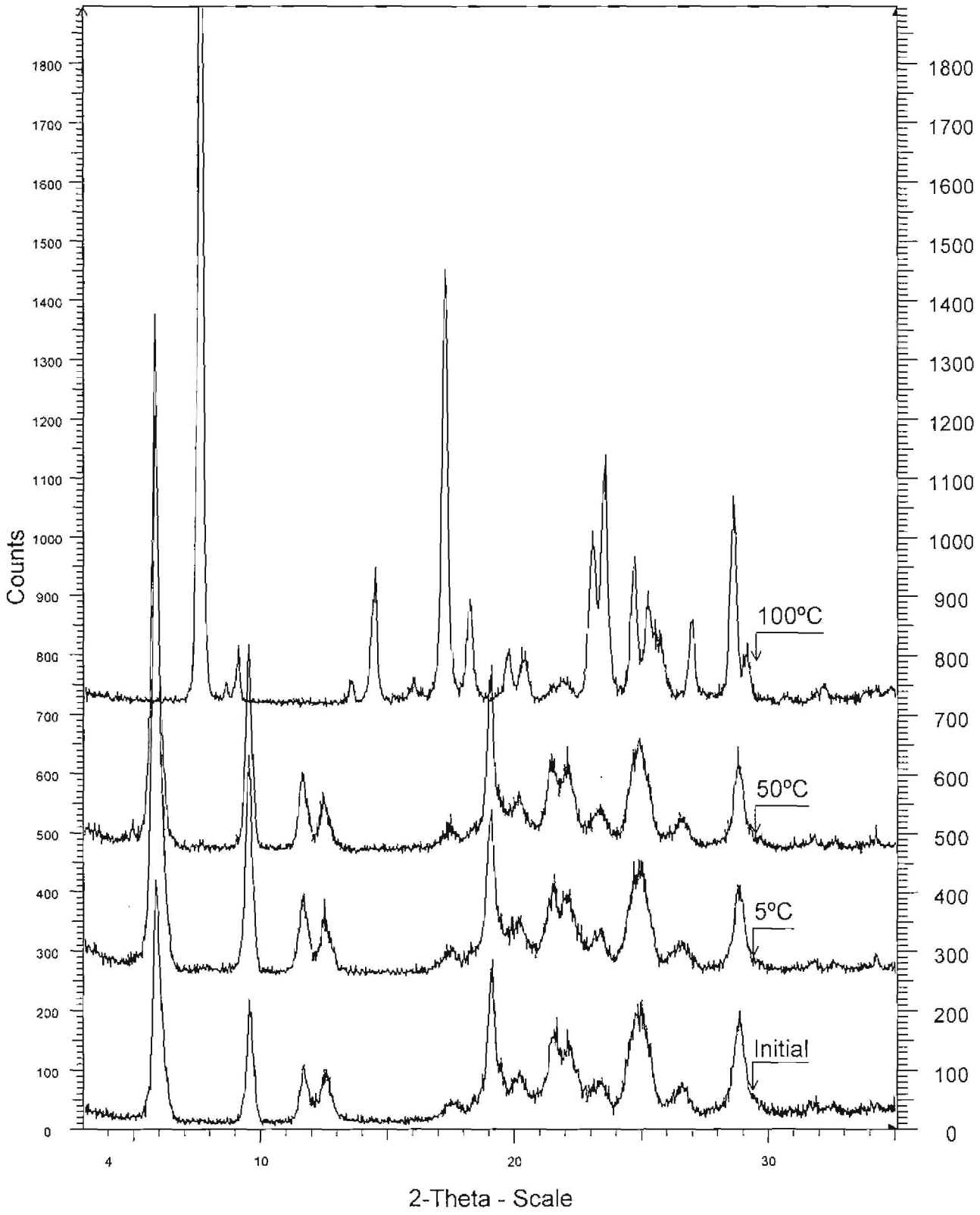


Figure 4.20 Overlay of the XRPD patterns of the suspended mebendazole polymorph B samples exposed to 5, 50 and 100°C for 75 hours.

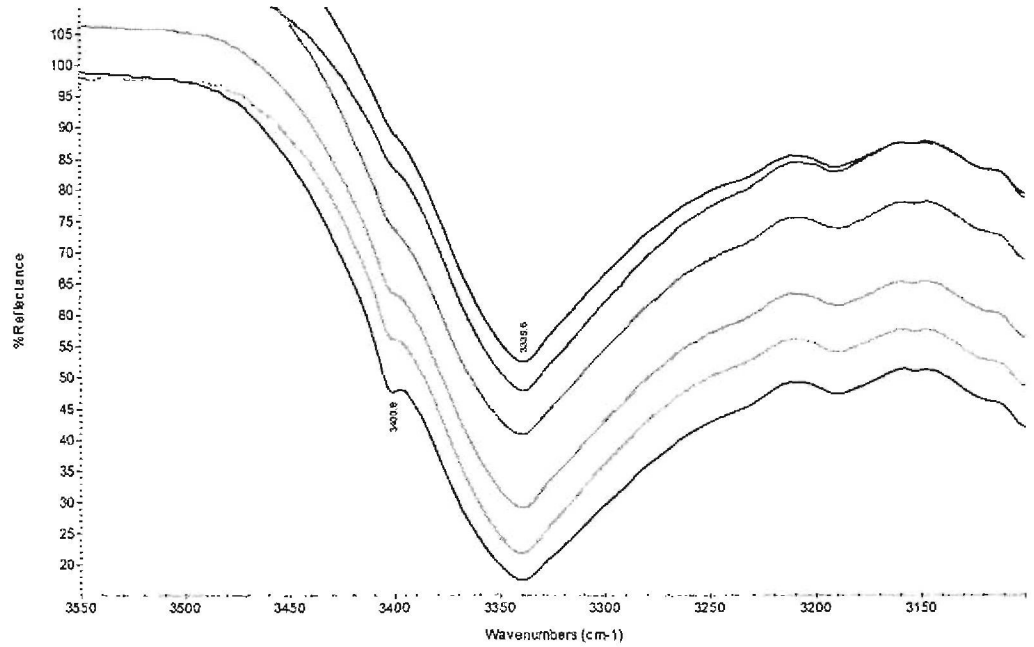


Figure 4.21 Overlay of DRIFT-IR spectra of the suspended mebendazole polymorph B sample – stored at 50°C over a period of 75 hours (initial, 1 hour, 6 hours, 25 hours, 50 hours, 75 hours) indicating differences in the main absorptions at the –NH stretch (3550-3150 cm^{-1}).

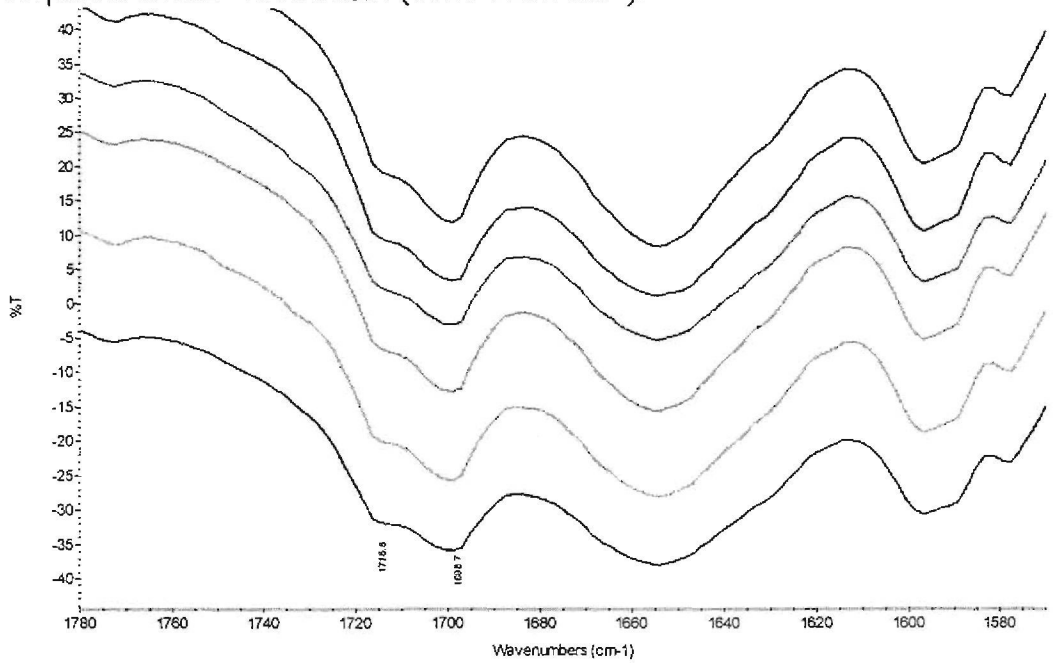


Figure 4.22 Overlay of DRIFT-IR spectra of the suspended mebendazole polymorph B sample – stored at 50°C over a period of 75 hours (initial, 1 hour, 6 hours, 25 hours, 50 hours, 75 hours) indicating differences in the main absorptions at the >C=O stretch (1780-1580cm^{-1}).

The XRPD patterns of the suspended samples stored at 50°C are depicted in figure 4.23. The XRPD analysis confirmed that no polymorphic transformations occurred during the first six hours of the study. Traces of mebendazole polymorph C were detected in the samples after 25 hours. The relative intensities of the Bragg peak present at 4.93±0.1°2θ increased from 5.5 – 6.9 % during the period 25-75 hours. At the end of the 75 hour study the sample consisted primarily of mebendazole polymorph B and contained traces of polymorph C (due to the presence of the small peak at 4.93±0.1°2θ).

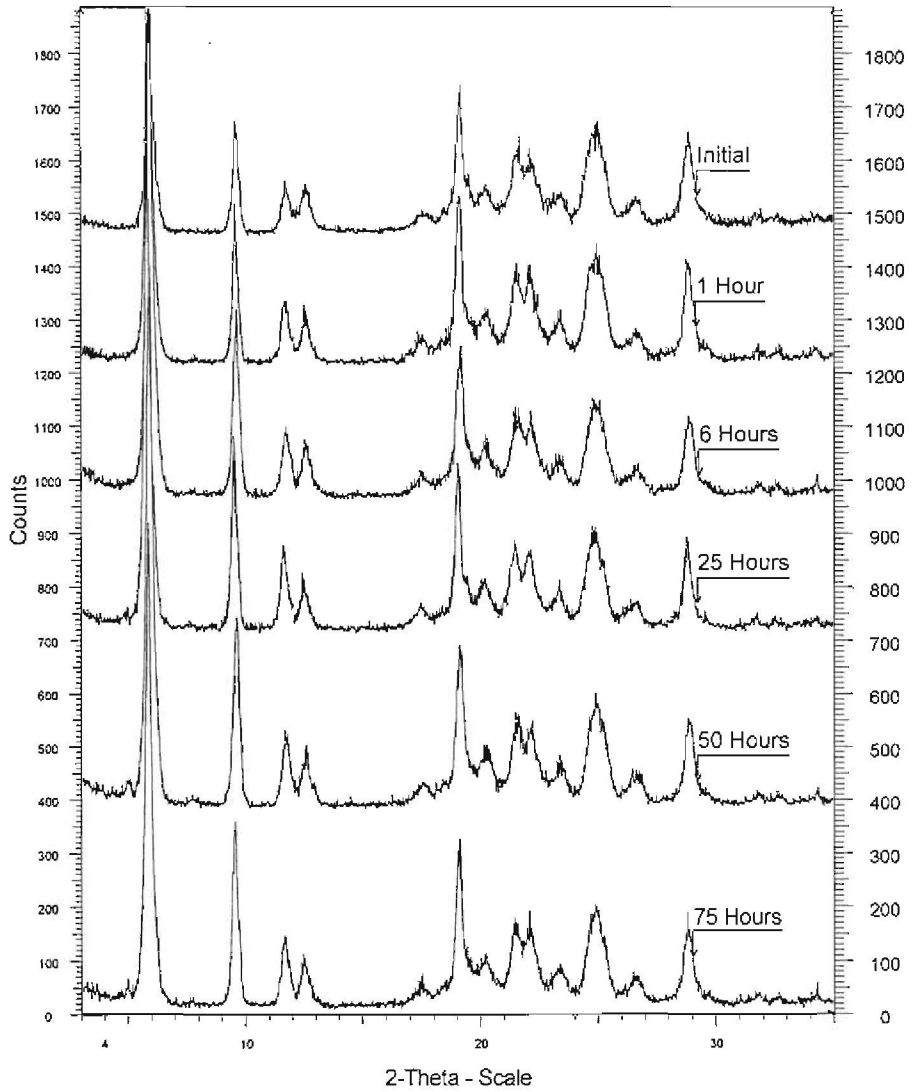


Figure 4.23 Overlay of the XRPD patterns of the suspended mebendazole polymorph B samples exposed to 50°C at various time intervals.

The results for the suspended mebendazole polymorph B at 50°C suggested that polymorph B might transform into polymorph C. This hypothesis was further investigated when a suspended sample was exposed to 100°C for 75 hours.
The characteristic absorption bands of the mebendazole polymorph B samples exposed to 100°C for 75 hours are summarised in table 4.4.

Table 4.4 Position of the –NH and >C=O stretch observed in the DRIFT-IR spectra of the suspended mebendazole polymorph B samples exposed to 100°C at various time intervals (⊙ indicates that traces of the specific polymorph were present in the sample)

	-NH			>C=O		
	C	A	B	A	C	B
	3410 cm^{-1}	3370 cm^{-1}	3340 cm^{-1}	1730 cm^{-1}	1720 cm^{-1}	1700 cm^{-1}
Initial			3340 •			1700 •
1 Hour			3340 •			1699 •
6 Hours	3404 ⊙		3339 •		1716 ⊙	1700 •
25 Hours	3404 •	3369 •	3340 ⊙	1732 •	1716 •	1699 ⊙
50 Hours	3404 ⊙	3369 •	3341 ⊙	1732 •	1716 ⊙	1699 ⊙
75 Hours	3404 ⊙	3369 •	3341 ⊙	1732 •	1716 ⊙	1699 ⊙

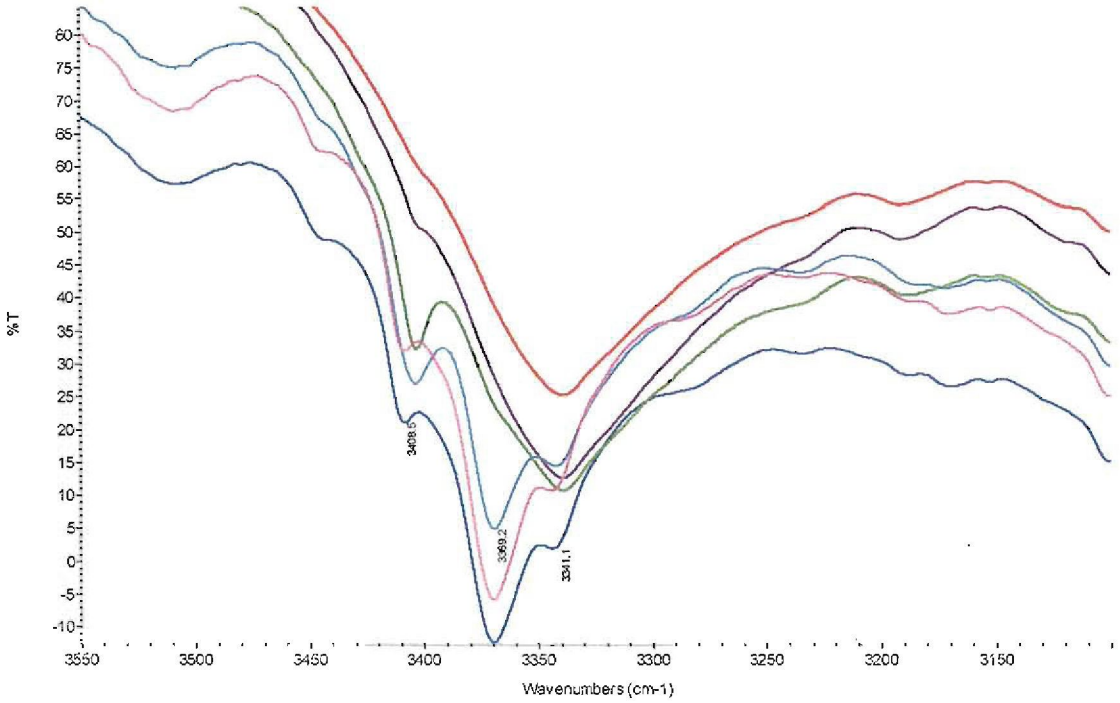


Figure 4.24 Overlay of DRIFT-IR spectra of the suspended mebendazole polymorph B sample – stored at 100°C over a period of 75 hours (initial, 1 hour, 6 hours, 25 hours, 50 hours, 75 hours) indicating differences in the main absorptions at the –NH stretch.

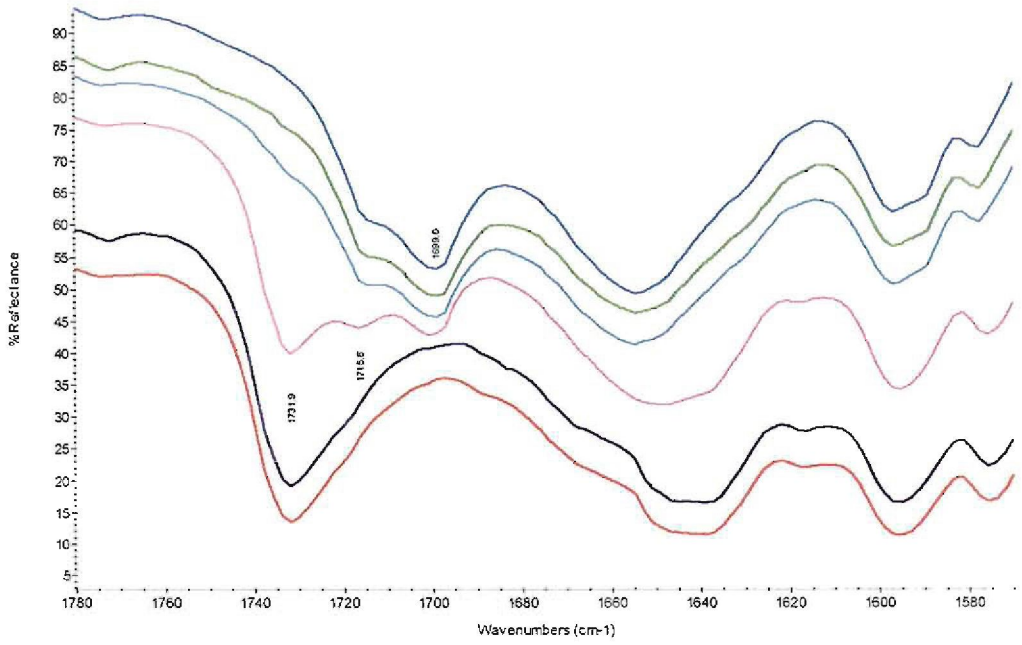


Figure 4.25 Overlay of DRIFT-IR spectra of the suspended mebendazole polymorph B sample – stored at 100°C over a period of 75 hours (initial, 1 hour, 6 hours, 25 hours, 50 hours, 75 hours) indicating differences in the main absorptions at the –NH stretch.

From the DRIFT-IR spectra (figure 4.24 and figure 4.25) it can be concluded that during the first hour of the study the sample mainly contained polymorph B. After 6 hours the sample consisted of a mixture of polymorphs B and C: polymorph B >>> polymorph C.

The IR spectrum of the 25 hours sample suggested that the sample consisted primarily of mebendazole polymorph C and traces of mebendazole polymorphs A and B: polymorph C >>> polymorph A >>> polymorph B.

The IR spectrum of the 50-75 hours samples suggested that it consisted primarily of mebendazole polymorph A and traces of mebendazole polymorph B and C: polymorph A >>> polymorph B >>> polymorph C.

The XRPD patterns of the suspended sample stored at 100°C are illustrated in figure 4.26. The XRPD patterns confirmed the presence of polymorph C, B and A in the samples after 6 hours (figure 4.27). Polymorph B traces were not detected in the 50 and 75 hours samples due to the poor-crystalline properties of mebendazole polymorph B. The XRPD pattern of the sample at 75 hours resembled that of mebendazole polymorph A, as illustrated in figure 4.27.

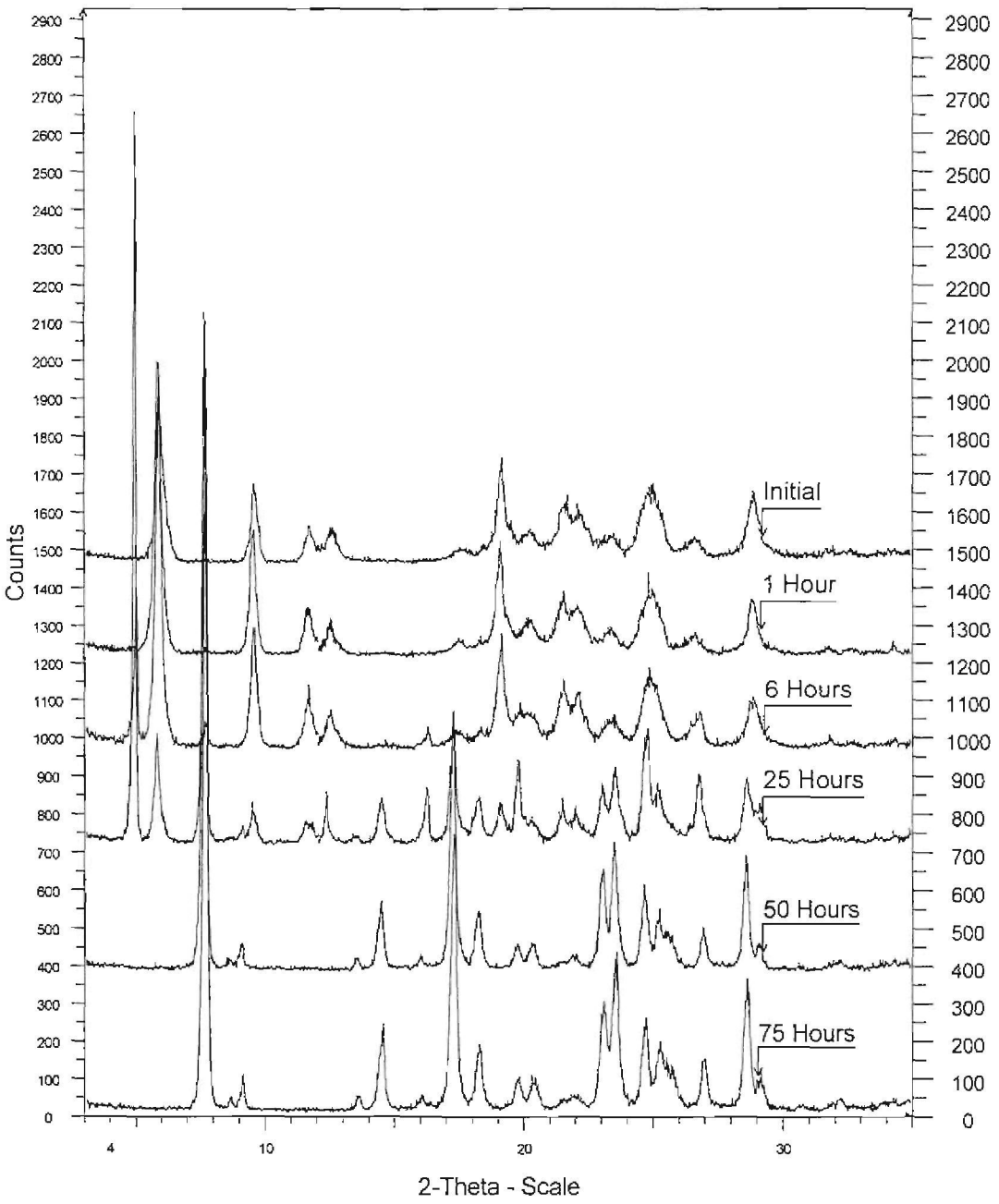


Figure 4.26 Overlay of the XRPD patterns of the suspended mebendazole polymorph B samples exposed to 100°C at various time intervals illustrating the polymorph transition.

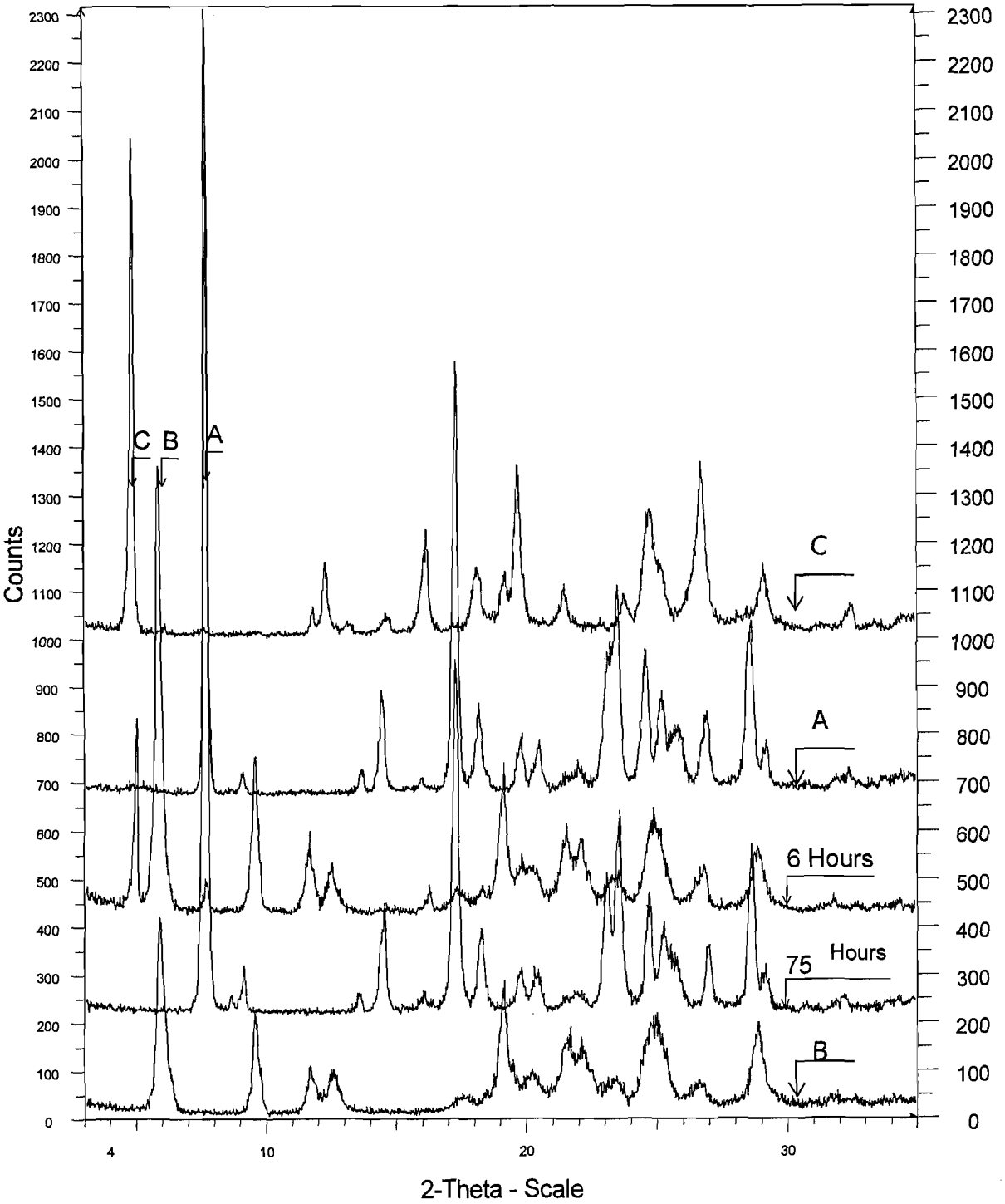


Figure 4.27 Overlay of the XRPD patterns of the suspended mebendazole polymorph B samples exposed to 100°C for 6 and 75 hours and polymorphs A, B and C.

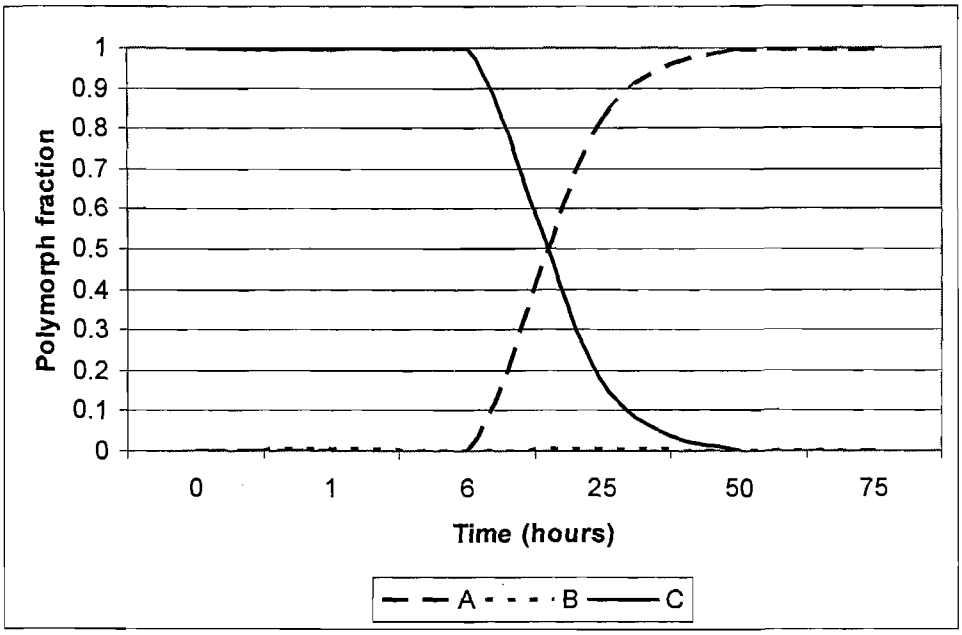
4.1.4 The effect of moisture on the stability of mebendazole polymorphs

The results for the exposed and unexposed Product 2, discussed in chapter 3, suggested that moisture played a significant role in the rate at which mebendazole polymorph C transforms to polymorph A. To investigate the effect on moisture on the transformation kinetics, suspensions of polymorphs B and C were subjected to elevated temperatures.

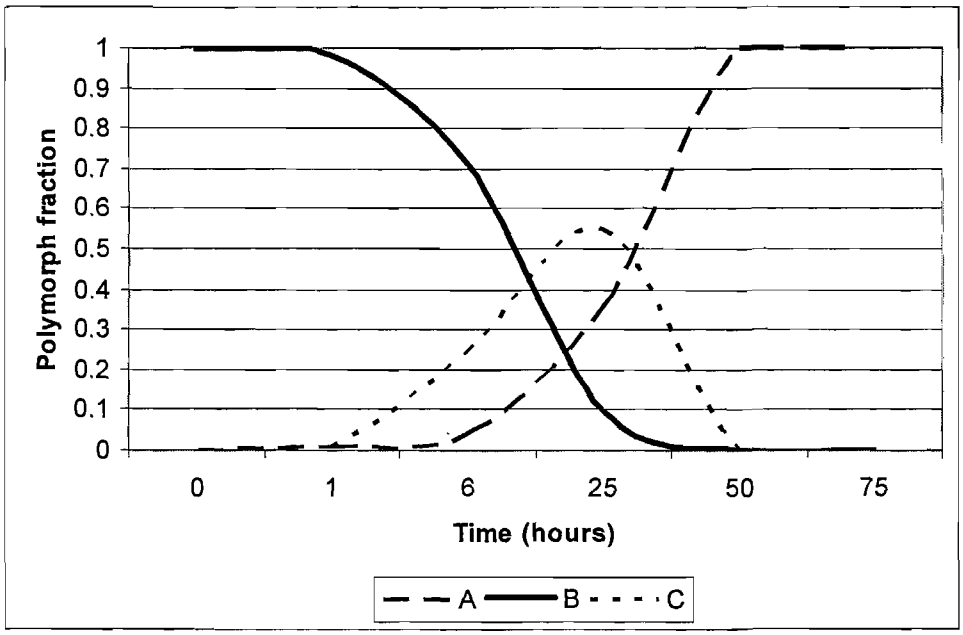
The polymorphic stability of the meta-stable mebendazole polymorphs (i.e. polymorph C and polymorph B) was investigated using DRIFT-IR and XRPD. The relative ratios of mebendazole polymorph A and C present at the various intervals were calculated from the XRPD and DRIFT-IR data using the principals discussed in section 3.3.1.1.

The ratios of polymorph A and C content relative to the total polymorph content in a sample were calculated from the DRIFT-IR and XRPD data. For the purpose of this study the polymorph fraction present relative to the total polymorph content present in the samples derived from the intensities (i) of the characteristic peaks [for example, polymorph A fraction = $i_A/\Sigma(i_A, i_B, i_C)$] will be discussed (figure 4.28).

As seen in figure 4.29 the decrease in polymorph C and the increase in polymorph A followed sigmoidal paths. However, with time a small amount of polymorph B was also present in the samples after 25 hours. This complicated the kinetics of the conversion and although the Avrami fits were reasonable with correlation coefficients around 0.9 it was not reliable.



(a)



(b)

Figure 4.28 Polymorph fractions present in the suspended mebendazole (a) polymorph C and (b) polymorph B at the various intervals when stored at 100°C derived from XRPD data.

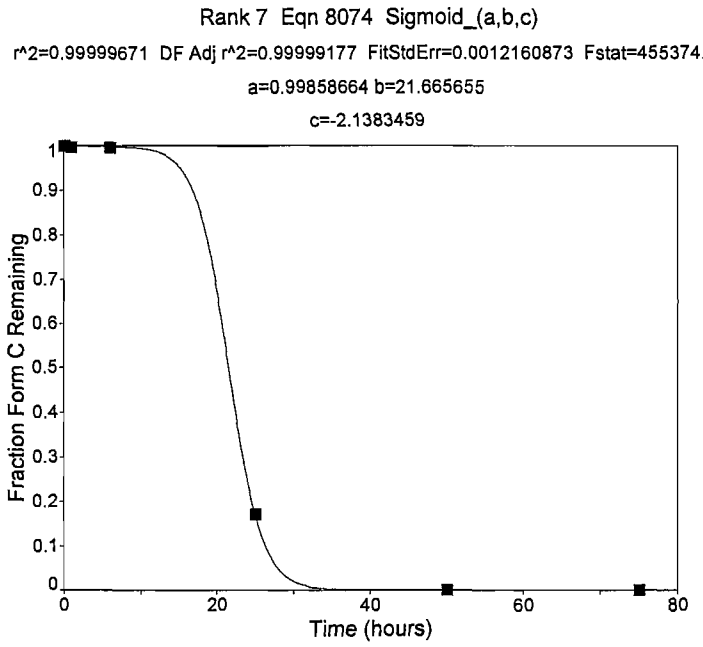
Fitting the data to a more generic sigmoidal equation gave very high correlation coefficients and allowed for the prediction of half-lives and shelf-lives for the decrease and growth in form C and A. The following equation was used:

$$\alpha = \frac{a}{1+\exp\left(-\frac{t-b}{c}\right)}$$

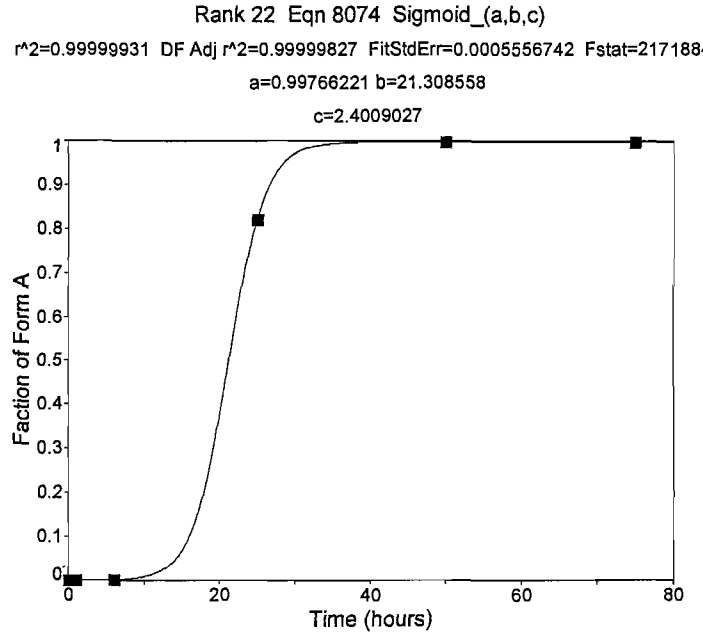
Where *a* is the transition height, *b* is the transition center (half-life) and *2.197c* is the transition width (*c* is negative for decay and positive for growth). The conversion of polymorph B (suspended in water and stored at 100°C) also followed a sigmoidal path characteristic of autocatalytic reactions.

The symbols in figures 4.29 and 4.30 represent experimental data and the lines the best fit according to abovementioned equation (data fitted using TableCurve 2D version 5.01, Systat, Richmond, CA, USA).

Table 4.5 illustrates the data obtained from fits of the polymorphic transformations using the data in figures 4.29 and 4.30 and the mentioned equation.

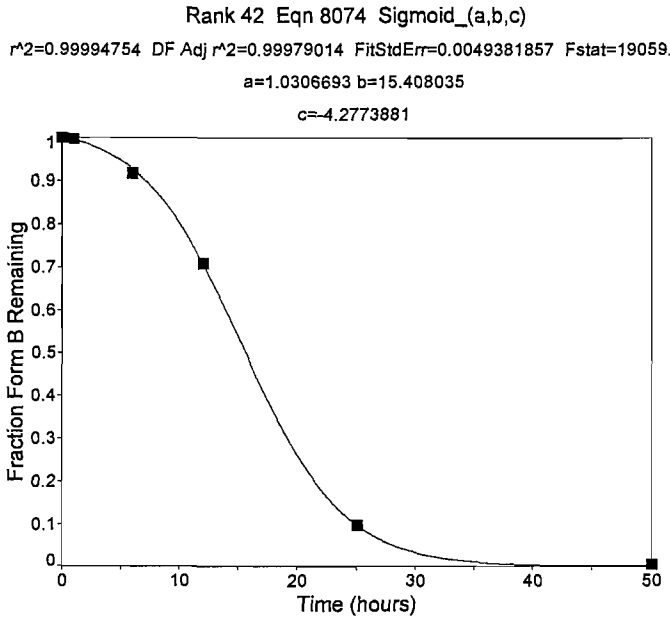


(A)

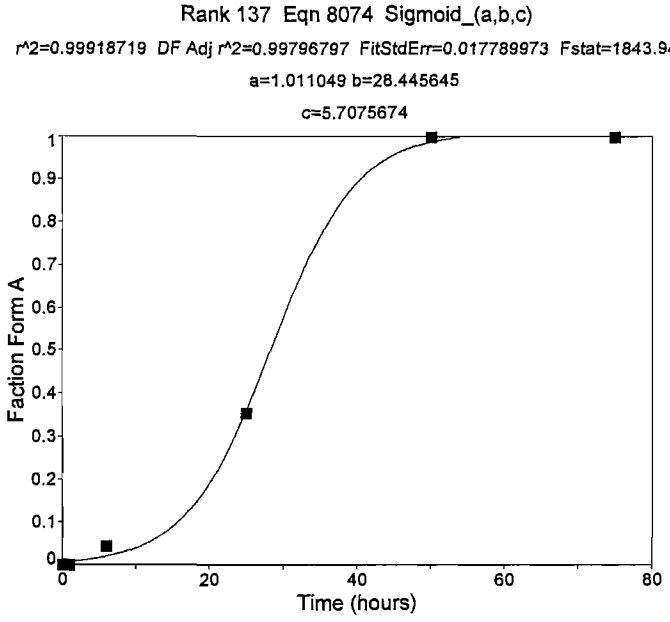


(B)

Figure 4.29 (A) Sigmoidal decrease in the content of mebendazole polymorph C when suspended in water at 100°C (B) Increase in content of mebendazole polymorph A when polymorph C was stored at the same conditions.



(A)



(B)

Figure 4.30 (A) Decrease in polymorph B when suspended in water at 100°C. (B) Increase in polymorph A when polymorph B was suspended in water at 100°C.

Table 4.5 Fit parameters for the polymorphic transformation of mebendazole polymorphs when suspended in water and stored in sealed containers at 100°C

Transformation	Curve Fit		a	b	c
	Shape	r^2			
C decay	Sigmoidal	0.9999	0.998	21.666	-2.138
A growth from C	Sigmoidal	0.9999	0.998	21.309	2.401
B growth from C	Sigmoidal	0.9977	0.0817	5.846	0.362
B decay	Sigmoidal	0.9997	1.031	15.408	-4.277
C growth from B	Bell shape	-	-	-	-
A growth from B	Sigmoidal	0.9980	1.011	28.445	5.707

For all the transformations, except for the growth of polymorph B from C, the transition heights, a, approached 1 (table 4.5). This means that in all these cases the polymorphic transformations were completed within the time the tests were performed. At 100°C when suspended in water, polymorph C quickly transformed to polymorph A with a $t_{0.5}$ = 22 hours. For this transformation the induction period of around 7-10 hours it took less than 5-6 hours for the conversion to be completed. The growth of polymorph A from polymorph C closely mirrored the decay in polymorph C because the $t_{0.5}$ for the formation of B was also 21 hours. In contrast the $t_{0.5}$ for polymorph B when suspended in water at 100°C was around 15 hours. In this case the induction period was markedly shorter at around 1-2 hours while the time necessary for completion of the conversion was longer at around 9-12 hours. In addition the formation of polymorph A from polymorph B was delayed with a $t_{0.5}$ = 28 hours and an even

longer transition time of more than 12 hours and almost no induction period. The reason for this could be that polymorph B transformed also to polymorph C which then transformed to polymorph A. This could explain why the curve following the transformation of polymorph C is a bell shape curve. Initially polymorph C is present and its content increase but then it decrease rapidly and eventually no polymorph C is detected.

4.1.5 Theory of the aqueous mediated phase transformation of mebendazole polymorphic forms

Swanepoel *et al.* (2003:348) indicated that polymorph C went into solution faster (70% in 120 minutes) compared to polymorph B (37% in 120 minutes) and polymorph A (20% in 120 minutes) when dissoluted in 0.1 N HCl at 25±2°C. The mentioned authors also indicated that the order of the solubility of the mebendazole polymorphs is: B > C > A. The order of the dissolution rate (C > B > A) does not correlated with the reported differences in the reported solubilities of the various forms (figure 4.31).

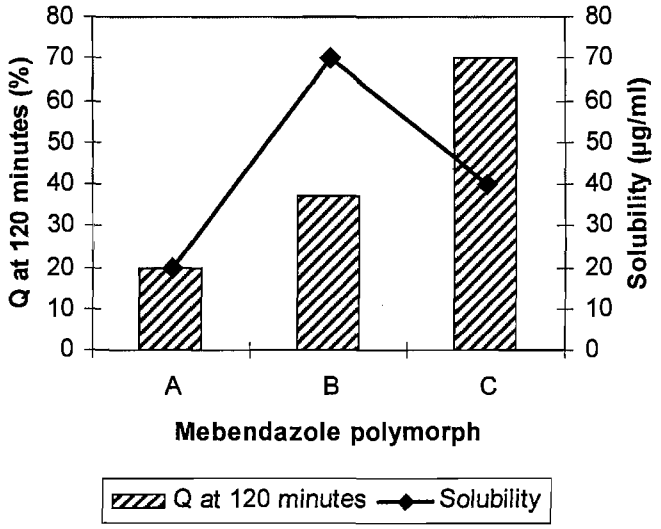


Figure 4.31 Q at 120 minutes for mebendazole polymorph A, B and C in 0.1 N HCl (reproduced from data published by Swanepoel *et al.*, 2003:347-348).

From this study it became clear that this incongruity could be attributed to the solvent mediated transformation of the metastable forms (polymorphs B and C) during the prolonged exposure (48 hours) to the aqueous solvent used during the solubility studies performed by Swanepoel *et al.*, 2003:478).

The Gibbs free energy is defined as the enthalpy (H) of the system minus the product of the temperature (T) times the entropy (S) of the system:

$$G = H - TS$$

The changes in the free energy of a system during dissolution can be measured at a predetermined temperature and is expressed in the following equation:

$$\Delta G = \Delta H - T\Delta S$$

ΔG is negative for a reaction in which ΔH is negative and ΔS is positive. Thus ΔG is negative for any reaction that is favoured by both the enthalpy and entropy terms, and this reaction could be considered spontaneous.

Mebendazole reveals a negative Gibbs free energy (G) in an aqueous solution (Shehatta, 2004:1239), utilising the solvent mediated phase transformation theory of Cardew and Davey (1985:418) and Ostwald's Rule. One can consider the theoretical phase diagram (which could be viewed as a monotropic / enantiotropic system (far away from the transition temperature)) for the mebendazole polymorphs (figure 4.32) to describe the solvent mediated transformation of mebendazole polymorph B.

W. Ostwald (1897) (as cited in Schmeltzer *et al.*, 1998):

"...in the course of transformation of an unstable (or metastable) state into a stable one the system does not go directly to the most stable conformation (corresponding to the modification with the lowest free energy) but prefers to reach intermediate stages (corresponding to other metastable modifications) having the closest free energy to the initial state".

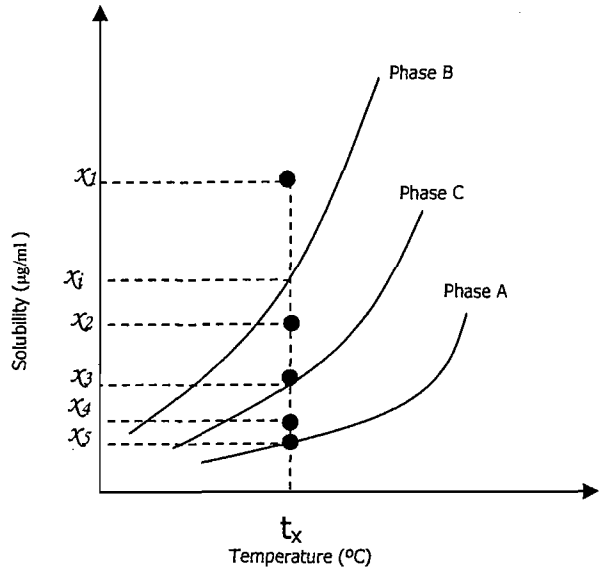


Figure 4.32 Theoretical solubility curves for mebendazole polymorphs.

In the phase diagram (figure 4.32) the stability of the mebendazole polymorphs are in the order: B > C > A as illustrated by Himmelreich *et al.* (1979:124).

For a solution with composition x_2 at t_x, it is supersaturated with respect to phases A & C, whilst for a solution of composition x_i at the same temperature (t_x) it is possible that al three phases could precipitate.

Thus according to Ostwald's Rule the metastable form will appear first (polymorph B) causing the solution composition to drop to x_1 (i.e. the solubility of polymorph B). At his point the solution is supersaturated with respect to phases C and A, so it is not unreasonable to suppose that phase B is the foremost solid phase appearing. Some nuclei of phase C and A might also be present (Cardew and Davey, 1985:418) in the solution.

The presence of the phase C and phase A nuclei will thus initiate the transformation process, namely a slurry of uniformly sized crystals of phase B in contact with the saturated solution containing equi-sized nuclei of the more stable phases, i.e. A and C.

As the nuclei growth proceeds the solubility of the system falls towards X_5 causing the system to become undersaturated with phase B, causing the phase B crystals to dissolve and thereby promoting the growth of the phase C and phase A crystals. The simultaneous dissolution of the metastable phase and growth of the more stable phase will continue until the metastable phases have been totally conformed into the stable phase and the solubility of the solution will decrease to X_5.

It is thus clear that the change in the volume fractions of the metastable phases (B and C) causes a change in the supersaturation (σ) of the system due to the growth-controlled transformation. Thus, it can be concluded that during the prolonged exposure of the metastable polymorphs to the aqueous solubility media, a fraction of the polymorph B phase transformed to polymorph C which contained a smaller fraction polymorph A, compared to the polymorph C fraction

which converted to the stable (and less soluble) polymorph A phase. It thus seems as if the rate of conversion from the metastable phases (polymorphs B & C) into the stable phase (polymorph A) is faster for the polymorph C, due to the direct conversion of polymorph C → polymorph A.

Figure 4.33 illustrates the change in volume fraction of each phase and the supersaturation for a growth-controlled transformation with second order kinetics (k_D/k_G = 10 and σ_1/σ_{12} = 10), in a system where phase 2 is the stable form and phase 1 the metastable form.

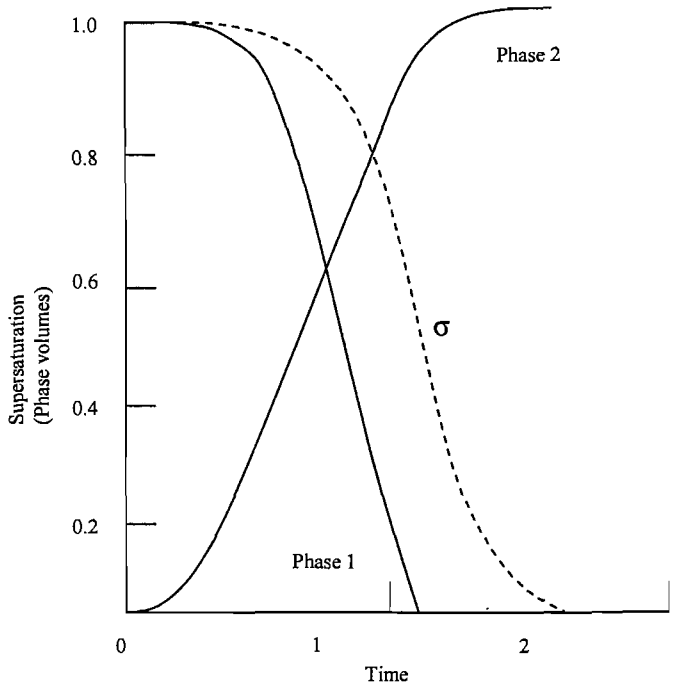


Figure 4.33 The change in volume fraction of each phase and the supersaturation for a growth-controlled transformation with second order kinetics (k_D/k_G = 10 and σ_1/σ_{12} = 10), in a system where phase 2 is the stable form and phase 1 the metastable form (reproduced from Cardew and Davey, 1985:421).

Conclusion

The influence of moisture and heat on the stability of mebendazole polymorph C and polymorph B in raw materials revealed that moisture was indeed a catalyst for the transformation process.

The exposure of mebendazole polymorph C to increased temperatures (up to 100°C) for a period of 75 hours did not induce polymorphic transition. In the presence of moisture (water) polymorphic transformations were observed at 100°C after only 25 hours, which produced polymorph A as final product after 50 hours. The presence of the polymorph B traces in the samples could be attributed to the solvent mediated transformation of polymorph C which lead to the formation of the thermodynamically least stable form (i.e. polymorph B). It is know that a system will always tend to produce only the most stable form (i.e. polymorph A), thus converting the most soluble form (i.e. polymorph B) to the most stable (least soluble) form, i.e. polymorph A (Byrn *et al.*, 1999:18-19). Thus the polymorph B traces will undergo rapid conversion to the more stable polymorphic forms, polymorphs C and A.

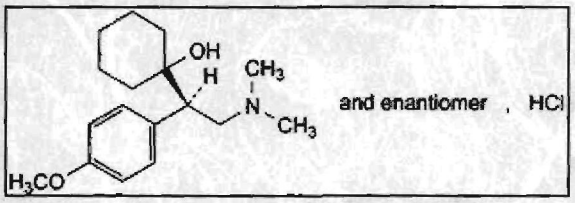
Exposure of mebendazole polymorph B to increased temperatures (up to 100°C) for a period of 75 hours did not reveal a significant polymorphic transition. In the presence of moisture (water) polymorphic transformations were observed at 50°C after 25 hours, when traces of polymorph C were detected in the samples, thus suggesting that polymorph B converted to polymorph C. After 75 hours the sample primarily consisted of mebendazole polymorph C and traces of mebendazole polymorph B.

The exposure of suspended mebendazole polymorph B to 100°C revealed that a fraction of polymorph B transformed into polymorph C. The IR spectrum of the 25 hours sample suggested that the sample consisted primarily of mebendazole polymorph C and traces of polymorphs A and B: polymorph C >>> polymorph A >>> polymorph B. The XRPD pattern of the sample at 75 hours resembled that of mebendazole polymorph A.

In addition the formation of polymorph A from polymorph B was delayed with a $t_{0.5}$ = 28 hours and an even longer transition time of more than 12 hours and almost no induction period which suggested that polymorph B transformed to polymorph C which then transform to polymorph A.

Future studies will focus on the influence of water and water-associated excipients used during the manufacturing process on the stability of mebendazole containing pharmaceutical products.

PART 2
Venlafaxine HCl



This sketch illustrates depression, a quiet fear. The fear is an unspoken, unconscious fear of Self. It is a time of paralysis where there is no emotion or any real movement or growth. It is a time of mind-numbing sameness, routine, and the stubborn refusal to face one's Self. Depression is a refusal to turn around, face the light and begin the slow ascent up the stairs.

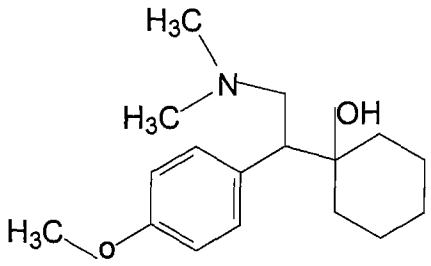
Words and Sketch, "Depression" by Jan Jennings www.janjenningsart.com

CHAPTER 5

Venlafaxine Hydrochloride

Introduction

Venlafaxine hydrochloride (venlafaxine HCl): (R,S)-1-[(2-Dimethylamino)-1-(4-methoxyphenyl)ethyl]cyclohexanol hydrochloride, is a structurally novel phenethylamine antidepressant, which inhibits monoamine re-uptake, with the greatest effect on serotonin, a substantial effect on norepinephrine, and relatively minor effects on dopamine (Potter *et al., 1998:483).*



The pharmacological activity of the (-)-isomer, is similar to that of the racemate, whereas the (+)-isomer, primarily inhibits serotonin uptake. There is no evidence for any stereoselective metabolism of venlafaxine HCl in the majority of subjects (Muth *et al.*, 1986:4493-4497).

The aim of this chapter is to provide an overview of the polymorphic behaviour of venlafaxine HCl and to describe the physico-chemical properties of the crystal forms investigated in this study.

5.1 Intellectual property: Venlafaxine HCl polymorphic and pseudopolymorphic forms

Venlafaxine HCl seems to be relatively free of the side-effects, associated with the known SSRI's (selective serotonin reuptake inhibitors, such as fluoxetine,

sertraline, paroxetine, fluvoxamine), and from the impact on both serotonin and norepinephrine that is associated with the tricyclic antidepressants (amitryptyline, imipramine, etc.) (Goldberg, 2002).

The patenting of the synthesis of venlafaxine in the mid 1980's induced a cascade of intellectual property claims of the polymorphic and pseudopolymorphic forms thereof. Table 5.1 provides a summary of the chronology of venlafaxine HCl polymorphs.

Table 5.1 Chronology of venlafaxine hydrochloride polymorphs (adapted from Roy *et al.*, 2005:2269)

No	Patent application no. and publication date	CAS reference	Crystal form
1	US 4,535,186 - 13 August 1985	CA 102:5895	Preparation of venlafaxine base and its HCl salt
2	WO 02/46140 A1 - 13 June 2002	CA 137:20211	Form 1, Form 2
3	US 2002/0183553 A1 - 5 December 2002	CA 138:8362	Form 1, Form 2
4	WO 03/048082 A2 - 12 June 2003	-	Form 3, Form 4
5	WO 03/042161 A1 - 22 May 2003	CA 138:406926	Three forms
6	US 2003/0105359 A1 – 5 June 2003	CA 136:355063	Form C, Form A, Form B, Form D
7	US 2003/0109585 A1 - 12 June 2003	CA 139:41803	Form 1, Form 2, Form 3
8	US 2003/0114536 A1 - 19 June 2003	CA 139:57923	Monohydrate form
9	WO 03/050074 A1 - 19 June 2003	CA 139:41833	Form 1, Form 2, Form 3

For the purpose of this study only the applicable venlafaxine hydrochloride polymorphic / pseudopolymorphic forms (i.e. Form 1, Form 2, monohydrate and its dehydrated crystal form) will be discussed, as well as a newly synthesized form, Form 5.

Rao *et al.* (2002:1) claimed intellectual property of venlafaxine crystal Forms 1 and 2, and a mixture of the two aforementioned crystal forms in the patent: WO03/46140. A summary of the thermal events of Form 1, 2 and the mixture thereof is presented in table 5.2 and figure 5.1.

Table 5.2 Thermal events in the DSC thermograms of venlafaxine hydrochloride Form 1, 2 and the mixture of Forms 1 and 2 (Adapted from Rao *et al.* 2002:3)

Form	**Thermal events**
Form 1	211°C – Melting endotherm 245°C – Decomposition endotherm
Form 2	221°C – Melting endotherm 255°C – Decomposition endotherm
Mixture of Form 1 and 2	211°C – Melting endotherm 219°C – Melting endotherm 251°C – Decomposition endotherm

The characteristic absorption bands (cm^{-1}) of the polymorphic forms in potassium bromide pellets are presented in table 5.4.

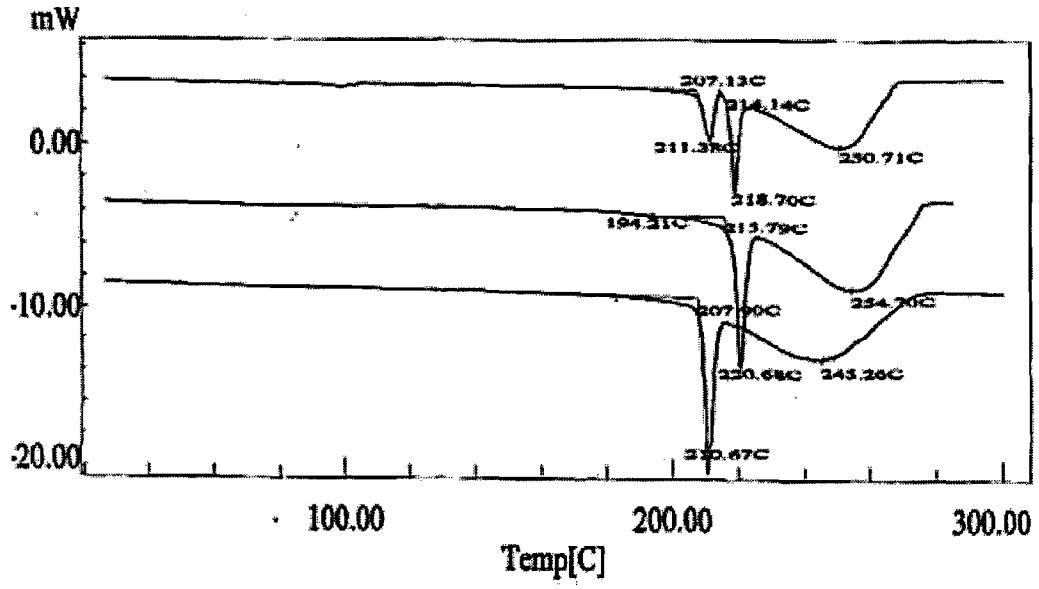


Figure 5.1 Overlay of venlafaxine hydrochloride DSC thermograms of Form 2 (middle), mixture of Form 1 and 2 (top) and Form 1 (bottom) (Adapted from Rao *et al.* 2002:5).

The DSC thermogram of Form 1 reveals a characteristic melting endotherm at 211°C with an onset temperature at 208°C followed by a decomposition endotherm at 245°C. Form 2 has a characteristic melting endotherm at 221°C (onset temperature at 216°C) followed by a decomposition endotherm at 255°C.

The DSC thermogram of the mixture (Form 1 and Form 2) has two melting endotherms at 211°C and 219°C respectively, and reveals a decomposition endotherm at 251°C. The authors of the patent (WO03/46140) also characterised Form 1 and 2 by means of single crystallography. The crystal parameters of Form 1 and Form 2 are presented in table 5.3 and the XRPD pattern data of Form 1, Form 2 and the mixture thereof are presented in figure 5.2 and table 5.5 respectively.

Table 5.3 Single crystal data for Form 1 and Form 2 (adapted from Rao *et al.* 2002:3)

Crystal data		**Form 1**	**Form 2**
Unit cell dimensions:	a	26.191(2)	5.797(6)
	b	5.875(2)	26.074(7)
	c	11.430(1)	11.722(3)
	α	90.00	90.00
	β	90.00	100.72(5)
	γ	90.00	90.00
Unit cell volume: V		1758.7(0.6)	1740.9(2.0)
Crystal system		Orthorhombic	Monoclinic
Space group		$Pca2_1$	$P2_1/n$
Density (g/ml)		1.18	1.20

Table 5.4 FT-IR absorption maxima of Form 1, 2 and the mixture of Form 1 and 2 (adapted from Rao *et al.* 2002:7)

Form 1	**Form 2**	**Mixture of Form 1 & 2**
3365	-	-
-	3352	3353
3324	-	3326
-	3016	3016
3003	-	-
2944	-	2943
2936	2936	-
-	2857	2856
2851	-	2851
-	2835	2832
2674	-	-
2587	2583	2585
-	-	-
2522	-	2519
-	2515	-
2484	-	2483
-	2480	-
-	-	-
1612	1614	1613
-	-	1583
1583	1582	-
1513	1514	1513

Table 5.4 continued ...

1474	1473	1473
1442	1439	1441
1404	1401	1403
1388	1385	1387
1366	1367	1366
1303	1307	1303
1275	1275	1275
1243	1247	1246
1180	1179	1179
-	1169	-
1153	1153	1153
1141	1141	1141
1108	1110	1109
1081	1083	1081
1061	1062	1062
-	1043	1040
1039	1035	-
981	982	-
970	972	971
959	957	958
928	929	929
909	909	909
-	837	-
830	-	831
818	-	818
-	811	-
-	778	-
770	768	769
-	740	-
735	-	736
594	-	592
-	581	-
547	553	-
528	-	-
-	523	525

Table 5.5 Main XRPD pattern peak positions (°2θ) of Form 1, 2 and the mixture of Form 1 and 2 (adapted from Rao *et al.* 2002:9)

Form 1	**Form 2**	**Mixture of Form 1 & 2**
6.74	-	6.72
-	6.84	-
-	8.44	8.34
10.26	10.30	10.20
-	12.80	12.68
13.50	-	13.50
-	13.62	-
15.06	-	15.00

Table 5.5 continued...

15.48	-	15.42
-	15.66	-
-	16.06	15.94
-	16.40	16.32
16.48	-	-
-	-	16.80
16.90	16.88	16.90
17.30	-	17.32
-	17.44	-
18.24	-	18.20
-	18.52	-
-	19.04	18.94
19.76	19.84	19.74
-	-	-
20.30	20.48	20.30
-	-	-
21.20	21.30	21.18
-	-	-
21.70	21.88	21.68
-	-	-
22.70	22.82	22.68
23.98	25.14	-
-	-	25.04
25.60	-	25.36
-	25.80	25.60
-	26.24	-
-	26.38	26.26
26.56	-	-
-	26.98	-
27.18	-	-
-	27.40	27.16
27.58	-	27.28
-	-	27.58
28.20	-	28.04
-	28.62	28.18
28.74	-	25.52
-	28.96	-
29.28	-	28.86
29.74	-	29.26
-	31.08	-
31.22	31.24	-
31.54	-	31.16
-	31.82	31.56
31.98	-	-
32.20	-	32.04
-	-	32.42
32.80	32.84	32.76
33.08	-	33.00
-	33.34	33.24
-	34.06	33.96
34.16	-	34.16
35.06	-	35.06

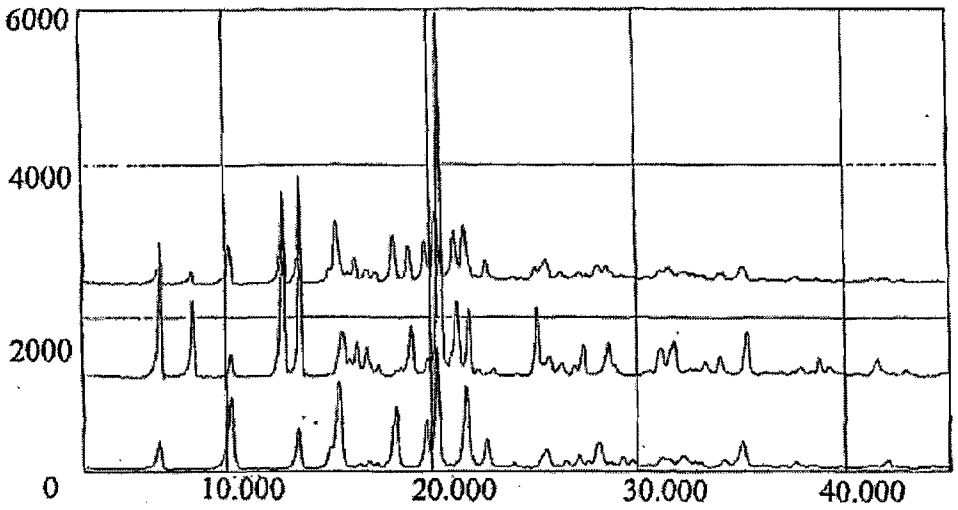


Figure 5.2 XRPD overlay of venlafaxine hydrochloride: mixture of Form 1 and Form 2 (top), Form 2 (middle), and Form 1 (bottom) (adapted from Rao *et al.* 2002:3).

Brits (2003:104) prepared two monohydrated crystal forms (i.e. polymorphic pseudopolymorphs), $\mathbf{H_{\alpha\beta}}$ and $\mathbf{H_{\beta}}$ (figure 5.3). In June 2003 a patent application was filed for a venlafaxine hydrochloride monohydrate by Jun & Jai (2003:1) which showed resemblances to form $\mathbf{H_{\beta}}$.

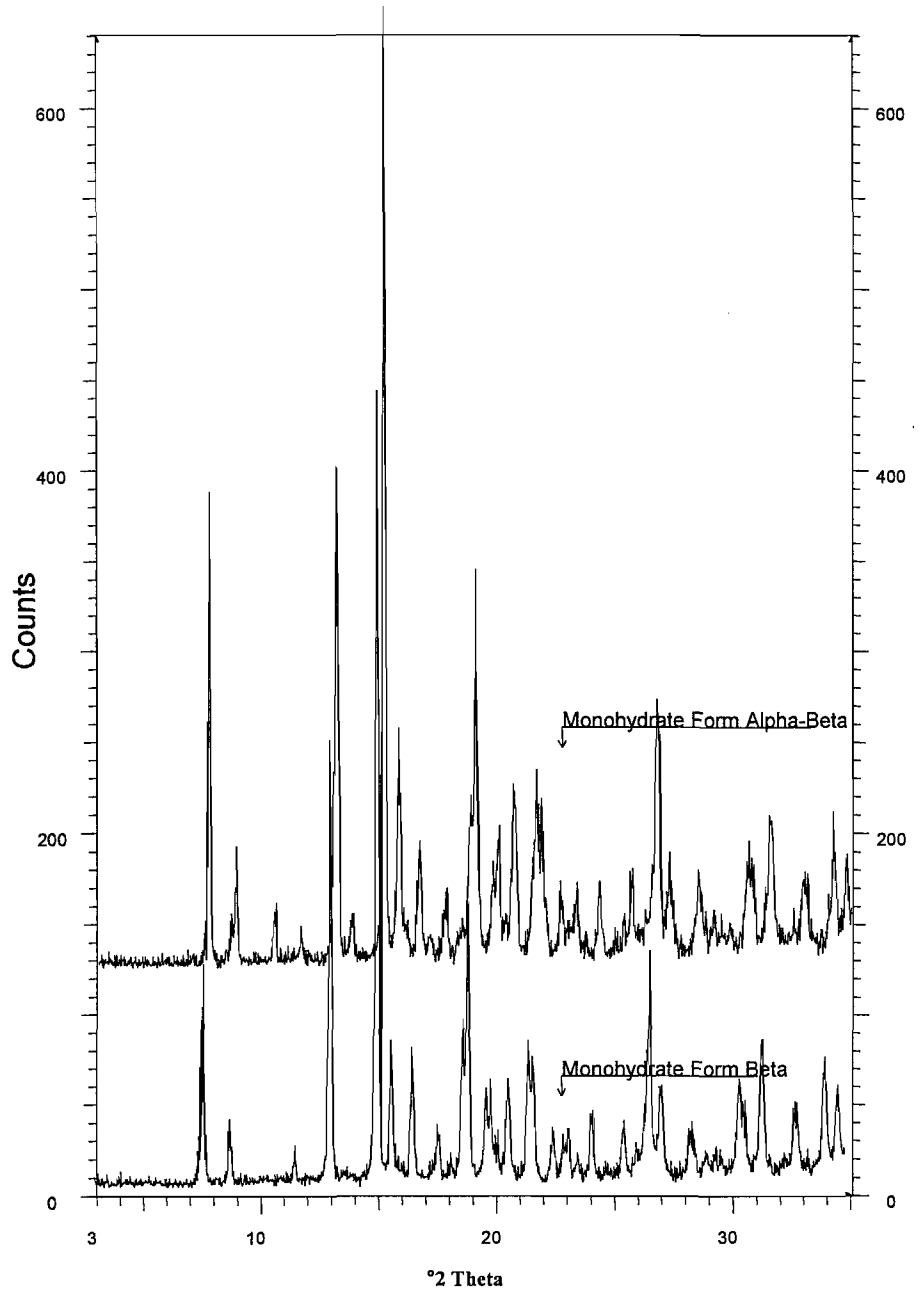


Figure 5.3 The XRPD patterns of pseudopolymorphic Form $\mathbf{H}_{\beta}$ and Form $\mathbf{H}_{\alpha\beta}$ (Brits, 2003:104).

Brits (2003:175) described the dehydration process of Form $\mathbf{H}_{\alpha\beta}$ using VT-XRPD, and characterised the dehydration product (Form γ) – figure 5.4.

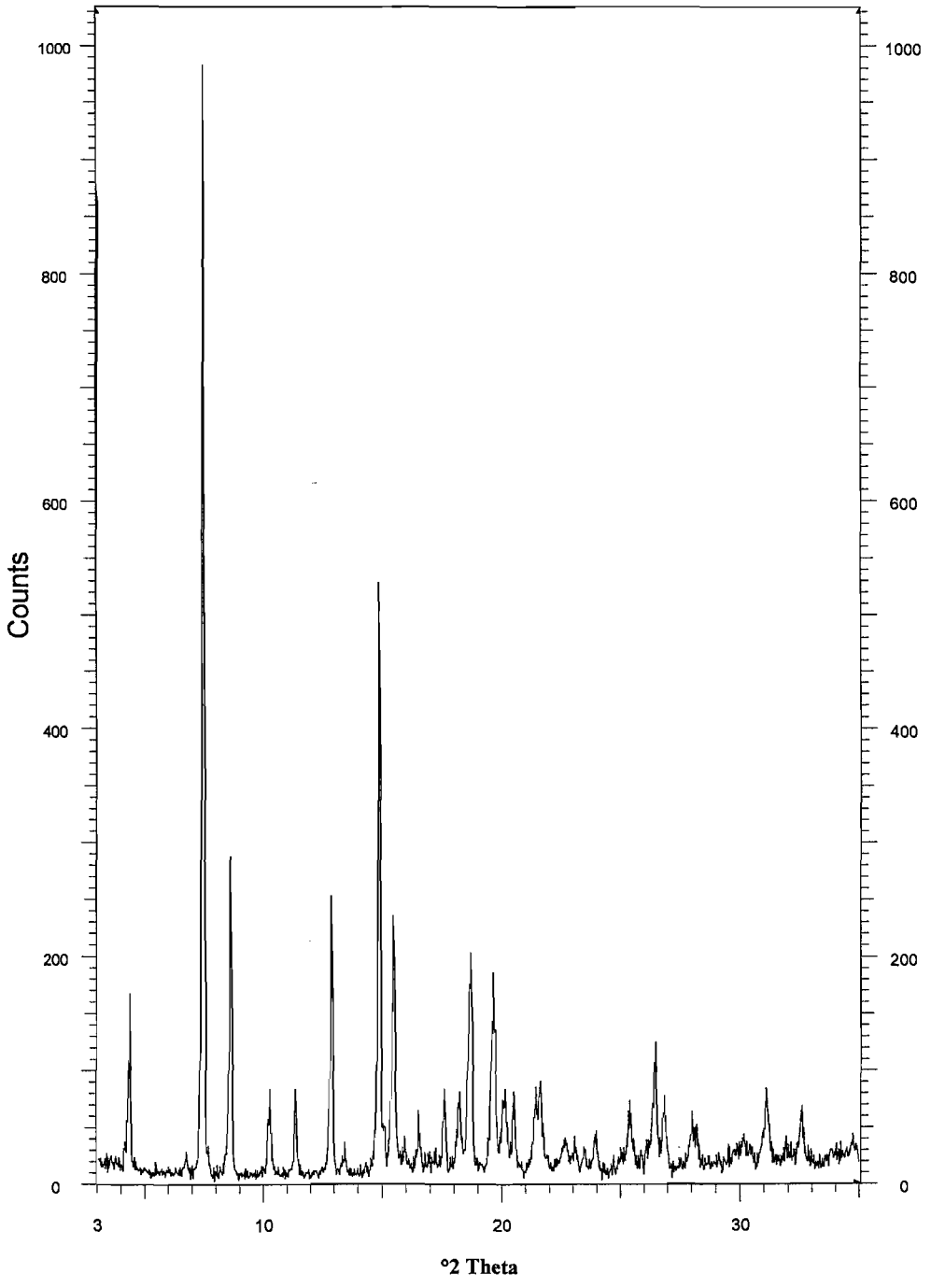


Figure 5.4 The XRPD pattern of Form γ (Brits, 2003:106).

5.2 Introduction to venlafaxine hydrochloride Form 1 and Form 5

The purpose of this section is to provide a general overview of the method of preparation, solid state properties and thermodynamic stability of venlafaxine hydrochloride Form 1 and Form 5.

In Part I of this study (Chapters 3 & 4), the thermodynamic stability and moisture induced polymorphic transitions of a practically water-insoluble API, mebendazole, were investigated. Venlafaxine HCl Form 1 and Form 5 were selected as prototype crystal forms due to the significant differences in their thermodynamic and crystallographic properties, to investigate the moisture-sorption susceptibility and thermodynamic stability of these two anhydrous polymorphic forms.

Form 5 is a new polymorph prepared by the addition of an anti-solvent (ethyl-acetate) to a saturated venlafaxine solution (solvent: methanol). This study revealed that here seems to be some structural correlations between Form 2 and Form 5, however the thermodynamic properties of these two, high-melting polymorphic forms differ. Form 5 is a metastable crystal form, whereas Form 1 and Form 2 are thermodynamic stable crystal forms (patent WO/02/46140:12). Thus, for the purpose of this study, a thermodynamically stable (Form 1) and metastable (Form 5) crystal form were selected.

5.2.1 Preparation of venlafaxine hydrochloride Form 1 and Form 5

Form 1

The following recrystallisation method was used to prepare Form 1. Analytical grade methanol (ACE (Pty) Ltd, South Africa) was used for the recrystallisation of venlafaxine HCl.

A saturated solution was prepared by dissolving venlafaxine HCl in the methanol, while heating to the boiling point of methanol (64°C). The solution was prepared under constant magnetic stirring. A rotary evaporator attached to a vacuum was used to evaporate the solvent from the saturated solution. A Buchi Rotavapor

R110 rotation evaporator (Buchi, Flawil, Switzerland) was used. The heating bath temperature was set at 100±5°C.

Form 5

The following recrystallisation method was used to prepare Form 5. Analytical grade methanol (ACE (Pty) Ltd, South Africa) was used for the recrystallisation of venlafaxine HCl.

A saturated solution was made by dissolving venlafaxine HCl in methanol at room temperature. The solution was prepared under constant magnetic stirring. The process of recrystallisation was accelerated by the addition of an anti-solvent (ethyl acetate – obtained from Saarchem, Merck chemicals (PTY) LTD., South Africa) while cooling the solution in an acetone-ice bath. The fine needles were filtered after 24 hours and dried at ambient conditions.

5.2.2 Solid state properties of Form 1 and Form 5

A well-balanced set of analytical techniques was used to investigate the solid state properties of the prepared venlafaxine HCl Form 1 and Form 5 which included: XRPD, DRIFT-IR, DSC, KF, VT-XRPD, TM, SEM and heat of solution investigations.

The recrystallised samples were dried in a vacuum oven at 90°C for 1 hour. It was found that the dried Form 1 sample showed greater resemblances to the published data (section 5.1) of Form 1.

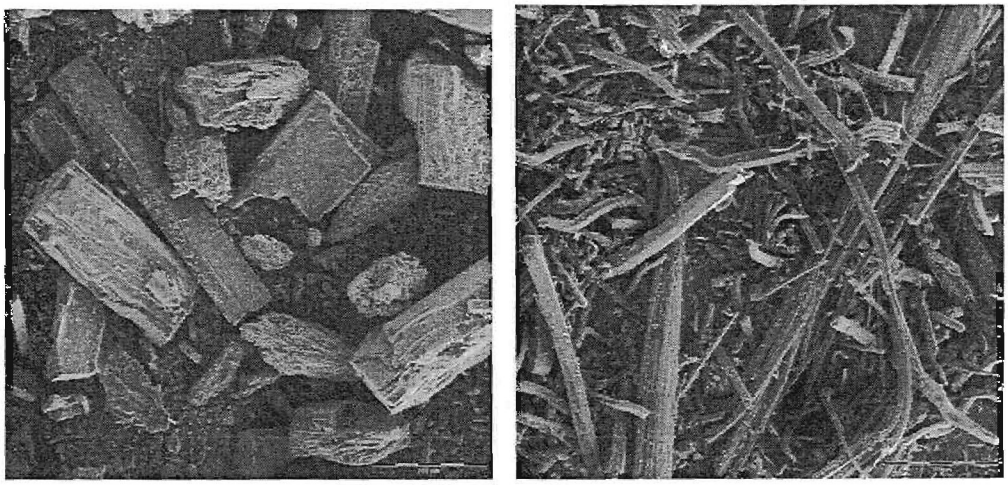
5.2.2.1 X-ray powder diffractometry (XRPD)

The XRPD patterns of the two venlafaxine HCl crystal forms are shown in figure 5.6. Peak angles (°2θ) and relative intensities (I/Io) of the main XRPD peaks are listed in table 5.6.

This study points out that venlafaxine hydrochloride Form 1 and Form 5 exhibits preferred orientation, and care should be taken during the sample preparation for XRPD recordings and the interpretation of XRPD patterns.

Preferred orientation in powder diffraction experiments is a common problem experienced by crystallographers. In powder crystallography, the ideal sample consists of crystals or crystal fragments oriented completely at random, thus the loci of end points of individual reciprocal vectors (i.e. H_{hkl}) are on the surfaces of concentric spheres and orientation of the samples is independent on direction of the primary beam. However, it is know that real samples present non-spherical crystal morphologies that cause preferred orientation of particles in polycrystalline specimens (Fejdi & Holocsy, 2001:23).

Anisotropic shaped crystals (e.g. platelet-like, needle-like, rod-like etc.) results in the introduction of distinctly non-random crystallite orientations (i.e. preferred orientation) and XRPD recordings reveal diffractograms with power lines completely missing or intensity lines with very misleading intensities (Bernstein, 2002:118). Thus preferred orientation can substantially alter the appearance of XRPD patterns. SEM photomicrographs of the prepared venlafaxine hydrochloride Form 1 and Form 5 revealed columnar (i.e. rod-like particle, having a width and thickness exceeding that of needle-type particles) and avicular (i.e. needle-like) crystal structures respectively (figure 5.5).



(a) **(b)**

Figure 5.5 SEM photomicrograph of venlafaxine hydrochloride crystal (a) Form 1 and (b) Form 5.

Table 5.6 Main XRPD pattern intensity ratios (I/Io) of venlafaxine HCl: Form 1 and Form 5

Form 1		Form 5	
Peak angles (°2θ)	**Relative intensities (I/Io)**	**Peak angles (°2θ)**	**Relative intensities (I/Io)**
6.7	18.9	6.8	14.9
-	-	7.4	8.7
-	-	8.4	21.5
10.2	14.9	10.2	6.3
-	-	12.7	100.0
13.5	37.8	13.6	38.1
-	-	14.9	13.6
15.1	1.2	-	-
15.5	15.4	15.6	21.9
-	-	16.0	5.1
-	-	16.4	12.7
-	-	16.8	13.8
16.9	1.5	-	-
17.3	0.8	17.4	3.9
18.2	5.2	18.5	10.3
-	-	19.0	17.7
19.8	6.3	19.8	8.4
20.3	100.0	20.4	78.9
-	-	21.2	25.7
21.7	16.6	21.8	25.3
22.7	3.2	-	-
-	-	23.0	3.9
24.0	0.5	-	-
-	-	25.1	25.5
25.6	2.4	-	-
-	-	25.7	7.5
-	-	26.3	6.8
26.5	1.0	-	-
-	-	26.9	5.9
27.2	9.5	27.3	7.9
27.6	1.0	-	-
28.2	2.6	-	-
28.7	0.6	28.6	12.8
-	-	28.9	5.8
29.3	1.2	-	-
29.7	0.9	-	-
-	-	-	-
31.1	1.7	31.2	11.7
31.5	3.1	-	-
-	-	31.7	10.8
32.0	1.4	-	-
32.3	1.4	-	-
32.7	0.9	-	-
-	-	33.3	8.0
-	-	34.0	10.0
34.2	1.8	-	-

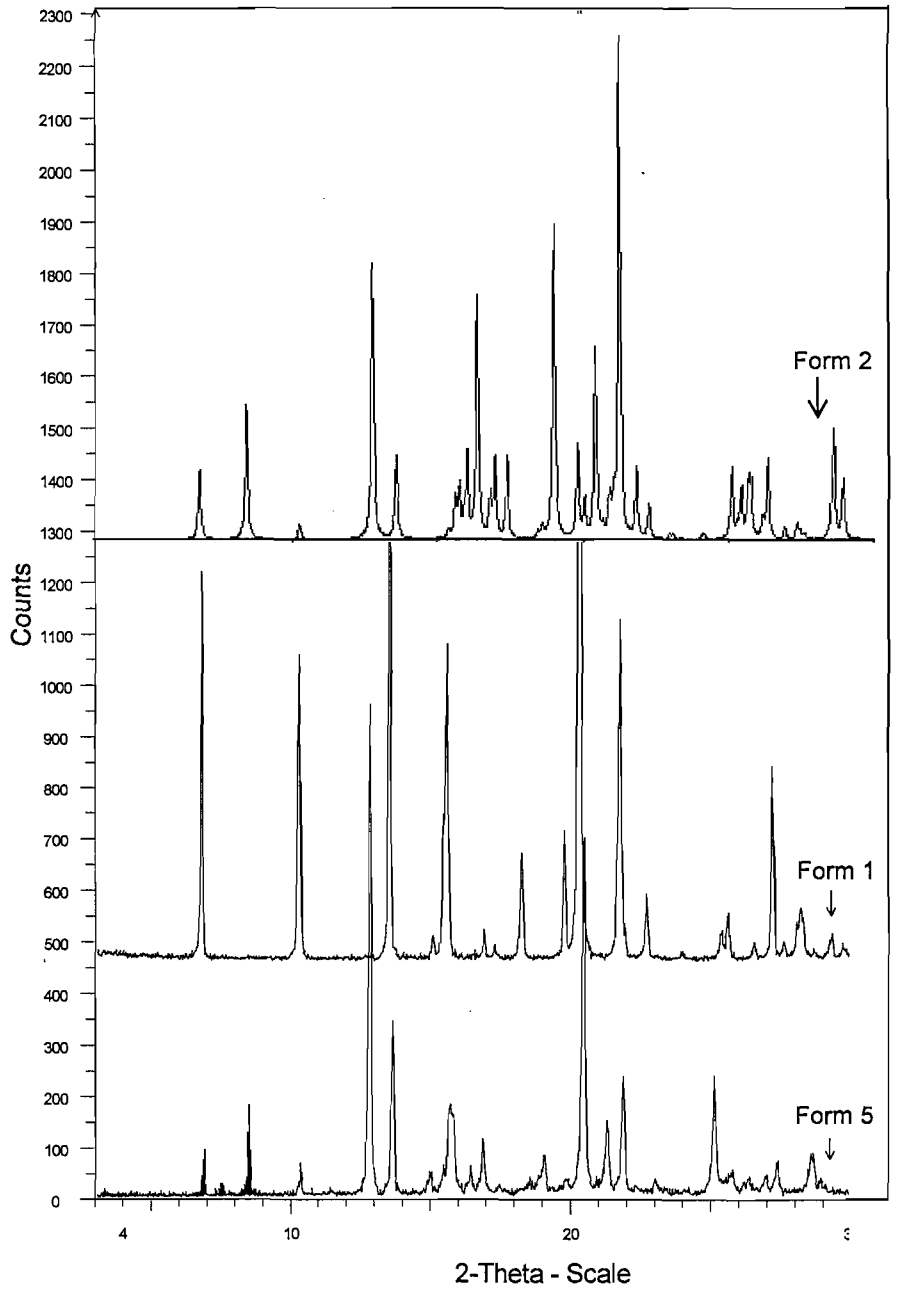
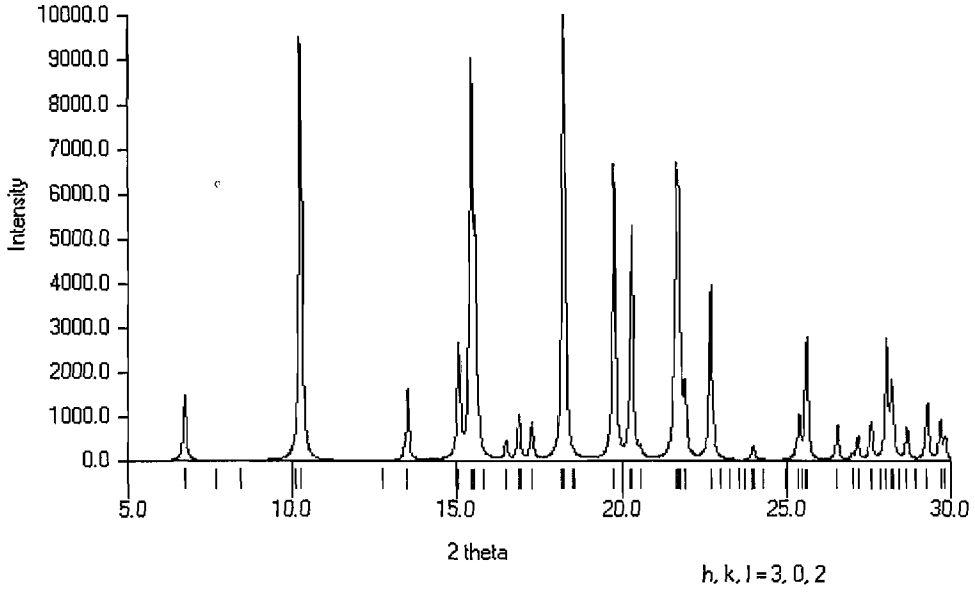
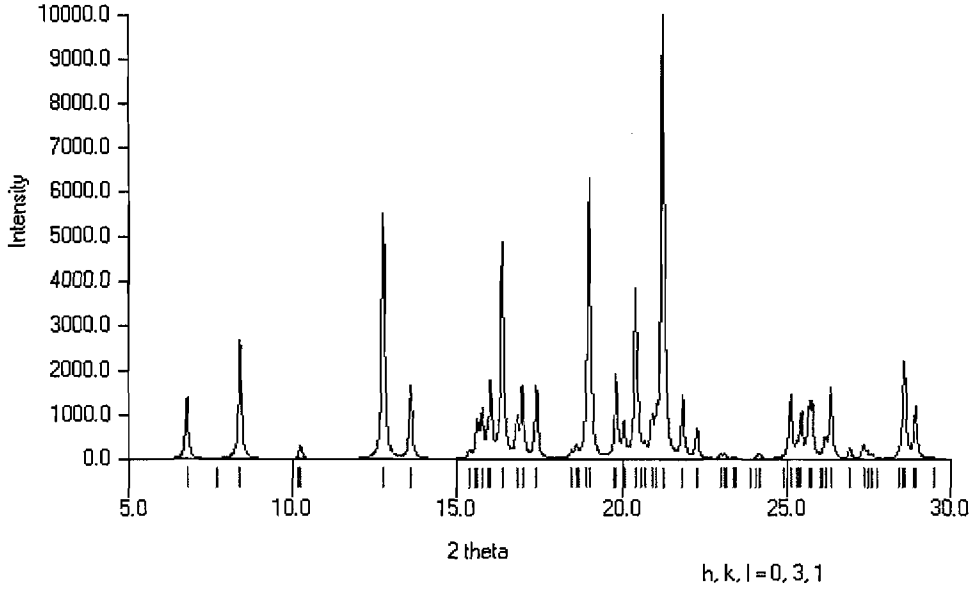


Figure 5.6 XRPD patterns of venlafaxine HCl crystal Form 1, Form 2 and Form 5.

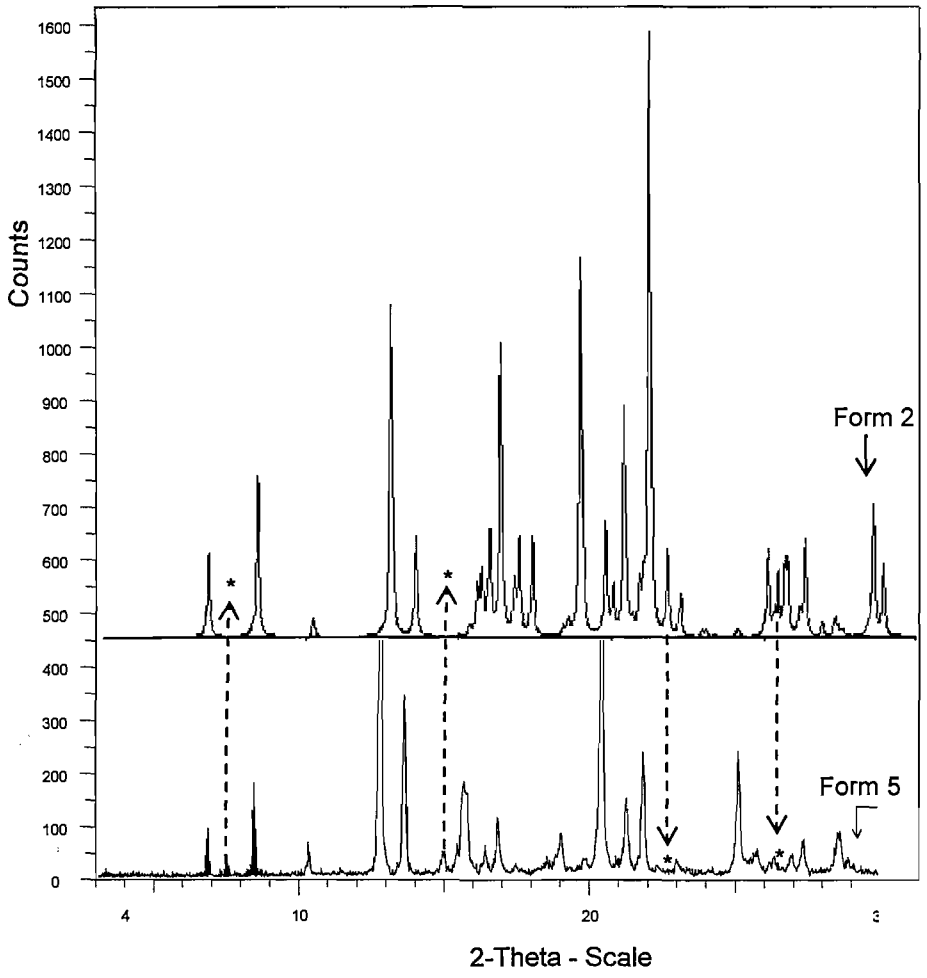


(a)



(b)

Figure 5.7 Theoretical X-ray powder diffractogram of venlafaxine HCl (a) Form 1 and (b) Form 2 derived form single crystal data published.



(C)

Figure 5.7 (c) XRPD overlay of the theoretical X-ray powder diffractogram of venlafaxine HCl Form 2 derived form single crystal data published, and Form 5 (* - indicates most significant differences in peak angular positions).

Comparing the XRPD patterns of Form 5 (Figure 5.6) and the theoretical powder diffraction pattern of Form 2 (derived form the single crystal data in table 5.3 using Mercury® Software) in Figure 5.7 (c), it was observed that there was a good correspondence as far as the peak angular positions are concerned for the main diffraction peaks, however discrepancies were detected at the angular peak positions for the weaker diffraction peaks of the mentioned two forms.

Regardless of all precautionary steps taken during the sample preparation (particle size reduction of sample by means of sample grinding, rotation of sample during XRPD recording) preferred orientation was observed. The observed preferred orientation is evident from the generally poor agreement in relative intensities of corresponding peaks in the patterns (figure 5.7 (c)). There were also examples of 'intensity reversals' where peak X had a larger intensity than peak Y in e.g. the experimental pattern, but the reverse was found in the calculated pattern (figure 5.7 (c)).

The diffraction peaks at 7.4, 14.9 and 23.0°2θ in the XRPD pattern of Form 5 which were absent in the XRPD pattern of Form 2 and the presence of peaks at 22.8 and 25.8°2θ in the XRPD pattern of Form 2 and the absence thereof in the XRPD pattern of Form 5 (figure 5.7 (c)) enthused the possibility of the existence of a mixture of crystal forms (i.e. Form 2 and other venlafaxine hydrochloride polymorphs) or that Form 2 and Form 5 might show some resemblances in crystal conformation but can not be considered to be the same polymorphic forms.

The Bragg peaks present at 7.4, 14.9 and 23.0°2θ in the XRPD pattern of Form 5 are also present in the XRPD pattern of venlafaxine hydrochloride crystal Form γ described by Brits (2003:105), but the absence of the characteristic Form γ peak at 4.2°2θ out-ruled the possibility that Form 5 could be a mixture of Form 2 and Form γ. The XRPD pattern of Form 5 differed significantly compared to that of the high-melting point polymorph (Form **β**) prepared by Brits (2003:100).

It is thus clear that there seems to be some structural correlations between Form 2 and Form 5, however in section 5.2.2.5 it will be indicated that Form 5 is a metastable crystal form (that converts to Form 2 upon exposure to heat) and from the literature it is evident that Form 2 is considered to be the thermodynamic stable form, based on the fact that it shows the highest unit cell density (table 5.3) (Rao *et al.* 2002:3).

5.2.2.2 Diffuse reflectance infrared Fourier transform spectroscopy (DRIFT-IR)

The superimposed IR spectra of the two polymorphs (Form 1 and Form 5) are shown in figure 5.8. The main IR-absorption peaks and their corresponding wavenumbers (cm^{-1}) are listed in table 5.7.

A close examination of the IR spectra of Form 1 and Form 5 showed significant differences. The specific peaks and their corresponding wavenumbers (cm^{-1}) of Form 5 (table 5.7) and that of Form 2 (table 5.4) may have varied two or three wavenumber units (cm^{-1}) either way, but overall the spectra of Form 2 and Form 5 were comparable. Thus, it can be concluded that the small differences between the crystal lattice of Form 2 and Form 5 did not have a profound influence of the vibrational energies in the mentioned crystal modifications. IR analysis can therefore not be used to differentiate between Form 5 and Form 2.

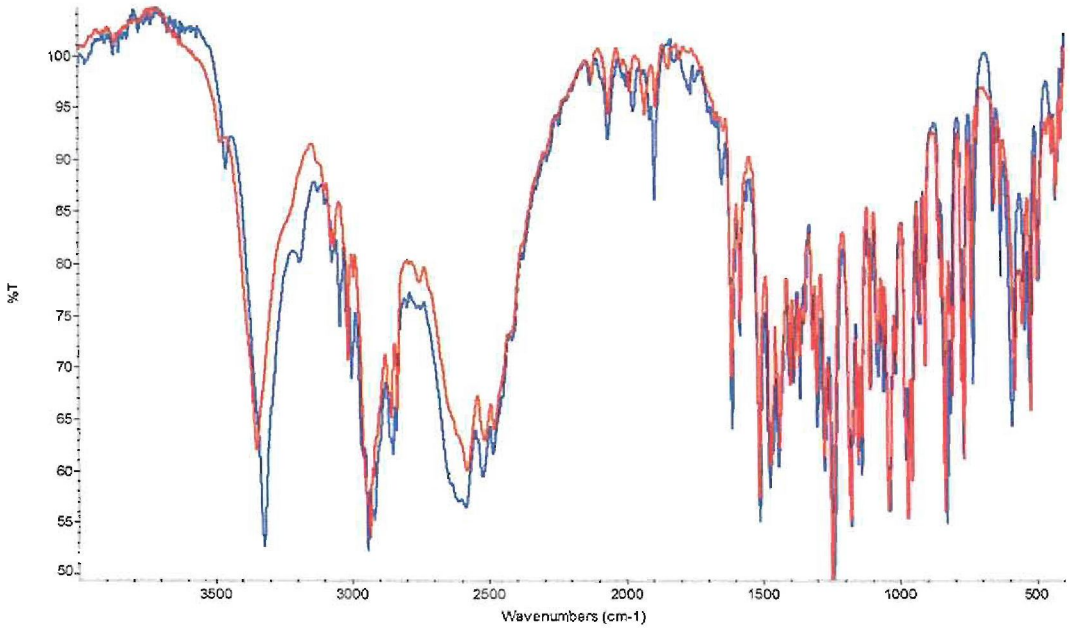


Figure 5.8 IR spectra (superimposed) of venlafaxine HCl crystal forms (Form 1 [blue] and Form 5 [red]).

Table 5.7 Main absorptions in the IR spectra of venlafaxine HCl: Form 1 and Form 5

Main absorptions	Wavenumbers (cm^{-1})	
	Form 1	Form 5
1	3871	-
2	3780	-
3	3462	3350
4	3323	3064
5	3073	3016
6	3045	2996
7	3002	2935
8	2943	2856
9	2919	2834
10	2851	2583
11	2838	2515
12	2587	2482
13	2524	2125
14	2486	2065
15	2131	1985
16	2067	1930
17	-	1891
18	1973	1844
19	1896	-
20	1763	-
21	1647	1613
22	1612	1582
23	1582	1514
24	1512	1473
25	1474	1438
26	1442	1401
27	1402	1384
28	1388	1366
29	1365	1319
30	1346	1305
31	1322	1274
32	1303	1247
33	1274	1180
34	1242	1153
35	1179	1141
36	1153	1110
37	1141	1083
38	1107	1062
39	1080	1043
40	1061	1016
41	1038	972
42	1018	957
43	981	929
44	970	908
45	959	860
46	927	850
47	909	836
48	859	811
49	844	777
50	829	768

5.2.2.3 Thermal analysis

The thermal properties of the venlafaxine HCl crystal forms were investigated, using DSC, TGA and thermomicroscopy (TM). TGA analysis was conducted on samples of which their DSC results indicated a tendency of possibly being solvated.

The DSC thermogram of crystal Form 1 (figure 5.9) exhibited a single melting endotherm at 211°C, followed by a decomposition endotherm. The absence of any desolvation endotherms indicated that crystal Form 1 was a true polymorph. The heat of fusion (ΔH_{f1}) was calculated to be approximately 109.31 J/g. A summary of the thermal events of Form 1 and Form 5 is given in table 5.8.

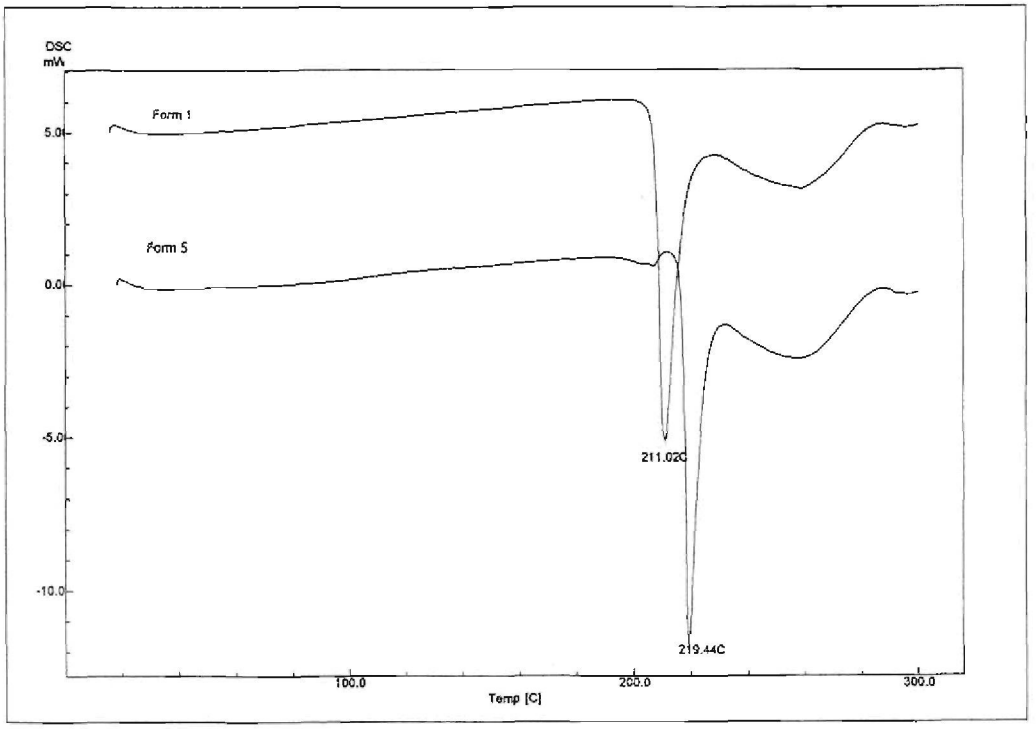


Figure 5.9 DSC thermograms of venlafaxine HCl crystal Form 1 and crystal Form 5.

Table 5.8 Summary of thermal properties of venlafaxine HCl crystal Form 1 and Form 5

Form	Melting point (°C)	Heat of fusion (J/g)
Form 1	211.02	109.31
Form 5	219.44	85.35

The DSC thermogram of crystal Form 5 (figure 5.9) exhibited a melting endotherm in the region of 219-221°C, followed by a decomposition endotherm. The absence of any desolvation endotherms indicated that crystal Form 5 was a true polymorph. The heat of fusion (ΔH_{f5}) was calculated to be approximately 85.35 J/g. The melting point of Form 2 is 221°C (table 5.2) and is thus comparable to that of Form 5. No heat of fusion data was available in the literature at the time of this study.

TM revealed that crystal Form 1 underwent crystal growth at ± 178°C (table 5.9). These plate-like, intergrowth crystals could clearly be seen on the thermomicroscope images. The crystal growth was not detectable in the DSC thermogram, since the energy needed for this growth might be below the detection limit of the apparatus used for the DSC analysis.

At 196°C melting of the smaller crystals was observed, and at 200°C the melting of the transparent, plate-like crystals. The initial melting of Form 1 was observed at 206°C, followed by complete melting of the sample at 209°C. The TM results supported the DSC results, i.e. that the melting of venlafaxine HCl crystal Form 1 occurred at 208–211°C.

Table 5.9 Summary of the TM results of venlafaxine HCl crystal Form 1 at a temperature range of 25-209°C

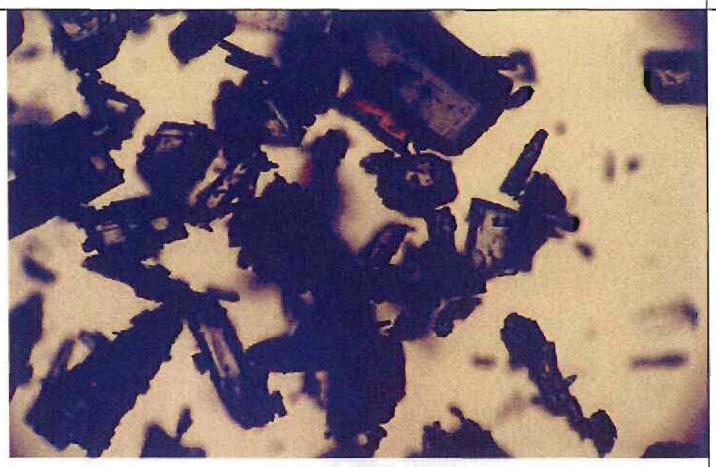
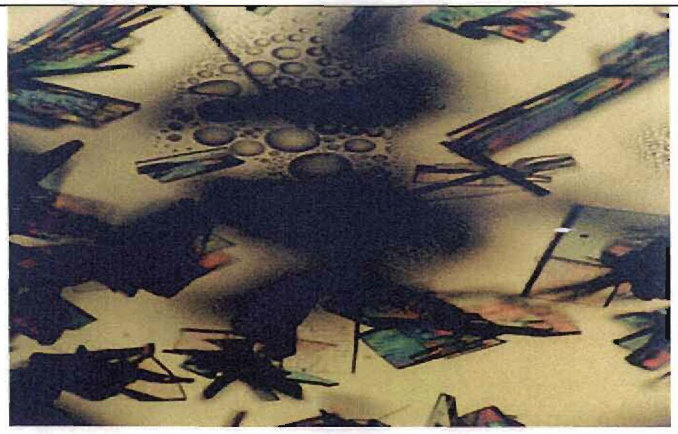
Temperature (°C)	Photomicrograph	Remarks
25		Crystal Form 1 at room temperature.
178		Plate-like, intergrowth crystals forming.
200		Transparent, plate-like crystals crystallised from the melt at 196°C.

Table 5.9 continued...

209		Complete melting of crystal Form 1.

TM revealed that crystal Form 5 also underwent crystal growth at ± 174°C. These plate-like, intergrowth crystals could clearly be seen on the photomicrographs (table 5.10). The crystal growth was not detected in the DSC thermogram, since the energy needed for this growth might be below the detection limit of the apparatus used for the DSC analysis.

Thermomicroscopy revealed that the crystals showed moderate movements at 75-100°C which could be attributed to an inter-crystal rearrangement. The DSC thermogram of Form 5 showed that the base-line of the thermogram was relatively unstable up to approximately 200°C, which may support the inter-crystal rearrangement observed using TM. This phenomenon will be discussed in section 5.2.2.5.2 using VT-XRPD.

At 210°C the inter-growth crystals started to melt, and complete melting of the sample occurred at 222°C. The TM results supported the DSC results, i.e. that the melting of venlafaxine HCl crystal Form 5 occurred at 219–221°C.

Table 5.10 Summary of the TM results of venlafaxine HCl crystal Form 5 at a temperature range of 25-222°C

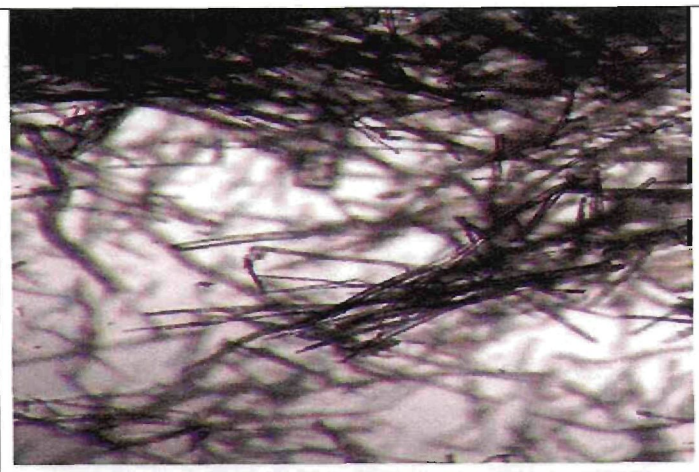
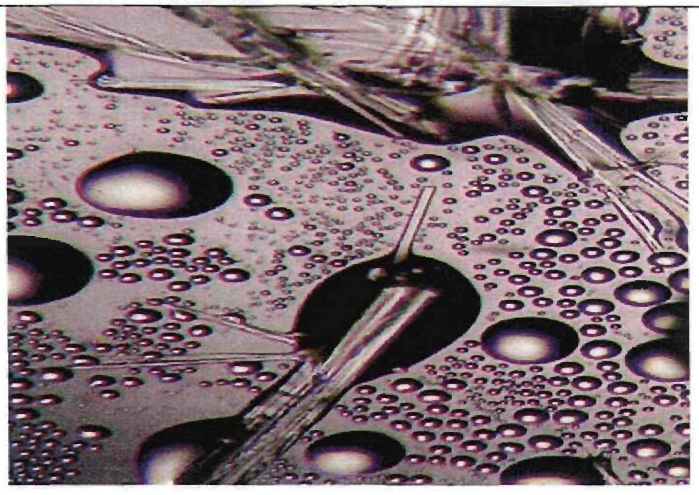
Temperature (°C)	Photomicrograph	Remarks
25		Form 5 at room temperature.
174		Plate-like, intergrowth crystals forming.

Table 5.10 continued...

188		Plate-like, intergrowth crystals.
210		Melting of intergrowth crystals initiated.
222		Melting of crystal Form 5.

5.2.2.4 Heat of Solution of Venlafaxine HCl polymorphs – Form 1 and Form 5

The heats of solution of the velafaxine HCl polymorphs were determined by isothermal high sensitivity microcalorimetry (MicroDSC III, Setaram, France) at 20, 30 and 40°C. Samples weighing approximately 2 mg were analysed in a mixing "batch" vessel under nitrogen purging with about 0.15 g deionised water used as the solvent (Nanopure, Barnstead International, Dubuque, Iowa). The vessel is composed of a cylinder and a set of parts mounted on a rod provided for dividing the experimental volume into two distinct chambers with a volume of 0.2 cm^3 for the upper chamber and 0.55 cm^3 for the lower chamber. The powder was placed in the bottom of the mixing vessel while the solvent was added to the top reservoir. Once the instrument was equilibrated at 20, 30 or 40°C, the rod was pushed down allowing the solvent to come in contact with the venlafaxine HCl powder. The heat measured, once corrected for the heat involved in stirring (second peak in figure 5.10), represent the heat involved in the dissolution of the venlafaxine powders in water. All measurements were repeated 6 times.

The heat of solution, ΔH, is calculated using the following equation:

$$\Delta H = \frac{q}{mol}$$

Since the heat (q) comes from the chemical reaction of the solute, ΔH is per moles solute, not per mol solution.

The effect of temperature on the solubility of a solid in water may be predicted using *Le Principe du Chatelier* if it is known whether the process is endo- or exothermic. If the solution process is endothermic, solubility increases with increasing temperature; if exothermic, solubility decreases (Kotz & Treichel, 1996:772). As seen in figures 5.11 and 5.12, the heat of solution for the venlafaxine crystal forms were exothermic. As shown in table 5.11, the symbol ΔH is used to denote the enthalpy changes. If heat is evolved, the reaction is

exothermic ($\Delta H < 0$) as shown in figures 5.11 and 5.12; and if heat is absorbed, the reaction is *endothermic* ($\Delta H > 0$). When a salt such as venlafaxine HCl dissolves in water, energy is required to break up the crystal lattice (the attraction between ions is called the crystal lattice energy), called $\Delta H_{lattice}$. Since energy is added to the system to break the lattice, $\Delta H_{lattice}$ is always positive, i.e. endothermic. When the ions are solvated by water (surrounded by water) energy is released in the formation of intermolecular bonds between ions and water (energy of hydration). We call this energy $\Delta H_{hydration}$. Since energy is lost by the system $\Delta H_{hydration}$ is always negative, i.e. exothermic. The relationship between lattice energy ($\Delta H_{lattice}$), heat of hydration ($\Delta H_{hydration}$), and $\Delta H_{solution}$ is:

$$\Delta H_{solution} = -\Delta H_{lattice} + \Delta H_{hydration}$$

When the energy of hydration is greater than the crystal lattice energy, the dissolving process will be exothermic and causes a temperature increase as seen for the venlafaxine HCl polymorph ($\Delta H_{hydration} > \Delta H_{lattice}$ then, $\Delta H_{solution} < 0$, table 5.11 and figure 5.10) and therefore it's an exothermic reaction. In addition when the enthalpy of dissolution is exothermic, as in the case of venlafaxine HCl, a temperature increase will decrease solubility according to *Le Principe du Chatelier* (Kotz & Treichel, 1996:772).

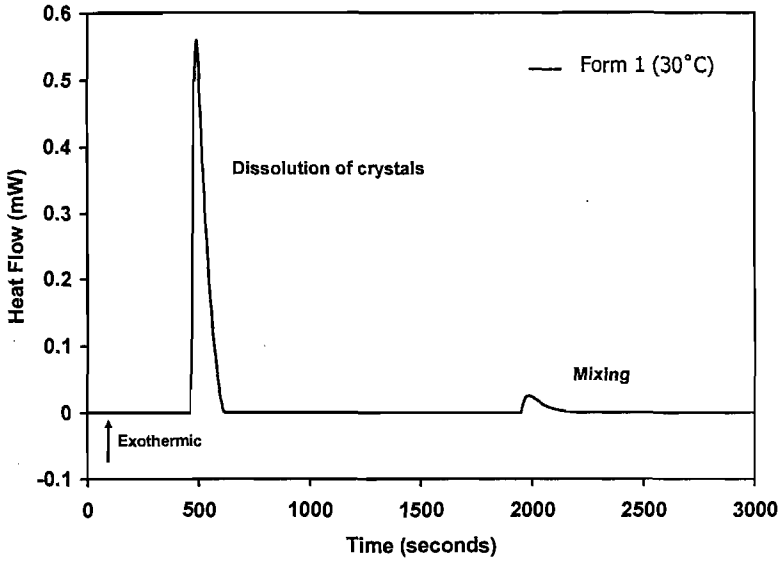


Figure 5.10 MDSC thermogram used for determining the heat of solution of venlafaxine HCl Form 1.

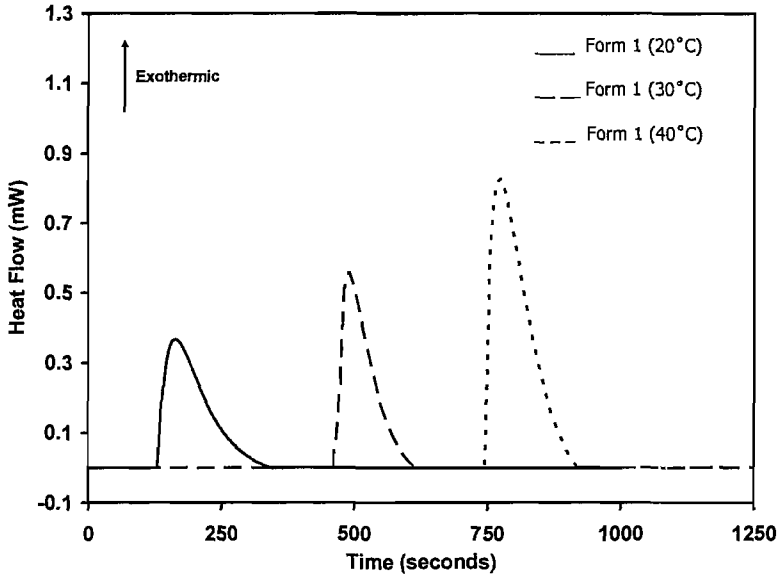


Figure 5.11 MDSC thermograms showing the exothermic heat generated at the dissolution of venlafaxine Form 1 at 20, 30 and 40°C.

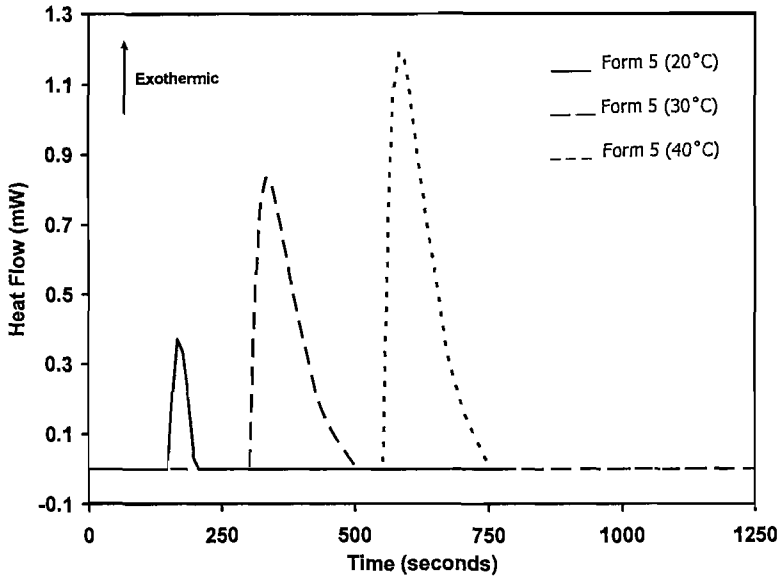


Figure 5.12 MDSC thermograms showing the exothermic heat generated at the dissolution of venlafaxine Form 5 at 20, 30 and 40°C.

Table 5.11 Heat of solution at increasing temperatures for venlafaxine HCl Form 1 and Form 5

Temperature (°C)	Form 1		Form 5	
	ΔH_{sol} (J/g)	ΔH_{sol} (kJ/mol)	ΔH_{sol} (J/g)	ΔH_{sol} (kJ/mol)
20	-18.22±1.78	-5.71±0.56	-17.29±2.31	-5.42±0.72
30	-40.93±2.22	-12.84±0.70	-115.17±3.62	-36.16±1.13
40	-61.82±2.65	-19.40±0.83	-159.98±5.12	-50.21±1.61

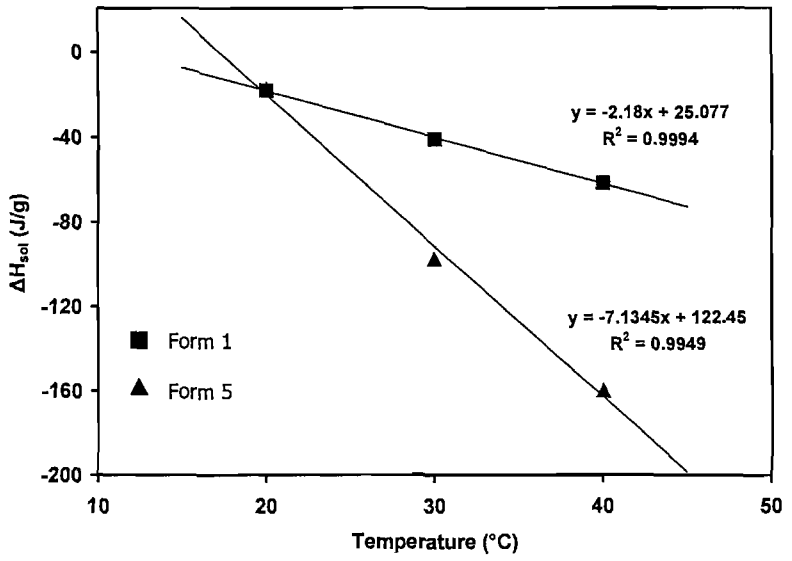


Figure 5.13 Change in the exothermic heat of solution of Form 1 and Form 5 of venlafaxine HCl with an increase in temperature.

To see this effect the heats of solution at increasing temperatures were measured as illustrated in figures 5.11, 5.12 and 5.13. Elevation of the temperature for the same concentration of API polymorph resulted in a linear increase in the exothermic heats of solution. This is because there is a greater destruction of the primary structure of the API caused by thermal effects at higher temperature. This effect was less pronounced for lower melting crystals of Form 1.

Spontaneous reactions depend on two forces, enthalpy (ΔH) and entropy (ΔS). The Gibbs free energy (G) relates this effect:

$$\Delta G = \Delta H - T\Delta S$$

where G is Gibbs free energy, H is enthalpy, S is entropy, and T is the Kelvin temperature. When ΔG for a reaction is negative, the reaction will be spontaneous. When ΔG for a reaction is positive, the reaction will not be spontaneous. When ΔG is zero, the reaction is at equilibrium. If both enthalpy

and entropy decrease the energy of the system (-ΔH and +ΔS), the reaction will be spontaneous. If both of these forces increase the energy of the system (+ΔH and -ΔS), the reaction will be non-spontaneous. If one force increases the energy of the system and the other decreases it, spontaneity will be determined by the larger force. Since entropy is linked to temperature, higher temperatures increase the effect of entropy (Blaber, 2006).

The temperature dependence of solubility is usually explained using Le Chatelier's principle. The principle states that when a system at equilibrium is placed under stress, the equilibrium will shift in a way that relieves that stress (Blaber, 2006). In the case of venlafaxine HCl, the "stress" is the addition of heat. If the heat given off in the dissolving process is greater than the heat required to break apart the solid, the net dissolving reaction is exothermic as seen for venlafaxine HCl. The addition of more heat (increased temperature) inhibits the dissolving reaction (broader peaks at higher temperatures in figure 5.11 and 5.12) since excess heat is already being produced by the reaction. This decreases the solubility of the drug with an increase in temperature. This situation is not very common where an increase in temperature produces a decrease in solubility.

5.2.2.5 Thermodynamic stability of venlafaxine HCl polymorphs – Form 1 and Form 5

The thermodynamic stability of polymorphic and pseudopolymorphic forms is of great interest to researchers in the pharmaceutical research and development field. It is important to investigate and fully comprehend the physico-chemical properties and thermodynamics of the APIs that are to be used during the manufacturing process to avoid unwanted surprises during and after the manufacturing process, that may have financial implications for the manufacturer and potential efficacy and safety risks for the patient.

The aim of this section was to investigate the stability of Form 1 and Form 5 when exposed to increased temperatures using variable temperature x-ray powder diffraction.

Form 1 and Form 5 were exposed to increased temperatures (up to a maximum of 215°C) while investigating potential changes in the crystal lattice indicated by changes in the XRPD patterns of the mentioned samples.

5.2.2.5.1 Thermodynamic stability of Venlafaxine HCl Form 1

The VT-XRPD patterns of venlafaxine hydrochloride Form 1 are shown in figure 5.14.

No thermal events were observed in the DSC thermogram of Form 1 (figure 5.9) prior to the melting endotherm that could suggest any phase transitions or desolvation.

With an increase in the temperature of venlafaxine hydrochloride Form 1, no significant changes were observed in the VT-XRPD pattern (figure 5.14) up to 150°C except for the increase of the intensity of the Bragg diffraction peak at 34.2°2θ. A slight peak shift occurred, possibly as a result of slight differences in sample height caused due to thermal expansion of the powder bed.

An increase in the temperature above 175°C induced the following changes:

- The peak at 6.7 °2θ disappeared.
- The following peaks revealed a shift towards the left: 10.2, 13.5, 15.1, 15.5, 16.9, 17.3 and 18.2°2θ.
- A decrease in the intensity of the peak at 18.2°2θ was observed.
- The peaks between 22.0°2θ and 35.0°2θ revealed a decrease in intensity, leading to the extinction of peaks at: 25.4, 31.1, 31.5 and 34.2°2θ.

The changes in the XRPD patterns could be attributed to the crystal growth observed at 178°C (section 5.2.2.3).

The halo-shaped XRPD pattern observed at 200°C indicated that the melting of the sample had commenced. Exposure of the sample for a prolonged period to increased temperatures during the VT-XRPD study caused the sample to melt at a lower temperature than observed in the DSC thermogram (figure 5.9). The appearance of the peak at 28.2°2θ at 215°C could be attributed to a reflection caused by the sample holder, due to the shrinkage of the melted mass on the sample holder.

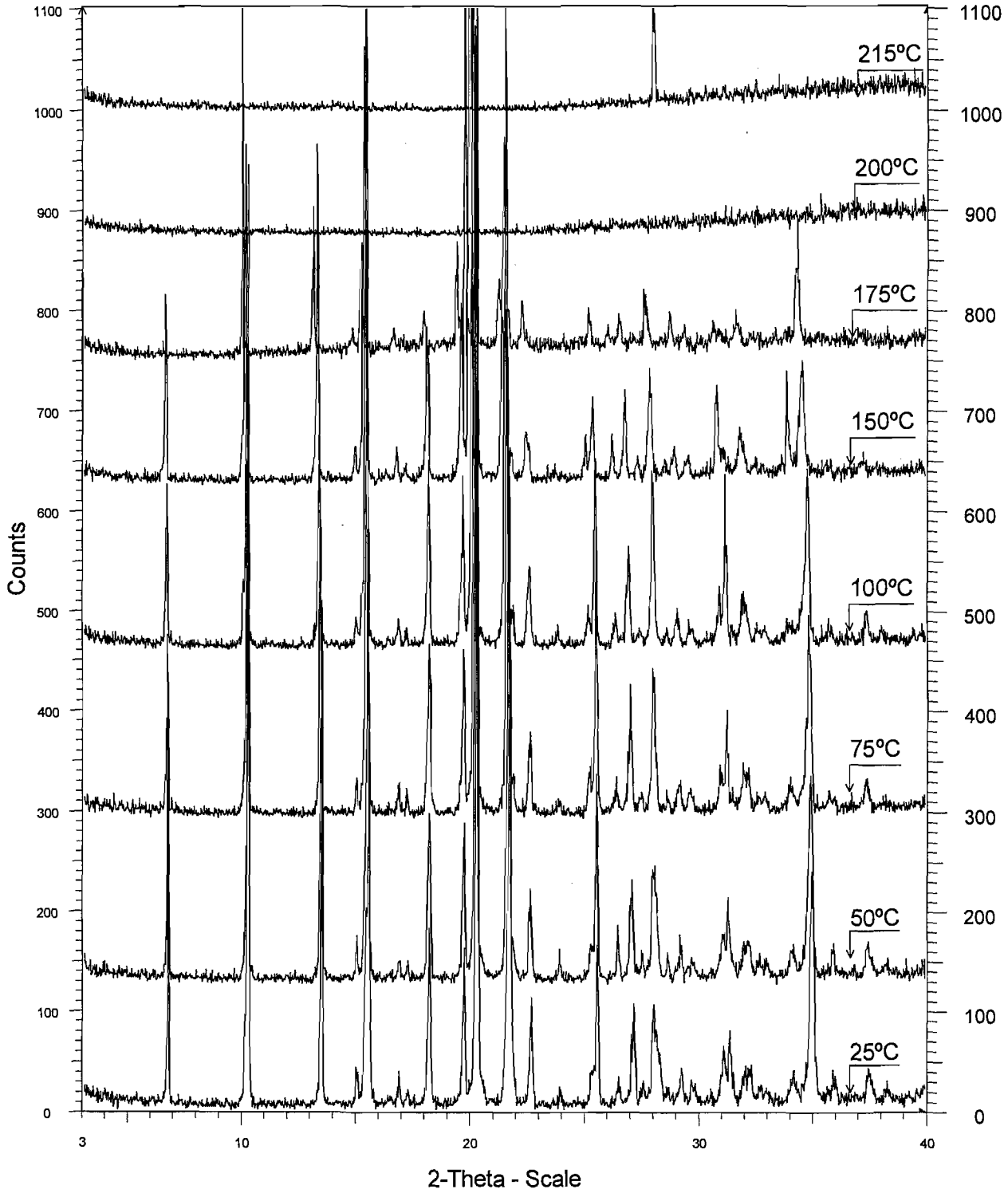


Figure 5.14 VT-XRPD patterns of venlafaxine hydrochloride Form 1 at temperatures: 25-215°C.

5.2.2.5.2 Thermodynamic stability of Venlafaxine HCl Form 5

The VT-XRPD patterns of venlafaxine hydrochloride Form 5 are shown in figure 5.15.

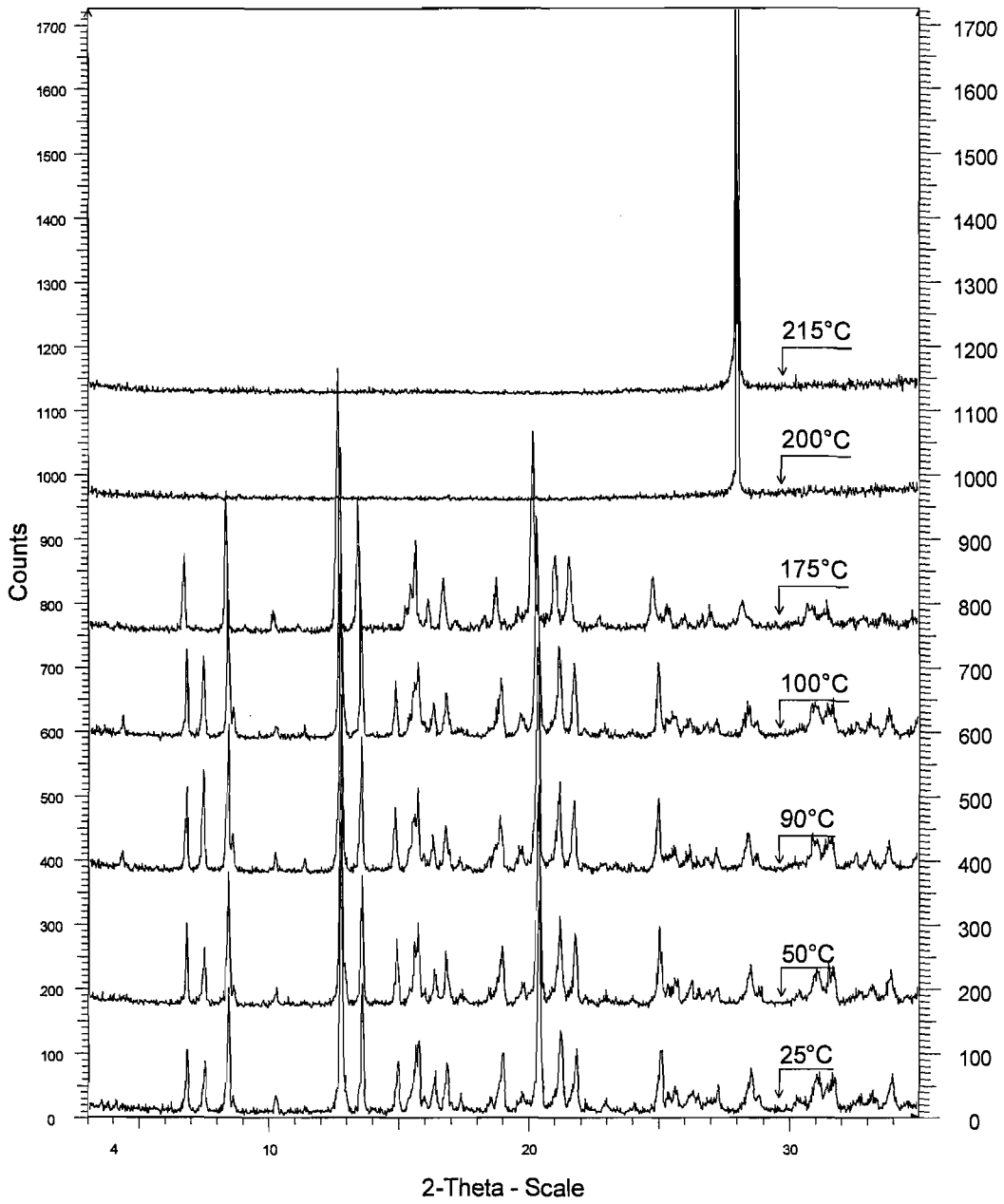


Figure 5.15 VT-XRPD patterns of venlafaxine hydrochloride Form 5 at various temperatures (25-215°C).

With an increase in the temperature of venlafaxine hydrochloride Form 5, no significant changes were observed in the VT-XRPD pattern (figure 5.15) up to

50°C. At 90 & 100°C two small diffraction peaks appeared at 4.3 & 11.5°2θ, which represented the internal-crystal rearrangements observed during the TM studies (section 5.2.2.3). Thermo-microscopy revealed the appearance of plate-like intergrowth crystals at 174°C (table 5.10).

The XRPD pattern obtained at 175°C revealed significant changes, which included the following:

- Disappearance of the diffraction peaks at 7.5 and 14.9°2θ;
- the intensities of the peaks found between 15.0-22.0°2θ revealed varying intensities; and
- a slight shift towards 4.0°2θ of all the diffraction peaks was observed, which could be attributed to a change in the powderbed-height induced by the formation of the intergrowth crystals.

The XRPD pattern of the sample at 175°C revealed resemblances to that of the XRPD pattern of Form 2 (figure 5.7). Figure 5.16 depicts an overlay of the theoretical XRPD pattern of Form 2 (derived from single crystal diffraction data) and the XRPD pattern of Form 5 at 175°C. The XRPD pattern of Form 1 at 175°C and that of Form 5 at 175°C differed significantly.

Heating the temperature stage to 200°C caused the sample to melt, as indicated by the lack of definite diffraction peaks.

Form 5 crystals were transferred into a Petri-dish and heated for two hours in a pre-heated oven at 150°C. The sample was then removed and placed in a desiccator containing silica-crystals (to prevent moisture sorption) allowing to cool to ambient temperature.

The XRPD pattern of the heated sample (figure 5.17) showed that the sample consisted of a mixture of Form 1 and Form 5. The XRPD pattern of the heated sample revealed diffraction peaks at: 6.7, 13.4, 17.2, 18.2, 22.6, 23.9, 26.5, 27.6, 28.2, 29.2 & 34.2°2θ, which are all characteristic to Form 1 (table 5.6),

and diffraction peaks at 8.3, 12.7, 16.8 & 31.2°2θ, which are characteristic to Form 5.

The DSC thermogram of the heated sample (figure 5.18) revealed two melting endotherms at 212 & 221°C respectively, supporting the phase transition observed in the XRPD pattern. The decomposition endotherm followed the two melting endotherms.

The DRIFT-IR spectrum of the heated sample was found to be concurrent to that of Form 1, as illustrated in figure 5.19.

The prolonged exposure of Form 5 to increased temperatures during the VT-XRPD studies (figure 5.15) weakened the crystal lattice causing the sample to melt at 200°C. The reason why the Form 5 → Form 1 transition was not observed (during the preliminary VT-XRPD studies) could be that the melting points of Form 1 and Form 5 are within close approximation, thus the transition could not be detected due to the rapid formation and melting of the mentioned two phases.

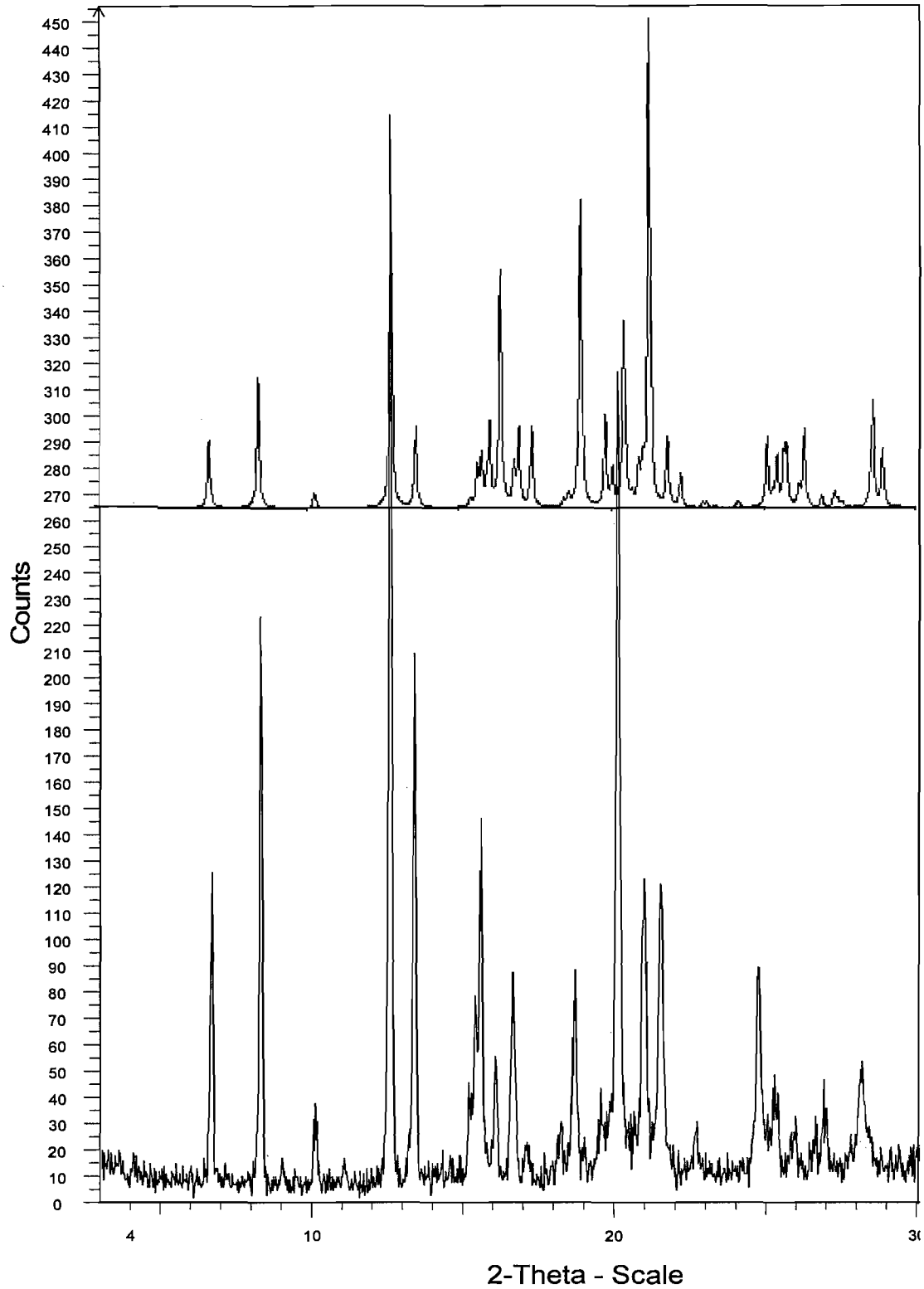


Figure 5.16 Theoretical XRPD pattern of Form 2 (derived from single crystal diffraction data - top) and the XRPD pattern of Form 5 at 175°C – bottom.

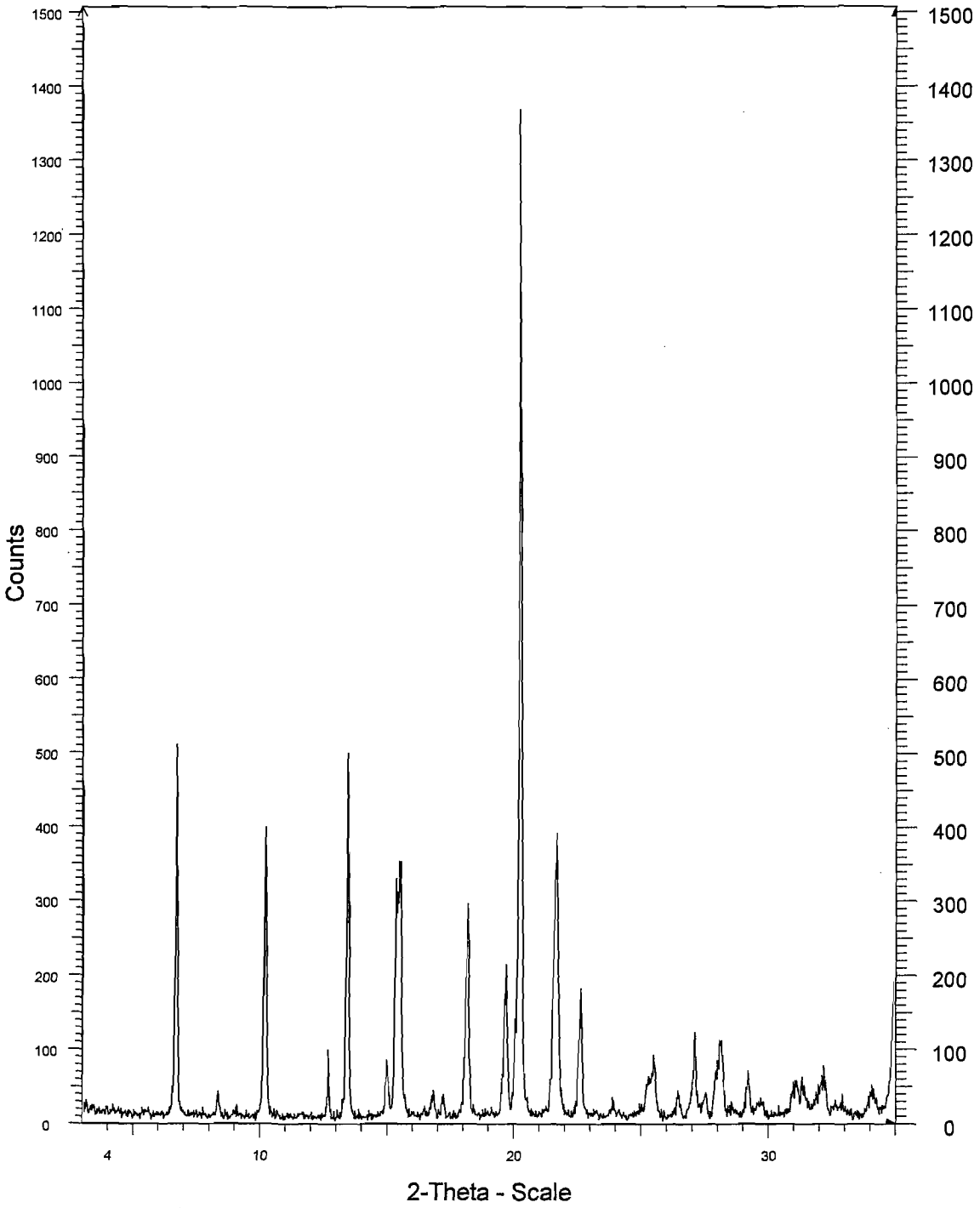


Figure 5.17 XRPD pattern of venlafaxine HCl Form 5, after being heated at 150°C for 2 hours.

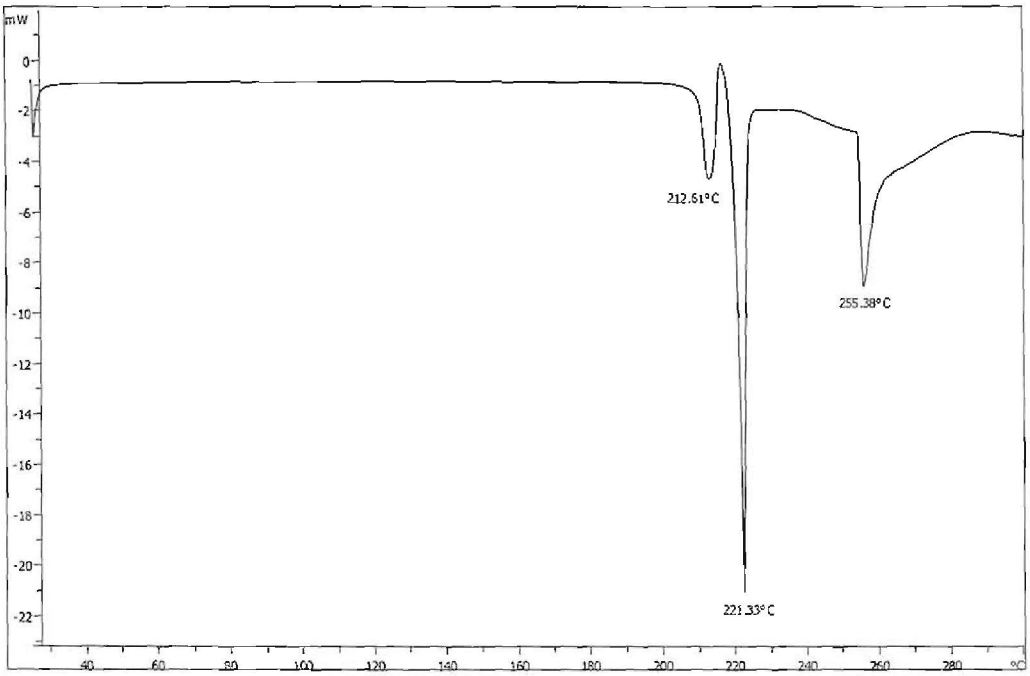


Figure 5.18 DSC thermogram of venlafaxine HCl Form 5, after being heated at 150°C for 2 hours.

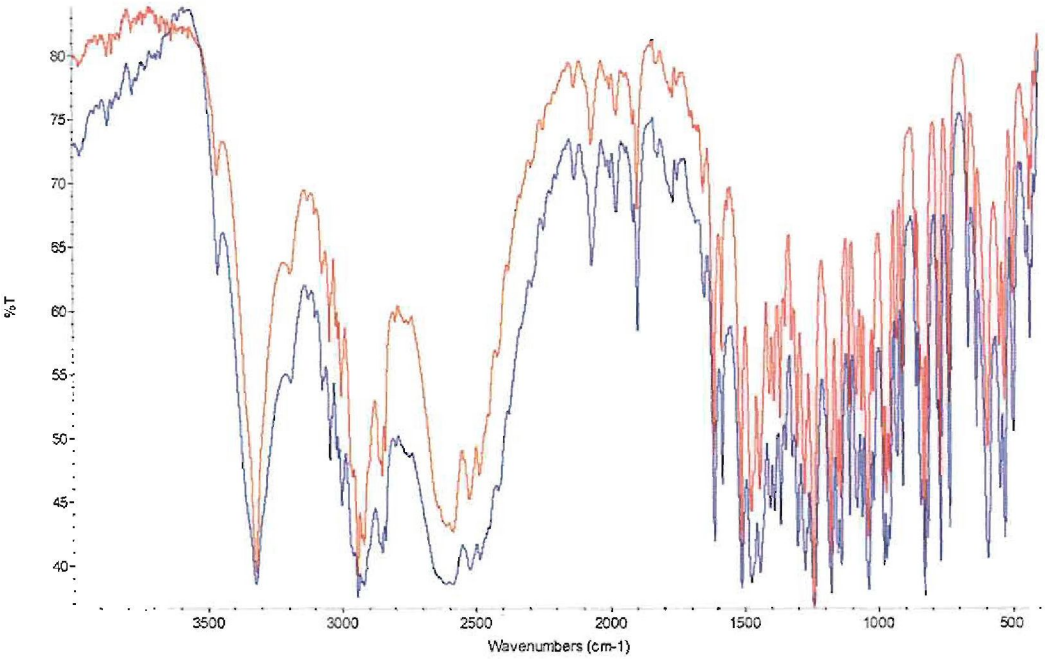


Figure 5.19 Overlay of DRIFT-IR spectra of venlafaxine HCl Form 5, after being heated at 150°C for 2 hours and that of Form 1.

It is thus suggested that prolonged exposure of venlafaxine HCl Form 5 (the higher-melting polymorph) to increased temperatures, induces a polymorphic transition which results in the formation of Form 1 (the lower-melting polymorph). In the past, various authors referred to a high melting polymorph, as the thermodynamically most stable crystal form, and the low melting polymorph, as the metastable crystal form (Rocco & Swanson, 1995:235) as a general rule for polymorphic thermodynamic stability. However, the melting point should not solely be used to predict the relative stability of polymorphic forms, since in an *enantiotropic system* (Chapter 1, section 1.2) the relative stability and solubility will change with temperature (Rocco and Swanson, 1995:235).

The relative thermodynamic stability of polymorphs can be determined by the measurement of their free energy difference (ΔG) which is defined by the following equation (Yu *et al.,* 1998:122):

$$\Delta G = \Delta H - T\Delta S$$

The enthalpy term (ΔH) results from the lattice energy difference between the polymorphs, and the entropy term ($T\Delta S$) from the difference in the lattice vibrations and disorder (Yu *et al.,* 1998:122).

Burger's heat of transition rule states the following:

(i) If an endothermic transition is observed at a certain temperature on heating, there must be an *enantiotropic* transition point at or bellow that temperature; but

(ii) If and exothermic transition is observed, then the transition point must lie above that temperature, or the two forms are related *monotropicaly* (Threlfall, 1995:2448).

However, if the transition cannot be clearly observed (due to the failure of the polymorphs to transform readily), Burger's *heat of fusion law* is of value which states that: the higher melting polymorph will have the lower heat of fusion if

the polymorphs are in an enantiotropic relationship, otherwise they are monotropically related (Burger & Ramberger, 1979a:266).

Table 5.8 confirms that an enantiotropic relationship exists due to the fact that the high melting form (Form 5) reveals a lower heat of fusion compared to the low melting form (Form 1).

Rocco & Swanson (1995:231) also indicated that the heat of fusion and the melting point data of polymorphs can be used to predict the relative solubility of the polymorphs. The polymorph with the lowest solubility will be the most thermodynamically stable form at a particular temperature.

Rocco and Swanson (1995:325) proposed the following equation to predict the relative solubilities of polymorphs:

$$RT\ln\left[\frac{Si}{Sii}\right]=\left[\frac{\Delta Hii\bullet(Tmii-T)}{Tmii}\right]-\left[\frac{\Delta Hi\bullet(Tmi-T)}{Tmi}\right]$$

Where:

Si = Relative solubility of the (i) high melting polymorph (Form 5).

Sii = Relative solubility of the (ii) low melting polymorph (Form 1).

ΔH = Heat of fusion for the polymorphic form.

Tm = Melting temperature of the polymorphic form.

T = Temperature of dissolution medium (23°C for the purpose of this study).

From the XRPD results obtained it was found that crystal Form 5 converted into crystal Form 1.

Table 5.8 shows the DSC data, used in the calculation of the theoretical solubility ratio of the high melting (Form 5) and low melting (Form 1) polymorphs.

The theoretical solubility ratio (Si/Sii) of polymorphic Form 1 and Form 5 was calculated as 1.12. Due to the fact that (Si/Sii) > 1 it can be considered that crystal Form 1 is the most stable form at room temperature by virtue of the lower solubility values observed and that Form 5, which revealed a higher solubility, could therefore be classified as a metastable crystal form at room temperature.

As mentioned polymorphic systems can be classified as either *monotropic* or *enantiotropic*. Byrn *et al.* (1999:20) defined these systems as follows:

- "**Monotropic systems** are defined as systems where a single form is always more stable regardless of the induced temperature."

- "**Enantiotropic systems** are defined as systems where the relative stability of the two forms inverts at some temperature" (figure 5.20 and figure 5.21).

The solubility values for different crystal forms (polymorphs) differ under a fixed set of conditions: temperature, pressure and solvent composition. The polymorph with the lowest solubility will be the most thermodynamically stable form at a particular temperature (Rocco & Swanson, 1995:231).

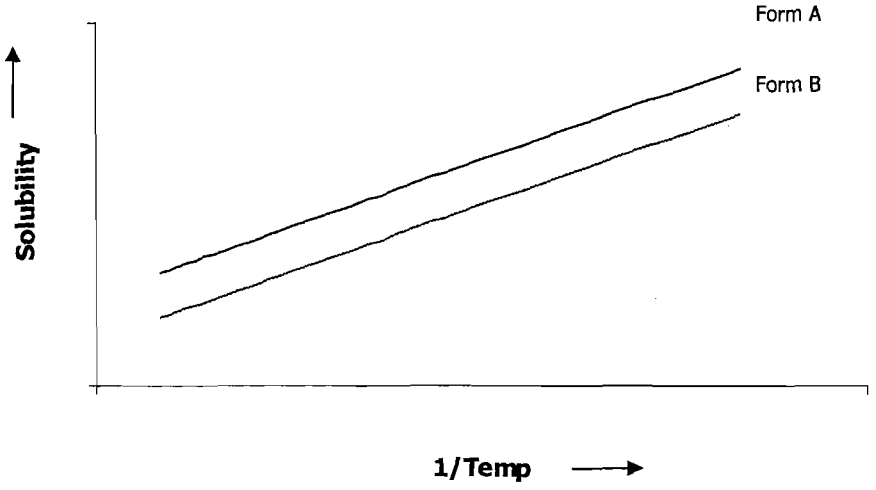


Figure 5.20 Schematic presentation of the solubility versus temperature for monotropic system (adapted and reproduced from Byrn *et al.*, 1999:20).

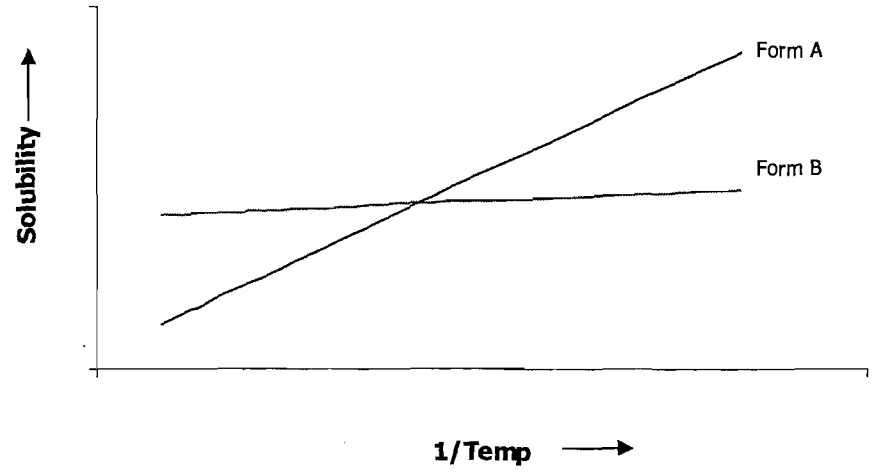


Figure 5.21 Schematic presentation of the solubility versus temperature for enantiotropic system (adapted and reproduced from Byrn *et al.*, 1999:20).

Figure 5.22 depicts the results obtained when the solubility ratios of the polymorphs (enantiotropic and monotropic) vs. the 1/temperature. For a monotropic system a non-linear relationship exists between the solubility ratios (Si/Sii) and the temperature. Construction of a logarithmic trendline produced a correlation coefficient (r^2) = 0.995.

A linear correlation exists between the solubility ratios and the temperature (r^2=0.998) for the enantiotropic system.

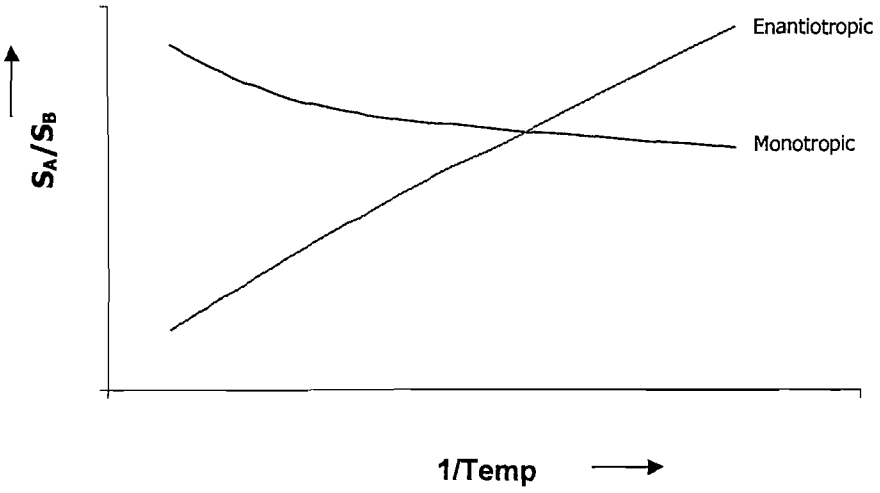


Figure 5.22 Solubility ratios (S_A/S_B) of the polymorphs (enantiotropic and monotropic) vs. the 1/temperature.

Results obtained when plotting the theoretically calculated solubility ratios of the venlafaxine HCl polymorphs (Form 1 and Form 5) at various temperatures are illustrated in figure 5.23.

The plot of the predicted solubility ratios (Si/Sii) vs. 1/temperature for the two polymorphs revealed that a linear correlation existed (r^2=0.999), thus supporting that an *enantiotropic* relationship exists.

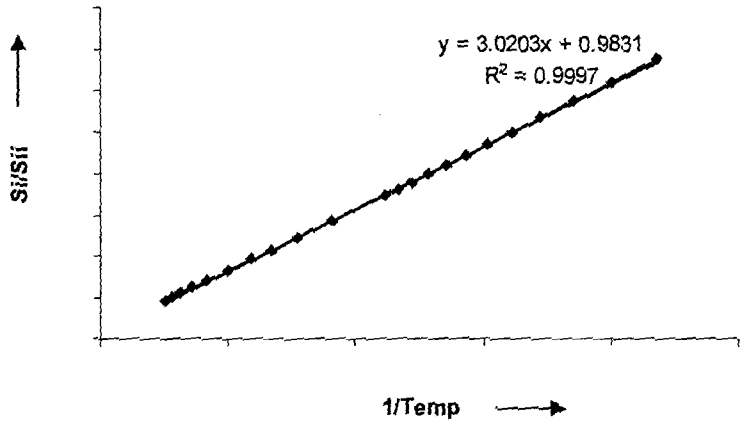


Figure 5.23 Solubility ratios of the venlafaxine HCl polymorphs (Si/Sii) vs. the 1/temperature.

Figure 5.24 provides a schematic summary of the thermodynamic stability of venlafaxine HCl Forms 1 and 5.

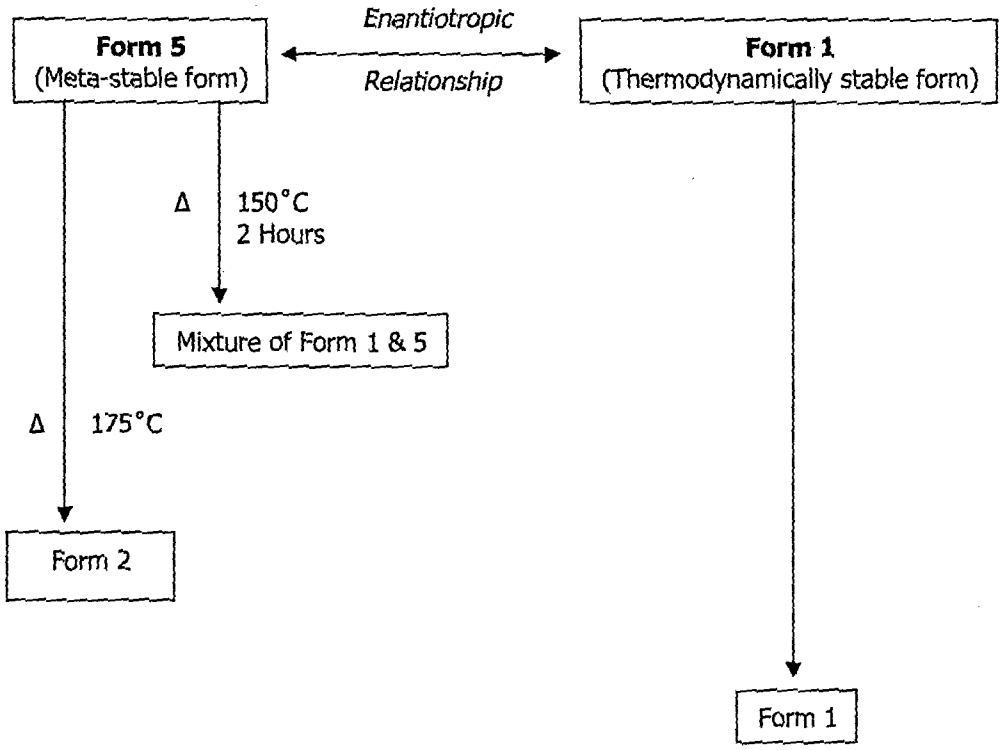


Figure 5.24 A schematic presentation of the thermodynamic stability of venlafaxine HCl Forms 5 and 1.

Conclusion

This chapter provided a general overview of the physico-chemical properties of venlafaxine HCl polymorphic forms. A new crystal form, Form 5, was prepared and characterised.

This study revealed that there seems to be some structural correlations between Form 2 and Form 5, however the thermodynamic properties of these two, high-melting polymorphic forms differ. Form 5 is a metastable crystal form that converts to Form 2 / Form 1 upon exposure to heat, whereas Form 2 is a thermodynamic stable crystal form (Rao *et al.* 2002:2). From the results obtained, it became clear that Form 5 revealed preferred orientation due to its anisotropic morphology.

Heat of solution studies (for Form 1 and Form 5) revealed that the dissolution of the crystals in water was an exothermic reaction ($\Delta H < 0$), and that an increase in temperature decreases the solubility of the polymorphic forms.

There was no polymorphic transformation observed for Form 1 when exposed to increased temperatures. Form 5, underwent internal-crystal rearrangements when heated to 90-100°C.

Both Form 1 and Form 5 exhibited crystal growth. The changes in the XRPD pattern of Form 5 at 175°C could be attributed to a phase transformation and probably the appearance of the intergrowth crystals.

Exposure of Form 5 crystals to 150°C (for two hours) showed that a fraction of the Form 5 crystals converted into Form 1, thus indicating that Form 5 is a meta-stable form and Form 1 is the thermodynamically stable form of venlafaxine HCl.

The theoretical solubility ratio (Si/Sii) was calculated to be 1.12, which signified that Form 1 and Form 5 was enantiotropic related. The linear correlation between the plot of the predicted solubility ratios (Si/Sii) vs. 1/temperature for the two polymorphs (Form 5 and Form 1) and the fact that the higher melting form (Form 5) revealed a lower heat of fusion compared to the lower melting

form (Form 1) supported the enantiotropic relationship between the mentioned polymorphic forms.

CHAPTER 6

Moisture sorption properties of venlafaxine hydrochloride crystal forms

Introduction

Water associated with pharmaceutical solids may greatly influence the physical, chemical and mechanical properties as discussed in chapter 1. It is known that the amount of water sorbed by a solid is a function of the affinity between the surface of the solid and the water molecules, relative humidity, temperature and in the case of adsorption (i.e. when water is interacting only at the surface of the solid) the surface area of the solid (chapter 1).

Generally, for polymorphic forms of the same API the unit cell volume differ, that may induce differences in the surface areas of the crystals. Exposure of two venlafaxine hydrochloride polymorphic forms, with similar particle sizes to similarly relative humidity conditions would provide an insight to the sorption- and phase-stability behaviour of the crystal forms.

Form 1 (a thermodynamically stable form) and Form 5 (metastable form) were selected as prototype crystal forms for this study to investigate the moisture sorption (ab-/adsorption) of the freely water soluble API, venlafaxine HCl, and to investigate the influence of moisture sorption on the physico-chemical properties of the crystal forms.

6.1 Method and materials for the moisture uptake measurement of venlafaxine hydrochloride polymorphic forms

Venlafaxine HCl raw material was obtained from Unichem Laboratories Ltd, Batch no: VEN/20301. The analytical results generated prior to the release date of the raw material, supplied by Unichem Laboratories (Ltd), revealed that the raw material complies with the prescribed quality specifications with respect to the above tests as per specification no: RO/FPS/VEN/026.REV00.

Form 1 and Form 5 were prepared according to the methods described in chapter 5 (section 5.2.1). The crystals obtained were sieved using a 106 µm and 250 µm sieve. The fraction between 106-250 µm was used during all the experiments. Sieving was performed to ensure uniformity of particle size. The sieved fraction was dried at 90°C for one hour to remove any residual solvent/moisture present. XRPD and DRIFT-IR analysis were done prior to, and after the drying process to ensure that no polymorphic conversion has occurred during the drying process.

Saturated solutions of NaCl and KNO_3 were prepared using the method described by Nyqvist (1983:47). Samples (500 mg) of both Form 1 and Form 5 were weighed into weighing boats and were stored in small % RH chambers within a 30°C & 65% RH regulated climatic chamber (see table 6.1 for a description of the % RH chambers). The samples were exposed to 0%, 65%, 75% and 85% RH conditions at 30°C respectively (figure 6.1). Samples were removed at 1, 2, 3, 4, 5, 6, 9, 14, 21, 28, 42 and 56 days and were analysed using the analytical methods discussed in chapter 2.

Table 6.1 %RH chambers prepared and stored in a 30°C & 65% RH regulated climatic chamber

	Saturated salt solution in chamber	**Measured % RH in chamber**
Chamber A	NaCl	75±5%
Chamber B	KNO_3	85±5%
Chamber C	No solution – Dried silica and air replaced with N_2 (g)	0±5%

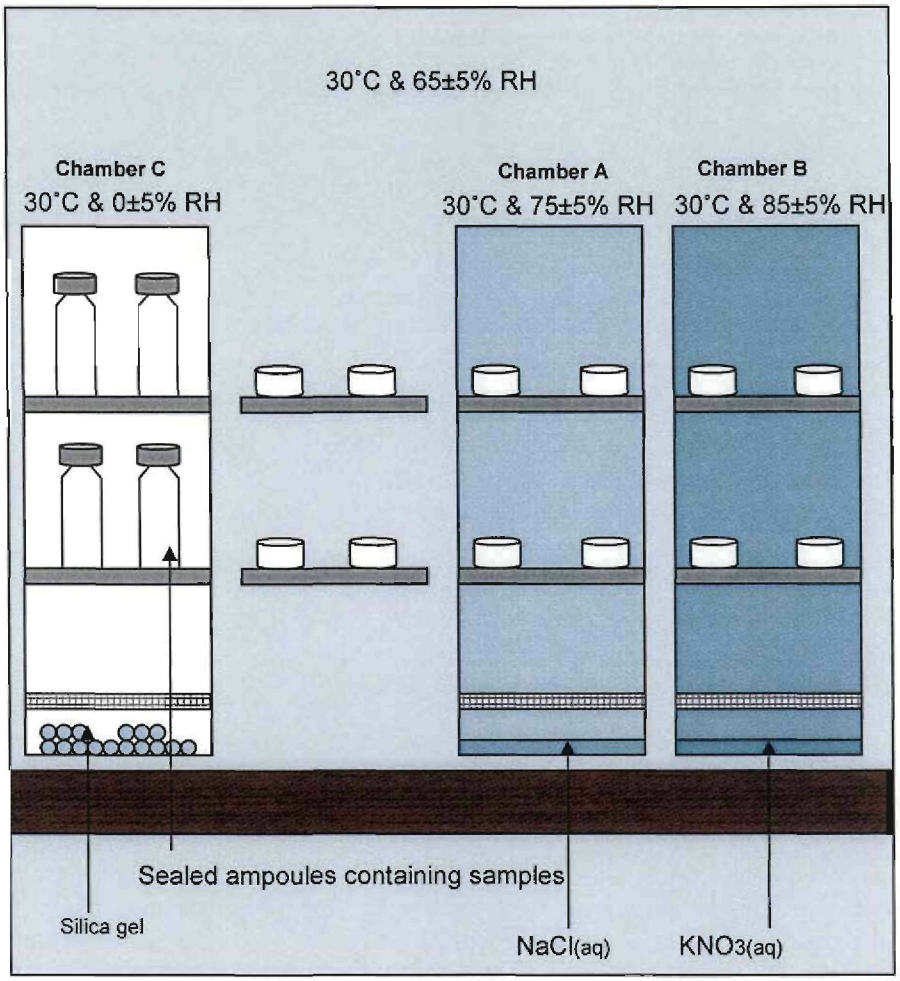


Figure 6.1 Schematic presentation of the storage conditions utilised during the study.

6.2 Moisture uptake measurement of venlafaxine hydrochloride polymorphic forms

6.2.1 Particle size and specific surface area analysis results

As mentioned (section 6.1), for the purpose of this study a sieved fraction of crystals was used. The particle size distributions were measured using a Galai-Cis-1 (Galai-Cis-1, Israel) particle size analyser, as described in chapter 2 (section 2.1.5). Samples of powder suspended in sedisperse (dispersing solution) were each placed in a small cuvette and fitted into the analyser. A small magnetic stirrer was placed inside the cuvette to prevent sedimentation of the

particles during the measurement. The acquired data was used to compute means, medians and standard deviations, based on the total particle population. The median diameters by volume are summarised in table 6.2.

Table 6.2 Median particle size by volume (mass) and specific surface area of venlafaxine HCl Form 1 and Form 5

Polymorphic form	Median diameter by volume (μm)	Specific surface area (m^2/g)
Form 1	134.55	0.49
Form 5	174.60	0.90

The median particle sizes of both polymorphic forms (Form 1 and Form 5) were within the sieved range: 106 μm - 250 μm. The median particle size of Form 5 sample was found to be slightly higher compared to that of Form 1.

Surface area analysis was performed using a high speed surface area analyser (Flowsorb11 2300) as described in chapter 2 (section 2.1.6). The specific surface area of Form 5 (table 6.2) was found to be 1.84 times higher compared to that of Form 1. Usually it will be assumed that smaller particles would present a higher specific surface area, however for these two forms the contradictory was observed, suggesting that the area of sorption sites on the Form 5 sample would be higher compared to that present in the Form 1 sample.

6.2.2 Moisture sorption analysis results

The anhydrous samples were vacuum dried at 50°C for over three days prior to inducing the sample in the sorption analyser. Moisture sorption isotherms were generated at 25°C using a Symmetric Vapor Sorption Analyzer (model SGA-100, VTI, Hialeah, Finland). The procedure involved drying the samples in the VTI instrument at 60 °C and ~ 0 % RH until the instrument recorded a weight loss of less than 1 μg over a period of 5 minutes. This was followed by exposing the

samples to 10 % steps in RH from 0 to 95 % RH. Equilibrium was assumed when there was no weight change of more than 1 µg over a period of 5 minutes.

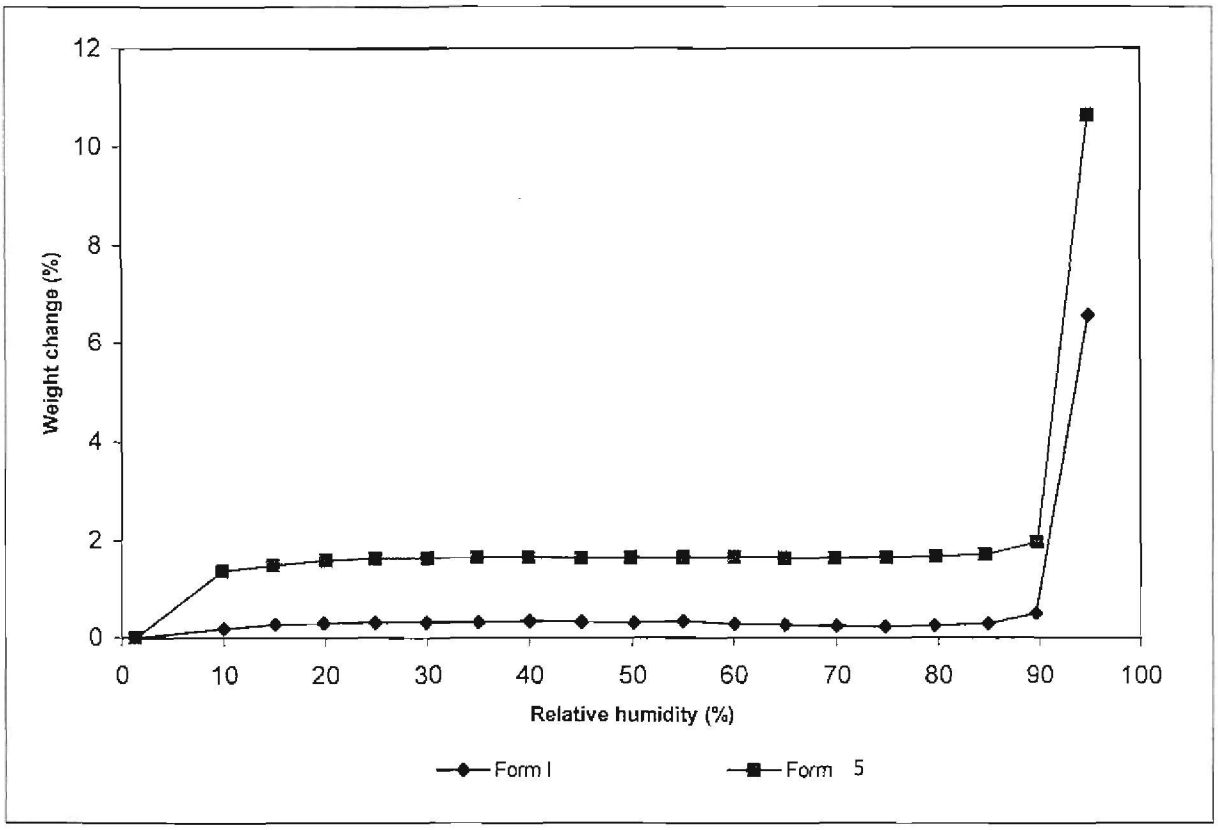


Figure 6.2 Moisture sorption isotherms of Form 1 and Form 5.

From the sorption analysis it became clear that both Form 1 and 5 are hygroscopic to the extent that they showed deliquescence at RH >85% (figure 6.2). The moisture sorption isotherms indicated that the rate and extend of moisture sorption for Form 5 was higher compared to that of Form 1.

Deliquescence could be considered to be the first stage of heterogeneous unary condensation on solid soluble nuclei, where the solid nucleus dissolves in a liquid film formed by the molecules of water vapour which condensed on the solid surface (figure 6.3) – Byrn *et al.*, 1999:23.

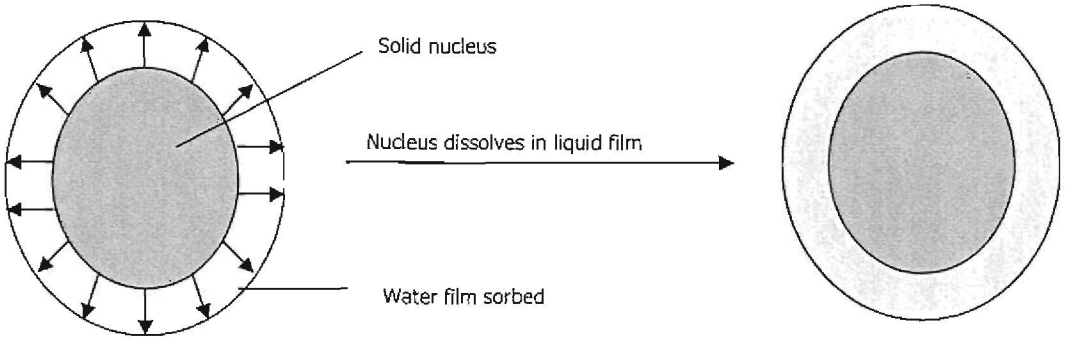


Figure 6.3 Schematic presentation of the deliquescence of a solid nucleus.

In the sections to follow, it will be illustrated that Form 5 undergoes a phase transition to form a monohydrated crystal phase. Upon complete conversion of the anhydrous form to the monohydrate, the system becomes bivariant. Since no higher hydrate forms are possible for venlafaxine, adventitious water will be absorbed which then leads to the deliquescence of the solid nucleus.

6.2.3 Total moisture content - Karl Fischer (KF) results

Tables 6.3 and 6.4 summarises the total moisture content of Form 1 and Form 5 at predetermined intervals when stored at 30°C – 0% RH, 65% RH, 75% RH & 85% RH respectively. The moisture sorption isotherms of Form 1 and Form 5 derived from moisture content using Karl Fischer titration results are displayed in figures 6.4 and 6.5 respectively.

Table 6.3 Average moisture content of Form 1 at predetermined intervals when stored at 30°C and different % RH's

% RH	Days						
	0	**9**	**14**	**21**	**28**	**42**	**56**
0±5	0.09	0.13	0.21	0.28	0.26	0.22	0.21
65±5	0.09	0.27	0.28	0.38	0.65	0.25	0.22
75±5	0.09	0.24	0.19	0.20	0.27	0.25	0.22
85±5	0.09	0.18	0.24	0.32	0.33	0.35	0.26

Table 6.4 Average moisture content of Form 5 at predetermined intervals when stored at 30°C and different % RH's

% RH	Days						
	0	**9**	**14**	**21**	**28**	**42**	**56**
0±5	0.71	0.72	0.70	1.12	0.83	0.68	0.63
65±5	0.71	0.89	1.20	1.24	1.00	0.99	0.71
75±5	0.71	0.98	1.19	1.32	0.93	0.52	0.61
85±5	0.71	3.66	4.36	4.49	4.34	4.91	5.46

The Karl Fischer results (tables 6.3 & 6.4) confirmed the moisture sorption isotherms (figure 6.2) that the rate and extend of moisture sorption for Form 5 was greater compared to that of Form 1.

Form 1 did not reveal a significant moisture uptake at the various relative humidities. Form 5 revealed comparable moisture sorption properties (moisture content) when stored at 0, 65 & 75% RH. At 85% RH, Form 5 however, showed a significant increase in moisture sorption over the 56 days period, with a total moisture content of 5.46% (m/m), which is comparable to the theoretical moisture content of a mono-hydrated venlafaxine hydrochloride crystal system (5.39%).

From the results obtained it could be suggested that Form 5 might have underwent a polymorphic / phase transition (anhydrate → monohydrate) when exposed to 85% RH at 30°C for 56 days and thus suggesting Form 1 to be the thermodynamically more stable crystal form (Form 1 vs. Form 5) when exposed to increased relative humidities.

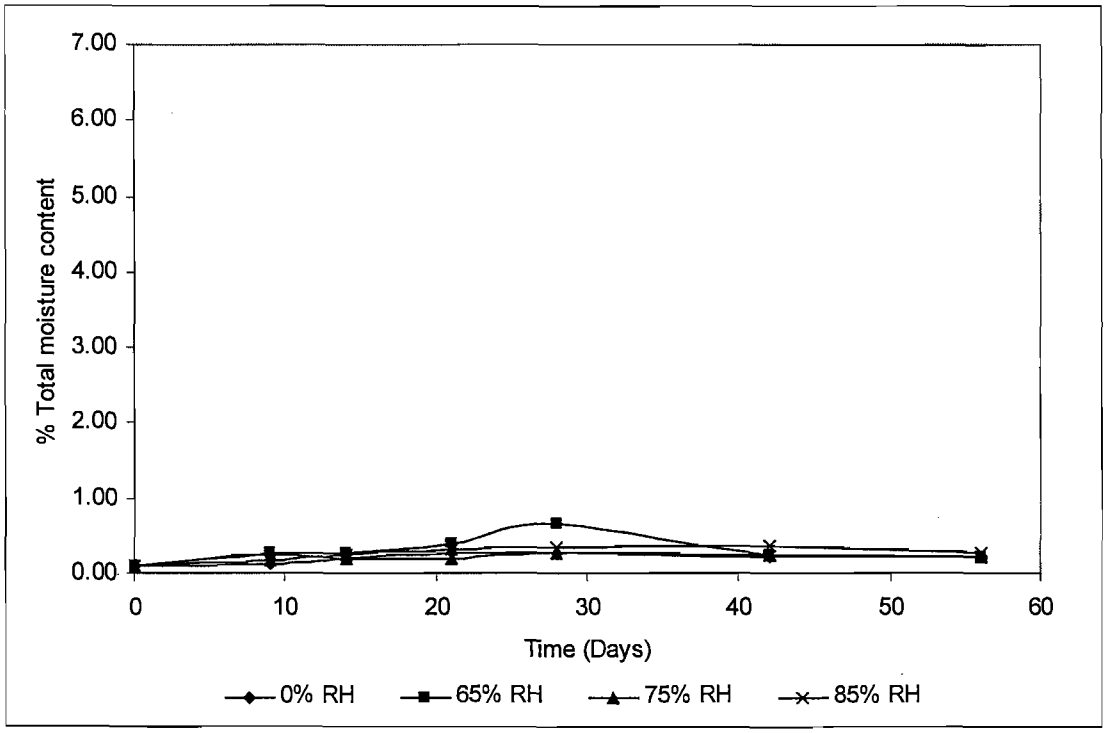


Figure 6.4 Moisture sorption isotherms of Form 1 derived from moisture content using Karl Fischer titration results.

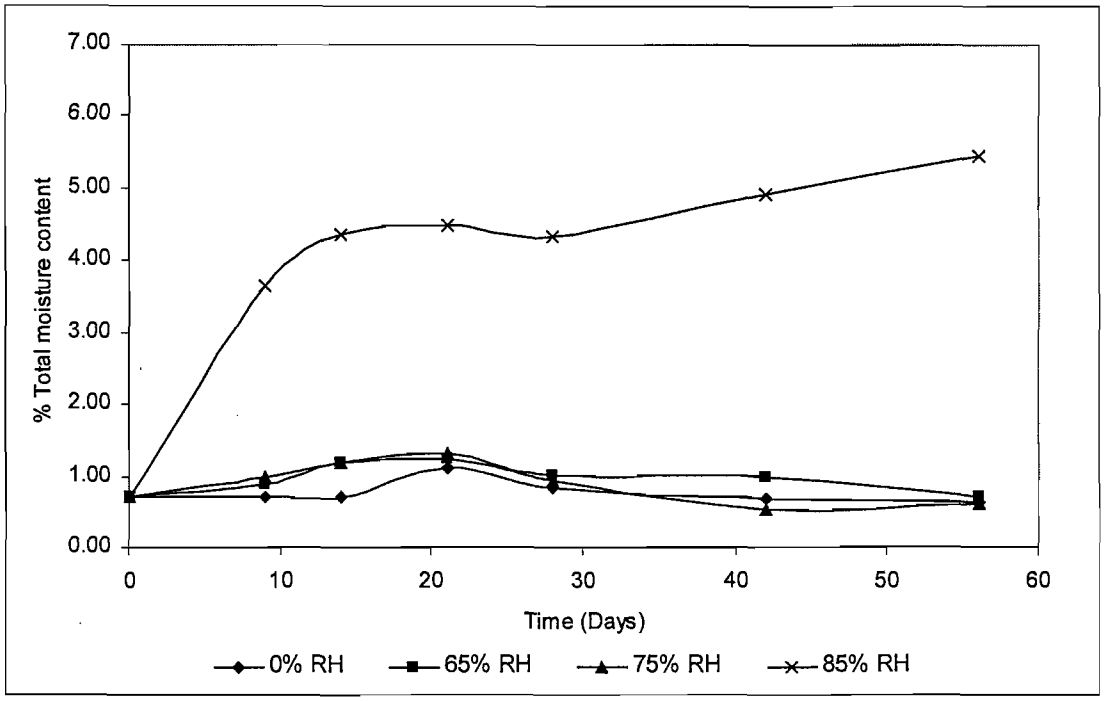


Figure 6.5 Moisture sorption isotherms of Form 5 derived from moisture content using Karl Fischer titration results.

6.2.4 Polymorphic stability of venlafaxine hydrochloride Form 1

The crystallographic behaviour of Form 1 and Form 5 during the moisture sorption study was investigated by means of XRPD and VT-XRPD.

An overlay of the XRPD patterns of Form 1 when exposed to 0, 65, 75 & 85% RH at 30°C over a 56 day period is displayed in figure 6.6. The XRPD data suggested that the crystal lattice of venlafaxine hydrochloride Form 1 remained relatively unchanged (small changes in the relative intensities of the Bragg reflections between 28-29°2θ and 31-32°2θ) when exposed to 30°C & 0±5% RH and 30°C & 65±5% RH over a period of 56 days. Exposure of Form 1 to higher humidity values at 30°C i.e. 75±5% RH and 85±5% RH for 56 days did also not induce any noticeable polymorphic phase transitions. Small variations in the relative peak intensities for the following conditions and peaks were observed:

- 30°C & 75±5% RH: A decrease in the peak intensities of the Bragg diffractions at 17.3°2θ and 32.0°2θ were observed on day 9.
- 30°C & 85±5% RH: Peaks at 15.1°2θ and 15.5°2θ revealed varying peak intensities.

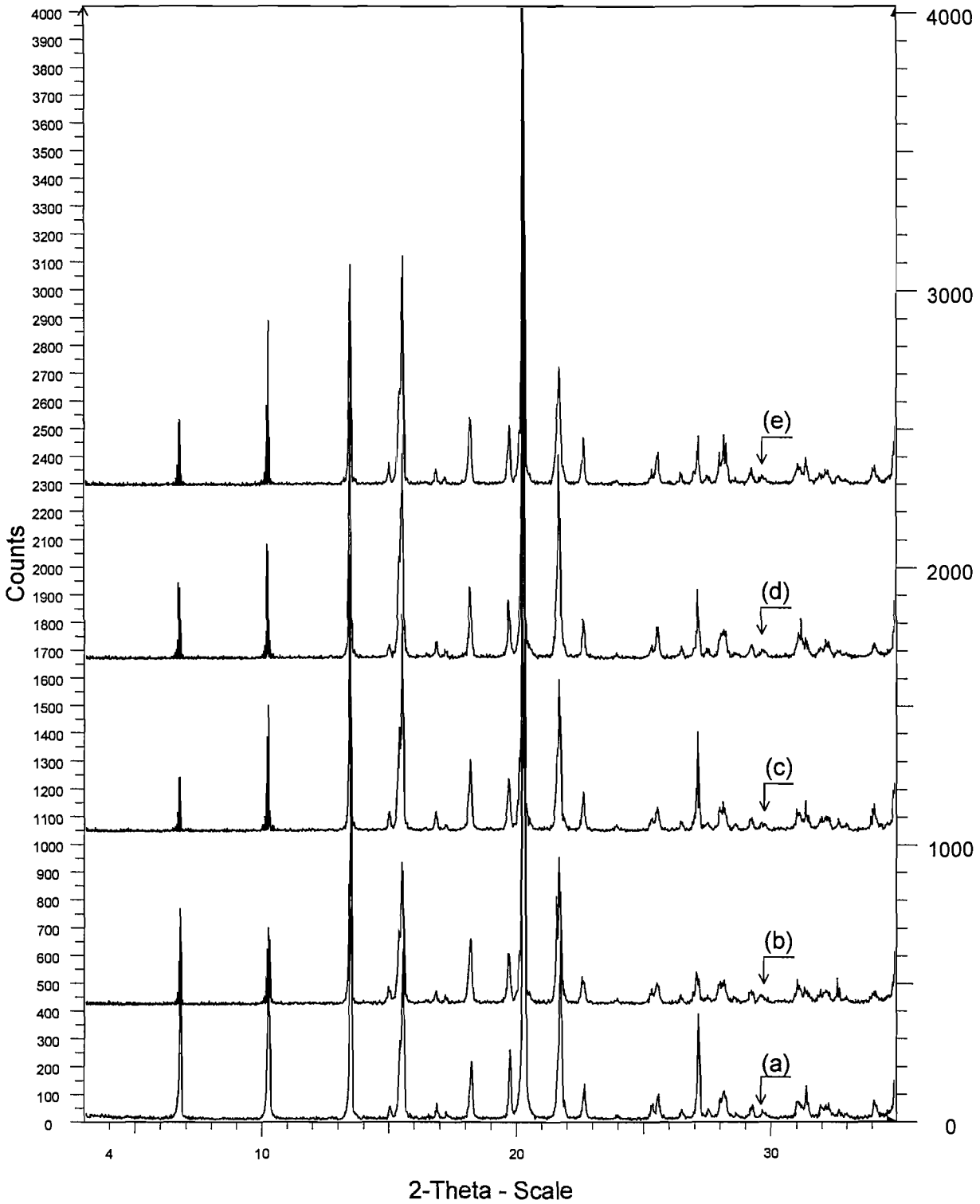


Figure 6.6 XRPD pattern overlay of venlafaxine HCl Form 1, (a) initial, and when exposed to 30°C & (b) 0, (c) 65, (d) 75 and (e) 85% RH at after 56 days.

Pecharsky and Zavalij (2005:184) stated that numerous factors play either central or secondary roles in the intensities of Bragg diffractions:

i) *Structural factors:* - depend on atomic structure (x,y,z, etc.) of the crystal which is described by the relative positions of atoms in the unit cell and their characteristics such as thermal motion and population parameters.

ii) *Specimen factors:* - shape, size, grain size and microstructure of the sample.

iii) *Instrumental factors:* - which includes the properties of the radiation type of focusing geometers, properties of detectors, slits and/or monochromator geometry.

In this study specimen and instrumental factors (ii and iii) may be disregarded due to the fact that equivalent samples (of the same batch crystals) were analysed using identical XRPD geometrical and radiation settings and equipment.

Structural factors (i) might be regarded as the primary rationale for the variance of diffraction intensities observed, due to the thermal motion of molecules or atoms in the molecules situated in the crystal unit cell or the preferred orientation effects (section 5.2.2.1).

The thermal properties of the two venlafaxine hydrochloride crystal forms were investigated, using DSC, TGA and thermomicroscopy (TM). TGA analysis was conducted only on the samples, of which their DSC results indicated a tendency of possibly being pseudo polymorphs (hydrates).

The DSC thermograms of Form 1, exposed to the various relative humidities are depicted in figure 6.7. No significant differences / changes were observed in the thermal behaviour of venlafaxine hydrochloride Form 1 when exposed for 56 days to the various conditions (0%, 65%, 75% & 85%) which confirmed the results obtained with XRPD, Karl Fischer etc. The melting endotherms (i.e. melting point) remained comparable and stable. No dehydration endotherms

were observed in the DSC thermograms of Form 1 during the study (figure 6.7), thus confirming the Karl Fischer results discussed in section 6.2.3 that Form 1 did not reveal any significant moisture sorption at the various relative humidities.

Thermal decomposition of venlafaxine hydrochloride usually occurs at temperatures exceeding 250°C and is associated with gas evolution. Slight differences in the sealing of the aluminium sample pans might attribute the differences in the position and shape for the decomposing endotherms observed in the DSC thermograms of Form 1 (figure 6.7).

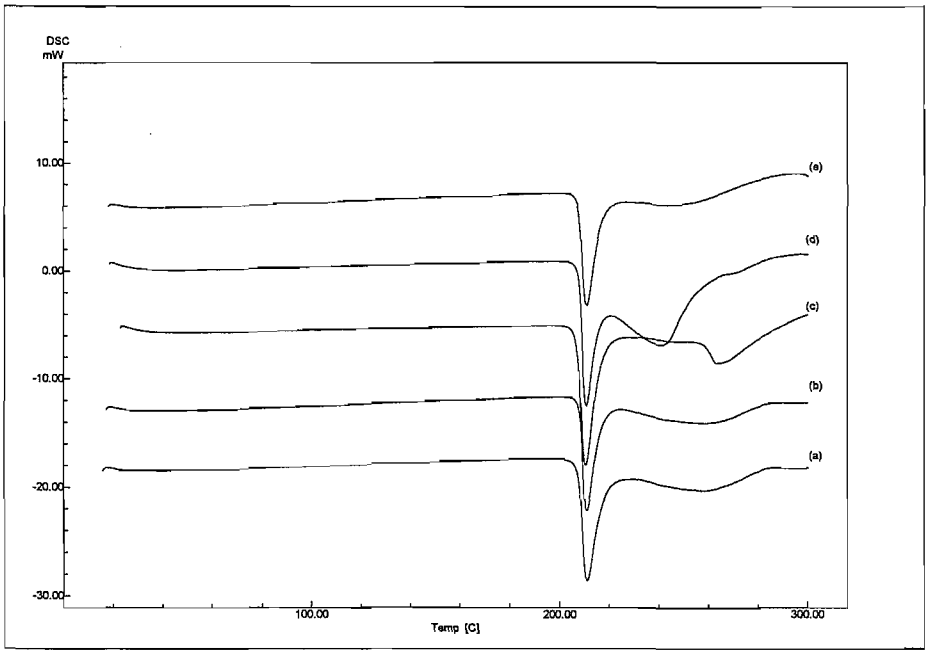


Figure 6.7 DSC thermograms of venlafaxine hydrochloride Form 1 (a) initially and when exposed to 30°C – (b) 0, (c) 65, (d) 75 & (e) 85% RH after 56 days.

The application of infra-red spectroscopy in qualitative and quantitative analysis of polymorphic forms in raw materials and solid dosage forms has become an important practice due to its simplicity and efficacy (Byrn *et al.*, 1999:111).

Brits (2003:112) indicated that the DRIFT-IR spectrum of the mono-hydrated venlafaxine hydrochloride differed considerably from that of the anhydrous forms. An overlay of the DRIFT-IR spectra of Form 1 when exposed to 0, 65, 75

& 85% RH at 30ºC over a 56 day period is displayed in figure 6.8. The DRIFT-IR spectra of Form 1 did not indicate any significant differences / changes when exposed for 56 days to the various conditions (0%, 65%, 75% & 85% RH), confirming the XRPD and DSC observations that Form 1 remained relatively stable and that no phase transitions occurred.

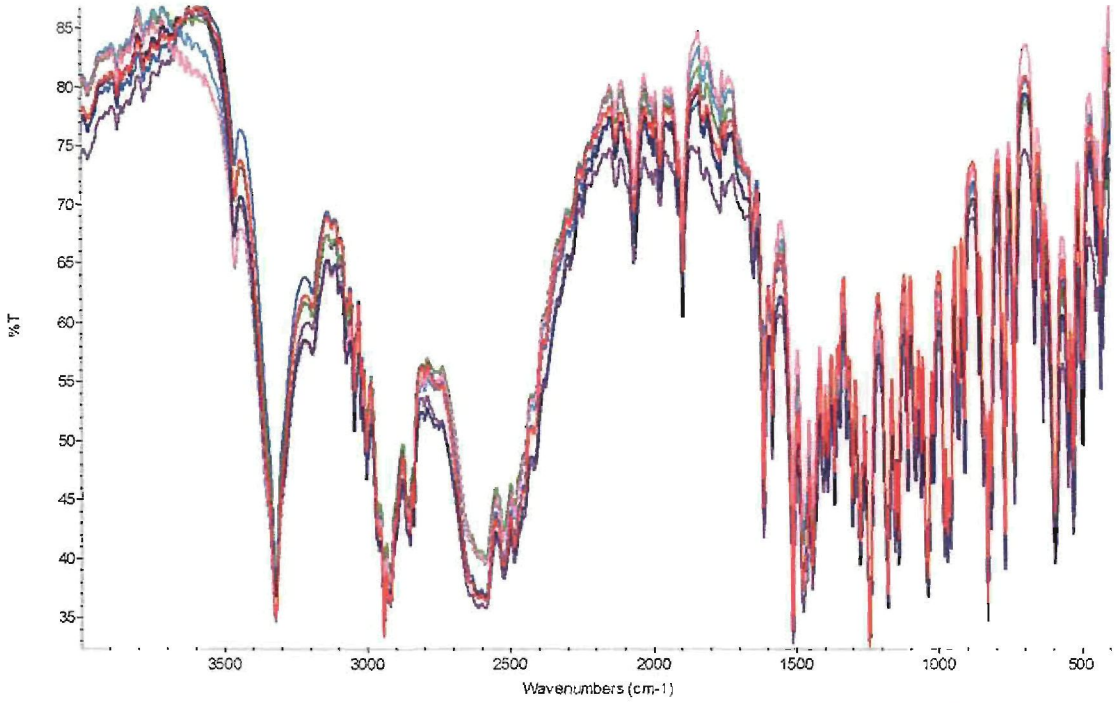


Figure 6.8 An overlay of the DRIFT-IR spectra of Form 1 at Initial, 0, 65, 75, and 85 % RH after 56 days.

6.2.5 Polymorphic stability of venlafaxine hydrochloride Form 5

The stability of the meta-stable, Form 5 when exposed to 0, 65, 75 & 85% RH at 30°C will now be discussed.

6.2.5.1 Venlafaxine hydrochloride Form 5 – 30°C & 0% RH

Minor changes were observed in the XRPD pattern of Form 5 when it was stored at 30°C & 0% RH (figure 6.9 and table 6.5). The most noticeable changes included the following:

- The intensity of the peak at 10.2 °2θ increased as a function of time, and showed a minor peak shift / peak replacement to a final peak position of 10.3 °2θ after 56 days.
- The intensities of the diffraction peaks between 14.8-16.0 °2θ showed varying intensities, and a gradual increase in the intensity of the peak at 18.4 °2θ.
- The intensities of the diffraction peaks in the 31.0 – 32.0 °2θ region showed varying intensities.

Upon closer inspection the gradual growth and repositioning of the 18.4-18.5°2θ peak (characteristic of Form 5) to 18.2 °2θ (characteristic of Form 1) suggested that a polymorphic phase transition occurred after 42 days at 30°C & 0% RH. This observation was indeed substantiated with DRIFT-IR and DSC analysis. The presence of diffraction peaks at: 22.7, 28.0, 29.3 and 29.7 °2θ suggested that the sample consisted of Form 1 or a mixture of Form 1 and Form 5 (the mentioned peaks are highlighted in table 6.5).

An overlay of the XRPD patterns of venlafaxine hydrochloride Form 5, Form 5 exposed to 30°C & 0% RH for 42 and 56 days and Form 1 is shown in figure 6.9, that clearly indicates the presence of peaks at, 18.2 & 22.7°2θ i.e. traces of Form 1 in the Form 5 sample exposed to 30°C & 0% RH for 56 days.

Table 6.5 Main XRPD pattern peak positions (°2θ) of venlafaxine HCl Form 5 at different time intervals when stored at 30°C & 0%RH

Main peak positions (°2θ) at time intervals						
Initial	**9 Days**	**14 Days**	**21 Days**	**28 Days**	**42 Days**	**56 Days**
6.8	6.7	6.7	6.7	6.8	6.7	6.8
7.4	7.4	7.3	7.4	7.5	7.4	7.4
8.4	8.3	8.3	8.3	8.4	8.3	8.4
-	8.6*	8.6*	8.6*	-	8.7*	8.6*
10.2	10.2	10.2	10.2	10.3	10.3	10.3
12.7	12.7	12.7	12.7	-	12.7	12.7
13.6	13.5	13.5	13.5	13.6	13.5	13.6
14.9	14.9	14.8	14.9	15.0	14.9	14.9
15.6	15.6	15.6	15.6	15.7	15.6	15.6
16.0	15.9*	15.9	15.9*	15.9*	15.9*	15.9*
16.4	16.3	16.3	16.4	16.4	16.3	16.4
16.8	16.7	16.7	16.8	16.8	16.8	16.8
17.4	17.3	17.3	17.4	17.5	17.4	17.4
18.5	18.4	18.4	18.5	18.5	18.2	18.2
19.0	18.9	18.9	19.0	19.0	19.0	19.0
19.8	19.7	19.7	19.8	19.8	19.7	19.8
20.4	20.3	20.3	20.4	20.4	20.4	20.4
21.2	21.2	21.1	21.2	21.3	21.2	21.2
21.8	21.8	21.7	21.8	21.8	21.8	21.8
-	-	-	-	-	-	22.7
23.0	23.0	22.9	22.9	23.0	22.9	23.0
-	24.0	24.0	24.1	24.1	24.1	24.1
25.1	25.0	25.0	25.1	25.1	25.0	25.1
25.7	25.6	25.6	25.7	25.7	25.6	25.7
-	26.2	26.2	26.3	26.3	26.2	26.3
26.3	26.5	26.5	26.5	26.5*	26.5*	26.5
26.9	26.8	26.8	26.9	26.9	26.9	26.9
27.3	27.3	27.3	27.3	27.4	27.3	27.3
-	-	-	-	-	-	28.0
28.6	28.5	28.5	28.5	28.6	28.5	28.6
28.9	28.9	28.8	28.9	28.9	28.8	28.9
-	-	-	-	-	-	29.3
-	-	-	-	-	-	29.7
-	30.5	30.4	30.4	30.4	30.5	30.5
31.2	31.0	31.0	31.0	31.0	31.0	31.1
31.7	31.7	31.7	31.7	31.7	31.7	31.6
-	32.7	32.7	32.8	32.8	32.7	32.8
33.3	33.2	33.2	33.2	33.3	33.2	33.2
34.0	33.9	33.9	34.0	34.0	34.0	34.0

(* Peak revealed weak intensity).

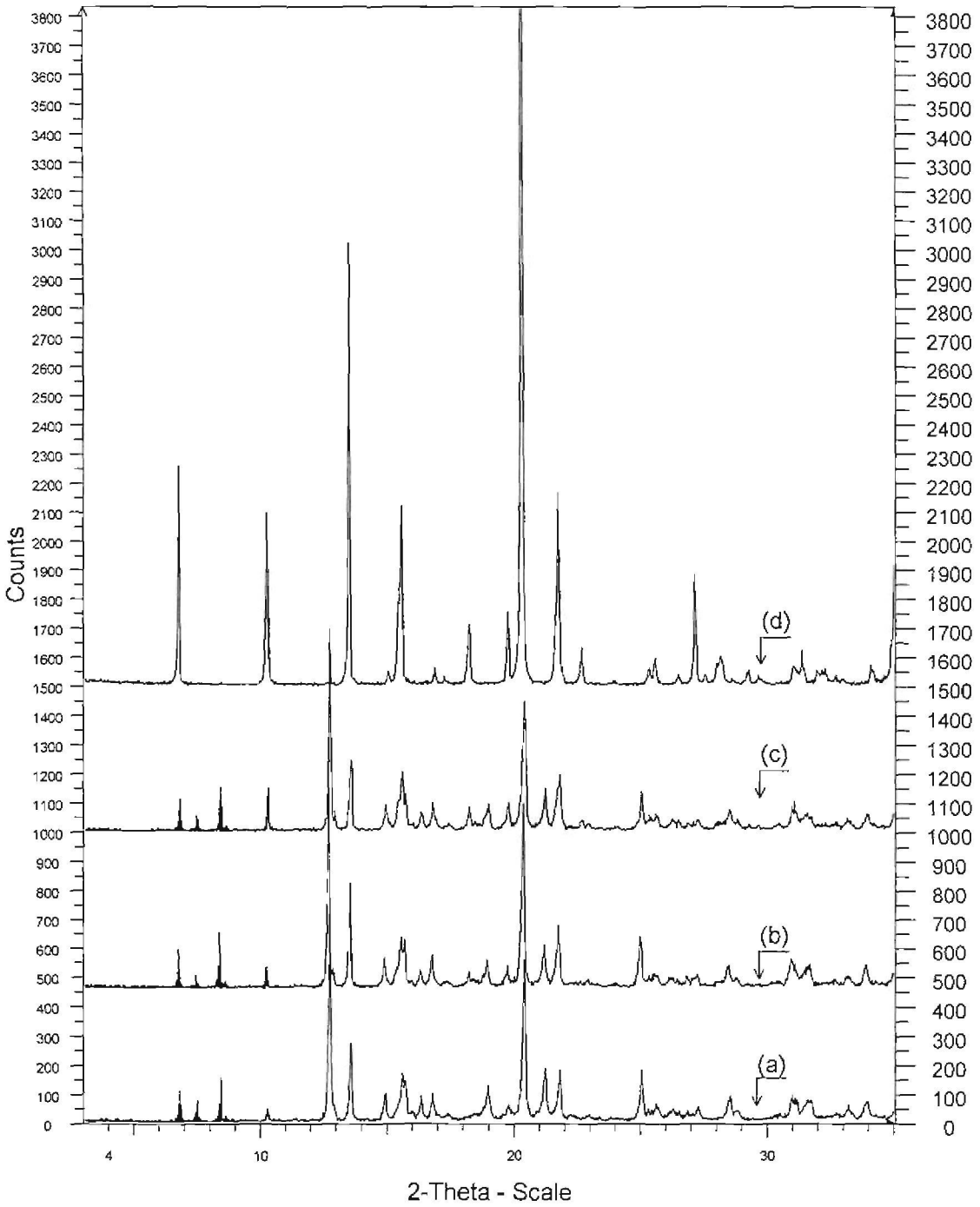


Figure 6.9 XRPD overlay of venlafaxine hydrochloride: (a) Form 5, Form 5 exposed to 30 ºC & 0% RH for (b) 42 days, (c) 56 days and (d) Form 1.

The DSC thermograms for Form 5, exposed to 0% RH at 30°C are depicted in figure 6.10. The DSC thermograms revealed significant changes during this study at 30 °C & 0% RH, which included the following:

- A small endotherm appeared at 76-91°C on days: 9, 28, 42 and 56. TGA on the mentioned samples did not reveal any significant mass loss, thus it can not be attributed to a dehydration process. Thermomicroscopy revealed that the crystals showed moderate movements between 75-100°C that could be construed to thermal induced inter-crystal rearrangements. VT-XRPD of Form 5 (chapter 5 – section 5.2.2.5) confirmed the observed rearrangements which occurred between 85-91°C. The DSC thermograms of Form 5 at: initial, 14 and 21 days did not reveal a definite endotherm representing the inter-crystal rearrangement, due to the presence of a moderate drift in the baseline of the DSC thermograms.
- The melting-point of venlafaxine hydrochloride Form 5 remained relatively unchanged (i.e. varied between 219-220°C – see figure 6.10) when exposed to 30°C & 0% RH for 21 days.
- The melting point of the sample on day 28 was slightly lower (i.e. 217 °C).
- On day 42 the DSC thermogram of Form 5 showed two melting endotherms: 210°C and 216°C respectively (normally associated with the mixture of Form 1 and Form 2 – see chapter 5). The DRIFT-IR spectrum of this sample (figure 6.11) clearly indicated the appearance of the IR-absorbance peaks at: 3326, 2943 & 2483 cm^{-1} (characteristic to Form 1) thus confirming that after 42 days at 30°C & 0% RH a fraction of Form 5 converted to Form 1 (which corresponded with the observations in section 5.2.2.5.2).

- On day 56 the sample revealed a melting endotherm at 210°C. The thermally induced rearrangement endotherm appeared at 76°C. The melting point at 210°C is characteristic of Form 1. XRPD (figure 6.9) indicated that the sample consisted of a probable mixture of Form 1 and Form 5 due to the presence of the following characteristic peaks of Form 1 in the XRPD pattern: 18.2, 22.7, 29.3 and 29.7 °2θ.

Brits (2003:123) showed that DSC is not always a discriminating tool to distinguish between the lower melting point polymorph and mixtures of the higher and lower melting point polymorphs. XRPD and DRIFT-IR can clearly distinguish between pure and mixtures of venlafaxine HCl polymorphs.

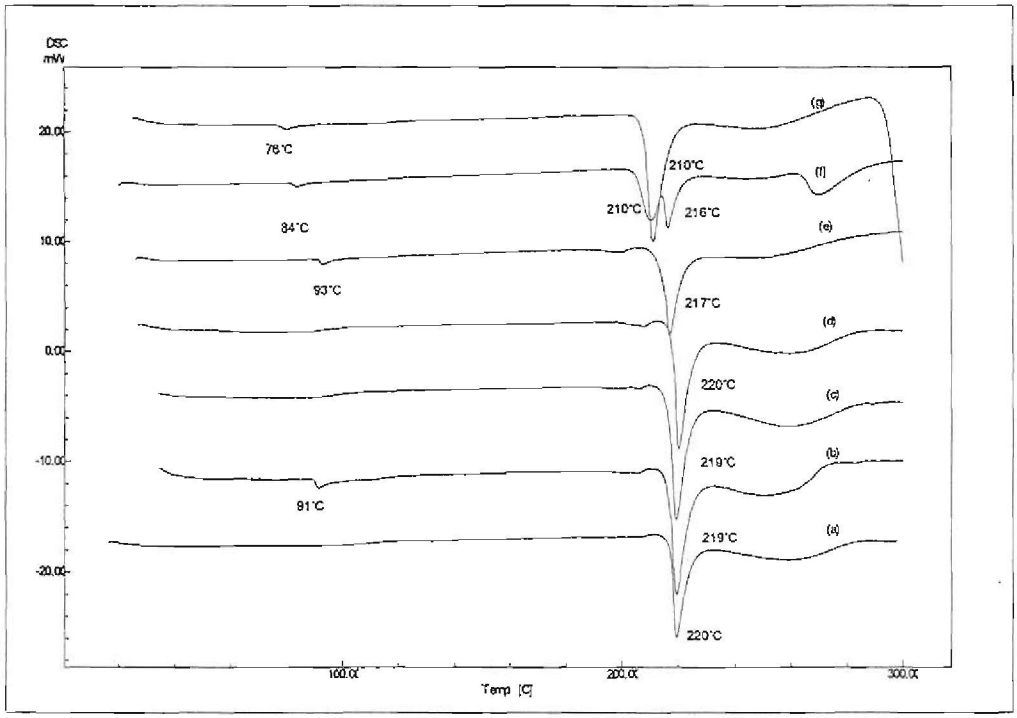


Figure 6.10 DSC thermograms of venlafaxine hydrochloride Form 5 when exposed to 30°C – 0% RH at the following intervals: (a) Initial, (b) 9 days, (c) 14 days, (d) 21 Days, (e) 28 days, (f) 42 days & (g) 56 days.

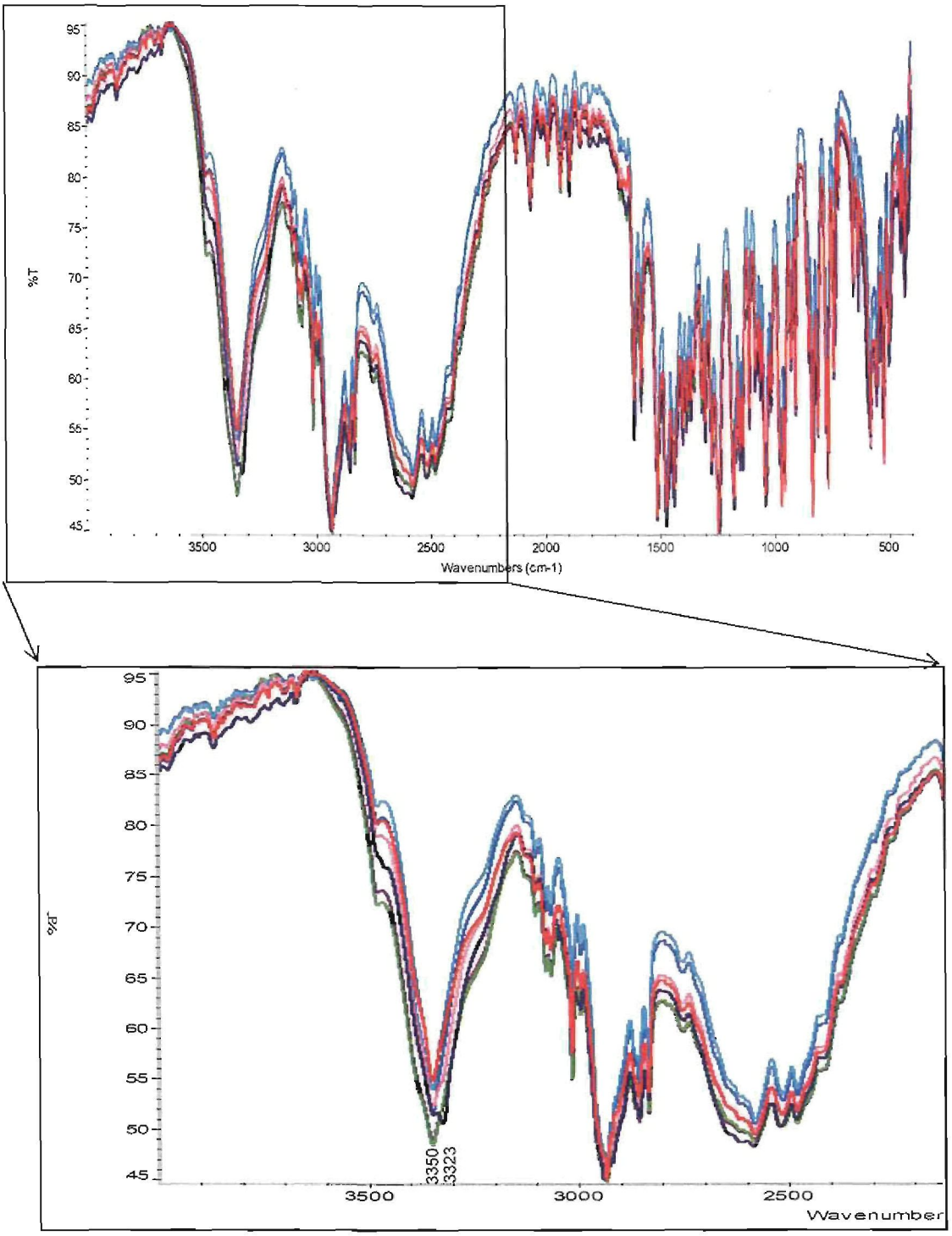


Figure 6.11 An overlay of the DRIFT-IR spectra of Form 5 when exposed to 0% RH at 30°C during a 56 day period: Initial, 9 days, 14 days, 21 days, 28 days, 42 days, 56 days.

An overlay of the DRIFT-IR spectra of venlafaxine HCl Form 5, Form 5 exposed to 30 °C & 0% RH for 56 days and Form 1 is shown in figures 6.11 and 6.12, which indicates the presence of traces of Form 1 in the Form 5 sample, exposed to 30°C & 0% RH for 56 days. Evidence of the phase transition that occurred is visible in the 4000-2500 cm^{-1} range, where the appearance of the absorption band at 3323 cm^{-1} (after 56 days) is indicative of the Form 1 traces, and the presence of the absorption band at 3350 cm^{-1} indicative of the Form 5 traces (figure 6.11 & 6.12).

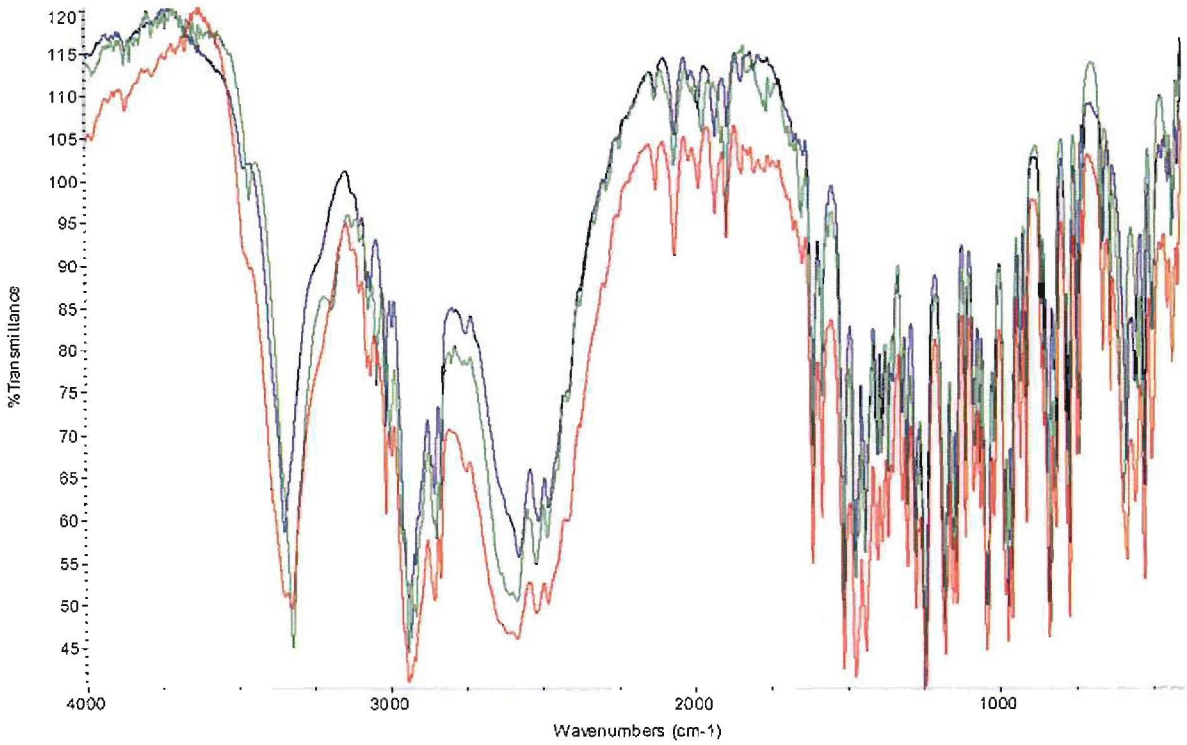


Figure 6.12 DRIFT-IR spectra overlay of venlafaxine hydrochloride: Form 5, Form 5 exposed to 30 °C & 0% RH for 56 days and Form 1.

6.2.5.2 Venlafaxine hydrochloride Form 5 – 30°C & 65 %RH

XRPD patterns and DRIFT-IR spectra of Form 5 when exposed to 30°C & 65 % RH did not reveal any significant changes.

The DSC thermogram of Form 5 (figure 6.14) remained relatively unchanged during the first 14 days of the study when exposed 30°C & 65% RH. The DSC thermogram of the sample evaluated on day 21 revealed a small endotherm at 99°C, which might have suggested a dehydration process, however thermogravimetric analysis revealed a weight loss of approximately 0.65% (m/m) when the sample was heated to 160°C, indicating that this endotherm did not necessarily indicate dehydration.

Thermomicroscopy revealed that the crystals showed moderate movements between 75-100°C that could be construed to the thermal induced rearrangements. VT-XRPD of Form 5 (section 5.2.2.5.2) confirmed the observed rearrangement that occurred between 75-100°C. The DSC thermograms for Form 5 at: initial, 9 and 14 days did not reveal a definite endotherm representing the inter-crystal rearrangement due to the presence of a moderate drift in the baseline of the DSC thermograms.

The thermal induced rearrangements in the samples on day 28 and 42 revealed the rearrangement endotherm at lower temperatures compared to the rearrangement temperatures at day 21 and 56 (figure 6.13 & 6.14). XRPD analysis of the samples (at ambient conditions) did not reveal any significant changes in the crystal lattices of the mentioned samples thus it can be assumed that all the samples contained Form 5.

Variation of the position of the thermal rearrangement endotherm in the DSC thermograms could be attributed to the fact that the Form 5 polymorph, when stored at 30°C & 65% RH, revealed a meta-stable phase which was temperature dependant where the amount of energy needed for the inter-crystal rearrangement (ΔH_{trans}) varied between the samples (table 6.6).

From the DSC thermograms obtained it can be suggested that the higher the temperature at which the rearrangement occurred, the higher the final melting point of the sample (figure 6.19).

Table 6.6 Heat of transition (ΔH_{trans}) needed for the inter-crystal rearrangement observed in venlafaxine HCl Form 5 samples stored at 65% RH – 30°C

Age (days)	**ΔH_{trans} (J/g)**
21	9.49
28	4.97
42	3.70
56	5.58

Based on these observations we can divide the observed DSC thermograms into 3 groups:

(i) **No rearrangement endotherm visible:** initial, 9 and 14 days.

(ii) **Low temperature rearrangement endotherms present:** 28 and 42 days.

(iii) **High temperature rearrangement endotherms present:** 21 and 56 days.

VT-XRPD studies were not able to discriminate between the three groups. The XRPD patterns of Form 5 samples, stored at 30°C & 65% RH: initial, 3 and 6 weeks were investigated at increased temperatures (figure 6.15 – 6.16).

The VT-XRPD studies indicated that all three samples revealed a similar behaviour (Form 5 in section 5.2.2.5.2). The XRPD pattern observed at 200°C revealed only one peak at 28.0 °2θ. The samples removed from the diffractometer at the end of the VT-XRPD study were melted and black in colour which suggested that melting and decomposition has occurred during the 200-215°C range. Thus, VT-XRPD was not able to distinguish between the melting behaviour of the mentioned samples.

The DSC thermograms of the samples evaluated on days: 28 and 42 revealed two melting endotherms with significantly lower melting endotherms at 201-202°C and 214-215°C respectively (see figures 6.13 & 6.14).

TM studies indicated that the endotherms observed at 201-202°C in the DSC thermogram of the sample (Form 5 – 42 days) were due to the crystal growth and melting of the intergrowth crystals (table 6.7). The endotherm at 215°C indicated the melting of the Form 5 fraction.

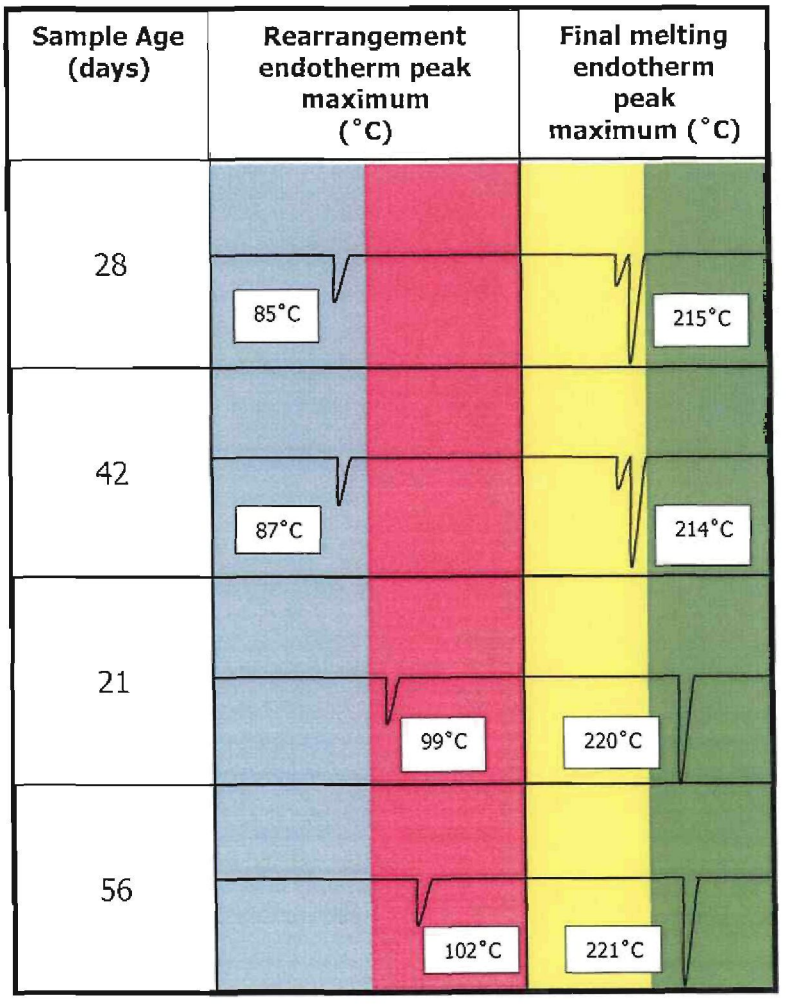


Figure 6.13 Schematic presentation of rearrangement endotherm temperature and final melting point of the venlafaxine hydrochloride Form 5 samples stored at 30 °C & 65% RH.

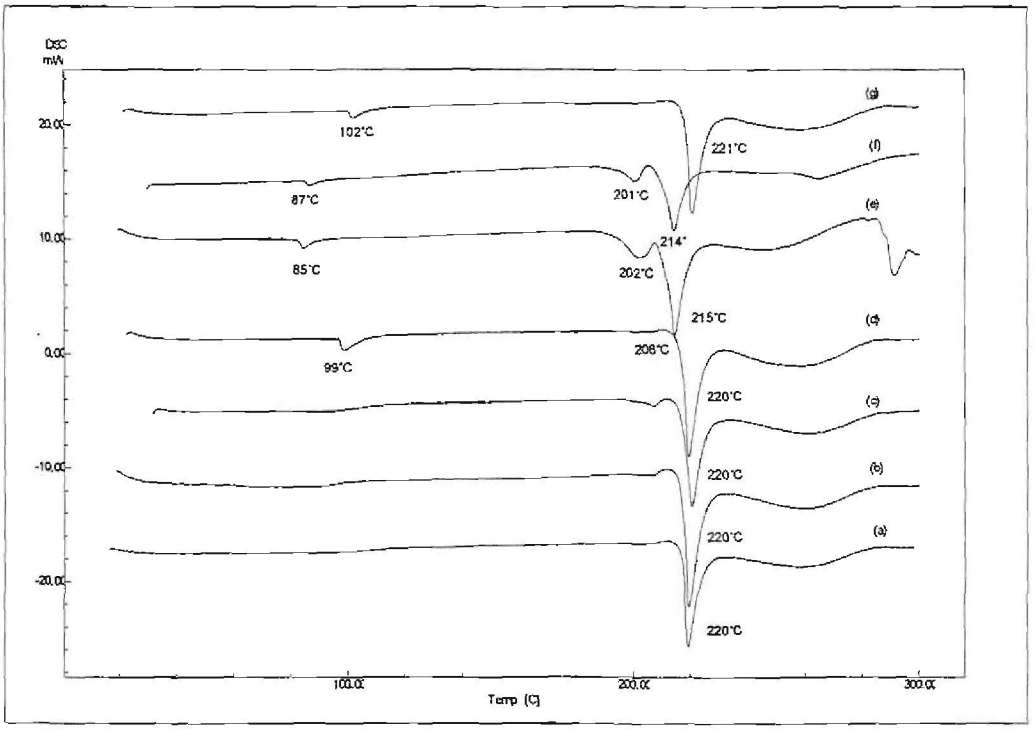


Figure 6.14 DSC thermograms of Form 5 when exposed to 30°C – 65% RH at the following intervals: (a) Initial, (b) 9 days, (c) 14 days, (d) 21 Days, (e) 28 days, (f) 42 days & (g) 56 days.

TM studies indicated that the small endotherm observed at 206°C in the DSC thermogram of the sample (Form 5 – 21 days) were due to the crystal growth and melting of the intergrowth crystals (table 6.7). The endotherm at 220°C indicated the melting of the Form 5 fraction.

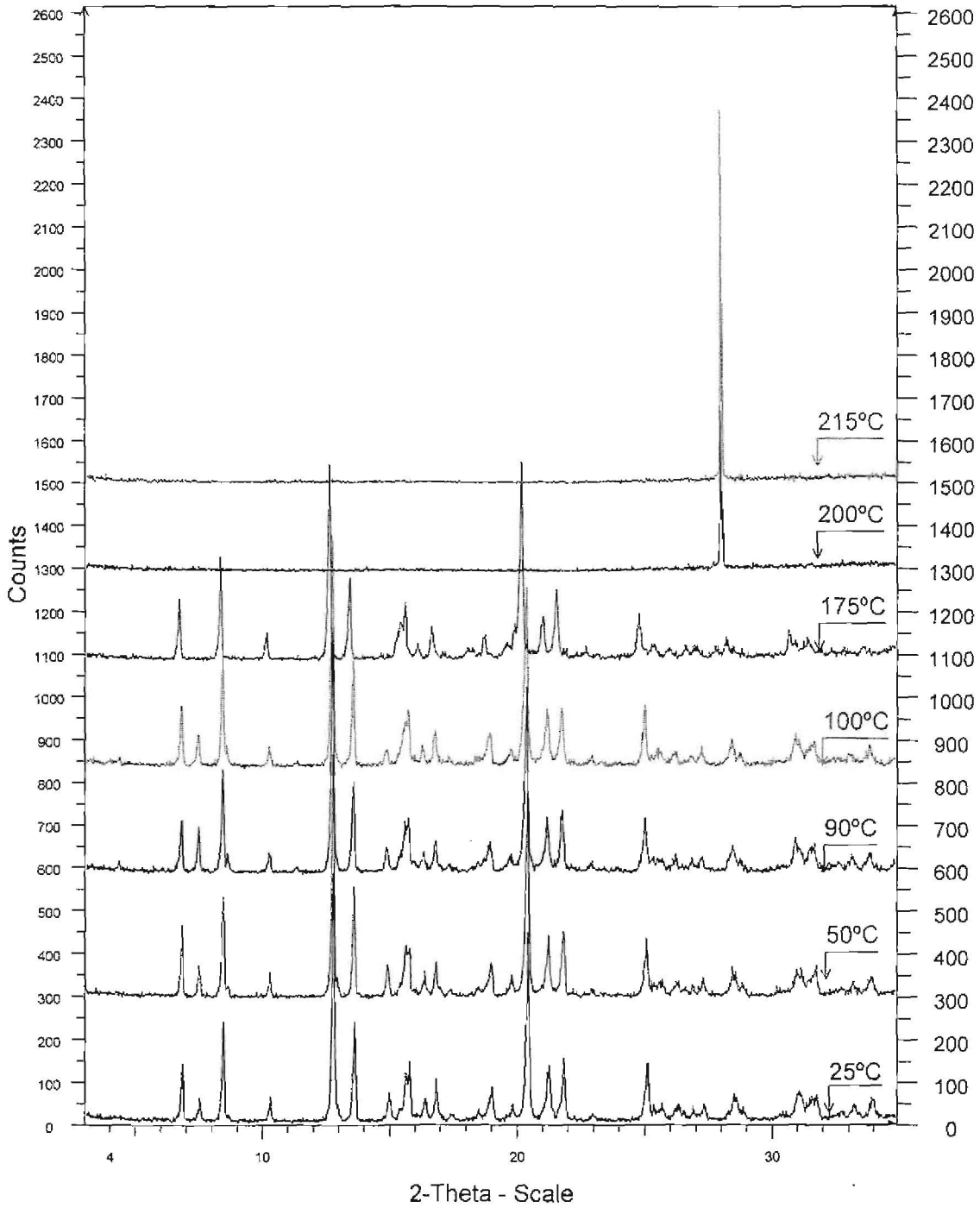


Figure 6.15 VT-XRPD patterns of venlafaxine hydrochloride Form 5 stored at 30°C & 65% RH for 3 weeks.

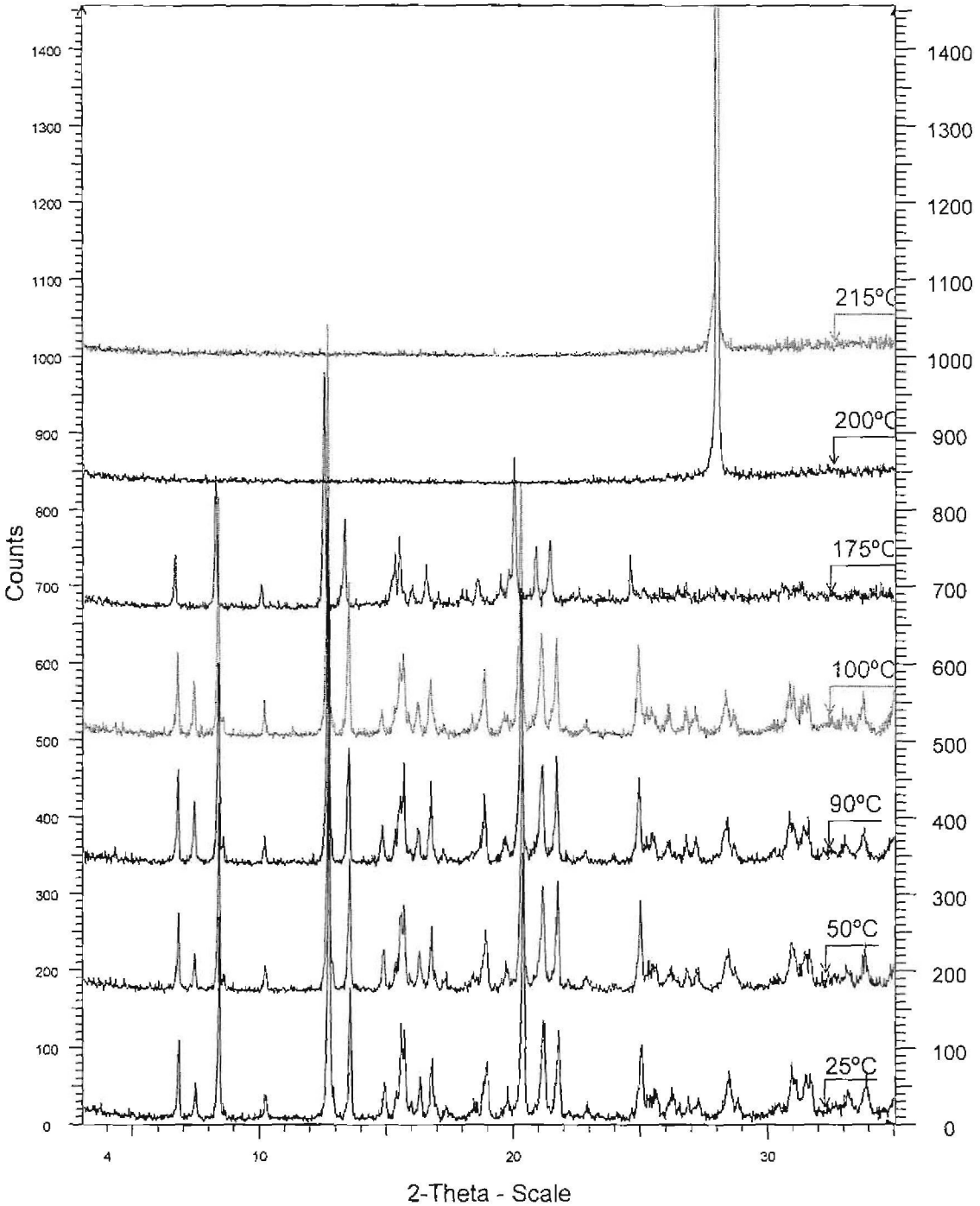


Figure 6.16 VT-XRPD patterns of venlafaxine hydrochloride Form 5 stored at 30°C & 65% RH for 6 weeks.

Table 6.7 Summary of the TM results of venlafaxine HCl crystal (a) Form 5 – stored at 30°C & 65% RH for 42 days, at a temperature range of 25-220°C and (b) Form 5 – stored at 30°C & 65% RH for 21 days, at a temperature range of 25-220°C

Temp. (°C)	(a) Photomicrograph	Temp. (°C)	(b) Photomicrograph	Remarks
25 to 78		25 to 78		Form 5 at room temperature. Some crystals displayed moderate movements at 78 °C.
185		181		Droplets (on the cover slip, suggesting sublimation) and needle-like intergrowth crystals appeared.

Table 6.7 Continued...

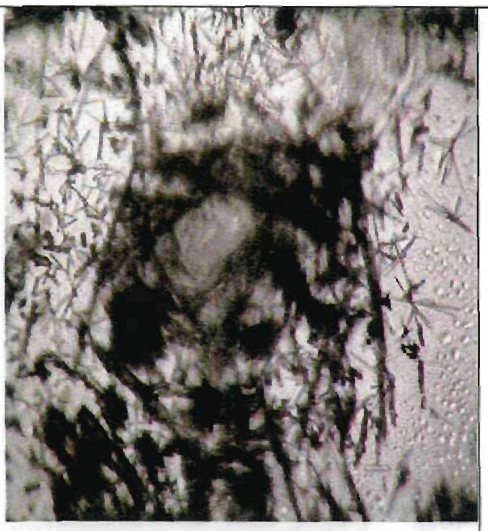
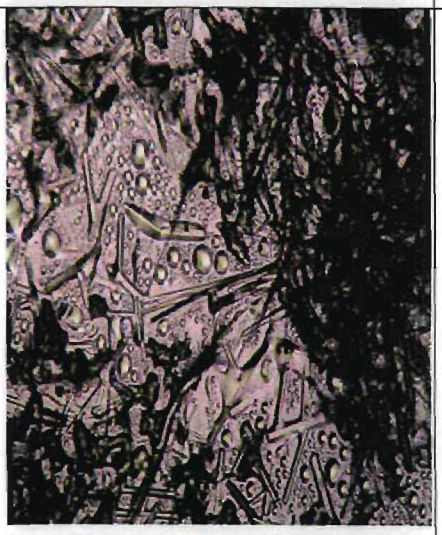
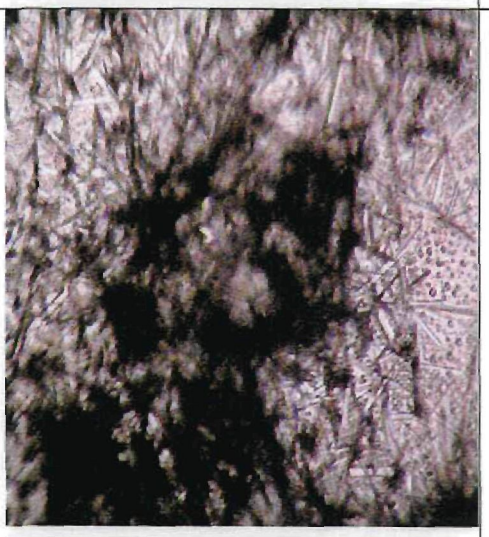
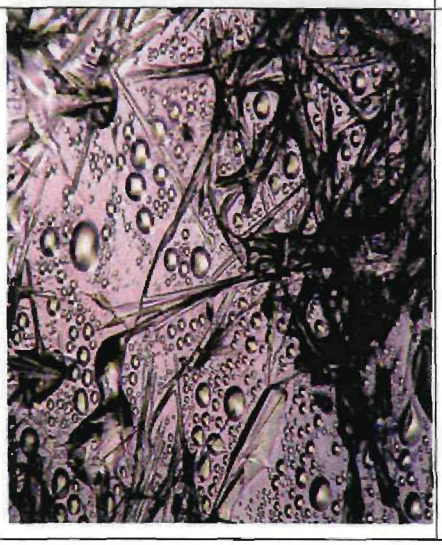
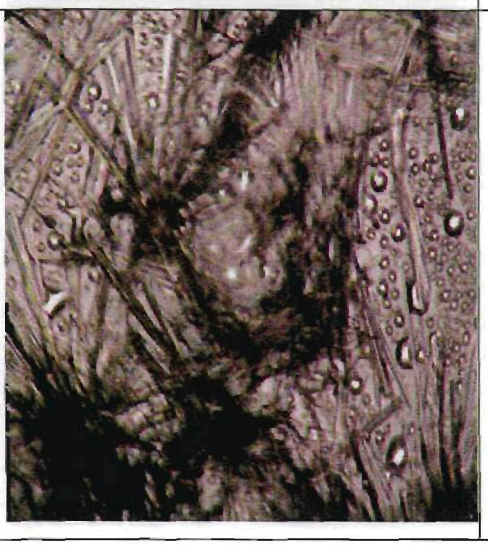
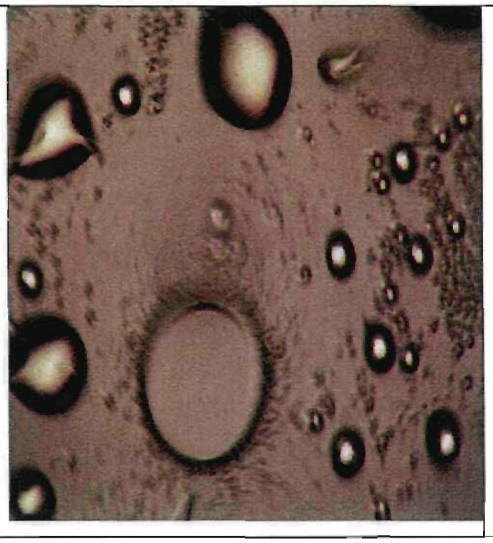
197		195		Intergrowth crystals.
206		206		Melting of intergrowth crystals initiated.
213-220		215		Melting of crystal Form 5 fraction.

Table 6.7 Continued...

-		220		Melting of crystal Form 5.

From the results obtained it can be concluded that the exposure of venlafaxine hydrochloride Form 5 to 30°C & 65% RH did not have a profound influence on the polymorphic behaviour (i.e. no polymorphic transition occurred). DSC results suggested that Form 5 revealed a meta-stable phase (possibly induced by the adsorbed water, which acted as molecular loosener) which influenced the thermal behaviour significantly causing unpredictable thermal events which can be classified into three groups. The XRPD and DRIFT-IR spectra of the samples appearing in the three groups did not reveal any significant differences, suggesting that the variable thermal behaviour was caused by differences in the thermodynamic stabilities of the three groups and was not primarily related to polymorphic transitions.

6.2.5.3 Venlafaxine hydrochloride Form 5 – 30°C & 75 %RH

The total moisture content of Form 5 – exposed to 30°C & 75% RH varied between 0.71-1.32% (m/m). The maximum moisture content sorbed was observed after 21 days (1.32%). The final moisture content (on day 56) was found to be 0.61% (m/m). The variation of moisture sorbed by the sample illustrates the dynamic behaviour of moisture *adsorption*, where adsorption and desorption occurs intercurently. The XRPD patterns of the samples did not reveal any significant changes (figure 6.17).

Minor variations in the peak intensities were observed which could be attributed to the preferred orientation effect of the crystals and small differences in the sample powder-bed height:

- A small diffraction peak at 8.6-8.7°2θ was detected during days: 9, 14, 42 and 56 which revealed very low intensities (maximum relative intensity exhibited = 1.7%). This peak (8.7°2θ) is characteristic of the venlafaxine monohydrate (Brits, 2003:129).
- The broad doublet diffraction peak between 15-16°2θ diverged and produced a small shoulder peak at 15.3°2θ, which revealed a variance in intensity. This observation suggested that a range of diffraction peaks might be overlapped in this region.
- The preferred orientation of the crystals could have been responsible for the variations in the intensities of the following diffraction peaks: 16.0, 18.4-18.5, 26.5 and 30.4°2θ. The Bragg peak at 30.4°2θ was first detected on day 9 of the study.

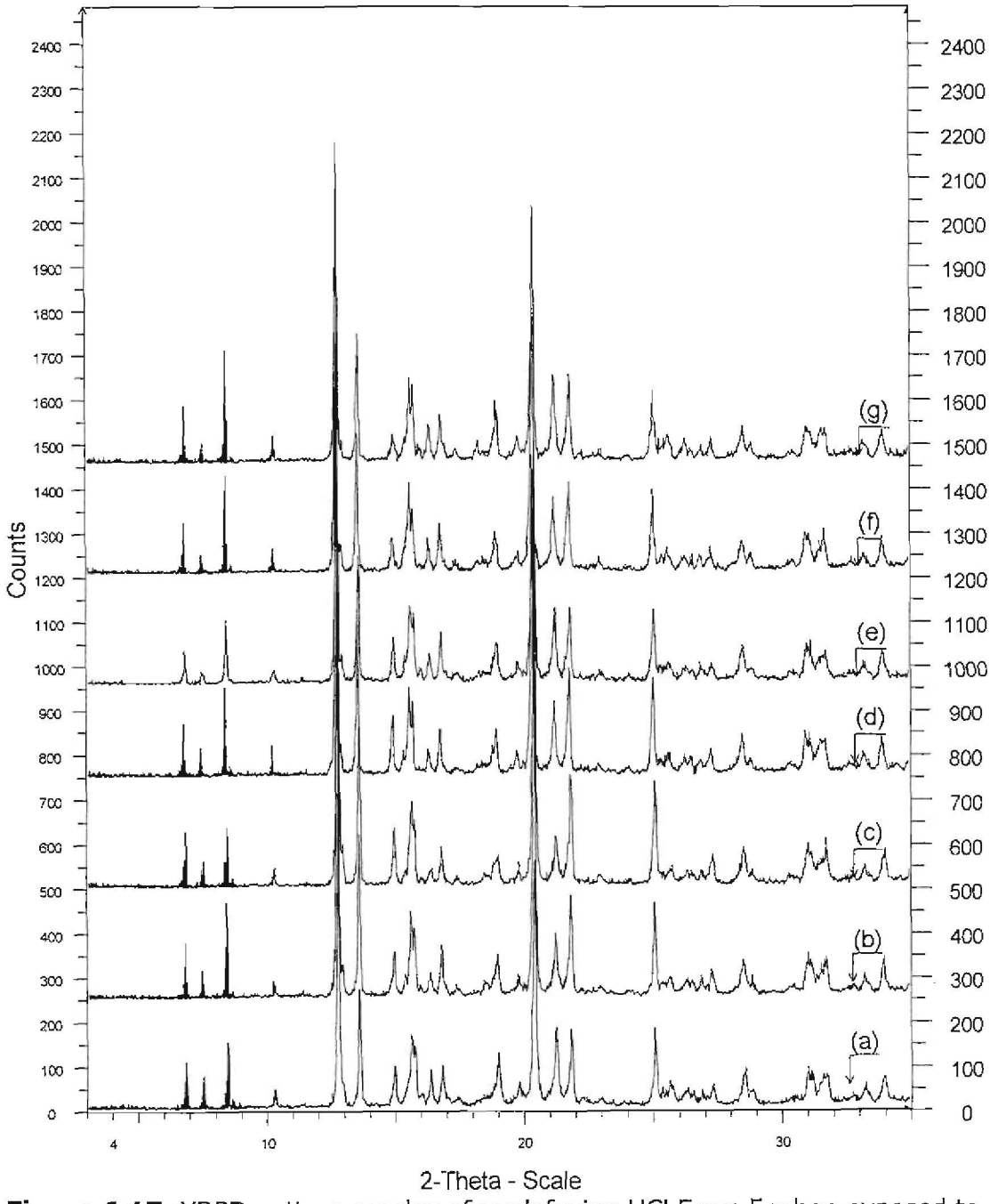


Figure 6.17 XRPD pattern overlay of venlafaxine HCl Form 5 when exposed to 30°C & 75% RH at the intervals: (a) 0, (b) 9, (c) 14, (d) 21, (e) 28, (f) 42 & (g) 56 days.

An overlay of the DRIFT-IR spectra of Form 5 exposed to 75% RH at 30°C during the 56 day test period is displayed in figure 6.18.

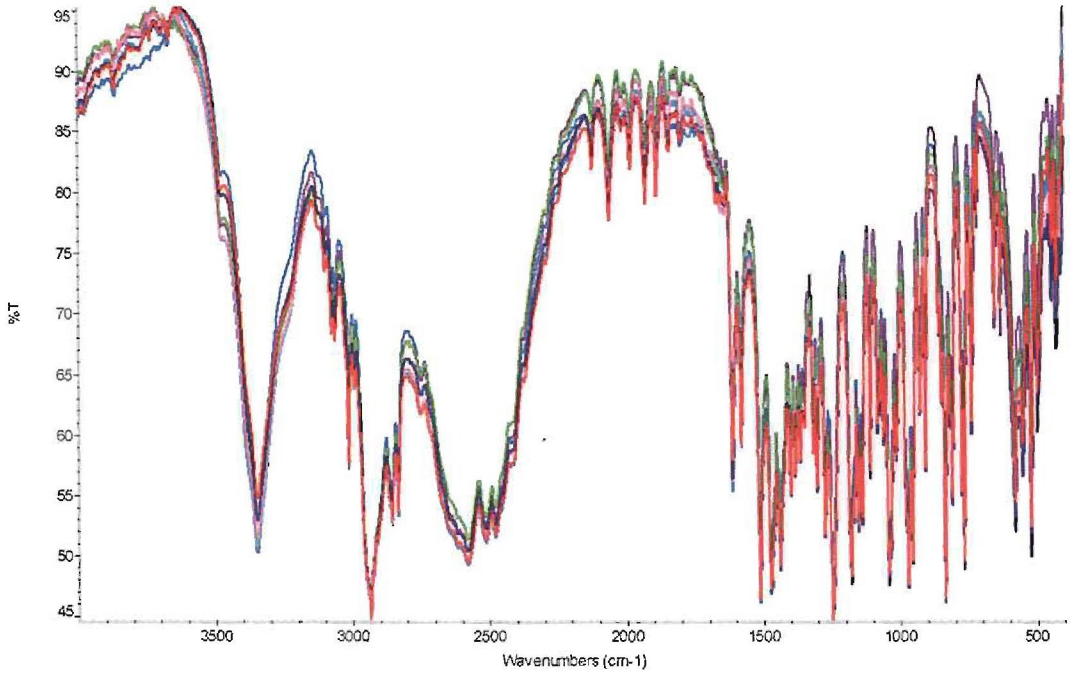


Figure 6.18 An overlay of the DRIFT-IR spectra of Form 5 when exposed to 75% RH at 30°C during a 56 day period: Initial, 9 days, 14 days, 21 days, 28 days, 42 days, 56 days.

The DRIFT-IR spectrum of venlafaxine hydrochloride Form 5 remained concomitant to the DRIFT-IR spectrum of Form 5 at the start of the study, supporting the XRPD observations that no significant polymorphic transformation occurred.

The thermal behaviour of venlafaxine hydrochloride Form 5 exposed to 30°C & 75% RH (figure 6.19) was found to be comparable to that observed for Form 5 exposed to 30°C & 65% RH (figure 6.14).

Based on the observations we can divide the observed DSC thermograms into 3 groups:

(i) **No rearrangement endotherm visible:** initial, 14 and 21 days.

(ii) **Low temperature rearrangement endotherms present:** 9, 28 and 42 days.

(iii) **High temperature rearrangement endotherms present:** 56 days.

The rearrangement endotherms were present in some of the samples at temperatures ranging between: 80-98°C (see figure 6.19). The rearrangement endotherm was not clearly detectable in all samples due to a drift in the baseline of the DSC thermograms, as illustrated in figure 6.20. The crystal growth and melting of the intergrowth crystals were clearly detected in the samples evaluated on days: 9, 14, 21, 28 and 42.

The melting temperature of the Form 5 fraction remained relatively unchanged (218-220°C) during the first 21 days of the study. The DSC thermograms of the samples investigated on day 28 and 42 revealed lower rearrangement and melting endotherms compared to those observed in the other thermograms in figure 6.19. A similar behaviour was revealed in figure 6.13 for Form 5 exposed to 30°C & 65% RH.

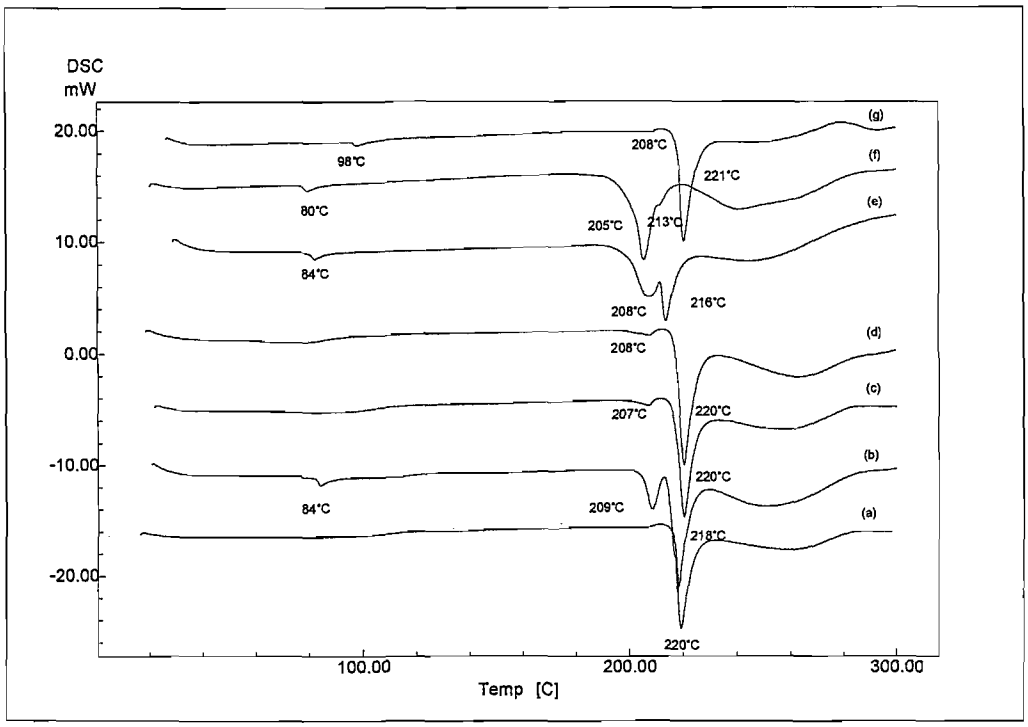


Figure 6.19 DSC thermograms of venlafaxine hydrochloride Form 5 when exposed to 30°C & 75% RH at the following intervals: (a) Initial, (b) 9 days, (c) 14 days, (d) 21 Days, (e) 28 days, (f) 42 days & (g) 56 days.

The DSC thermogram of the sample on day 42 revealed endotherms at 205°C and 213°C, this might suggest that the sample consisted of a probable mixture of Form 5 and Form 1, but XRPD and DRIFT-IR did not detect any significant traces of Form 1 present in the sample. The DSC thermogram was once again recorded but the heating rate decreased (from 10°C/min) to 5°C/min and the DSC thermogram obtained was found to be comparable to that of the sample analysed on day 28 (figure 6.20).

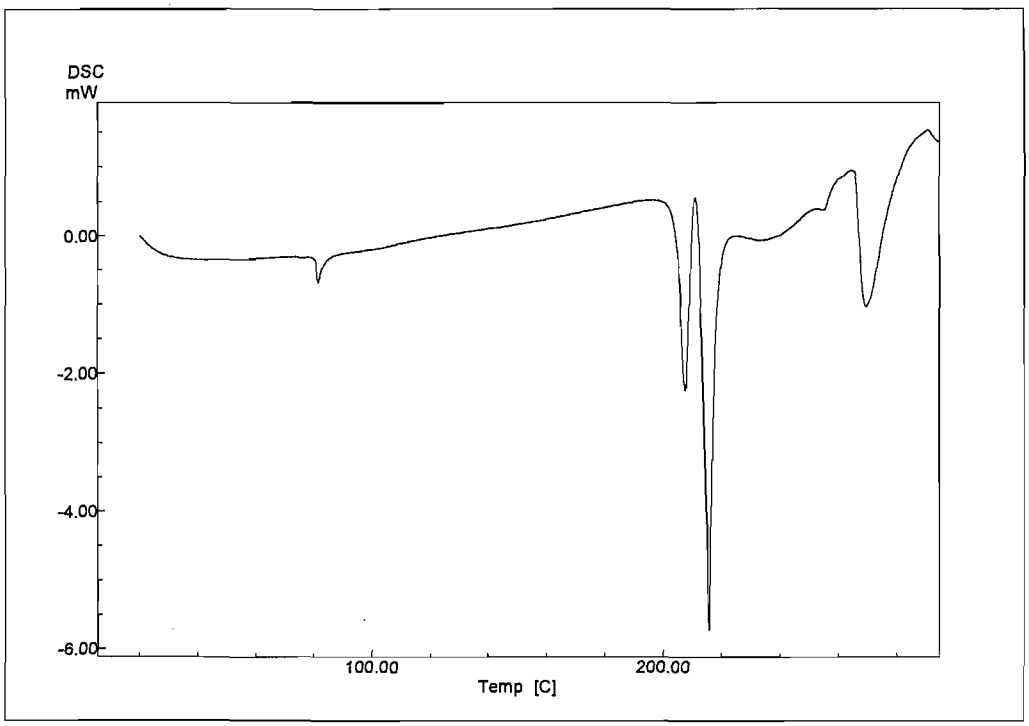


Figure 6.20 DSC thermogram of venlafaxine hydrochloride Form 5 when exposed to 30°C & 75% RH for 42 days, recorded at a heating rate: 5°C/min.

The sample evaluated on day 56 revealed a DSC thermogram comparable to that of the initial sample Form 5.

DSC results once again suggested that Form 5 revealed a meta-stable phase (induced by the adsorbed water), as observed for the Form 5 samples stored at 65% RH & 30°C, which influenced the thermal behaviour significantly causing unpredictable thermal events which can be classified into three groups. The XRPD and DRIFT-IR spectra (of the samples appearing in the three groups) did not reveal any significant differences, suggesting that the variable thermal behaviour was caused by differences in thermodynamic stability of the three groups, and is not primarily related to the structural properties of their lattices (i.e. differences in crystal structure).

From the results obtained it can be concluded that the exposure of venlafaxine hydrochloride Form 5 to 30°C & 75% RH did not induce a polymorphic transition.

6.2.5.4 Venlafaxine hydrochloride Form 5 – 30°C & 85 %RH

As mentioned previously in section 6.2.1 – the moisture sorption isotherms of venlafaxine hydrochloride Form 5 showed deliquescence at %RH > 85%. The stability of Form 5 was investigated by exposing samples of Form 5 to 30°C & 85% RH for a period of 56 days.

The total moisture content of Form 5 – exposed to 30°C & 85% RH varied between 0.71-5.46 % (m/m) – see table 6.4. The maximum moisture content sorbed was observed after 56 days. The ascending slope of the moisture sorption isotherm in figure 6.5 indicated that the moisture sorption process was continuous, supporting the observation in section 6.2.1 that the sample underwent continuous moisture sorption which resulted in deliquescence at %RH > 85%.

The XRPD patterns of the venlafaxine hydrochloride Form 5 crystals exposed to 30°C & 85% RH are displayed in figure 6.21, changes in the XRPD peak positions are summarised in table 6.8 and the changes could be summarised as follows:

- The intensity of the diffraction peak at 6.8°2θ showed a decrease in intensity as a function of the exposure time to the testing conditions (i.e. 30°C & 85% RH). The intensity of the peak decreased until no longer detectable on day 56.
- The peak at 7.4°2θ revealed a slight shift to 7.5°2θ after 28 days.
- The intensity of the peak at 8.4°2θ decreased until no longer detectable on day 46.
- The peak at 8.5°2θ was detected after 9 days, and revealed an increase in intensity. The peak showed a peak-shift (from 8.5°2θ) to 8.7°2θ on day 56.

- A diffraction peak was detected after 9 days at 11.3°2θ which revealed a peak-shift towards 35°2θ with time.

Major changes occurred in the 12.0-14.0°2θ region which included the following:

- The peak at 12.7°2θ showed tailing which suggested overlapping of more than one peak. After 9 days the peak segregated and displayed a doublet with peak maxima at 12.6-12.7 and 12.9°2θ respectively. The intensity of the peak at 12.7°2θ decreased and disappeared on day 56. The intensity of the 12.9°2θ peak increased and shifted to a final peak position of 13.0°2θ after 56 days.
- The intensity of the diffraction peak at 13.6°2θ decreased.
- The doublet at 16.4-16.8°2θ revealed the following changes:
    - 16.4°2θ, a decrease in intensity and shifted to a final peak position of 16.5°2θ.
    - 16.8°2θ, a decrease in intensity until it disappeared after 56 days.
- A decrease in intensity of the peak at 20.4°2θ and shifted to a final peak position of 17.6°2θ.
- A diffraction peak appeared at 18.7°2θ on day 9 and showed an increase in intensity.
- A decrease in intensity of the peak at 20.4°2θ and minor peak position shifts during the course of this study.
- The peaks at 21.2°2θ and 21.8°2θ disappeared after 9 days and formed a collection of overlapping peaks ranging between 21.7-22.5°2θ.
- A peak appeared at 24.0°2θ after 9 days when exposed to 30°C & 85% RH.

The discussed changes in the XRPD pattern of Form 5 are illustrated in the overlay of the Guinier plates in figure 6.22.

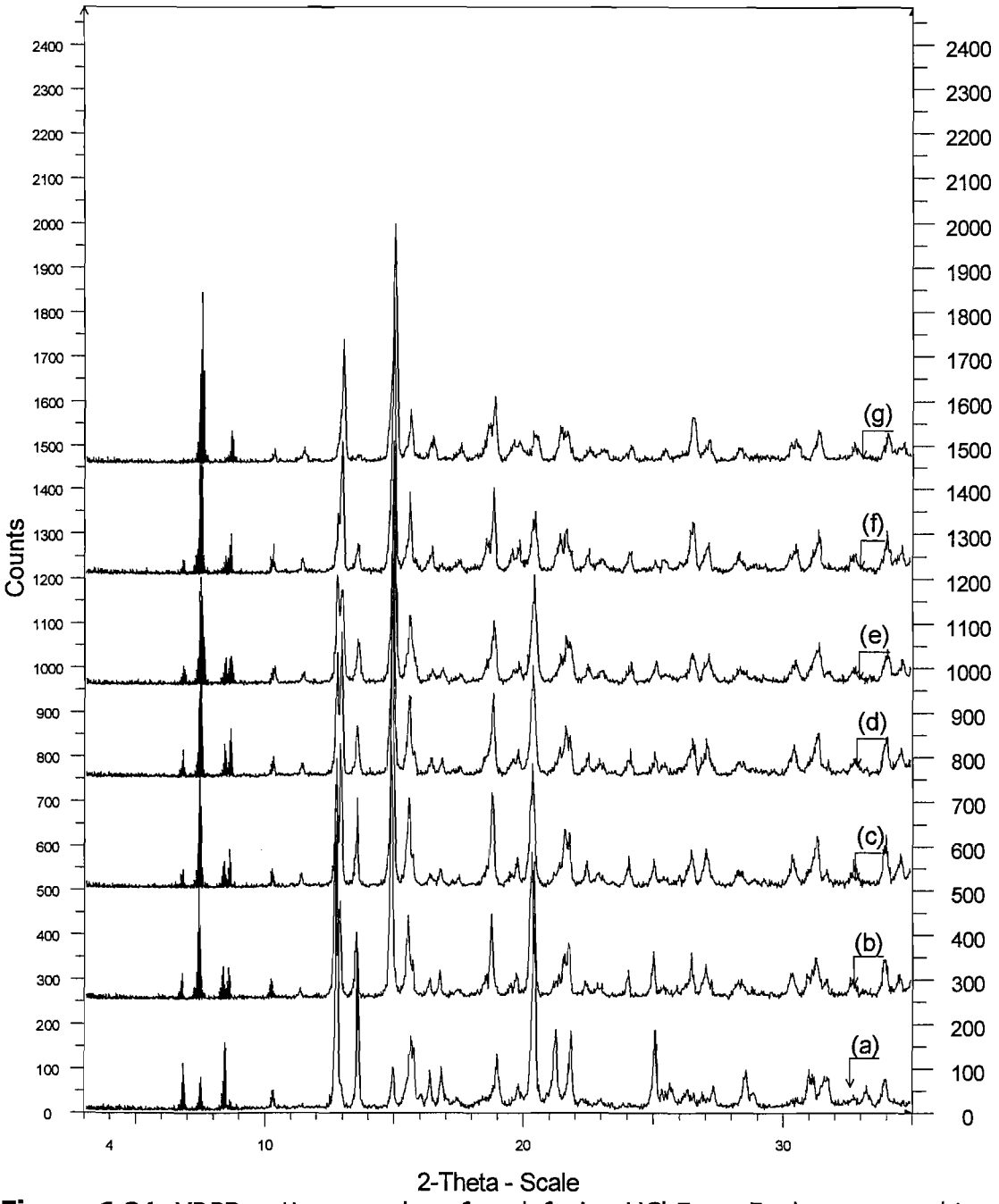


Figure 6.21 XRPD pattern overlay of venlafaxine HCl Form 5 when exposed to 30°C & 85% RH at the intervals: (a) 0, (b) 9, (c) 14, (d) 21, (e) 28, (f) 42 & (g) 56 days.

Table 6.8 Main XRPD pattern peak positions (°2θ) of venlafaxine HCl Form 5 at various time intervals when stored at 30°C & 85% RH

Main peak positions (°2θ) at time intervals						
Initial	**9 Days**	**14 Days**	**21 Days**	**28 Days**	**42 Days**	**56 Days**
6.8	6.7	6.7	6.8	6.8	6.8	-
-	-	-	-	-	-	7.1
7.4	7.4	7.4	7.4	7.5	7.5	7.5
-	-	-	7.8	-	-	-
8.4	8.3	8.4	8.4	8.4	-	-
-	8.5	8.6	8.6	8.6	8.6	8.7
10.2	10.2	10.2	10.3	10.3	10.3	10.3
-	11.3	11.4	11.4	11.4	11.4	11.5
12.7	12.6	12.7	-	12.8	12.9	13.0
-	12.9	12.9	12.8	12.9	-	-
13.6	13.5	13.5	13.5	13.6	13.6	13.6
14.9	14.9	14.9	14.9	15.0	14.9	15.0
15.6	15.5	15.5	15.6	15.6	15.6	15.6
16.4	16.3	16.4	16.4	16.4	16.4	16.5
16.8	16.7	16.8	16.8	16.8	16.8	-
17.4	17.4	17.5	17.5	17.5	17.5	17.6
-	18.5	-	-	-	18.6	18.7
19.0	18.7	18.8	18.8	18.8	18.8	18.9
-	-	-	-		-	-
-	-	19.5	19.6	-	19.6	19.6
19.8	19.7	19.8	19.8	19.8	19.8	19.8
20.4	20.3	20.3	20.4	20.4	20.4	20.4
21.2	-	-	21.4	21.4	21.4	21.4
21.8	21.7	21.6	21.6	21.7	21.6	21.7
-	22.4	22.4	22.5	22.5	22.4	22.5
23.0	22.9	22.9	22.9	23.0	23.0	23.1
-	-	-	23.5	-	-	-
-	24.0	24.1	24.1	24.1	24.1	24.2
25.1	25.0	25.0	25.1	25.1	25.1	-
25.7	25.4	-	25.4	-	25.4	25.5
26.3	-	-	26.5	26.5	26.5	26.6
-	26.5	26.5	-	-	-	-
26.9	27.0	27.1	27.1	27.1	27.1	27.1
27.3	-	-	-	-	-	-
28.6	28.4	28.3	-	28.3	28.3	28.3
28.9	-	-	-	-	28.9	-
-	-	29.3	29.6	-	-	-
-	30.4	30.4	30.4	30.5	30.5	30.5
-	30.9	-	-	-	-	-
31.2	31.3	31.4	31.4	31.4	31.4	31.4
31.7	31.7	31.7	31.8	31.8	-	32.8
-	32.7	32.8	32.8	32.8	32.7	-
33.3	-	-	-	32.9	-	-
-	-	-	-	-	33.4	-
34.0	34.0	34.0	34.0	34.1	34.1	34.1
-	34.6	34.6	34.6	34.7	34.6	34.7

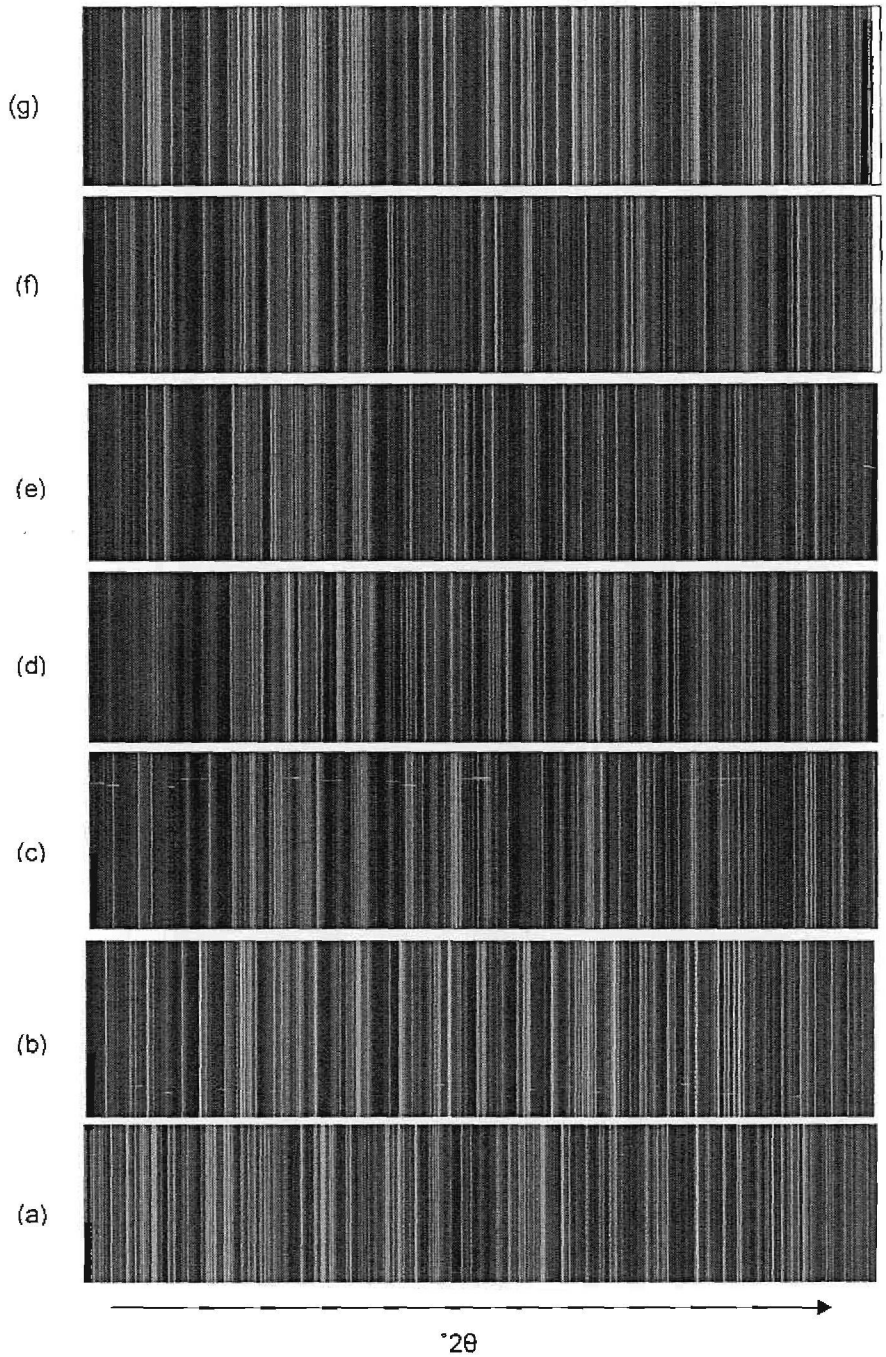


Figure 6.22 XRPD Guinier plates overlay of venlafaxine HCl Form 5 when exposed to 30°C & 85% RH at the intervals: (a) 0, (b) 9, (c) 14, (d) 21, (e) 28, (f) 42 & (g) 56 days.

The changes in the XRPD patterns could be attributed to the hydration process of the anhydrous form, to produce a monohydrated crystal form. The XRPD pattern of the sample at 56 days represents the XRPD pattern of the monohydrate which showed resemblances to that of the monohydrate prepared previously by Brits (2003:104) i.e. Form $\mathbf{H}_{\alpha\beta}$. The XRPD patterns of the 9-42 days samples represent XRPD patterns of mixtures of the hydrated and anhydrous form (Form 5).

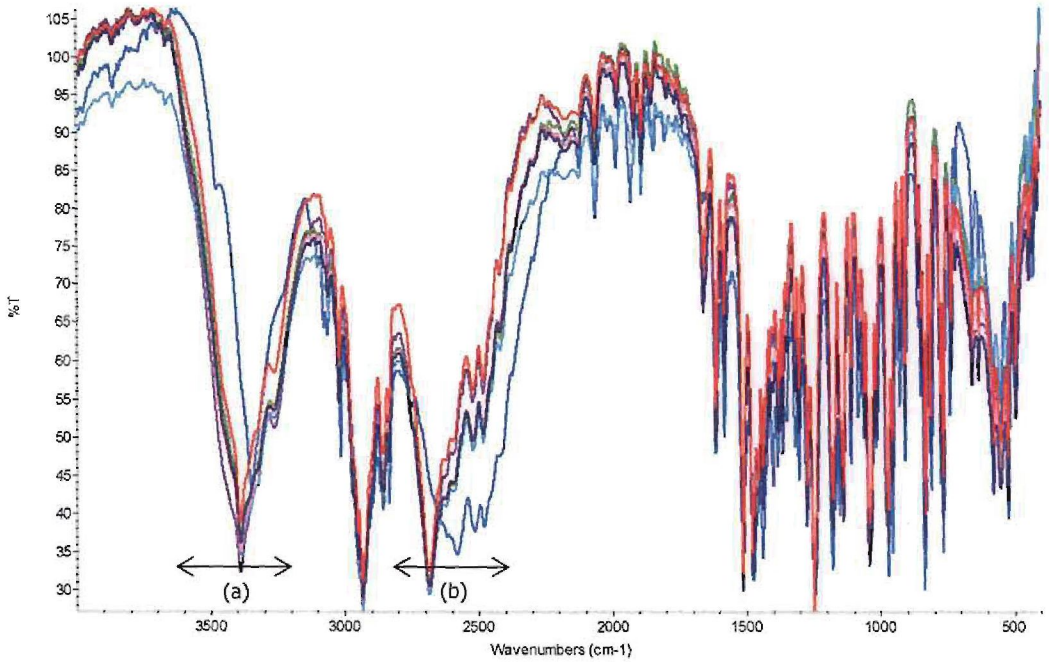


Figure 6.23 An overlay of the DRIFT-IR spectra of Form 5 when exposed to 85% RH at 30°C during a 56 day period: Initial, 9 days, 14 days, 21 days, 28 days, 42 days, 56 days.

The DRIFT-IR spectrum of Form 5 displayed significant changes in the (a) 3200-3700 cm^{-1} and (b) 2350-2900 cm^{-1} absorption regions (figure 6.23). A summary of the main absorption positions (wavenumbers, cm^{-1}) is tabulated in table 6.9.

The 2700-3800 cm^{-1} absorption region is usually associated with O-H, C-H and N-H stretching frequencies in organic molecules (McMurry, 1995:442). In this

particular case, the change in stretching frequency observed after 9 days at 3389 / 3390 and 2686 cm^{-1} indicated the presence of water in the hydrated crystal lattice.

Table 6.9 Main absorptions in the DRIFT-IR spectra of venlafaxine HCl Form 5 at various time intervals when stored at 30°C & 85% RH

Main absorptions	Wavenumbers (cm^{-1})						
	Initial	9 Days	14 Days	21 Days	28 Days	42 Days	56 Days
1	-	3389	3390	3390	3390	3390	3390
2	3350	-	-	-	-	-	-
3	3064	3062	3062	3061	-	-	3061
4	3016	3020	3020	3020	3020	3021	3021
5	-	-	-	-	-	2951	2951
6	2935	2935	2935	2935	2935	2935	2935
7	2856	2855	2855	2854	2854	2854	2854
8	2834	2834	2834	2834	2834	2834	2834
9	2583	2686	2686	2686	2686	2686	2687
10	-	2523	2523	2523	2523	2523	2523
11	2515	-	-	-	-	-	-
12	2482	2484	2484	2484	2484	2484	2484
13	-	-	-	-	-	2173	2172
14	2125	-	-	-	-	-	-
15	2065	2065	2065	2065	2065	2065	2066
16	1985	1983	1983	1982	1982	1982	1981
17	1930	-	-	-	-	-	-
18	-	1919	1919	1919	1919	1918	1918
19	1891	1891	1891	1891	1891	1891	1891
20	-	1855	1854	1855	1856	1856	1857
21	1844	-	-	-	-	-	-
22	1613	1613	1613	1613	1613	1613	1613
23	1582	1582	1582	1582	1582	1582	1583
24	1514	1514	1514	1514	1514	1514	1514
25	1473	1478	1478	1478	1478	1478	1478
26	-	-	-	-	-	1455	1455
27	1438	1438	1438	1438	1438	1438	1438
28	1401	1412	1412	1412	1412	1412	1412
29	1384	1380	1379	1379	1379	1379	1379
30	1366	1366	1365	1365	1365	1365	1365
31	-	-	-	-	-	1347	1347
32	1319	1319	1319	1319	1319	1319	1318
33	1305	1305	1305	1305	1305	1305	1305
34	1274	1273	1273	1273	1273	1272	1272
35	1247	1248	1248	1248	1248	1248	1248
36	1180	1179	1179	1179	1179	1180	1180
37	1153	-	-	-	-	-	-
38	1141	1141	1141	1141	1141	1142	1141
39	1110	1111	1111	1111	1111	1111	1111
40	1083	1083	1083	1083	1083	1083	1083
41	1062	1061	1061	1061	1061	1061	1061
42	1043	1043	1043	1043	1043	1043	1043
43	1016	1017	1017	1017	1017	1018	1018
44	972	972	972	972	972	972	973
45	957	958	958	958	958	958	958
46	929	929	929	928	928	928	928
47	908	908	908	908	908	908	908
48	860	860	860	860	860	860	860
49	850	846	846	846	846	846	846
50	836	834	833	833	833	833	833
51	811	816	816	816	816	816	816
52	777	778	778	778	778	778	778
53	768	768	768	768	768	768	768
54	740	736	736	736	736	735	735
55	719	720	720	720	-	-	-
56	657	659	659	659	659	659	659
57	635	635	635	635	635	635	635

The incorporation of water molecules into the crystal lattice was indicated by the disappearance of the 3350, 2514, 1930, 1844 and 1153 cm^{-1} wavenumbers and the appearance of new wavenumbers at 2523, 1919, 1855 and 553 cm^{-1} after 9 days at 85% RH & 30°C.

The following wavenumbers could be considered characteristic of the monohydrated crystals produced after 56 days: 2951, 2523, 2172, 1857, 1455 and 1347 cm^{-1}. The DRIFT-IR spectrum of the hydrated samples could be considered similar to that of the monohydrate previously prepared, Form $\mathbf{H}_{\alpha\beta}$ (Brits 2003:111).

The DSC thermograms of venlafaxine HCl crystal Form 5, exposed to 30°C & 85% RH are depicted in figure 6.24.

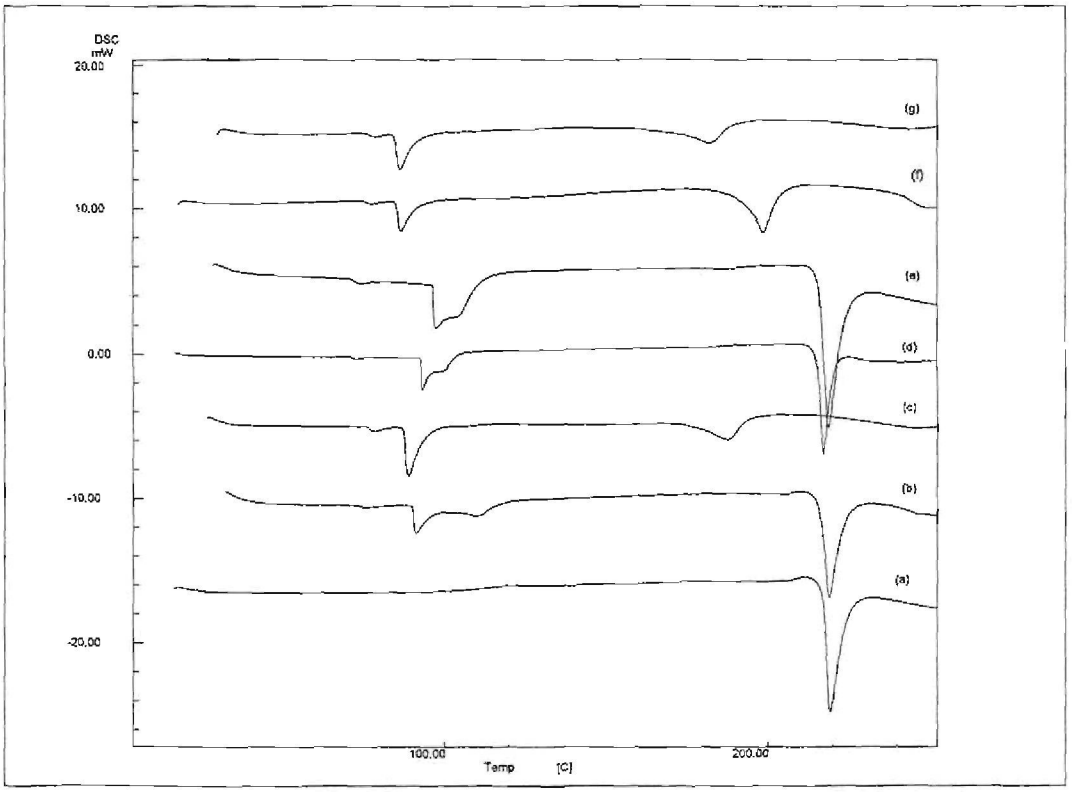


Figure 6.24 DSC thermograms of venlafaxine hydrochloride Form 5 when exposed to 30°C – 85% RH at the following intervals: (a) Initial, (b) 9 days, (c) 14 days, (d) 21 Days, (e) 28 days, (f) 42 days & (g) 56 days.

Han *et al.* (1997:209-218) described the different steps in the dehydration process as follows:

(D = drug, s = solid, l = liquid, v = vapor).

$$D \bullet nH_2O(s) \rightarrow D(s) + nH_2O(l)$$

The enthalpy of the dehydration (ΔHd): Step 1

$$D(s) + nH_2O(l) \rightarrow D(s) + nH_2O(v)$$

The enthalpy of vaporisation of water (ΔHv): Step 2

$$D \bullet nH_2O(l) \rightarrow D(s) + nH_2O(v)$$

Enthalpy of overall transition (ΔHt): Step 3

$$\Delta Ht = \Delta Hd + \Delta Hv$$

Thermogravimetric analysis of the Form 5 samples (figure 6.25) revealed that a mass loss occurred when the samples where heated to 160°C, correlating with the moisture content of the various samples determined with Karl Fischer titrations. Table 6.10 summarises the % weight loss observed in the samples.

The TGA results (table 6.10) confirmed that the Form 5 sample, 9-42 days, consisted of a mixture of Form 5 and a monohydrate, and that the sample after 56 days was a monohydrate.

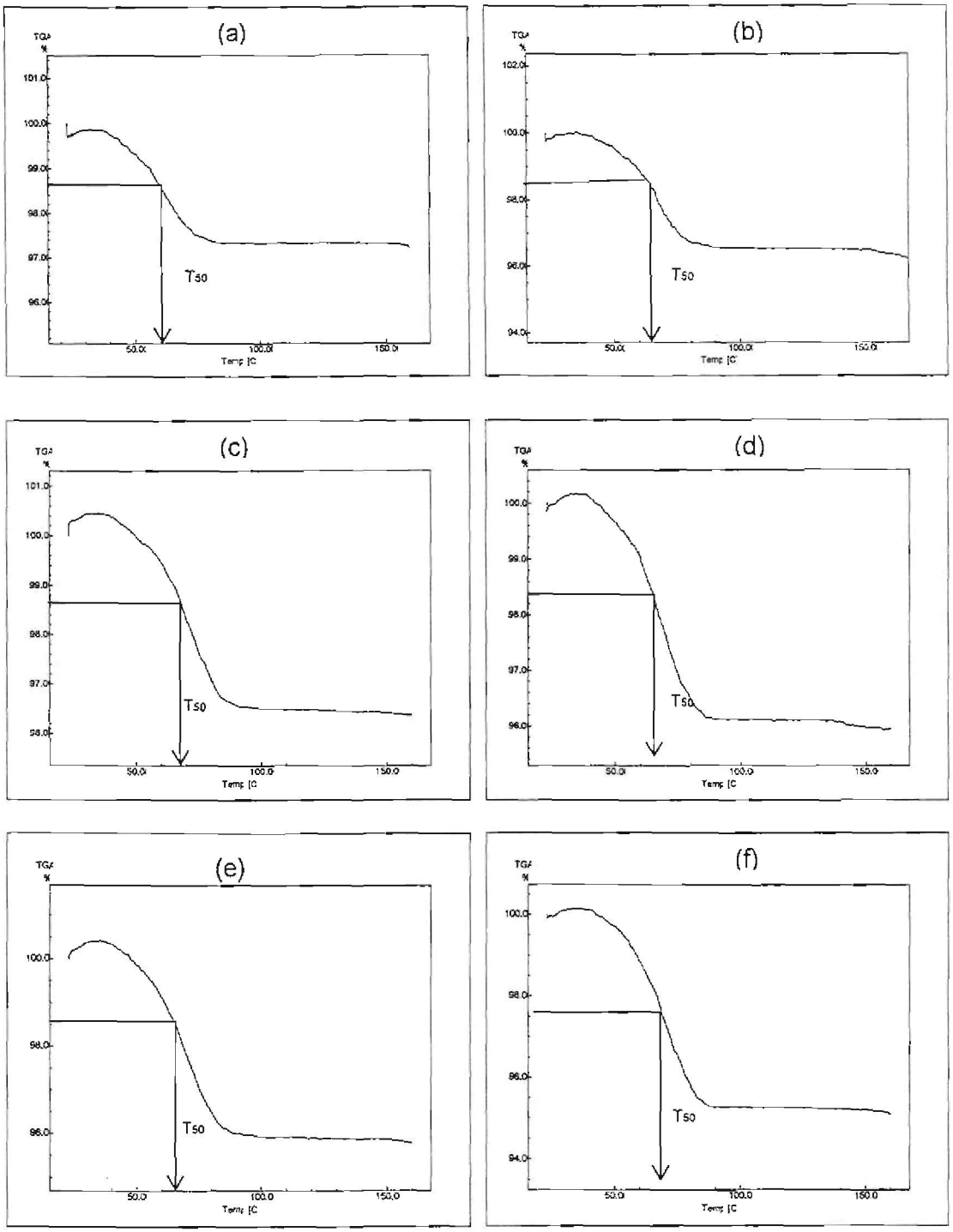


Figure 6.25 TGA thermograms of venlafaxine hydrochloride Form 5 when exposed to 30°C – 85% RH at the following intervals: (a) 9 days, (b) 14 days, (c) 21 days, (d) 28 days, (e) 42 days & (f) 56 days.

Table 6.10 TGA results indicating the % mass loss (m/m) when venlafaxine HCl Form 5 at various time intervals (stored at 30°C & 85% RH) was heated to 160°C

Age (days)	% mass loss (% m/m)
9	2.56
14	3.49
21	4.07
28	4.17
42	4.51
56	4.85

The T_{50} values were calculated for all samples. The T_{50} values indicate the temperature where 50% of the total mass loss occurred when the samples were heated from ambient temperature to 160°C. The T_{50} values (figure 6.25 and table 6.11) during the first 9 days were lower compared to the T_{50} values of the samples at 14-56 days, and increased to a maximum of 69.04°C indicating the stabilisation of the water molecules into the crystal lattice via hydrogen bonding.

Table 6.11 T_{50} values, indicating the temperature where 50% of the total mass loss occurred when venlafaxine HCl Form 5 at various time intervals (stored at 30°C & 85% RH) was heated to 160°C

Age (days)	T_{50} value (°C)
9	60.27
14	66.68
21	69.04
28	66.50
42	67.43
56	68.57

The DSC thermograms of the 28, 42 and 56 days samples (figure 6.24) revealed unpredictable DSC thermograms with significantly lower melting endotherms not previously observed or reported. The thermal behaviour of the samples was investigated utilising thermal microscopy (TM).

TM provides a visual image of the processes and stages that the crystals undergo prior to complete fusion. It is a unique method that is also used to investigate crystal growth. TM can also be applied to determine the melting point of solids with great accuracy, and to investigate the loss of solvent molecules in pseudopolymorphic crystal forms (Byrn *et al.*, 1999:69). The TM observations of the 21-56 days samples were found to be similar and all correlated to the thermal events observed in the DSC thermograms of the samples at 9, 14 and 21 days. Table 6.12 summarises the TM observations for the 21-56 days samples.

Table 6.12 Summary of the TM results of venlafaxine HCl crystal Form 5 (stored at 30°C & 85% RH for 8 weeks) at a temperature range of 25-219°C

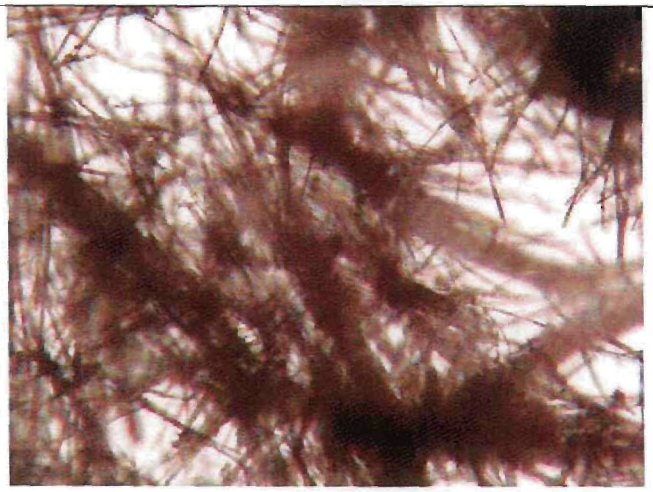
Temperature (°C)	Photomicrograph	Remarks
25		Form 5 at room temperature.

Table 6.12 continued...

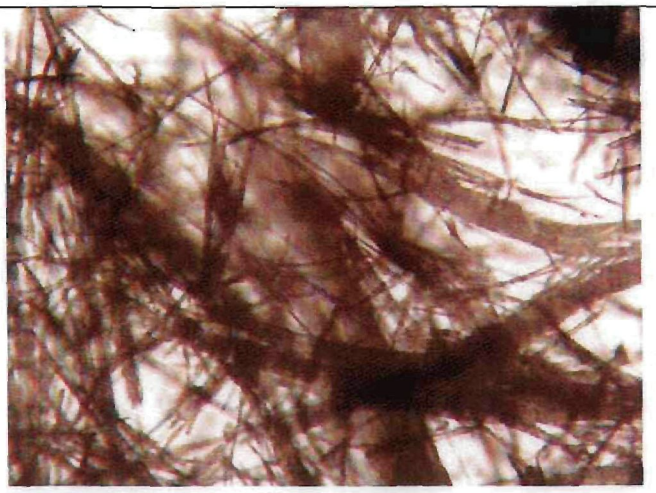
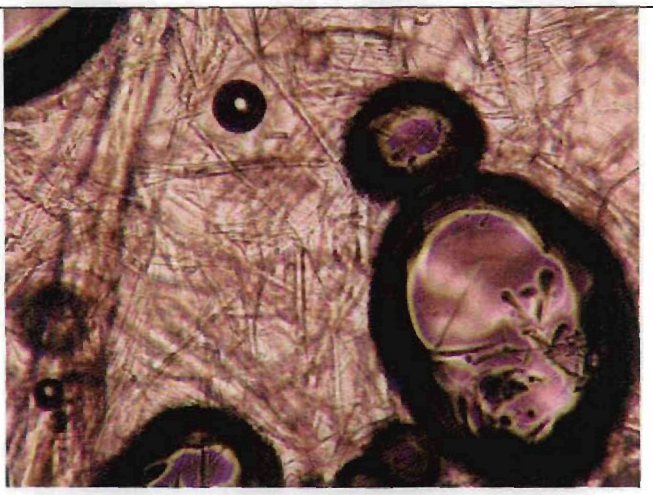
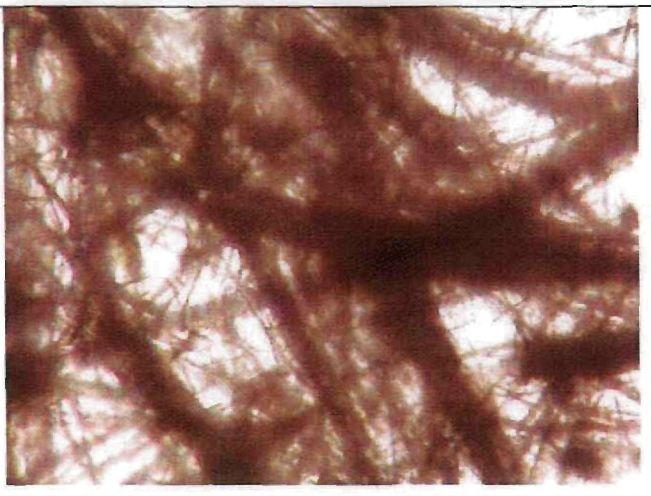
78		Crystals revealed moderate movements associated with the rearrangement of the crystals.
100		Evolution of bubbles when the sample was emerged in silicon oil, indicated the dehydration of the sample.
185		Intergrowth crystals which formed.

Table 6.12 continued...

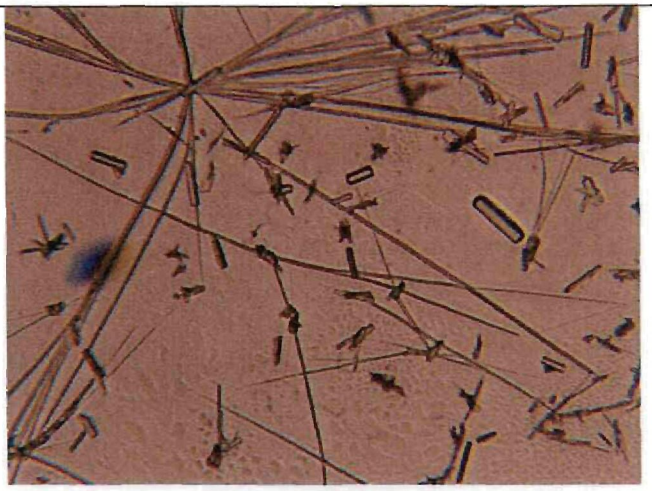
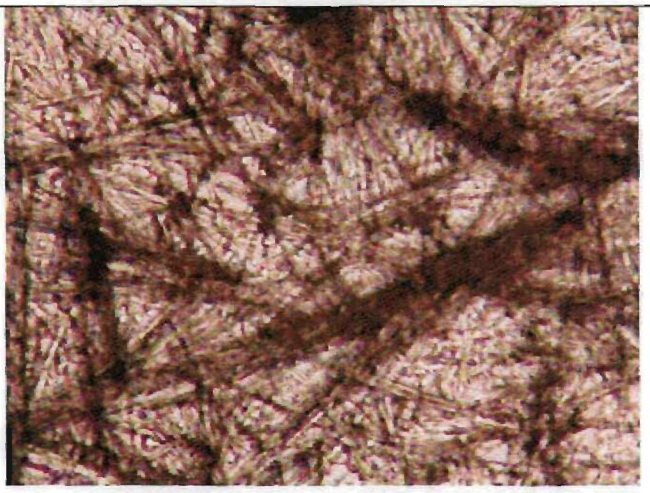
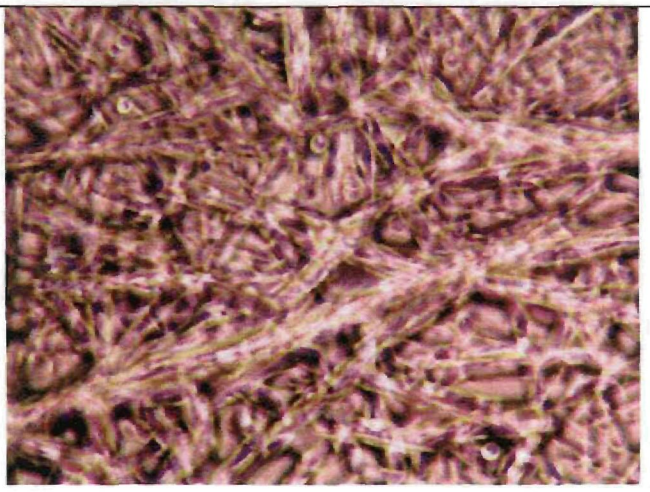
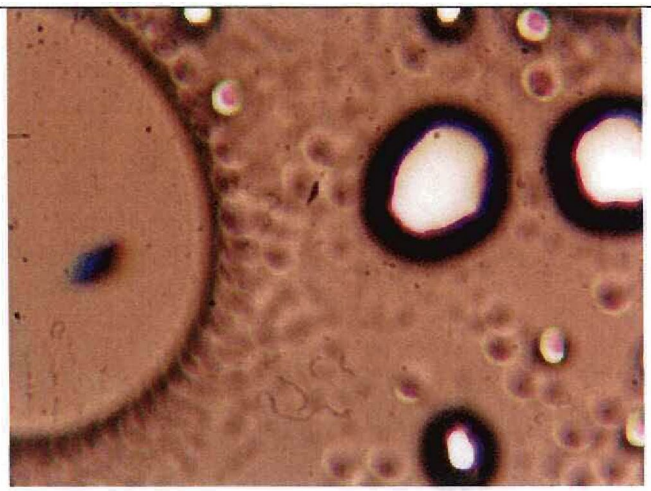
188		View of the intergrowth crystals at an increased focus.
211		Melting of the intergrowth crystals was observed between 206-211°C.
215		Melting of the dehydrated Form 5 crystals started at 215°C.

Table 6.12 continued...

217-219		Melting of Form 5 was completed at 219°C.

When the 21-56 days samples were stored at ambient conditions (allowing surface moisture to evaporate) and recording the DSC thermograms using pierced-lid aluminium sample pans (allowing the evaporation of the dehydrated moisture from the sample environment) a DSC thermogram was produced similar to that of the 9 & 14 days sample (figure 6.26). Allowing the vaporised moisture to escape from the sample pan prevented the pressure cooker effect, as observed in figure 6.26.

The TM observations were not influenced by the accumulation of the vaporised moisture, due to the fact that the cover slip allowed the dehydrated / vaporised moisture to escape.

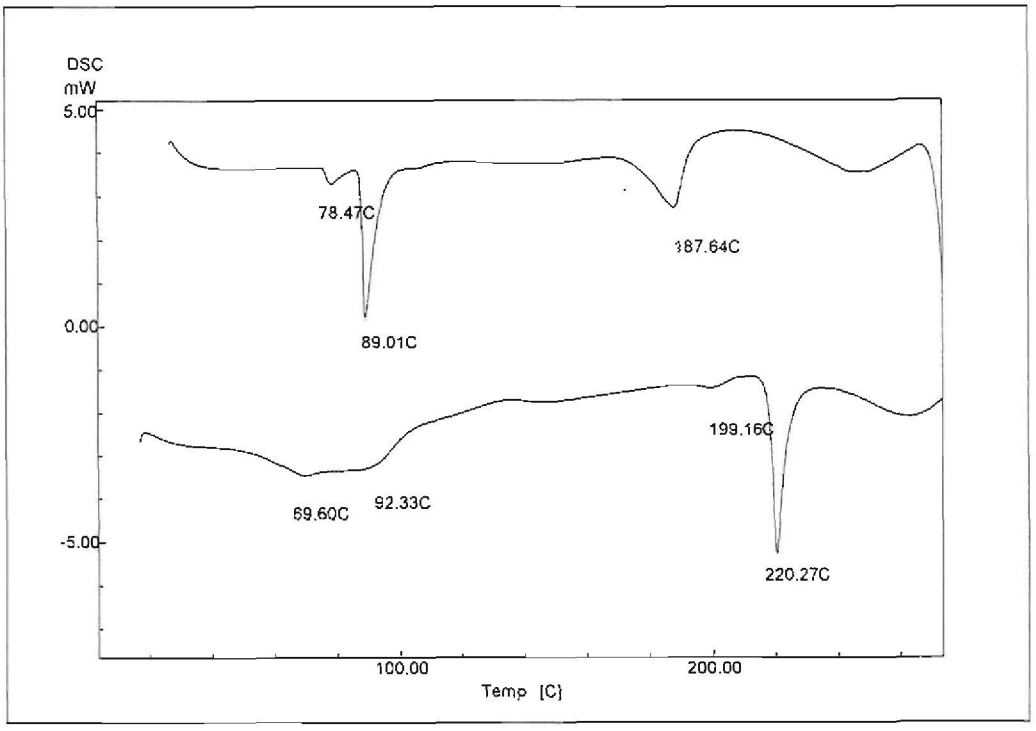


Figure 6.26 Overlay of the DSC thermograms of the hydrated Form 5 in a sealed sample pan (top), and the hydrated Form 5 in a pierced-lid sample pan (bottom).

6.2.5.5 Morphological behaviour of the venlafaxine hydrochloride polymorphs when exposed to increased relative humidities

As mentioned in chapter 5 (section 5.2.2.1) the SEM photomicrographs of the prepared venlafaxine hydrochloride Form 1 and Form 5 revealed columnar (i.e. rodlike particles, having a width and thickness exceeding that of needle-type particles) and avicular (i.e. needlelike) crystal structures respectively.

SEM photomicrographs of Form 1 and Form 5 samples exposed to the various relative humidities (30°C – 0, 65, 75 & 85% RH) were taken after the 56 day period and are displayed in figure 6.27 and 6.28 respectively.

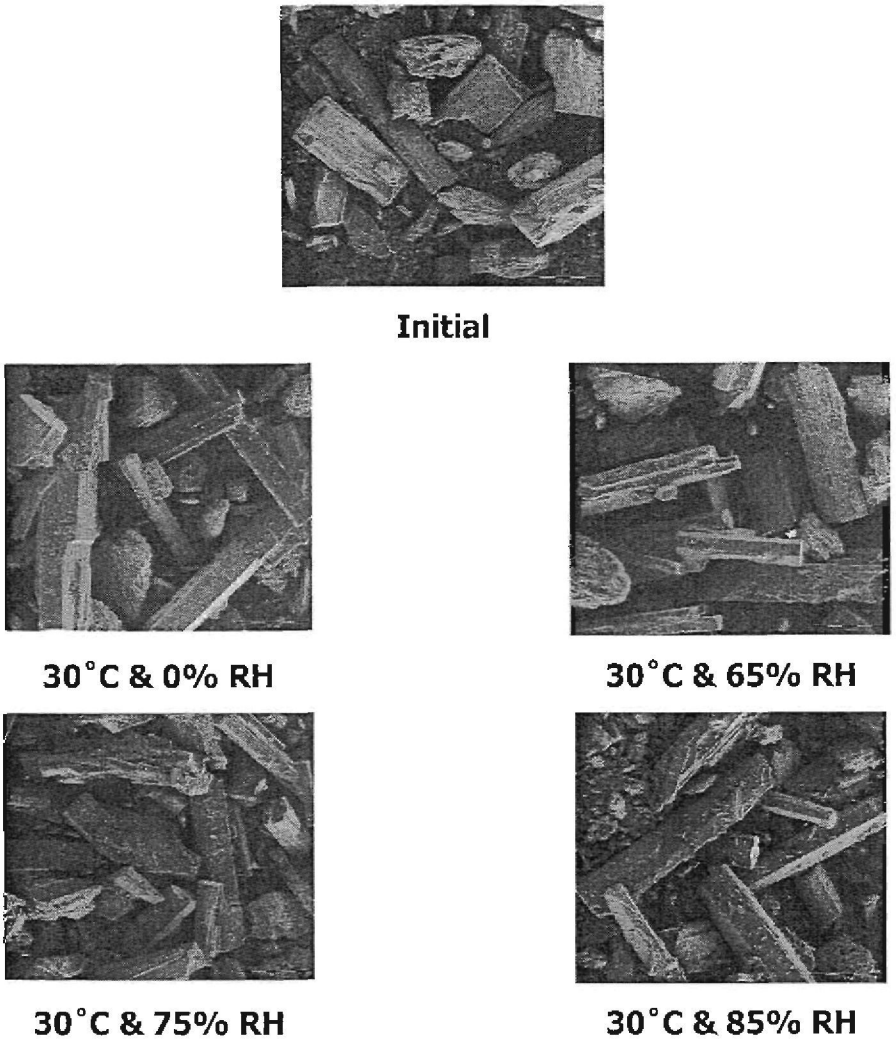
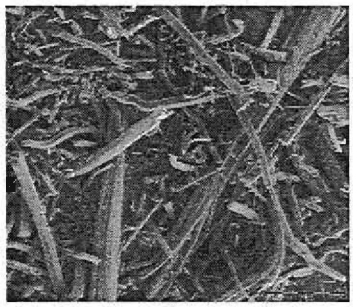


Figure 6.27 SEM photomicrographs of Form 1 exposed to various relative humidities at 30°C after day 56.

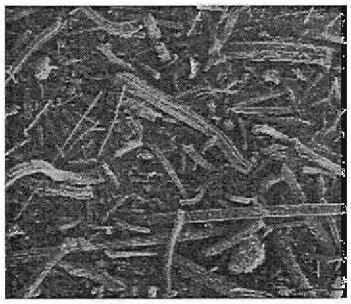
As depicted in figure 6.27, no morphological changes occurred which supported the XRPD, DRIFT-IR and DSC observations that venlafaxine HCl Form 1 did not reveal any polymorphic conversion during this study.



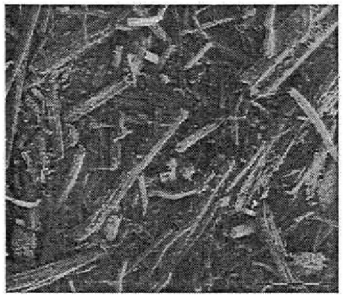
Initial



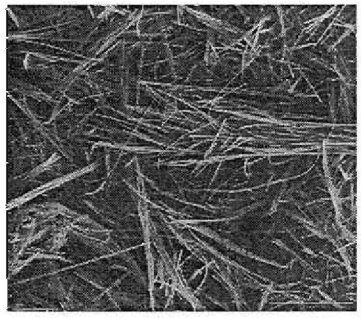
30°C & 0% RH



30°C & 65% RH



30°C & 75% RH



30°C & 85% RH

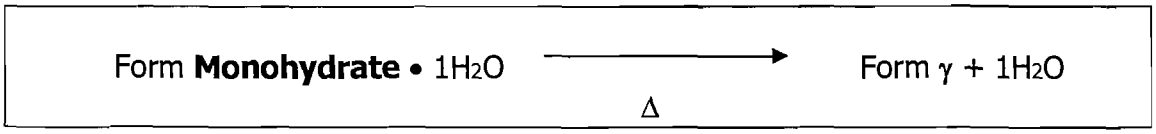
Figure 6.28 SEM photomicrographs of Form 5 exposed to various relative humidities at 30°C after day 56.

Figure 6.28, illustrates that no significant morphological changes occurred in the venlafaxine HCl Form 5 samples exposed to 30°C – 0, 65 & 75% RH for 56 days. However the samples exposed to 85% RH revealed a significant change. The avicular (i.e. needle-like) crystal structure of Form 5 transformed into a fibrous (i.e. needle-like particles which are very thin) structure, thus the polymorphic conversion (anhydrous form → monohydrated form) was accompanied by a

morphological change to accommodate the absorbed water molecules in the hydrated Form 5.

6.2.5.6 Dehydration of the hydrated venlafaxine hydrochloride Form 5

Brits (2003:175) discussed the thermally induced transformation (dehydration) of a monohydrate into an anhydrous form, Form γ:



The influence of an increase in temperature on the stability of the hydrated Form 5 was investigated, using VT-XRPD, thermal analysis (DSC, TGA) and DRIFT-IR spectroscopy.

The VT-XRPD pattern of the hydrated venlafaxine HCl Form 5 was recorded at 25–175°C, using an environmental chamber, with a low temperature camera being attached to the X-ray diffractometer. With an increase in the temperature of the sample, several changes were observed in the VTXRPD pattern (figure 6.29).

The VTXRPD pattern seemed to remain stable in the temperature range of 25°C to 50°C. A slight peak shift occurred, possibly as a result of slight differences in sample height caused by the dehydration process. An increase in the temperature above 50°C led to the appearance of a peak at 4.3°2θ and an increase in the relative intensity of the 11.4°2θ peak.

The XRPD pattern at 75°C resembled a mixture of the hydrated and anhydrous form (Form γ). The XRPD pattern obtained at 100°C resembled that of Form γ observed and described by Brits (2003:175).

The XRPD pattern at 150°C revealed diffraction peaks at the main peak positions characteristic to Form 1, suggesting that Form γ converted to the thermodynamically stable Form 1. The peaks in the 22-35°2θ region were not

clearly visible. Due to the prolonged exposure to the increased temperatures the crystal lattice was weakened causing the weak diffraction peaks in the 22-35°2θ region and the sample to melt at 175°C.

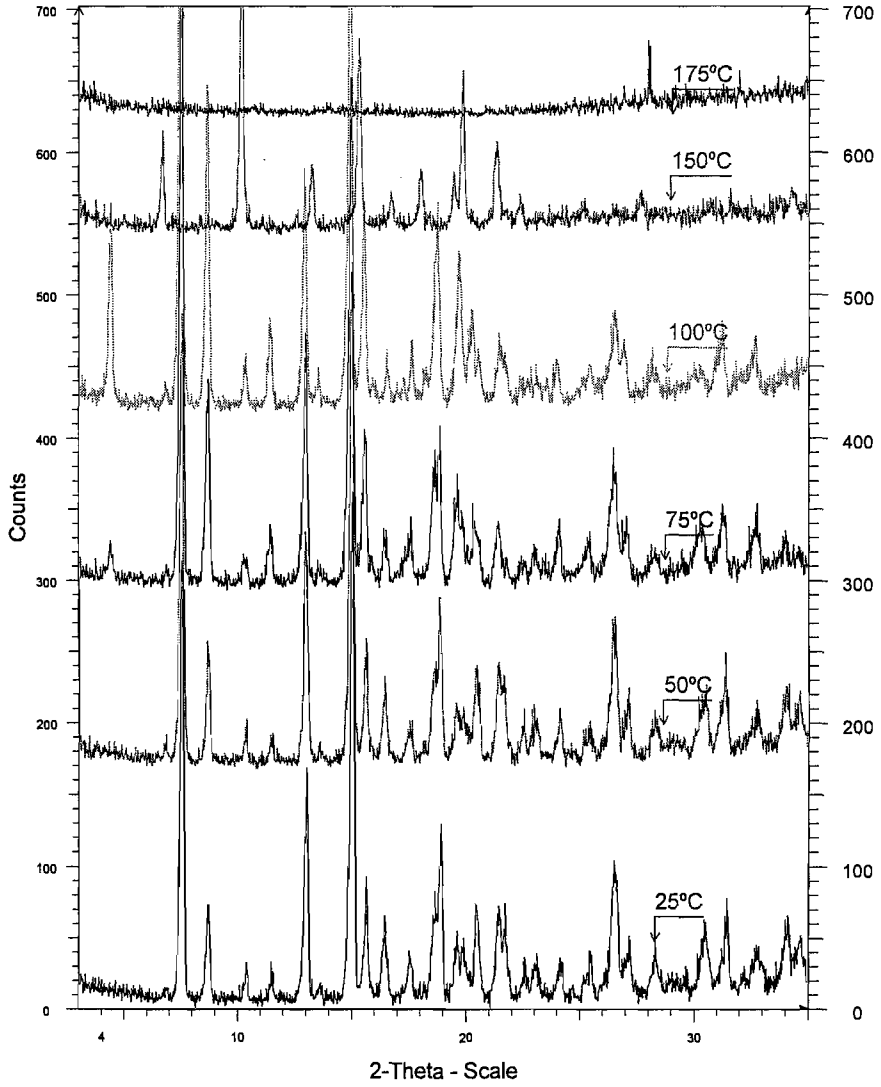


Figure 6.29 VT-XRPD patterns of the hydrated venlafaxine HCl crystal Form 5 at various temperatures (25–175°C).

6.3 Hydration kinetics of Form 5

Several models have been developed to account for the dehydration kinetics of crystalline hydrates. All of these methods assume a certain geometry and rely on some consistency of the system as the process proceeds. Table 6.13

provides a summary of the kinetic equations used for the most common solid state decomposition mechanisms.

The process of the hydration of Form 5 (stored at 30°C & 85% RH) was studied using XRPD. Rastogi *et al.* (1999:623-632) investigated the inter-conversions of AG337, an antitumor agent, using ambient and variable temperature X-ray powder diffractometry (VTXRPD).

Rastogi *et al.* (2001:267) published an article on the dehydration kinetics of aspertame hemihydrate. In this study they revealed that XRPD was successfully used to simultaneously quantify the disappearance of aspartame hemihydrate (ASH) and the appearance of aspartame anhydrate (ASA), using VTXRPD.

Rastogi *et al.* (2001:267) stated that many solid state reactions can be described by the general relation, $f(\alpha) = kt$, where α (or x - in the equations in table 6.13) is the mole fraction of solid that has reacted at time t, and k is the rate constant.

Table 6.13 Kinetic equations used for the most common solid state decomposition mechanisms (Agbada *et al.*, 1994:33-40)

Rate controlling process and equation describing the process	Rate controlling process and equation describing the process
1. Prout Tompkins equation $\ln\left(\frac{x}{1-x}\right) = kt + c$	7. Two-dimensional diffusion equation $(1-x) \bullet \ln(1-x) + x = kt$
2. Avrami Efofe'ev equations $[-\ln(1-x)]^n = kt$ n = ¼ n = 1/3 n = 1/2 n = 2/3 n = 1	8. Three-dimensional diffusion equation $1-\frac{2}{3}x-(1-x)^{\frac{2}{3}} = kt$
3 One-dimensional advancement of a phase boundary equation $1-x = kt$	9. Power law equation $x^n = kt$ n = ¼ n = 1/3 n = ½ n = 1
4. Two-dimensional advancement of a phase boundary equation $1-(1-x)^{1/2} = kt$	10. Equations based on the concept of the order of the reaction (a) Zero order reaction $1-x = kt$
5. Three-dimensional advancement of a phase boundary equation $1-(1-x)^{1/3} = kt$	(b) First order reaction $\ln(x) = kt$
6. One-dimensional diffusion equation $x^2 = kt$	(c) Second order reaction $\frac{1}{(1-x)} = kt$

In kinetic studies the α (or x) values are plotted against time t. The results of these plots are then fitted to several kinetic equations (table 6.13). The values of $f(\alpha)$ are plotted against t for the kinetic equations and the best fitting straight line is used to calculate of the rate constant (k).

Klug and Alexander (1974:531-566) developed the theoretical basis of quantification of crystalline phases in a mixture. In a two component mixture, the intensity of line I of component 1 (I_{i1}) in the XRPD pattern, is related to its weight fraction x_1, according to the equation:

$$\frac{Ii_1}{(Ii_i)_0} = \frac{X_1\mu_1^*}{X_1(\mu_1^* - \mu_2^*) + \mu_2^*}$$

Where $(I_i)_0$ is the intensity of line I, in a sample containing only component 1, and μ_1^* and μ_2^* are the mass attenuation coefficients of component 1 and 2 respectively. If $\mu_1^* \cong \mu_2^*$ then the above equation approximates to:

$$\frac{Ii_1}{(Ii_1)_0} = x_1$$

XRPD analysis (figure 6.21) revealed that the appearance of a peak at 13.6 °2θ was a characteristic peak which signified the presence of Form 5 and the disappearance thereof indicated the formation of the hydrated Form 5. Figure 6.30 is an illustration of the XRPD patterns (in the range 13.2 – 13.8 °2θ) showing the decrease in the peak intensity as a function of time.

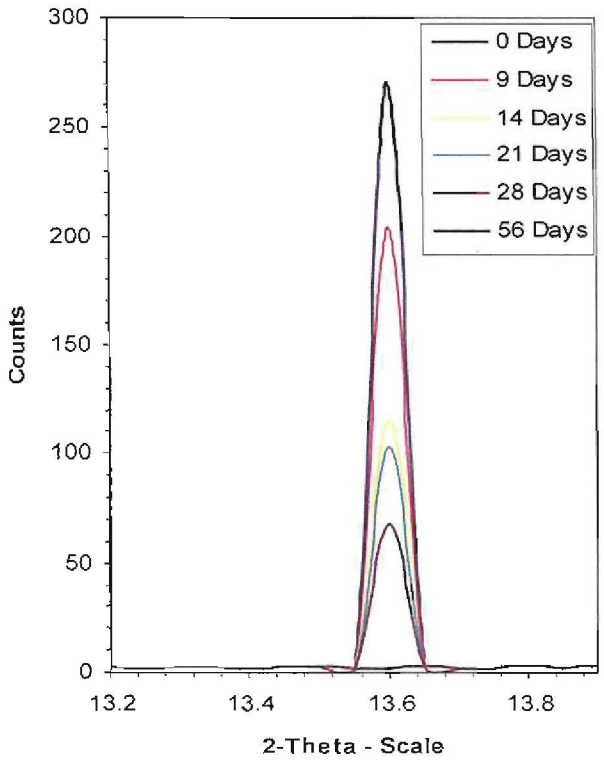


Figure 6.30 XRPD patterns of Form 5 stored at 30°C & 85% RH over a period of 56 days. The decrease in the intensity of the peak at 13.6°2θ was characteristic of the hydration process.

The quantification of the formation of the hydrated Form 5 weight fraction (x_1) as a result of the hydration process, was based on the calculation of the decrease in the characteristic peak (13.6 °2θ) as a function of time (Figure 6.31), as described by the equation developed by Klug and Alexander (1974:5331-556).

Rastogi *et* al., (2001:269) and (2002:1268) revealed that for the purpose of quantitative analysis, the mass attenuation coefficients of hydrated and anhydrated species are compareable, thus it can be assumed that $\mu_1^* \cong \mu_2^*$.

With the disappearance of the peak at 13.6 °2θ (Figure 6.30), the hydration process was completed. The intensity of the characteristic peak (13.6 °2θ) was determined in the pure Form 5 sample, and this intensity was used as the $(I_{i1})_0$

value. The intensity of the peak (I_{i1}) was determined at each time interval. The weight fraction of the hydrated Form 5 for each time interval was calculated using the following equation:

$$\text{Hydrated fraction} = 1 - \frac{I_{i1}}{(I_{i1})_0}$$

Figure 6.31 indicates the calculated weight fraction of the hydrated Form 5 as a function of time

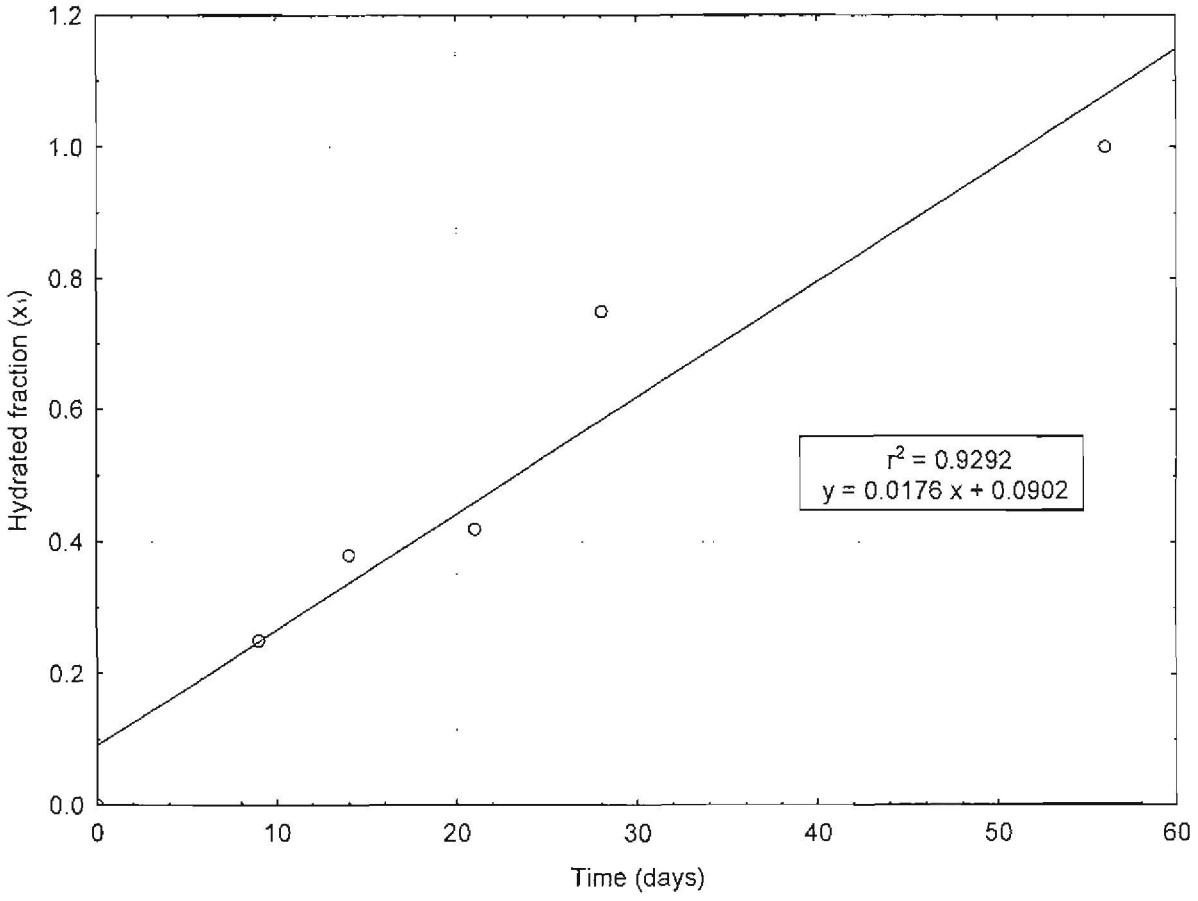


Figure 6.31 Weight fraction of the hydrated Form 5 as a function of time.

The various equations listed in table 6.13, were used to analyse the plots of the weight fraction (x_1) versus the time, in order to classify the hydration process.

The slope, intercept, and correlation coefficient for all the equations were calculated.

The results obtained revealed that the increase in the concentration of the hydrated Form 5 as a function of time, could be considered being a zero order process (r^2=0.9292).

Byrn *et al.* (1999:447) stated that equations that give good fits to data, show a correlation greater than 0.990. The reason for the calculated correlation coefficient (r^2=0.9292) not being greater than 0.990 could be attributed to the preferred orientation effects which Form 5 exhibit, that could have influenced the accuracy of the analysis.

6.4 Summary of results

From the results presented it can be concluded that From 1 did not reveal any polymorphic transition when exposed 30°C – 0, 65, 75 and 85 %RH. Form 5 however demonstrated unpredictable thermal behaviour and polymorphic conversions at the various relative humidities (figure 6.32).

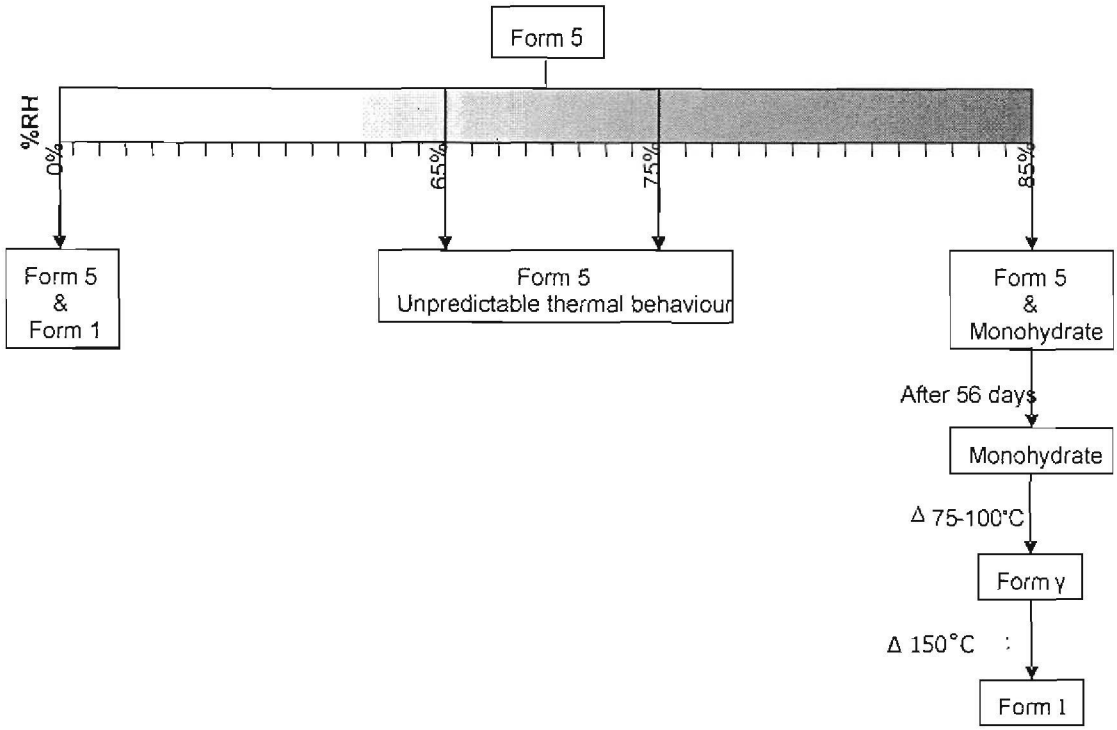


Figure 6.32 Polymorphic conversions observed when Form 5 was stored at 30°C at various relative humidities, and conversions of the monohydrated form at elevated temperatures during a VT-XRPD study.

When Form 5 was stored at 0% RH a fraction thereof converted to the thermodynamic stable Form 1, which supported the enantiotropic behaviour of Form 5 as described in section 5.2.2.5.2.

When Form 5 was stored at 65% RH the inter-crystal rearrangement at 75-100°C became more prominent in the DSC thermograms of the samples. Variation of the position of the thermal rearrangement endotherm in the DSC thermograms could be attributed to the fact that Form 5, when stored at 30°C & 65% RH, revealed a meta-stable phase which was temperature dependant, where the amount of energy needed for the inter-crystal rearrangement (ΔH_{trans}) varied between the samples DSC results. This suggested that the meta-stable phase (possibly induced by the adsorbed water, which acted as molecular loosener) influenced the thermal behaviour significantly causing unpredictable

thermal events which can be classified into three groups. The XRPD and DRIFT-IR spectra of the samples appearing in the three groups did not reveal any significant differences, suggesting that the variable thermal behaviour was caused by differences in the thermodynamic stabilities of the three groups and was not primarily related to a polymorphic conversion.

When Form 5 was stored at 75% RH it adsorbed moisture ranging between 0.71-1.32 % (m/m). The appearance of a diffraction peak in the XRPD pattern at 8.6 - 8.7 °2θ (with low intensities) suggested the possible incorporation of water within the crystal lattice to form a monohydrate. The samples stored at 75% RH also revealed unpredictable thermal behaviour as the samples stored at 65% RH did.

The water absorption and hydration of Form 5 (following zero-order kinetics) was illustrated when it was stored at 85% RH. Significant changes in the XRPD patterns, DRIFT-IR spectra and DSC and TGA spectra indicated the systematic incorporation of water molecules into the crystal lattice after 9 days.

The T_{50} values (figure 6.25 and table 6.11) during the first 9 days were lower compared to the T_{50} values of the samples aged, 14-56 days, and increased to a maximum of 69.04°C indicating the stabilisation of the water molecules into the crystal lattice.

The polymorphic conversion (anhydrous form → monohydrated form) was accompanied by a morphological change to accommodate the absorbed water molecules in the hydrated Form 5.: the avicular (i.e. needle-like) crystal structure of Form 5 transformed into a fibrous (i.e. needle-like particles which are very thin) structure.

VT-XRPD studies revealed that the dehydrated product of the hydrated was Form γ, which converted to Form 1 when heated to 150°C.

Conclusion

This chapter revealed that the moisture sorption and thermodynamic properties of the two venlafaxine HCl polymorphic forms (i.e. Form 1 and Form 5) studied, differed significantly.

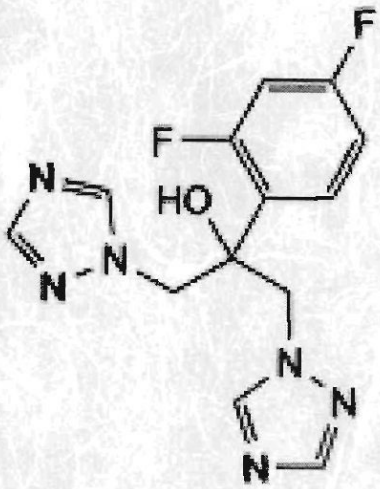
Moisture adsorbed on the surface of the thermodynamic stable form, Form 1, without any polymorphic conversions during 56 days. The metastable form, Form 5, revealed a specific surface area that was 1.84 times greater compared to that of Form 1, which suggested that Form 5 will sorb a greater amount of moisture due to the presence of more acceptor sites on the surface of Form 5.

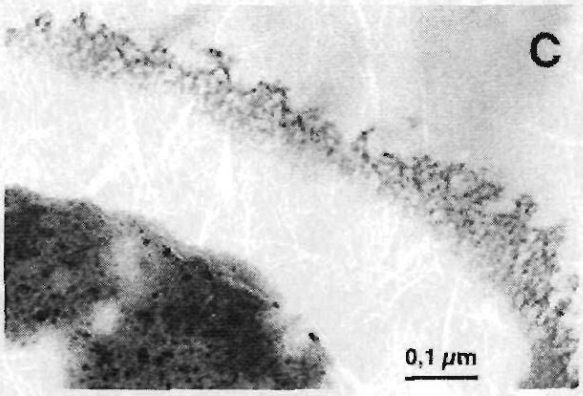
To conclude: venlafaxine HCl, Form 1 adsorbed low levels of moisture (not more than 0.65% m/m) and did not reveal any polymorphic conversions when exposed to increased relative humidities. The instability of Form 5 was soundly demonstrated by the unpredictable thermal behaviour (at 65% and 75% RH) and polymorphic conversions (at 85% RH) observed at the various relative humidities. It is therefore recommended that Form 1 should be used for pharmaceutical manufacturing, due to its thermodynamically stable profile and permanence when exposed to increased relative humidities.



PART 3
Fluconazole







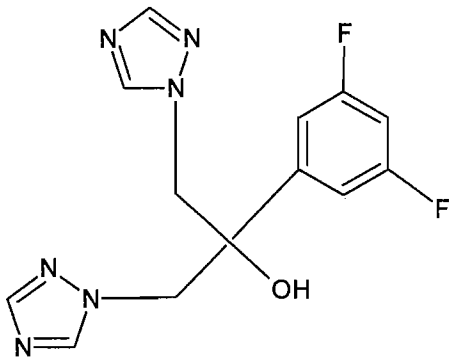
Transmission electron micrographs of ultrathin sections of *Candida albicans* fixed with DMSO:
A: An image of a 25°C-grown cell revealing intracellular organelles;
B: Brush-like fibrillar structure on the outermost surface of a C. albicans cell grown at 37°C.
Note the interconnections of the long fibrils between two cells (arrow);
C: A cell grown at 37°C showing distinct, long individual fibrils
Photographs obtained from: MA Jabra-Rizk, WA Falkler, JrWG Merz, JI Kelley, AAMA Baqui, TF Meiller. Candida dubliniensis and Candida albicans display surface variations consistent with observed intergeneric coaggregation.
Rev Iberoam Micol 1999; 16: 187-193.

CHAPTER 7

Fluconazole

Introduction

Fluconazole is a water-soluble triazole antifungal agent (an imidazole derivative) that has shown activity against several organisms (Dollerey, 1999:f63).



Therapeutic indications of fluconazole include the following: superficial candidal infections such as oral or vaginal thrush, esophagitis caused by *Candida* or other susceptible species, maintenance therapy for cryptococcal meningitis, cryptococcal meningitis, dissenubared candidiasis, prophylaxis for fungal infection in neutropenic cancer patients, acute treatment of systemic fungal infections such as coccidiodomycoses and histoplasmosis in selected cases, dermatophyte and *Candida* skin infections and fungal urinary tract infections (Dollerey, 1999:f63). Fluconazole plays an important role in the treatment regimen for oral and esophageal candidiasis in patients with AIDS (Dollerey, 1999:f66).

The complexity of polymorphic interconversions due to moisture sorption has been demonstrated in sections 1.3.6.2-1.3.6.3. In this last part of the study

(chapter 7 and chapter 8), the focus will be on the polymorphic stability of the slightly water soluble API, fluconazole. The aim of this chapter is to provide an overview of the polymorphic behaviour of fluconazole and to describe the physico-chemical properties of the crystal forms investigated in this study.

7.1 Literature overview of fluconazole

The systemic administration of fluconazole causes the inhibition of sterol 14-α-demethylase (the microsomal cytochrome P450-dependant enzyme system), thus impairing the biosynthesis of ergosterol for the cytoplasmic membrane and leading to the accumulation of 14-α-methylsterols. The methylsterols disrupt the close packing of acyl chains of phospholipids, thus impairing the functions of membrane-bound enzyme systems such as ATPase and certain enzymes involved in the electron transport system, thus inhibiting fungi-growth (Bennet, 1996:1180).

The exceptional antifungal activity of fluconazole in the early 1980's enthused various scientists to investigate the solid-state and chemical properties of this promising antifungal. Han *et al.*, (1993:263) studied the structural conformation of fluconazole by means of conformational free energy calculations using an empirical potential function and hydration shell model. The mentioned authors suggested the most feasible conformations i.e. lowest free energy conformations of fluconazole in the hydrated and unhydrated states (figure 7.1).

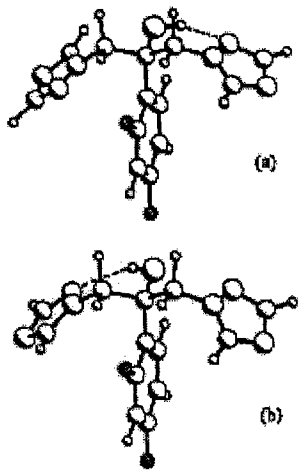


Figure 7.1 The lowest free energy conformations of fluconazole in the unhydrated (a) and hydrated (b) states. The F atoms are indicated by shading and hydrogen bonds are represented by dotted lines (Han *et al.*, 1993:265).

Han *et al.* (1993:263) indicated that in the lowest free energy conformation (b) in the hydrated state, a weak intramolecular hydrogen bond exists between N3 and H8 with a distance 2.26 Å similar to that of H8 of the isopropyl hydroxyl group and N17 of the triazole ring with the distance 2.27 Å. It was also stated that the overall conformation of fluconazole in the hydrated and unhydrated state is governed by the weak intramolecular hydrogen bonds, but that the structural flexibility plays a greater role in the stabilizing of the molecule.

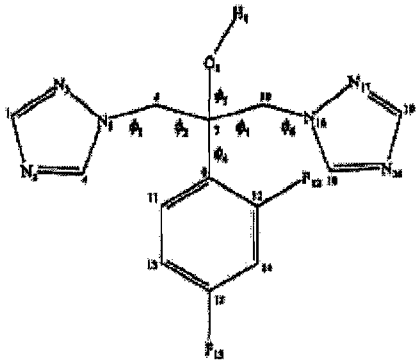


Figure 7.2 Chemical structure and torsion angles of fluconazole (Han *et al.*, 1993:265).

The inclination of fluconazole towards polymorphism was identified by Gu & Jaing (1995:1438) in the early 1990's when they observed differences in the FT-Raman spectra, DSC thermal behaviour and XRPD patterns of two fluconazole samples (Sample A & Sample B) obtained form two different suppliers.

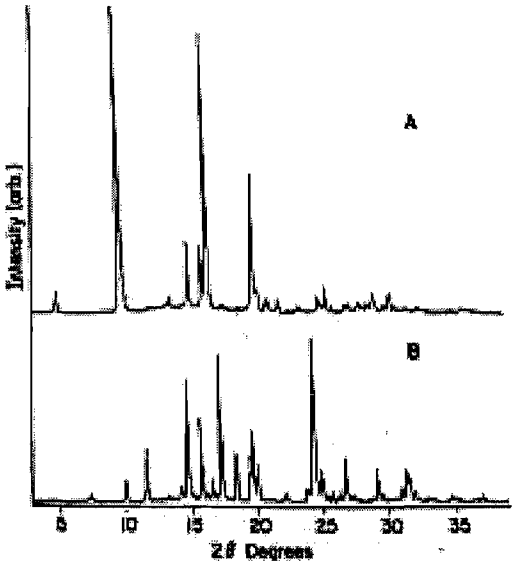
Gu & Jaing (1995:1438) identified and classified the two forms as: Form I and Form II. Table 7.1 indicates the differences in the main vibrational modes observed in the FT-raman spectra of the two fluconazole samples.

Table 7.1 Main vibrational modes observed in the FT-raman spectra of the two fluconazole samples Gu & Jaing (1995:1438)

Wavenumber (cm^{-1})		
Sample A	**Sample B**	**Assignment**
Triazole Group		
3129s	3129s	CH Stretch
1368s	1368s	Ring Stretch
1253s	1257s	Ring Stretch
1135s	1136s	Ring Breath
965m	9660	Ring Bend
2,4-Difluorobenzyl Group		
3089s	3097s	CH Stretch
3015s	3022s	CH Stretch
16160	1618m	C=C Stretch
1273s	1279s	CF Stretch
1075s	1076s	CH Deform
734vs	737vs	Ring Breath
5870	585m	Ring Deform
Propane Backbone		
2975s	2968s	CH_2-Strecth
2963s	-	-
1464m	1451m	CH_2-Sissor
1453m	-	-
1353m	1355m	CH Bend
1117s	1106m	C-C Stretch
1026m	1018s	C-(OH) Stretch

Gu & Jaing (1995:1438) found that the DSC thermogram for Sample A had one endothermic peak at 139.7°C and Sample B had a main endothermic peak at 138.9°C followed by a secondary endotherm at 139.7°C, suggesting that Sample A was the pure Form I and Sample B consisted of a mixture of Form I and Form

II. Gu & Jaing (1995:1438) also suggested that it was also possible that a small amount of Form II transformed into Form I during the heating process of Sample B. The crystallographic properties (XRPD) of Form I and the Form I and II mixture as published by Gu & Jaing (1995:1438) are summarised and illustrated in Figure 7.3.



X-ray diffraction patterns of fluconazole: Sample A & Sample B

Main diffraction peak positions (°2θ) for Sample A & Sample B

Sample A	Sample B
10.0	11.6
15.0	14.7
16.0	15.8
16.6	17.3
20.0	18.4
-	19.5
-	24.4

Figure 7.3 X-ray powder diffraction pattern and peak list of sample A (Form I) and sample B (Form I & Form II mixture) - Gu & Jaing (1995:1438).

In 2002, Kreidl *et al.* (2002:1) submitted an intellectual property patent claim. In their claim, the inventors claimed the inventions relating to the process for the preparation of fluconazole and the preparation of the two crystal modifications (I & II).

The inventors (Kreidl *et al.*, 2002:2-3) mentioned two critical aspects to consider during the preparation process of Forms I & II, i.e. cooling temperature and drying temperature of the hydrated forms:

Cooling temperature – It was found that if the solution of the anhydrous or fluconazole monohydrate (dissolved in a C1-C4 straight or branched chain alcohol at boiling temperature) was slowly cooled (5-15 °C/hour), Form II crystals were prepared. If the solution was cooled fast (35-65 °C/hour), Form I crystals precipitated.

Drying temperature – Drying of the fluconazole monohydrate after seeding with crystals of Form II (preferably in vacuum between 30-70°C) produced Form II crystals. Fast drying at 80°C of the monohydrate produced crystals with a modification similar to Form I.

Dash & Elmquist (2001:77) reported the existence of three polymorphic forms of fluconazole and a monohydrate. The anhydrous forms have been named: Form I, II & III. The x-ray powder diffractograms are displayed in figure 7.4.

The melting ranges for the three polymorphs were reported by Dash & Elmquist (2001: 77) – see table 7.2.

Table 7.2 Melting ranges for Form I, II & III as reported by Dash & Elmquist (2001: 77)

Form	Melting range (°C)
I	135-136
II	138-140
III	137-138

During 2002 Alkhamis *et al.* (2002:491) isolated and classified two new polymorphs and three solvates of fluconazole. The x-ray powder diffraction patterns for the five solid modifications exhibited substantial differences in the position and intensities of the peaks (figure 7.5). The DSC thermogram of anhydrate Form I showed a single melting point at 139.2°C. Anhydrate Form II showed two endothermic peaks at 136.5 and 139.2°C and one exothermic peak in between. The ¼ acetone solvate exhibited a desolvation endotherm at 75.5°C and a melting endotherm at 139.2°C. The 1/7 benzene solvate displayed two endothermic peaks at 131.5 and 138.8°C. The monohydrate displayed a dehydration endotherm at 102.7°C and a melting peak at 139.2°C (figure 7.6).

The XRPD pattern and melting behaviour of Form II prepared by Alkhamis *et al.* (2002:491) differed from the anhydrous Form II prepared by Gu & Jaing (1995:1438), however the physico-chemical properties of Form I was similar to those mentioned by Gu & Jaing (1995:1438) for Form I.

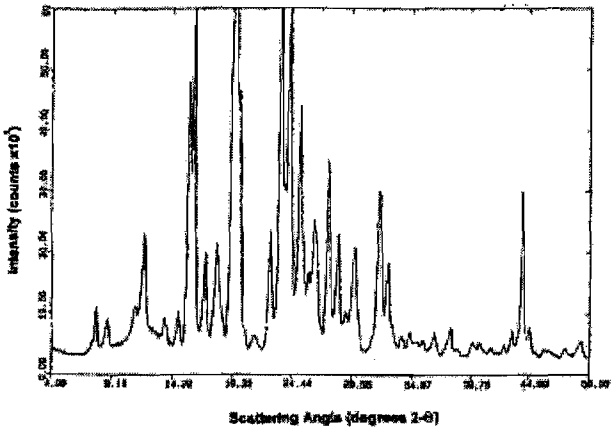
The solubilities of the different modifications (in water) were reported as: amorphous > acetone ¼ solvate > anhydrate Form II > anhydrate Form I > benzene 1/7 solvate > monohydrate (table 7.3)

Table 7.3 Solubility data for the characterisation of polymorphic modifications of fluconazole as reported by Alkhamis *et al.* (2002:491) in water

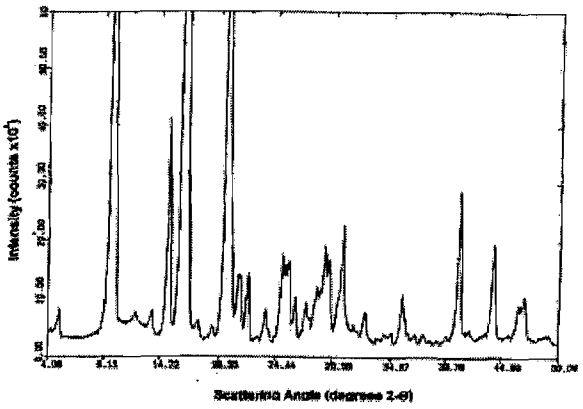
Form	Solubility (mg/ml)	S.D.
Anhydrate Form I	4.29	0.08
Anhydrate Form II	4.60	0.14
Acetone ¼ solvate	5.18	0.11
Benzene 1/7 solvate	3.77	0.06
Monohydrate	3.56	0.08
Amorphous	5.2	0.10

Anhydrous Form II was identified as a meta-stable polymorph which converted to the stable anhydrous Form I at ambient temperature and pressure (Alkhamis *et al.*, 2002:491).

(A)



(B)



(C)

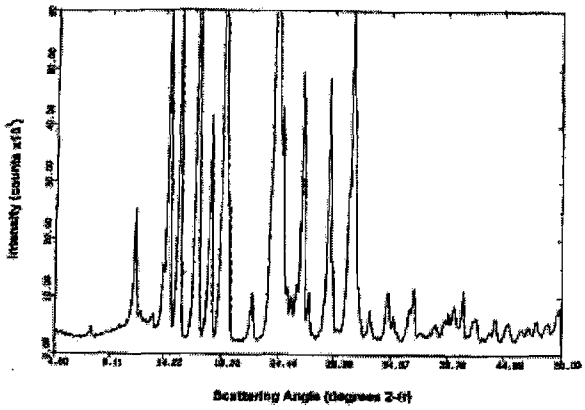


Figure 7.4 XRPD patterns of fluconazole solid modifications: (A) Form I, (B) Form II, (C) Form III – as described by Dash & Elmquist (2001:78).

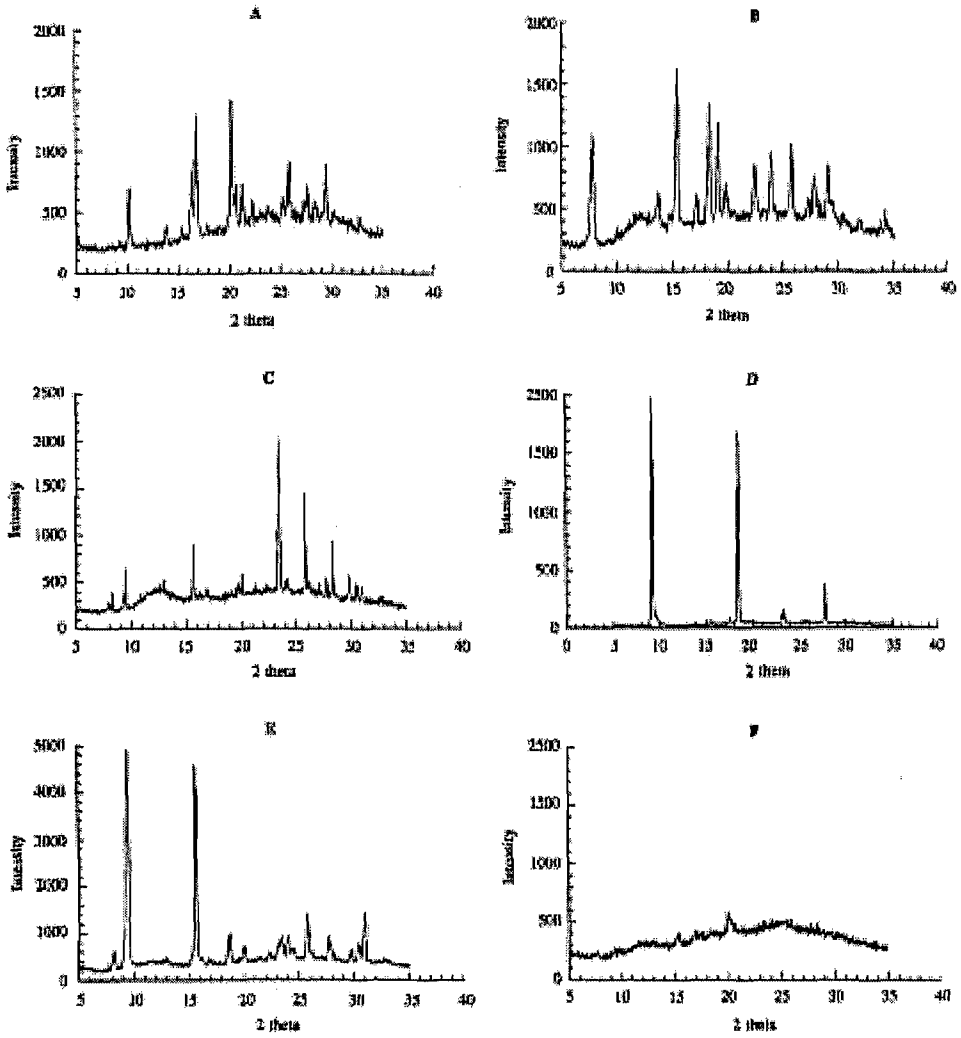


Figure 7.5 XRPD patterns of fluconazole solid modifications: (A) anhydrate Form I, (B) anhydrate Form II, (C) acetone ¼ solvate, (D) benzene 1/7 solvate, (E) monohydrate, and (E) amorphous form (Alkhamis *et al.*, 2002:494).

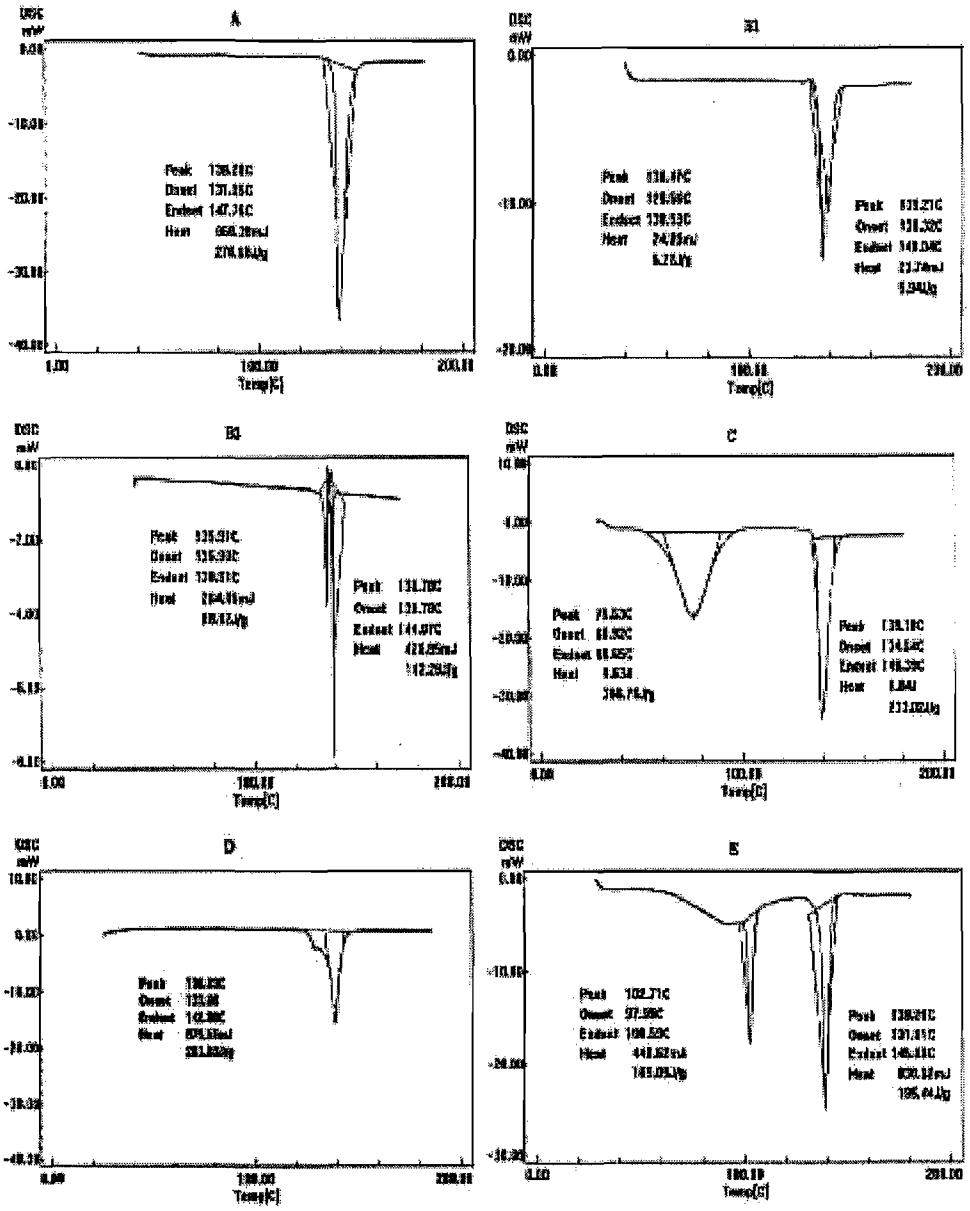


Figure 7.6 DSC thermograms of fluconazole polymorphs and solvates: (A) anhydrate Form I, (B1) anhydrate Form II 10°C/min heating rate, (B2) anhydrate Form II 1°C/min heating rate, (C) acetone ¼ solvate, (D) benzene 1/7 solvate, and (E) monohydrate (Alkhamis *et al.*, 2002:499).

Desai *et al.* (2002:89) performed a thermoanalytical study on the polymorphic transformation of fluconazole Form I. It was found that the melt of Form I

solidified to a glassy mass after heating Form I to 150°C and allowing the melt to solidify (figure 7.7a). The glassy mass was reheated to a maximum temperature of 150°C. The second heating step revealed a small endotherm at 31°C which was attributed to a glass transition. The DSC thermogram revealed a recrystallisation endotherm at 88°C signifying the transformation of the glassy mass into Form II, which transformed to Form I prior to melting (figure 7.7b) (Desai *et al.*, 2002:89).

(A)

(B)

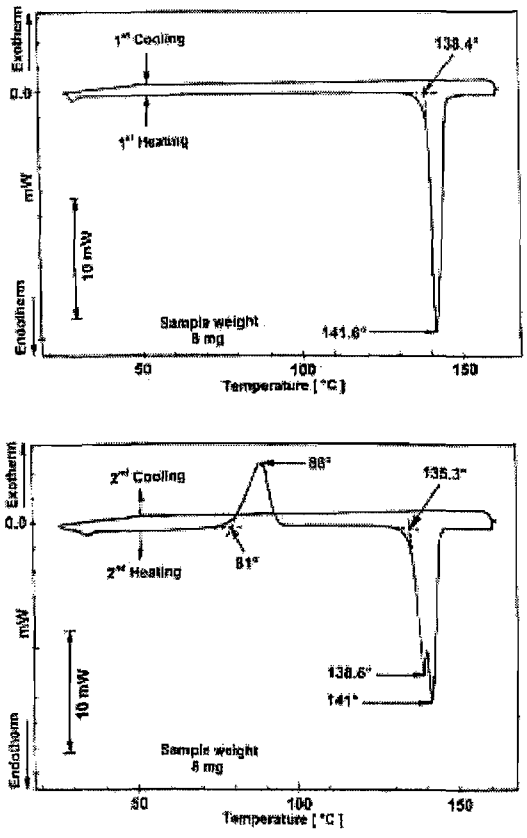


Figure 7.7 (a) DSC thermogram of fluconazole Form I for a heating and cooling sequence at a heating and cooling rate of 5°C/min. **(b)** DSC thermogram for fluconazole sample (a) for a heating and cooling sequence at a heating and cooling rate of 5°C/min (Desai *et al.*, 2002:89).

7.2 Introduction to fluconazole crystal forms investigated in this study: Form I, and monohydrate (Form MH)

The purpose of this section is to provide a general overview of the method of preparation, and supplementary information on the solid state properties and thermodynamic stability of the following fluconazole crystal forms: anhydrous Form I and the monohydrate (Form MH).

7.2.1 Preparation of fluconazole Form I and the monohydrate (Form MH)

Fluconazole Form I

Fluconazole Form I is commercially available and was purchased from Matrix Laboratories Ltd, Batch no: FLP 0170405. A more comprehensive description of the raw material obtained will be discussed in chapter 8 – section 8.1.

The raw material was dried in a vacuum oven at 90°C for 1 hour to ensure that the sample to be used during the moisture studies is free from potential surface moisture / solvent.

Fluconazole monohydrate (Form MH)

The following recrystallisation method (described by Caira *et al.*, 2004:602) was used to prepare fluconazole monohydrate:

Fluconazole was dissolved in HPLC grade water under constant stirring at 40°C to prepare a supersaturated solution. The supersaturated solution was filtered to remove all nuclei, and the filtered solution was cooled in a refrigerator at 5°C.

After 48 hours, the resulting crystals were rapidly surface dried at ambient conditions and slightly ground with a mortar and pestle. The powder was sieved to obtain a 250-106 µm fraction, which was used during the study.

7.2.2 Solid state properties of fluconazole Form I and monohydrate (Form MH)

The solid state properties of the prepared fluconazole forms were investigated using the following set of techniques: XRPD, DRIFT-IR, DSC, KF, VT-XRPD, TM and SEM.

7.2.2.1 X-ray powder diffractometry (XRPD)

The XRPD patterns of the fluconazole crystal forms prepared and used in these studies are shown in figure 7.8. Peak angles (°2θ) and relative intensities (I/Io) of the main XRPD peaks are listed in table 7.4.

Both crystal forms show definite diffraction peaks characteristic of crystalline materials. The single crystal x-ray diffraction properties of the monohydrate (Form MH) have been discussed by Caira *et al.* (2003: 601-611). Figure 7.9 illustrates the computed XRPD pattern and an illustration of the unit-cell packing of Form MH computed from the x-ray crystallographic data obtained from the Cambridge Crystallographic Data Center (CCDC 208862), using Dash® and Mercury® software to prepare the illustrations.

Caira *et al.* (2003: 601-611) illustrated that both the triazolyl rings of each fluconazole molecule in the monohydrate engage in hydrogen bonding (as illustrated in figure 7.9 - a) that gives rise to infinite arrays.

The water molecules are localized in layers corresponding to the 001 crystal planes, occupying isolated sites. Isolated site hydrates represent structures with water molecules isolated from direct contact with other water molecules by intervening drug molecules (Morris, 1999:142). The packing of isolated site hydrates influences the thermodynamic behaviour of the API and will be discussed in section 7.2.2.3.

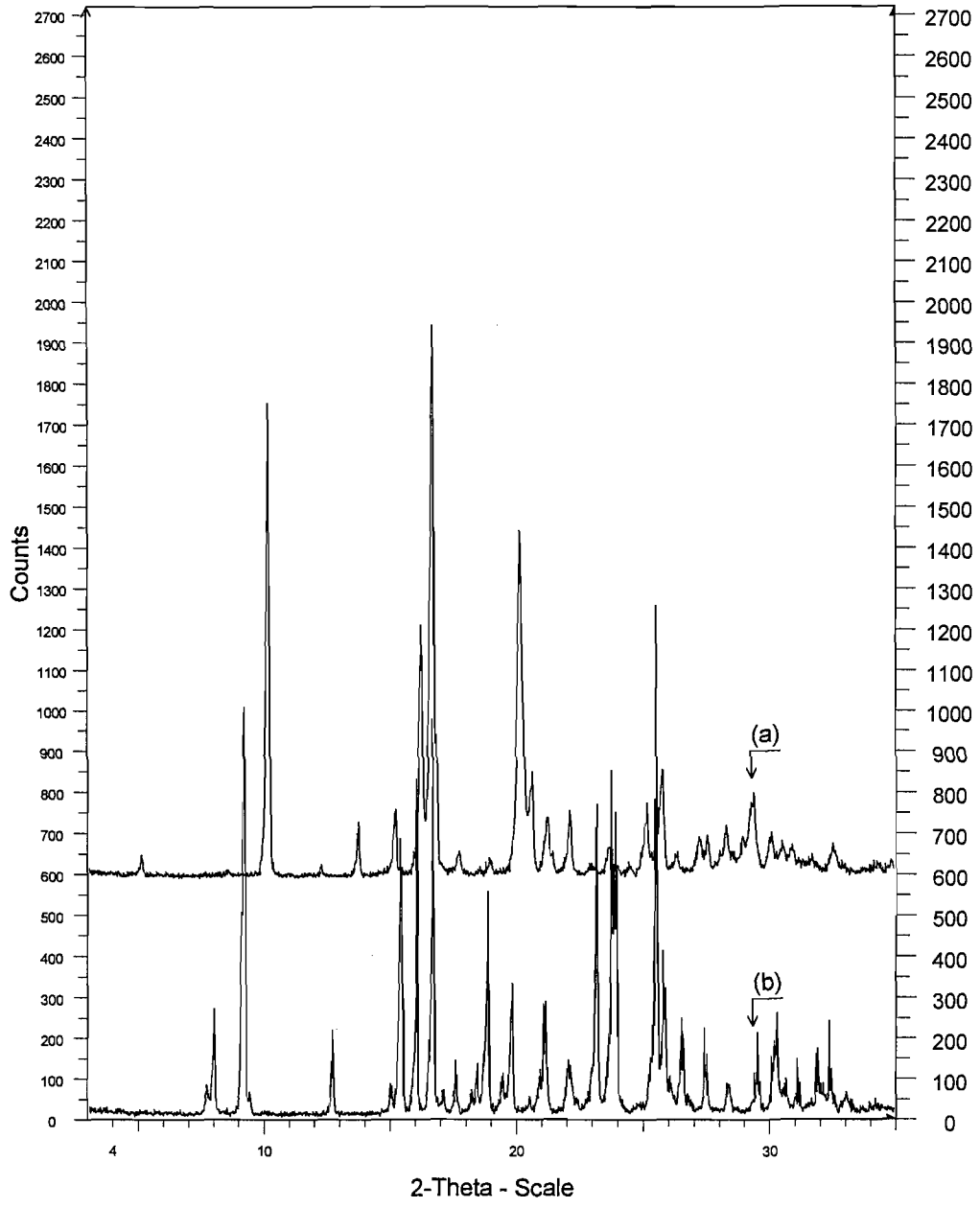
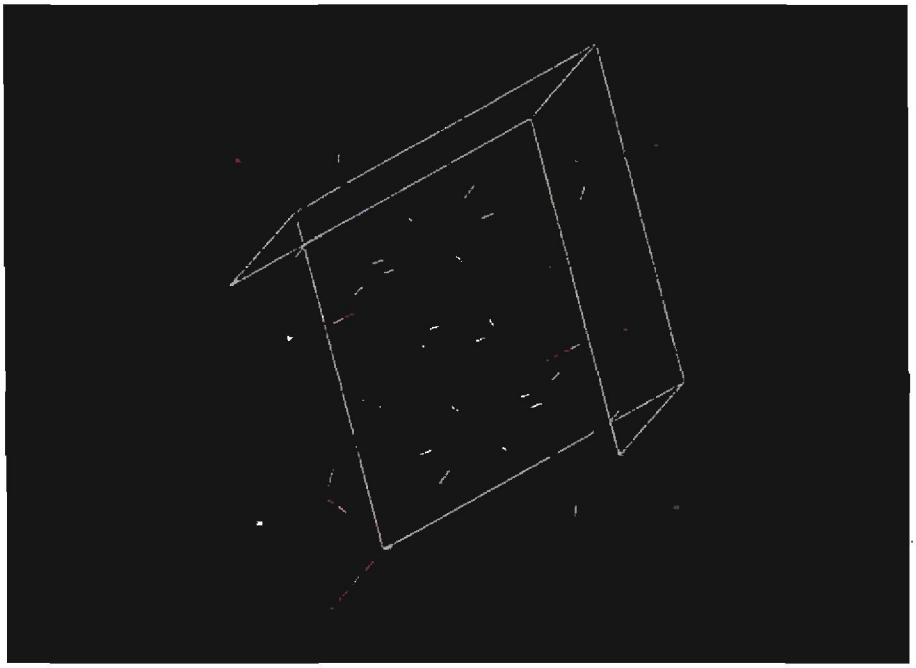


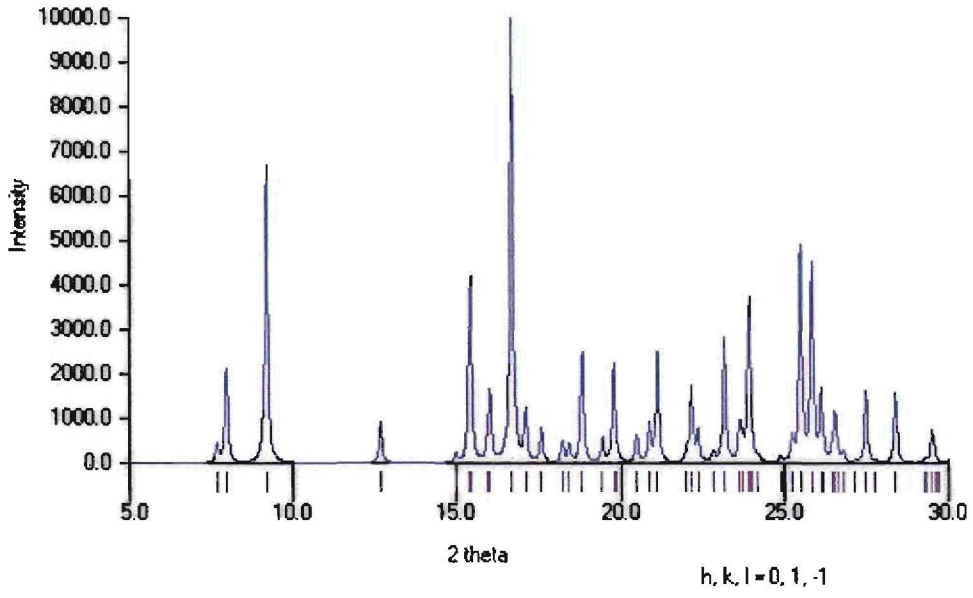
Figure 7.8 Overlay of fluconazole (a) Form I and (b) Form MH XRPD patterns.

Table 7.4 Peak angles (°2θ) and relative intensities (I/Io) of the main XRPD peaks for fluconazole Form I and Form MH

FORM I		Form MH	
Peak angles (°2θ)	**Relative intensities (I/Io)**	**Peak angles (°2θ)**	**Relative intensities (I/Io)**
5.1	4.4	**-**	-
-	-	**7.7**	19.2
-	-	**7.9**	6.1
8.5	1.8	**-**	-
-	-	**9.2**	47.3
10.1	86.0	**-**	-
12.2	2.7	**12.7**	17.2
-	-	**-**	-
13.7	10.4	**15.0**	6.6
15.2	12.6	**15.4**	54.4
-	-	**16.0**	66.0
16.2	46.0	**16.7**	77.6
16.7	100.0	**17.1**	5.3
-	-	**17.6**	11.1
17.7	5.1	**18.2**	5.4
-	-	**18.4**	10.5
18.5	2.4	**18.8**	44.0
19.0	3.6	**19.5**	8.7
-	-	**19.8**	23.2
20.1	63.1	**20.5**	4.1
20.6	19.5	**20.9**	8.0
-	-	**21.1**	21.8
21.2	11.2	**22.1**	11.3
22.1	12.4	**23.2**	61.1
22.9	3.0	**23.9**	49.4
23.7	6.0	**24.8**	2.8
-	-	**-**	-
25.1	13.8	**25.5**	100.0
-	-	**25.8**	25.5
25.7	19.9	**26.5**	19.5
26.3	4.4	**26.8**	3.8
-	-	**-**	-
27.2	7.8	**27.5**	17.6
27.5	8.2	**28.4**	6.6
28.3	9.9	**-**	-
28.9	7.9	**29.6**	16.7
29.4	15.7	**30.3**	20.5
30.1	8.6	**30.7**	7.6
30.9	6.4	**31.1**	11.5
-	-	**31.6**	3.2
31.7	4.6	**31.9**	13.6
-	-	**32.4**	12.6
32.5	6.5	**33.0**	5.0
-	-	**-**	-
34.4	3.2	**-**	-
34.9	3.7	**-**	-



(a)

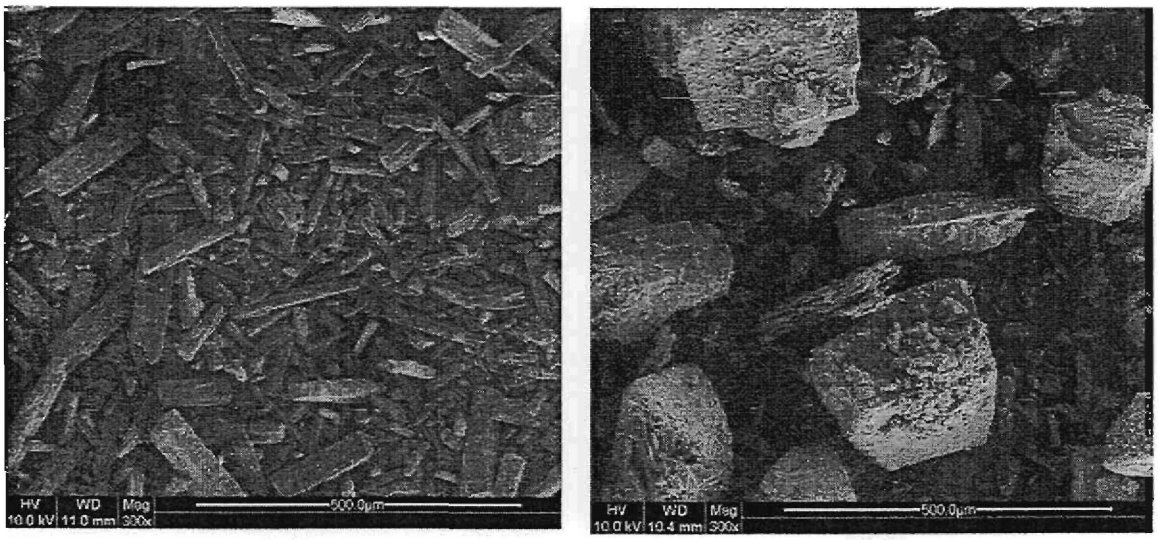


(b)

Figure 7.9 (a) Unit-cell packing of fluconazole monohydrate, illustrating hydrogen bonding properties and (b) calculated XRPD pattern thereof using x-ray crystallographic data obtained from the Cambridge Crystallographic Data Center (CCDC 208862).

The peak angular positions in the experimental XRPD pattern (figure 7.8) is in good agreement with those in the computed XRPD pattern (figure 7.9 – b). The intensity reversals observed for some of the peaks (15.4, 23.2, 23.9 and 25.5°2θ) in the experimental pattern (figure 7.8) indicated that the peak intensities suffered severely from preferred orientation effects.

Figure 7.10 illustrates the SEM photomicrographs of Form I and Form MH. The acicular habit of both forms is clearly visible in the mentioned figure. The preferred orientation could definitely be attributed to the acicular habits as suggested by Caira *et al.* (2004:607). Despite all precautionary steps taken (i.e. particle size reduction, rotation of sample stage at 75 rpm and random packing of the sample holder) the preferred orientation effects were clearly visible.



(a) **(b)**

Figure 7.10 SEM photomicrographs of fluconazole (a) Form I and (b) Form MH.

7.2.2.2 Diffuse reflectance infrared Fourier transform spectroscopy (DRIFT-IR)

The IR spectra of the two fluconazole crystal modifications are shown in figure 7.11. The main IR absorption peaks and their corresponding wavenumbers (cm^{-1}) are listed in table 7.5.

Examination of the IR spectrum of fluconazole crystal Form I showed significant differences when compared to the IR spectrum of fluconazole Form MH.

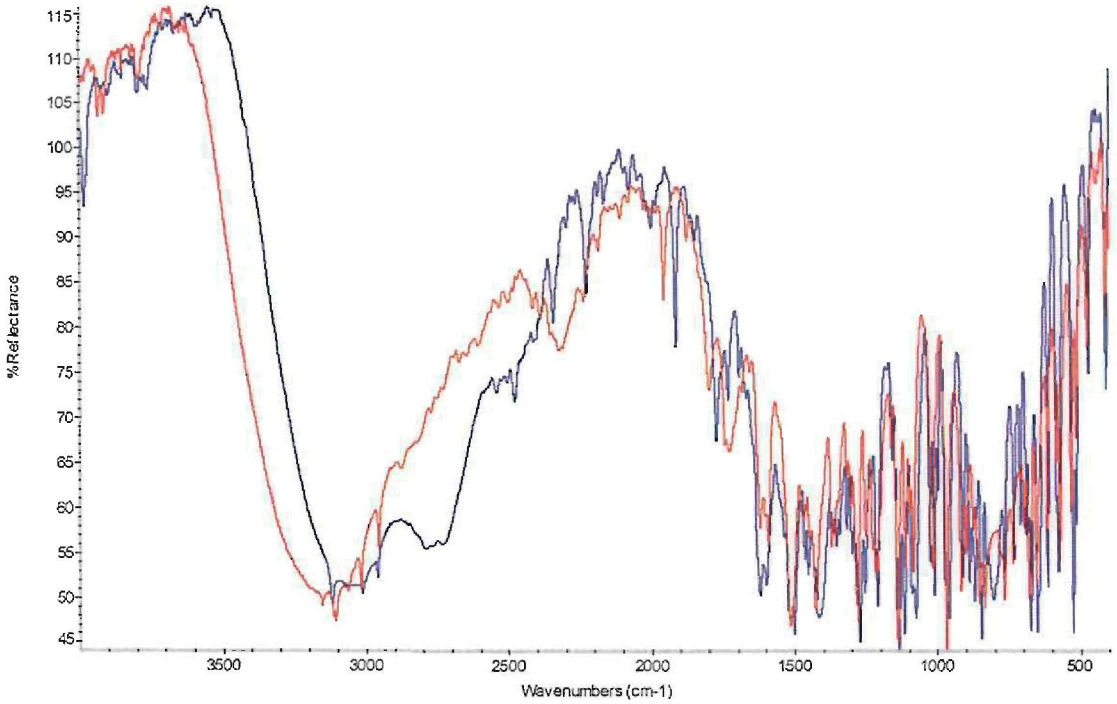


Figure 7.11 IR spectra (superimposed) of fluconazole crystal modifications (Form I [blue] & Form MH [red]).

Table 7.5 Main absorptions in the IR spectra of the crystal modifications of fluconazole: Form I and Form MH

Main absorptions	Wavenumbers (cm^{-1})	
	Form I	Form MH
1	3984	3935
2	3796	3916
3	3121	3795
4	2791	3155
5	2479	3107
6	2343	3019
7	2228	2956
8	2166	2320
9	2080	1957
10	2002	1798
11	1916	1729
12	1850	1619
13	1774	1592
14	1733	1515
15	1695	1425
16	1619	1370
17	1502	1305
18	1463	1276
19	1452	1249
20	1417	1217
21	1353	1163
22	1318	1139
23	1300	1112
24	1271	1083
25	1253	1016
26	1210	968
27	1160	916
28	1137	898
29	1116	853
30	1075	833
31	1026	766
32	1011	735
33	999	697
34	967	680
35	911	654
36	888	617
37	869	587
38	846	571
39	804	532
40	769	514
41	733	478
42	711	447
43	691	413
44	674	404
45	652	-
46	616	-
47	576	-
48	525	-
49	514	-
50	472	-
51	413	-

Both forms (Form I and Form MH) had a characteristic DRIFT-IR spectrum. The IR-spectra indicated that the bands associated the triazole group, 2,4-difluorobenzyl group and the propane backbone were sensitive to the structural differences.

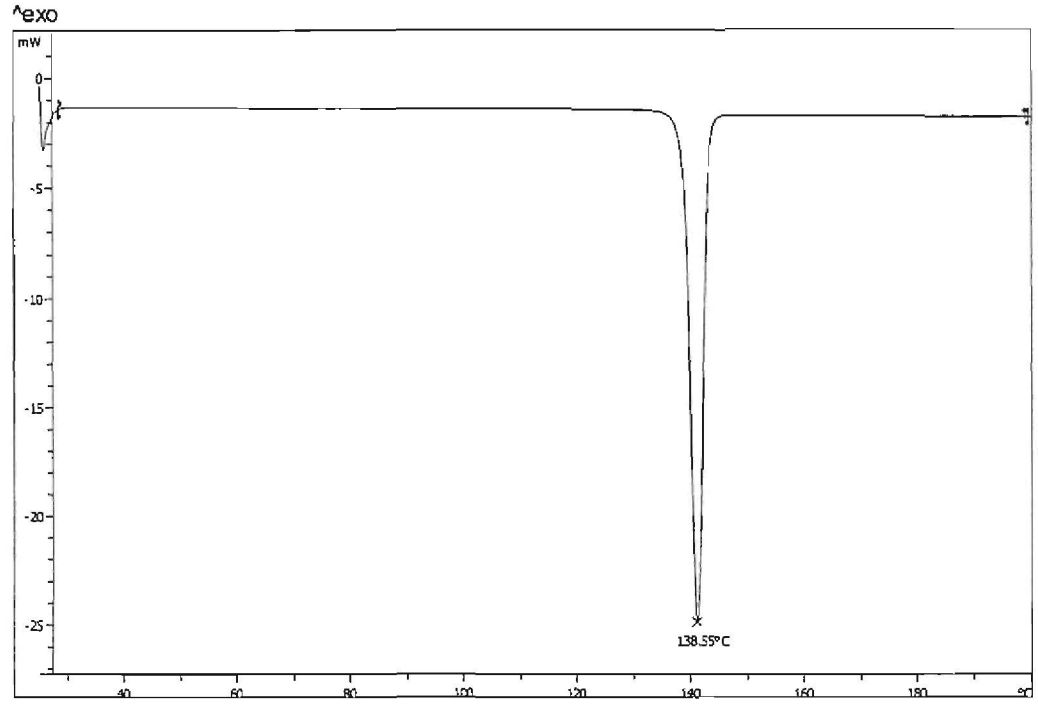
The most significant differences are visible in the 3500-3000 cm^{-1} region where the presence of the incorporated water molecules could be detected due to the presence of the absorption band at 3155 cm^{-1} in Form MH and absent in Form I and the hydrogen bonding of the tiazolyl-rings (as discussed in the XRPD data in section 7.2.2.1).

The presence of the absorption band at approximately 1957 cm^{-1} could be attributed to a combination of the OH-stretching and bonding vibrations (Caira *et al.*, 2004:607).

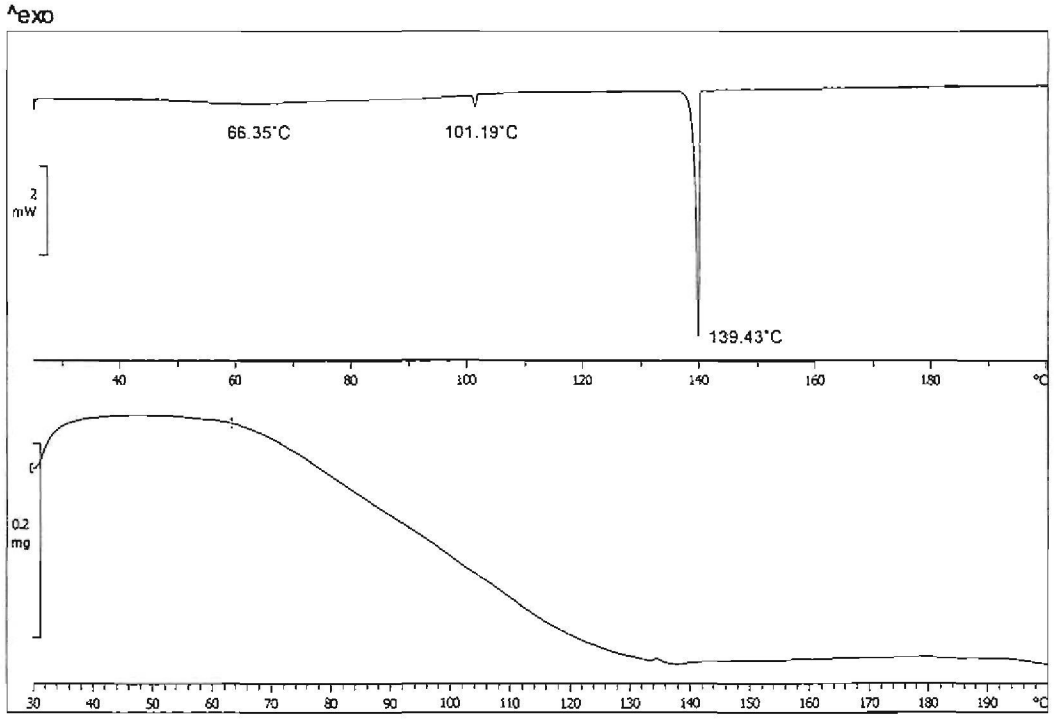
7.2.2.3 Thermal analysis

The thermal properties of the various fluconazole crystal modifications were investigated, using DSC, TGA and TM. TGA analysis was conducted on all the samples, of which their DSC results indicated a tendency of possibly being pseudopolymorphs.

The DSC thermogram of crystal Form I (figure 7.12) exhibited a single melting endotherm with a peak maximum (melting point) at 139.50°C. The absence of any desolvation endotherms confirmed that crystal Form I was a true polymorph. The heat of fusion was calculated to be 122 J/g. A summary of the thermal events observed using TM, when Form I was heated is given in table 7.6.



(a)

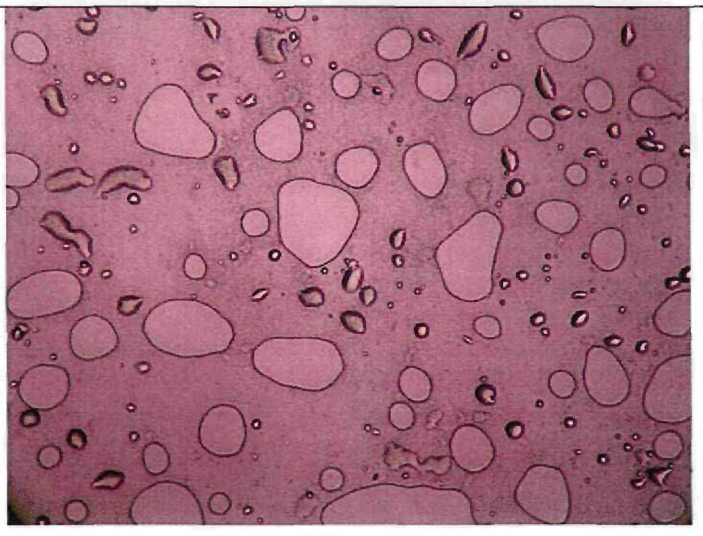


(b)

Figure 7.12 DSC thermogram of fluconazole (a) Form I and an overlay of the DSC and TGA thermogram of (b) Form MH.

The TM results supported the DSC results, i.e. that the melting of fluconazole Form 1 commenced at 140°C and ceased at 142°C.

Table 7.6 Summary of the TM results of fluconazole Form I at a temperature range of 25-142°C

Temperature (°C)	Photomicrograph	Remarks
25		Form I at room temperature.
140-142		Onset of melting was observed at 140°C and complete melting of the sample was observed at 142°C.

Caira *et al.*, 2004:602 stated that the dehydration process is indicated by the sharp melting endotherm at 101°C. The DSC thermogram of fluconazole monohydrate (Figure 7.12 – b) exhibited a broad dehydration endotherm with a peak minimum at 66.35°C and a small sharp endotherm at 101.19°C associated with dehydration, followed by a sharp melting endotherm at 139.43ºC. TGA confirmed that the broad endotherm at 66.35°C and sharp endotherm at 101.19ºC could be attributed to the dehydration of the sample and revealed a total mass loss of 4.79% (m/m) when heated. The heat of fusion for the dehydrated Form MH was found to be 116 J/g, which did not differ significantly from that of the heat of fusion of Form I, which suggested that the dehydration of Form MH produced Form I. The thermodynamic stability of Form I and Form MH will be discussed in section 7.2.2.4.

The average moisture content of Form MH was determined as 5.52% using Karl Fischer (KF) titrations. This value was slightly higher compared to the TGA results, and could be attributed to the presence of surface moisture that was detected during the KF titrations.

The thermal behaviour of the monohydrated fluconazole crystals (Form MH) was investigated by means of TM (table 7.7). Bubble formation was observed at 107ºC when Form MH crystals were submerged in silicon oil and heated. The evolution of gas in mineral oil or silicon oil when hydrated or solvated crystal forms are heated can be considered to be a positive identification for the dehydration or desolvation process (Kuhnert-Brandstätter, 1971:16). The impact of the dehydration process on the crystal lattice will be discussed in section 7.2.2.4.2 using VT-XRPD as analytical technique.

The TM results supported the DSC results, i.e. that the melting of the dehydrated Form MH commenced at 137°C and ceased at 141°C.

Table 7.7 Summary of the TM results of fluconazole Form MH at a temperature range of 25-141°C

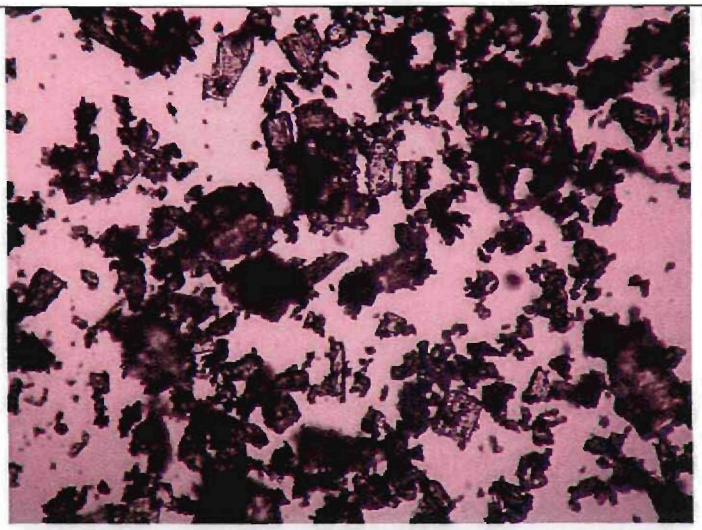
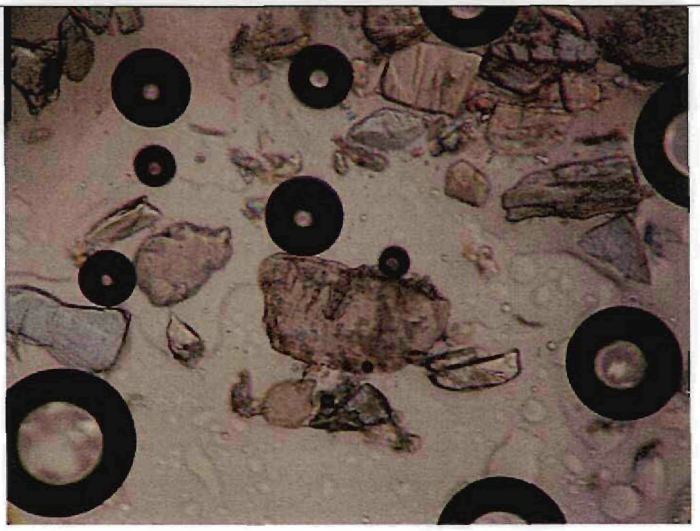
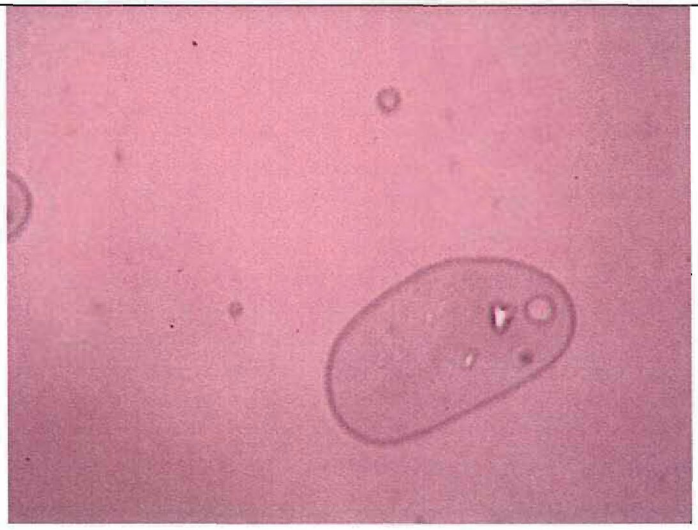
Temperature (°C)	Photomicrograph	Remarks
25		Fluconazole Form MH at room temperature.
107		Gas evolution (bubble formation) at 107°C when Form MH crystals were submerged in silicon oil.

Table 7.7 continued ...

137		Onset of melting was observed at 137°C.
141		Complete melting of the sample was observed at 141°C.

7.2.2.4 Thermodynamic stability of fluconazole crystal modifications – Form I and Form MH

The aim of this section was to investigate the thermodynamic stability of two fluconazole crystal modifications (Form I and Form MH) when exposed to increased temperatures using variable temperature x-ray powder diffraction as exploratory technique.

7.2.2.4.1 Thermodynamic stability of fluconazole Form I

As mentioned previously (section 7.2.1), the raw material (Form I) purchased was dried in a vacuum oven at 90°C for 1 hour to ensure that the sample to be used during the moisture studies was free from potential surface moisture / solvent. The XRPD pattern of the originally procured raw material and that of the thermally treated sample were found to be comparable, thus it can be concluded that the drying process did not induce any polymorphic transition / transformation (figure 7.13). A slight shift in the peak positions could be attributed to differences in the powder-bed heights.

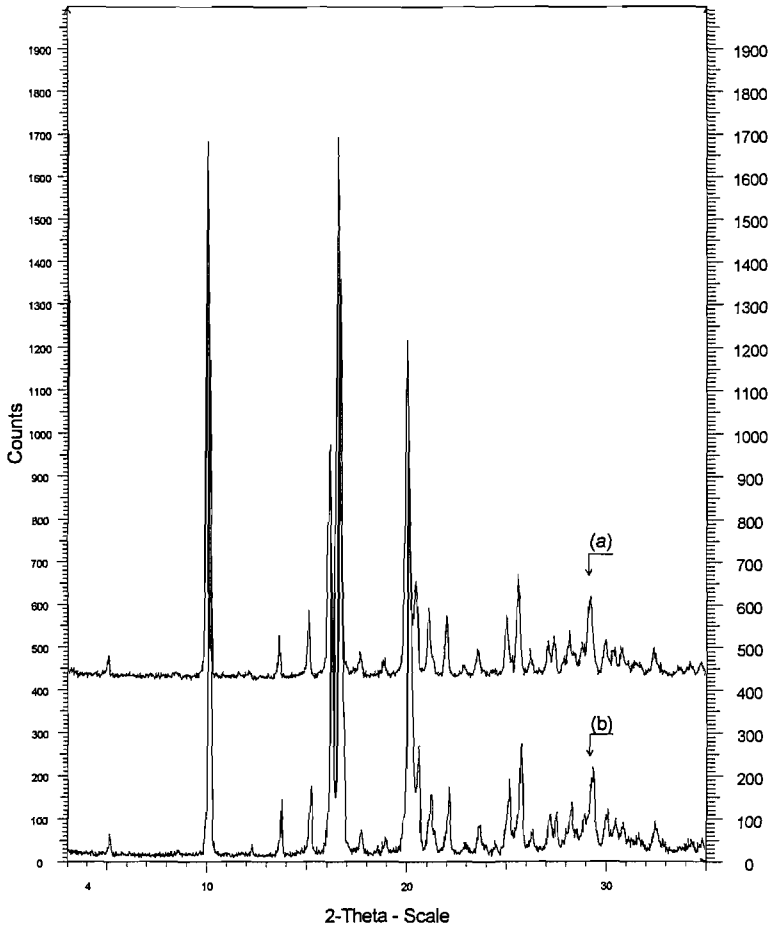


Figure 7.13 Overlay of fluconazole Form I (a) prior to and (b) after drying at 90°C for 1 hour.

The DSC thermogram of Form I did not reveal any thermal events prior to / after the melting of the phase which suggests that no polymorphic / phase transitions occurs when exposed to increased temperatures. The thermodynamic stability of Form I was investigated by means of VT-XRPD.

The sample was exposed to increased temperatures ranging between 25-145°C. An overlay of the XRPD patterns recorded at the predetermined temperatures is illustrated in figure 7.14.

The XRPD pattern of Form I (figure 7.14) did not reveal any significant changes when exposed to increasing temperatures (25-130°C). The intensities of the Bragg peaks reduced significantly between 130-140°C due to the molecular loosening in the lattice, associated with the melting process, which lead to the formation of a less crystalline phase which finally underwent complete melting at temperatures exceeding 140°C, producing a halo-shaped XRPD pattern with no prominent diffraction peaks at 145°C.

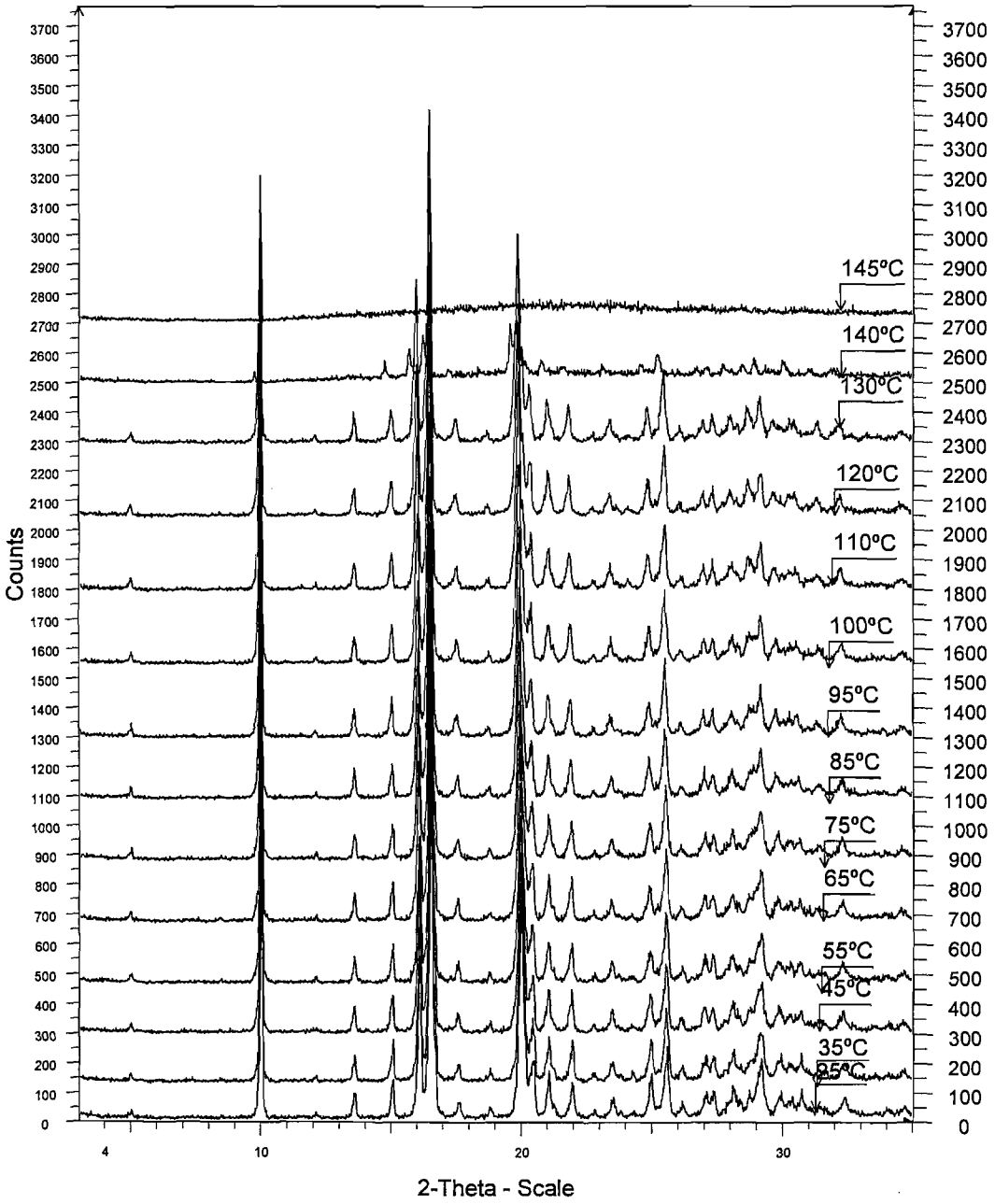


Figure 7.14 VT-XRPD patterns of fluconazole Form I exposed to increasing temperatures ranging between 25-145°C.

It is thus confirmed that fluconazole Form I is the thermodynamic stable form, which does not reveal any phase / polymorphic transitions prior to the melting thereof.

7.2.2.4.2 Thermodynamic stability of fluconazole Form MH

Khouloud *et al.* (2006:859-869) studied the thermal dehydration of fluconazole Form MH using FT-IR and TGA analysis. It was concluded that the dehydration process abided the three-dimensional phase boundary reaction model and that the properties of the anhydrate resembled that of Form I. No XRPD data was supplied to support the observations made, thus this study provides the supplementary information to substantiate their observations.

Due to the stabilisation role of the water molecules in the hydrated lattice, it could be suggested that the dehydration process will cause a disturbance of the crystal structure and that this thermodynamically unstable lattice will rearrange into the thermodynamically stable Form I lattice.

The VT-XRPD patterns of fluconazole Form MH when heated from ambient to 140°C is illustrated in figure 7.15. The most significant lattice changes occurred in the 3-15°2θ region as illustrated by the overlay of the Guinier-plates (figure 7.16).

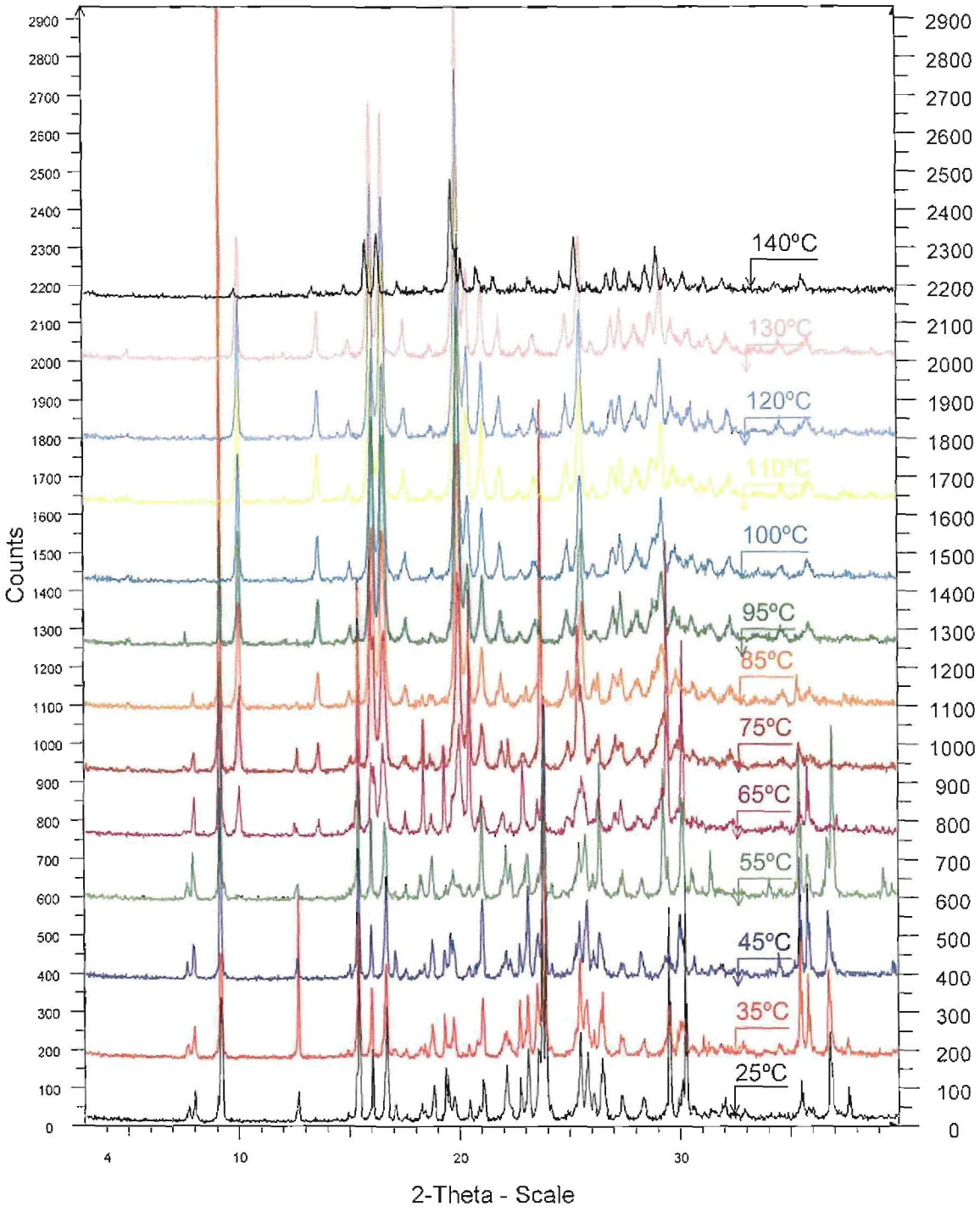


Figure 7.15 VT-XRPD patterns of fluconazole Form MH when exposed to increasing temperatures ranging from 25-140°C.

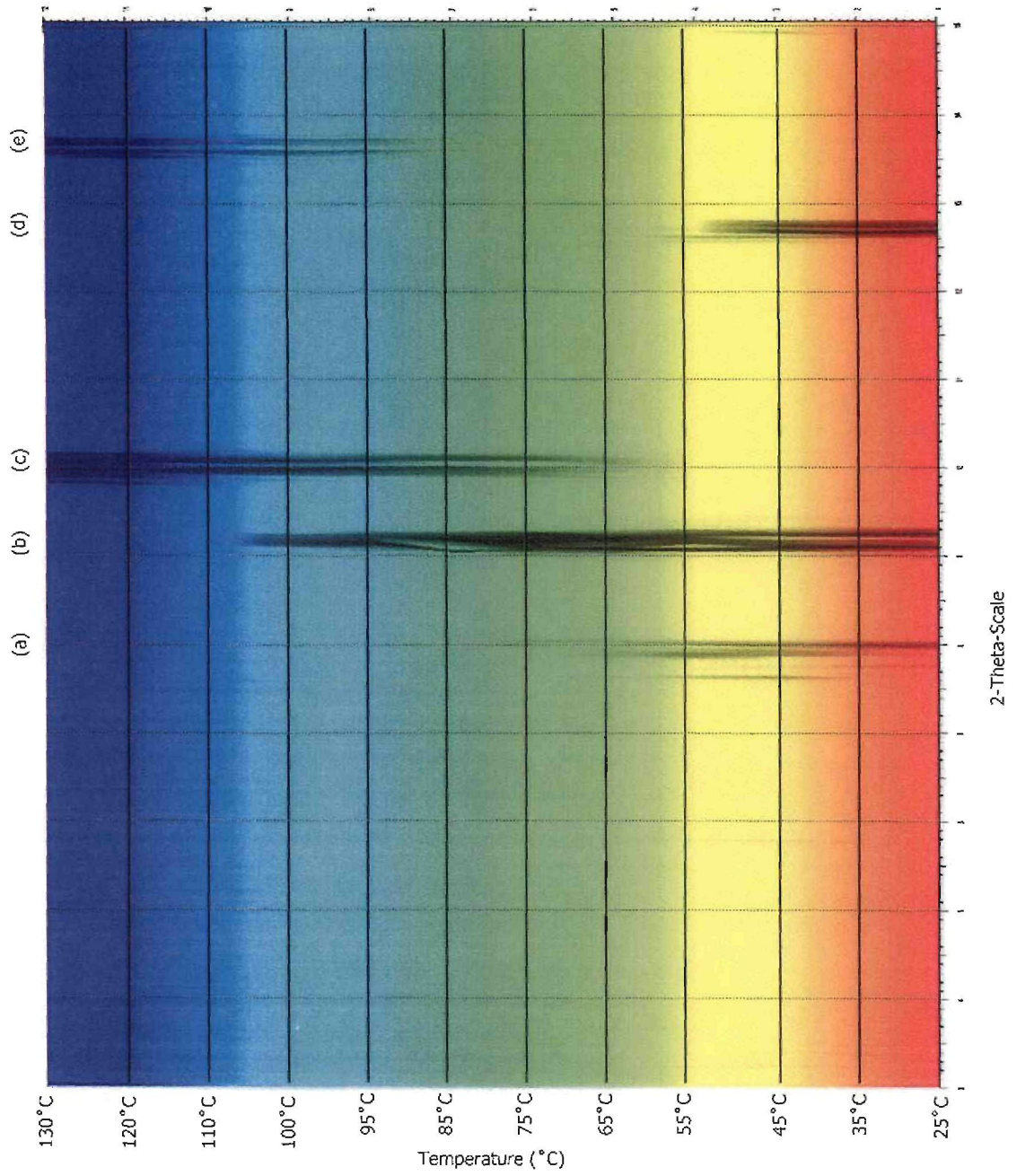


Figure 7.16 Overlay of the Guinier plate of fluconazole Form MH when exposed to increasing temperatures ranging from 25-130°C, in the 3-15°2θ region.

The following observations were made from the variable temperature Guinier plates depicted in figure 7.16:

(a) The intensities of the peak at 7.7 and 7.9°2θ (characteristic of Form MH) decreased when exposed to the increased temperature and disappeared at 55-65°C and 95-110°C respectively.

(b) The intensity of the strongest diffraction peak, characteristic of Form MH, located at 9.2°2θ, revealed a notable decrease in intensity between 85-100°C and disappeared at 110°C indicating that the dehydration process has concluded.

(c) The diffraction peak at 10.1°2θ (characteristic of Form I) was detected in the sample from 55°C and revealed an increase of the anhydrous fraction (i.e. Form I) with an increase of temperature.

(d) The diffraction peak at 12.7°2θ (characteristic to Form MH) revealed a decreased intensity when heated and disappeared between 55-65°C.

(e) The appearance of the 13.7°2θ diffraction peak at 65°C (and the increasing intensity thereof) indicated the increasing fraction of the anhydrous phase (Form I) in the sample.

The TGA thermogram of the Form MH revealed that the dehydration process has commenced at approximately 50°C and concluded at approximately 130°C. Considering the abovementioned observations and the TGA thermogram (figure 7.12) it can be concluded that dehydration occurs between 50-130°C. Considering the dehydration model described for Form MH by Khouloud *et al.* (2006:864) i.e. the three dimensional boundary reaction model, the dehydration process consists of two steps: (a) dissociation of water molecules from the crystal lattice (which is the rate-limiting step due to larger energy barrier associated with hydrogen-bond dissociation), and then the (b) release of these water molecules by diffusion through the channels. Sufficient energy supply (i.e. heat) to the isolated site hydrate leads to the liberation of water from all the sites due to the similar energetic environments (uniformly hydrogen bonding of

the water molecules to drug molecules) wherein the water molecules are found in (figure 7.9).

The moisture sorption behaviour of fluconazole Form I and Form MH and the dehydration behaviour of Form MH will be discussed in chapter 8.

Conclusion

This chapter provided an overview of the polymorphic behaviour of fluconazole and described the physico-chemical properties of the crystal forms investigated in this study.

SEM studies confirmed that the preferred orientation of Form I and MH could be attributed to the acicular habits of the mentioned crystal forms as suggested by Caira *et al.* (2004:607).

VT-XRPD studies confirmed that Form I is the thermodynamic stable form. VT-XRPD and TGA studies indicated that Form MH the dehydration process has commenced at approximately 50°C and concluded at approximately 130°C. After dehydration the unstable, dehydrated lattice converted to the thermodynamic form. The heat of fusion for the dehydrated Form MH was found to be 116 J/g, which did not differ significantly from that of the heat of fusion of Form I.

CHAPTER 8

Moisture sorption properties of fluconazole crystal forms

Introduction

The thermodynamic behaviour and stability of two fluconazole crystal modifications (a polymorphic and a pseudopolymorphic form) will be investigated in this chapter to compare the stability / instability thereof when exposed to moisture.

Khouloud *et al.* (2002:501) indicated that the dissolution rate of the fluconazole anhydrate, Form I, was higher compared to that of the monohydrate, Form MH. The dissolution rate constant of the monohydrate was 15% higher compared to that of Form I. Form I is thus the preferred crystal form to be used in pharmaceutical dosage forms due to its thermodynamic stability (section 7.2.2.4.1) and the favoured dissolution behaviour. Hydration of the anhydrous Form I to produce Form MH should be prevented during the storage of the raw material manufacturing of dosage forms, to ensure optimal bio-availability.

An investigation of the physico-chemical properties of Form I and the monohydrate at predetermined intervals provided insight into the moisture-sorption susceptibility of the two fluconazole crystal modifications and the thermodynamic behaviour of the two forms.

8.1 Moisture uptake measurement of fluconazole Form I and Form MH

Fluconazole raw material was obtained from Matrix Laboratories Ltd, Batch no: FLP 0170405.

One of the aims of this study was to prepare the monohydrate (hereafter referred to as Form MH) from the recrystallisation of Form I.

Form MH was prepared according to the methods described in literature (Caira *et al.*, 2004:602). A particle size fraction between 106-250 µm was used during all the experiments to ensure uniformity of particle size.

Form I crystals were dried at 90°C for one hour to remove any residual solvent / moisture from the samples. XRPD and DRIFT-IR studies revealed that no polymorphic transition occurred during the drying process of the Form I crystals (figure 7.13). Form MH was rapidly surface dried at ambient conditions to prevent dehydration.

Saturated solutions of NaCl and KNO_3 were prepared using the method described by Nyqvist (1983:47). 500 mg samples of Form I and Form MH were weighed into weighing boats and were stored in separate small RH chambers (0±5%, 65±5%, 75±5% and 85±5%) within a 30°C & 65% RH regulated climatic chamber (see table 6.1 for a description of the % RH chambers).

Samples were removed at predetermined intervals (i.e. 1,2,3,4,5,6,7,14,21, and 28 days) and were analysed using the methods discussed in chapter 2.

8.2 Moisture uptake measurement of the fluconazole polymorphic forms

The particle size distributions were measured using a Galai-Cis-1 (Galai-Cis-1, Israel) particle size analyser, as described in chapter 2. Samples of powder suspended in sedisperse (dispersing solution) were each placed in a small cuvette and fitted into the analyser. A small magnetic stirrer was placed inside the cuvette to prevent sedimentation of the particles during the measurement. The acquired data was used to compute means, medians and standard deviations, based on the total particle population. The median diameters by volume are summarised in table 8.1.

Table 8.1 Median particle size by volume (mass) and specific surface area of fluconazole Form I and Form MH

Polymorphic form	Median diameter by volume (μm)	Specific surface area (m^2/g)
Form I	80.27	0.807
Form MH	55.13	0.814

It is clear that the median particle sizes of both forms (Form I and Form MH) were lower than the sieved range: 106 μm - 250 μm. During the sieving process it was observed that both samples revealed a tendency to conglomerate due to static friction buildup during sieving. Thus, once the conglomerates (sized: 106-250 μm) were suspended in the suspending agent, it dispersed and the smaller particles were in suspension. The median diameter by volume of Form MH was found to be lower compared to that of Form I.

Surface area analysis was performed using a high speed surface area analyser (Flowsorb11 2300) as described in chapter 2. The specific surface area of Form I and Form MH was comparable (table 8.1) at standard conditions (outgas temperature: 100°C & outgas time: 3 hours). However it is known that Form MH dehydrates at these conditions, thus the specific surface area reported for Form MH was actually that of the dehydrated sample i.e. Form I. Irreproducible results were obtained when the specific surface areas were determined for Form MH at lower temperatures, thus no bona fide results can be reported for comparison purposes.

The specific surface analysis of Form MH at the following conditions (outgas temperature 40°C & outgas time: 80 hours) revealed that the specific surface area of the sample increased as the sample dehydrated, indicating that dehydration of Form MH increases the specific surface area of the sample (figure 8.1).

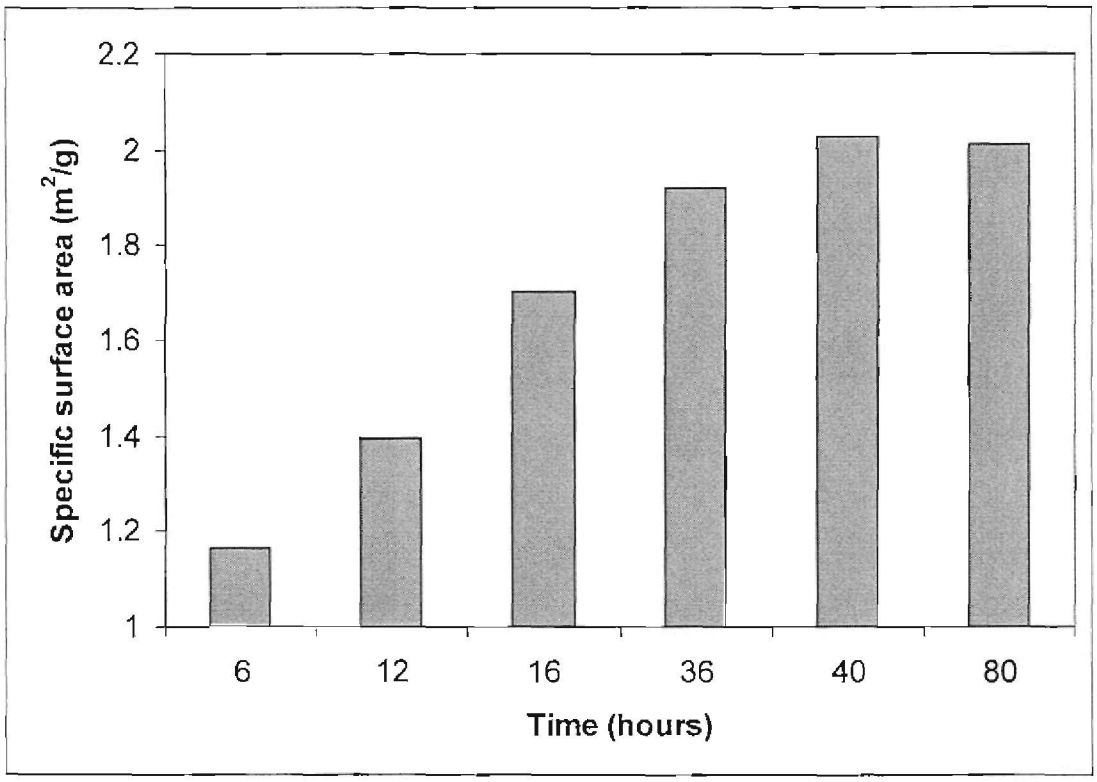
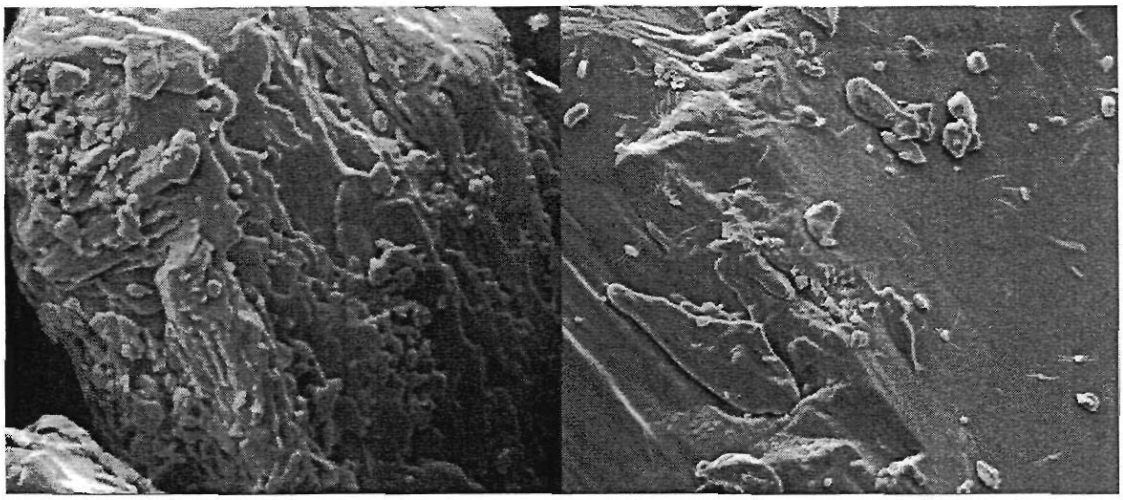


Figure 8.1 Specific surface area of Form MH at various intervals at the following conditions: outgas temperature: 40°C & outgas time 80 hours.

SEM photomicrographs of Form I revealed that the sample consisted of needle-like crystals and the Form MH sample revealed non-specific shapes. The surfaces of the crystal forms differed significantly (figure 8.2). The surface of Form I appeared to be plate-like structures stacked upon each other, creating a greater exposure surface compared to the flat, smooth surface of Form MH.



(a) (b)

Figure 8.2 SEM photomicrographs of fluconazole (a) Form I and (b) Form MH, revealing significant differences in the surface properties of these crystal forms.

The effect of increased temperatures on the surface properties of Form I and Form MH will be discussed in section 8.2.5.

8.2.1 Moisture sorption analysis results

Samples of Form I were vacuum dried at 50°C for over three days prior to inducing the sample in the sorption analyser. Moisture sorption isotherms were generated at 25°C using a Symmetric Vapor Sorption Analyzer (model SGA-100, VTI, Hialeah, Finland). The procedure involved drying the samples in the VTI instrument at 60 °C and ~ 0 % RH until the instrument recorded a weight loss of less than 1 µg over a period of 5 minutes. This was followed by exposing the samples to 10 % steps in RH from 0 to 95 % RH. Equilibrium was assumed when there was no weight change of more than 1 µg over a period of 5 minutes.

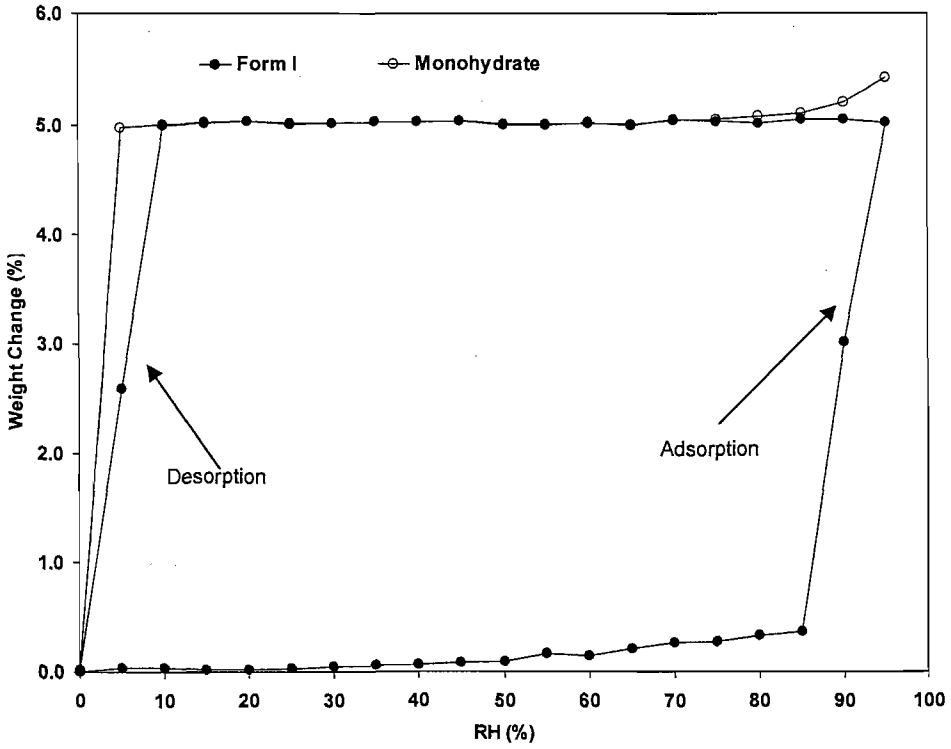


Figure 8.3 Moisture sorption isotherms of Form I and Form MH of fluconazole.

From the sorption analysis (figure 8.3) it became clear that Form I did not show any significant moisture sorption (< 1.0%) when exposed to relative humidities ranging between 0-84% RH. When exposed to RH > 85% it revealed a significant increase in moisture sorption and revealed a maximum water sorption capacity of approximately 5.0 %, suggesting that Form I converted to a monohydrated crystal form. When the relative humidity was reduced from 90 – 0 % RH (desorption cycle) it became clear that the hydrated Form I remained stable in the range of 90 – 10 % RH, and revealed a 5.0 % weight loss at RH < 10.0%, suggesting the dehydration of the hydrated Form I.

The desorption isotherm of Form MH (figure 8.3) revealed that dehydration occurred at RH < 5.0 %, thus suggesting that the hydrated Form I was less stable compared to the crystallised, monohydrate, Form MH. This observation will be further investigated and discussed in this chapter.

8.2.2 Total moisture content - Karl Fischer results

Tables 8.2 and 8.3 summarise the total moisture content of Form I and Form MH at predetermined intervals when stored at 30°C – 0% RH, 65% RH, 75% RH & 85% RH respectively. The moisture sorption isotherms of the mentioned forms derived from moisture content using Karl Fischer titration results are displayed in figures 8.4 and 8.5 respectively.

Table 8.2 Average moisture content of Form I at predetermined intervals when stored at 30°C – 0% RH, 65% RH, 75% RH & 85% RH respectively

	Days				
% RH	**0**	**7**	**14**	**21**	**28**
0±5	0.07	0.11	0.09	0.11	0.08
65±5	0.07	0.14	0.09	0.11	0.17
75±5	0.07	0.11	0.15	0.17	0.16
85±5	0.07	5.52	5.55	5.64	5.46

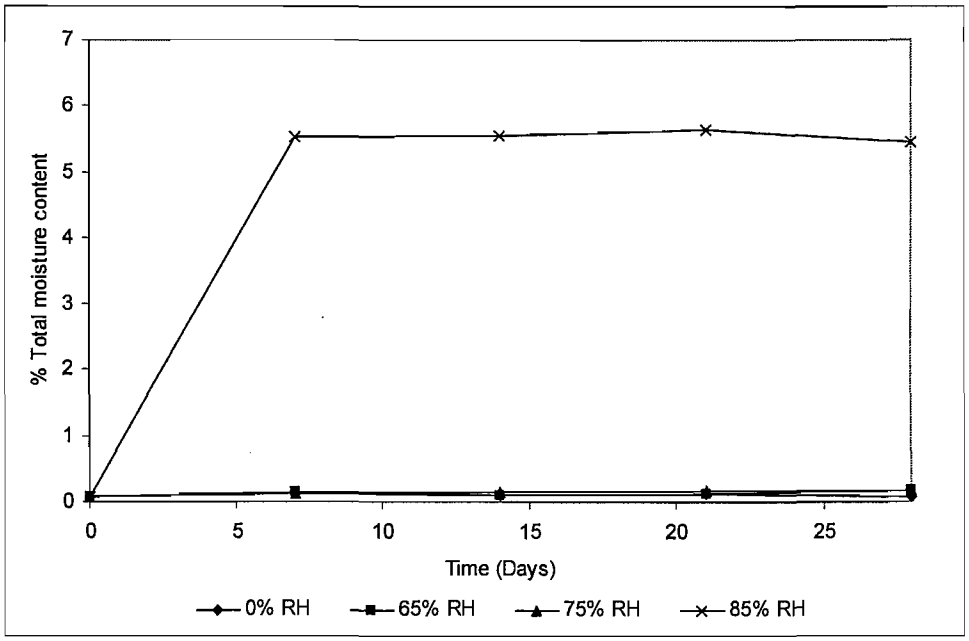


Figure 8.4 Moisture sorption isotherms of Form I derived from moisture content using Karl Fischer titration results.

The moisture sorption isotherms derived from the KF results for Form I (table 8.2 and figure 8.4) indicated that the no significant moisture sorption occurred when exposed to 0-75% RH. However, when Form I was exposed to 85% RH a considerable amount of moisture was sorbed by the samples (5.52% (m/m) after 7 days). The moisture content of the samples after 7 days, were found to correlate with the theoretical moisture content of a fluconazole monohydrated crystal system [5.84% (m/m)]. The moisture content of the samples exposed to 85% RH showed small variances (5.46-5.64%) which could be attributed to the dynamic process of moisture sorption and desorption.

Table 8.3 Average moisture content of Form MH at predetermined intervals when stored at 30°C – 0% RH, 65% RH, 75% RH & 85% RH respectively

	Days				
% RH	**0**	**7**	**14**	**21**	**28**
0±5	5.52	5.47	5.48	5.58	5.51
65±5	5.52	5.55	5.45	5.50	5.48
75±5	5.52	5.51	5.53	5.56	5.56
85±5	5.52	5.55	5.49	5.64	5.52

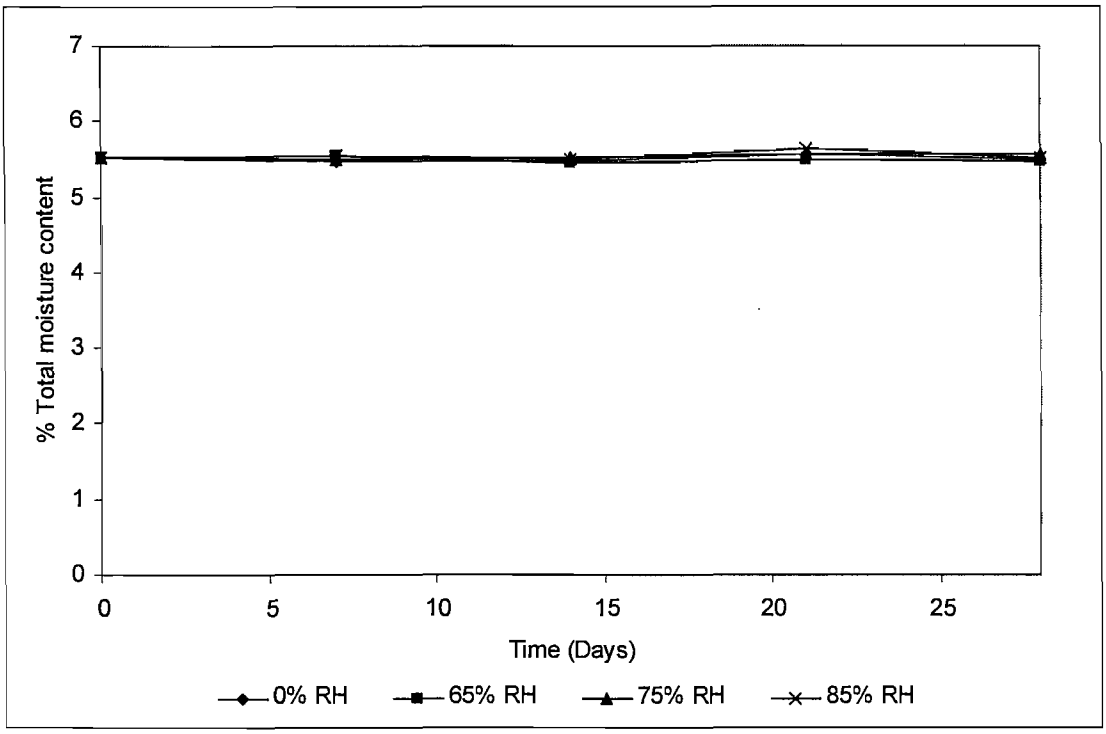


Figure 8.5 Moisture sorption isotherms of Form MH derived from moisture content using Karl Fischer titration results.

The moisture sorption isotherms derived from the KF results for Form MH (table 8.3 and figure 8.5) indicated that the no significant moisture sorption occurred when exposed to 0-85% RH during the 28 days.

8.2.3 Polymorphic stability of fluconazole Form I

The crystallographic behaviour and properties of Form I and Form MH during the moisture sorption study was investigated by means of XRPD and VT-XRPD studies.

Exposure of fluconazole Form I to 0-75% RH for a period of 28 days did not induce any significant changes in the XRPD patterns of the samples (figure 8.6). The intensity of the small peak at 5.0°2θ varied considerably at the various time intervals, which could be attributed to preferred orientation or minor differences in crystal habit (discussed in section 7.2.2.1).

The XRPD patterns of Form I (figure 8.7) exposed to 85% RH for 28 days revealed that a polymorphic transition occurred after 7 days. A summary of the peak appearances and disappearances is tabulated in table 8.4. It can thus be concluded that the moisture sorption (described in section 8.2.2) could be classified as moisture *absorption* rather than moisture *adsorption*, due to the significant crystal-lattice changes that occurred in order to compensate for the water molecule(s) incorporated into the crystal lattice.

The XRPD pattern of fluconazole Form I (exposed to 85% RH) at day seven is in good agreement with that of fluconazole Form MH (figure 7.9). The crystal packing of fluconazole monohydrate (Form MH) revealed that water molecules occupy isolated cavities in the crystal structure (Caira *et al.*, 2004:601).

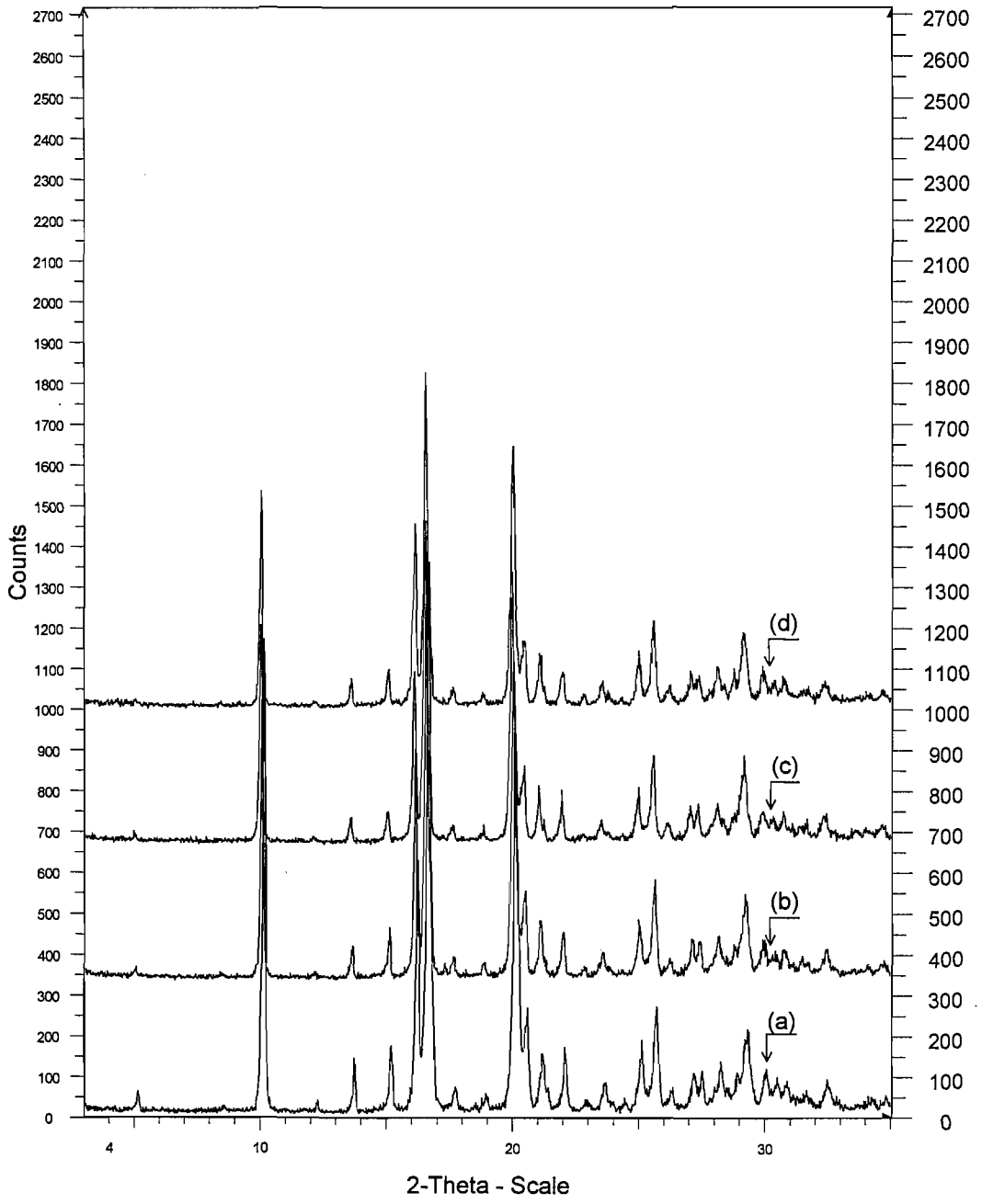


Figure 8.6 XRPD pattern overlay of fluconazole (a) Form I when exposed to 30°C & (b) 0, (c) 65 & (d) 75% RH for 28 days.

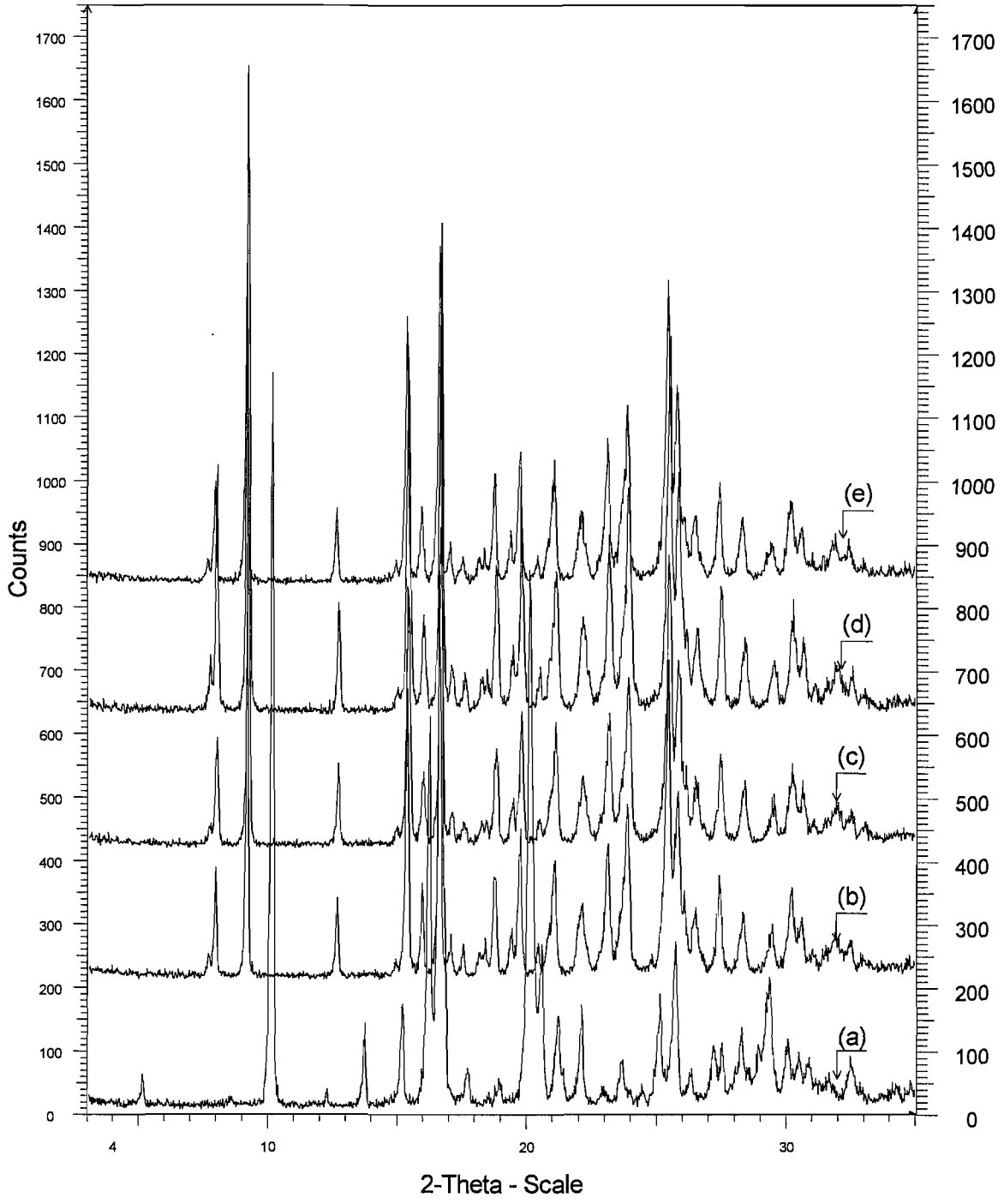


Figure 8.7 XRPD pattern overlay of fluconazole Form I when exposed to 30°C & 85% RH at the intervals: (a) 0, (b) 7, (c) 14, (d) 21 & (e) 28 days.

Table 8.4 Main XRPD pattern peak positions (º2θ) of fluconazole Form I at various time intervals when stored at 30ºC & 85% RH

Main peak positions (º2θ) at time intervals				
Initial	**7 Days**	**14 Days**	**21 Days**	**28 Days**
5.1	-	-	-	-
-	7.7	7.7	7.7	7.6
-	7.9	8.0	8.0	7.9
8.5	-	-	-	-
-	9.1	9.2	9.2	9.1
10.1	-	-	-	-
12.2	12.6	12.7	12.7	12.6
13.7	-	-	-	-
-	14.9	14.9	14.9	14.9
15.2	15.4	15.4	15.4	15.4
16.2	16.0	16.0	16.0	15.9
16.7	16.6	16.7	16.7	16.6
-	17.1	17.1	17.1	17.0
17.7	17.5	17.6	17.6	17.5
-	18.2	18.2	18.3	18.2
18.5	18.4	18.5	18.5	18.5
-	18.8	18.8	18.8	18.8
19.0	19.4	19.4	19.5	19.4
-	19.7	19.7	19.8	19.7
20.1	20.4	20.5	20.5	20.4
20.6	-	-	-	-
21.2	21.1	21.1	21.1	21.1
22.1	22.1	22.2	22.2	22.1
22.9	23.1	23.2	23.2	23.1
23.7	23.9	23.9	23.9	23.9
25.1	-	-	-	-
25.7	25.5	25.5	25.5	25.4
-	25.8	25.9	25.9	25.8
26.3	26.1	26.2	26.1	26.1
-	26.5	26.5	26.6	26.5
27.2	27.4	27.5	27.5	27.4
27.5	-	-	-	-
28.3	28.4	28.4	28.4	28.3
28.9	29.5	29.5	29.6	29.5
29.4	-	-	-	-
30.1	30.2	30.3	30.3	30.2
30.5	30.6	30.7	30.7	30.6
30.9	-	-	-	-
31.7	31.1	31.1	31.1	31.5
-	31.9	32.0	32.0	31.9
32.5	32.5	32.6	32.6	32.5
-	33.0	33.1	33.1	33.0

The DSC thermogram of Form I (figure 8.8) revealed a sharp melting endotherm at 139°C. The DSC thermogram of Form I remained relatively unchanged during the 28 days when stored at 0%, 65% and 75% RH respectively, confirming that no phase transformation has occurred (figure 8.8).

The DSC thermogram of Form I exposed to 85% RH changed significantly after 7 days (figure 8.9). A broad, weak dehydration endotherm appeared in the 50-100°C region. Thermogravimetric analysis (figure 8.10) confirmed that the broad endotherm at 50-100°C was due to the dehydration of the sample.

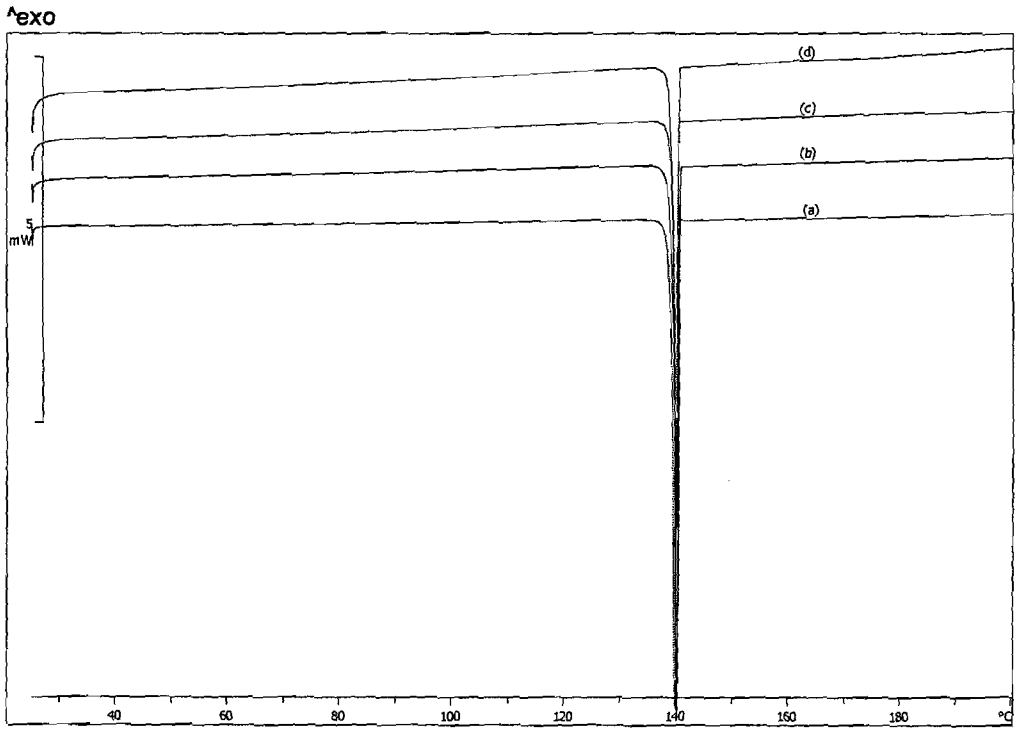


Figure 8.8 DSC thermograms of fluconazole (a) Form I when exposed to 30°C – (b) 0, (c) 65 & (d) 75% RH after 28 days.

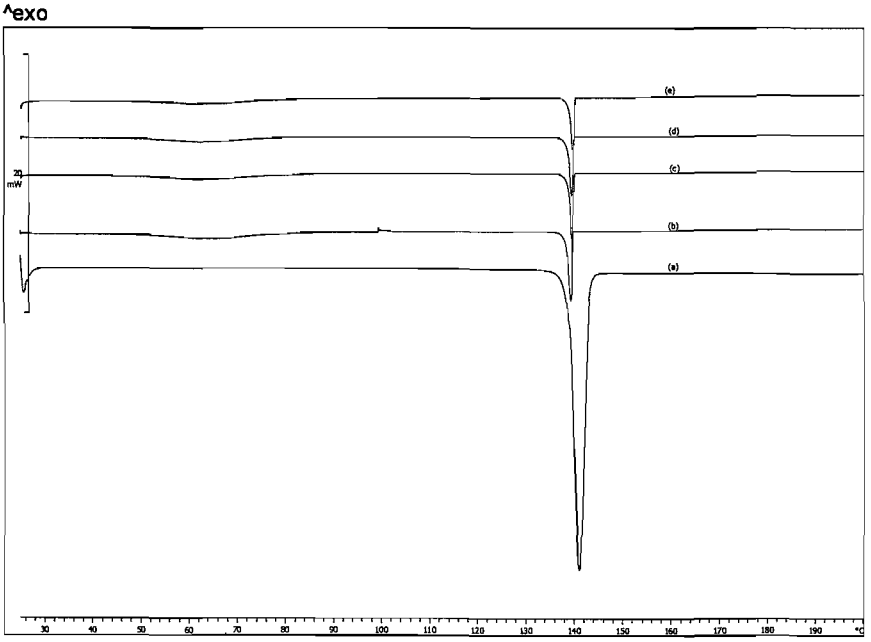


Figure 8.9 DSC thermograms of fluconazole Form I when exposed to 30°C – 85% RH at the following intervals: (a) Initial, (b) 7 days, (c) 14 days, (d) 21 days & (e) 28 days.

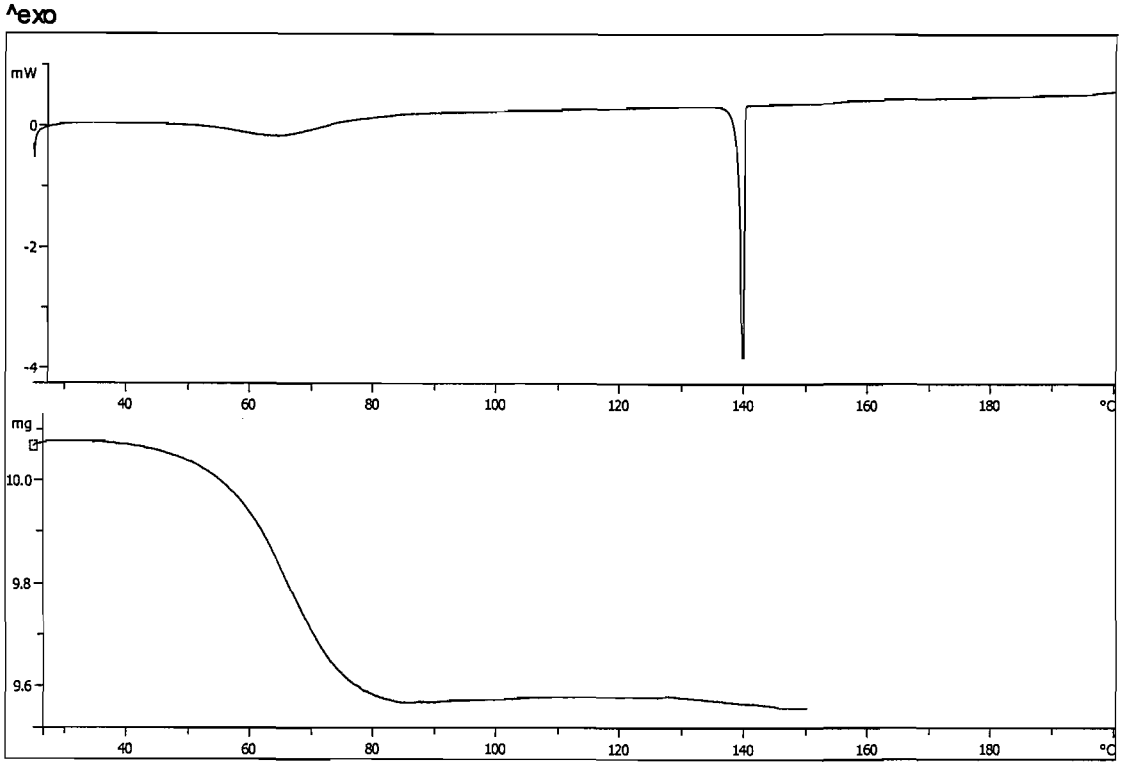


Figure 8.10 Overlay of DSC (top panel) and TGA (lower panel) thermogram of fluconazole Form I when exposed to 30°C – 85% RH for 28 days.

The DRIFT-IR spectra of the fluconazole Form I samples exposed to 0-75% RH for a period of 28 days (figure 8.11) did not reveal any significant differences confirming the XRPD and DSC observations that no polymorphic transitions occurred.

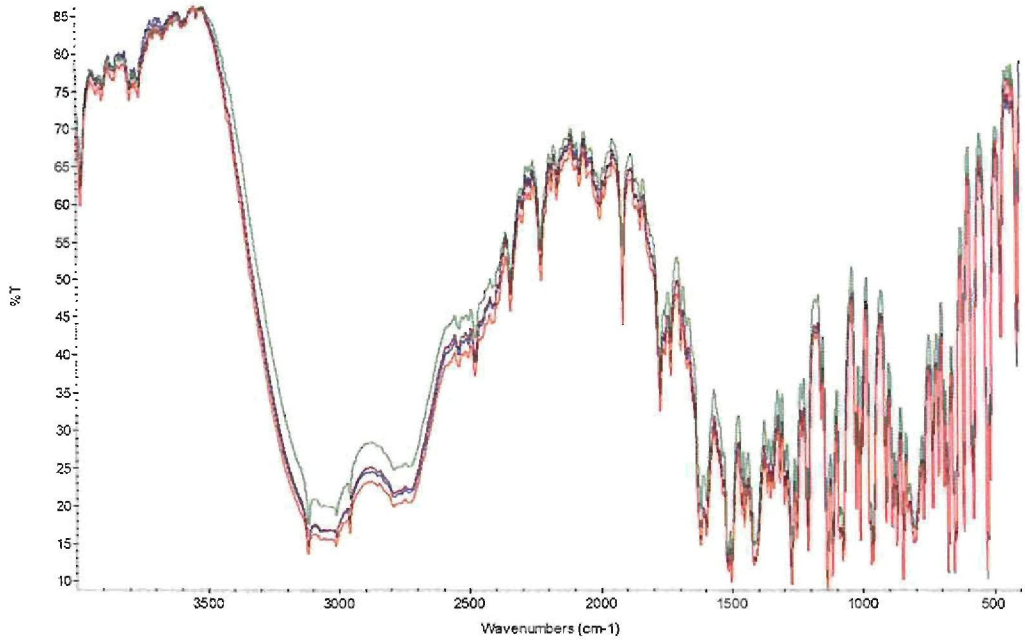


Figure 8.11 An overlay of the DRIFT-IR spectra of fluconazole Form I when exposed to 30°C – 0, 65, 75% RH.

The DRIFT-IR spectra of Form I exposed to 85% RH for a period of 28 days (figure 8.12) revealed significant changes in the main absorption peak positions. The DRIFT-IR spectra of the samples after 7, 14, 21 and 28 days were found to be comparable to that of fluconazole monohydrate (Form MH – figure 7.11), thus suggesting that the new crystal modification (hydrated Form I) remained stable at 30°C & 85% RH during the 28 day period.

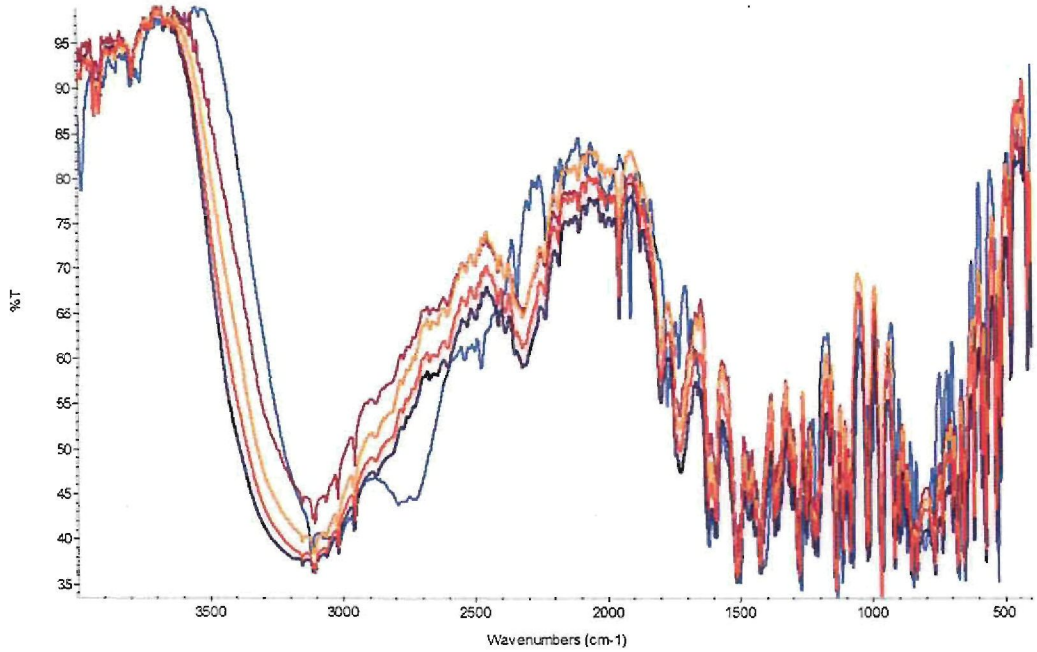


Figure 8.12 An overlay of the DRIFT-IR spectra of fluconazole Form I when exposed to 85% RH at 30°C during a 28 day period: Initial, 7 days, 14 days, 21 days, 28 days.

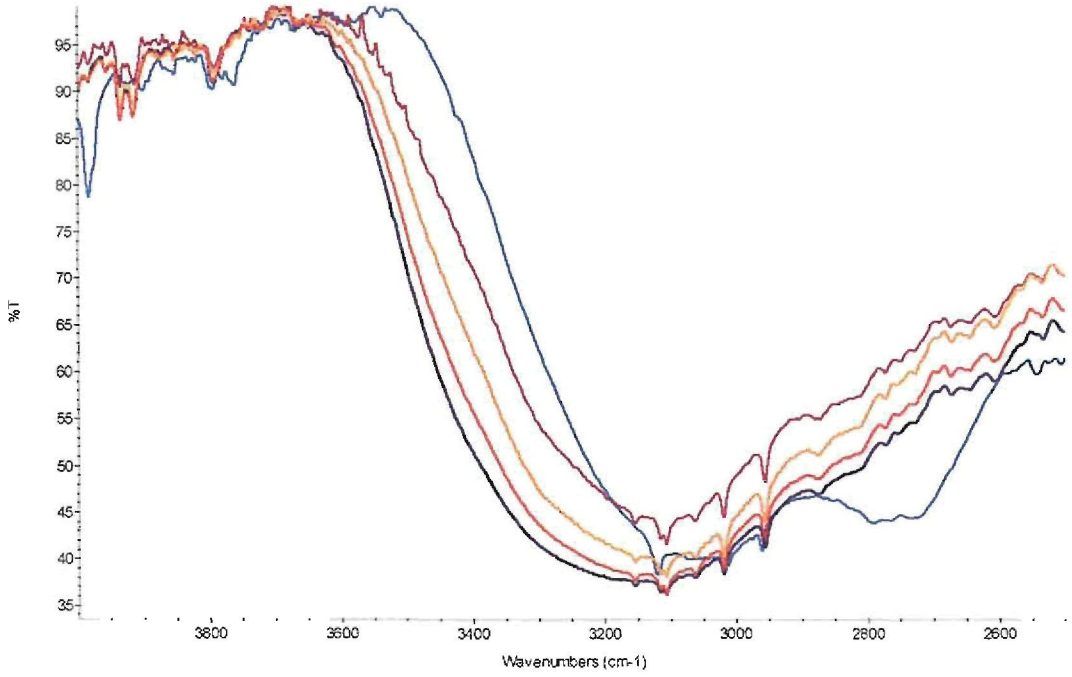


Figure 8.13 An overlay of the DRIFT-IR spectra of fluconazole Form I when exposed to 85% RH at 30°C during a 28 day period in the 4000-2600 cm^{-1} region: Initial, 7 days, 14 days, 21 days, 28 days.

The most remarkable differences or changes in the DRIFT-IR spectra were observed in the 4000-2600 cm^{-1} region (figure 8.13). The appearance of various Form MH characteristic absorption bands supported the XRPD observations that Form I transformed into the monohydrated Form MH upon exposure to 30°C & 85% RH for 7 days (table 8.5).

The stability of fluconazole monohydrate (Form MH) when exposed to various relative humidities was investigated and will now be discussed.

Table 8.5 Appearance of Form MH characteristic peaks in the fluconazole Form I samples stored at 30°C & 85% RH after 7 days

Wavenumbers (cm^{-1}) of absorptions which appeared	**Assignment**
3155	Water molecules
3019	CH - stretch of 2,4-Difluorobenzyl group
2956	CH_2 – stretch of propane backbone
1619	C=C – stretch of 2,4-difluorobenzyl group
1468	CH_2 – scissor of propane backbone
1370	Ring stretch of triazole group
1249	Ring stretch of triazole group
1139	Ring breathing of triazole group
1112	C-C – stretch of propane backbone
1020	C-(OH) – stretch of propane backbone
968	Ring-bend of triazole group

8.2.4 Polymorphic stability of fluconazole Form MH

The XRPD patterns of Form MH when exposed to 0, 65, 75 & 85% RH at 30°C for 28 days are displayed in figure 8.14.

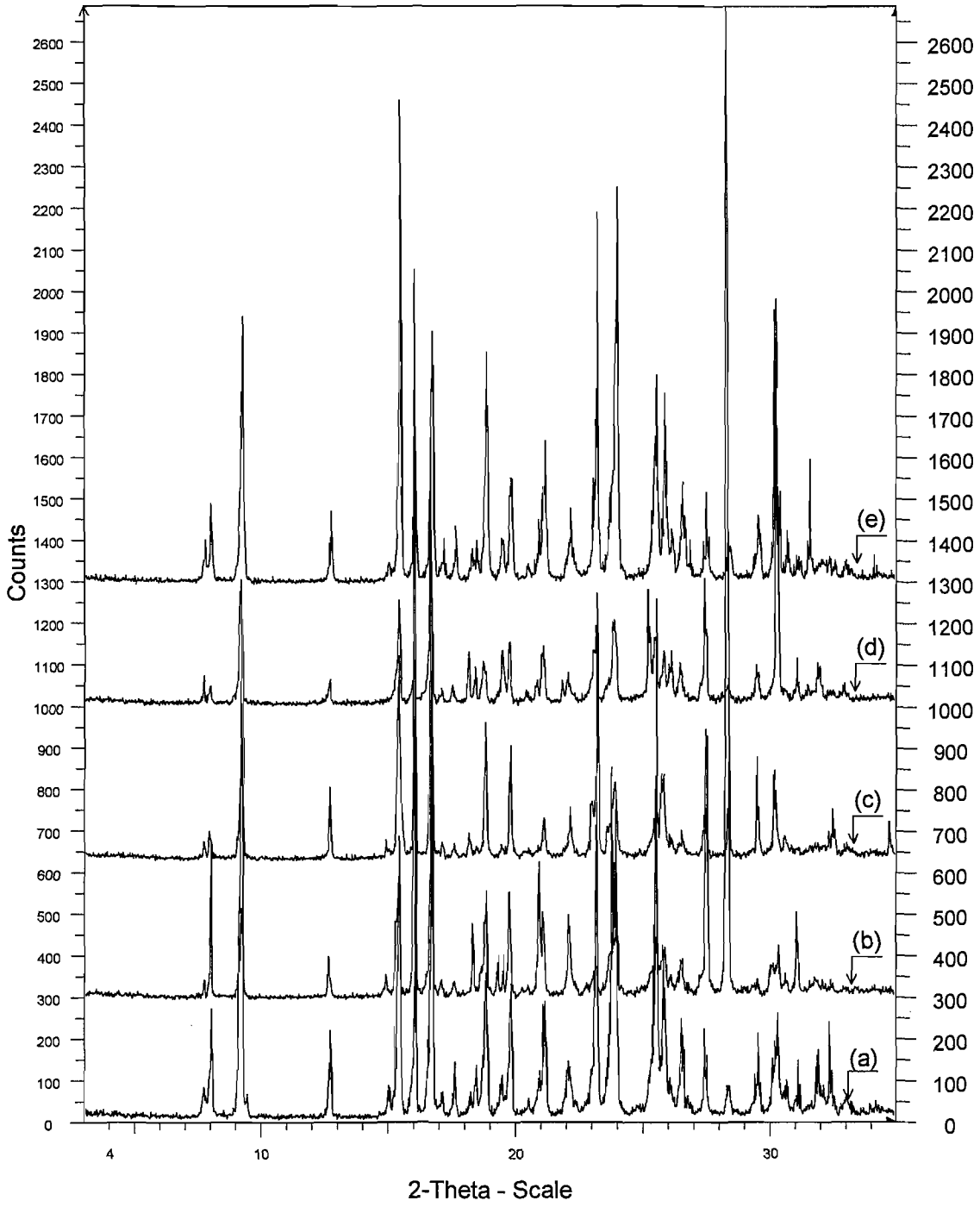


Figure 8.14 XRPD pattern overlay of fluconazole (a) Form MH when exposed to 30°C at (b) 0, (c) 65, (d) 75 and (e) 85% RH for 28 days.

The experimental XRPD pattern (figure 8.14 (a)) for the monohydrate (Form MH) and that computed from the single-crystal XRPD pattern was found to be in close agreement (figure 7.9).

As mentioned in section 7.2.2.1 the peak intensities in the XRPD patterns of fluconazole monohydrate suffer severely from preferred orientation effect due to the pronounced acicular habit of this crystal form. The variation in the peak intensities, especially decrease in some intensities that may suggest false peak disappearances, is clearly detectable in figure 8.14.

The XRPD patterns of fluconazole monohydrate did not reveal any significant changes in peak positions when exposed to 0, 65, 75 & 85% RH at 30°C for 28 days. The "absence" of some of the Bragg peaks, as illustrated in figure 8.14 could be attributed to the preferred orientation effects of the crystals. An example of preferred orientation is shown for Form III of sulphathiazole (figure 8.15). A comparison of the experimental XRPD pattern with that of the XRPD pattern calculated from the crystal structure of sulphathiazole indicated that the intensities of almost all of the expected diffraction peaks have been suppressed (Bernstein, 2002:118).

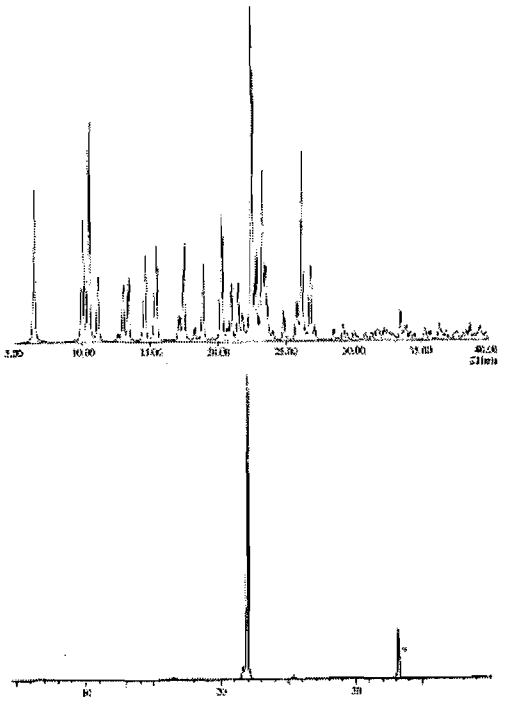


Figure 8.15 Calculated XRPD pattern of Form III of sulphathiazole – upper pattern. Experimental XRPD pattern – lower pattern (Bernstein, 2002:118).

In the sections to follow, it will be illustrated that the physico-chemical properties of the crystals remained relatively unchanged; supporting the XRPD observation that Form HM did not reveal any polymorphic transitions during this study.

The thermal properties of the various fluconazole crystal forms were investigated using DSC, TGA and TM.

The broad endotherms present in the 62-66°C region and the sharp endotherm at 101°C regions are indicative of the dehydration process of the monohydrate. These dehydration temperatures did not vary significantly as illustrated in figure 8.16.

In section 7.2.2.4.2 it was illustrated that upon dehydration the monohydrate converts to the thermodynamically stable Form I (figure 7.15). The melting endotherms observed in figure 8.16 at 139°C are characteristic of fluconazole Form I (the dehydration product of Form MH).

TGA analysis of the various samples confirmed the Karl Fischer observations, that no significant moisture sorption or desorption occurred.

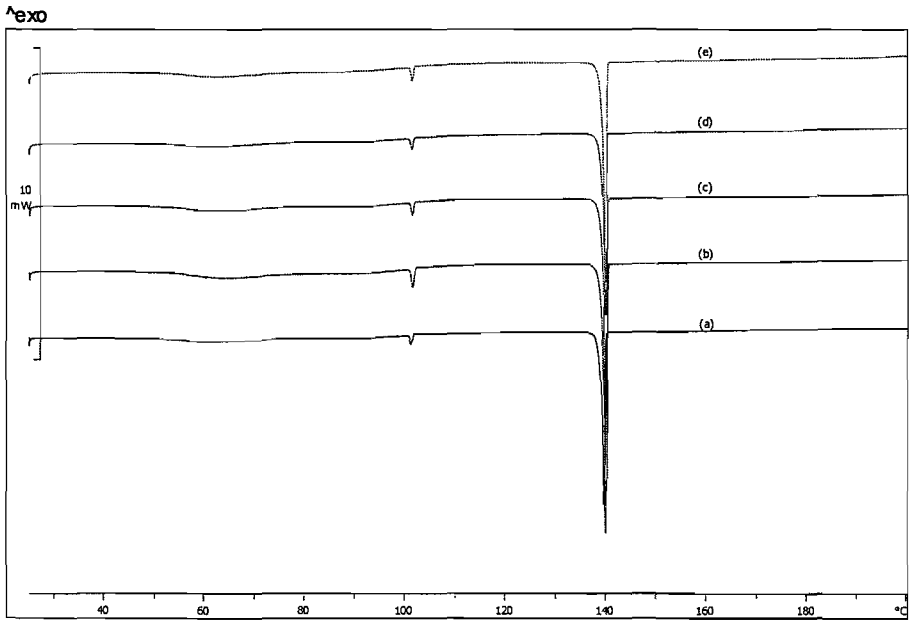


Figure 8.16 DSC thermograms of fluconazole (a) Form MH when exposed to 30°C and (b) 0, (c) 65, (d) 75 and (e) 85% RH after 28 days.

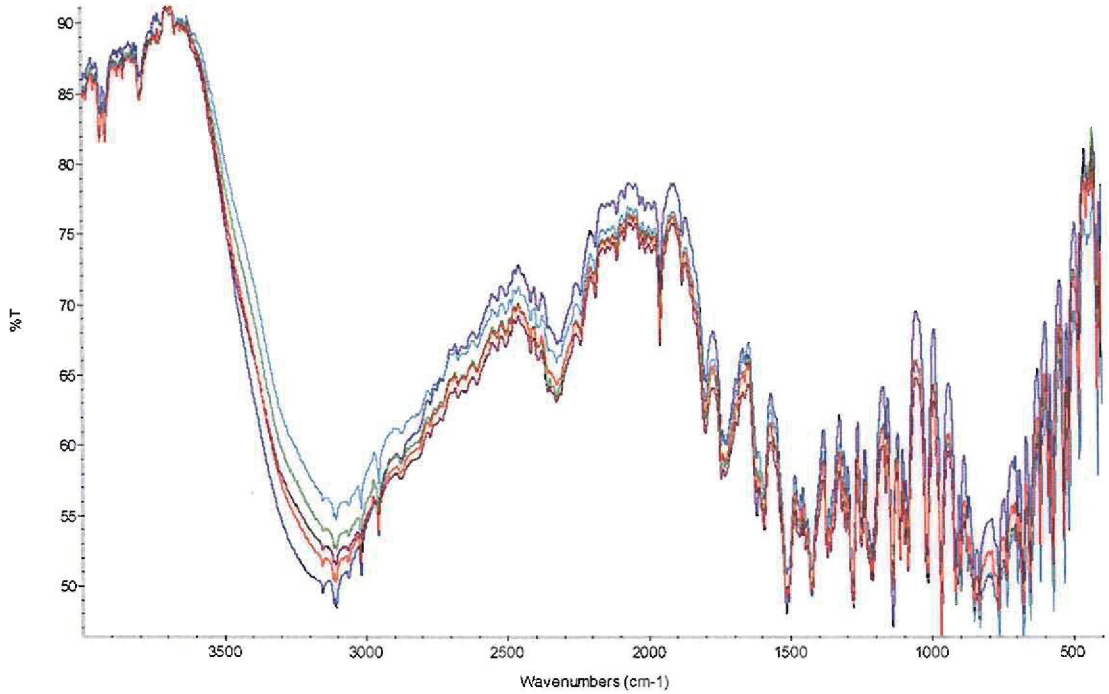


Figure 8.17 An overlay of the DRIFT-IR spectra of Form MH when exposed to 30°C at 0, 65, 75 and 85 % RH after 28 days.

The DRIFT-IR spectra of Form MH when exposed to 0, 65, 75 & 85% RH at 30°C over a 28 day period (figure 8.17) did not display any change in the position of the absorption bands, thus supporting the XRPD, DSC, TGA and KF observations that the exposure of fluconazole Form MH to the mentioned conditions for 28 days did not induce any polymorphic conversion.

8.2.5 Comparison of fluconazole Form MH and the hydrated Form I

Khouloud *et al.* (2006:859) studied the dehydration of fluconazole monohydrate (Form MH). Figure 8.18 (a) illustrates the seven TGA thermograms used in the Ozawa kinetic analysis method and (b) illustrates the plots of log A versus T^{-1} used in the calculation of the dehydration activation energy (E_A).

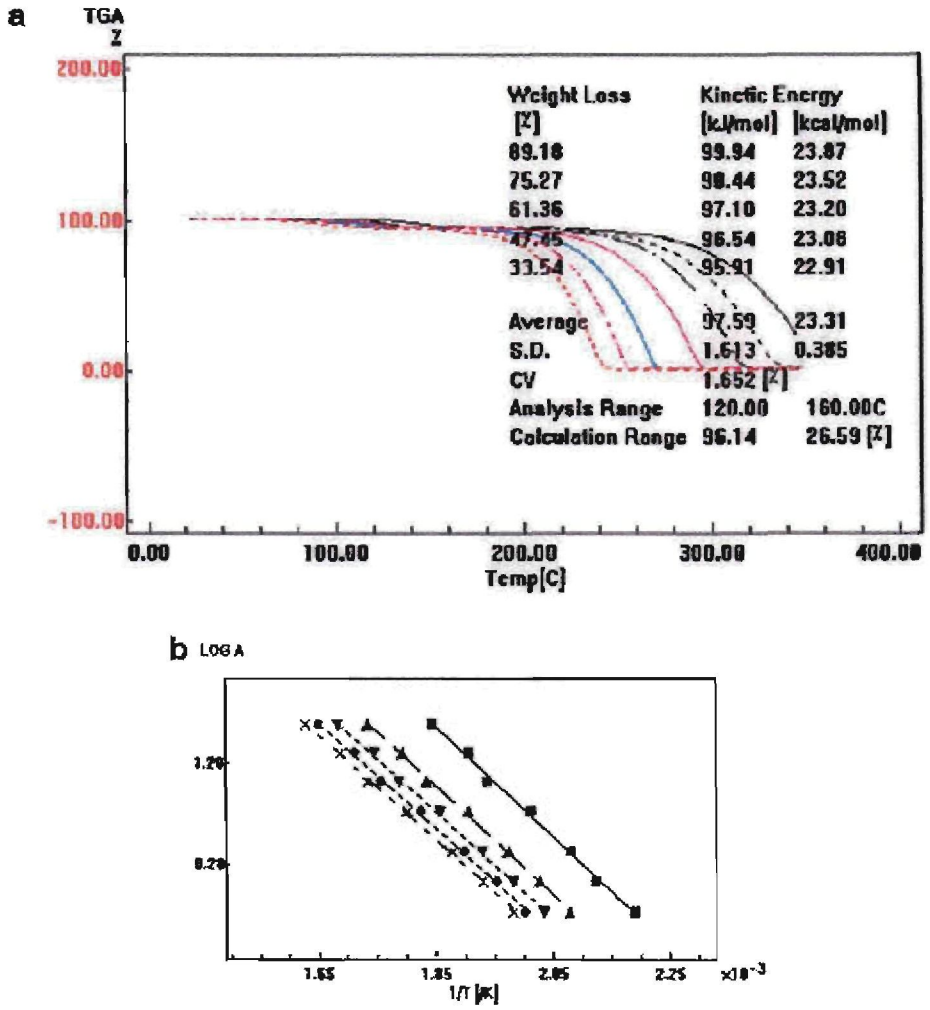


Figure 8.18 The seven TGA thermograms selected for applying the Ozawa kinetic method of analysis and (b) illustrates the plots of log A versus T^{-1} for fluconazole monohydrate (Khouloud *et al.*, 2006:865).

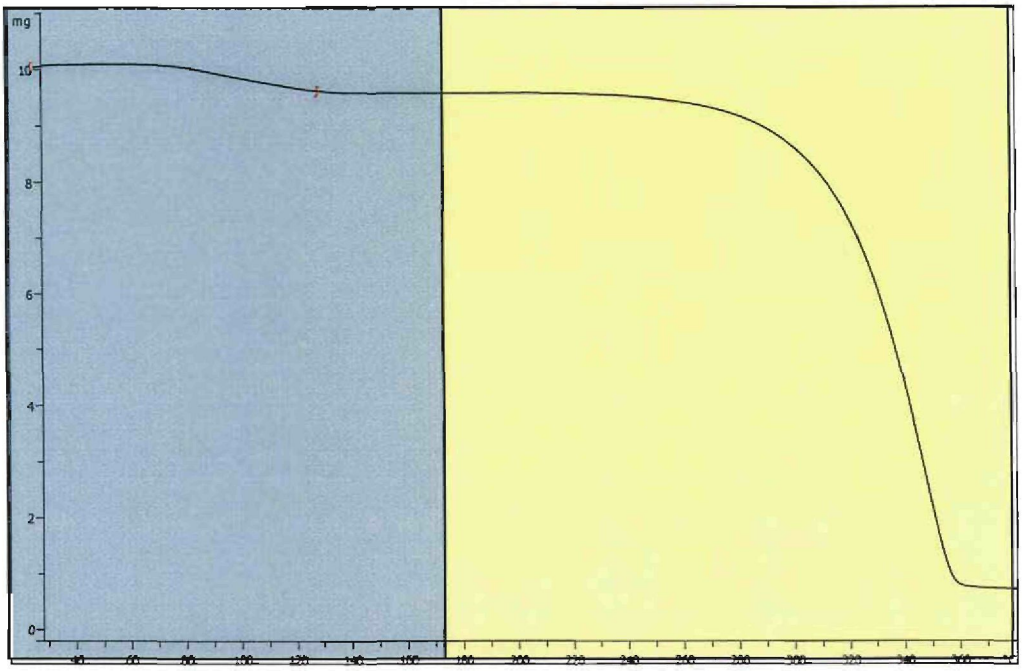
The authors, Khouloud *et al.* (2006:865) stated that the temperature range used in the study was 80.82-157.55°C, however upon closer inspection of the plots in figure 8.18 b – it was clear that the absolute temperature range wherein the calculations were performed was actually between 171.3°C – 332.9°C, which did not correlate with the range of dehydration, but rather the thermal decomposition of the sample.

Figure 8.19 a - illustrates a TGA thermogram of Form MH when heated from 25°C to 380°C. From this figure it is clear that two mass-loss events occurred in the sample i.e. (b) & (c). The first mass loss (b) occurred between 30°C and 150°C and was calculated to be 5.08% (m/m) which could be attributed to the dehydration of the sample. The second mass loss (c) observed occurred between 160°C and 380°C and was calculated to be 88.36% (m/m) which could be attributed to the thermal decomposition of the sample.

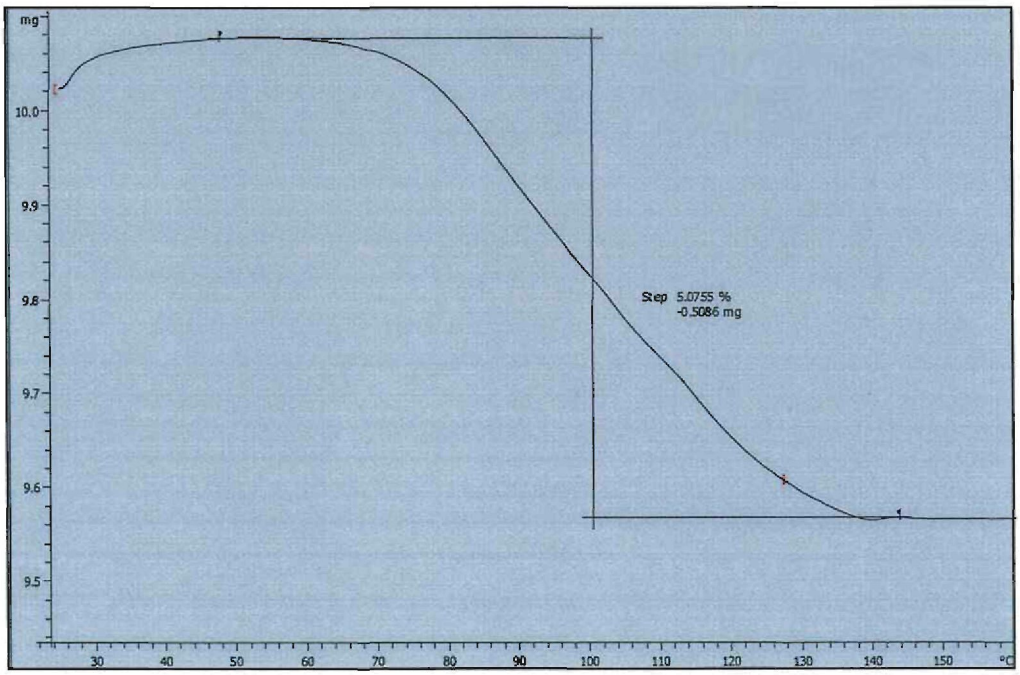
The kinetic parameters for the dehydration of fluconazole Form MH and the hydrated Form I were determined using TGA. The Ozawa method (Ozawa, 1965:1881) was used in this study to determine the dehydration activation energy (E_A) for the mentioned hydrates.

This method involved the analysis of the weight loss *vs.* temperature thermograms, at different heating rates (β), in order to determine the corresponding temperatures (temperatures in Kelvin) at a constant weight loss (C).

The dehydration of fluconazole Form MH and the hydrated Form I was studied, by exposing the hydrated crystal forms to five different TGA heating rates of 1, 2, 3, 5, and 10°C/min, respectively. The TGA thermograms of fluconazole Form MH and the hydrated Form I, at different heating rates, are depicted in figure 8.20.

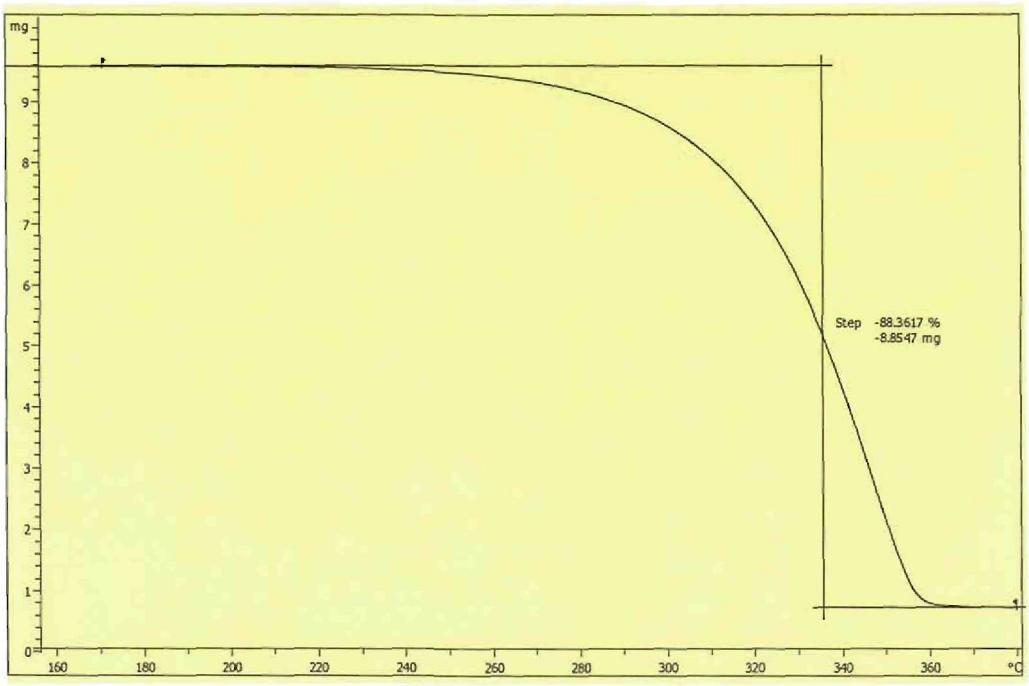


(A)



(B)

Figure 8.19 The (a) TGA thermogram of Form MH when heated from 25-380°C. (b) TGA trace between 25-150°C.



(C)

Figure 8.19 (c) The TGA trace between 160-380°C of Form MH when heated from 25-380°C.

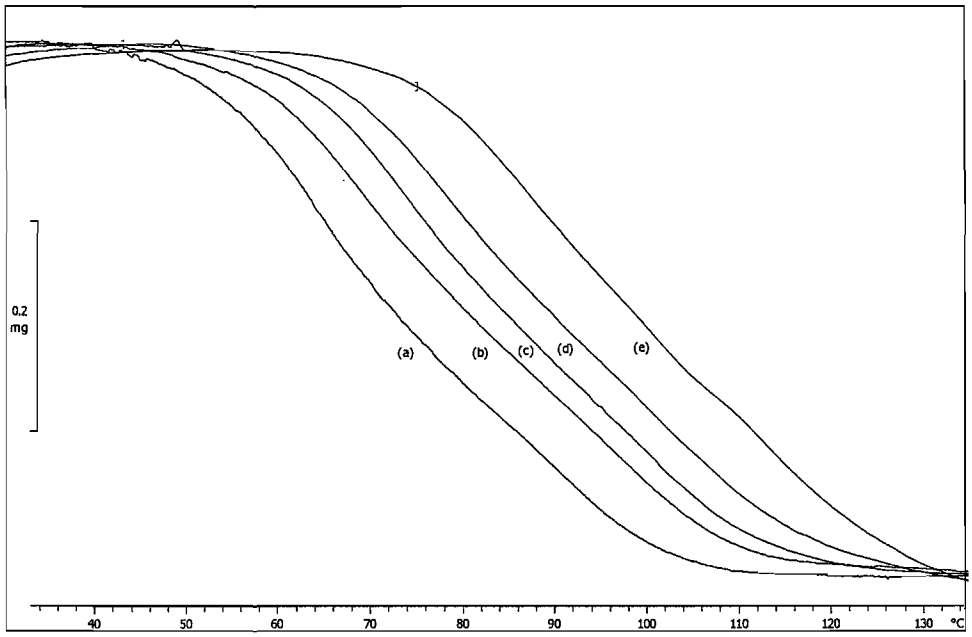
The dehydration activation energy (E_A) was calculated using the following equation and the derivatives thereof:

$$\log \beta = \log\left(\frac{AE_A}{R}\right) - 2.315 - 0.4567\left(\frac{E_A}{RT}\right) - \log g(\alpha)$$

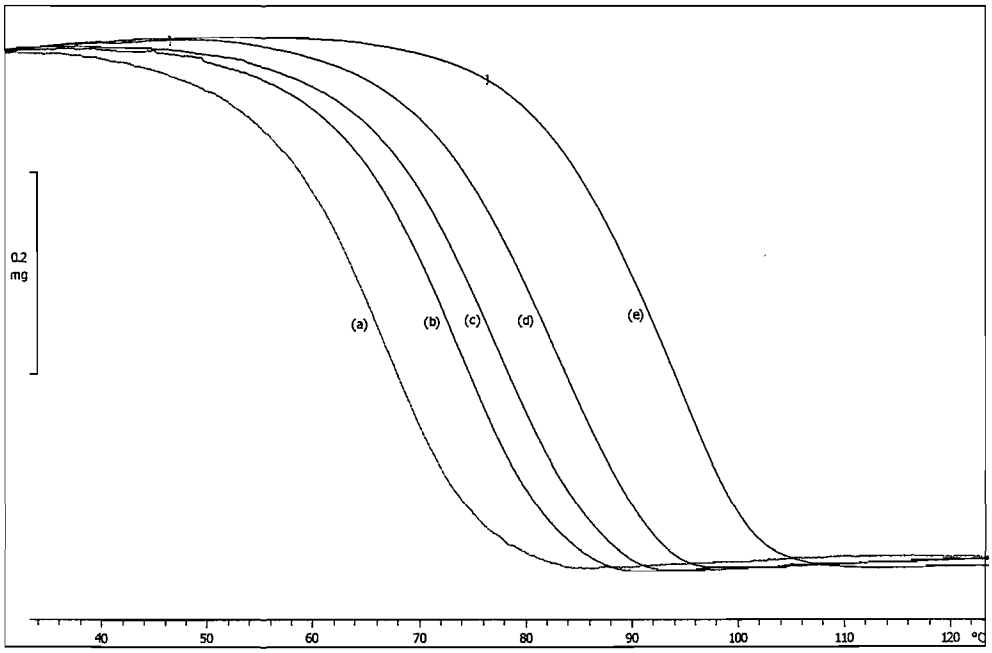
Where β is the heating rate ($K.min^{-1}$), A is the pre-exponential factor (min^{-1}), R is the universal gas constant (8.314 $J.mol^{-1}.K^{-1}$) and:

$$g(\alpha) = \left(\frac{AE_A}{\beta R}\right) P(x)$$

And $x = \frac{E_A}{RT}$



(i)



(ii)

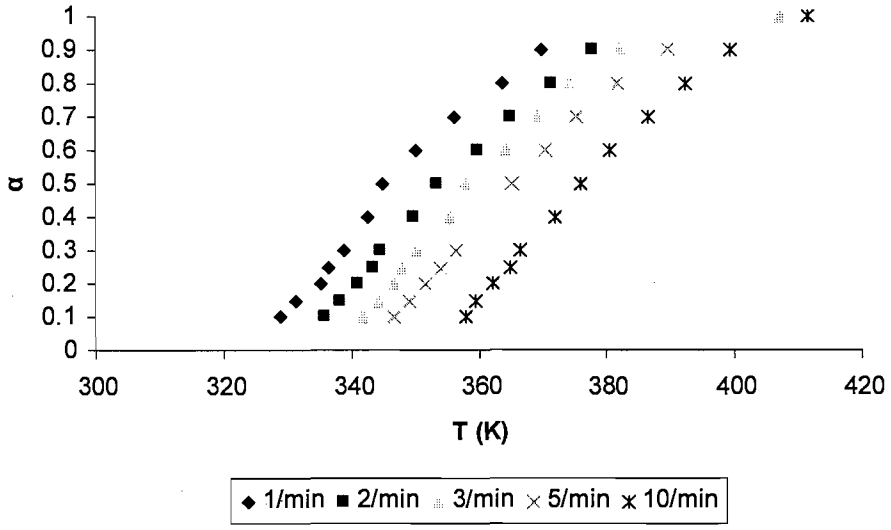
Figure 8.20 TGA thermograms of fluconazole (i) Form MH and the (ii) hydrated Form I at heating rates of (a) 1, (b) 2, (c) 3, (d) 5 and (e) 10°C/min.

α is the fraction reacted (i.e. dehydrated fraction), which was calculated using the following equation:

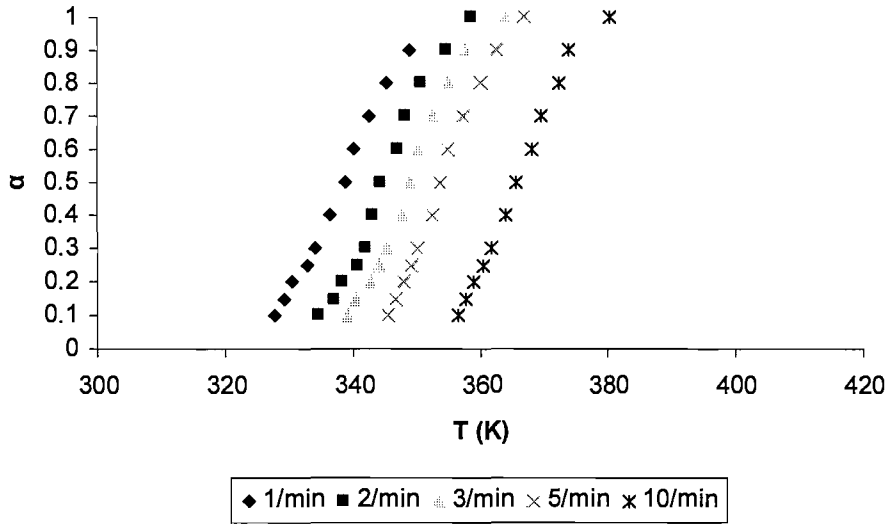
$$\alpha = \frac{(W_0 - W_t)}{(W_0 - W_f)}$$

Where W_0 is the initial mass of the sample, W_t the mass of the sample at temperature *t*, and W_f is the final mass at a temperature at which the mass loss of the sample is approximately unchanged.

The plots of dehydrated fraction (α) versus the absolute temperature (T) for Form MH and the hydrated Form I at various heating rates (β) are depicted in figure 8.21.



(a)



(b)

Figure 8.21 The plots of dehydrated fraction (α) versus the absolute temperature (T) for (a) Form MH and the (b) hydrated Form I at various heating rates: 1, 2, 3, 5 & 10 °C/minute.

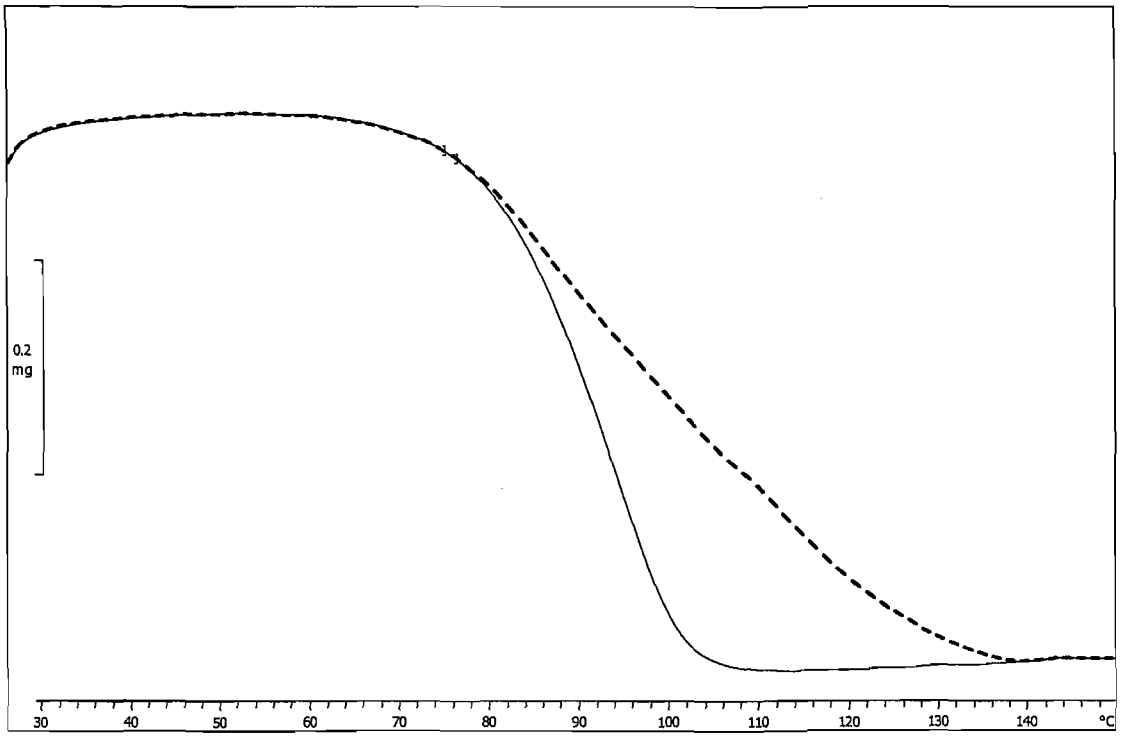
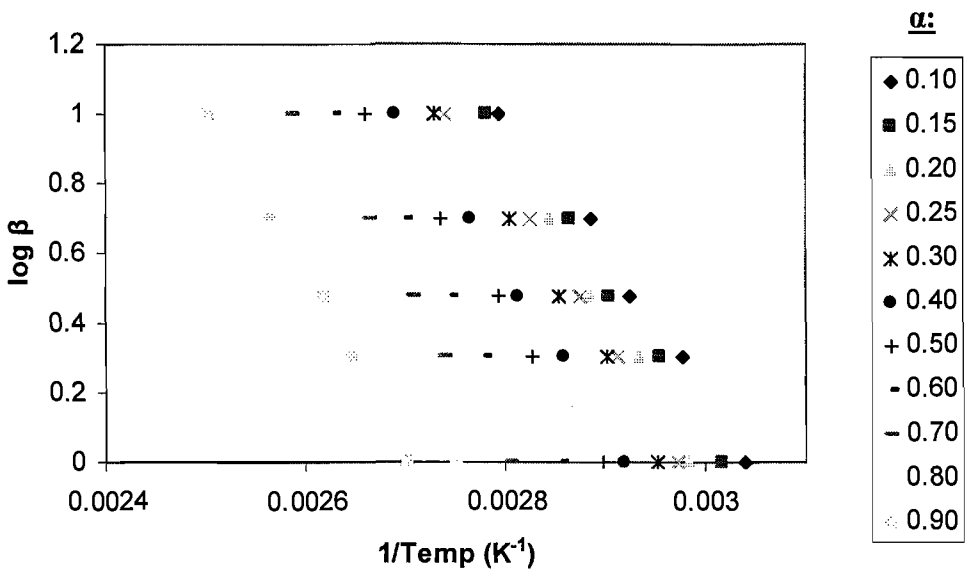


Figure 8.22 TGA thermograms of fluconazole Form MH (-------) and the hydrated Form I (_____) at a heating rate (β) of 10°C/minute.

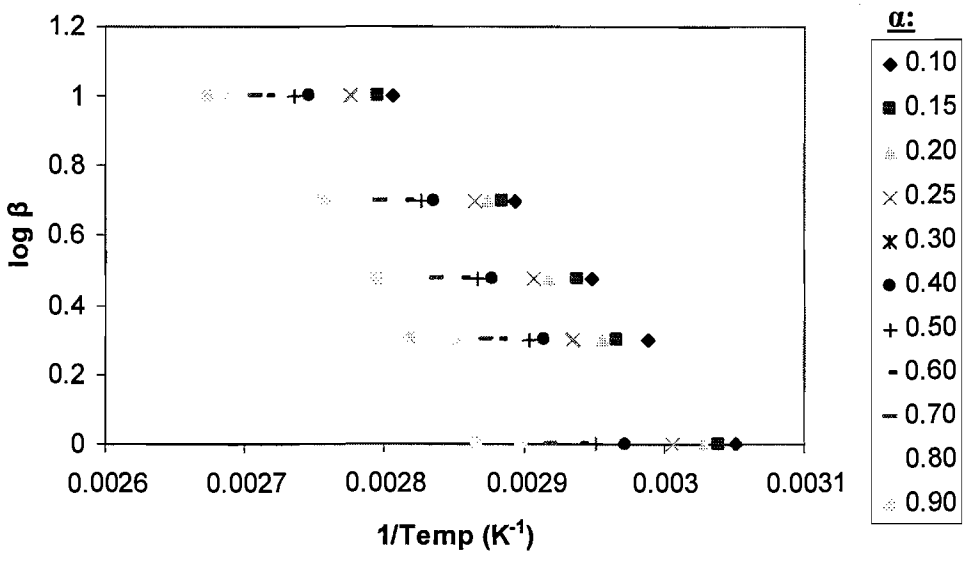
Figures 8.21 indicated that the dehydration process in both crystal forms was initiated at T > 320 K and that the dehydration process in the Form MH sample terminated at higher a temperature (T > 380 K) compared to that observed for the hydrated Form I (T < 380 K).

Plots of log β versus 1/T for Form MH and the hydrated Form I gave parallel lines for each α value (figure 8.23). The dehydration activation energies for the two samples were calculated from the slopes (m) of these parallel lines using the following calculation:

$$m = \frac{-0.4567\, E_A}{R}$$



(a)



(b)

Figure 8.23 Plots of log β versus 1/T for (a) Form MH and the (b) hydrated Form I for each α value ranging between 0.10-0.90.

The dehydration activation energy for the hydrated Form I was found to be 0.4 kJ/mol higher compared to that of monohydrate Form MH (table 8.6).

Table 8.4 Dehydration activation energy (E_A) calculated from the Ozawa method for fluconazole Form MH and the hydrated Form I

Form MH	Hydrated Form I
81.9±5.9 kJ/mol	82.3±5.6 kJ/mol

The DSC thermogram of Form MH (figure 8.16) revealed a sharp endotherm at 101°C (ΔH_{trans}=1.33±0.22 kJ/mol) which could be attributed to an endothermic rearrangement of the dehydrated lattice to transform in the thermodynamic stable Form I (section 7.2.2.4.2) rather than a sheer dehydration endotherm as suggested by previous authors [Alkhamis *et al.*, (2002:496)]. However, this endotherm was not detected in the DSC thermogram of the hydrated Form I.

VT-XRPD studies (figure 8.24) revealed that the stabilisation of the dehydrated lattice of the hydrated Form I was concluded at a lower temperature (85°C) compared to that observed for Form MH (130°C), suggesting that the dehydration and endothermic rearrangement occurred simultaneously (for the hydrated Form I), contributing the slightly higher dehydration activation energy observed for the hydrated Form I, and the absence of the rearrangement endotherm in the DSC thermogram of the hydrated Form I at 101°C.

The effect of the dehydration on the surface properties of Form MH is illustrated in figure 8.25.

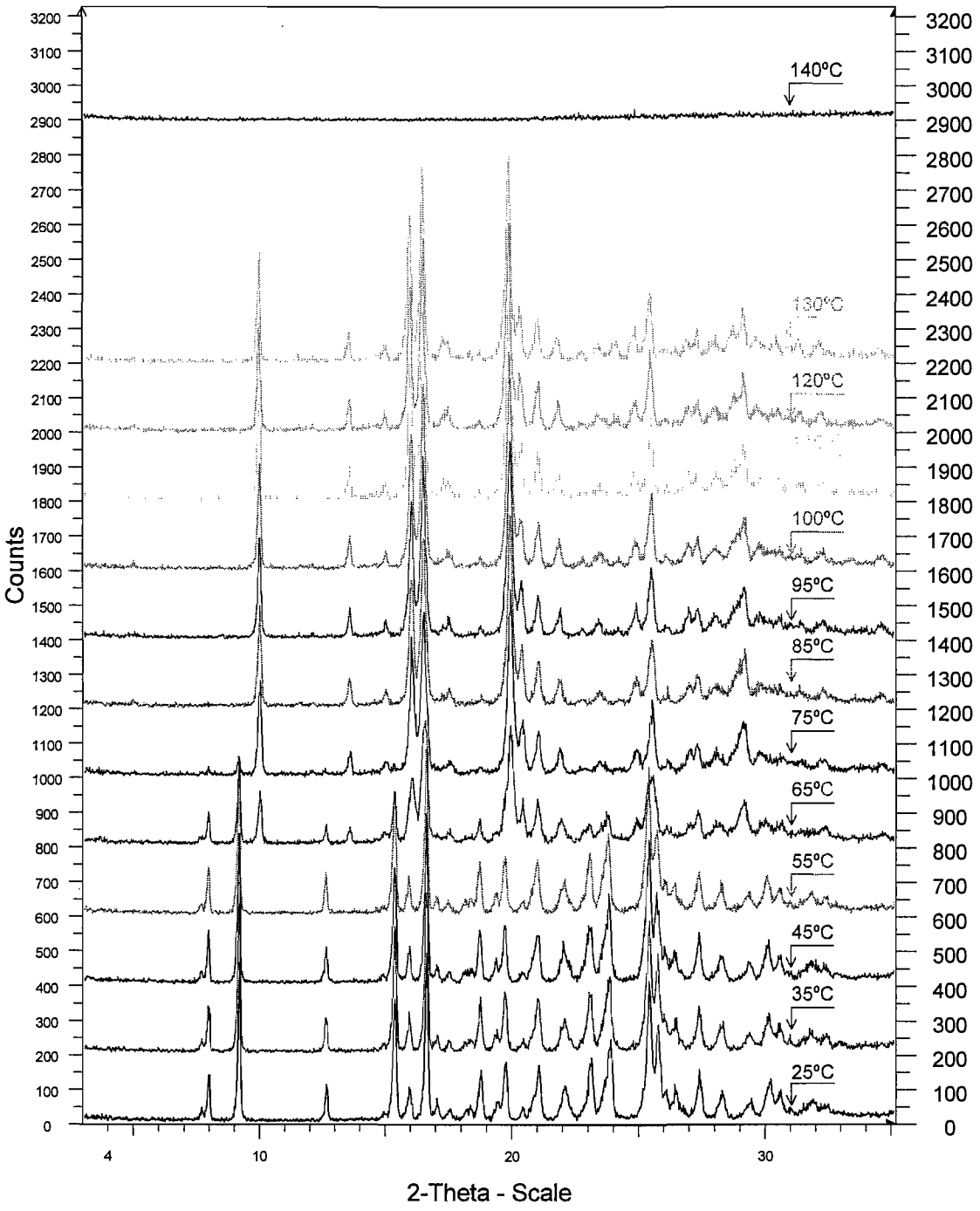


Figure 8.24 Overlay of the VT-XRPD patterns for hydrated Form I sample of fluconazole at increased temperatures ranging between 25-140°C.

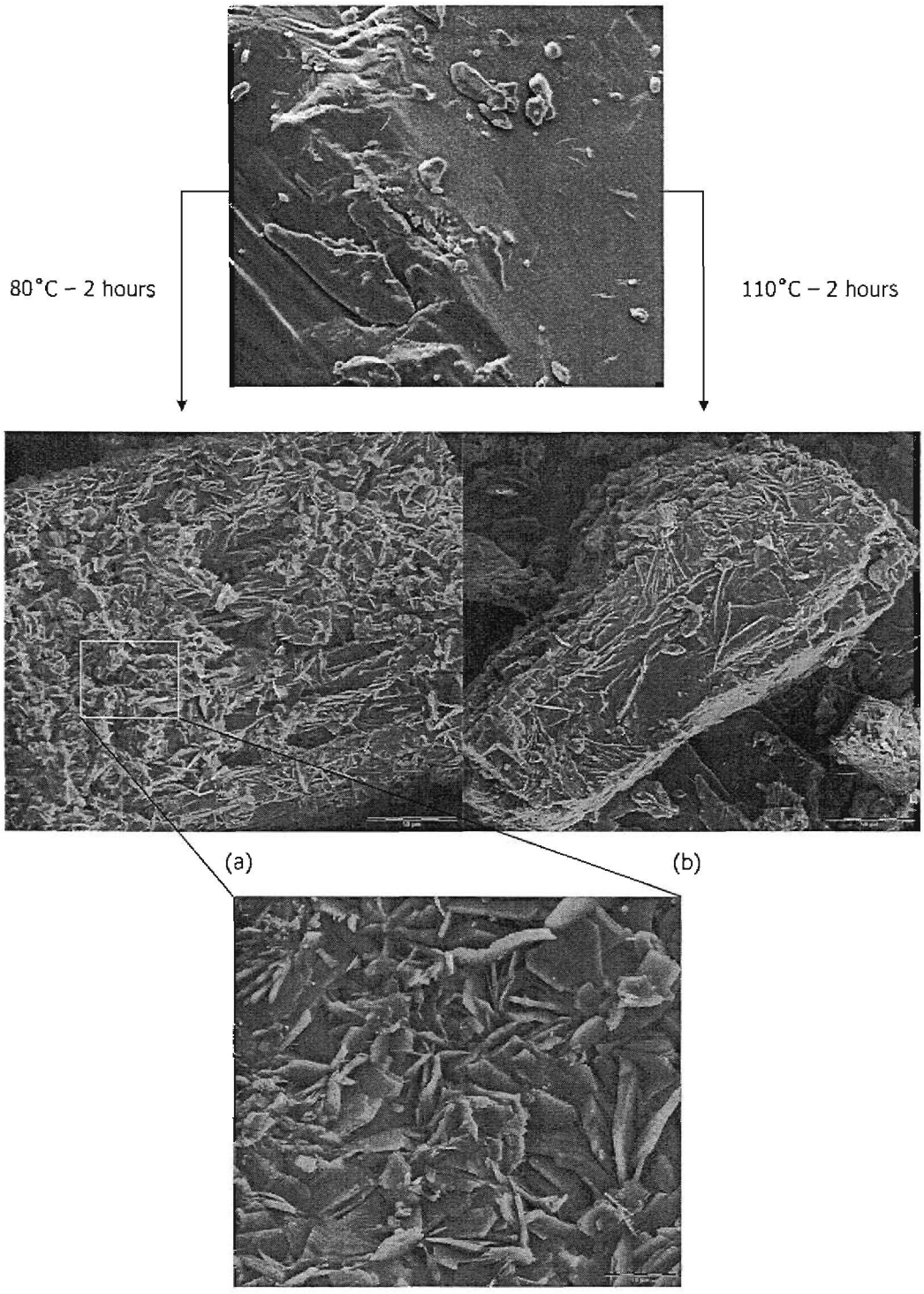


Figure 8.25 SEM photomicrograph of fluconazole Form MH (top) at ambient conditions. SEM photomicrographs after exposure to 80°C (a) and 110°C (b) for 2 hours, (c) is a magnification of the surface of the sample exposed to 80°C for 2 hours.

From figure 8.25 it is clear that dehydration of Form MH caused a disruption in the initial smooth surface of the crystal producing a rough, conglomerated surface. Once the sample has been heated past the crystal rearrangement temperature (101°C) the surface of the crystal is transformed into a more flattened surface with plate-like structures stacked upon each other, similar to that observed for the recrystallised Form I (figure 8.2).

8.3 Summary of results

Hydration of the anhydrous form of fluconazole (Form I) to produce Form MH should be prevented during the storage of the raw material and manufacturing of dosage forms to ensure the optimal bio-availability of this antifungal, due to the fact that the dissolution rate of anhydrate (Form I) is higher compared to that of the monohydrate, Form MH (Khouloud *et al.,* 2002:501).

This study revealed that the monohydrated crystal from (Form MH) and the anhydrous form (Form I) remained stable when exposed to 0-85% RH (30°C) and 0-75% RH respectively. When Form I was exposed to 30°C – 85% RH it showed an affinity for water molecules, and incorporated the water molecules into the crystal lattice. The water absorption induced a polymorphic conversion, and the physico-chemical properties of the hydrated crystal form were found to be comparable to that of Form MH (figure 8.26).

The XRPD pattern, moisture content and IR-spectrum of the hydrated Form I was comparable with that of monohydrate, Form MH. However, the DSC thermogram of the hydrated Form I did not reveal the rearrangement endotherm at 101°C, which is characteristic to the recrystallised Form MH (table 8.7).

When the dehydration process of the hydrated Form I and Form MH was compared it became clear that the activation energy for dehydration of the hydrated Form I was slightly higher compared to that for Form MH due to the fact that the dehydration and endothermic rearrangement event occurred simultaneously (for the hydrated Form I), contributing the slightly higher

dehydration activation energy observed for the hydrated Form I, explaining the absence of the rearrangement endotherm in the DSC thermogram of the hydrated Form I at 101°C.

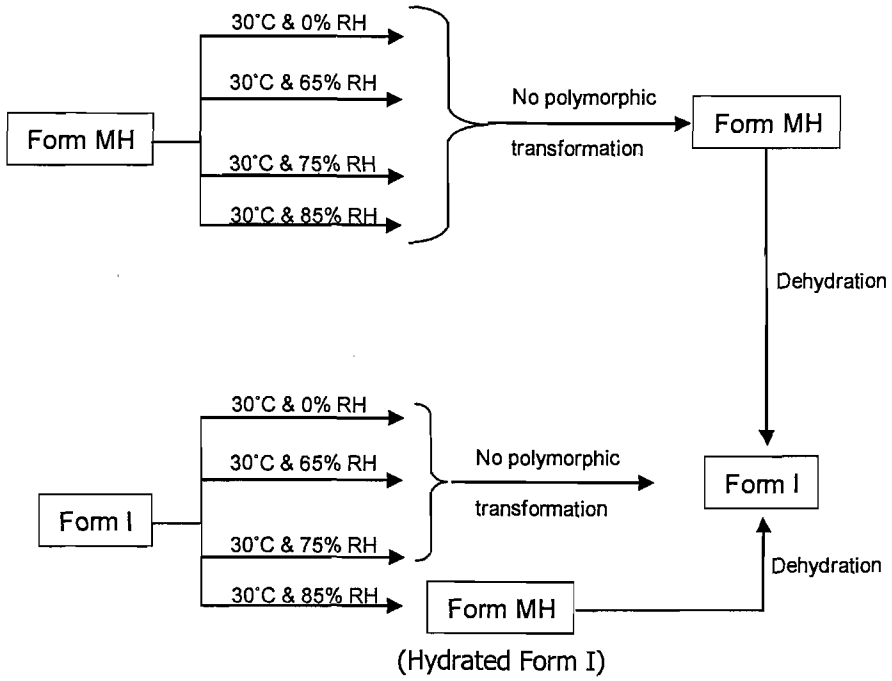


Figure 8.26 Schematic presentation of fluconazole Form I and Form MH stability when exposed to 0, 65, 75 and 85% RH at 30°C for 28 days.

VT-XRPD studies also revealed that the dehydration process for the hydrated Form MH terminated at a lower temperature (85°C) compared to that for Form MH (130°C), suggesting that the bond-strength between the incorporated water molecules and the fluconazole molecules in the hydrated Form I lattice was weaker compared to that in the recrystallised monohydrate (Form MH). Moisture sorption studies revealed that the desorption isotherm of Form MH (figure 8.3) showed that dehydration occurred at RH < 5.0 %, thus supporting that the hydrated Form I was less stable compared to the recrystallised, monohydrate, Form MH. When the hydrated Form I and monohydrate (Form MH) was

dehydrated by means of heat, both converted to the thermodynamic stable Form I.

Table 8.7 Properties of the hydrated Form I and Form MH

	Form MH	**Hydrated Form I**
XRPD patterns:	Comparable XRPD patterns	
IR spectra:	Comparable IR spectra	
DSC thermograms:		
• Dehydration endotherm range:	50-90°C	50-90°C
• Rearrangement endotherm:	101°C	None
• Melting point:	139-141°C	139-141°C
VT-XRPD pattern:		
• Dehydration commenced at:	50°C	65°C
• Dehydration terminated at:	130°C	85°C
Dehydration activation energy:	81.9±5.9 kJ/mol	82.3±5.6 kJ/mol

Conclusion

Due to the thermodynamic stability and favoured dissolution profile of Form I, it is considered to be the crystal form of choice for pharmaceutical manufacturing, compared to Form MH. However, this chapter revealed that Form I converts to the Form MH when exposed to relative humidities > 85%. It can thus be suggested that Form I should be protected from high humidity conditions to prevent the hydration thereof that might jeopardize the optimal bio-availability of this antifungal.

Form MH did not reveal any significant moisture sorption and could be considered non-hygroscopic.

CHAPTER 9

Summary and Conclusion

The vast majority of pharmaceutical dosage forms that are available for administration are presented as solid dosage forms. The implementation of Quality Assurance Systems (QAS) and Good Manufacturing Procedures (GMP) in the manufacturing process of these solid dosage forms require that the crystalline form used during manufacturing should be well interrogated prior to the use thereof to ensure the safety and efficacy of the final product. These quality measures aim to refine and control the manufacturing process and were instated by national and international governing bodies.

Chapter 1 provided a short introduction to the art of crystal engineering (polymorphism, pseudopolymorphism, amorphism and pharmaceutical co-crystals) and indicated that the structure adopted by a given compound would have a profound effect on the physico-chemical properties of the solid. To avoid inter-batch variations during the manufacturing process the thermodynamic relationship (monotropic or enantiotropic) between the various crystalline forms of API's should be well understood and used to ensure the stability of the favoured crystal form in the final dosage form.

Chapter 1 also highlighted the importance of the early and comprehensive exploration of novel crystalline forms to enable pharmaceutical companies to take a proactive and value-maximizing approach to product life cycle management and to secure appropriate and timely intellectual property protection of the newly identified crystal forms.

The complexity of polymorphic interconversions emphasized the need for a well defined study to characterize and explore the effect of heat and moisture on the stability of polymorphic forms. It was decided to embark on such studies for venlafaxine HCl (freely water soluble), fluconazole (slightly water soluble) and mebendazole (practically insoluble in water).

A complementary battery of tests was used to identify, characterise, and evaluate the influence of moisture and heat on the solid state properties of the mentioned API's (Chapter 2).

PART I – Mebendazole

Mebendazole polymorph A has no anthelmintic activity when administered alone or when present above 30% in polymorphic mixtures (Ren *et al.* 1987:356). It is troublesome to report that three of the seven mebendazole containing tablet products which are available in South Africa contained traces of polymorph A.

From the results presented in Chapter 3 it became clear that (i) moisture and increased temperatures and the (ii) presence of polymorph A traces in the product played an integral role in the thermodynamic stability of mebendazole polymorph C, which influenced the dissolution behaviour significantly. The polymorph C → A conversion in the tablets caused a significant decrease in the rate and extend of the mebendazole dissolution.

The fact that the current USP (2007) dissolution test conditions are not able to distinguish between the dissolution properties of the various mebendazole polymorphs could easily hoax manufacturers during stability testing trials by suggesting that the mebendazole polymorph C remains stable in the product due to the fact that no changes in the dissolution behaviour of the tablets are detected.

(i) Effect of moisture on stability of mebendazole polymorph C in tablets

When the tablets of Product 2 were removed from their blisters and stored at 30°C & 65% RH polymorphic transitions were observed after 5 months (traces of mebendazole polymorph A were detected in the tablets) which lowered the rate and extend of dissolution of the tablets.

The rate of the polymorph C → polymorph A conversion was investigated and found to be higher for tablets stored at 40°C & 75% RH, compared to the

samples at 30°C & 65% RH. After 4 months polymorphic transitions in Product 2 caused significant changes in the dissolution profiles of the samples.

(ii) Effect of traces of mebendazole polymorph A in the product on stability of mebendazole polymorph C in tablets

Products (Products 2, 4 and 7) which did not contain any traces of polymorph A did not reveal any polymorph C → polymorph A transformations when stored at 30°C & 65% RH for 6 months. Products which contained traces of polymorph A revealed a higher rate of polymorph transformation (polymorph C → polymorph A) compared to those who initially contained only polymorph C. This fact reinforces the importance for manufacturers to ensure that the initially procured mebendazole raw material is 100% pure polymorph C, and free from polymorph A traces.

Product 7 didn't contain any traces of mebendazole polymorph A and was packed in a HDPE securitainer. This product did not reveal any polymorph transformation when stored at 30°C & 65% RH nor at 40°C & 75% RH for 6 months. It was postulated that the stability of this formulation could be attributed to the fact that the polymorph C fraction in Product 7 was protected from moisture-induced polymorph transition by a dual mechanism: (1) the formulation contained monohydrate lactose (a less hygroscopic tablet excipient) and (2) was stored in a container with low water vapour permeation (i.e. HDPE securitainer).

The transpiring parasitic-resistance towards mebendazole and the distressing consequences thereof urges medical practitioners to promote patient compliance when mebendazole is prescribed as choice drug. This study highlighted the importance to ensure that mebendazole products contain the active polymorph i.e. polymorph C, and to ensure the stability of the polymorph in the pharmaceutical dosage form to ensure the efficacy and safety of the mebendazole. It is suggested that the current monographs should include a polymorphic identification (via DRIFT-IR) as a compulsory test during stability testing of mebendazole containing products to limit the

polymorph A content allowed in tablets in accordance with ICH-guidelines (ICH, 1999:27 – see section 1.3).

Aqueous mediate phase transformation of mebendazole polymorphs B and C

The influence of moisture and heat on the stability of the metastable polymorphs of mebendazole (i.e. polymorph C and polymorph B) was further investigated in Chapter 4 which revealed that moisture was indeed a catalyst for the transformation process.

When mebendazole polymorph C was exposed to increased temperatures (5 - 100°C) for a period of 75 hours no polymorphic conversions were observed. However, in the presence of moisture (water) polymorphic transformations were observed at 100°C after only 25 hours, which produced polymorph A as final product after 50 hours. The presence of the polymorph B traces in the samples could be attributed to the solvent mediated transformation of polymorph C which led to the formation of the thermodynamically least stable form (i.e. polymorph B). It is know that a system will always tend to produce only the most stable form (i.e. polymorph A), thus converting the most soluble form (i.e. polymorph B) to the most stable (least soluble) form, i.e. polymorph A (Byrn *et al.,* 1999:18-19). Thus the polymorph B traces will undergo rapid conversion to the more stable polymorphic forms, i.e. polymorphs A and C.

When mebendazole polymorph B was exposed to increasing temperatures (for a period of 75 hours) it did not reveal any polymorphic transition. In the presence of moisture (water), polymorphic transformations were observed at 50°C after 25 hours, when traces of polymorph C were detected in the samples, thus suggesting that polymorph B converted to polymorph C. After 75 hours the sample primarily consisted of mebendazole polymorph C and traces of mebendazole polymorph B.

The exposure of suspended mebendazole polymorph B to 100°C revealed that a fraction of polymorph B transformed into polymorph C. The IR spectrum of the sample stored at 100°C for 25 hours suggested that the sample consisted primarily of mebendazole polymorph C and traces of

mebendazole polymorphs A and B: polymorph C >>> polymorph A >>> polymorph B. The XRPD pattern of the sample for 75 hours resembled that of mebendazole polymorph A.

In addition, the formation of polymorph A from polymorph B was delayed with a $t_{0.5}$ = 28 hours and an even longer transition time of more than 12 hours and almost no induction period which suggested that polymorph B transformed to polymorph C which then transform to polymorph A.

Future studies will focus on the influence of water and water-associated excipients in tablets and the choice of suitable suspending agents for suspensions.

In parts II and III of this study, we focused on the solid state properties of two newer API's (i.e. venlafaxine HCl and fluconazole) and the effect of moisture on the thermodynamic stability of different crystal forms of the mentioned API's.

PART II – Venlafaxine HCl

A new crystal form of venlafaxine HCl (Form 5) was successfully prepared and characterised in chapter 5. Form 5 revealed preferred orientation due to its anisotropic morphology, and it was revealed that the dissolution of the venlafaxine HCl Form 1 and Form 5 in water was an exothermic reaction ($\Delta H < 0$), and that an increase in temperature decreases the solubility of the polymorphic forms.

Form 1 did not reveal any polymorphic transformation when exposed to increased temperatures, however From 5, underwent an internal-crystal rearrangements when heated to 90-100°C. Form 5 was classified as a metastable polymorph of venlafaxine HCl which is enantiotropically related to Form 1, due to the fact that: (i) the theoretical solubility ratio (Si/Sii) was calculated to be greater than one (>1), (ii) The linear correlation between the plot of the predicted solubility ratios (Si/Sii) vs. 1/temperature for the two polymorphs (Form 5 and Form 1) and (iii) the higher melting form (Form 5) revealed a lower heat of fusion compared to the lower melting form (Form 1).

Thermal studies indicated that the polymorphic conversion product of Form 5 is temperature dependant. When Form 5 was heated to 175°C it converted to Form 2, when exposed to 150°C for two hours it converted to Form 1. Exposure of Form 5 crystals to 150°C (for two hours) revealed that a fraction of the Form 5 crystals converted into Form 1, thus indicating that Form 5 is a meta-stable form and confirming that Form 1 is the thermodynamically most stable form.

Figure 9.1 provides a schematic presentation of the thermodynamic stability of venlafaxine HCl Forms 1 and 5.

Exposure of venlafaxine HCl Form 1 to moisture did not induce any polymorphic transition. However the metastable form, Form 5 (with a specific surface area 1.84 times greater compared to that of Form 1) *absorbed* moisture and transformed into a monohydrate when exposed to 85% RH at 30°C.

When Form 5 was stored at 0% RH a fraction thereof converted to the thermodynamic stable Form 1.

When Form 5 was stored at 65% RH the inter-crystal rearrangement at 75-100°C became more prominent in the DSC thermograms of the samples. Variation of the position of the thermal rearrangement endotherm in the DSC thermograms could be attributed to the fact that Form 5, when stored at 30°C & 65% RH, revealed a meta-stable phase which was temperature dependant, where the amount of energy needed for the inter-crystal rearrangement (ΔH_{trans}) varied between the samples. This suggested that the meta-stable phase (possibly induced by the adsorbed water, which acted as molecular loosener) influenced the thermal behaviour significantly causing unpredictable thermal events which can be classified into three groups. The XRPD and DRIFT-IR spectra of the samples appearing in the three groups did not reveal any significant differences, suggesting that the variable thermal behaviour was caused by differences in the thermodynamic stabilities of the three groups, and was not primarily related to differences in the structural properties of their lattices.

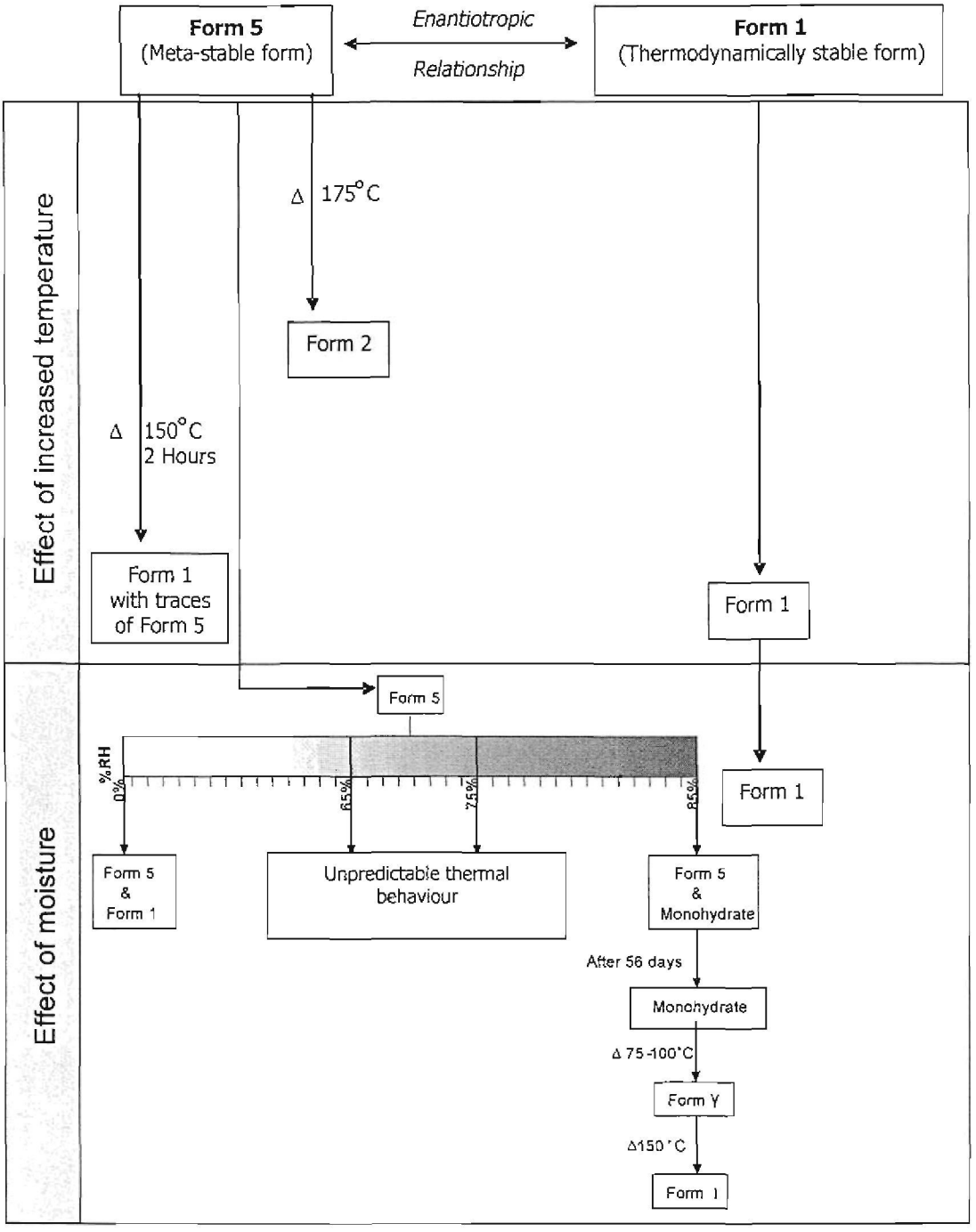


Figure 9.1 A schematic presentation of the thermodynamic stability of venlafaxine HCl Forms 1 and 5 and the effect of moisture on the stability of the mentioned crystal forms.

When Form 5 was stored at 75% RH it adsorbed moisture ranging between 0.71-1.32 % (m/m). The appearance of a diffraction peak in the XRPD pattern at 8.6 - 8.7 °2θ (with low intensities) suggested the possible

incorporation of water within the crystal lattice to form a monohydrate. The samples stored at 75% RH also revealed unpredictable thermal behaviour as the samples stored at 65% RH did.

The polymorphic conversion of Form 5 when exposed to 85% RH – 30°C (anhydrous form → monohydrated form) was accompanied by a morphological change to accommodate the absorbed water molecules in the hydrated Form 5. The avicular (i.e. needle-like) crystal structure of Form 5 transformed into a fibrous (i.e. needle-like particles which are very thin) structure. The XRPD patterns, DRIFT-IR spectra and DSC and TGA spectra confirmed the systematic incorporation of water molecules into the crystal lattice after 9 days. An increase in the T_{50} values indicated the stabilisation of the water molecules into the crystal lattice. Kinetics studies (using XRPD) revealed that the hydration process of Form 5 was a zero order reaction.

VT-XRPD studies revealed that when the hydrated Form 1 was heated to 100°C dehydration occurred and an anhydrous lattice was produced with a XRPD pattern comparable to that of Form γ. When heated to 150°C the Form γ sample converted to the thermodynamic stable, Form 1.

It is recommended that Form 1 should be used for pharmaceutical manufacturing, due to its thermodynamically stable profile and permanence when exposed to increased relative humidities.

PART III – Fluconazole

Chapter 7 provided an overview of the polymorphic behaviour of fluconazole and described the physico-chemical properties of the anhydrous Form I and monohydrate (Form MH) investigated in this study.

VT-XRPD studies confirmed that fluconazole Form I is the thermodynamic stable form, and that Form MH converted to Form I upon dehydration.

Khouloud *et al.* (2002:501) indicated that the dissolution rate of anhydrate, Form I, was higher compared to that of the monohydrate, Form MH. The dissolution rate constant of the monohydrate was 15% higher compared to that of Form I. Form I is thus the preferred crystal form to be used in pharmaceutical dosage forms due to its thermodynamic stability (section 7.2.2.4.1) and the favoured dissolution behaviour thereof. Hydration of the anhydrous Form I to produce Form MH should be prevented during the storage of the raw material, manufacturing of dosage forms, to ensure the optimal bio-availability of this antifungal.

This study revealed that the monohydrated crystal from (Form MH) and the anhydrous form (Form I) remained stable when exposed to 0 - 85% RH - 30°C and 0 - 75% RH – 30°C respectively. Upon exposure to 30°C – 85% RH, Form I incorporated water molecules into the crystal lattice and transformed into Form MH after 7 days (figure 9.2).

The dehydration mechanism of the hydrated Form I and Form MH was compared and revealed that the activation energy for dehydration of the hydrated Form I was slightly higher compared to that for Form MH due to the fact that the dehydration and endothermic rearrangement occurred simultaneously, contributing the slightly higher dehydration activation energy observed for the hydrated Form I, also explaining the absence of the rearrangement endotherm in the DSC thermogram of the hydrated Form I at 101°C. The rearrangement endotherm at 101°C is thus characteristic to the recrystallised Form MH.

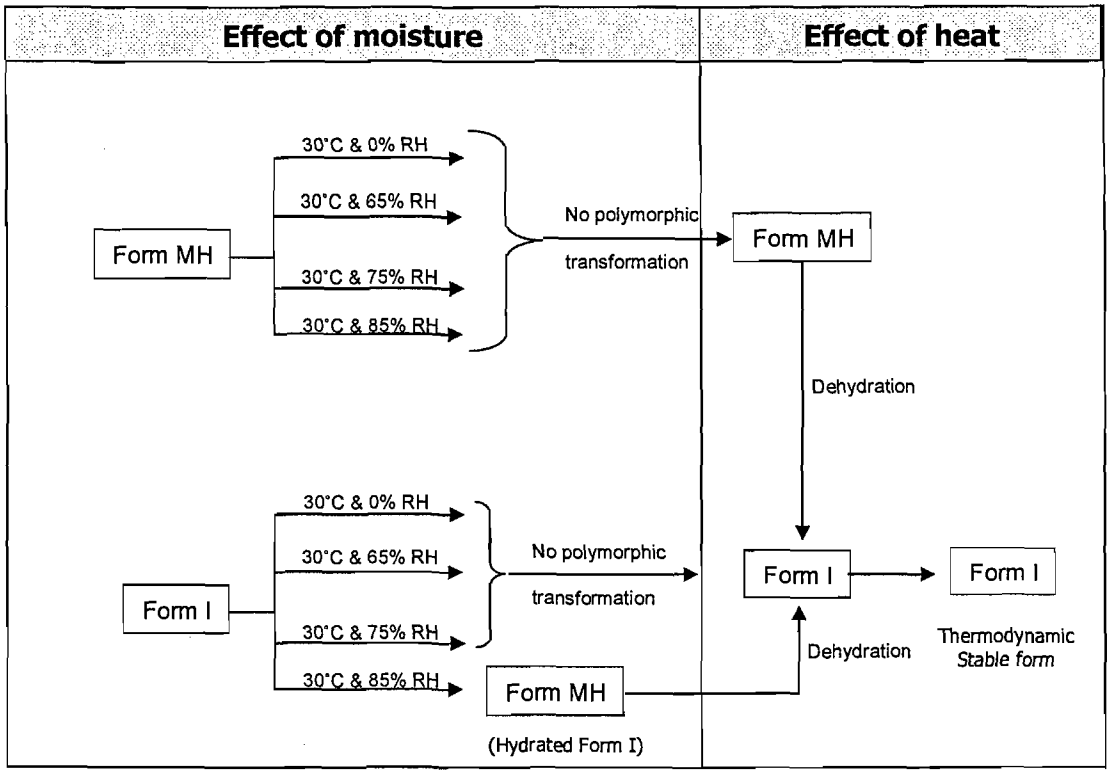


Figure 9.2 Schematic presentation of fluconazole Form I and Form MH stability when exposed to 0, 65, 75 and 85% RH at 30°C for 28 days.

VT-XRPD studies also revealed that the dehydration process of the hydrated Form I terminated at a lower temperature (85°C) compared to that for Form MH (130°C), suggesting that the bond-strength between the incorporated water molecules and the fluconazole molecules in the hydrated Form I lattice was weaker compared to that present in the recrystallised monohydrate (Form MH). Moisture sorption studies revealed that the desorption isotherm of Form MH showed that dehydration occurred at RH < 5.0 %, thus supporting that the hydrated Form I was less stable compared to the recrystallised, monohydrate, Form MH.

When the hydrated Form I and monohydrate (Form MH) was dehydrated, both converted to the thermodynamic stable Form I.

It can thus be suggested that Form I should be protected from high humidity conditions during manufacturing and storage to prevent the hydration thereof that might jeopardize the optimal bio-availability of this antifungal.

"There are many mysteries of nature that we have not yet solved. Hurricanes, for example continue to occur and often cause massive devastation. Meteorologists cannot predict months in advance when and with what velocity a hurricane will strike a specific community. Polymorphism is a parallel phenomenon. We know that it will probably happen. But not why or when. Unfortunately, there is nothing we can do today to prevent a hurricane from striking any community or polymorphism from striking any drug."

(Sun 1998 – referenced by Bernstein, 2002:241)

It is true that one can't always predict the behaviour of pharmaceuticals, however it remains the social responsibility of all pharmaceutical scientists to explore the rich mine-field of the solid state properties of pharmaceuticals to ensure the safety and efficacy of API's.

"After the discovery of the first cases of polymorphism with dramatic differences in biological activity between two forms of the same drug ... no pharmaceutical manufacturer could neglect the problem."

(Borka 1999 – referenced by Bernstein, 2002:241)

BIBLIOGRAPHY

AGBADA, C.O. & YORK, P. 1994. Dehydration of theophylline monohydrate powder: effects of particle size and sample weight. *International journal of pharmaceutics,* 106:33-40.

AIRAKSINEN, S., LUUKKONEN, P., JØRGENSEN, A., KARRJALAINEN, M., RANTANEN, J. & YLIRUUSI, J. 2003. Effects of excipients on hydrate formation in wet masses containing theophylline. *Journal of Pharmaceutical Sciences,* 92(2):516-528.

AIRAKSINEN, S., KARJALAINEN, M., KIVIKERO, N., WESTERMARCK, S., SHEVCHENKO, A., RATANEN, J. & YLIRUUSI, J. 2005. Excipient selection can significantly affect solid-state phase transformation in formulation during wet granulation. *AAPS Pharmaceutical Science and Technology,* 6(2):E311-E322.

A-KARIM, E.F.I., AHMED, M. H. & SALAMA, R.B. 1996. Studies on the thermal and photochemical decomposition of mebendazole. *International Journal of Pharmaceutics,* 142:251-255.

AL-BADR, A.A. & TARIQ, M. 1987. Mebendazole. (*In* Florey, K., *ed. Analytical Profiles of Drug Substances,* Fifteenth Volume. New York: Academic Press. pp. 292-326.

ALKHAMIS. K.A., A.A. OBAIDAT. & A.F. NUSEIRAT. 2002. Solid-State Characterization of Fluconazole. *Pharmaceutical Development and Technology,* 7(4):491-503.

AL-KURDI, Z., AL-JALLAD, T., BADWAN, A. & JABER, A.M.Y. 1999. High performance liquid chromatography method for determination of methyl-5-benzoyl-2-benzimidazole carbamate (mebendazole) and its main degradation product in pharmaceutical dosage forms. *Talanta,* 50:1089-1097.

ANDRADE, S.R.C., SCARMINIO, I.S., NERY, M.M.F. & de OLIVEIRA, A.C. 2003. Comparison of multivariate calibration method to determine simultaneously mebendazole-cambendazole and mebendazole-thiabendazole in pharmaceutical preparations by UV-visible specytophotometry. *Journal of Pharmaceutical and Biomedical Analysis,* 33:655-665.

AVRAMI, M. 1939. Kinetics of phase change. I: General theory. *The Journal of Chemical Physics,* 7:1103-1112.

AVRAMI, M. 1940. Kinetics of phase change. II: Transformation-time relations for random distribution of nuclei. *The Journal of Chemical Physics,* 8:212-224.

AVRAMI, M. 1941. Kinetics of phase change. III: Granulation, phase change, and microstructures. *The Journal of Chemical Physics,* 9:177-184.

BAUER, J., SPANTON, S., HENRY, R., QUICK, J., DZIKI, W., PORTER, W. & MORRIS, J. 2001. Ritonavir: an extraordinary example of conformational polymorphism. *Pharmaceutical Research,* 18(6):859-866.

BAUER, J., MORLEY, J., SPANTON, S., LEUSEN, F.J.J., HENRY, R., HOLLIS, S., HEITMANN, W., MANNINO, A., QUICK, J. & DZIKI, W. 2006. Identification, preparation and characterization of several polymorphs and solvates of terazosin hydrochloride. *Journal of Pharmaceutical Sciences,* 95(4):917-928.

BENNET, J.E. 1996. Antimicrobial agents. (*In* Hardman, J.G. & Limbird, L.E., *ed. Goodman & Gilman's The pharmacological basis of therapeutics,* Ninth Edition. New York: McGraw-Hill. 1905p.

BERNSTEIN, J. 2002. *Polymorphism in molecular crystals.* Oxford: Clarendon press. 410p.

BETTINETTI, G., SORRENTI, M., CATENACCI, L., FERRARI, F. & ROSSI, S. 2006. Polymorphism, pseudopolymorphism, and amorphism of peracetylated α-, β-, and γ-cyclodextrins. *Journal of Pharmaceutical and Biomedical Analysis,* 41:1205-1211.

BLABBER, M. 2006. Chemical Thermodynamics: Gibbs Free Energy (Gibbs Energy). [Web] http://wine1.sb.fsu.edu/chm1046/notes/Thermody/Gibbs/Gibbs.htm. [Date of access: 11 November 2006].

BLOMSMA, E. 2006. Drug life cycle management through solid form discovery – the new game in the industry. *Drug development. Clinical Outsourcing,* (1):32-43.

BOLDYREVA, E.V., DMITRIEV, V. & HANCOCK, B.C. 2006. Effect of pressure up to 5.5 GPa on dry powder samples of chlorpropamide form-A. *International Journal of Pharmaceutics,* 327(1-2):51-57.

BP see BRITTISH PHARMACOEPIAE.

BRITS, M. 2003. Crystal polymorphism and pseudopolymorphism of Venlafaxine hydrochloride. Potchefstroom: Potchefstroom University for Christian Higher Education (PU for CHE). (Dissertation – M.Sc.) 212p.

BRITTAIN, H.G. 2007. Polymorphism and solvatomorphism 2005. *Journal of Pharmaceutical Sciences,* 96(4):705-728.

BRITTISH PHARMACOEPIAE. 2007. London : HMSO. 2473p.

BROWN, M.E. & GLASS, B.D. 1999. Pharmaceutical applications of the Prout-Tompkins rate equation. *International Journal of Pharmaceutics,* 190:129-137.

BUNACIU, A.A., FLESCHIN, S. & ABOUL-ENEIN, H.Y. 2002. Analysis improvement of drugs using modern methods. *Romanian biotechnology letters,* 7(2):647-654.

BURGER, A. & RAMBERGER, R. 1979a. On the polymorphism of pharmaceuticals and other molecular crystals. Theory of thermodynamic rules. *Mikrochimica Acta,* II:259-272.

BURGER, A. & RAMBERGER, R. 1979b. On the polymorphism of pharmaceuticals and other molecular crystals. *Mikrochimica Acta,* II:273-316.

BURGER, A. 1982a. Thermodynamic and other aspects of polymorphism of drug substances. *Pharmaceutical International Journal,* 3:158-163.

BURGER, A. 1982b. Interpretation of polymorphism studies. *Acta Pharmaceutics and Technology,* 28:1-20.

BYRN, S., PFEIFER, M., GANEY, M., HOIBERG, C. & POOCHIKIAN, G. 1995. Pharmaceutical solids: a strategic approach to regulatory considerations. *Pharmaceutical Research,* 12(7):945-954.

BYRN, S.R., PFEIFFER, R.R. & STOWELL, J.G. 1999. Solid State Chemistry of drugs. 2nd edition. West Lafayette, Indiana: SSCI Inc. 576p.

CAHN, J.W. 1999. Challenges of Paradigm Building for Solid-State Transformations. PTM'99, *The Japan Institute of Metals,* p.3-14.

CAIRA, M.R., ALKHAMIS, K.A. & OBAIDAT, R.M. 2004. Preparation and characterization of a polymorph, monohydrate and an ethyl acetate solvate of the antifungal fluconazole. *Journal of pharmaceutical sciences,* 93(3):601-611.

CAIRA, M.R., DEKKER, T.G. & LIEBENBERG, W. 1998. Structure of a 1:1 complex between the anthelmintic drug mebendazole and propionic acid. *Journal of Chemical Crystallography,* 28(1):11-15.

CAIRA, M.R., PIENAAR, E.W. & LÖTTER, A.P. 1996. Polymorphism and pseudopolymorphism of the antibacterial nitrofurantoin. *Molecular Crystals and Liquid Crystal Science and Technology,* 279:241-264.

CAMBRIDGE STRUCTURAL DATABASE AND STRUCTURAL DATABASE SYSTEM. 2002. Version 5.24. Cambridge, UK: Cambridge Crystallographic Data Centre. University Chemical Laboratory.

CHAN, H.K. & DOELKER. E. 1985. Polymorphic transformation of some drugs under compression. *Drug Development and Industrial Pharmacy,* 11:315-332.

CARDEW, P.T & DAVEY, R.J. 1985. The kinetics of solvent-mediated transformations. *Proceedings of the Royal Society of London, Series A, Mathematical and Physical Sciences,* 389(1815):415-428.

CASTILLO, R. 2003. Synthesis and antiparacitic activity of albendazole and mebendazole analogues. *Bio-organic and Medicinal Chemistry,* 11:4615-4622.

CHAROENLARP, P., WAIKAGUL, J., MUENNOO, C., SRINOPHAKUN, S. & KITAYAPORN, D. 1993. Efficacy of single-dose mebendazole polymorphic forms A and C, in the treatment of hookworm and *Thrichuis* infections. *South-east Asian Journal of Tropical Medicines and Public Health,* 24:712-716.

CHRISTIAN, J.W. 1975. The Theory of Transformation in Metals and Alloys. 2nd edition, Part I. New York: Pergammon 479p.

CLEMENTE, R.A. & SALEH, A.M. 2002. Crystallization kinetics: A solution for geometrical impingement. *Physics Review – B,* 65(13):132102-132105.

COSTA, J., FRESNO, M., GUZMAN, L., IGUAL, A., OLIVA, J., VIDAL, P., PEREZ, A. & PUJOL, A. 1991. Polymorphic form of mebendazole: Analytical Aspects & Toxicity. *Circular of Farm,* 49:415-424.

DASH. A.K. & W.F. ELMQUIST. 2001. Fluconazole. (*In* Analytical profiles of drug substances and excipients. 27. 67-113. New York: Academic Press).

DASH SOFTWARE. 2007. CCDC Software Ltd and CCLRC Mecury Dash. Cambridge Crystallographic Data Centre. Cambridge.

DAWOODBHAI, S. & RHODES, C.T. 1989. The effect of moisture on powder flow and on physical stability of tablets. *Drug Development and Industrial Pharmacy,* 15(10):1577-1600.

DEBNATH, S. & SURYANARAYANAN, R. 2003. Influence of processing-induced phase transformations on the dissolution of theophylline tablets. *AAPS Pharmaceutical Sciences and Technology,* 5(1):1-11.

DESAI. S.R., SHAIKH. M.M. & DHARWADKAR. S.R. 2003. Thermoanalytical study of polymorphic transformation in fluconazole drug. *Thermochimica Acta,* 399:81-89.

DESCAMPS, M., WILLART, J.F., DUDOGNON, E. & CARON, V. 2007. Transformation of pharmaceutical compounds upon milling and comilling: the role of Tg. *Journal of Pharmaceutical Sciences,* 96(5):1398-1407.

DE VILLIERS, M.M., TERBLANCHE, R.J., LIEBENBERG, W., SWANEPOEL, E., DEKKER, T.G. & SONG, M. 2005. Variable-temperature X-ray powder diffraction analysis of the crystal transformation of the pharmaceutically preferred polymorph C of mebendazole. *Journal of Pharmaceutical and Biomedical Analysis,* 38:435-441.

DE VILLIERS, M.M., VAN DER WATT, J.G. & LÖTTER, A.P. 1991. The conversion of the polymorphic forms of chloramphenicol palmitate (CAP) as a function of environmental temperature. *Drug Development and Industrial Pharmacy,* 17(10):1295-1303.

DOLLERY, C. 1999. Fluconazole. (*In.* DOLLERY, C. *ed.* Therapeutic drugs, 2nd Ed. 1999). London : Churchill Livingstone. f62-f68.

EROFEEV, B.V. 1946. Generalized equation of chemical kinetics and its application in reactions involving solids. *Compt. Rend. Acad. Sci,* USSR (Dokl. Akad. Nauk SSSR) 52, 511-514.

FACHAUX, J.M., GUYOT-HERMAN, A.M., GUYOT, J.C., CONFLANT, P., DRACHE, M., VLEESLER, S & BOISTELLE, R. 1995. Pure paracetamol for direct compression Part II. Study of the physicochemical and mechanical properties of sintered-like crystals of paracetamol. *Powder technology,* 82(2):129-133.

FEJDI, P. & HOLOCSY, A. 2001. Relationship between crystal morphology and preferred orientation in polycrystalline specimens for diffraction experiments. *Materials Structure,* 8(1):22-24.

FINCHAM, J.E., MARKUS, M.B., NGOBENI. J.T., MAYOSI. B.N., ADAMS, V.J., KWITSHANA, Z.L., OBIHARA, C.C., DHANSAY, M.A. & JACKSON, T.F.H.G. 2005. Synchronized and regular deworming of children an women in South Africa: policy and practice. *South African Journal of Science,* 101:13-17.

FOKKENS, J.G. & BLAEY, C.J., 1984. Drug release from non-aqueous suspensions IIII - the release of methylxanthines from paraffin suspensions. *International Journal of Pharmaceutics,* 18:127-138.

GALWEY, A.K. & JACOBS, P.W.M. 1960. The thermal decomposition of ammonium perchlorate at low temperatures. *Proceedings of the Royal Society of London. Series A. Mathematical and Physical Sciences,* 254(1279):455-469.

GERBER, J.J. 1989. Die bereiding en fisiese karakterisering van siklopentasied-kristalvorms. Potcheftroom: PU vir CHO. (Tesis – D.Sc.) 161p.

GIBBON, C.J. 2000. South African Medicines Formulary. 4th edition. Cape Woodstock. South Africa: INCE 537p.

GIRON, D. 1995. Thermal analysis and calorimetric methods in the characterisation of polymorphs and solvates. *Thermochimica Acta,* 248:1-59.

GIRON-FOREST, D., GOLDBRONN, C.H. & PIECHON. P. 1989. Thermal analysis methods for pharmacopoeial materials. *Journal of Pharmaceutical and Biomedical Analysis,* 7(12):1421-1433.

GOLDBERG, I. 2002. Focus on venlafaxine. [Web] http://www.piory.com/focus1.htm. [Date of access: 2 April 2002].

GOMES, A.R. & NAGARAJU. V. 2001. High-performance liquid chromatographic separation and determination of the process related impurities of mebendazole, fenbendazole and albendazole in bulk drugs. *Journal of Pharmaceutical and Biomedical Analysis,* 26:919-927.

GRANT, D.J.W. 1999. Theory and Origin of Polymorphism. (*In* Brittain. H.G, *ed.* Polymorphism in Pharmaceutical Solids). New York, Basel: Marcel Dekker Inc. 427p.

GRANT, D.J.W. & BRITTAIN, H.G. 1995. Solubility of Pharmaceutical Solids. (*In* Brittain. H.G. *ed.* Physical Characterization of Pharmaceutical Solids). New York, Basel, Marcel Dekker Inc., 424p.

GU, C.H. & GRANT, D.J.W. 2001. Estimating the relative stability of polymorphs and hydrates from heats of solution solubility data. *Journal of Pharmaceutical Sciences,* 90(9):1277-1287.

GU. X.J. & JIANG. W. 1995. Characterization of polymorphic forms of fluconazole using Fourier transform raman spectroscopy. *Journal of Pharmaceutical Sciences,* 84(12):1438-1441.

HALTTUNEN, H., HURTTA, M., PITKÄNEN, I. & NURMI, I. 2005. The Sorption and desorption of water in lactitols. *Journal of thermal analysis and calorimetry,* 81(2):285-290.

HAN. S.J., KANG. K.L., LEE. S.H., CHUNG. U.T. & KANG. Y.K. 1993. Conformation of antifungal agent fluconazole. *Bulletin of Korean Chemistry Society,* 14(2):262-265.

HAN, J. & SURYANARAYANAN, R. 1997. Applications of pressure scanning calorimetry in the study of pharmaceutical hydrates. I. Carbamazepine dihydrate. *International Journal of Pharmaceutics,* 157:209-218.

HANCOCK, B.C. & ZOGRAFI, G. 1997. Characteristics and significance of the amorphous state in pharmaceutical systems. *Jounal of Pharmaceutical Sciences,* 86(1):1-12.

HILFIKER. R. 2006. Polymorphism in the pharmaceutical industry. Germany: Wiley-VCH. 433p.

HIMMELREICH, M., RAWSON, B.J. & WATSON, T.R. 1979. Polymorphic forms of mebendazole. *Australian Journal of Pharmaceutical Sciences,* 6(4):123-125.

ICH – See International conference on harmonisation

INTERNATIONAL CONFERENCE ON HARMONISATION OF TECHNICAL REQUIREMENTS FOR REGISTRATION OF PHARMACEUTICALS FOR HUMAN USE. 1999. Specifications: Test procedures and acceptance criteria for new drug substances and new drug products: Chemical substances. Q6A. 31p.

INTERNATIONAL CONFERENCE ON HARMONIZATION OF PHARMACEUTICALS FOR HUMAN USE. 2003. ICH stability testing guidelines - Q1A. Revision 2, 26p.

JOHNSON, W. & MEHL, R. 1939. Reaction kinetics in processes of nucleation and growth. *Transactions of the American Institute of Mineral and Metallurgy,* 135:416-46.

JUN, H. & JAI, Y. 2003. Venlafaxine hydrochloride monohydrate and methods for the preparation thereof. US 2003/0114536 A1. Patent. 15p.

KACHRIMANIS, K., NOISTERING, M.F., GRIESSER, U.J. & MALAMATARIS, S. 2006. Dynamic moisture sorption and desorption of standard and silicified microcrystalline cellulose. *European Journal of Pharmaceutics and Biopharmaceutics,* 64:307-315.

KHOULOUD, A., ALKHAMIS, SALEM, M.S. & OBAIDAT, R.M. 2006. Comparison between dehydration and desolvation kinetics of fluconazole monohydrate and fluconazole ethylacetate solvate using three different methods. *Journal of Pharmaceutical Sciences,* 95(4):859-870.

KITAIGORODSKII, A.I. 1961. Organic chemical crystallography. New York: Consultants Bureau. 326p.

KLUG, P.L. & ALEXANDER, L.E. 1974. X-Ray Diffraction Procedure for Polycrystalline and Amorphous Materials. 2nd ed. New York : Wiley, 966 p.

KOLMOGOROV, A. 1937. A statistical theory for the recrystallization of metals. *Bulletin of Academy of Science, USSR Material Sciences,* 1:355-359.

KONTNY, M.J. & ZOGRAFI, G. 1995. Sorption of water by solids. (*In.* BRITTAIN, H. G. *ed.* Physical Characterization of Pharmaceutical Solids). New York : Marcel Dekker Inc. 387-418.

KOTZ, J.C. & TREICHEL, P. 1996. Principals of Reactivity: Chemical Equilibria. (*In.* KOTZ, J.C. & TREICHEL, P. *ed.* Chemistry and Chemical Reactivity, 3rd Ed.). New York : Saunders College Publishing. 749-793.

KRIEDL. J., CZIBULA. L., SZÁNTAY. C., FRAKAS. J., DEUTSCHNÉ JUHÁSZ. I., HEGEDUS. I., WERKNÉ PAPP. E., NAGYNÉ BAGDY. J. & PILLER. A. 2002. Process for preparing fluconazole and its crystal modifications. WO 02/076955 A1. Patent. World Intellectual Property Organization. 19p.

KRISHNAIAH, Y.S.R., RAJU, P.V., KUMAR, B.D., BHASKAR, P. & SATYANARARYANA, V. 2001. Development of colon targeted drug delivery systems for mebendazole. Journal of Controlled Release, 77:87-95.

KRISNAIAH, Y.S.R., RAJU, P.V., KUMAR, B.D., SATYANARAYANA, V., KARTHIKEYAN, R.S. & BHASKAR, P. 2003. Pharmacockinetic evaluation of guar gum-based colon-targeted drug delivery systems of mebendazole in healthy volunteers. *Journal of Controlled Release,* 88:95-103.

KUHNERT-BRANDSTÄTTER, M. 1971. Thermomicroscopy in the analysis of pharmaceuticals. Oford: Pergamon Press Ltd. 409p.

LEHTO, V., LAINE, E. 2000. Simultaneous determination of heat and the quantity of vapour sorption using a novel microcalorimetric method. *Pharmaceutical Research,* 27:701-706.

LIEBENBERG, W., DEKKER. T.G., LŐTTER, A.P. & DE VILLIERS, M.M. 1998. Identification of the mebendazole polymorphic form present in raw materials and tablets available in South Africa. *Drug Development and Industrial Pharmacy,* 24(5):485-488.

LOHANI, S. & GRANT, D.J.W. 2006. Thermodynamics of Polymorphs. (*In.* HILFIKER, R. *ed.* Polymorphism in the Pharmaceutical Industry. 2006). Weinheim, Germany : Wiley-VCH Verlag GmbH & Co.. 21-44.

LUCAS, J. & BURGESS, P. 2004. When form equals substance: the value of form screening in product life cycle management. *PharmaVoice,* February 2004:54-57.

MANEK, R.V. & KOLLING, W.M. 2004. Influence of moisture on the crystal forms of Niclosamide obtained from acetone and ethyl acetate. *AAPS Pharmaceutics and Technology,* 5(1):1-8.

MATSUDA, Y., ETSUKO, T., ETSUKO, C. & YUKIE, M. 1984. Kinetic study of the polymorphic transformations of phenylbutazone. *Journal of Pharmaceutical Sciences,* 73:1453-1460.

MATSUO, K. & MATSUOKA, M. 2007. Solid-state polymorphic transition of theophylline anhydrate and humidity effect. *Crystal Growth and Design,* 7(2):411-415.

MERCURY SOFTWARE. 2007. CCDC Software Ltd and CCLRC Mecury Dash. Cambridge Crystallographic Data Centre. Cambridge.

MOORE, J.W. & FLANNER, H.H. 1996. Mathematical comparison of dissolution profiles. *Pharmaceutical Technology,* 20:64-74.

MORIBE, K., WONGMEKIAT, A., HYAKUTAKE, Y., TOZUKA, Y., OGUCHI, T., YAMAMOTO, K. 2005. Influence of dehydration temperature on water vapor adsorption, dissolution behavior and surface property of ampicillin. *International Journal of Pharmaceutics,* 288:245-252.

MORRIS, K.R. 1999. Structural aspects of hydrates and solvates. (*In* Brittain. H.G. *ed.* Polymorphism in Pharmaceutical Solids). New York, Basel, Marcel Dekker Inc., 427p.

MUTH, E.A., HASKINS, J.T. & MOYERS. J.A. 1986. Antidepressant biochemical profile of the novel biciclic compounds Wy-45,030, an ethylcyclohexanol derivate. *Biochemical Pharmacology,* (35):4493-4497.

MWAMBETE, K.D., TORRADO. S., BANDERA, C.C., GORDO, F.P. & TORRADO, J.J. 2004. The effect of solubilization on the oral bioavailability of three benzimidazole carbamate drugs. *International Journal of Pharmaceutics,* 272:29-36.

NAVARRETE-VáZQUEZ, G., YEPEZ. L., CAMPOS, A.H., TAPIA, A., LUIS, F.H., CEDILLO, R., GONZALEZ, J., FERNANDEZ, A.M., GRUEIRO, M.M. & NEWMAN, A.W. & BRITTAIN, H.G. 1995. Particle morphology: Optical and electron Microscopics (*In* Brittain. H.G. *ed.* Physical Characterization of Pharmaceutical Solids). New York, Basel, Marcel Dekker Inc., 424p.

NYQVIST, H. , 1983. Saturated salt solutions for maintaining specified relative humidities. *International Journal of Pharmaceutical Technology and Product Manufacture,* 4(2):47-48.

OTSUKA, M. & MATSUDA, Y. 1994. The effect of humidity on hydration kinetics of mixtures of nitrofurantoin anhydride and diluents. *Chemical Pharmaceutical Bulletin,* 42:156-159.

OTSUKA, M., KATO, F. & MATSUDA, Y. 2004. Effect of temperature and kneading solution on polymorphic transformation of mefenamic acid during granulation. *Solid State Ionics,* 172:451-453.

OZAWA, T. 1965. A new method of analyzing thermogravimetric data. *Bulletin of the Chemical Society of Japan,* 38:1881-1887.

PECHARSKY, V.K. & ZAVALIJ, P.Y. 2005. Fundamentals of diffraction (*In* Fundamentals of powder diffraction and structural characterization of materials.) New York: Springer Science and Business Media Inc. 713p.

PETERSON, M.L., HICKEY, M.B., ZAWOROTKO, M.J. & ALMARSSON, Ö. 2006. Expanding the scope of crystal form evaluation in pharmaceutical science. *Journal of Pharmaceutical Sciences,* 9(3):317-326.

PIDWIRNY, M. 2007. Physical properties of water. [Web] http://www.physicalgeography.net/fundamentals/8a.htm. [Date of access: 2 April 2007].

PIENAAR, E.W., CAIRA, M.R. & LÖTTER, A.P. 1993. Polymorphs of nitrofurantoin I. Preparation and X-ray crystal structures of two monohydrated forms of nitrofurantoin. *Journal of Crystal Spectroscopic Research,* 23:739-744.

PIENAAR, E.W., CAIRA, M.R. & LÖTTER, A.P. 1993. Polymorphs of nitrofurantoin 2. Preparation and X-ray crystal structures of two anhydrous forms of nitrofurantoin. *Journal of Crystal Spectroscopic Research,* 23:785-790.

PIENAAR, E.W. 1994. Characterisation of anhydrous and monohydrous crystal forms of nitrofurantoin. Potchefstroom: PU vir CHO. (Tesis – D.Sc.) 196p.

PIRTTIMAKI, J. & LAINE, E. 1994. The transformation of anhydrate and hydrate forms of caffeine at 100-percent RH and 0-percent RH. *European Journal of Pharmaceutical Sciences,* 1:203-208.

POTTER, W.Z. & HOLLISTER, L.E. 1998. Antidepressant Agents. (*In.* ed. KATZUNG, B.G. *ed.* Basic & Clinical Pharmacology). USA, Appleton & Lange, 1151p.

PRICE, R., YOUNG, P.M. 2004. Visualization of the crystallization of lactose from the amorphous state. *Journal of Pharmaceutical Sciences,* 93(1):155-164.

PROUT, E.G. & TOMPKINS, F.C. 1944. Thermal decomposition of $KMnO_4$. *Trans. Faraday Society,* 40:448-498.

RAO, S.M., VYAS, K., LAKSHMI, A.S.L. & REDDY, G.M. 2002. Novel crystalline polymorphic forms of venlafaxine hydrochloride and a process for their preparation. Patent: WO 02/46140 A1. 31 p.

RASTOGI, S., ZAKREWESKI, M. & SURYANARAYANAN, R. 2001. Investigation of solid-state reactions using variable temperature x-ray powder diffractometry. I. Aspertame Hemihydrate, *Pharmaceutical Research,* 18(3):267-273.

RASTOGI, S., ZAKREWESKI, M. & SURYANARAYANAN. 2002. Investigation of solid-state reactions using variable temperature x-ray powder diffractometry. I. Aminophylline Monohydrate, *Pharmaceutical Research,* 19(9):1265-1273.

RASTOGI, S., ZAMANSKY, I., ROY, S. & SURYANARAYANAN, R. 1994. Solid-state phase transitions of AG337, an antitumor agent. *Pharmaceutical Development and Technology,* 4(4):623-632.

RAW, A.S., FURNESS, M.S., GILL, D.S., ADAMS, R.C., HOLCOMBE (JR), F.O. & YU, L.X. 2003. Regulatory considerations of pharmaceutical solid polymorphism in abbreviated new drug applications (ANDAs). *Advanced Drug Delivery Reviews,* 56:397-414.

REN, H., CHENG, B., MA, J. & HUA, D. 1987. Yiyao Gongye, 18:356-359.

REQUADT, S. 2004. The importance of crystalline forms to product development and life cycle management. *Transform Pharmaceutical,* April 2004:2-5.

ROCCO, W.L & SWANSON, J.R. 1995. Win 63843 polymorphs: prediction of enantiotropy. *American Journal of Pharmaceutics,* 117:231-236.

RODRIGUEZ-HERNANDO. N., LECHUGA-BALLESTEROS, D., WU. H. 1992. Phase transition and heterogeneous/epitaxial nucleation of hydrayed and anhydrous theophylline crystals. *International Journal of Pharmaceutics,* 85:149-162.

RÖMER, M., HEINÄMÄKI, J., MIROSHNYK, I., SANDLER, N., RANTANEN, J. & YLIRUUSI, J. 2007. Phase transformations of erythromycin A dihydrate during pelletisation and drying. *European Journal of Pharmaceutics and Biopharmaceutics,* 67:246-252.

ROY, S., AITIPAMULA, S. & NANGIA, A. 2005. Venlafaxine hydrochloride polymorphs. *Crystal Growth and Design,* 5:2268-2276.

SCHEMELZER, J. 1998. Ostwald's rule of stages. The effect of elastic strains and external pressure.: MOELLER, J. & GUTZOW, I. *Physical Chemistry,* 204(1/2):171-181.

SHEHATTA, I. 2004. Cyclodextrins as enhancers of the aqueous solubility of the anthelmintic drug mebendazole: thermodynamic conciderations. *Chemical Monthly,* 133(9):1239-1247.

SILVERSTEIN, R.M., BASSLER, G.C. & MORRIL, T.C. 1991. Spectrometric identification of organic compounds. Fifth edition. New York : John Wiley & sons. 419 p.

SMITH, K.W., CAIN, F.W. & TALBOT, G. 2005. Kinetic Analysis of Nonisothermal Differential Scanning Calorimetry of 1,3-Dipalmitoyl-2-oleoylglycerol. *Journal of Agricultural and Food Chemistry,* 53:3031-3040.

SNIDER, D.A., ADDICKS, W. & OWENS, W. 2004. Polymorphism in generic drug product development. *Advanced Drug Delivery Reviews,* 56:391-395.

SUMPTER, M.L. 2004. Johnson-Mehl-Avrami kinetics of intracellular ice formation in confluent tissue constructs. Gorgia: Gorgia Institute of Technology. (Thesis – M.Sc.) 95p.

SWANEPOEL, E., LIEBENBERG, W. & DE VILLIERS. M.M. 2003. Quality evaluation of generic drugs by dissolution test: changing the USP dissolution medium to distinguish between active and non-active mebendazole polymorphs. *European Journal of Pharmaceutics and Biopharmaceutics,* 55:345-349.

TERBLANCHE, R.J. 2001. Thermo-mechanical transformation of drug polymorphs and pseudopolymorphs characterised by differential scanning calorimetry and x-ray powder diffraction. Potchefstroom: PU vir CHO. (Thesis – PHD.) 250p.

THRELFALL, T.L. 1995. Analysis of organic polymorphs. *Analyst,* October, 120:2435-2460.

TRAINI, D., YOUNG, P.M., JONES, M., EDGE, S. & PRICE, R. 2006 Comparative study of erythriol and lactose monohydrate as carriers for inhalation: Atomic force microscopy and in vitro correlation. *European Journal of Pharmaceutical Sciences,* 27:243-251.

USP – see United States Pharmacopeial Convention.

UNITED STATES PHARMACOPEIAL CONVENTION. 2006. USP29:NF25 Online. Available: www.uspnf.com.

UNITED STATES PHARMACOPEIAL CONVENTION. 2007. USP30:NF25 Online. Available: www.uspnf.com.

VAN SICLEN, C.D. 1996. Random nucleation and growth kinetics. *Physical Review B,* 54(17):11845-11848.

VOET. M.A. 2005. The generic challenge: Understanding patents, FDA and pharmaceutical life cycle management. USA: Brown Walker press. 105p.

WARDROP, J., LAW, D., QIU, I., ENGH, K., FAITSCH, L. & LING, C. 2006. Influence of solid phase and formulation processing on stability of Abboyy-232 tablet formulations. *Journal of Pharmaceutical Sciences,* 95(11):2380-2392.

WEINBERG, M. & KAPRAL. R. 1989. Phase transformation kinetics in finite inhomogeneously nucleated systems. *The Journal of Chemical Physics,* 91(11):7146-7152.

WHO – see World health organization.

WIKSTRÖM, H., MARSAC, P.J. & TAYLOR. L.S. 2005. In-line monitoring of hydrate formation during wet granulation using Raman spectroscopy. *Journal of Pharmaceutical Sciences,* 94(1):209-219.

WORLD HEALTH ORGANIZATION. 2002. Guidance on the selection of comparator pharmaceutical products for equivalence assessment of interchangeable multisource (generic) products. (*In* WHO Technical Report Series). Annexure 11(902):161-180.

YOSHINARI, T., FORBES, R.T., YORK, P. & KAWASHIMA, Y. 2002. Moisture induced polymorphic transition of mannitol and its morphological transformation. *International Journal of Pharmaceutics,* 247:69-77.

YOSHINARI, T., FORBES, R.T., YORK, P. & KAWASHIMA, Y. 2003. The improved compaction properties of mannitol after a moisture-induced polymorphic transition. *International Journal of Pharmaceutics,* 258:121-131.

YU, L. 1995. Inferring thermodynamic stability relationship between polymorphs from melting data. *Journal of Pharmaceutical Sciences,* 84:966-974.

YU, L., REUTZEL, S.M. & STEPHENSON, G.A. 1998. Physical characterization of polymorphic drugs: an integrated characterization strategy. *PSTT,* 1(3):118-127.

ZHANG, G.G.Z., LAW, D., SCMITT, E.A. & QUI, Y. 2004. Phase transformation considerations during process development and manufacture of solid oral dosage forms. *Advanced Drug Delivery Reviews,* 56:371-390.

ZHU, H., YUEN, C., GRANT, D.J.W. 1996. Influence of water activity in organic solvent & water mixtures on the nature of the crystallizing drug phase 1. Theophylline. *International Journal of Pharmaceutics,* 135:151-160.

ZOGRAFI, G., LAUGCHIN, S.M., PIKAL, M.J, SCHWARTZ, J.P., VAN CAMPEN, L. 1991. Report of the advisory panel on moisture specifications. *Pharmacopeial Forum,* Jan-Feb 1991:1459.

Acknowledgements

This study would not have been possible without the assistance and encouragement of several people. I would like to make use of this opportunity to express my sincerest and heartfelt gratitude to the following persons:

- Prof. W. Liebenberg for her constant assistance, support, motivation and friendship during the duration of my study. During the completion of this manuscript she has sustained as critic, proofreader and source of calm commonsense.

- Prof. M.M. de Villiers for his support, assistance, and motivation to broaden my views and thoughts.

- My friends and colleagues at the Research Institute for Industrial Pharmacy, for their interest, friendship, and support throughout the years, in particular Mari-Alet, Marique, André, Marina, Stefan, Dr Erna Swanepoel, Prof. Theo Dekker and Dr Elsa van Tonder and her dissolution team.

- My friends: Izak, René, Lindie, Rudi, Zak, Emtia, Carel, Janine and Tiny for your support, friendship and encouragement. Sue – you're a star!

- Mrs. A. Pretorius for her assistance way beyond the call of duty, and interest in my personal life.

- My loving (and always praying) parents, Gerrit and Enet, my brothers Gerrit and Chris and their wives Janine and Helen and their beautiful children, for their undivided love, support, encouragement and prayers during the whole of my life. Grandpa Chris & Grandma Baby your prayers where the fuel for this study. Grandma Martie, I know that you are smiling down from heaven, I miss you. The rest of my family for their support and encouragement. You raised me up ....

- Dr. M.W. Kolling for your assistance with the heat of solution and moisture sorption studies.

Most importantly I thank my Heavenly Father, Almighty GOD for His Love and Blessings, for giving me the time, opportunity and strength to complete this task. Thank you Lord-Jesus for revealing to me some of the wonders of the molecular-world. For it was in the small things, that I saw and experienced the greatness of Your love.

ANNEXURES

Articles in the process of being submitted for publication

Thermodynamic stability of mebendazole polymorph C in solid dosage forms

Marius Brits [a,*], Melgardt de Villiers [b], Wilna Liebenberg [c]

[a] Research Institute for Industrial Pharmacy®, North West University, Potchefstroom campus, Potchefstroom, South Africa
[b] School of Pharmacy, University of Wisconsin, Madison, WI, USA
[c] Unit for Drug Research and Development, Faculty of Health Sciences, North West University, Potchefstroom campus, Potchefstroom, South Africa

Abstract

The thermodynamic stability of mebendazole polymorph C in tablets was investigated. The three polymorphic forms of mebendazole (i.e. A, B and C) display significant differences in solubility and therapeutic efficacy. Polymorph C is the preferred form to be used clinically due to its optimal bioavailability and reduced toxicity compared to the more soluble form B [1]. It was shown [2] that polymorph C transformed into the thermodynamically more stable polymorph A at temperatures exceeding 175°C, thus suggesting that mebendazole polymorph C would remain stable in tablets stored at ambient conditions. This study revealed that the polymorph C present in tablets converted to polymorph A at when stored at 30°C & 65% RH and 40°C 75% RH respectively. The polymorph C → A conversion was found to be preceded by a temperature-dependent incubation time, and that the JMAEK model described this conversion best. The results obtained showed that conversion in some tablets (when stored in original packaging at high temperatures and high humidities) had shelf-lives of less than 7 months. Direct exposure of a product to the environmental conditions increased the polymorph C → A conversion by a factor of 5.

Keywords: Mebendazole polymorphs; Polymorphic transitions; Polymorphism; Thermodynamic stability

* Corresponding author. Tel.: +2718-299-2323; fax: +2718-299-2291.
E-mail address: Marius.Brits@nwu.ac.za

1. Introduction

Mebendazole (methyl-5-benzoyl-2-benzimidazole carbamate) is a benzimidazole antihelmintic which is commonly used in the treatment of roundworm, hookworm, pinworm (threadworm), whipworm and *Strongyloides sercoralis* infestations [3]. This anthelmintic is known to act through the irreversible inhibition of glucose uptake by the parasite that leads to glycogen depletion in the parasite, which finally results in decreased adenosine triphosphate activity [4].

Fincham *et al.* [5] discussed the relevance and importance of synchronized and regular deworming of children and women in South Africa and stressed the importance that all batches of deworming medicine to be tested independently to ensure safety, quality and efficacy. Fincham *et al.* [5] stated that on two occasions it was found that South African generic mebendazole tablets profiles did not match that of the specified polymorph C profile.

The transpiring parasitic-resistance towards mebendazole and the distressing consequences thereof urges medical practitioners to promote patient compliance when mebendazole is prescribed as choice drug. It is of utmost importance to ensure that mebendazole products contain the active polymorph i.e. polymorph C, and to ensure the stability of the polymorph in the pharmaceutical dosage form to ensure the efficacy and safety of the mebendazole. The fact that the current USP dissolution test conditions are not able to distinguish between the dissolution properties of the various mebendazole polymorphs [6] could hoax manufacturers during stability testing trials by suggesting that the mebendazole polymorph C remains stable in the product due to no changes in the dissolution behaviour of the tablets. The aim of this study was to investigate the thermodynamic stability of mebendazole polymorph C in commercially available products.

2. Materials and methods

2.1 Materials

Various commercially available mebendazole tablets in South Africa were obtained. The products were randomly numbered: Product 1 – Product 7, to conceal the product identity.

2.2 Stability testing conditions

The products were stored in temperature and relative humdity controlled climate rooms at conditions in accordance to ICH stability guidelines [7] for intermediate and accelerated stability testing at : 30°C & 65% RH and 40°C & 75% RH respectively.

Product 2 (which contained only polymorph C) and was removed from its original packaging (and will be referred to as "Product 2 - open") and exposed to the stability testing conditions (30°C & 65% RH and 40°C & 75% RH). The polymorphic transition kinetics in the exposed product to that of the unexposed product (Product 2 in original packaging) was compared to investigate the effect of moisture on the stability of mebendazole polymorph C in the tablets.

2.3 Methods

XRPD and DRIFT-IR spectroscopy were used to evaluate the polymorphic composition of the various tablets. The dissolution profiles of the various tablets were also evaluated at monthly intervals to determine the influence of polymorphic conversions on the dissolution behaviour of the various tablets.

2.3.1 Infrared absorption spectroscopy (DRIFT-IR)

The IR-spectra of the various products were recorded on a Nicolet Nexus 470-FT-IR spectrometer (Nicolet intrument corporation, Madison, USA) over a range of 400 – 4000 cm^{-1}. The diffuse reflectance method was used. KBr was used as background material.

Infrared spectroscopy has emerged as the preferred method to identify the mebendazole polymorphic forms [8,9].

The areas of the characteristic absorption bands of the different polymorphs in the DRIFT-IR spectra of the products were determined and used to calculate the relative polymorph A and polymorph C ratios present in the tablets at the various intervals and to investigate the rate of the polymorphic conversions.

2.3.2 X-ray powder diffraction (XRPD)

From the XRPD results published by de Villiers *et al,* [10] it was observed that the main XRPD peaks for mebendazole polymorphs A, B and C were at the following positions: 7.67, 19.07 and 19.80 °2θ respectively. The XRPD patterns of the mebendazole polymorphs indicated that the following peaks (in the 3–10 °2θ region) may be regarded as characteristic peak positions for polymorph A, B and C: 7.67, 5.84 and 4.93 °2θ respectively.

The X-ray powder diffraction patterns of the products were recorded at room temperature using a Bruker D8 Advance diffractometer (Bruker, Germany). Approximately 200 mg the powdered samples were transferred into aluminium sample holders, taking care not to induce a preferential orientation of crystals. The measurement conditions were: target, Cu; voltage, 40 kV; current, 30 mA; divergence slit, 2 mm; antiscatter slit, 0.6 mm; detector slit, 0.2 mm; monochromator; scanning speed, 2°/min (step size, 0.025°; step time, 1.0 sec.).

The intensities of the characteristic peaks were used to calculate the relative polymorph A and polymorph C ratios present in the tablets during the various intervals of the stability testing.

2.3.3 Dissolution testing

Dissolution studies were conducted on the tablets according to the USP [11] specifications for mebendazole tablets, excluding sodium lauryl sulphate (SLS) from the dissolution medium.

Swanepoel *et al.* [6] suggested changes to be made to the USP dissolution medium to be able to distinguish between the active and favoured (polymorph C) and non-favoured and inactive mebendazole polymorphs (polymorphs A and B). The change suggested, the exclusion of SLS from the USP dissolution medium (0.1 N HCl & 1% SLS). When SLS was removed from the dissolution medium, the percentage dissolved versus time profiles changed and indicated that the dissolution rate to be: C > B > A.

The dissolution conditions were as follows:

Apparatus: USP paddle assembly. Medium: 900 ml 0.1 N HCl preheated and maintained at 37±0.5°C. Paddle speed: 75 rpm. Samples were withdrawn through 0.45 micrometer membrane syringe filters (MCE-Filters).

The amount of mebendazole dissoluted at the various intervals (i.e.: 7.5, 15, 30, 60, 90 and 120 minutes) was calculated from the uv-absorbance of the suitably diluted samples at 254 nm.

2.3.4 Calculations

2.3.4.1 Calculating the ratio of polymorph A and C content relative to the total polymorph content in the tablet from DRIFT-IR data

The ratios of polymorph A and C content relative to the total polymorph content in the product were calculated from the DRIFT-IR data using the equations (1) and (2):

$$Polymorph\ A/(A+C) = \frac{AUC_A}{AUC_A + AUC_C} \qquad (1)$$

$$Polymorph\ C/(A+C) = \frac{AUC_C}{AUC_A + AUC_C} \quad (2)$$

Where:

Polymorph A/(A+C) is the ratio of polymorph A content relative to the total mebendazole polymorph content in the product;

Polymorph C/(A+C) : ratio of polymorph C content relative to the total mebendazole polymorph content in the product;

AUC_A : Area of the absorption peak present at 3370 cm^{-1}, characteristic of polymorph A;

AUC_C : Area of the absorption peak present at 3410 cm^{-1}, characteristic of polymorph C.

2.3.4.2 Calculating the ratio of polymorph A and C content relative to the total polymorph content in the tablet from XRPD data

The ratios of polymorph A and C content relative to the total polymorph content in a product were calculated from the XRPD data using the equations (3) and (4):

$$Polymorph\ A/(A+C) = \frac{I_A}{I_A + I_C} \quad (3)$$

$$Polymorph\ C/(A+C) = \frac{I_C}{I_A + I_C} \quad (4)$$

Where:

Polymorph A/(A+C) is the ratio of polymorph A content relative to the total mebendazole polymorph content in the product;

Polymorph C/(A+C) is the ratio of polymorph C content relative to the total mebendazole polymorph content in the product;

I_A : Intensity of the 7.67±0.1°2θ diffraction peak, characteristic of polymorph A;

I_C : Intensity of the 4.93±0.1°2θ diffraction peak, characteristic of polymorph C.

Microsoft® Office Excel 2003 software was used for all calculations and graphs plotted.

Several models have been developed to account for the polymorphic transitions observed in solid-state studies. All of these methods assume a certain geometry and rely on some consistency of the system as the process proceeds. The kinetics of the polymorphic transition (polymorph C → polymorph A) observed in the tablets was investigated using various kinetic models summarised in table 1.

Table 1. Equations used during kinetic study [12]

Rate controlling process and equation describing the process	Rate controlling process and equation describing the process
1. Prout Tompkins equation $\ln\left(\frac{x}{1-x}\right) = kt + c$	7. Two-dimensional diffusion equation $(1-x) \bullet \ln(1-x) + x = kt$
2. Avrami Efofe'ev equations $[-\ln(1-x)]^n = kt$ n = ¼ n = 1/3 n = 1/2 n = 2/3 n = 1	8. Three-dimensional diffusion equation $1 - \frac{2}{3}x - (1-x)^{\frac{2}{3}} = kt$
3. One-dimensional advancement of a phase boundary equation $1 - x = kt$	9. Power law equation $x^n = kt$ n = ¼ n = 1/3 n = ½ n = 1
4. Two-dimensional advancement of a phase boundary equation $1-(1-x)^{\frac{1}{2}} = kt$	10. Equations based on the concept of the order of the reaction (a) Zero order reaction $1 - x = kt$
5. Three-dimensional advancement of a phase boundary equation $1-(1-x)^{\frac{1}{3}} = kt$	(b) First order reaction $\ln(x) = kt$
6. One-dimensional diffusion equation $x^2 = kt$	(c) Second order reaction $\frac{1}{(1-x)} = kt$

3. Results and discussion

3.1 Polymorph C → Polymorph A conversion in commercially available tablets

Three of the seven products (Products 3, 5 and 6) initially contained polymorph C and traces of polymorph A, the other four products (Products 1,2,4 & 7) contained mebendazole polymorph C. The stability testing revealed that rate of the polymorph C → polymorph A conversion was higher at 40°C & 75% RH compared to that observed at 30°C & 65% RH. Two of the products underwent polymorphic conversion at 30°C & 65% RH to form mixtures of polymorphs A and C whilst six of the products converted at 40°C & 75% RH producing mixtures of polymorphs A and C or primarily polymorph A in the various tablet matrix.

Fig. 1 illustrates the characteristic stretching frequencies at 3370 cm^{-1} 3410 cm^{-1} of polymorph A and polymorph C respectively and the areas thereof observed in the DRIFT-IR spectra of Product 3 at 0, 3 and 6 months respectively.

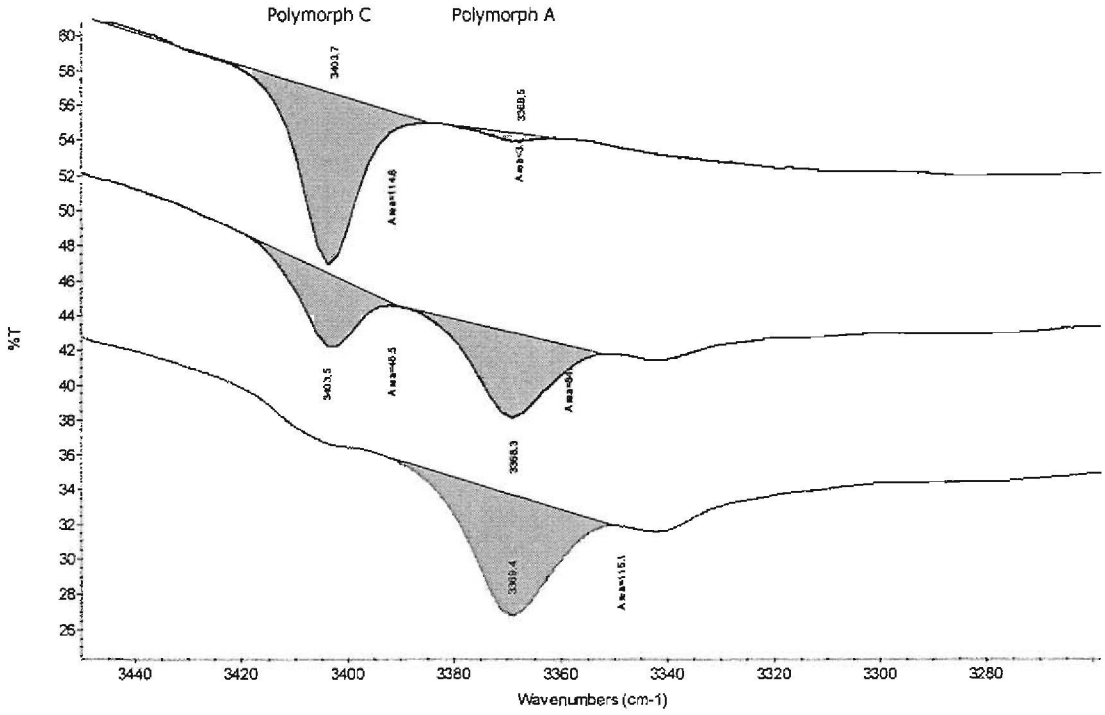


Fig. 1. Characteristic stretching frequencies (cm^{-1}) and the areas thereof in the DRIFT-IR spectra Product 3 at 0 (top), 3 (middle) and 6 (bottom) months respectively indicating the decreasing polymorph C and increasing polymorph A content.

Fig. 2 illustrates the characteristic diffraction peaks and their intensities for polymorphs A and C present in Product 3 at 0 (top), 3 (middle) and 6 (bottom) months when stored at 40°C & 75% RH, indicating the decrease of the polymorph C content and the increase in polymorph A content as a function of time.

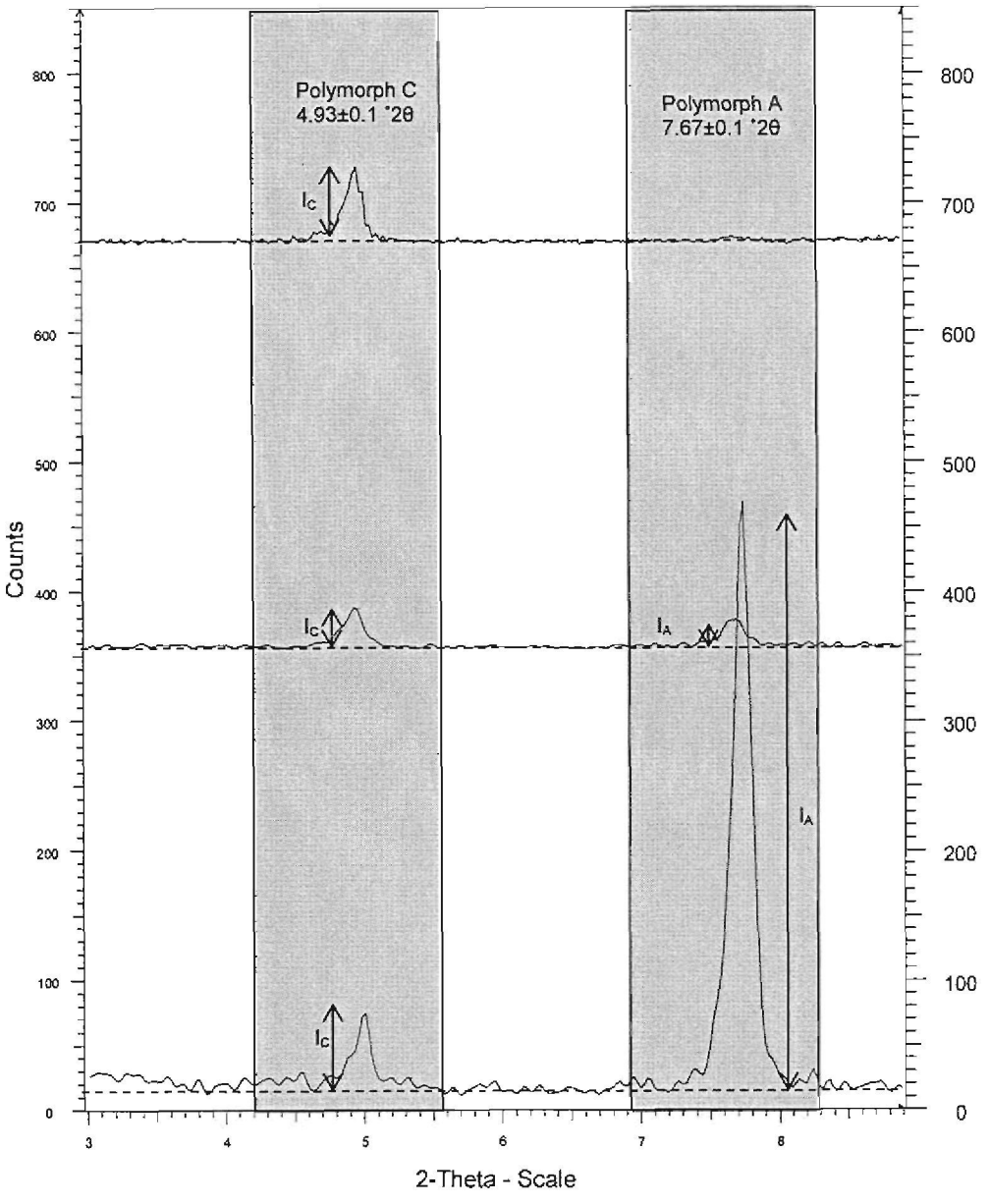
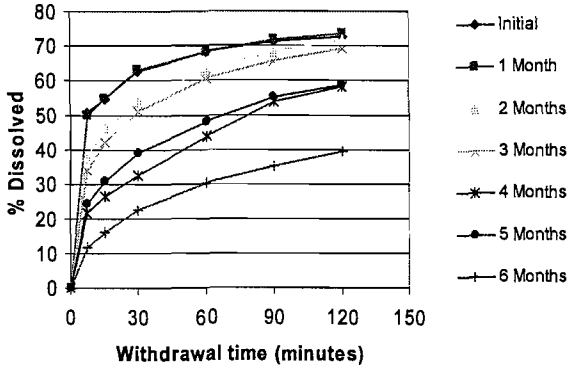
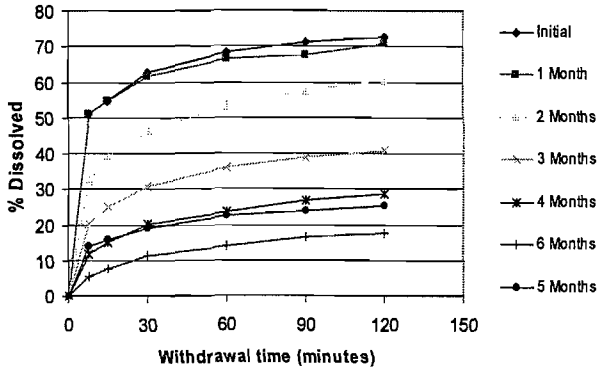


Fig. 2. Characteristic diffraction peaks and their intensities for mebendazole polymorphs A and C present in Product 3 at 0 (top), 3 (middle) and 6 (bottom) months when stored at 40°C & 75% RH.

The polymorph conversion influenced the dissolution behaviour of the various products significantly. The dissolution profiles of Product 3 stored at 30°C & 65% RH and 40°C & 75% RH at the various time intervals are illustrated in fig. 3. Both the dissolution rate and extend of dissolution were significantly reduced when Product 3 was stored at 40°C & 75% RH for 6 months. The initial and final dissolution profiles of products without any polymorphic conversions were comparable. Product 7 was taken as an example (fig.4).



(A)



(B)

Fig. 3. Dissolution profiles of tablets of Product 3 when stored at (a) 30°C & 65% RH and (b) 40°C & 75% RH respectively for a period of six months (in 0.1 M HCl).

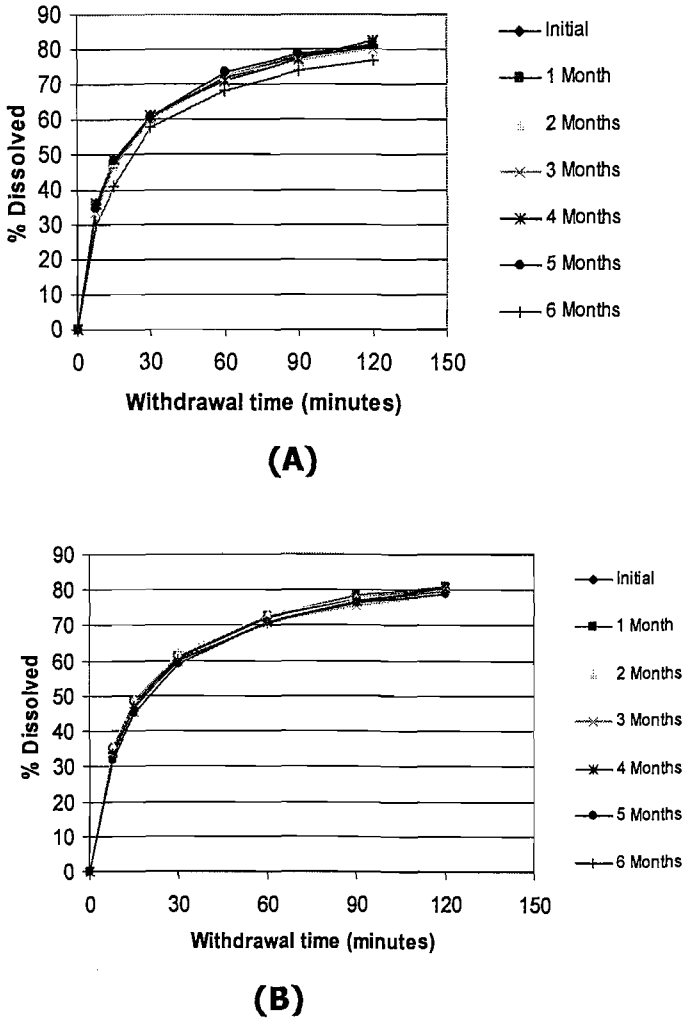


Fig. 4. Dissolution profiles of tablets of Product 7 when stored at (a) 30°C & 65% RH and (b) 40°C & 75% RH respectively for a period of six months (in 0.1 M HCl).

The ratios of polymorphs A and C present in the various products were calculated for all the products and plotted against time (0-6 months). This provided an indication of the relative mebendazole polymorph content in a product at a given time. Fig. 5 illustrates the ratio of polymorph A and C content relative to the total mebendazole polymorph content in Product 1 (at 30°C & 65% RH) and Product 3 (at 40°C & 75% RH) calculated from the DRIFT-IR and XRPD data respectively.

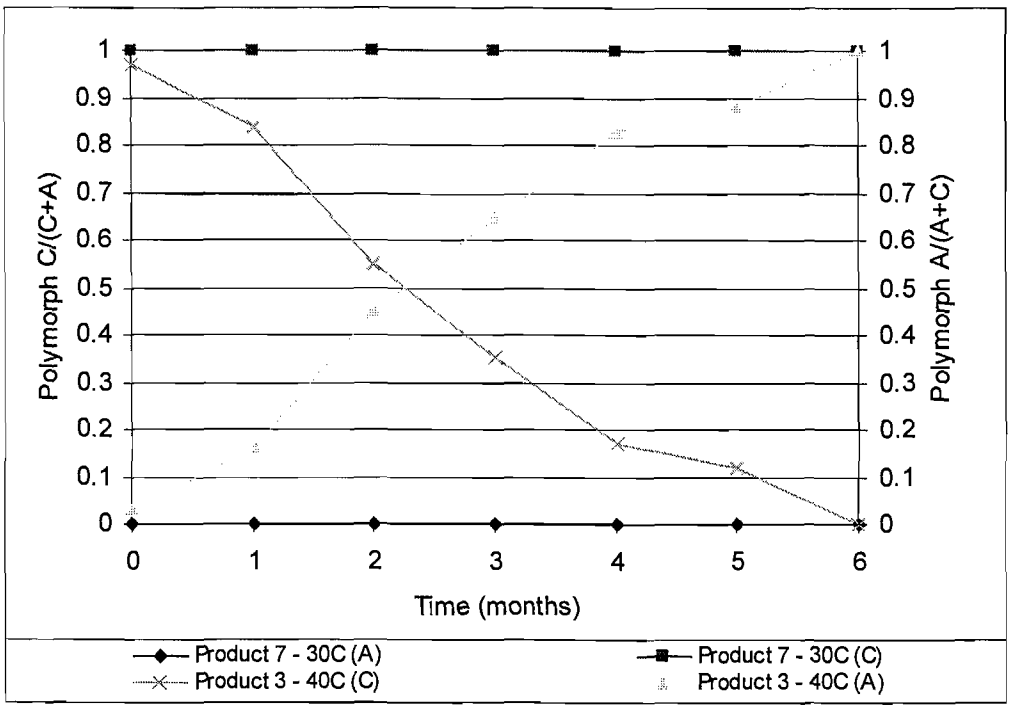
The polymorph A ratios present in Product 7 (calculated from the DRIFT-IR data) remained 0.00, and the polymorph C/(A+C) = 1.00 during the six months, which indicated that no polymorphic transition occurred when Product 7 was stored at 30°C & 65% RH. The transformation of the mebendazole polymorph C fraction into polymorph A in Product 3 (stored at 40°C & 75% RH) during the six months is

illustrated in fig. 5 (b). The decrease in the polymorph C content (polymorph C/(A+C): decreased from 0.97 to 0.00) and simultaneous increase in polymorph A content (polymorph A/(A+C): increased from 0.03 to 1.00) is illustrated.

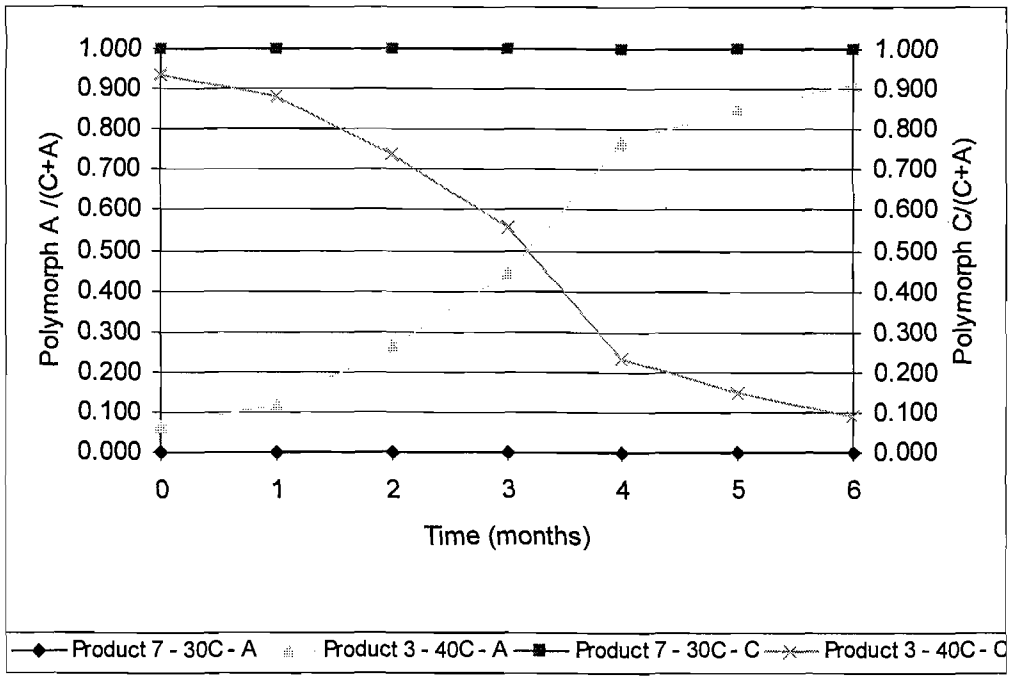
The overall-shape and distribution of the polymorph A/(A+C) and polymorph C/(A+C) vs. time graphs for Product 7 and Product 3 derived from the DRIFT-IR and that XRPD data were comparable.

The polymorph ratio (calculated from DRIFT-IR and XRPD data for polymorph A & C) at the various intervals differed slightly. Quantitative analysis of phases present in solids using XRPD techniques may be complicated due to the absorption effect which is normally different for phases with different chemical composition and gravimetric density [13]. The presence of the various unknown tablet excipients might have interfered with the detection of the mebendazole crystal phases.

However, due to the unique features of the infrared spectra of the mebendazole polymorphs it has emerged as the preferred method to identify mebendazole polymorphic forms [8,9]. These studies have also shown that DRIFT-IR data for the polymorphs are not influenced by commercially used pharmaceutical excipients.



(a)



(b)

Fig. 5. Ratio of the polymorph A and polymorph C content relative to the total mebendazole polymorph content in Product 7 (30°C & 65% RH) and Product 3 (40°C & 65% RH) calculated from (a) DRIFT-IR and (b) XRPD data.

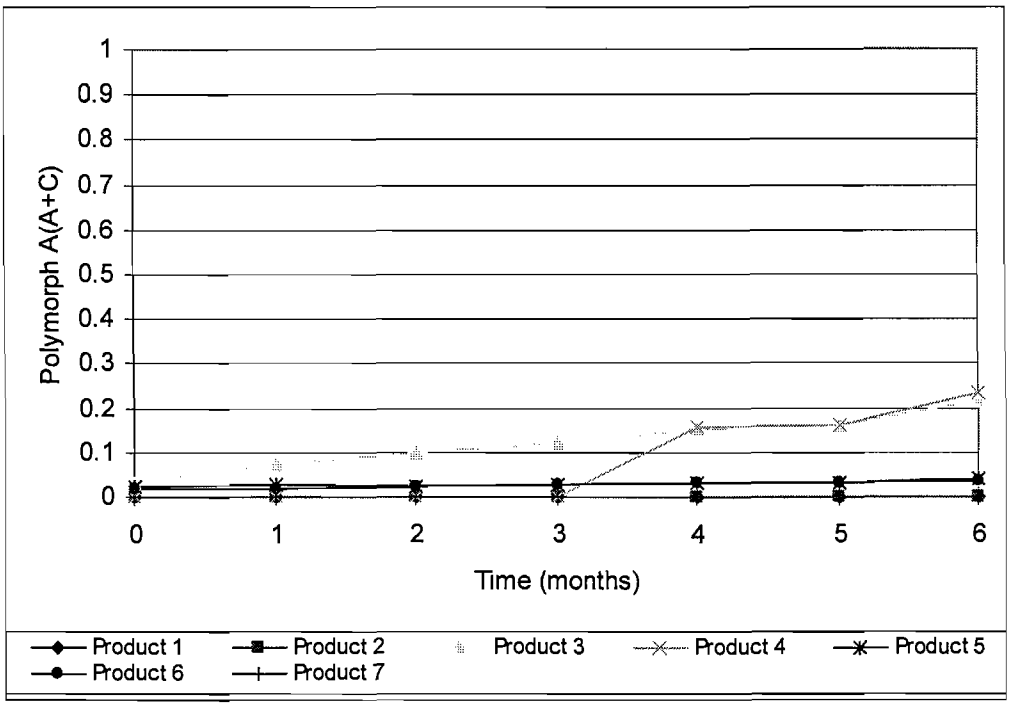
Based on these initial observations it was decided to use the polymorph A ratios (calculated from the DRIFT-IR data) vs. time to compare the conversion of polymorph C to polymorph A in the products. The polymorph A/(C+A) vs. time plots (fig. 6) indicates the progressive increase of the mebendazole polymorph A content in the products due to the polymorph transition (polymorph C → polymorph A). Overall the conversion of polymorph C → A was more pronounced in the products stored at 40°C & 75% RH compared to those stored at 30°C & 65% RH.

Upon closer inspection of the graphs the following observations were made regarding the polymorph stability testing of the various products at 30°C & 65% RH and 40°C & 75% RH (fig. 6):

- Products 1,2,4,5 and 7 did not reveal significant polymorphic transition during the 6 months when stored at 30°C & 65%RH.

  The polymorphic transition in Product 3 and Product 4 at 30°C & 65% RH was only detected after 1 month for Product 3 and after 3 months for Product 4. All the products, except Product 7 revealed polymorphic transitions when exposed to 40°C & 75% RH for 6 months.

- The rate and extend of the polymorphic transitions of polymorph C to polymorph A at 40°C & 75% RH was greater and more pronounced compared to the transitions observed at 30°C & 65% RH, for example the ratio of polymorph A relative to the total polymorph content (i.e. A/(A+C)) for Product 3 was found to be higher (1.00) at 40°C & 75% RH compared to the ratio (0.21) at 30°C & 65% RH.



(A)

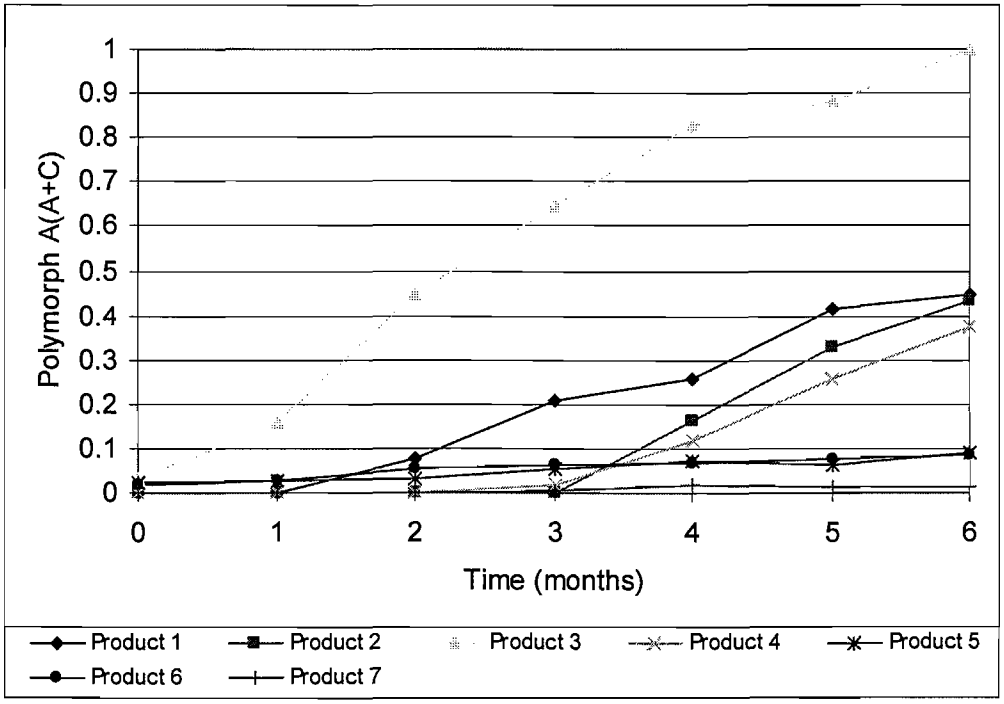


Fig. 6. Ratio of polymorph A relative to the total polymorph contents for products 1-7 using DRIFT-IR data at: (a) 30°C & (b) 40°C respectively.

3.2 Kinetics of mebendazole polymorph C → polymorph A conversion in the tablets

Recrystallisation occurs through nucleation as illustrated in fig. 7 which shows that overall crystallization, r_C, depends on nucleation and occurs at a temperature intermediate between the preferred temperatures for nucleation and growth [14]. Within this model, three types of recrystallisation can be distinguished: static recrystallisation, metadynamic recrystallisation and dynamic recrystallisation. A minimum strain (deformation) is needed to initiate *static recrystallisation.* This deformation must be sufficient to create the recrystallising nuclei and to sustain their growth. Increasing the deformation reduces the incubation period and increases the rate of recrystallisation. Eventually a critical strain is reached above which recrystallisation starts before the end of deformation. *Metadynamic recrystallisation* refers to the case in which, the nuclei are formed during deformation and consequently no incubation period is observed. In the case of *dynamic recrystallisation*, repeated nucleation and growth occur during deformation.

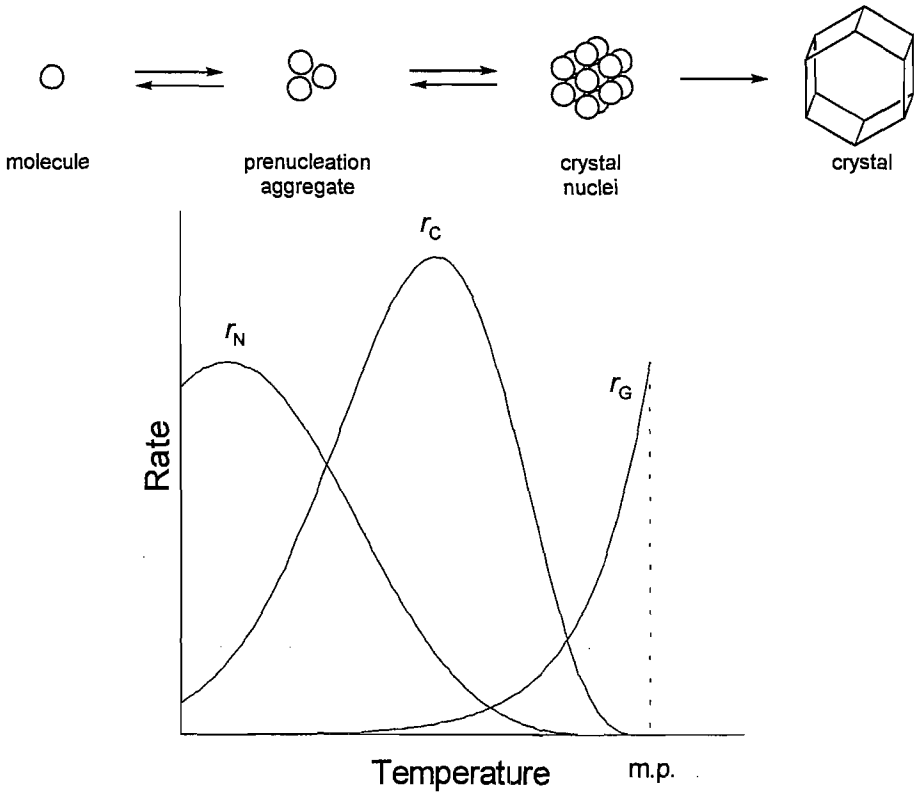


Fig. 7. Theoretical representation showing that recrystallisation occurs through nucleation (applicable to the Prout-Tompkins and JMAEK kinetic models). When the rate of crystallization is plotted as a function of temperature then the plot r_G represents the crystal growth rate, r_N the crystal nucleation rate, and r_C the overall crystallization rate (adapted and reproduced from [15]).

When we look at the transformation of mebendazole polymorph C it can be considered that the growth stage of the parent phase (polymorph C) will undergo a complete transformation to a new equilibrium phase (polymorph A). The amount of new equilibrium phase will depend on time, growth rate and the number of nuclei. Most often the equations used to describe the kinetics of transformation are grouped according to the shape of the isothermal extent of transformation (fraction, α) versus time curves as acceleratory, sigmoid or deceleratory. In the case of the transformation of mebendazole polymorph C to polymorph A in the tablets (figure 5 and figure 6) the shape of the curves approximates that of sigmoidal curves. Two equations for the kinetics of reactions involving nucleation according to sigmoidal α-time curves have been derived and are commonly used to describe the kinetics of polymorphic transformations [18].

(i) Prout-Tompkins model

If the rate of the polymorphic transformation is assumed to be controlled by linearly growing nuclei that branch into chains and are terminated more rapidly as the number of nuclei increase, then the kinetics of transformation can be described by the Prout-Tompkins equation [19,20].

$\frac{d\alpha}{dt} = k\alpha(1-\alpha)$	(1)

This equation upon integration gives

$\ln\left[\frac{\alpha}{1-\alpha}\right] = kt + c$	(2)

where c is a constant. This derivative form shows clearly the dependence of the rate on both the amount of original crystal form left and the amount of the new crystal form produced. The transformation is therefore an autocatalytic process. Sometimes the kinetics of certain transformations are better described by a *modified* Prout-Tompkins equation

$$\ln\left[\frac{\alpha}{1-\alpha}\right] = k\ln(t) + c \qquad (3)$$

Where sigmoid α-time curves have been obtained there has been a surprising lack of examination of alternative kinetic expressions, with the Prout-Tompkins equation being accepted as an empirical method of comparing this type of transformations [20]. However, the equation is not particularly convenient for application in kinetic analysis because of its indeterminate nature at small and large extremes of the extent of transformation, α. This is important for comparing the mebendazole polymorph C → A conversion in the tablets since this conversion was limited in some products, $\alpha_{max} \approx 10\ \%$.

(ii) Johnson-Mehl-Avrami-Erofeev-Kolmogorov (JMAEK) model

Another very popular kinetic model applied to solid state transformations has been the Avrami model, developed independently by several workers and thus referred to as the Johnson-Mehl-Avrami-Erofeyev-Kolmogorov (JMAEK) model [21,22,23,14,24,25]. First, for simplicity, suppose that all the nuclei grow as spheres with constant velocity, *v*, and are nucleated at some different time *T*. The nucleus which nucleated at some time *T* will have a volume at time, *t*:

$$V(t,T) = \frac{4\pi}{3}R^3 = \frac{4\pi}{3}v^3(t-T)^3 \qquad (4)$$

If the nuclei do not interfere (collide during growth), then the total volume of transformed material is the sum of all the nuclei (N) which have created at times T

$$V_{total}(t) = \int_0^t \frac{4\pi}{3}v^3(V_{total}N)(t-T)^3\,dt \qquad (5)$$

The volume fraction, α, of transformed material is:

$$\alpha = \frac{\pi}{3}Nv^3t^4 \qquad (6)$$

If the nuclei do interfere with each other, a condition which would apply at either high density of nucleation sites or long times, i.e. during stability testing, then the above equation must be modified to account for volumes of particles which are changing. If the particles are nucleated independently, then the volume fraction is given by the *Avrami* equation:

$\alpha = 1 - \exp(-\frac{\pi}{3} N v^3 t^4)$	(7)

This equation represent site saturated 3D growth. However, depending on whether all the nuclei appear at one time, or growths dimensionally, the general equation for volume transformed transformation looks like:

$\alpha = 1 - \exp(-kt^n)$	(8)

Upon integration

$[\ln(1-\alpha)]^n = kt$	(9)

This equation summarizes transformation kinetics for any case where $\alpha \rightarrow 1$ as $t \rightarrow \infty$. The characteristics of the kinetics is that of a "S-curve", i.e. slow at first, then accelerating, then decelerating. Values of k and n are diagnostic of the crystallisation mechanism. The equation has been derived for spheres, discs and line segments, representing three-, two- and one-dimensional form of isotropic constant rate growth. In the case of two dimensional (planar) growth $n = 3$ for sporadic nucleation and $n = 2$ for predetermined nucleation. A very useful way to analyze the kinetics of transformation is to plot the quantity $-\ln(1-\infty)$ versus time on a double logarithmic plot. The slope of the line is then the exponent n. To do this the Avrami equation can be linearized to:

$\ln\left(\ln\frac{1}{1-\alpha}\right) = \ln k + n \ln t$	(10)

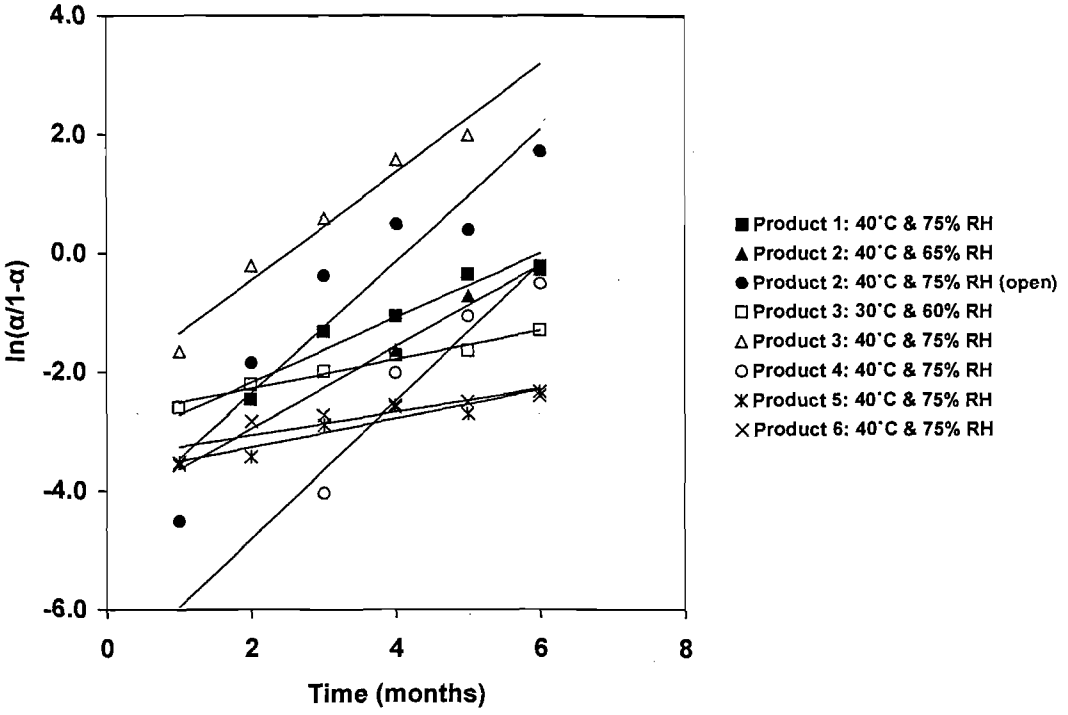


Fig. 8. Prout-Tompkins plots for mebendazole products. The slopes of the fitted lines represent the rate constant for polymorph C → polymorph A conversion.

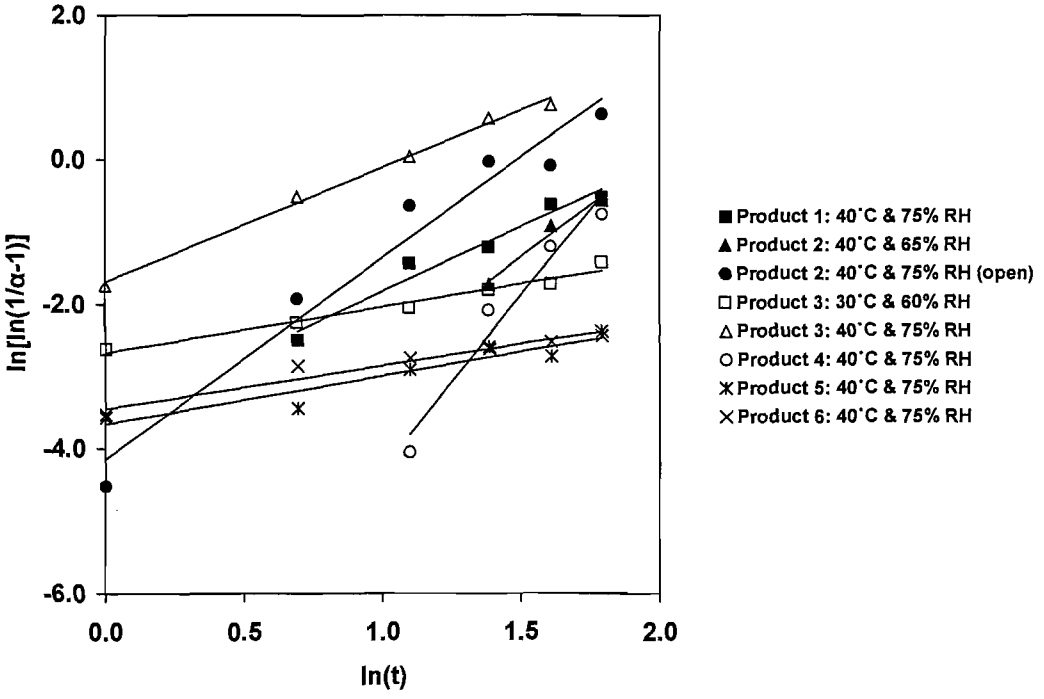


Fig. 9. Avrami plots for the mebendazole products. Data shown correspond to the transformed A volume fraction between 3% and 90%. The slopes of the lines represent the Avrami exponents, n, and the y-intercept the natural logarithm of the rate constant.

In fig. 8 and fig. 9 the Prout-Tompkins and JMAEK fits for the isothermal conversion of mebendazole polymorph C → polymorph A in the tablets are shown for those products where at least 5 % transformation was observed within 3 months. In table 2 the fit parameters for the two models are compared.

For several products at 30°C & 65% RH and some at 40°C & 75% RH no crystal transformation was observed. In addition for all the products that showed polymorph C → polymorph A conversion the start of the crystallization process was found to be preceded by a temperature-dependent *incubation time*, this leads to the sigmoidal curves shown in fig. 6. The *incubation time*, by definition, is the time that passes before the first nuclei of the new phase are formed. In table 2 the model fit results for those products showing significant transformation within 6 months, are listed. The data in table 2 show that for the transformation of mebendazole polymorph C to polymorph A in tablets, the JMAEK model gives better and less variable correlation constants (0.954±0.030) compared to the Prout-Tompkins model (0.927±0.037). For this reason the results obtained from the JMAEK model was used to calculate stability constants (table 3) and to determine difference in the rate of polymorph C → A conversion in the seven products stored at 30°C & 65 % RH and 40°C & 75 % RH. In table 3 for the JMAEK equation fit the isothermal parameters, k is known as the Avrami coefficient (also the rate constant) and n as the Avrami exponent.

Table 2. Comparison of the fit parameters for mebendazole polymorph C → polymorph A conversion in commercial products according to the Prout-Tompkins and JMAEK models of solid-state transformation

Product	Storage Conditions	Prout-Tompkins		JMAEK		
		k	r^2	ln*k*	*n*	r^2
1	40°C & 75% RH	0.547	0.9204	-3.623	1.8	0.9645
2	40°C & 75% RH	0.692	0.9625	-5.735	2.9	0.9746
2(open)	40°C & 75% RH	1.108	0.8788	-4.147	2.8	0.9603
3	30°C & 65% RH	0.318	0.9049	-2.675	0.6	0.9694
3	40°C & 75% RH	1.576	0.9943	-1.689	1.6	0.9943
4	40°C & 75% RH	1.158	0.9222	-6.871	1.1	0.9069
5	40°C & 75% RH	0.243	0.8955	-3.660	0.7	0.9420
6	40°C & 75% RH	0.600	0.9375	-3.728	0.3	0.9177

When the rate constants, *k*, calculated using JMAEK kinetics (table 3) are compared it is clear that the rate of polymorph C → A conversion was faster at 40°C & 75% RH than at 30°C & 65% RH and that Product 3 was the least stable. Even at 30°C & 65% RH the rate constant for polymorph transformation in Product 3 was 2.5 times faster than for the next fastest transformation Product 1 at 40°C & 75% RH. The fastest conversation was observed for Product 3 at 40°C & 75% RH. The rate of conversion when the tablets were stored under these conditions was 2.7 times faster than at 30°C & 65 % RH. Overall Product 7 was the most stable with no transition detected at both storage temperatures within the 6 months of testing. Product 4 was the second most stable with no polymorph C → A conversion at 30°C & 65% RH and the slowest measured conversion rate, 0.0011 $month^{-1}$, at 40°C & 75% RH. The third best product was Product 2 stored as sealed samples. However, at 40°C & 75% RH the polymorph C → A conversion in this product was almost 3 times faster than for

Product 4. For this product protecting it by storing it in a sealed container at 40°C & 75% RH slowed down the polymorph C → A conversion by a factor of 5.

Table 3. Stability parameters calculated using the JMAEK model for the mebendazole polymorph C → polymorph A conversion in the tablets

Product	Storage Conditions	JMAEK Stability Parameters		
		k (month^{-1})	$t_{1/2}$ (months)	t_{90} (months)
1	40°C & 75% RH	0.0267	26.0	3.9
2	40°C & 75% RH	0.0032	216.6	32.8
2(open)	40°C & 75% RH	0.0158	43.9	6.6
3	30°C & 65% RH	0.0689	10.1	1.5
3	40°C & 75% RH	0.1848	3.8	0.6
4	40°C & 75% RH	0.0011	630.0	95.5
5	40°C & 75% RH	0.0258	26.9	4.1
6	40°C & 75% RH	0.0240	28.9	4.4

In practical terms the importance of these results are shown by changes in the half-life ($t_{1/2} = 0.693/k$) and shelf-life ($t_{90} = 0.105/k$) listed in table 3. These values show that, except for Products 4 and 7 that showed little or no polymorph conversion, when stored at high temperature and high humidity conditions the mebendazole polymorph C → polymorph A conversion is so fast when the products are not completely sealed from the environment that most have shelf-lives of less than 7 months. This means that after these products enter the supply chain the possibility is there that patients will receive therapeutically ineffective tablets. This could explain the high variability in the success rate of treatment with mebendazole products [5] in third world countries

where environmental control of storage conditions in the supply chain is not always adequate.

The classic JMAEK model describes the kinetics of isothermal transformation from a parent phase to an equilibrium phase, by nucleation (the process by which the formation of a new phase begins), growth, and impingement (the restriction of transformed region growth by other transformed regions). This model decouples the kinetics of nucleation and growth from the geometric constraints of impingement, greatly simplifying analysis of the problem [16,17]. The theory is based on three main assumptions: an infinite volume available for transformation, random nucleation, and growth of transformed regions without preference of direction (see fig. 10). Specific simplifying assumptions have also been made about geometry and kinetics of nucleation and growth, in order to derive analytical solutions for special cases, such as zero-nucleation rate (pre-existing nuclei), constant nucleation rate, linear growth velocity, diffusion-limited growth, and growth of crystals in needle- or plate-like configurations [16,17].

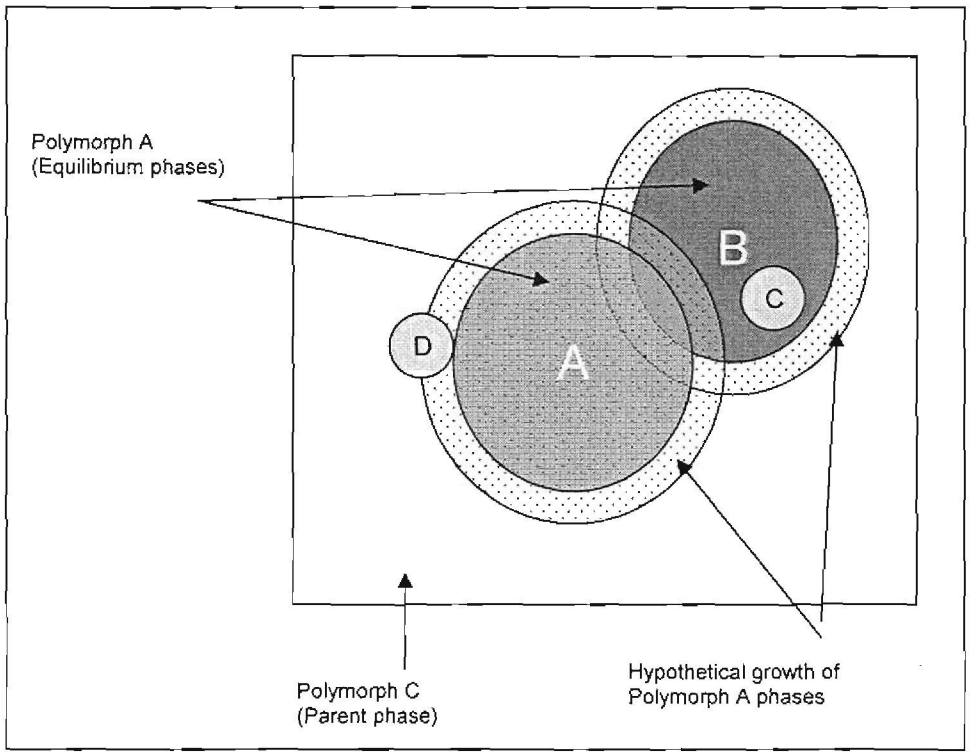


Fig. 10. Schematic presentation of a two-dimensional phase transformation according to JMAEK theory. The spheres A and B represent regions of the transformed phase (polymorph A), growing from the parent phase (polymorph C). The shells represent the hypothetical growth of A and B during an infinitesimal time interval, ignoring impingement. The spheres C and D represent nascent nuclei appearing during this

time interval, neglecting impingement (adapted and reproduced for mebendazole, using a schematic presentation by [17]).

Therefore, to get a better understanding of the actual process involved in mebendazole polymorph C → polymorph A conversion the results obtained from the JMAEK model should be studied closer, especially the importance of the Avrami exponent, *n*. According to the original theory this exponent, listed in table 2, should be an integer from 0.5 to 4 [25, 14; 21, 22; 23 & 24]. Values of $n \approx 0.5$ to 1 (Product 3 at 30°C & 65% RH and Products 4, 5 and 6 at 40°C & 75% RH) would be characteristic of linear (rodlike) crystal growth and athermal (spontaneous) nucleation rate-limited by diffusion (Smith *et al.,* 2005). Values of $n \approx 2$ (Products 1 and 3 at 40°C & 75% RH) could indicate either sporadic nucleation and linear growth with the rate limited by diffusion or spontaneous nucleation and spherical growth with the rate limited by diffusion. Both cases would suggest two-dimensional diffusion and a constant or decelerating nucleation rate. This means that the rate-limiting step for the formation of polymorph A in these products was diffusion. Product 2 at 40°C & 75% RH closed and exposed to the atmosphere represents an example of a case in which the (local) nucleation rate is a decreasing function of time ($n \approx 3$). In the limiting case of site-saturation the nucleation rate decreases very rapidly. As a result, one may assume that all of the nuclei were formed at the start of recrystallisation. The JMAEK exponent would lie between 3 and 4 if the decrease in the nucleation rate was finite.

In this study the observed values of n were not exact numbers. However, many authors have suggested possible causes for the observed discrepancies between the JMAEK model and experimental data, including non-linear growth of crystals [26], non-random nucleation [27], and effect of finite sample size [28]. However, recently Cahn [29] demonstrated that the JMAEK approach is accurate provided that the nuclei are randomly distributed. The requirement of a random distribution of nuclei is, therefore, the most serious limitation of the JMAK approach. Since the mebendazole in the products are randomly distributed throughout the tablet matrixes we assume that this requirement was met and therefore the JMAEK model is applicable to estimate the rate and type of polymorphic transformation observed for mebendazole because the basic assumptions of the model were met.

4. Conclusion

These results revealed the thermodynamic instability of mebendazole polymorph C in solid dosage forms (i.e. tablets) available in South Africa, when exposed to increased temperatures and high humidities. The polymorph C → A conversion in the tablets caused a significant decrease in the rate and extend of the mebendazole dissolution. These results showed the Avrami exponent, n, ranged from ~ 1 to 3 for mebendazole polymorph C in tablets with different compositions. Within the JMAEK approach differences in the calculated *n*-values for the polymorph C→ polymorph A conversion in the products could be explained by a difference in the number of nucleation sites, differences in nucleation rate compared to growth velocity, and the presence of an incubation time before the beginning of nucleation.

ACKNOWLEDGEMENTS

The authors would like to acknowledge financial assistance from the Research Institute for Industrial Pharmacy®, North-West University and the National Research Foundation of South Africa.

REFERENCES

[1] **CHAROENLARP, P., WAIKAGUL, J., MUENNOO, C., SRINOPHAKUN, S. & KITAYAPORN, D.** 1993. Efficacy of single-dose mebendazole polymorphic forms A and C, in the treatment of hookworm and *Thrichuis* infections. *South-east Asian Journal of Tropical Medicines and Public Health,* 24:712-716.

[2] **TERBLANCHE, R.J.** 2001. Thermo-mechanical transformation of drug polymorphs and pseudopolymorphs characterised by differential scanning calorimetry and x-ray powder diffraction. Potchefstroom: PU vir CHO. (Thesis – PHD.) 250p.

[3] **GIBBON, C.J.** 2000. South African Medicines Formulary. 4th edition. Cape Woodstock. South Africa: INCE 537p.

[4] **AL-KURDI, Z., AL-JALLAD, T., BADWAN, A. & JABER, A.M.Y.** 1999. High performance liquid chromatography method for determination of methyl-5-benzoyl-2-benzimidazole carbamate (mebendazole) and its main degradation product in pharmaceutical dosage forms. *Talanta,* 50:1089-1097.

[5] **FINCHAM, J.E., MARKUS, M.B., NGOBENI. J.T., MAYOSI. B.N., ADAMS, V.J., KWITSHANA, Z.L., OBIHARA, C.C., DHANSAY, M.A. & JACKSON, T.F.H.G.** 2005. Synchronized and regular deworming of children an women in South Africa: policy and practice. *South African Journal of Science,* 101:13-17.

[6] **SWANEPOEL, E., LIEBENBERG, W. & DE VILLIERS. M.M.** 2003. Quality evaluation of generic drugs by dissolution test: changing the USP dissolution medium to distinguish between active and non-active mebendazole polymorphs. *European Journal of Pharmaceutics and Biopharmaceutics,* 55:345-349.

[7] **INTERNATIONAL CONFERENCE ON HARMONIZATION OF PHARMACEUTICALS FOR HUMAN USE.** 2003. ICH stability testing guidelines - Q1A. Revision 2, 26p.

[8] **LIEBENBERG, W., DEKKER. T.G., LŐTTER, A.P. & DE VILLIERS, M.M.** 1998. Identification of the mebendazole polymorphic form present in raw materials and tablets available in South Africa. *Drug Development and Industrial Pharmacy,* 24(5):485-488.

[9] **BUNACIU, A.A., FLESCHIN, S. & ABOUL-ENEIN, H.Y.** 2002. Analysis improvement of drugs using modern methods. *Romanian biotechnology letters,* 7(2):647-654.

[10] **DE VILLIERS, M.M., TERBLANCHE, R.J., LIEBENBERG, W., SWANEPOEL, E., DEKKER, T.G. & SONG, M.** 2005. Variable-temperature X-ray powder diffraction analysis of the crystal transformation of the pharmaceutically preferred polymorph C of mebendazole. *Journal of Pharmaceutical and Biomedical Analysis,* 38:435-441.

[11] **UNITED STATES PHARMACOPEIAL CONVENTION.** 2007. USP30:NF25 Online. Available: www.uspnf.com.

[12] **AGBADA, C.O. & YORK, P.** 1994. Dehydration of theophylline monohydrate powder: effects of particle size and sample weight. *International journal of pharmaceutics,* 106:33-40.

[13] **PECHARSKY, V.K. & ZAVALIJ, P.Y.** 2005. Fundamentals of diffraction (*In* Fundamentals of powder diffraction and structural characterization of materials.) New York: Springer Science and Business Media Inc. 713p.

[14] **JOHNSON, W. & MEHL, R.** 1939. Reaction kinetics in processes of nucleation and growth. *Transactions of the American Institute of Mineral and Metallurgy,* 135:416-46.

[15] **HANCOCK, B.C. & ZOGRAFI, G.** 1997. Characteristics and significance of the amorphous state in pharmaceutical systems. *Jounal of Pharmaceutical Sciences,* 86(1):1-12.

[16] **CHRISTIAN, J.W.** 1975. The Theory of Transformation in Metals and Alloys. 2nd edition, Part I. New York: Pergammon 479p.

[17] **SUMPTER, M.L.** 2004. Johnson-Mehl-Avrami kinetics of intracellular ice formation in confluent tissue constructs. Gorgia: Gorgia Institute of Technology. (Thesis – M.Sc.) 95p.

[18] **BYRN, S.R., PFEIFFER, R.R. & STOWELL, J.G.** 1999. Solid State Chemistry of drugs. 2nd edition. West Lafayette, Indiana: SSCI Inc. 576p.

[19] **PROUT, E.G. & TOMPKINS, F.C.** 1944. Thermal decomposition of $KMnO_4$. *Trans. Faraday Society,* 40:448-498.

[20] **BROWN, M.E. & GLASS, B.D.** 1999. Pharmaceutical applications of the Prout-Tompkins rate equation. *International Journal of Pharmaceutics,* 190:129-137.

[21] **AVRAMI, M.** 1939. Kinetics of phase change. I: General theory. *The Journal of Chemical Physics,* 7:1103-1112.

[22] **AVRAMI, M.** 1940. Kinetics of phase change. II: Transformation-time relations for random distribution of nuclei. *The Journal of Chemical Physics,* 8:212-224

[23] **AVRAMI, M.** 1941. Kinetics of phase change. III: Granulation, phase change, and microstructures. *The Journal of Chemical Physics,* 9:177-184.

[24] **EROFEEV, B.V.** 1946. Generalized equation of chemical kinetics and its application in reactions involving solids. *Compt. Rend. Acad. Sci,* USSR (Dokl. Akad. Nauk SSSR) 52, 511-514.

[25] **KOLMOGOROV, A.** 1937. A statistical theory for the recrystallization of metals. *Bulletin of Academy of Science, USSR Material Sciences,* 1:355-359.

[26] **VAN SICLEN, C.D.** 1996. Random nucleation and growth kinetics. *Physical Review B,* 54(17):11845-11848.

[27] **CLEMENTE, R.A. & SALEH, A.M.** 2002. Crystallization kinetics: A solution for geometrical impingement. *Physics Review – B,* 65(13):132102-132105.

[28] **WEINBERG, M. & KAPRAL. R.** 1989. Phase transformation kinetics in finite inhomogeneously nucleated systems. *The Journal of Chemical Physics,* 91(11):7146-7152.

[29] **CHAN, H.K. & DOELKER. E.** 1985. Polymorphic transformation of some drugs under compression. *Drug Development and Industrial Pharmacy,* 11:315-332.

Aqueous mediated phase transformation of mebendazole polymorphic forms

Marius Brits[1*], Melgardt de Villiers[2], Wilna Liebenberg[3]

[1]Research Institute for Industrial Pharmacy®, North-West University, Potchefstroom campus, Potchefstroom, South Africa

[2]School of Pharmacy, University of Wisconsin, Madison, WI, USA

[3]Unit for Drug Research and Development, Faculty of Health Sciences, North-West University, Potchefstroom campus, Potchefstroom, South Africa

ABSTRACT

The aim of this study was to investigate the influence of moisture and heat on the stability of mebendazole polymorph B and C. Mebendazole polymorphs B & C underwent polymorphic conversions (converted to the thermodynamic form, polymorph A) when exposed to increased temperatures when suspended in water. The study revealed that moisture was a catalyst and mediator for the transformation process observed at accelerated temperatures.

Keywords: Mebendazole polymorphs; Polymorphic transitions; Polymorphism; Thermodynamic stability

* Corresponding author. Tel.: +2718-299-2323; fax: +2718-299-2291.

E-mail address: Marius.Brits@nwu.ac.za

INTRODUCTION

Mebendazole (methyl-5-benzoyl-2-benzimidazole carbamate) is a benzimidazole antihelmintic which is commonly used in the treatment of roundworm, hookworm, pinworm (threadworm), whipworm and *Strongyloides sercoralis* infestations [1]. This anthelmintic is known to act through the irreversible inhibition of glucose uptake by the parasite that leads to glycogen depletion in the parasite, which finally results in decreased adenosine triphosphate activity [2].

The thermo-mechanical stability of mebendazole polymorph C has been described by Terblanche [3]. It has been indicated that mebendazole polymorph C remained stable between room temperature and ± 179°C, and revealed that no crystal transformation seemed to occur between the mentioned temperatures. It was also showed that polymorph C transformed into the thermodynamically more stable polymorph A at higher temperatures. This transformation is a first-order process with activation energy of 238±16 kJ/mole [3].

The aim of this study was to investigate the influence of moisture and heat on the stability of mebendazole polymorph B and polymorph C.

MATERIALS AND METHODS

Materials

Mebendazole polymorph C (batch number: F10958) and polymorph B (batch number: MWB/M-007/2006) were obtained from Rolab, South-Africa and Exim-Pharm International, Mumbai, India respectively.

Methods

Approximately 500 mg portions of the mebendazole polymorph raw material were transferred into 30 amber 30 glass bottles each with tight fitting caps. Water was added to 15 of these bottles (will be referred to as *suspended samples*), the other 15 bottles (will be referred to as *dry samples*) were tightly sealed. The samples were then divided into 3 temperature groups: 5±3°C, 50±3°C and 100±2°C. Five suspended samples and five dry samples were stored at the

mentioned temperatures in incubators for 75 hours. Two bottles (one dry sample and one suspended sample) were removed from each incubator at the following intervals: 1, 6, 50 and 75 hours. The suspended samples were filtered and the mebendazole residues were allowed to dry at ambient conditions for 12 hours. XRPD and DRIFT-IR analysis were performed on all samples.

Infrared absorption spectroscopy (DRIFT-IR)

The IR-spectra of the samples were recorded on a Nicolet Nexus 470-FT-IR spectrometer (Nicolet intrument corporation, Madison, USA) over a range of 400 – 4000 cm^{-1}. The diffuse reflectance method was used. KBr was used as background material.

Infrared spectroscopy has emerged as the preferred method to identify the mebendazole polymorphic forms [4,5].

The areas of the characteristic absorption bands of the different polymorphs in the DRIFT-IR spectra of the samples were determined and used to calculate the relative polymorph A, B and C ratios present in the samples at the various intervals and to investigate the rate of the polymorphic conversions. Table 1 lists the characteristic absorption bands of polymorphs A, B and C used to calculate the polymorph ratios.

Table 1 Characteristic stretching frequencies (cm^{-1}) of the carbonyl (carbamate) and –NH stretching [6] and XRPD diffraction peak positions [7] of mebendazole polymorph A, B and C used to calculate the polymorph ratios present in the samples

Polymorph	**IR stretching frequencies (cm^{-1})**		**XRPD peaks in 3-10°2θ region**
	-NH	**>C=O**	
A	3370 cm^{-1}	1730 cm^{-1}	7.67°2θ
B	3340 cm^{-1}	1700 cm^{-1}	5.84°2θ
C	3410 cm^{-1}	1720 cm^{-1}	4.93°2θ

X-ray powder diffraction (XRPD)

The XRPD patterns of the mebendazole polymorphs indicated that the following peaks (in the 3–10 °2θ region) may be regarded as characteristic peak positions for polymorph A, B and C: 7.67, 5.84 and 4.93 °2θ respectively (table 1).

The x-ray powder diffraction patterns of the various products were recorded at ambient conditions using a Bruker D8 Advance diffractometer (Bruker, Germany). Approximately 200 mg the powdered samples were transferred into aluminium sample holders, taking care not to induce a preferential orientation of crystals. The measurement conditions were: target, Cu; voltage, 40 kV; current, 30 mA; divergence slit, 2 mm; antiscatter slit, 0.6 mm; detector slit, 0.2 mm; monochromator; scanning speed, 2°/min (step size, 0.025°; step time, 1.0 sec.).

The intensities of the characteristic peaks were used to calculate the relative polymorph A, B and C ratios present in the samples during the various intervals of the stability testing.

Microsoft® Office Excel 2003 software was used for all calculations and graphs plotted.

Several models have been developed to account for the polymorphic transitions observed in solid-state studies [8]. All of these methods assume certain geometry and rely on some consistency of the system as the process proceeds. The kinetics of the polymorphic transitions observed in the samples were investigated using the mentioned kinetic models.

RESULTS AND DISCUSSION

Effect of heat on the thermodynamic stability of mebendazole polymorph B & C in the absence of moisture

Mebendazole polymorph C

The DRIFT-IR and XRPD results indicated that the exposure of mebendazole polymorph C to 5°C, 50°C and 100°C in the absence of water for 75 hours, did not induce a polymorphic

transition. This correlated with the observations made by Terblanche [3] that mebendazole polymorph C remains stable between room temperature and ± 179 °C.

Mebendazole polymorph B

An investigation into the behaviour of solid drugs at elevated environmental temperatures is important in ensuring the stability, efficacy and safety of the drug [9]. The thermodynamic stability of mebendazole polymorph B was investigated by means of VT-XRPD.

An overlay of the XRPD patterns obtained during the VT-XRPD study is depicted in figure 1.

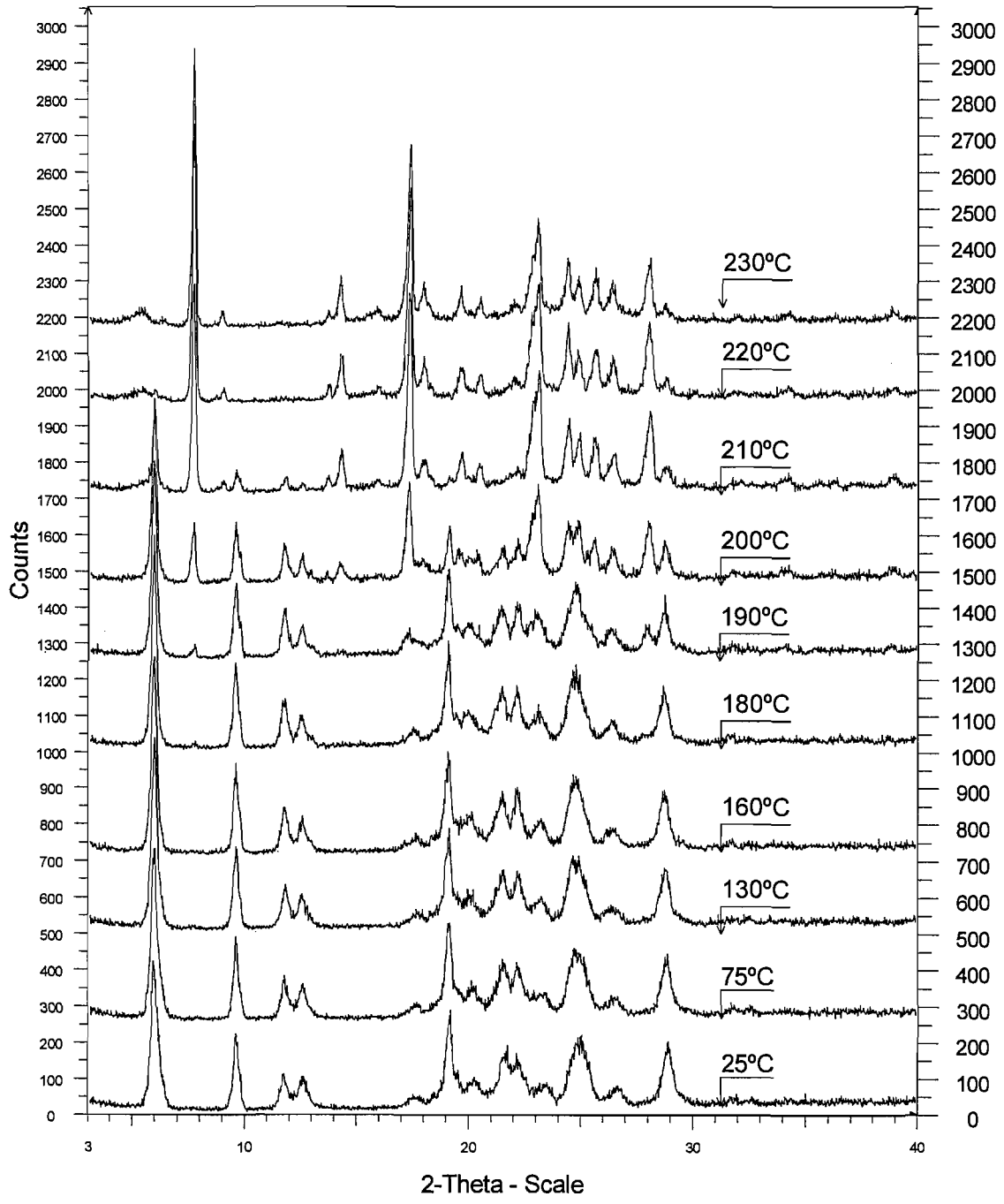


Figure 1 VT-XRPD patterns of mebendazole polymorph B at temperatures: 25-230°C.

Himmelreich *et al.* [6] stated that the heating of polymorph B below 235°C caused the transformation to polymorph A; however no VT-XRPD data was available to illustrate this transformation process.

The XRPD pattern of polymorph B remained relatively unchanged when exposed to 25-180°C. At temperatures exceeding 190°C polymorph B converted to the more stable polymorph A. At 220°C the coversion of polymorph B to polymorph A was completed.

The DRIFT-IR and XRPD results showed that the exposure of mebendazole polymorph B to 5°C, 50°C and 100°C for 75 hours did not induce any polymorphic transitions. The position of the –NH stretch and >C=O band was detected at 3340 cm^{-1} and 1700 cm^{-1} respectively, which is characteristic of mebendazole polymorph B throughout the study. No traces of polymorphs A or C were detected in any of the samples. This correlated with the results observed in the VT-XRPD study (figure 1) which indicated that mebendazole polymorph B remained stable between room temperature and ± 220°C.

Effect of heat on the thermodynamic stability of mebendazole polymorph B & C in the presence of moisture

Mebendazole polymorph C

No changes were observed in the DRIFT-IR spectra and XRPD patterns when the suspended mebendazole polymorph C samples were exposed to 5°C and 50°C over for a period of 75 hours. However, polymorphic transitions occurred when the suspended mebendazole polymorph C samples were exposed to 100°C for 75 hours.

The DRIFT-IR spectra of the samples revealed significant changes during the 75 hours in the 3550-3150 cm^{-1} (-NH stretch) region (figure 2). Initially the sample revealed a sharp absorption peak at 3403 cm^{-1}, which indicated that the sample consisted of mebendazole polymorph C. After one hour the spectrum revealed a sharp absorption peak at 3403 cm^{-1} and minor peak broadening in the 3420-3440 cm^{-1} region, which indicated the presence of surface moisture in the sample.

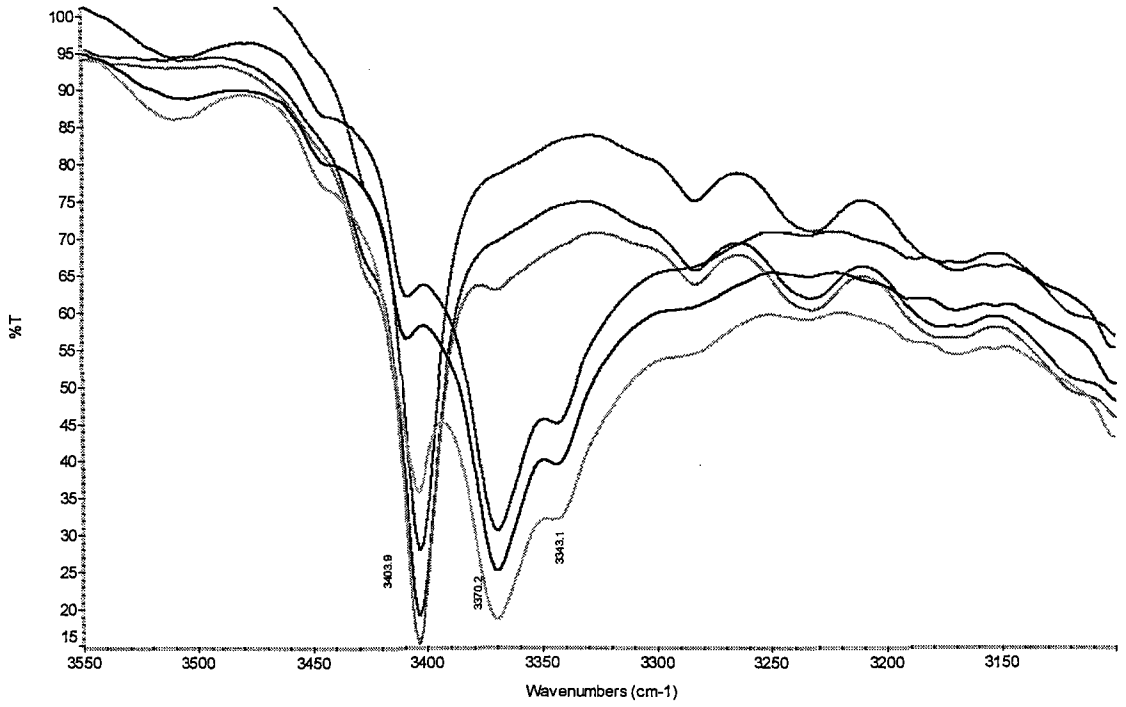


Figure 2 Overlay of DRIFT-IR spectra of the suspended mebendazole polymorph C sample – stored at 100°C over a period of 75 hours (initial, 1 hour, 6 hours, 25 hours, 50 hours, 75 hours) indicating differences in the main absorptions at the –NH stretch.

The commencement of the polymorphic transformation was observed after six hours, with the appearance of a shoulder peak at 3370 cm^{-1} which indicated that the sample contained traces of mebendazole polymorph A. After 25 hours the intensity of the 3403 cm^{-1} peak decreased significantly and the intensity of the 3370 cm^{-1} peak increased. The appearance of a shoulder peak at 3343 cm^{-1} was also observed after 25 hours, which suggested that the sample might have contained polymorph A and traces of polymorphs C and B (polymorph A >>> polymorph C >>> polymorph B).

The spectra of the samples after 50 and 75 hours were comparable in the 3550-3150 cm^{-1} region which indicated that the fraction of polymorph C in the sample has decreased significantly and mainly consisted of polymorph A and possible small traces of polymorph B.

The following observations were made in the >C=O band (1780-1700 cm^{-1}) region (figure 3):

The band present at 1717 cm^{-1} in the initial sample indicated that the sample consisted of polymorph C. After 6 hours at 100°C no changes were observed in the mentioned region. After 25 hours the intensity of the 1717 cm^{-1} band was reduced and the absorption band at 1731 cm^{-1} appeared which confirmed the polymorphic transition observed in the –NH stretch region. The band at 1717 cm^{-1} disappeared after 50 hours which indicated that the sample primarily contained polymorph A. After 75 hours no absorption peak was detected at 1717 cm^{-1}. The >C=O absorption band of polymorph B (1700 cm^{-1}) was not clearly detected during the 75 hours.

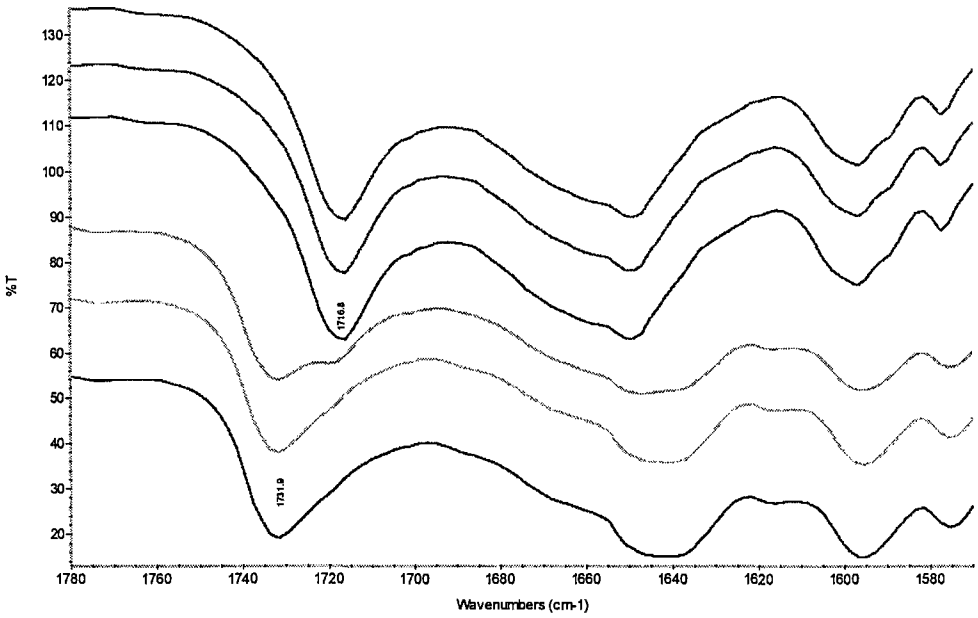


Figure 3 Overlay of DRIFT-IR spectra of the suspended mebendazole polymorph C sample – stored at 100°C over a period of 75 hours (initial, 1 hour, 6 hours, 25 hours, 50 hours, 75 hours) indicating differences in the main absorptions at the >C=O band.

The characteristic Bragg peaks of mebendazole polymorph A, B and C in the 3.1 - 9.8°2θ region are listed in table 1. The intensities of these three peaks are in the order: A > C > B. The following observations were made:

(i) The detection of mebendazole polymorph B in the presence of amorphous solids or in the presence of highly crystalline solids (such as tablet excipients) will be

complicated due to the fact that polymorph B reveals an XRPD pattern with weak intensities.

(ii) Weak intensities usually signify the absence of numerous crystal faces, for example: a sample with an XRPD pattern with low peak intensities could be considered to be less crystalline compared to a sample with an XRPD pattern with well-defined, intensified Bragg peaks. It can thus be proposed that the order of crystalinity (and therefore the order of stability) for the three polymorphs is: A > C > B. Himmelreich *et al.* [6] also stated that the order of thermal stability of the polymorphic forms is: A > C > B.

The XRPD pattern of the suspended sample exposed to 100°C for 1 hour (figure 4) was comparable to the XRPD pattern of the initial sample with the exception that the 1 hour sample revealed a peak shift of all the peaks towards the right, which could be attributed to differences in sample bed height. As mentioned the DRIFT-IR spectra of the 1 hour and initial sample were comparable.

A general decrease in the intensities of the peaks in the region of 15-30 °2θ was observed after 6 hours, which suggested the initiation of phase transformations within the crystal lattice. The effect of the polymorphic transition was clearly detectable after 25 hours. Figure 4 indicates that the XRPD pattern of the sample is characteristic to both polymorph A and polymorph C, supporting the DRIFT-IR observations.

The XRPD patterns of the 50 & 75 hours samples were comparable and resembled that of polymorph A. No traces of polymorphs C and B were detected in the diffractograms after 25 hours.

The fact that DRIFT-IR only detected the –NH stretch absorption peaks, and that neither the >C=O band nor clearly detectable crystallographic (XRPD) traces of polymorph B were detected could indicate that the presence of polymorph B could be considered trivial.

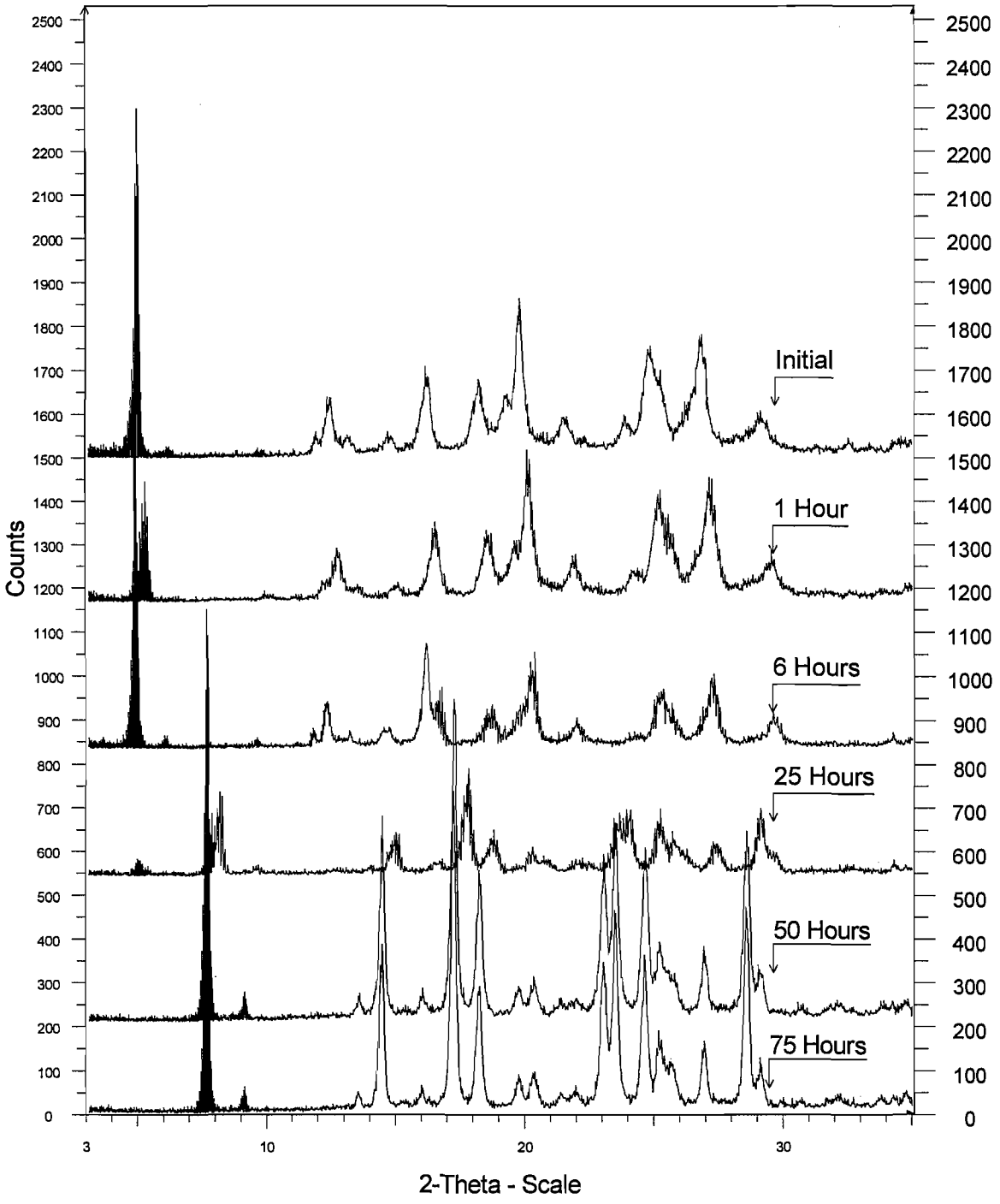


Figure 4 Overlay of the suspended mebendazole polymorph C samples exposed to 100°C at various time intervals.

It can thus be concluded that the exposure of mebendazole polymorph C to increased temperatures (up to 100°C) for a period of 75 hours in the absence of moisture did not induce any polymorphic transition, which correlated well with the observations made by Terblanche [3]. However when suspended in water, polymorphic transformations were observed at 100°C after only 6 hours, which resulted in polymorph A as final product after 50 hours.

Mebendazole polymorph B

XRPD and VT-XRPD analysis revealed that the storage of the suspended mebendazole polymorph B samples at 5°C for 75 hours did not induce any polymorphic transition.

The DRIFT-IR spectra of the suspended mebendazole polymorph B exposed to 50°C revealed that the crystal form remained unchanged during the first six hours of the study, and minor shoulder peaks appeared after 25 hours at 3401 and 1716 cm^{-1} respectively, which suggested that a fraction of the mebendazole polymorph B transformed into polymorph C.

The XRPD patterns of the suspended samples stored at 50°C confirmed that no polymorphic transformations occurred during the first 6 hours of the study. Traces of mebendazole polymorph C were detected in the samples after 25 hours. The relative intensities of the Bragg peak present at 4.93±0.1°2θ increased from 5.5 – 6.9 % during the period 25-75 hours. At the end of the 75 hour study the sample consisted primarily of mebendazole polymorph B and contained traces of polymorph C (due to the presence of the small peak at 4.93±0.1°2θ).

The XRPD patterns of the suspended sample stored at 100°C are illustrated in figure 5. The XRPD patterns confirmed the presence of polymorph C, B and A in the samples after 6 hours (figure 5). No polymorph B traces were detected in the 50 and 75 hours samples. The poor-crystalline properties of mebendazole polymorph B make the detection thereof diffucult. The XRPD pattern of the sample at 75 hours resembled only that of mebendazole polymorph A.

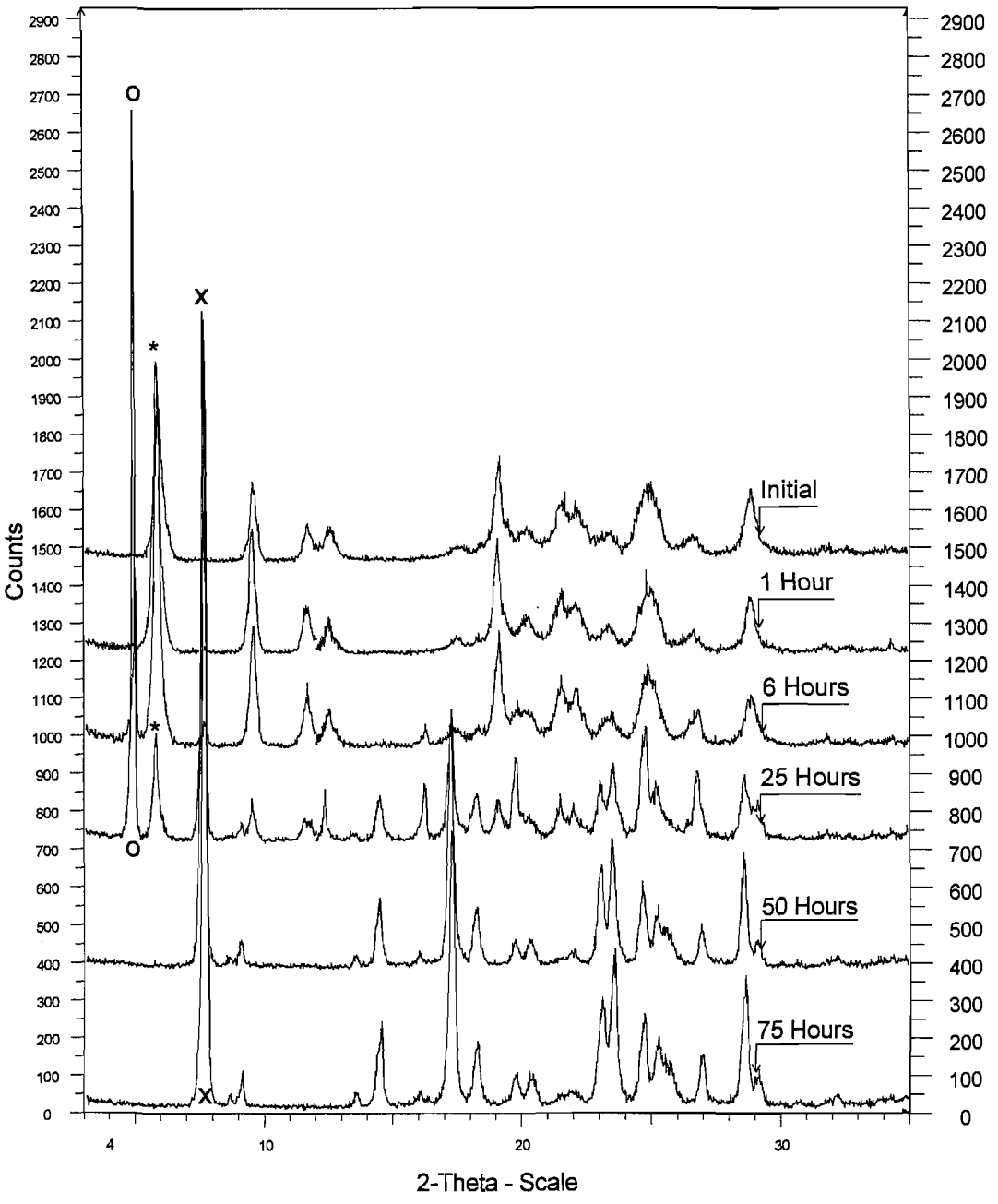
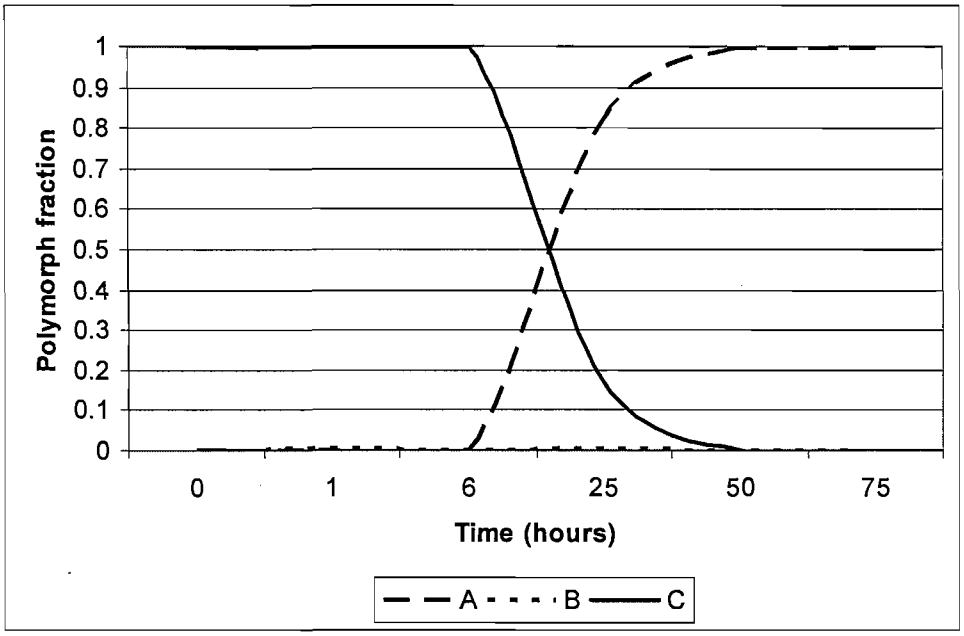


Figure 5 Overlay of the XRPD patterns of the suspended mebendazole polymorph B samples exposed to 100°C at various time intervals illustrating the polymorph transition. Characteristic peaks of polymorphs A (x), B (*) and C (o) in the 3 – 40°2θ range are indicated.

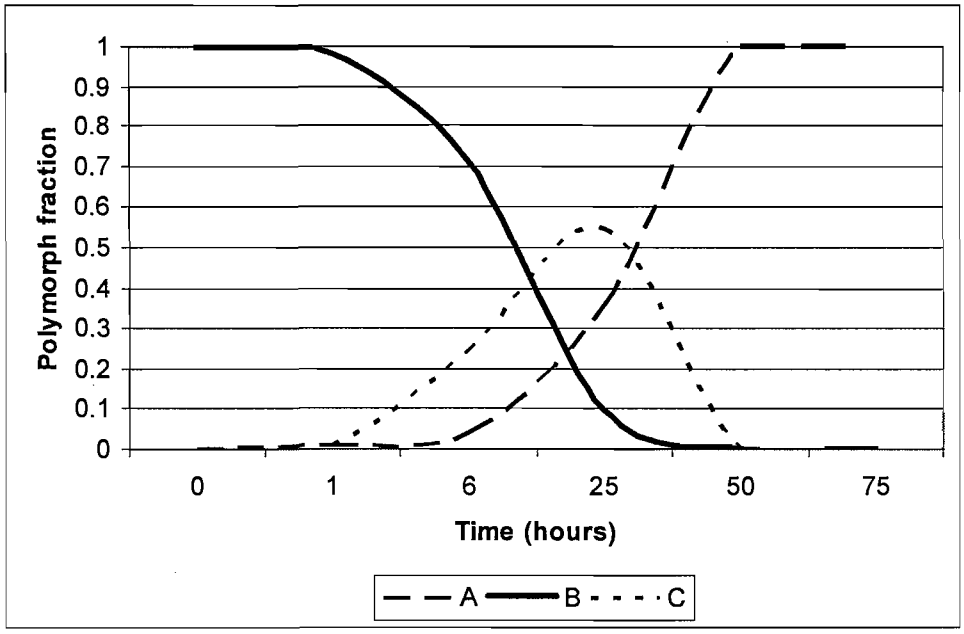
Quantitative investigation of the aqueous mediated phase transformation of mebendazole polymorph B and C

The ratios of polymorph A and C content relative to the total polymorph content in a product were calculated from the DRIFT-IR and XRPD data. For the purpose of this study the polymorph fraction present relative to the total polymorph content present in the samples derived from the intensities (i) of the characteristic peaks [for example, polymorph A fraction = $i_A/\Sigma(i_A, i_B, i_C)$] will be discussed.

As seen in figure 6 the decrease in polymorph C and the increase in polymorph A followed sigmoidal paths. However, with time a small amount of polymorph B was also present in the samples after 25 hours. This complicated the kinetics of the conversion and although the Avrami fits were reasonable with correlation coefficients around 0.9 it was not reliable.



(a)



(b)

Figure 6 Polymorph fractions present in the suspended mebendazole (a) polymorph C and (b) polymorph B at the various intervals when stored at 100°C derived from XRPD data.

Fitting the data to a more generic sigmoidal equation gave very high correlation coefficients and allowed for the prediction of half-lives and shelf-lives for the decrease and growth in form C and A. The following equation was used:

$$\alpha = \frac{a}{1+\exp\left(-\frac{t-b}{c}\right)}$$

Where a is the transition height, b is the transition center (half-life) and $2.197c$ is the transition width (c is negative for decay and positive for growth). The conversion of polymorph B (suspended in water and stored at 100°C) also followed a sigmoidal path characteristic of autocatalytic reactions.

The symbols in figure 7 represent experimental data and the lines the best fit according to abovementioned equation (data fitted using TableCurve 2D version 5.01, Systat, Richmond, CA, USA).

Table 2 illustrates the data obtained from fits of the polymorphic transformations using the data in figure 7 and the mentioned equation.

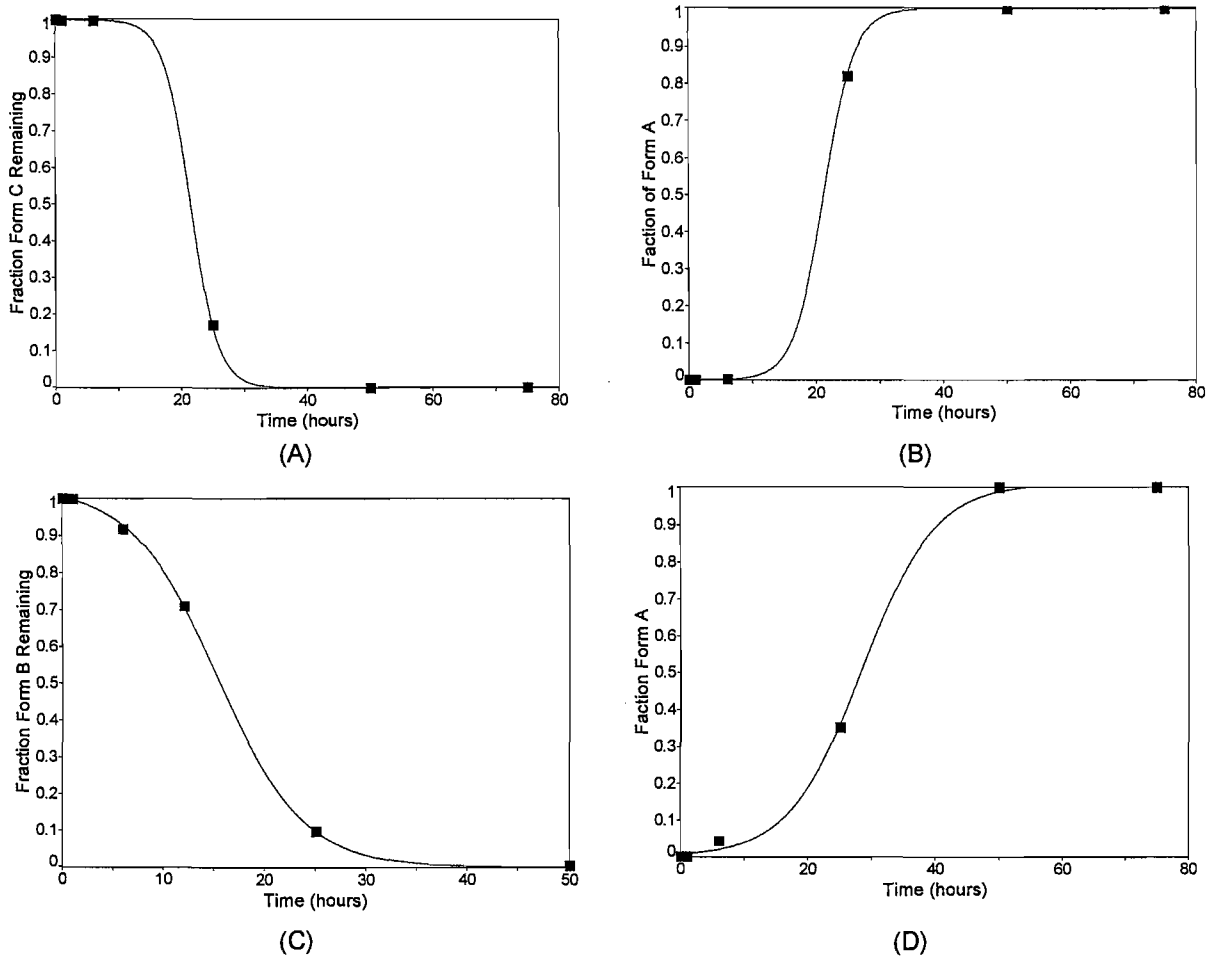


Figure 7 (A) Sigmoidal decrease in the content of mebendazole polymorph C when suspended in water at 100°C. (B) Increase in content of mebendazole polymorph A when polymorph C was stored at the same conditions. (C) Decrease in polymorph B when suspended in water at 100°C. (D) Increase in polymorph A when polymorph B was suspended in water at 100°C.

Table 2 Fit parameters for the polymorphic transformation of mebendazole polymorphs when suspended in water and stored in sealed containers at 100°C.

Transformation	Curve Fit		a	b	c
	Shape	r^2			
C decay	Sigmoidal	0.9999	0.998	21.666	-2.138
A growth from C	Sigmoidal	0.9999	0.998	21.309	2.401
B growth from C	Sigmoidal	0.9977	0.0817	5.846	0.362
B decay	Sigmoidal	0.9997	1.031	15.408	-4.277
C growth from B	Bell shape	-	-	-	-
A growth from B	Sigmoidal	0.9980	1.011	28.445	5.707

For all the transformations, except for the growth of polymorph B from C, the transition heights, a, approached 1 (table 2). This means that in all these cases the polymorphic transformations were completed within the time the tests were performed. At 100°C when suspended in water, polymorph C rapidly transformed to polymorph A with a $t_{0.5}$ = 22 hours. For this transformation, the induction period was around 7-10 hours and it took less than 5-6 hours for the conversion to be completed. The growth of polymorph A from polymorph C closely mirrored the decay in polymorph C because the $t_{0.5}$ for the formation of B was also 21 hours. In contrast the $t_{0.5}$ for polymorph B when suspended in water at 100°C was around 15 hours. In this case the induction period was markedly shorter at around 1-2 hours while the time necessary for completion of the conversion was longer at around 9-12 hours. In addition the formation of polymorph A from polymorph B was delayed with a $t_{0.5}$ = 28 hours and an even longer transition time of more than 12 hours and almost no induction period. The reason for this could be that polymorph B transformed also to polymorph C which then transformed to polymorph A. This could explain why the curve following the transformation of polymorph C is a bell shape curve. Initially

polymorph C is present and its content increase but then it decrease rapidly and eventually no polymorph C is detected.

Theory of the aqueous mediated phase transformation of mebendazole

Swanepoel *et al.* [10] indicated that polymorph C went into solution faster (70% in 120 minutes) compared to polymorph B (37% in 120 minutes) and polymorph A (20% in 120 minutes) when dissoluted in 0.1 N HCl at 25±2°C. The mentioned authors also indicated that the order of the solubility of the mebendazole polymorphs is: B > C > A. The order of the dissolution rate (C > B > A) does not correlated with the reported differences in the reported solubilities of the various forms.

From this study it became clear that this incongruity could be attributed to the solvent mediated transformation of the metastable forms (i.e. polymorphs B and C) during the prolonged exposure (48 hours) to the aqueous solvent used during the solubility studies performed by Swanepoel *et al.* [10].

The Gibbs free energy is defined as the enthalpy (H) of the system minus the product of the temperature (T) times the entropy (S) of the system:

$$G = H - TS$$

The changes in the free energy of a system during dissolution can be measured at a predetermined temperature and is expressed in the following equation:

$$\Delta G = \Delta H - T\Delta S$$

ΔG is negative for a reaction in which ΔH is negative and ΔS is positive. Thus ΔG is negative for any reaction that is favoured by both the enthalpy and entropy terms, and this reaction could be considered spontaneous.

Mebendazole reveals a negative Gibbs free energy (G) in an aqueous solution [11], utilising the solvent mediated phase transformation theory of Cardew and Davey [12] and Ostwald's Rule (W. Ostwald (1897) (as cited in Schmeltzer *et al.*[13]):

"...in the course of transformation of an unstable (or metastable) state into a stable one the system does not go directly to the most stable conformation (corresponding to the modification with the lowest free energy) but prefers to reach intermediate stages (corresponding to other metastable modifications) having the closest free energy to the initial state".

One can consider the theoretical phase diagram (which could be viewed as a monotropic / enantiotropic system (far away from the transition temperature)) for the mebendazole polymorphs (figure 8) to describe the solvent mediated transformation of mebendazole polymorph B.

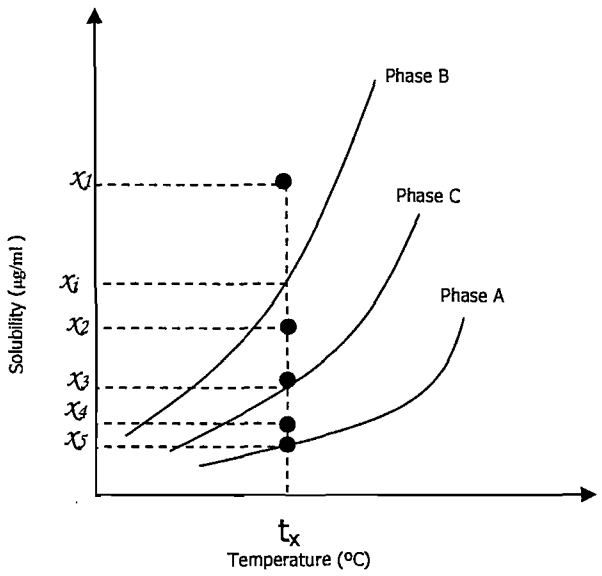


Figure 8 Theoretical solubility curves for mebendazole polymorphs.

In the phase diagram (figure 8) the stability of the mebendazole polymorphs are in the order: B > C > A as reported by Himmelreich *et al.* [6].

For a solution with composition x_2 at t_x, it is supersaturated with respect to phases A & C, whilst for a solution of composition x_i at the same temperature (t_x) it is possible that al three phases could precipitate.

Thus according to Ostwald's Rule the metastable form will appear first (polymymorph B) causing the solution composition to drop to x_1 (i.e. the solubility of polymorph B). At this point the solution is supersaturated with respect to phases A and C, so it is not unreasonable to suppose that phase B is the foremost solid phase appearing. Some nuclei of phase C and A might also be present [13] in the solution.

The presence of the phase C and phase A nuclei will thus initiate the transformation process, namely a slurry of uniformly sized crystals of phase B in contact with the saturated solution containing equi-sized nuclei of the more stable phases, i.e. A and C.

As the nuclei growth proceeds the solubility of the system falls towards X_5, causing the system to become undersaturated with phase B, causing the phase B crystals to dissolve and thereby promoting the growth of the phase C and phase A crystals. The simultaneous dissolution of the metastable phase and growth of the more stable phase will continue until the metastable phases have been totally conformed into the stable phase and the solubility of the solution will decrease to X_5.

It is thus clear that the change in the volume fractions of the metastable phases (B and C) causes a change in the supersaturation of the system due to the growth-controlled transformation. Thus it can be concluded that during the prolonged exposure of the metastable polymorphs to the aqueous solubility media, a fraction of the polymorph B phase transformed to polymorph C which contained a smaller fraction polymorph A, compared to the polymorph C fraction which converted to the stable (and less soluble) polymorph A phase. It thus seems as if the rate of

conversion from the metastable phases (polymorphs B & C) into the stable phase (polymorph A) is faster for the polymorph C, due to the direct conversion of polymorph C → polymorph A.

CONCLUSION

Mebendazole polymorphs B & C underwent polymorphic conversions (converted to the thermodynamic form, polymorph A) when exposed to increased temperatures when suspended in water. The study revealed that moisture was a catalyst and mediator for the transformation process observed at accelerated temperatures.

ACKNOWLEDGEMENTS

The authors would like to acknowledge financial assistance from the Research Institute for Industrial Pharmacy®, North-West University and the National Research Foundation of South Africa.

REFERENCES

[1] GIBBON, C.J. 2000. South African Medicines Formulary. 4th edition. Cape Woodstock. South Africa: INCE 537p.

[2] AL-KURDI, Z., AL-JALLAD, T., BADWAN, A. & JABER, A.M.Y. 1999. High performance liquid chromatography method for determination of methyl-5-benzoyl-2-benzimidazole carbamate (mebendazole) and its main degradation product in pharmaceutical dosage forms. *Talanta,* 50:1089-1097.

[3] **TERBLANCHE, R.J.** 2001. Thermo-mechanical transformation of drug polymorphs and pseudopolymorphs characterised by differential scanning calorimetry and x-ray powder diffraction. Potchefstroom: PU vir CHO. (Tesis – PHD.) 250p.

[4] LIEBENBERG, W., DEKKER. T.G., LŐTTER, A.P. & DE VILLIERS, M.M. 1998. Identification of the mebendazole polymorphic form present in raw materials and tablets available in South Africa. *In.* Drug development and industrial pharmacy. 24(5):485-488.

[5] BUNACIU, A.A., FLESCHIN, S. & ABOUL-ENEIN, H.Y. 2002. Analysis improvement of drugs using modern methods. *In.* Roumanian biotechnology letters. 7(2):647-654.

[6] HIMMELREICH, M., RAWSON, B.J. & WATSON, T.R. 1979. Polymorphic forms of mebendazole. *In.* Australian journal of pharmaceutical sciences. 6(4):123-125.

[7] DE VILLIERS, M.M., TERBLANCHE, R.J., LIEBENBERG, W., SWANEPOEL, E., DEKKER, T.G. & SONG, M. 2005. Variable-temperature X-ray powder diffraction analysis of the crystal transformation of the pharmaceutically preferred polymorph C of mebendazole. *In.* Journal of pharmaceutical and biomedical analysis. 38:435-441.

[8] **AGBADA, C.O. & YORK, P.** 1994. Dehydration of theophylline monohydrate powde — effects of particle size and sample weight. International journal of pharmaceutics. 106:33 - 40.

[9] BYRN, S.R., PFEIFFER, R.R. & STOWELL, J.G. 1999. Solid-state chemistry of drugs. West Lafayette, Indiana: SSCI, Inc. 575p.

[10] SWANEPOEL, E., LIEBENBERG, W. & DE VILLIERS. M.M. 2003. Quality evaluation of generic drugs by dissolution test: changing the USP dissolution medium to distinguish between active and non-active mebendazole polymorphs. *In.* European journal of pharmaceutics and biopharmaceutics. 55:345-349.

[11] SHEHATTA, I. 2004. Cyclodextrins as enhancers of the aqueous solubility of the anthelmintic drug mebendazole: thermodynamic conciderations. *Chemical Monthly,* 133(9):1239-1247.

[12] SCHEMELZER, J. 1998. Ostwald's rule of stages. The effect of elastic strains and external pressure.: MOELLER, J. & GUTZOW, I. *Physical Chemistry,* 204(1/2):171-181.

[13] CARDEW, P.T & DAVEY, R.J. 1985. The kinetics of solvent-mediated transformations. *Proceedings of the Royal Society of London, Series A, Mathematical and Physical Sciences,* 389(1815):415-428.

Thermodynamic stability of two venlafaxine HCl polymorphic forms

Marius Brits[1*], Melgardt de Villiers[2], Wilna Liebenberg[3]

[1]Research Institute for Industrial Pharmacy®, North West University, Potchefstroom campus, Potchefstroom, South Africa
[2]School of Pharmacy, University of Wisconsin, Madison, WI, USA
[3]Unit for Drug Research and Development, Faculty of Health Sciences, North-West University, Potchefstroom campus, Potchefstroom, South Africa

ABSTRACT

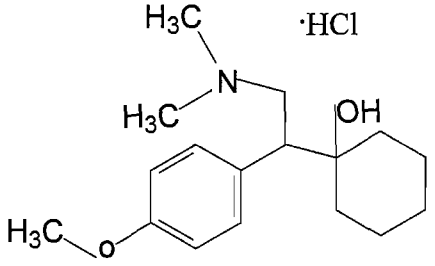
Venlafaxine hydrochloride is a phenethylamine antidepressant wich is widely used for the treatment of depression. The aim of this study was to investigate the thermodynamic stability of two polymorphic forms of venlafaxine HCl and to investigate the influence of increased temperatures on the solubility of these crystal forms.

Keywords: Venlafaxine, polymorph, crystal forms, thermodynamic stability, solid-state properties

* Corresponding author. Tel.: +2718-299-2323; fax: +2718-299-2291. E-mail address: Marius.Brits@nwu.ac.za

1. INTRODUCTION

Venlafaxine hydrochloride (venlafaxine HCl): (R,S)-1-[(2-Dimethylamino)-1-(4-methoxyphenyl)ethyl]cyclohexanol hydrochloride, is a structurally novel phenethylamine antidepressant, which inhibits monoamine re-uptake, with the greatest effect on serotonin, a substantial effect on norepinephrine, and relatively minor effects on dopamine (1).



Venlafaxine HCl is a chiral molecule and is therefore optically active, the racemate is being used clinically. Venlafaxine HCl is currently not available in any combination preparations.

The pharmacological activity of the (-)-isomer, is similar to that of the racemate, whereas the (+)-isomer, primarily inhibits serotonin uptake. There is no evidence for any stereoselective metabolism of venlafaxine HCl in the majority of subjects (2).

The patenting of the synthesis of venlafaxine in the mid 1980's induced a cascade of intellectual property claims of the polymorphic and pseudopolymorphic forms thereof.

2. MATERIALS AND METHODS

2.1 Materials

Venlafaxine HCl raw material was obtained from Unichem Laboratories Ltd, South Africa, Batch no: VEN/20301. Analytical grade methanol (ACE (Pty) Ltd, South Africa) and ethyl acetate (Saarchem, Merck chemicals (PTY) LTD., South Africa) were used as solvents for recrystallisation.

2.2 Methods

2.2.1 X-ray powder diffractometry

The X-ray powder diffraction profiles were obtained at room temperature with a Bruker D8 advance diffractometer (Bruker, Germany). The measurement conditions were: target, Cu, voltage, 40 kV; current, 30 mA; divergence slit, 2 mm; anti scatter slit, 0.6 mm: detector slit, 0.2 mm; monochromator, scanning speed, 2°/min (step size 0.025°, step time, 1.0 sec). Approximately 200 mg sample was loaded into an aluminium sample holder, taking care not to introduce a preferential orientation of the crystals.

2.2.2 Differential Scanning Calorimetry

DSC thermograms of the venlafaxine hydrochloride samples were recorded with a Shimadzu DSC-50 instrument (Shimadzu, Kyoto, Japan). Samples weighing 3-5 mg were heated in closed aliminium crimp cells at a rate of 10°C/min under a nitrogen purge of 35 ml/min.

2.2.3 Scanning electron microscopy (SEM)

The information obtained from SEM is visual and descriptive of nature. The particle morphology of the pharmaceutical solids was investigated using SEM. A FEI Quanta 200 ESEM & Oxford INCA 400 EDS system (FEI, USA) was used to obtain photomicrographs of the various crystal forms studied. The samples were adhered to a small piece of carbon tape, mounted onto a metal stub and coated with a gold-palladium film (Eiko Engineering ion Coater IB-2, USA).

3. RESULTS

3.1 Preparation of the polymorphic crystal phases

The following methods were used to prepare venlafaxine HCl Form 1 and Form 5:

Form 1

The following recrystallisation method was used to produce venlafaxine HCl Form 1 crystals. Analytical grade methanol (ACE (Pty) Ltd, South Africa) was used for the recrystallisation of venlafaxine HCl.

Venlafaxine HCl powder was added to small volumes of the solvent (methanol). A saturated solution was prepared by dissolving venlafaxine HCl in the solvent, while heating the solution to the boiling point of the solvent (64°C). The solution was prepared under constant magnetic stirring.

The saturated solution was prepared and the process of recrystallisation was accelerated by using a rotary evaporator attached to a vacuum to evaporate all the solvent from the saturated

solution. A Buchi Rotavapor R110 rotation evaporator (Buchi, Flawil, Switzerland) was used. The heating bath temperature was set at 100±5°C.

Form 5

The following recrystallisation method was used to produce venlafaxine HCl Form 5 crystals. Analytical grade methanol was used for the recrystallisation of venlafaxine HCl.

Venlafaxine HCl powder was added to small volumes of the solvent (methanol). A saturated solution was made by dissolving venlafaxine HCl in the solvent at room temperature. The solution was prepared under constant magnetic stirring.

The saturated solution was prepared and the process of recrystallisation was accelerated by the addition of an anti-solvent (ethyl acetate) while cooling the solution in an acetone-ice bath. The fine needles were filtered after 24 hours and dried at ambient conditions.

3.2 Characterisation of polymorphic crystal phases

3.2.1 X-ray powder diffraction

The XRPD patterns of the two venlafaxine HCl crystal forms prepared are shown in figure 1. The XRPD pattern of the recrystallised Form 1 was concurrent to that described in the literature (3). The XRPD patterns of Form 5 and that of Form 2 (3) showed some resemblances.

The diffraction peaks at 7.4, 14.9 and 23.0 °2θ in the XRPD pattern of Form 5 which are absent in the XRPD pattern of Form 2 enthused the possibility of the existence of a mixture of crystal forms (i.e. Form 2 and other venlafaxine hydrochloride polymorphs). Bragg peaks at 7.4, 14.9 and 23.0 °2θ appear in the XRPD pattern of venlafaxine hydrochloride crystal Form γ described by Brits (4), but the absence of the distinct diffraction peak at 4.2 °2θ out-ruled this possibility.

The presence of peaks at 7.4, 14.9 and 23.0 °2θ that are absent in the XRPD pattern of Form 2 might be attributed to preferred orientation displayed by the crystal form but it can not be assumed with confidence that Form 5 was indeed concomitant to Form 2 described in literature, and was therefore regarded as a novel crystal form and dubbed venlafaxine Form 5.

SEM photomicrographs of the prepared venlafaxine hydrochloride Form 1 and Form 5 revealed columnar (i.e. rod-like particle, having a width and thickness exceeding that of needle-type particles) and avicular (i.e. needle-like) crystal structures respectively (figure 1).

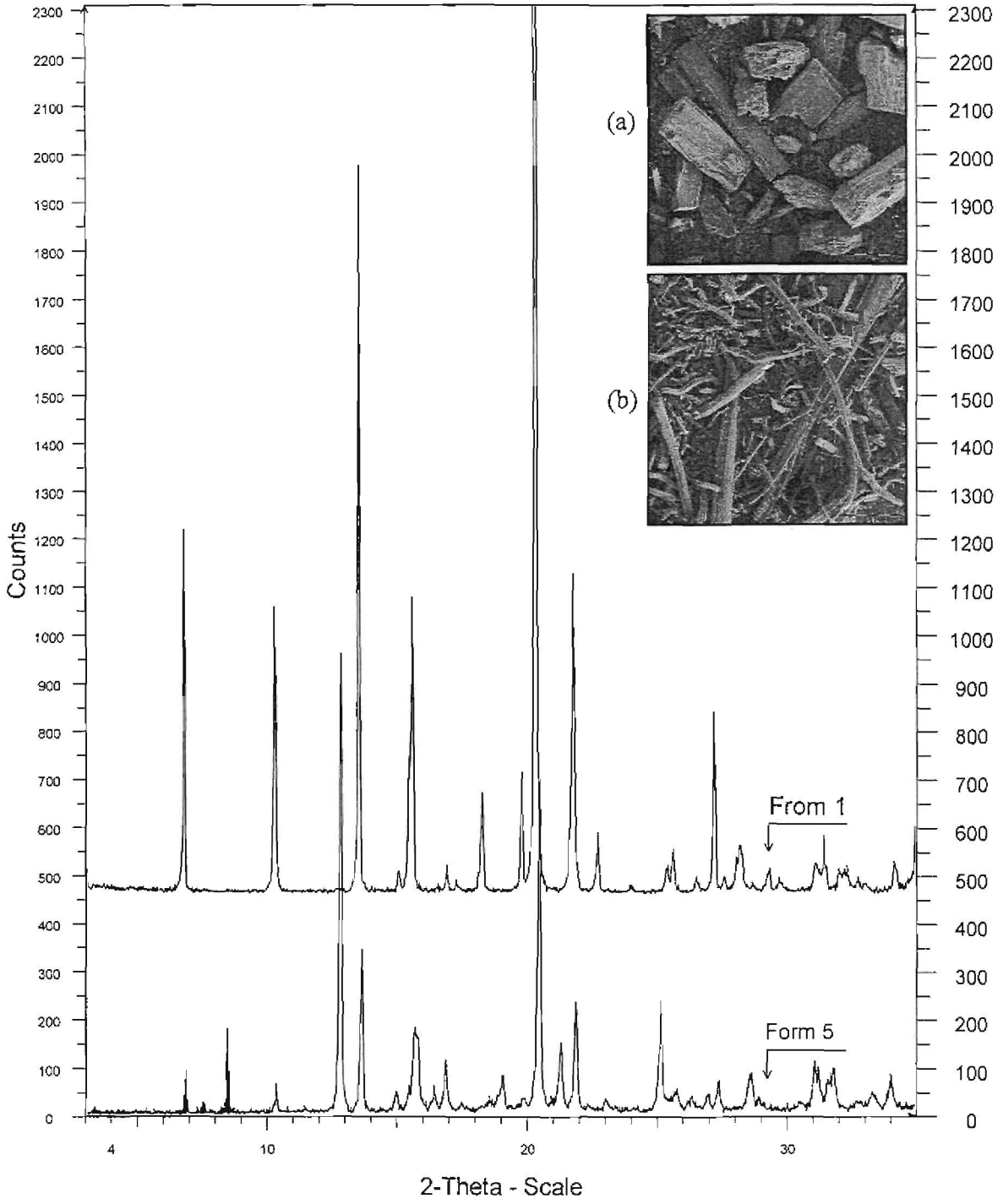


Figure 1 XRPD patterns of venlafaxine HCl crystal Form 1 and Form 5 and SEM photomicrographs of (a) Form 1 and (b) Form 5.

3.2.2 Thermal analysis

The DSC thermogram of crystal Form 1 (figure 2) exhibited a single melting endotherm at 211°C, followed by a decomposition endotherm. The absence of any desolvation endotherms indicated that crystal Form 1 was an anhydrous form. The heat of fusion (ΔH_{fl}) was calculated to be approximately 109.31 J/g. A summary of the thermal events that the two venlafaxine HCl polymorphs (i.e Form 1 and Form 5) exhibited is summarized in table 1.

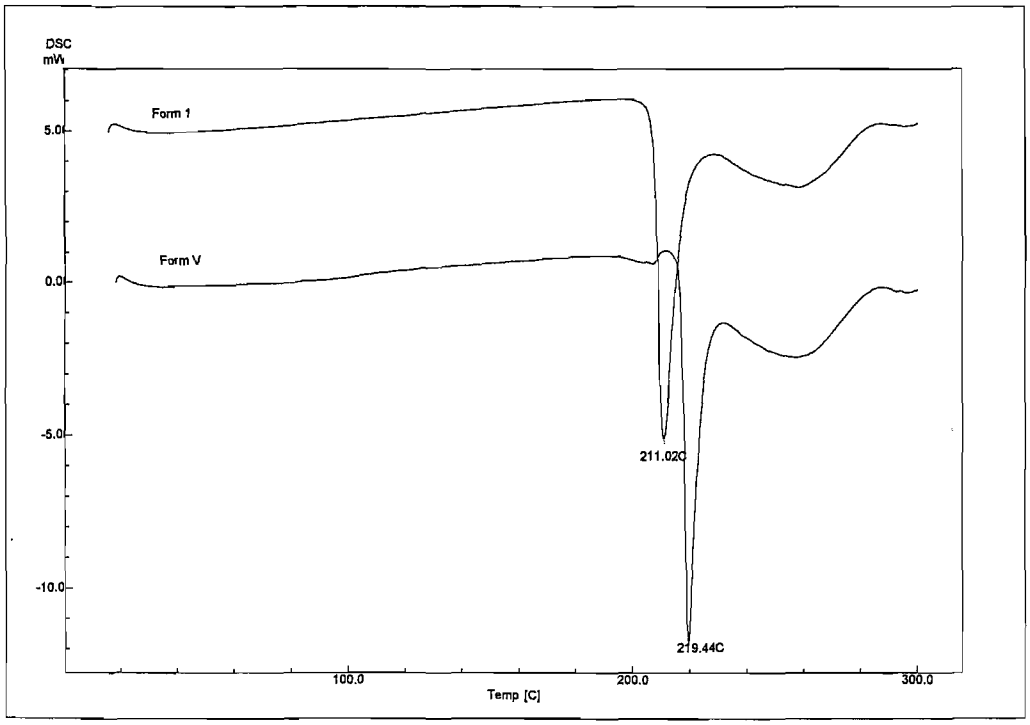


Figure 2 DSC thermograms of venlafaxine HCl crystal Form 1 and crystal Form 5.

Table 1 Summary of thermal properties of venlafaxine HCl crystal Form 1 and Form 5

Form	Melting point (°C)	Heat of fusion (J/g)
Form 1	211.02	109.31
Form 5	219.44	85.35

The DSC thermogram of crystal Form 5 (Figure 2) exhibited a melting endotherm in the region of 219-221°C, followed by a decomposition endotherm. The absence of any desolvation endotherms indicated that crystal Form 5 was a true polymorph. The heat of fusion (ΔH_{fv}) was calculated to be approximately 85.35 J/g.

3.2.3. Solution microcalorimetry

The heats of solution of the velafaxine HCl polymorphs were determined by isothermal high sensitivity microcalorimetry (MicroDSC III, Setaram, France) at 20, 30 and 40°C. Samples weighing approximately 2 mg were analysed in a mixing "batch" vessel under nitrogen purging with about 0.15 g deionised water used as the solvent (Nanopure, Barnstead International, Dubuque, Iowa). The vessel is composed of a cylinder and a set of parts mounted on a rod provided for dividing the experimental volume into two distinct chambers with a volume of 0.2 cm^3 for the upper chamber and 0.55 cm^3 for the lower chamber. The powder was placed in the bottom of the mixing vessel while the solvent was added to the top reservoir. Once the instrument was equilibrated at 20, 30 or 40°C, the rod was pushed down allowing the solvent to come in contact with the venlafaxine HCl powder. The heat measured, once corrected for the heat involved in stirring (second peak in figure 3), represent the heat involved in the dissolution of the venlafaxine powders in water. All measurements were repeated 6 times.

The heat of solution, ΔH, is calculated using the following equation:

$$\Delta H = \frac{q}{mol}$$

Since the heat (q) comes from the chemical reaction of the solute, ΔH is per moles solute, not per mol solution.

The effect of temperature on the solubility of a solid in water may be predicted using *Le Principe du Chatelier* if it is known whether the process is endo- or exothermic. If the solution process is endothermic, solubility increases with increasing temperature; if exothermic, solubility decreases. As seen in figures 4 and 5, the heat of solution for the venlafaxine crystal forms were exothermic. As shown in table 2, the symbol ΔH is used to denote the enthalpy changes. If heat is evolved, the reaction is *exothermic* ($\Delta H < 0$) as shown in figures 4 and 5; and if heat is absorbed, the reaction is *endothermic* ($\Delta H > 0$). When a salt such as venlafaxine HCl dissolves in water, energy is required to break up the crystal lattice (the attraction between ions is called the crystal lattice energy), called $\Delta H_{lattice}$. Since energy is added to system to break the lattice, $\Delta H_{lattice}$ is always positive, i.e. endothermic. When the ions are solvated by water (surrounded by water) energy is released in the formation of intermolecular bonds between ions and water (energy of hydration). We call this energy $\Delta H_{hydration}$. Since energy is lost by the system $\Delta H_{hydration}$ is always negative, i.e. exothermic. The relationship between lattice energy ($\Delta H_{lattice}$), heat of hydration ($\Delta H_{hydration}$), and $\Delta H_{solution}$ is:

$$\Delta H_{solution} = -\Delta H_{lattice} + \Delta H_{hydration}$$

When the energy of hydration is greater than the crystal lattice energy, the dissolving process will be exothermic and causes a temperature increase as seen for the venlafaxine HCl polymorph ($\Delta H_{hydration} > \Delta H_{lattice}$ then, $\Delta H_{solution} < 0$, table 2 and figure 3) and therefore it's an exothermic reaction. In addition when the enthalpy of dissolution is exothermic, as in the case of venlafaxine HCl, a temperature increase will decrease solubility.

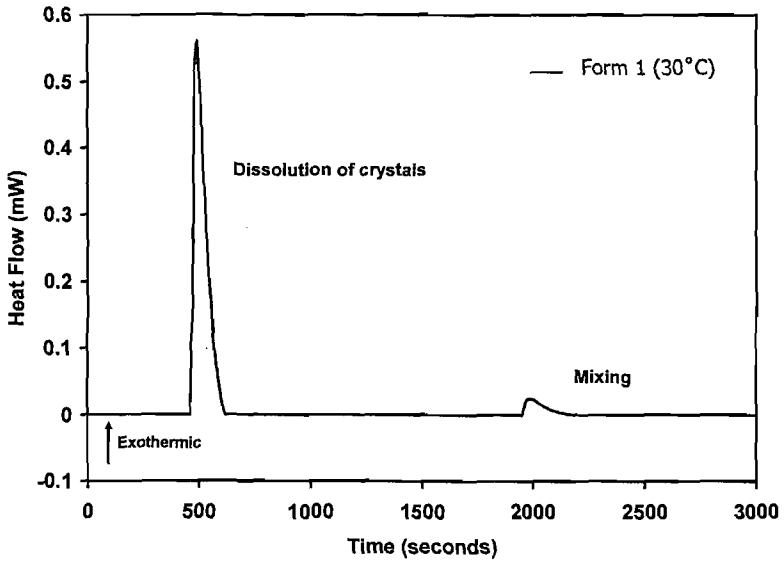


Figure 3 MDSC thermogram used for determining the heat of solution of venlafaxine HCl Form 1.

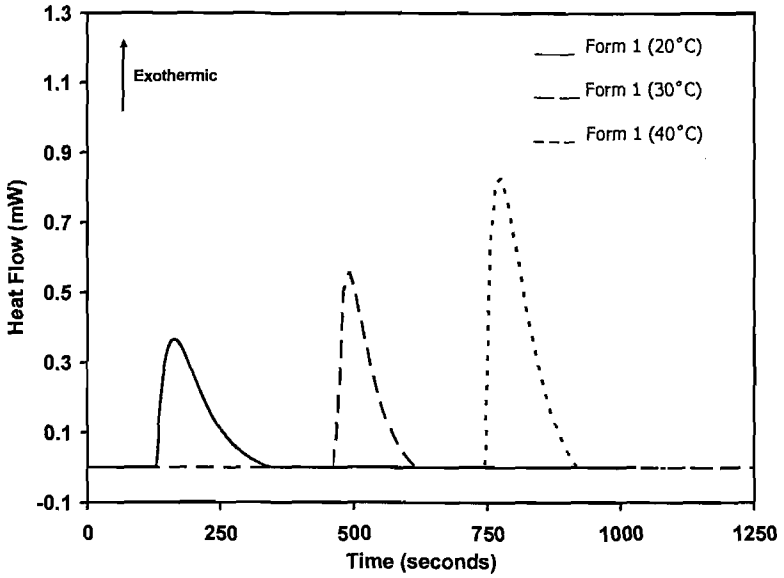


Figure 4 MDSC thermograms showing the exothermic heat generated at the dissolution of venlafaxine Form 1 at 20, 30 and 40°C.

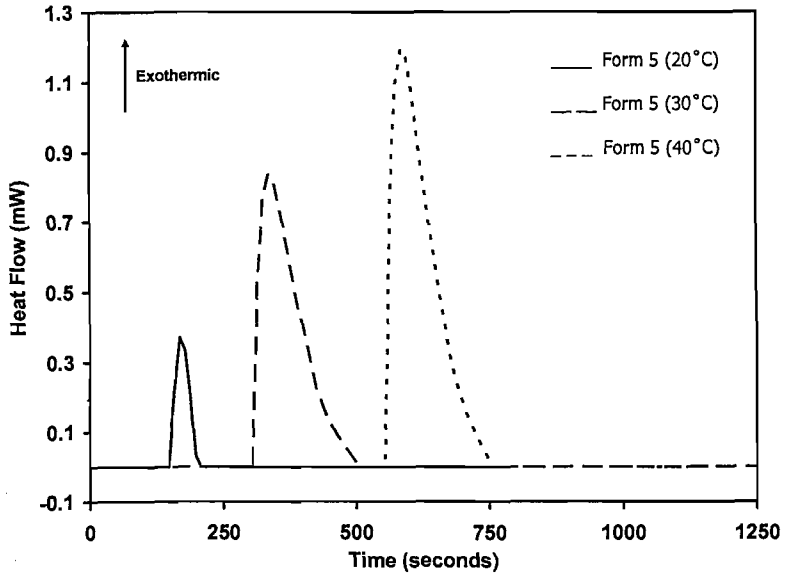


Figure 5 MDSC thermograms showing the exothermic heat generated at the dissolution of venlafaxine Form 5 at 20, 30 and 40°C.

Table 2 Heat of solution at increasing temperatures for venlafaxine HCl Form 1 and Form 5

Temperature (°C)	Form 1		Form 5	
	ΔH_{sol} (J/g)	ΔH_{sol} (kJ/mol)	ΔH_{sol} (J/g)	ΔH_{sol} (kJ/mol)
20	-18.22±1.78	-5.71±0.56	-17.29±2.31	-5.42±0.72
30	-40.93±2.22	-12.84±0.70	-115.17±3.62	-36.16±1.13
40	-61.82±2.65	-19.40±0.83	-159.98±5.12	-50.21±1.61

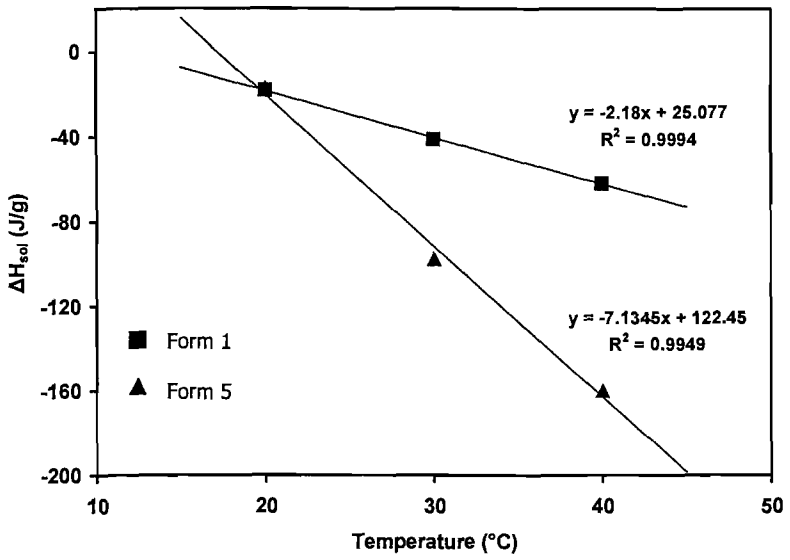


Figure 6 Change in the exothermic heat of solution of Form 1 and Form 5 of venlafaxine HCl with an increase in temperature.

To see this effect the heats of solution at increasing temperatures were measured as illustrated in figures 4, 5 and 6. Elevation of the temperature for the same concentration of drug polymorph resulted in a linear increase in the exothermic heats of solution. This is because there is a greater destruction of the primary structure of the water structure caused by thermal effects at higher temperature. This effect was less pronounced for lower melting crystals of Form 1.

Spontaneous reactions depend on two forces, enthalpy (ΔH) and entropy (ΔS). The Gibbs free energy (G) relates this effect:

$$\Delta G = \Delta H - T\Delta S$$

where G is Gibbs free energy, H is enthalpy, S is entropy, and T is the Kelvin temperature. When ΔG for a reaction is negative, the reaction will be spontaneous. When ΔG for a reaction is positive, the reaction will not be spontaneous. When ΔG is zero, the reaction is at equilibrium. If both enthalpy and entropy decrease the energy of the system ($-\Delta H$ and $+\Delta S$),

the reaction will be spontaneous. If both of these forces increase the energy of the system (+ΔH and -ΔS), the reaction will be non-spontaneous. If one force increases the energy of the system and the other decreases it, spontaneity will be determined by the larger force. Since entropy is linked to temperature, higher temperatures increase the effect of entropy.

The temperature dependence of solubility is usually explained using Le Chatelier's principle. The principle states that when a system at equilibrium is placed under stress, the equilibrium will shift in a way that relieves that stress. In the case of venlafaxine HCl, the "stress" is the addition of heat. If the heat given off in the dissolving process is greater than the heat required to break apart the solid, the net dissolving reaction is exothermic as seen for venlafaxine HCl. The addition of more heat (increased temperature) inhibits the dissolving reaction (broader peaks at higher temperatures in figures 4 and 5) since excess heat is already being produced by the reaction. This decreases the solubility of the drug with an increase in temperature.

This situation is not very common where an increase in temperature produces a decrease in solubility.

3.3 Thermodynamic relationship between polymorphic crystal phases

The thermodynamic stability of polymorphic and pseudopolymorphic forms is of great interest to researchers in the pharmaceutical research and development field. It is of utmost importance to investigate and fully comprehend the physico-chemical properties and thermodynamics of the APIs that are to be used during the manufacturing process to avoid unwanted surprises during and after the manufacturing process, that may have financial implications for the manufacturer.

Rocco & Swanson (5) indicated that the heat of fusion and the melting point data of polymorphs can be used to predict the relative solubility of the polymorphs. The polymorph with the lowest solubility will be the most thermodynamically stable form at a particular temperature.

Rocco and Swanson (5) proposed the following equation to predict the relative solubilities of polymorphs:

$$RT\ln\left[\frac{Si}{Sii}\right]=\left[\frac{\Delta Hii\bullet(Tmii-T)}{Tmii}\right]-\left[\frac{\Delta Hi\bullet(Tmi-T)}{Tmi}\right]$$

Where:

Si = Relative solubility of the (i) high melting polymorph.

Sii = Relative solubility of the (ii) low melting polymorph.

ΔH = Heat of fusion for the polymorphic form.

Tm = Melting temperature of the polymorphic form.

T = Temperature of dissolution medium (23°C for the purpose of this study).

From the XRPD results obtained it was found that crystal Form 5 converted into the crystal Form 1 when heated at 150°C.

Table 1 shows the DSC data, used in the calculation of the theoretical solubility ratio of the high melting (Form 5) and low melting (Form 1) polymorphs. The theoretical solubility ratio (Si/Sii) of polymorphic Form 1 and Form 5 was calculated as 1.12. Due to the fact that the theoretical solubility ratio (Si/Sii) > 1.0 it can be concluded that Form 1 and Form 5 is enantiotropically related. Crystal Form 1 was the most stable form at room temperature by virtue of the lower solubility values observed for crystal Form 1. Crystal Form 5 revealed a higher solubility and could therefore be classified as a metastable crystal form at room temperature.

Polymorphic systems can be classified as either *monotropic* or *enantiotropic*. Byrn *et al.* (6) defined these systems as follows:

- "**Monotropic systems** are defined as systems where a single form is always more stable regardless of the induced temperature."

- "**Enantiotropic systems** are defined as systems where the relative stability of the two forms inverts at some temperature (figure 7 and figure 8)".

The solubility values for different crystal forms (polymorphs) differ under a fixed set of conditions: temperature, pressure and solvent composition. The polymorph with the lowest solubility will be the most thermodynamically stable form at a particular temperature (5).

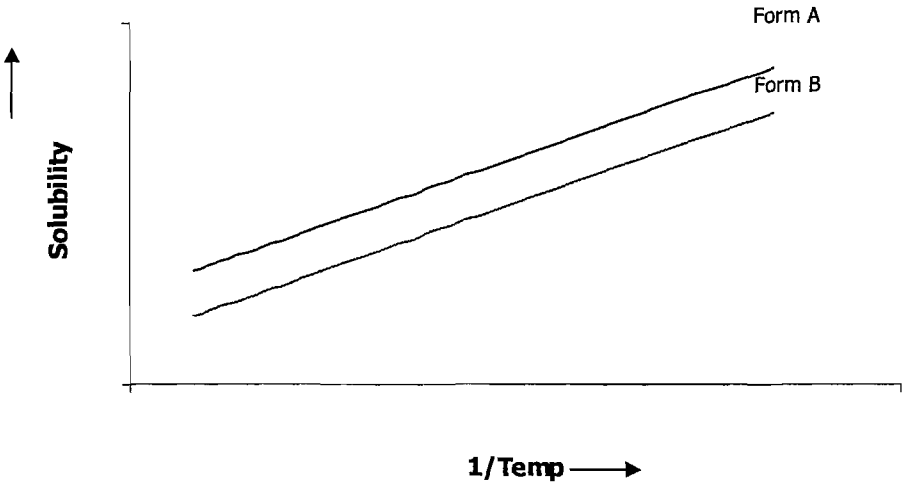


Figure 7 Schematic presentation of the solubility versus temperature for monotropic system (adapted and reproduced from [10]).

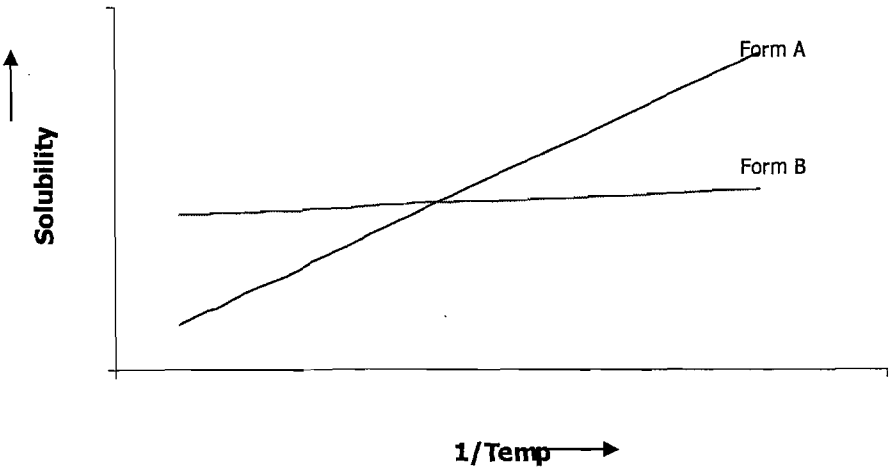


Figure 8 Schematic presentation of the solubility versus temperature for enantiotropic system (adapted and reproduced from [10]).

Figure 9 depicts the results obtained when the solubility ratios of the polymorphs (enantiotropic and monotropic) vs. the 1/temperature are plotted. For a monotropic system a non-linear relationship exists between the solubility ratios (Si/Sii) and the temperature. Construction of a logarithmic trendline produced a correlation coefficient (r^2) = 0.995.

A linear correlation exists between the solubility ratios and the temperature (r^2=0.998) for the enantiotropic system.

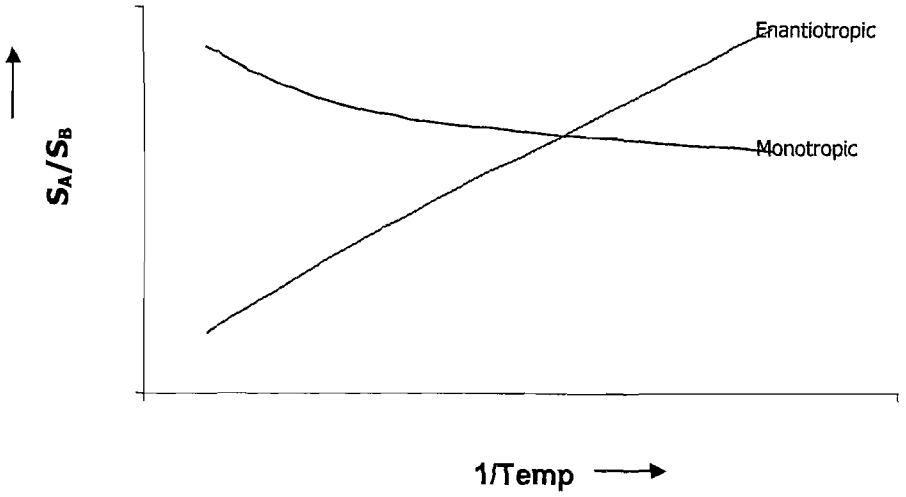


Figure 9 Solubility ratios (S_A/S_B)of the polymorphs (enantiotropic and monotropic) vs. the 1/temperature.

Results obtained when plotting the theoretically calculated solubilities of the venlafaxine hydrochloride polymorphs (Form 1 and Form 5) at various temperatures are illustrated in figure 10.

The plot of the predicted solubility ratios (Si/Sii) vs. 1/temperature for the two polymorphs revealed that a linear correlation existed (r^2=0.999), thus supporting that an enantiotropic relationship exists.

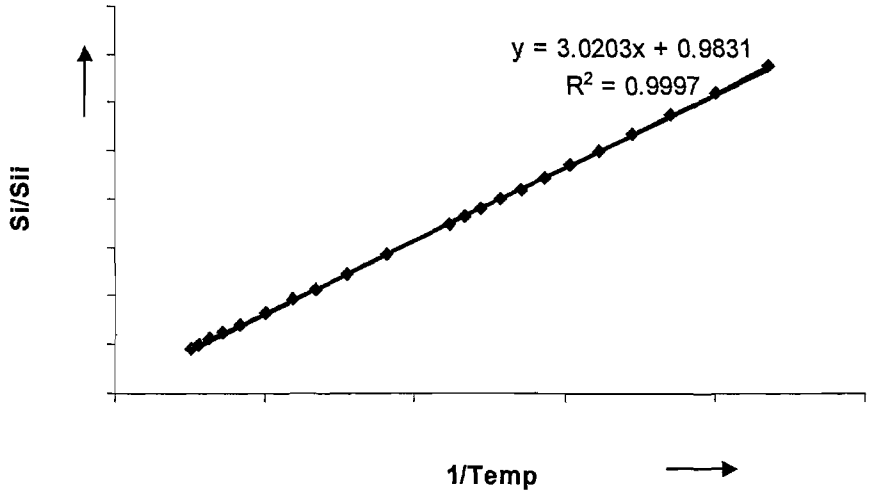


Figure 10 Solubility ratios of the venlafaxine HCl polymorphs (Si/Sii) vs. the 1/temperature.

One of the most important concidderations of a polymorphic drug is the relative thermodynamic stability thereof. The relative thermodynamic stability of polymorphs can also be determined by the measurement of their free energy difference (ΔG) which is defined by the following equation (7):

$$\Delta G = \Delta H - T\Delta S$$

The enthalpy term (ΔH) results from the lattice energy difference between the polymorphs, and the entropy term ($T\Delta S$) from the difference in the lattice vibrations and disorder (7).

Burger's heat of transition rule states the following:

(i) If an endothermic transition is observed at a certain temperature on heating, there must be an *enantiotropic* transition point at or bellow that temperature; but

(ii) If and exothermic transition is observed, then the transition point must lie above that temperature, or the two forms are related *monotropicaly* (8).

However, if the transition cannot be clearly observed (owing to the failure of the polymorphs to transform readily), Burger's *heat of fusion law* is of value which states that: the higher melting polymorph will have the lower heat of fusion if the polymorphs are in an enantiotropic relationship, otherwise they are monotropically related (9).

Table 1 confirms that an enantiotropic relationship exists due to the fact that the high melting form (Form 5) reveals a lower heat of fusion compared to the low melting form (Form 1).

4. CONCLUSIONS

Heat of solution studies (for Form 1 and Form 5) revealed that the dissolution of the crystals in water was an exothermic reaction ($\Delta H < 0$), and that an increase in temperature decreases the solubility of the polymorphic forms.

Exposure of Form 5 crystals to 150°C (for two hours) revealed that a fraction of the Form 5 crystals converted into Form 1, thus indicating that Form 5 is a meta-stable form and confirming that Form 1 is a thermodynamically stable form.

The theoretical solubility ratio (Si/Sii) was calculated to be 1.12, which signified that Form 1 and Form 5 was enantiotropic related. The linear correlation between the plot of the predicted solubility ratios (Si/Sii) vs. 1/temperature for the two polymorphs (Form 5 and Form 1) and the fact that the higher melting form (Form 5) revealed a lower heat of fusion compared to the lower melting form (Form 1) supported the enantiotropic relationship between the mentioned polymorph forms.

ACKNOWLEDGEMENTS

The authors would like to acknowledge financial assistance from the Research Institute for Industrial Pharmacy®, North-West University and the National Research Foundation of South Africa and the assistance and great input and assistance of Dr. Kolling (University of Monroe) with the MDSC studies.

REFERENCES

1. **POTTER, W.Z. & HOLLISTER, L.E.** 1998. Antidepressant Agents. (*In.* ed. KATZUNG, B.G. *ed.* Basic & Clinical Pharmacology). USA, Appleton & Lange, 1151p.

2. **MUTH, E.A., HASKINS, J.T. & MOYERS. J.A.** 1986. Antidepressant biochemical profile of the novel biciclic compounds Wy-45,030, an ethylcyclohexanol derivate. *Biochemical Pharmacology,* (35):4493-4497.

3. **SIRIPRAGADA, M.R., KRISHNAMURTHI, V., ARIKATLA, S.L.D. & GADDAM, O.M.** 2000. Novel crystalline polymorphic forms of venlafaxine hydrochloride and a process for their preparation. Patent: WO 02/46140 A1. 52p.

4. **BRITS, M.** 2003. Crystal polymorphism and pseudopolymorphism of Venlafaxine hydrochloride. Potchefstroom: Potchefstroom University for Christian Higher Education (PU for CHE). (Dissertation – M.Sc.) 212p.

5. **ROCCO, W.L. & SWANSON, J.R.** 1995. Win 63843 polymorphs: prediction of enantiotropy. *American Journal of pharmaceutics,* 117:231-236.

6. **BYRN, S.R., PFEIFFER, R.R. & STOWELL, J.G.** 1999. Solid-state chemistry of drugs. West Lafayette, Indiana: SSCI, Inc. 575p.

7. **YU, L., REUTZEL, M. & STEPHENSON, G.A.** 1998. Physical characterization of polymorphic drugs: an integrated characterization strategy. PSTT. 1(3):118-127.

8. **THRELFALL, T.L.** 1995. Analysis of organic polymorphs. Analyst. October 1995. 120:2435-2460.

9. **BURGER, A. & RAMBERGER, R.** 1979a. On the polymorphism of pharmaceuticals and other molecular crystals. Theory of thermodynamic rules. Mikrochimica Acta. II:259-272.

10. **BYRN, S.R., PFEIFFER, R.R. & STOWELL, J.G.** 1999. Solid State Chemistry of drugs. 2nd edition. West Lafayette, Indiana: SSCI Inc. 576p.

Moisture sorption properties of fluconazole crystal forms and stability of the transformed crystal forms

Marius Brits [a,*], Melgardt de Villiers [b], Wilna Liebenberg [c]

[a] Research Institute for Industrial Pharmacy®, North West University, Potchefstroom campus, Potchefstroom, South Africa

[b] School of Pharmacy, University of Wisconsin, Madison, WI, USA

[c] Unit for Drug Research and Development, Faculty of Health Sciences, North-West University, Potchefstroom campus, Potchefstroom, South Africa

Abstract

The thermodynamic behaviour and stability of two fluconazole crystal modifications (an anhydrous and a monohydrated form) will be investigated in this paper to compare the stability / instability thereof when exposed to moisture. It was found that the anhydrous form (Form I) converted to a monohydrate when exposed to 85% RH at 30°C. The XRPD pattern, moisture content and IR-spectrum of the hydrated Form I was comparable with that of monohydrate, Form MH. However, the DSC thermogram of the hydrated Form I did not reveal the rearrangement endotherm at 101°C, which is characteristic to Form MH. The thermodynamic stability of the monohydrate (Form MH) and the hydrated Form I was in vestigated using XRPD, VT-XRPD, DSC, TGA and SEM analysis.

Keywords: Fluconazole polymorphs; Polymorphic transitions; Polymorphism; Thermodynamic stability, Moisture,

* Corresponding author. Tel.: +2718-299-2323; fax: +2718-299-2291.

E-mail address: Marius.Brits@nwu.ac.za

1. Introduction

Fluconazole is a water-soluble triazole antifungal agent (an imidazole derivative) that has shown activity against several organisms [1].
Therapeutic indications of fluconazole include the following: superficial candidal infections such as oral or vaginal thrush, esophagitis caused by *Candida* or other susceptible species, maintenance therapy for cryptococcal meningitis, cryptococcal meningitis, dissenubared candidiasis, prophylaxis for fungal infection in neutropenic cancer patients, acute treatment of systemic fungal infections such as coccidiodomycoses and histoplasmosis in selected cases, dermatophyte and *Candida* skin infections and fungal urinary tract infections [1]. Fluconazole plays an important role in the treatment regimen for oral and esophageal candidiasis in patients with AIDS [1].

It was indicated that the dissolution rate of the fluconazole anhydrate, Form I, was higher compared to that of the monohydrate, Form MH. The dissolution rate constant of the monohydrate was 15% higher compared to that of Form I [2]. Form I is thus the preferred crystal form to be used in pharmaceutical dosage forms due to its thermodynamic stability and the favoured dissolution behaviour. Hydration of the anhydrous Form I to produce Form MH should be prevented during the storage of the raw material manufacturing of dosage forms, to ensure the optimal bio-availability of this antifungal.

An investigation of the physico-chemical properties of Form I and the monohydrate at predetermined intervals using a well-balanced set of analytical techniques provided insight into the moisture-sorption susceptibility of the two fluconazole crystal modifications and the thermodynamically behaviour of the two forms.

2. Materials and methods

2.1 Materials

Fluconazole raw material, Form I, was obtained from Matrix Laboratories Ltd, Batch no: FLP 0170405.

2.2 Methods

2.2.1 Preparation of crystal forms of fluconazole

Form MH was prepared according to the methods described in literature and methods described in literature [3]. The crystals obtained were sieved using a 250 μm and 106 μm sieve. The fraction between 106-250 μm was used during all the experiments to ensure uniformity of particle size.

Form I crystals were dried at 90°C for one hour to remove any residual solvent / moisture from the samples. XRPD and DRIFT-IR studies confirmed that no polymorphic transition occurred during the drying process of the Form I crystals. Form MH was rapidly surface dried at ambient conditions to prevent dehydration.

The XRPD patterns of the crystal forms (Form I and Form MH) were concurrent with the XRPD patterns published [3].

2.2.2 Stability testing conditions

Saturated solutions of NaCl and KNO_3 were prepared using the method described by Nyqvist [4]. The saturated solutions were transferred into glass boxes with tight fitting lids. The glass boxes (% RH chaimbers) were allowed to equilibriate in a 30°C & 65% RH - regulated climatic chamber and the relative humidity was recorded to be 75±5% and 85±5% respectively at 30°C. 500 mg Samples of Form I and Form MH were weighed into weighing boats and were stored in a 30°C & 65% RH regulated climatic chamber and in various % RH chambers. 500 mg Samples were sealed in glass vials. The air present in the vials was displaced with nitrogen. The sealed vials

were then stored in a desiccator (containing silica gel) at 30°C.The samples were thus exposed to 0%, 65%, 75% and 85% RH conditions at 30°C respectively.

Samples were removed at predetermined intervals (i.e. 1,2,3,4,5,6,7,14,21, and 28 days) and were analysed.

2.3 Methods

XRPD, DSC, TGA, KF and DRIFT-IR spectroscopy were used to evaluate the polymorphic composition of the various samples.

2.3.1 Infrared absorption spectroscopy (DRIFT-IR)

The IR-spectra of the various samples were recorded on a Nicolet Nexus 470-FT-IR spectrometer (Nicolet intrument corporation, Madison, USA) over a range of 400 – 4000 cm^{-1}. The diffuse reflectance method was used. KBr was used as background material. The main absorptions in the IR-spectral results of all the samples were compared to determine possible significant differences with regard to polymorphic form or polymorphic modifications.

2.3.2 X-ray powder diffraction (XRPD)

The X-ray powder diffraction patterns of the various samples were recorded at room temperature using a Bruker D8 Advance diffractometer (Bruker, Germany). Approximately 200 mg the powdered samples were transferred into aluminium sample holders, taking care not to induce a preferential orientation of crystals. The measurement conditions were: target, Cu; voltage, 40 kV; current, 30 mA; divergence slit, 2 mm; antiscatter slit, 0.6 mm; detector slit, 0.2 mm; monochromator; scanning speed, 2°/min (step size, 0.025°; step time, 1.0 sec.).

The XRPD patterns of the various samples were compared with respect to the peak position and relative intensities of the characteristic peaks in the XRPD patterns of the fluconazole polymorphs.

2.3.3 Particle size analysis

For the purpose of this study a sieved fraction of crystals was used. The particle size distributions were measured using a Galai-Cis-1 (Galai-Cis-1, Israel) particle size analyser. Samples of powder suspended in sedisperse (dispersing solution) were each placed in a small cuvette and fitted into the analyser. A small magnetic stirrer was placed inside the cuvette to prevent sedimentation of the particles during the measurement. The acquired data was used to compute means, medians and standard deviations, based on the total particle population.

3. Results and discussion

The physical transformations of crystalline solids from one solid phase to another can occur between (a) polymorphs, (b) solvates of different stoichiometry, (c) solvated and unsolvated forms and (d) amorphous and crystalline forms [5].

Moisture and solution mediated phase transitions are well-known [6]. As mentioned by Byrn *et al.* [5] the kinetics of solution mediated transformations are not well-understood.

This article will focus on the moisture mediated transformation of fluconazole Form I and the stability of the hydrated Form I.

3.1 Particle size and specific surface area analysis

The median particle sizes of both polymorphic forms (Form I and Form MH) were lower than the sieved range: 106 μm - 250 μm (table 1). During the sieving process it was observed that both samples revealed a tendency to conglomerate due to the static

friction build-up during sieving. Thus, once the conglomerates (sized: 106-250 μm) were suspended in the suspending agent, it dispersed and the smaller particles were in suspension. The median particle size of the Form MH sample was found to be lower compared to that of Form I.

Table 1 Median particle size by volume (mass) and specific surface area of fluconazole Form I and Form MH

Polymorphic form	**Median diameter by volume (μm)**	**Specific surface area (m^2/g)**
Form I	80.27	0.807
Form MH	55.13	0.814

The specific surface areas of Form I and Form MH were comparable (table 1) at standard conditions (outgas temperature: 100°C & outgas time: 3 hours). However it is known that Form MH dehydrates at these conditions, thus the specific surface area reported for Form MH was actually that of the dehydrated sample i.e. Form I. Irreproducible results were obtained when the specific surface areas were determined for Form MH at lower temperatures, thus no bona fide results can be reported for comparison purposes.

The specific surface analysis of Form MH at the following conditions (outgas temperature 40°C & outgas time: 80 hours) revealed that the specific surface area of the sample increased as the sample dehydrated, suggesting that dehydration of Form MH increases the specific surface area of the sample (figure 1).

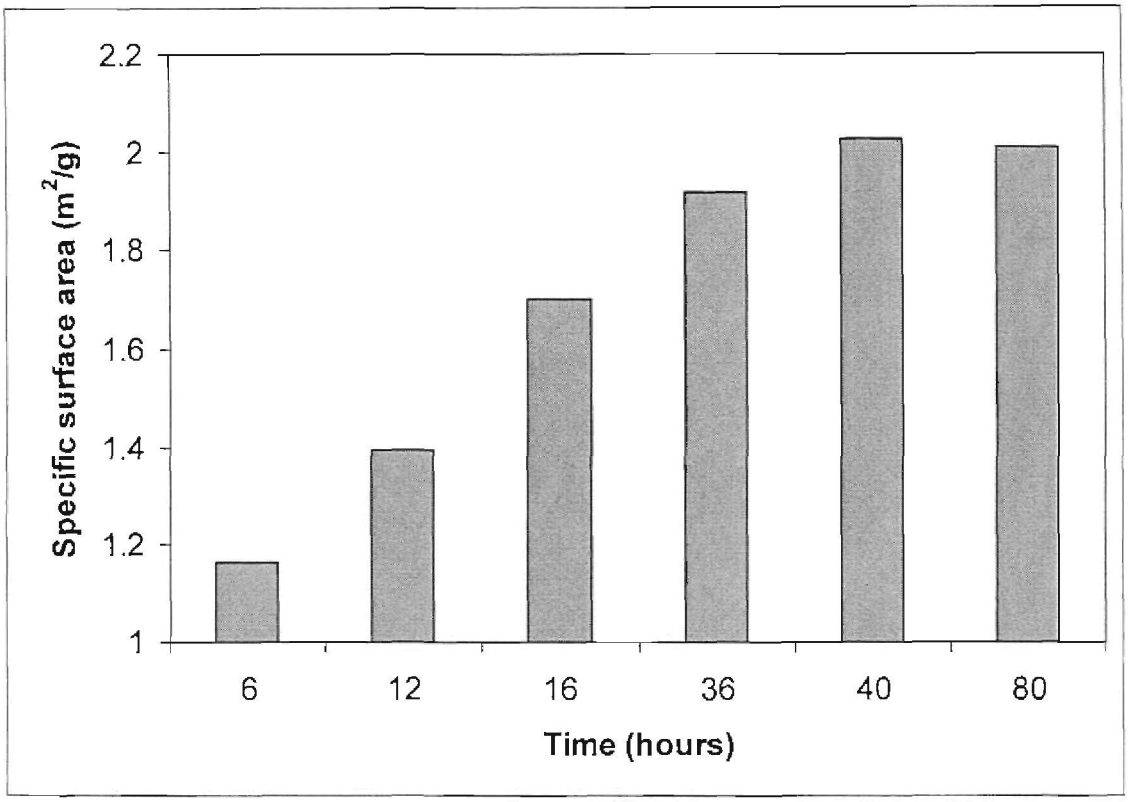
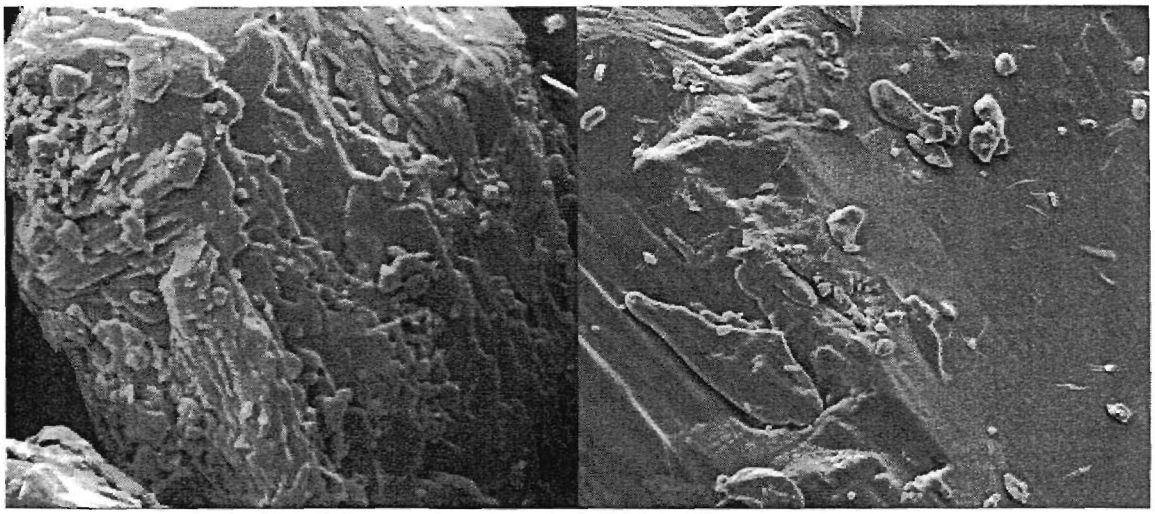


Figure 1 Specific surface area of Form MH at various intervals at the following conditions: outgas temperature: 40°C & outgas time 80 hours.

SEM photomicrographs of Form I revealed that the sample consisted of needle-like crystals and the Form MH sample revealed non-specific shapes. The surfaces of the crystal forms differed significantly (figure 2). The surface of Form I appeared to consist of plate-like structures stacked upon each other, creating a greater exposure surface compared to the flat, smooth surface of Form MH.



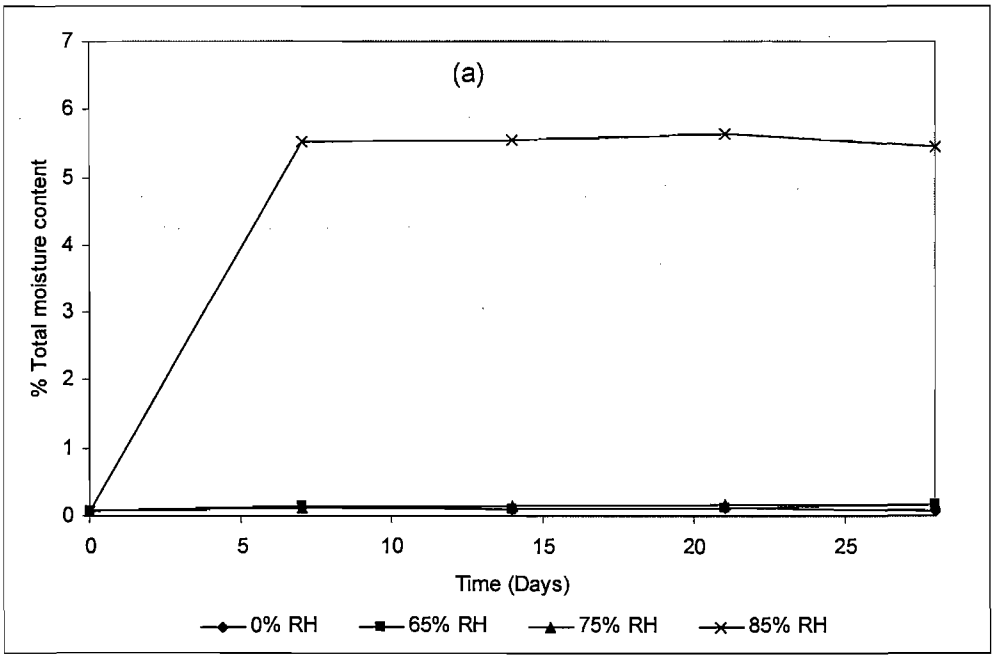
(a) (b)

Figure 2 SEM photomicrographs of fluconazole (a) Form I and (b) Form MH, revealing significant differences in the surface properties of these crystal forms.

3.2. Moisture sorption analysed using Karl Fischer analysis

The moisture sorption isotherms of the mentioned forms derived from moisture content using Karl Fischer titration results are displayed in figure 3.

The moisture sorption isotherms derived from the KF results for Form I (figure 3) indicated that the no significant moisture sorption occurred when exposed to 0-75% RH. However, when Form I was exposed to 85% RH a considerable amount of moisture was sorbed by the samples (5.52% (m/m) after 7 days). The moisture content of the samples after 7 days, were found to correlate with the theoretical moisture content of a fluconazole monohydrated crystal system [5.84% (m/m)]. The moisture content of the samples exposed to 85% RH showed small variances (5.46-5.64%) which could be attributed to the dynamic process of moisture sorption and desorption.



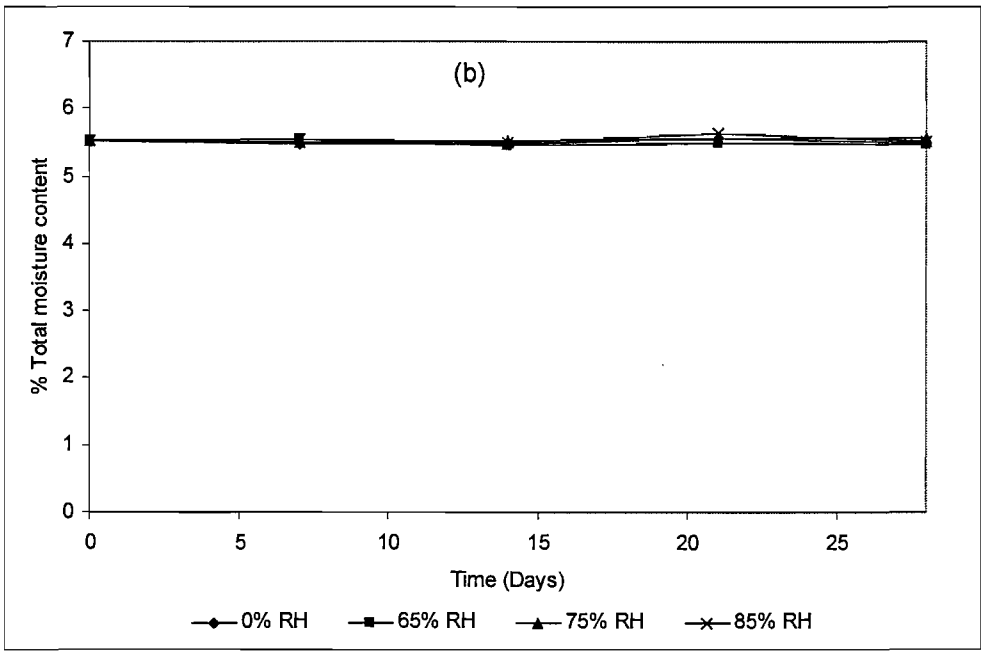


Figure 3 Moisture sorption isotherms of (a) Form I and (b) Form MH, derived from moisture content using Karl Fischer titration results.

The moisture sorption isotherms derived from the KF results for Form MH (figure 3) indicated that the no significant moisture sorption occurred when exposed to 0-85% RH during the 28 days. Thus, the monohydrate form (Form MH) did not undergo any significant moisture *absorption.*

3.3. Influence of moisture sorption of the crystalline properties of Form I and Form MH

Exposure of fluconazole Form I to 0-75% RH for a period of 28 days did not induce any significant changes in the XRPD patterns of the samples (figure 4) indicating that no polymorphic transition occurred. The intensity of the small peak at 5.0°2θ varied considerably at the various time intervals, which could be attributed to preferred orientation or minor differences in crystal habit.

The XRPD patterns of Form I (figure 5) exposed to 85% RH for 28 days revealed that a polymorphic transition occurred after 7 days. The moisture sorption could thus be classified as moisture *absorption* rather than moisture *adsorption*, due to the significant crystal-lattice changes that occurred in order to compensate the water molecule(s) incorporated into the crystal lattice.

The crystal packing of fluconazole monohydrate (Form MH) revealed that water molecules occupy isolated cavities in the crystal structure [3].

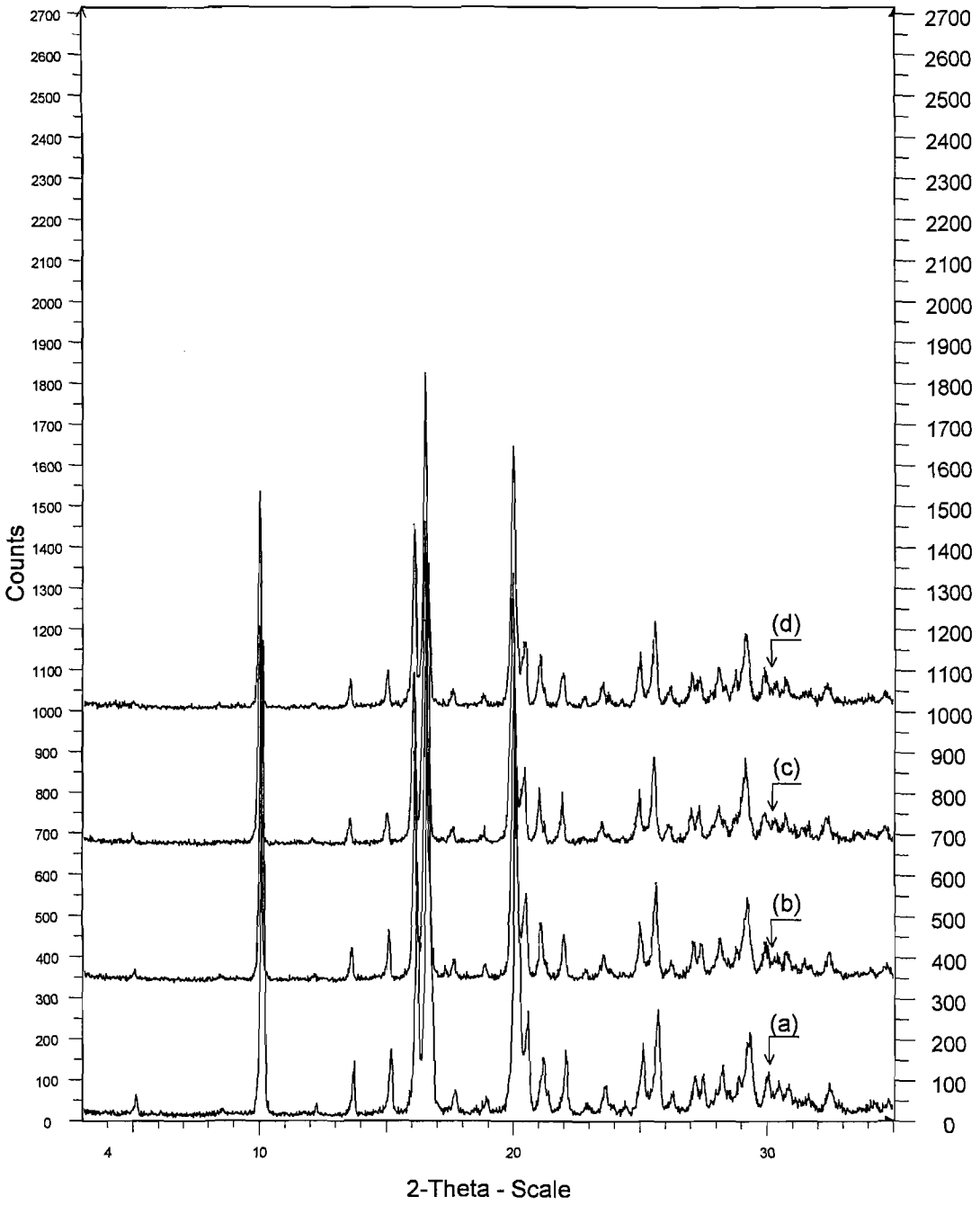


Figure 4 XRPD pattern overlay of fluconazole (a) Form I when exposed to 30°C & (b) 0, (c) 65 & (d) 75% RH for 28 days.

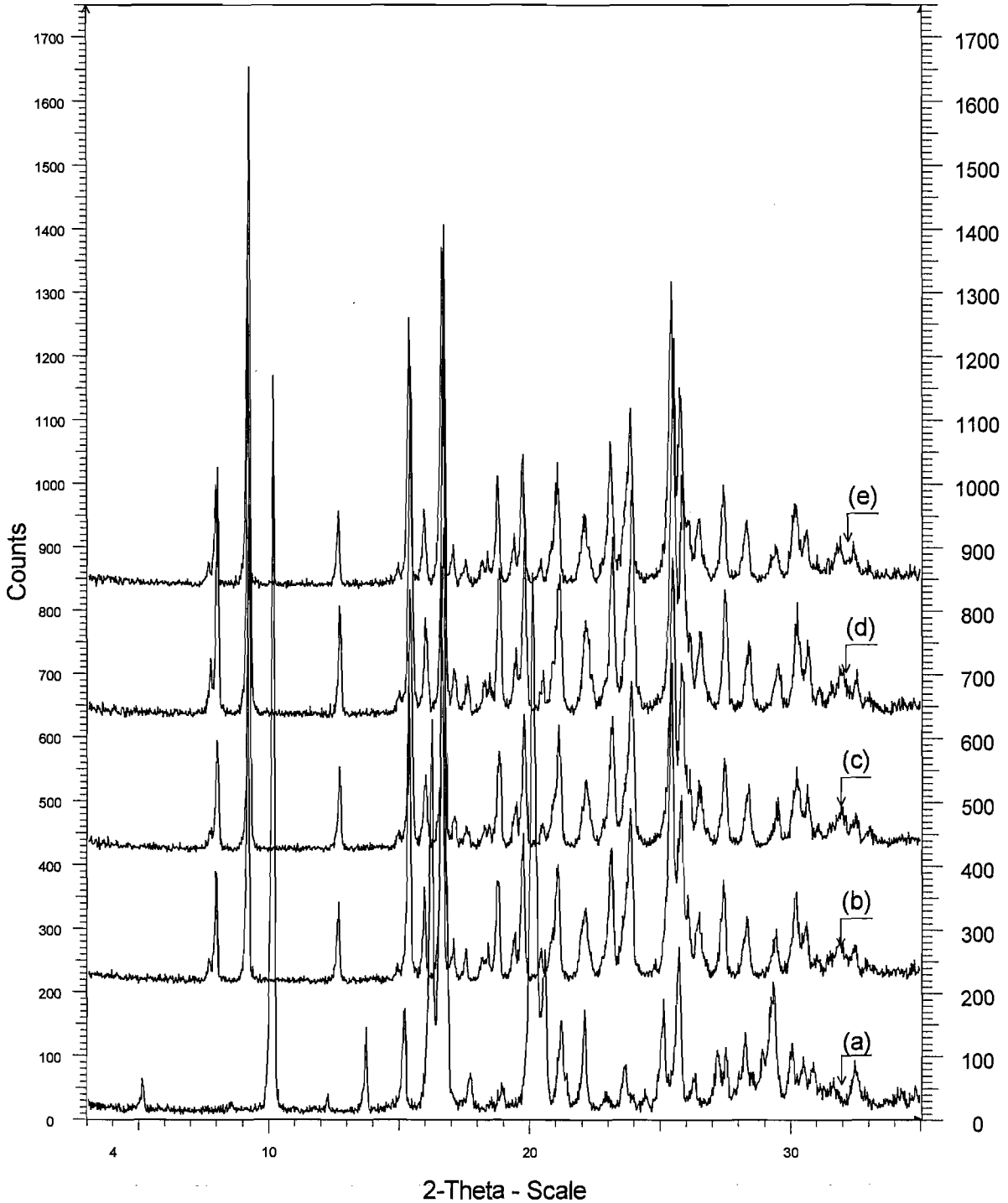


Figure 5 XRPD pattern overlay of fluconazole Form I when exposed to 30°C & 85% RH at the intervals: (a) 0, (b) 7, (c) 14, (d) 21 & (e) 28 days.

The peak intensities in the XRPD patterns of fluconazole monohydrate suffer severely from preferred orientation effect due to the pronounced acicular habit of this crystal form. The XRPD patterns of fluconazole monohydrate did not reveal any significant changes in peak positions when exposed to 0, 65, 75 & 85% RH at 30°C for 28 days.

3.4. Influence of moisture sorption of the thermal properties of Form I and Form MH

The DSC thermogram of Form I (figure 6) revealed a sharp melting endotherm at 139°C. The DSC thermogram of Form I remained relatively unchanged during the 28 days when stored at 0%, 65% and 75% RH respectively, confirming that no phase transformation has occurred (figure 6).

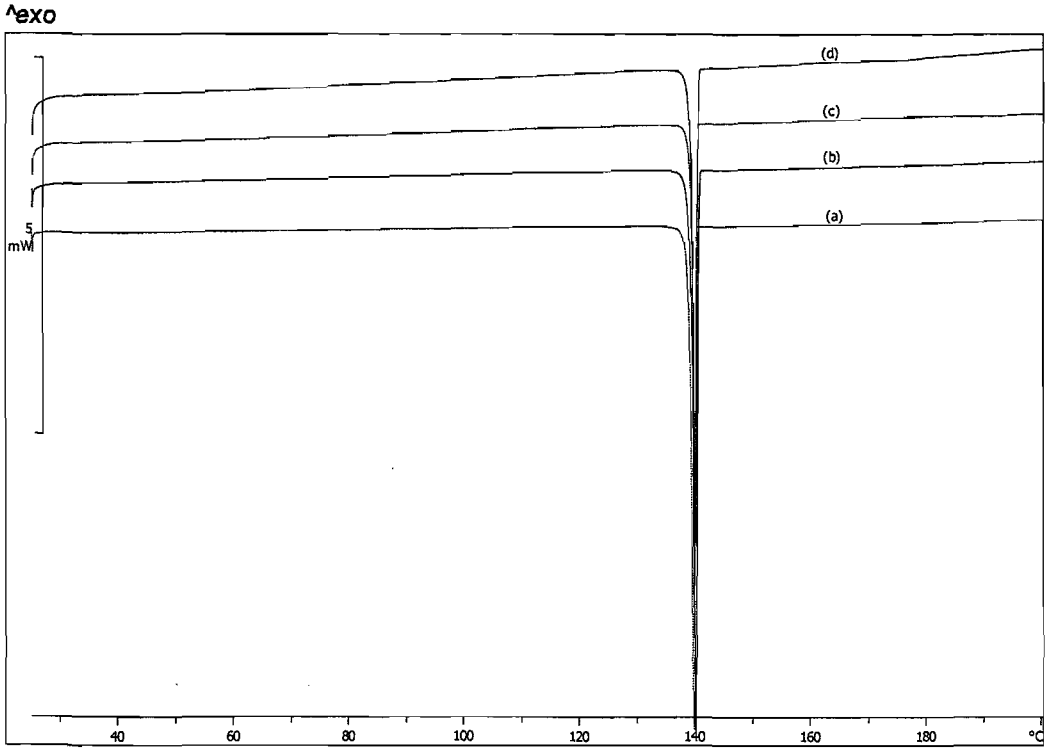


Figure 6 DSC thermograms of fluconazole (a) Form I when exposed to 30°C – (b) 0, (c) 65 & (d) 75% RH after 28 days.

The DSC thermogram of Form I exposed to 85% RH changed significantly after 7 days (figure 7). A broad, weak dehydration endotherm appeared in the 50-100°C region. Thermogravimetric analysis (figure 8) confirmed that the broad endotherm at 50-100°C was due to the dehydration of the sample.

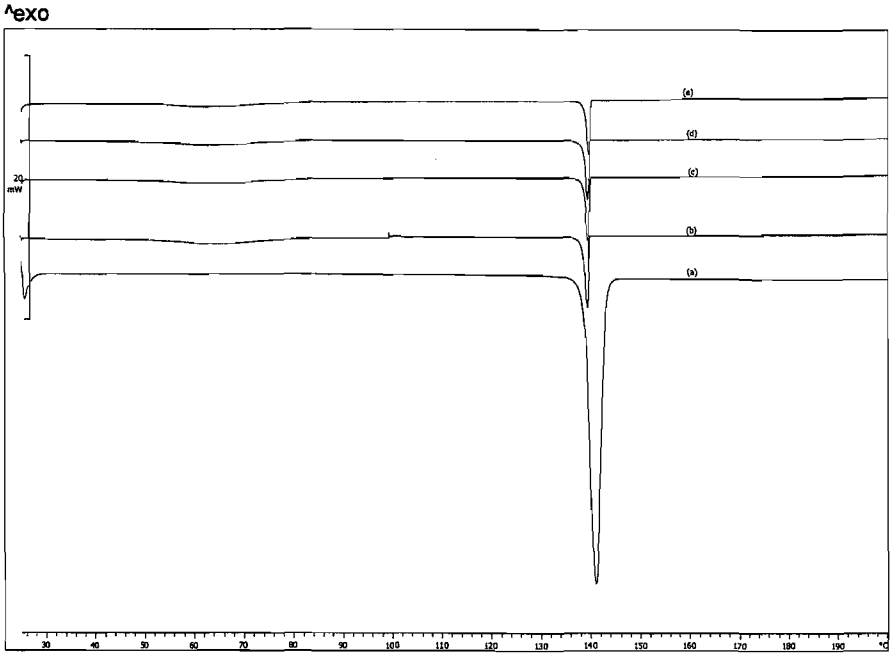


Figure 7 DSC thermograms of fluconazole Form I when exposed to 30°C – 85% RH at the following intervals: (a) Initial, (b) 7 days, (c) 14 days, (d) 21 days & (e) 28 days.

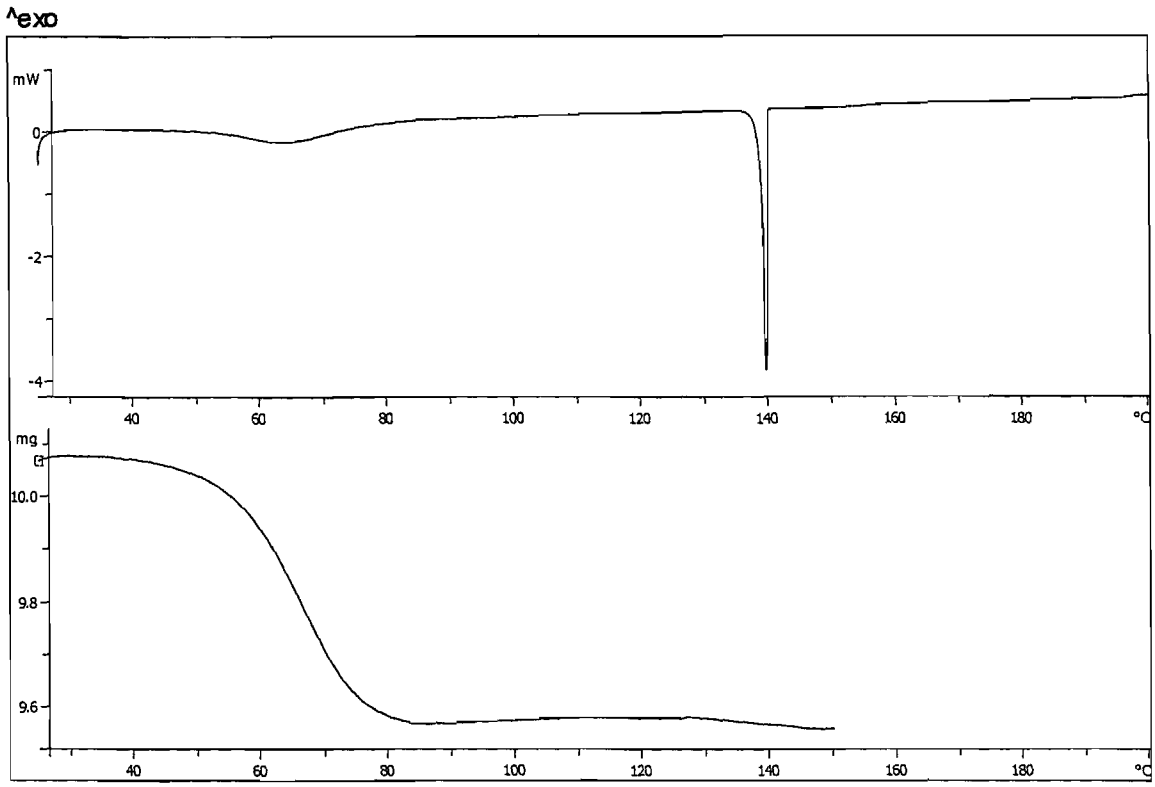


Figure 8 Overlay of DSC (top panel) and TGA (lower panel) thermogram of fluconazole Form I when exposed to 30°C – 85% RH for 28 days.

The broad endotherms present in the DSC thermograms of Form MH (figure 9) in the 40-70°C region and the sharp endotherm at 101°C regions are indicative of the dehydration process of the monohydrate. These dehydration temperatures did not vary significantly as illustrated in figure 9.

TGA analysis of the various samples confirmed the Karl Fischer observations, that no significant moisture sorption or desorption occurred.

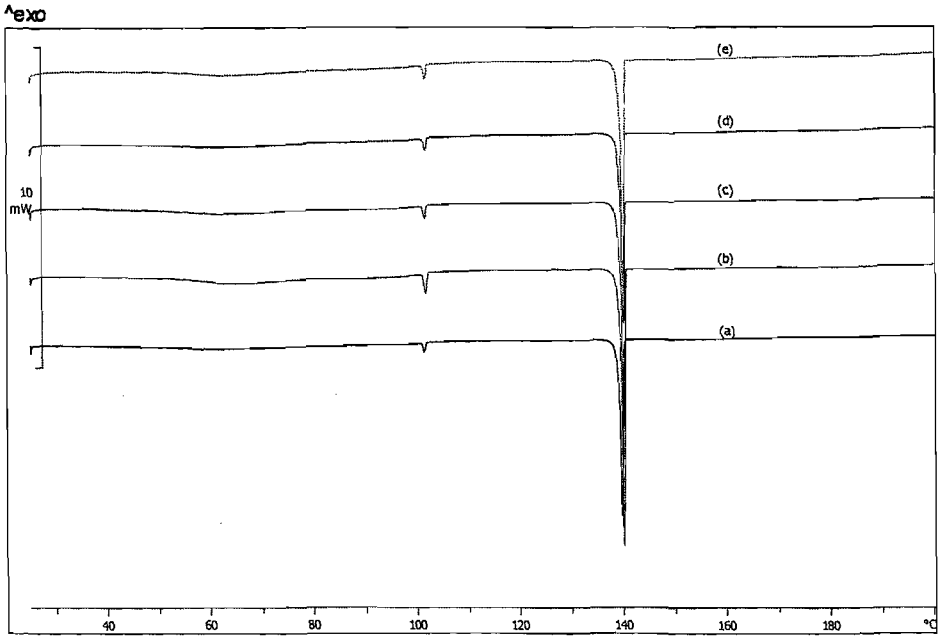


Figure 9 DSC thermograms of fluconazole (a) Form MH when exposed to 30°C and (b) 0, (c) 65, (d) 75 and (e) 85% RH after 28 days.

3.5. Influence of moisture sorption of the infra-red spectrum of Form I and Form MH

The DRIFT-IR spectra of Form MH when exposed to 0, 65, 75 & 85% RH at 30°C over a 28 day period did not display any change in the position of the absorption bands, thus supporting the XRPD, DSC, TGA and KF observations that the exposure of fluconazole Form MH to the mentioned conditions for 28 days did not induce any polymorphic conversion.

The DRIFT-IR spectra of Form I exposed to 85% RH for a period of 28 days (figure 10) revealed significant changes in the main absorption peak positions. The DRIFT-IR spectra of the samples after 7, 14, 21 and 28 days were found to be comparable to that of fluconazole monohydrate (Form MH), thus suggesting that the new crystal modification (hydrated Form I) remained stable at 30°C & 85% RH during the 28 day period.

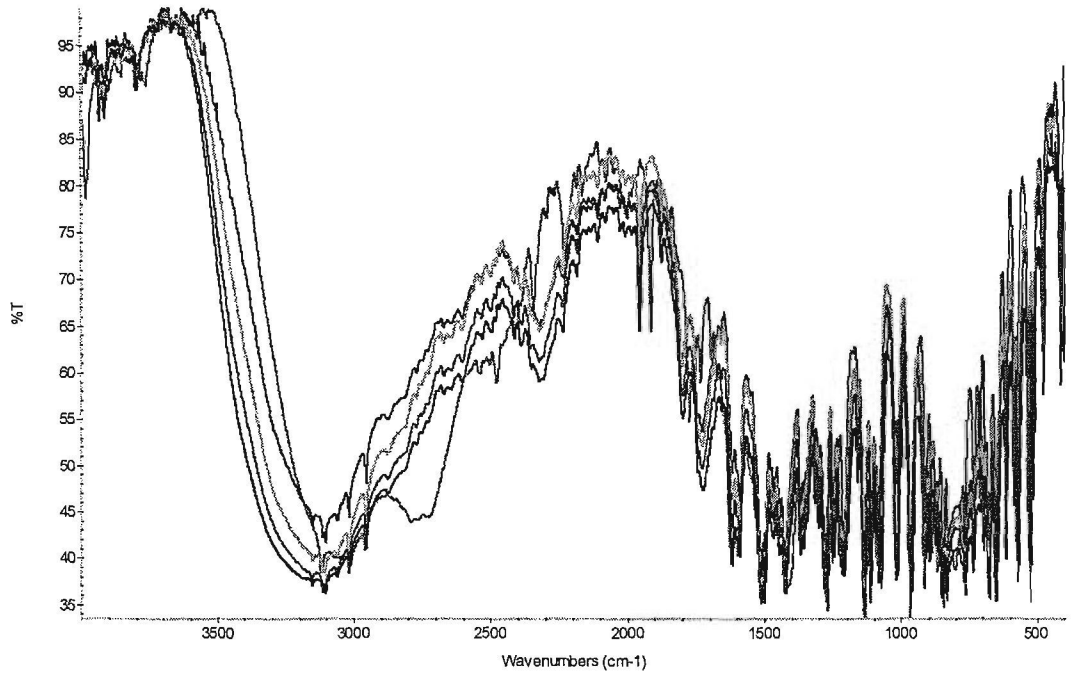


Figure 10 An overlay of the DRIFT-IR spectra of fluconazole Form I when exposed to 85% RH at 30°C during a 56 day period: Initial, 7 days, 14 days, 21 days, 28 days.

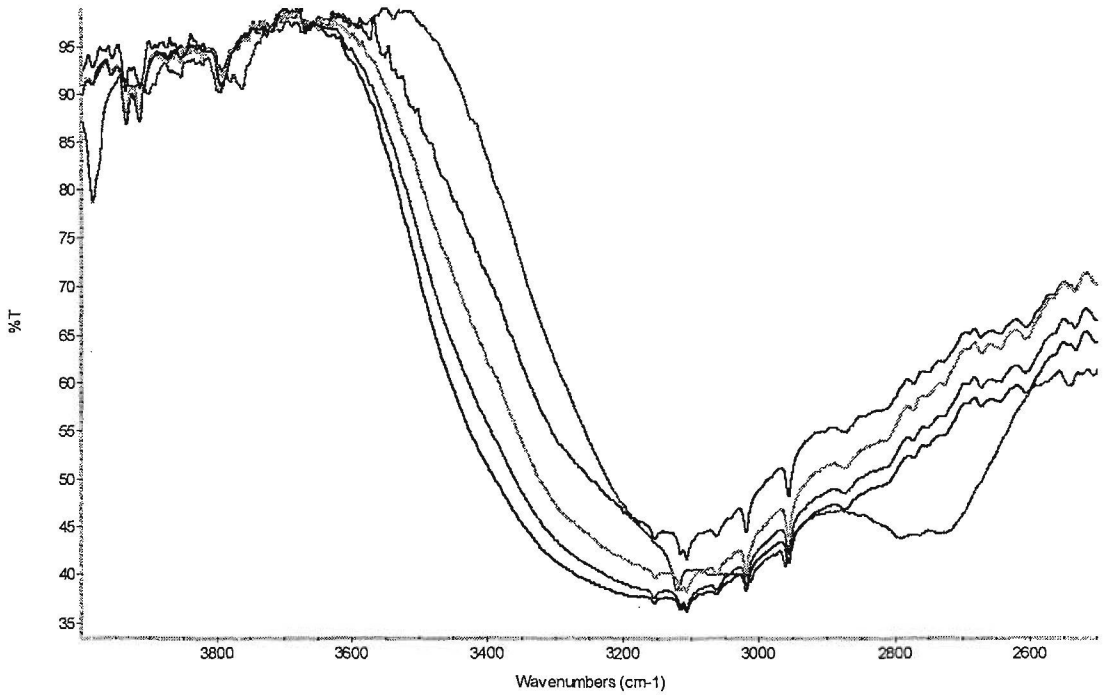


Figure 11 An overlay of the DRIFT-IR spectra of fluconazole Form I when exposed to 85% RH at 30°C during a 56 day period in the 4000-2600 cm^{-1} region: Initial, 7 days, 14 days, 21 days, 28 days.

The most remarkable differences or changes in the DRIFT-IR spectra were observed in the 4000-2600 cm^{-1} region (figure 11). The appearance of various Form MH characteristic absorption bands supported the XRPD observations that Form I transformed into the monohydrated Form MH upon exposure to 30°C & 85% RH for 7 days (table 2).

Table 2 Appearance of Form MH characteristic peaks in the fluconazole Form I samples stored at 30°C & 85% RH after 7 days

Wavenumbers (cm^{-1}) of absorptions which appeared	**Assignment**
3155	Water molecules
3019	CH - stretch of 2,4-Difluorobenzyl group
2956	CH_2 – stretch of propane backbone
1619	C=C – stretch of 2,4-difluorobenzyl group
1468	CH_2 – scissor of propane backbone
1370	Ring stretch of triazole group
1249	Ring stretch of triazole group
1139	Ring breathing of triazole group
1112	C-C – stretch of propane backbone
1020	C-(OH) – stretch of propane backbone
968	Ring-bend of triazole group

3.6. Thermodynamic stability of fluconazole monohydrate (Form MH) and the hydrated Form I

Khouloud *et al.* [7] studied the dehydration of fluconazole monohydrate (Form MH). Figure 12 (a) illustrates the seven TGA thermograms used in the Ozawa kinetic analysis method and (b) illustrates the plots of log A versus T^{-1} used in the calculation of the dehydration activation energy (E_A).

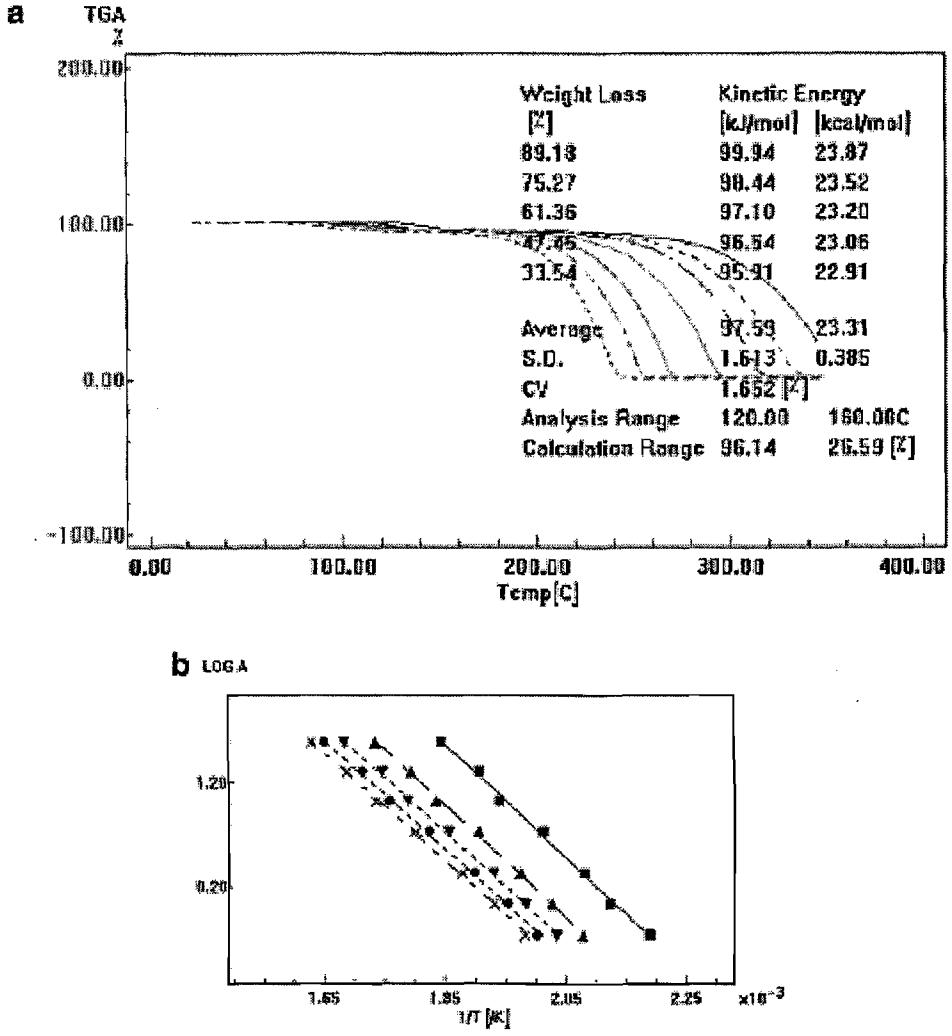


Figure 12 The seven TGA thermograms selected for applying the Ozawa kinetic method of analysis and (b) illustrates the plots of log A versus T^{-1} for fluconazole monohydrate [7].

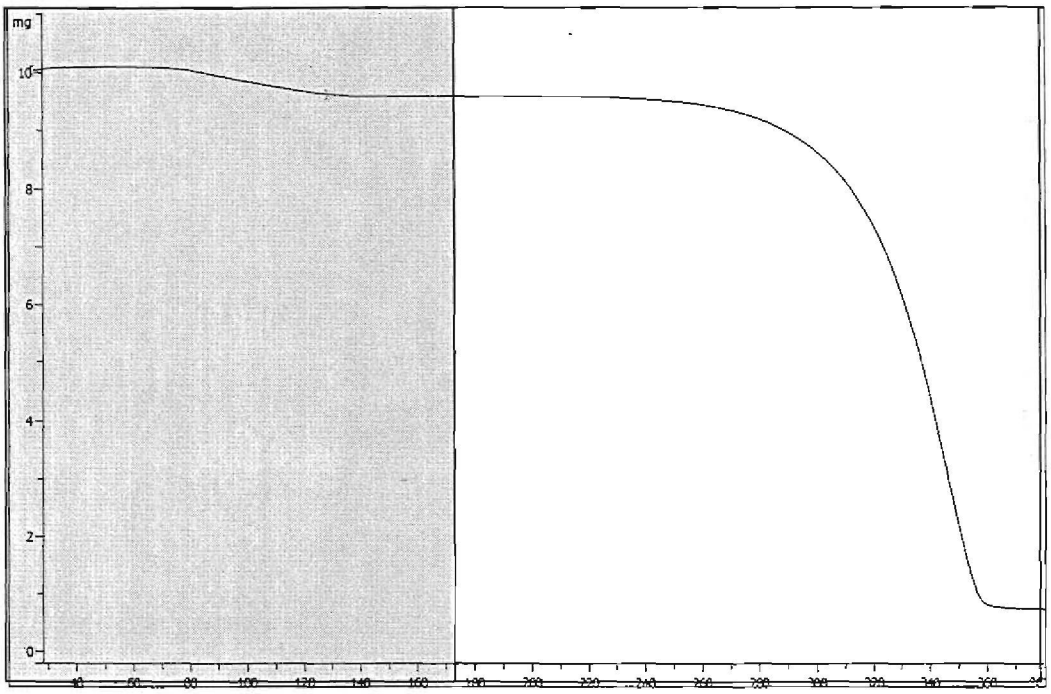
The authors [7] stated that the temperature range used in the study was 80.82-157.55°C [7] however upon closer inspection of the plots in figure 12 b – it was clear that the absolute temperature range wherein the calculations were performed was actually between 171.3°C – 332.9°C, which did not correlate with the range of dehydration, but rather the thermal decomposition of the sample.

Figure 13 a - illustrates a TGA thermogram of Form MH when heated from 25°C to 380°C. From this figure it is clear that two mass-loss events occurred in the sample i.e. (b) & (c). The first mass loss (b) occurred between 30°C and 150°C and was calculated to be 5.08% (m/m) which could be attributed to the dehydration of the sample. The second mass loss (c) observed occurred between 160°C and 380°C and was calculated to be 88.36°C (m/m) which could be attributed to the thermal decomposition of the sample.

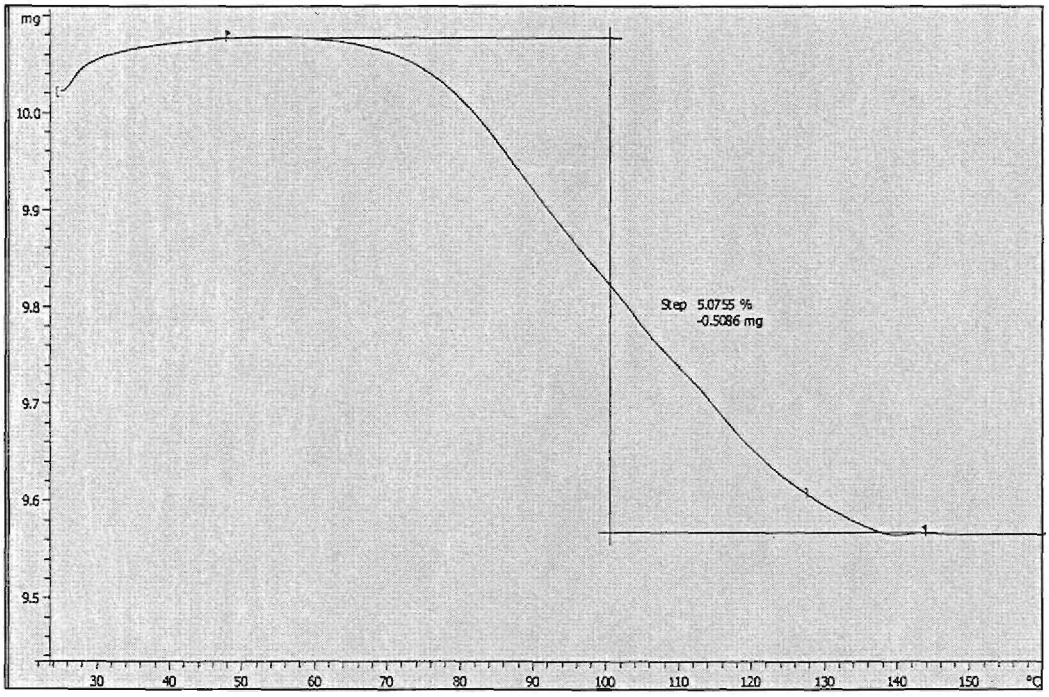
The kinetic parameters for the dehydration of fluconazole Form MH and the hydrated Form I were determined using TGA. The Ozawa method [8] was used in this study to determine the dehydration activation energy (E_A) for the mentioned hydrates.

This method involved the analysis of the weight loss *vs.* temperature thermograms, at different heating rates (β), in order to determine the corresponding temperatures (temperatures in Kelvin) at a constant weight loss (C).

The dehydration of fluconazole Form MH and the hydrated Form I was studied, by exposing the hydrated crystal forms to five different TGA heating rates of 1, 2, 3, 5, and 10°C/min, respectively. The TGA thermograms of fluconazole Form MH and the hydrated Form I, at different heating rates, are depicted in figure 14.

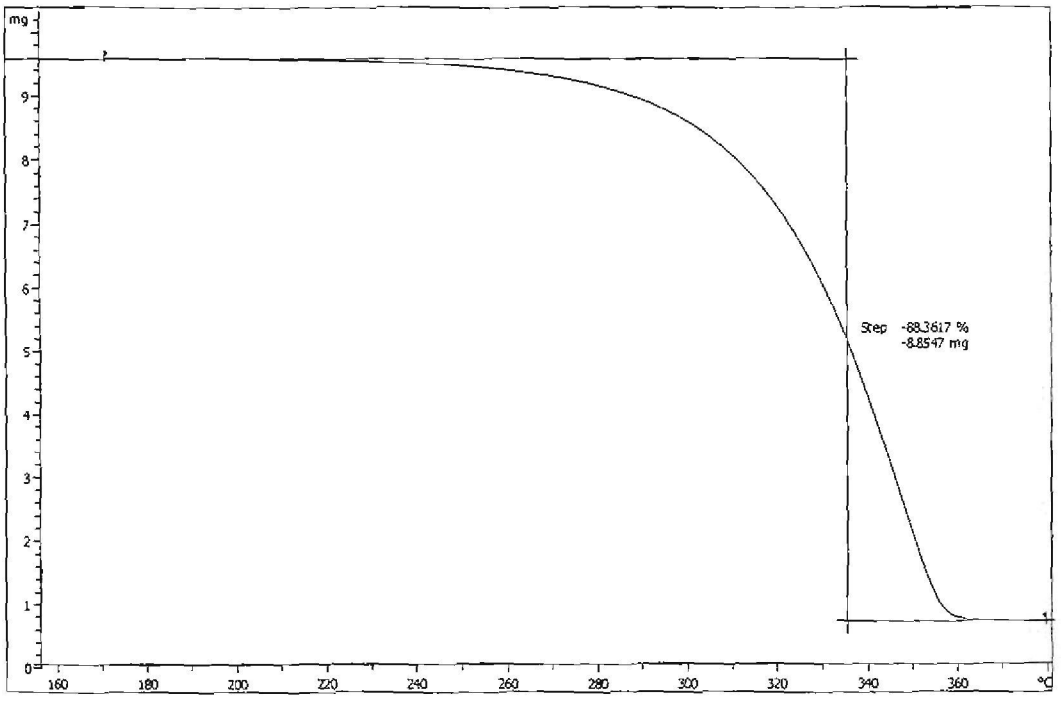


(A)



(B)

Figure 13 The (a) TGA thermogram of Form MH when heated from 25-380°C. (b) TGA trace between 25-150°C.



(C)

Figure 13 (c) The TGA trace between 160-380°C of Form MH when heated from 25-380°C.

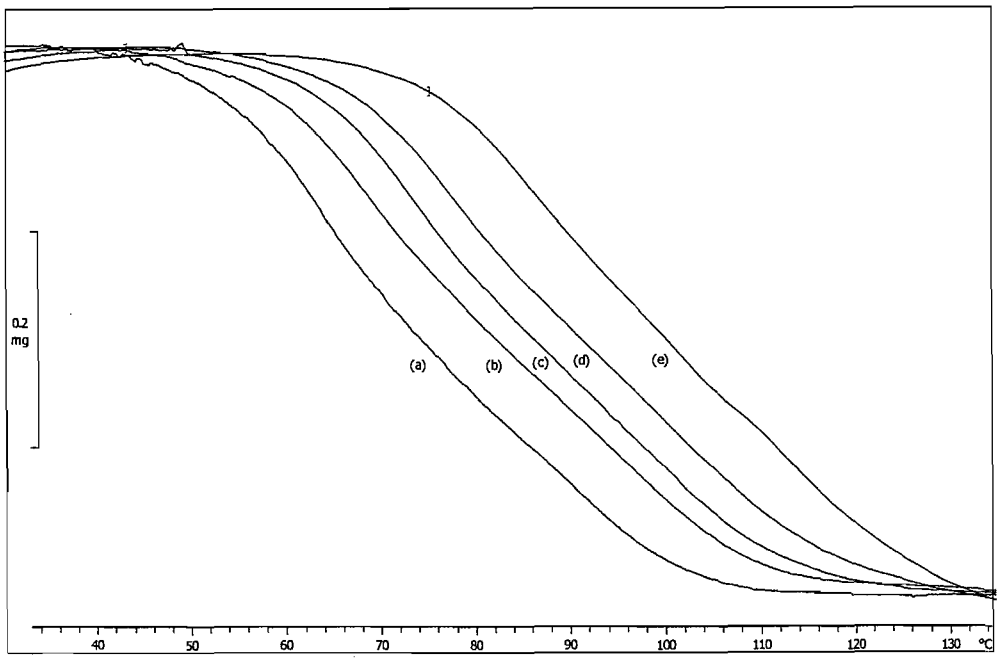
The dehydration activation energy (E_A) was calculated using the following equation and the derivatives thereof:

$$\log \beta = \log\left(\frac{AE_A}{R}\right) - 2.315 - 0.4567\left(\frac{E_A}{RT}\right) - \log g(\alpha)$$

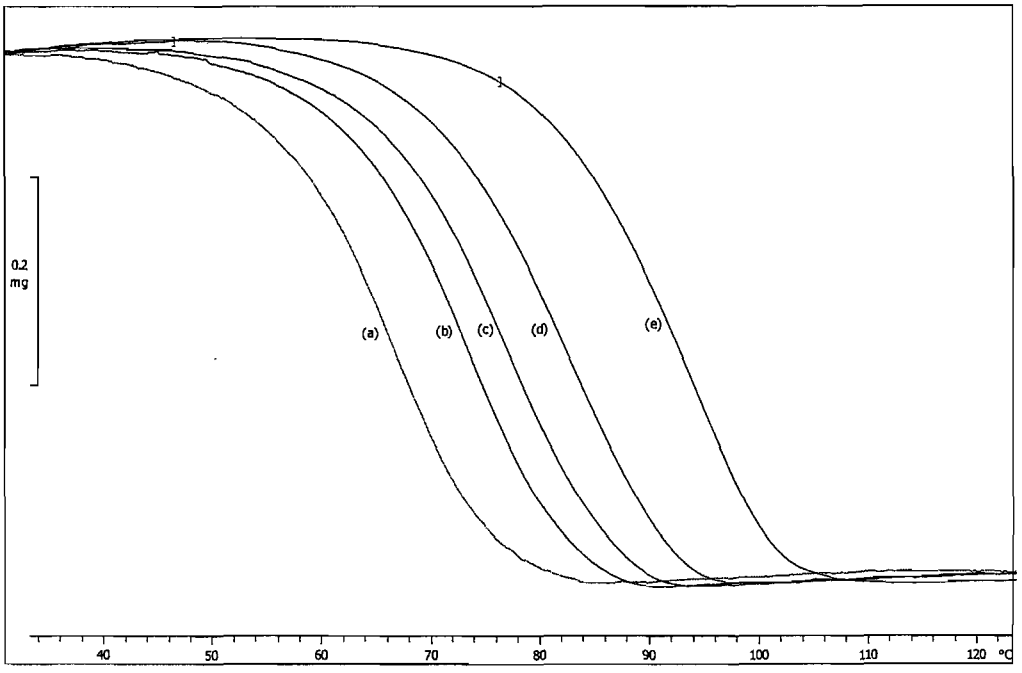
Where β is the heating rate ($K.min^{-1}$), A is the pre-exponential factor (min^{-1}), R is the universal gas constant (8.314 $J.mol^{-1}.K^{-1}$) and:

$$g(\alpha) = \left(\frac{AE_A}{\beta R}\right) P(x)$$

And $x = \frac{E_A}{RT}$



(a)



(b)

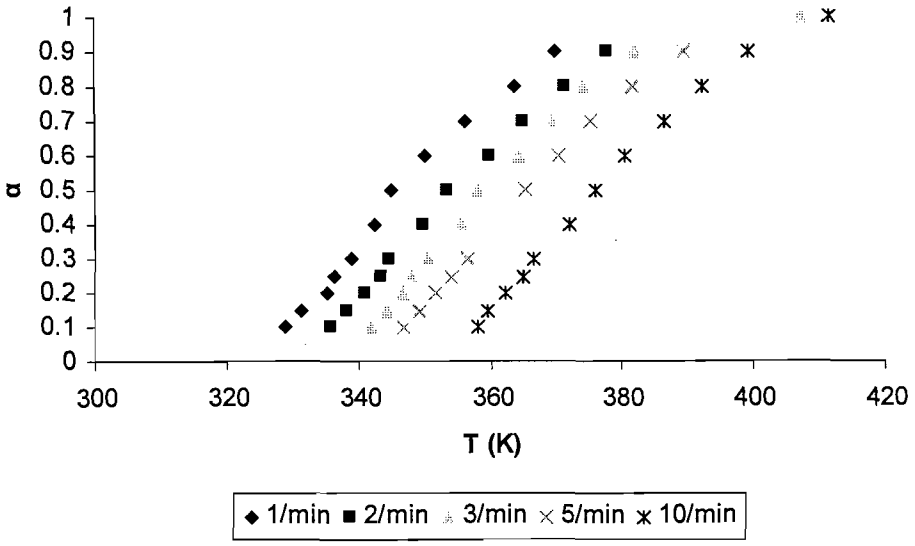
Figure 14 TGA thermograms of fluconazole (a) Form MH and the (b) hydrated Form I at heating rates of (a) 1, (b) 2, (c) 3, (d) 5 and (e) 10°C/min.

α is the fraction reacted (i.e. dehydrated fraction), which was calculated using the following equation:

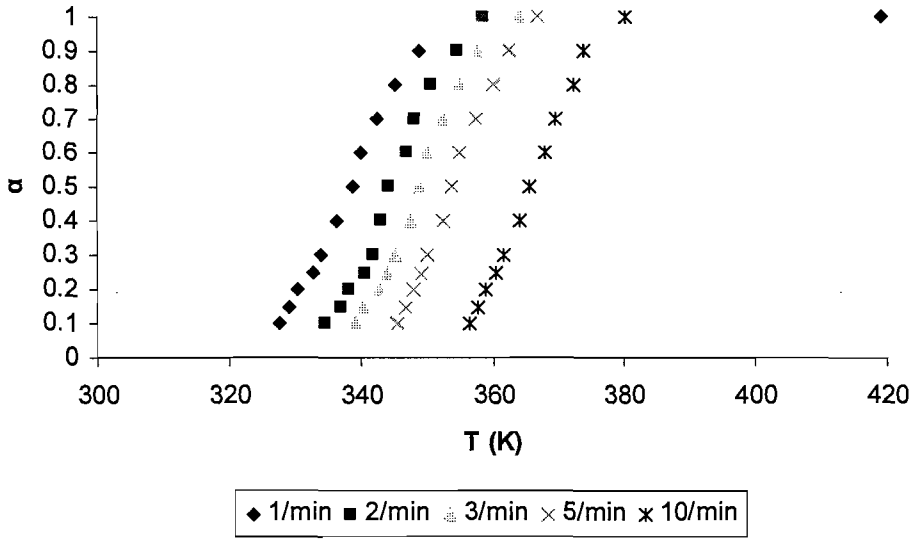
$$\alpha = \frac{(W_0 - W_t)}{(W_0 - W_f)}$$

Where W_0 is the initial mass of the sample, W_t the mass of the sample at temperature t, and W_f is the final mass at a temperature at which the mass loss of the sample is approximately unchanged.

The plots of dehydrated fraction (α) versus the absolute temperature (T) for Form MH and the hydrated Form I at various heating rates (β) are depicted in figure 15.



(a)



(b)

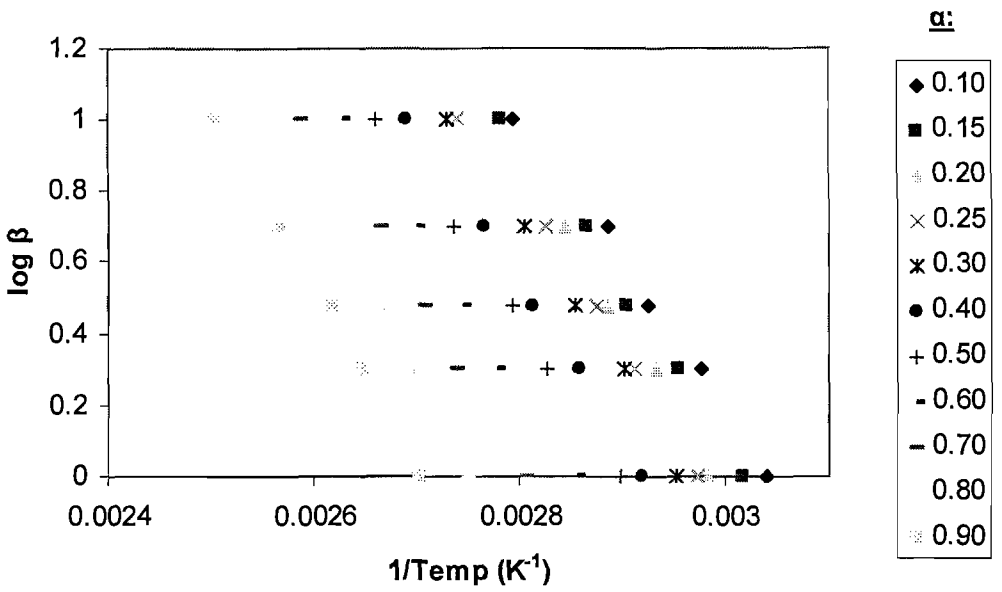
Figure 15 The plots of dehydrated fraction (α) versus the absolute temperature (T) for (a) Form MH and the (b) hydrated Form I at various heating rates: 1, 2, 3, 5 & 10 °C/minute.

Figures 15 (a) and (b) indicated that the dehydration process in both crystal forms was initiated at T > 320 K and that the dehydration process in the Form MH sample terminated at higher a temperature (T > 380 K) compared to that observed for the hydrated Form I (T < 380 K).

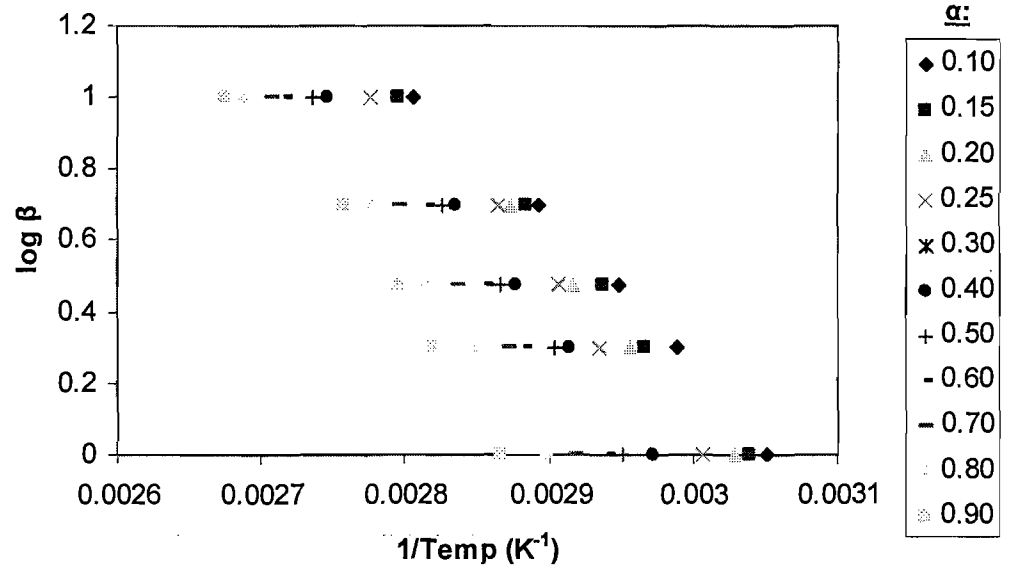
Plots of log β versus 1/T for Form MH and the hydrated Form I gave parallel lines for each α value (figure 16). The dehydration activation energies for the two samples

were calculated from the slopes (m) of these parallel lines using the following calculation:

$$m = \frac{-0.4567\, E_A}{R}$$



(a)



(b)

Figure 16 Plots of log β versus 1/T for (a) Form MH and the (b) hydrated Form I for each α value ranging between 0.10-0.90.

The dehydration activation energy for the hydrated Form I was found to be 0.4 kJ/mol higher compared to that of monohydrate Form MH (table 3).

Table 3 Dehydration activation energy (E_A) calculated from the Ozawa method for fluconazole Form MH and the hydrated Form I

Form MH	Hydrated Form I
81.9±5.9 kJ/mol	82.3±5.6 kJ/mol

The DSC thermogram of Form MH (figure 9) revealed a sharp endotherm at 101°C (ΔH_{trans}=1.33±0.22 kJ/mol) which could be attributed to an endothermic rearrangement of the dehydrated lattice to transform in the thermodynamic stable Form I rather than a sheer dehydration endotherm as suggested by previous authors [2]. However, this endotherm was not detected in the DSC thermogram of the hydrated Form I (figure 7).

VT-XRPD studies (figure 17) revealed that the stabilization of the dehydrated lattice of the hydrated Form I was concluded at a lower temperature (85°C) compared to that observed for Form MH (130°C), suggesting that the dehydration and endothermic rearrangement occurred simultaneously (for the hydrated Form I), contributing the slightly higher dehydration activation energy observed for the hydrated Form I, and the absence of the rearrangement endotherm in the DSC thermogram of the hydrated Form I at 101°C.

The effect of the dehydration on the surface properties of Form MH is illustrated in figure 18.

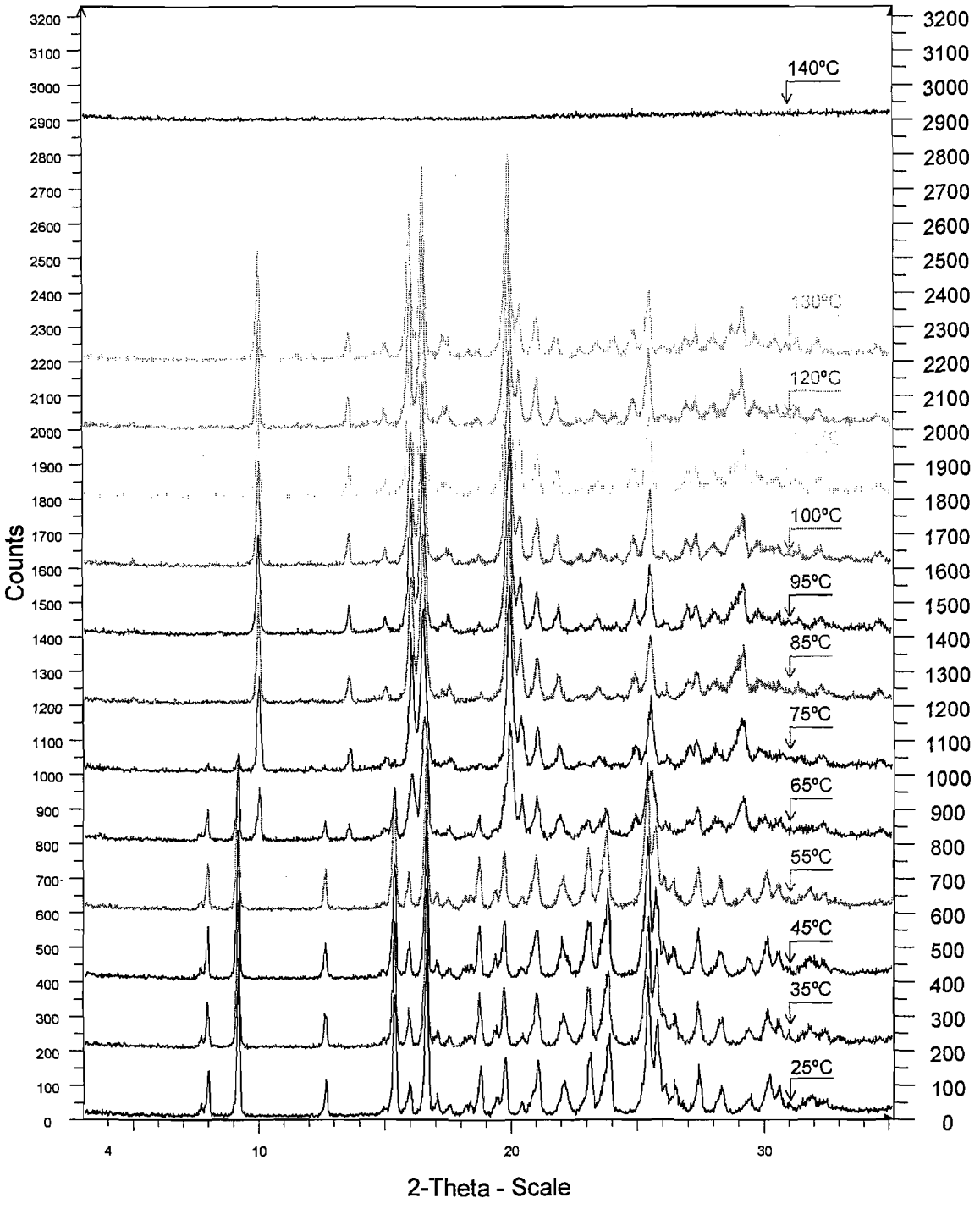


Figure 17 Overlay of the VT-XRPD patterns for hydrated Form I sample of fluconazole at increased temperatures ranging between 25-140°C.

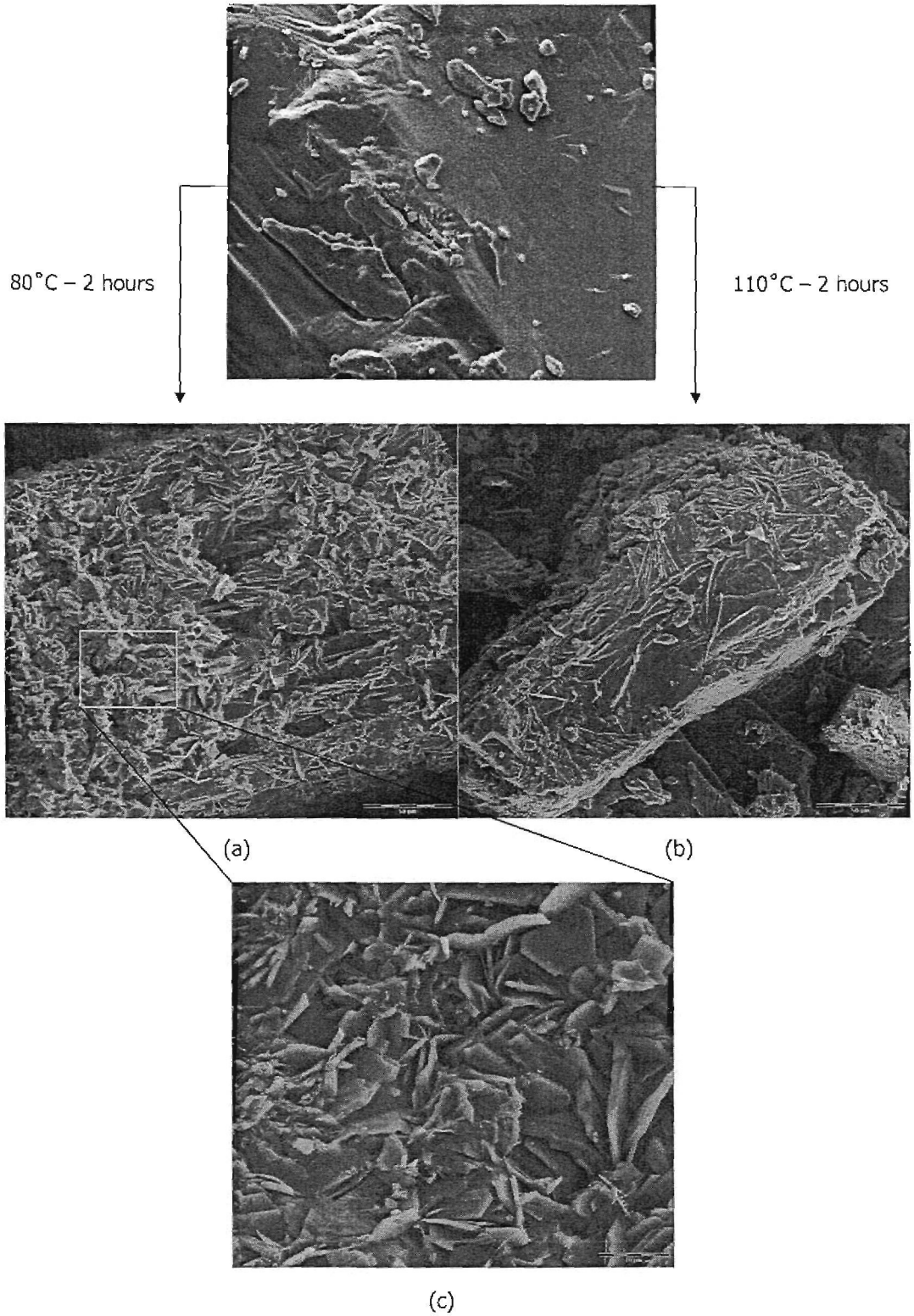


Figure 18 SEM photomicrograph of fluconazole Form MH (top) at ambient conditions. SEM photomicrographs after exposure to 80°C (a) and 110°C (b) for 2 hours, (c) is a magnification of the surface of the sample exposed to 80°C for 2 hours.

From figure 18 it is clear that dehydration of Form MH caused a disruption in the initial smooth surface of the crystal producing a rough, conglomerated surface. Once the sample has been heated past the crystal rearrangement temperature (101°C) the surface of the crystal is transformed into a more flattened surface with plate-like structures stacked upon each other, similar to that observed for the recrystallised Form I (figure 2(a)).

4. Conclusion

Hydration of the anhydrous form of fluconazole (Form I) to produce Form MH should be prevented during the storage of the raw material and manufacturing of dosage forms to ensure the optimal bio-availability of this antifungal, due to the fact that the dissolution rate of anhydrate (Form I) is higher compared to that of the monohydrate, Form MH [2].

This study revealed that the monohydrated crystal from (Form MH) and the anhydrous form (Form I) remained stable when exposed to 0-85% RH (30°C) and 0-75% RH respectively. When Form I was exposed to 30°C – 85% RH it showed an affinity for water molecules, and incorporated the water molecules into the crystal lattice. The water absorption induced a polymorphic conversion, and the physico-chemical properties of the hydrated crystal form were found to be comparable to that of Form MH (figure 19).

The XRPD pattern, moisture content and IR-spectrum of the hydrated Form I was comparable with that of monohydrate, Form MH. However, the DSC thermogram of the hydrated Form I did not reveal the rearrangement endotherm at 101°C, which is characteristic to Form MH (table 4).

When the dehydration process of the hydrated Form I and Form MH was compared it became clear that the activation energy for dehydration of the hydrated Form I was slightly higher compared to that for Form MH due to the fact that the dehydration and endothermic rearrangement event occurred simultaneously (for the hydrated Form I), contributing the slightly higher dehydration activation energy observed for the

hydrated Form I, explaining the absence of the rearrangement endotherm in the DSC thermogram of the hydrated Form I at 101°C.

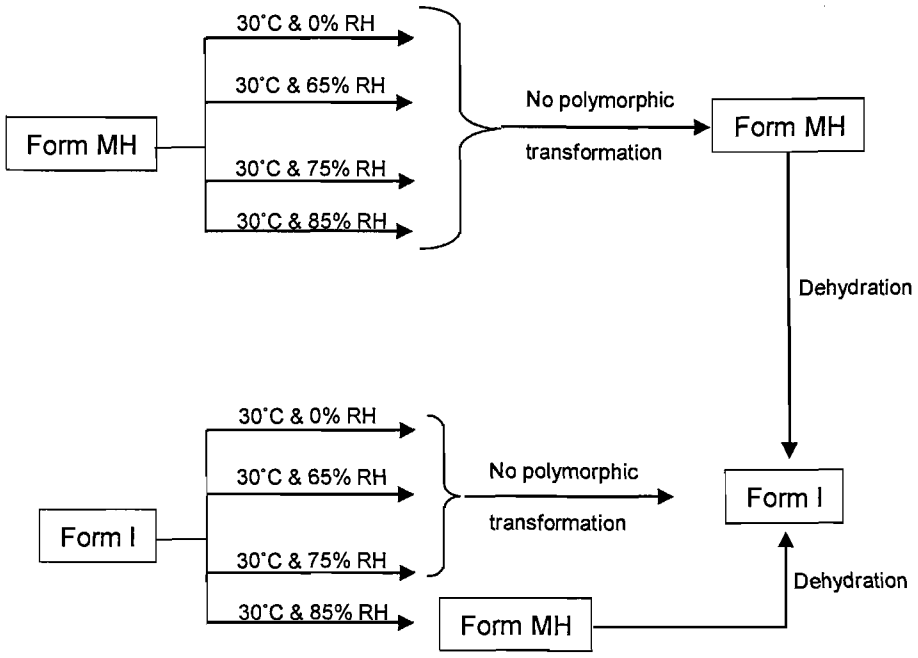


Figure 19 Schematic presentation of fluconazole Form I and Form MH stability when exposed to 0, 65, 75 and 85% RH at 30°C for 28 days.

VT-XRPD studies also revealed that the dehydration process for the hydrated Form MH terminated at a lower temperature (85°C) compared to that for Form MH (130°C), suggesting that the bond-strength between the incorporated water molecules and the fluconazole molecules in the hydrated Form I lattice was weaker compared to the recrystallised monohydrate (Form MH). When the hydrated Form I and monohydrate (Form MH) was dehydrated, both converted to the thermodynamic stable Form I.

Table 4 Properties of the hydrated Form I and Form MH

Property	Form MH	Hydrated Form I
XRPD patterns	Comparable XRPD patterns	
IR spectra	Comparable IR spectra	
DSC thermograms: • Dehydration endotherm range: • Rearrangement endotherm: • Melting point:	 50-90°C 101°C 139-141°C	 50-90°C None 139-141°C
VT-XRPD pattern: • Dehydration commenced at: • Dehydration terminated at:	 50°C 130°C	 65°C 85°C
Dehydration activation energy:	81.9±5.9 kJ/mol	82.3±5.6 kJ/mol

It can thus be concluded that Form I should be protected from high humidity conditions to prevent the hydration thereof that might jeopardize the optimal bio-availability of this antifungal.

5. Acknowledgements

The authors would like to acknowledge financial assistance from the Research Institute for Industrial Pharmacy®, North-West University and the National Research Foundation of South Africa.

5. References

[1] **DOLLERY, C.** 1999. Fluconazole. (*In.* DOLLERY, C. *ed.* Therapeutic drugs, 2nd Ed. 1999). London : Churchill Livingstone. f62-f68.

[2] **ALKHAMIA, K.A., OBAIDAT, A.A. & NUSEIRAT, A.F.** 2002. Solid-state characterization of fluconazole. Pharmaceutical development and technology.7(4):491-503.

[3] **CAIRA, M.R., ALKHAMIS, K.A. & OBAIDAT, R.M.** 2004. Preparation and characterization of a polymorph, monohydrate and an ethyl acetate solvate of the antifungal fluconazole. *Journal of pharmaceutical sciences.* 93(3):601-611p.

[4] **NYQVIST, H.** , 1983. Saturated salt solutions for maintaining specified relative humidities. *International journal of pharmaceutical technology and product manufacture*. 4(2):47-48.

[5] **BYRN, S.R., PFEIFFER, R.R. & STOWELL, J.G.** 1999. Solid-state chemistry of drugs. West Lafayette, Indiana: SSCI, Inc. 575p.

[6] **MATSUDA, Y., ESTUKO, T., ESTUKO, C. & YUKIE M.** 1984. Kinetic study of the polymorphic transformations of phenylbutazone. *Journal of pharmaceutical sciences*, 73:1453-1460.

[7] **ALKAHAMIS, K.A., SALEM, M.S. & OBIDAT, R.M.** 2006. Comparison between dehydration and desolvation kinetics of fluconazole monohydrate and fluconazole ethylacetate solvate using three different methods. Journal of pharmaceutical sciences. 95(4):859-870.

[8] **OZAWA, T.** 1965. A new method of analyzing thermogravimetric data. *Bulletin of the chemistry society of Japan*, 38:1881-1886.